ACTA CHIMICA

ACADEMIAE SCIENTIARUM HUNGARICAE

TOMUS 93 FASCICULUS 1

AKADÉMIAI KIADÓ, BUDAPEST

1977

ACTA CHIM. (BUDAPEST) ACASA 2 93 (1) 1–106 (1977)

ACTA CHIMICA

A MAGYAR TUDOMÁNYOS AKADÉMIA KÉMIAI TUDOMÁNYOK OSZTÁLYÁNAK IDEGEN NYELVŰ KÖZLEMÉNYEI

Acta Chimica is a journal for the publication of papers on all aspects of chemistry, in the English, German, French and Russian languages.

Acta Chimica is published in 4 volumes per year. Each volume consists of 4 issues of varying size.

Manuscripts should be sent to

Acta Chimica
H-1521 Budapest, Hungary

Correspondence with the Editors should be sent to the same address. Manuscripts are not returned to the Authors.

Subscription rate $ 32.00 per volume.

Hungarian subscribers should order from Akadémiai Kiadó, 1363 Budapest, P.O. Box 24. Account No. 215 11488.

Orders from other countries are to be sent to "Kultúra" Foreign Trade Company (H-1389 Budapest 62, P.O. Box 149. Account No. 218 10990) or to its representatives abroad.

ACTA CHIMICA

ACADEMIAE SCIENTIARUM HUNGARICAE

TOMUS 93

AKADÉMIAI KIADÓ, BUDAPEST

1977

ACTA CHIM. (BUDAPEST)

ACTA CHIMICA

TOMUS 93

FASCICULUS 1
FASCICULUS 2
FASCICULUS 3—4

INDEX

Acta Chimica Academiae Scientiarum Hungaricae, Tomus 93 (1), pp. 1—21 (1977)

EFFECT OF CYCLIC STRUCTURE ON THE RADIOLYSIS OF HYDROCARBONS, IV

RADIOLYISIS OF ALKYLCYCLOPENTANES AND ALKYLCYCLOHEXANES, II THE PROBLEMS OF BIRADICALS

L. WOJNÁROVITS and G. FÖLDIÁK

(Institute of Isotopes of the Hungarian Academy of Sciences)

Received October 11, 1975

On generalization of earlier results (Acta Chim. (Budapest) **82,** 285 (1974)), radiolysis of C_nH_{2n} cyclopentane and cyclohexane compounds containing normal and branched alkyl side chains revealed that, in accordance with the energy conditions, the open-chain alkenes C_nH_{2n} formed as the main products of C–C bond splitting are predominantly produced by the rupture of C–C bonds linked to carbon atoms situated at the positions of ring branching. The products include all those alkenes the double bonds of which are adjacent to such a carbon atom.

The yield of skeletal isomer products decreases with the increase in length of the side chain and its degree of branching. By their decompositions, the branched side chains protect the ring from breakdown 'intramolecularly'.

Investigations with radical scavengers show that some of the skeletal isomer products are formed in bimolecular reactions of open-chain alkyl monoradicals. The residual larger yield cannot be reduced with radical scavengers. The experimental results and various analogies strongly suggest that these 'monomolecular' reactions proceed *via* biradicals.

1. Introduction

By the splitting of a C–C bond in the ring, *cyclo*-C_nH_{2n} cycloalkenes containing 5 or more ring carbon atoms give rise mainly to open-chain alkenes C_nH_{2n}, *i.e.* to open-chain isomers of the initial cycloalkanes. It was reported earlier [1, 2] that the reactions of cyclopentane and of cyclohexane lead predominantly to 1-alkenes, whereas the methyl compounds yield larger proportions of 1- and 2-alkenes, and the ethylcyclohexanes give 1- and 3-alkenes.

In the present paper some further cycloalkanes, in part with longer and branched alkyl chains, have been studied in an attempt to discover how the yield of the alkenes depends on the structure of the molecule. The relatively large number of findings acquired to date have been used to clarify the mechanism of decomposition.

2. Possible reaction mechanisms

There are two fundamentally different reaction mechanisms for the formation of the open-chain alkenes: monomolecular and bimolecular.

The *monomolecular* reaction may in principle be a 'biradical' or a 'concerted' process. The majority of the publications [3—9] assume 'biradical'

processes, although the existence of these, and their role in the chemical transformations have at present not been completely proved. The contradictions are well characterized by the fact that even the definition [10] of the biradical itself is not unambiguous, for in a broader sense even individual triplet states can be regarded as biradicals. At the same time, according to the "narrower" definition of FREEMAN [11], biradicals are formations which react further as bifunctional radicals, but the closeness of the two radical sites inhibits bimolecular reactions.

The following reactions can be written for the formation of such a bifunctional radical intermediate from a cycloalkane, and for its subsequent transformations:

$$\textit{cyclo}\text{-}C_nH_{2n} \rightarrow \dot{C}H_2—(H_2)_{n-2}—\dot{C}H_2 \qquad (1)$$

$$\dot{C}H_2—(CH_2)_{n-2}—\dot{C}H_2 \begin{cases} \longrightarrow \textit{cyclo}\text{-}C_nH_{2n} & (2a) \\ \longrightarrow 1—C_nH_{2n} & (2b) \\ \longrightarrow C_2H_4 + \dot{C}H_2—(CH_2)_{n-4}—\dot{C}H_2 & (2c) \end{cases}$$

In principle, in addition to these, in the presence of a radical scavenger (S) it is also necessary to assume the reaction

$$\dot{C}H_2—(CH_2)_{n-2}—\dot{C}H_2 + S \rightarrow \text{scaveging product} \qquad (3)$$

If the overall rate constant for reactions (2) is k_2, and that for reaction (3) is k_3, while the yield of biradical formation is G_k molecules/100 eV, then we have the following expression for the yield of the scavenged product:

$$G(S_p) = G_k \frac{k_3[S]}{k_3[S] + k_2} \qquad (4)$$

The value of rate constant k_3 can be expected to be of the order of those for diffusion-controlled processes, *i.e.* $\sim 10^{10}\ M^{-1}s^{-1}$. If $[S] = 0.1\ M$, the sensitivity of determination of $G = 0.01$, and the yield of ring-opening $G_k = 1.0$, then the yield of the scavening product can be measured only if $k_2 < 10^{11}\ s^{-1}$, *i.e.* if the half-life of further transformation of the biradical is longer than $\sim 10^{-11}$ s.

In contrast with the foregoing, the transition state of the 'concerted' transformation is of a non-radical character. For example, this can be conceived in that an internal hydrogen bond is formed in the ring, and the hydrogen atom necessary for product formation migrates *via* this either before or simultaneously with the bond rupture. Thus, on the example of methylcyclopentane:

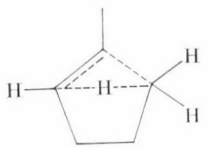

For *bimolecular* alkene formation, it is necessary that monoradicals first be produced, the further reactions of these leading to monoalkene. In the radiolysis of cyclopentane and cyclohexane, such radicals are 1-pentyl and 1-hexyl ($G = 0.15$ and 0.2, respectively) [12, 13].

3. Experimental

The hydrocarbons were Fluka products; before use they were freed from unsaturated contaminants by sulfuric acid washing, and then purified by redistillation.

Irradiations were carried out with a ^{60}Co source at room temperature, the dose rate being $2.6 \cdot 10^{16}$ eV $g^{-1}s^{-1}$ (1.5 Mrd h^{-1}), and the dose $2 \cdot 10^{20}$ eV g^{-1} (3 Mrd). The experimental technique was reported in detail previously [1, 2].

4. Results

Data as to the yields of the alkene products C_nH_{2n} from the cyclopentane and cyclohexane derivatives studied are given in Tables I—III, while the G values of the more important products of splitting of the alkyl group from the ring are to be found in Table IV. The yields were also investigated for some products of 1,1-dimethylcyclohexane, *cis*- and *trans*-1,2-dimethylcyclohexanes, 1,3-dimethylcyclohexane containing the *cis* and *trans* isomers in a ratio of 72 : 28, *cis*- and *trans*-1,4-dimethylcyclohexanes, and *cis*- and *trans*-decalins (Tables V—VI).

In addition to the tabulated compounds, all of the cycloalkanes also yield fragmentation hydrocarbons indicative of the cleavage of the rings. Analogously as reported earlier [14] in connection with cyclopentane, cyclohexane and their methyl and ethyl derivatives, these are predominantly open-chain monoalkenes. For cyclopentane the yield of decomposition to the fragments $G \approx 0.5$ molecule/100 eV, as compared with a value of ~ 0.1 for cyclohexane. The fragment formed in highest yield is generally ethylene ($G = 0.05$—0.4). Increase in the length of the side-chain is accompanied by a gradual decrease in the extent of fragmentation.

For cyclic hydrocarbons with side chains containing two or more carbon atoms, it is also possible to observe formation of products where rupture has occurred at a C–C bond in the side-chain: for example, on radiolysis of butylcyclohexane, methyl-, ethyl- and propylcyclohexanes are formed in small amounts, with individual G values of ~ 0.02. The probability of decomposition of the side chain is considerably higher in cycloalanes containing branched side chains:

(a) on radiolysis of isopropylcyclohexane, methyl groups are split off from the side chain with a yield of ~ 0.1;

Table I

G values of open-chain isomeric products of cyclopentanes

C atom number (n)	5	6	7	8	9	10
cycloalkane / product	cyclo-pentane	methyl-cyclo-pentane	ethyl-cyclo-pentane	propyl-cyclo-pentane	butyl-cyclo-pentane	pentyl-cyclo-pentane
1-C_nH_{n2}	0.70	0.75	0.40	0.30	0.21	0.30*
cis-2-C_nH_{2n}	0.02	0.10	0.23	0.03		
trans-2-C_nH_{2n}		0.23				
cis-3-C_nH_{2n}		~0.02	0.13	0.18	0.10	
trans-3-C_nH_{2n}			0.37			
cis-4-C_nH_{2n}				0.11	0.08	0.10
trans-4-$_nCH_{2n}$				0.35	0.31	
cis-5-C_nH_{2n}						0.05
trans-5-C_nH_{2n}						
Isoalkenes	—	0.10	0.09	~0.08	0.09	0.06
Σ C_nH_{2n}	0.72	1.20	1.22	1.05	0.79	0.51

* 1-decene + *trans*-4-decene

Table II

G values of open-chain isomeric products of cyclohexanes

C atom number (n)	6	7	8	9	10	11
cycloalkane / product	cyclo-hexane	methyl-cyclo-hexane	ethyl-cyclo-hexane	propyl-cyclo-hexane	butyl-cyclo-hexane	pentyl-cyclo-hexane
1-C_nH_{2n}	0.34	0.34	0.22	0.18	0.17	0.33*
cis-2-C_nH_{2n}	0.02	0.08	0.03			
trans-2-C_nH_{2n}		0.20				
cis-3-C_nH_{2n}	0.01		0.06	0.03		
trans-3-C_nH_{2n}			0.20			
cis-4-C_nH_{2n}				0.06	0.02	
trans-4-C_nH_{2n}				0.22		
cis-5-C_nH_{2n}					0.045	0.04
trans-5-C_nH_{2n}					0.18	
Isoalkenes	—	0.10	0.08	~0.04	~0.025	~0.02
Σ C_nH_{2n}	0.37	0.72	0.59	0.53	0.44	0.39

* 1-undecene + *trans*-5-undecene

Table III

Open-chain isomeric products of isobutylcyclopentane, isopropylcyclohexane and tert-butylcyclohexane

Isobutylcyclopentane	
product	G
7-methyl-1-octene	0.44*
trans-2-methyl-4-octene	
cis-2-methyl-4-octene	
trans-2-methyl-3-octene	0.13
cis-2-methyl-3-octene	0.04
other C_nH_{2n}	0.07
Total	0.68

* Due to the poor separation of the gas chromatographic peaks, the individual G values could not be determined

Isopropylcyclohexane	
product	G
cis-2-methyl-3-octene	0.01
trans-2-methyl-3-octene	0.075
7-methyl-1-octene	0.05
2-methyl-2-octene	0.02
other C_nH_{2n}	0.07
Total	0.22

tert-butylcyclohexane	
product	G
trans-2,2-dimethyl-3-octene	0.05
cis-2,2-dimethyl-3-octene	$\sim$0.006
7,7-dimethyl-1-octene	0.02
other C_nH_{2n}	$\sim$0.01
Total	0.08

(b) on decomposition of isobutylcyclopentane, the methyl and isopropyl groups split off from the side chain with G values of $\sim$0.12 and $\sim$0.4, respectively;

(c) on irradiation of *tert*-butylcyclohexane, detachment of one methyl group from the quaternary carbon atom leads to isopropyl-, isopropenyl- and isopropylidenylcyclohexane with a combined yield of $G \approx 0.2$.

As is known from the literature [15, 16], among the C_n products *n*-pentane and *n*-hexane are formed on radiolysis of cyclopentane and cyclohexane, respectively ($G = 0.10$ and 0.06, respectively). Products of a similar nature are also formed on decomposition of the alkylcycloalkanes too, but the yield is fairly small.

Among the dimerized products, hydrocarbons C_nH_{2n+1}-*cyclo*-C_nH_{2n-1} indicate coupling of cyclic and open-chain molecules; for instance, the forma-

Table IV

G values for removal of the alkyl side chains of alkylcyclopentanes and alkylcyclohexanes, and bond energies

	G (cyclopentane) or G (cyclohexane)	G (cyclopentene) or G (cyclohexene)	product	G	G_{est}	D* kcal mol^{-1}
Methylcyclopentane	0.1	0.1	methane	0.13	~0.2	83
Ethylcyclopentane	0.16	0.06	ethane	0.16	~0.3	80
Propylcyclopentane	0.13	0.08	propane	0.15	~0.25	80
Butylcyclopentane	0.10	0.07	butane	0.15	~0.2	80
Pentylcyclopentane	0.07	0.03	pentane	0.12	0.1—0.2	80
Isobutylcyclopentane	0.15	0.08		0.2	~0.025	80
Methylcyclohexane	0.08	0.14	methane	0.08	~0.2	84
Ethylcyclohexane	0.2	0.1	ethane	0.13	~0.3	80
Propylcyclohexane	0.14	0.08	propane	0.2	0.2—0.3	80
Butylcyclohexane	0.12	0.08	butane	0.17	0.2—0.3	80
Pentylcyclohexane	0.11	0.06	pentane	0.2	~0.2	80
Isopropylcyclohexane	1.02	0.36	propane propene	1.1	~1.5	76
tert-butylcyclohexane	1.8	0.4	isobutane isobutene	2.0	2.0—2.5	71

* The bond dissociation energies were estimated on the basis of data in Refs [18—20]

tion of pentylcyclopentane ($G = 0.05$) can be established on irradiation of cyclopentane. These products could not be identified or determined separately in every case on irradiation of alkylcycloalkanes of higher molecular weight. In the case of cycloalkanes of lower carbon atom numbers, the yields vary in the range $G = 0.05$—0.12. For the alkylcycloalkanes containing more carbon atoms, the yields are to be expected to be somewhat less than this.

It was earlier reported [1] that for cyclopentane, cyclohexane and their methyl and ethyl derivatives the yield of the C_n alkene decreases by 20—40% in the presence of scavengers in a concentration of 0.01 — 0.1 M. Some more recent investigations, mainly with propylcyclopentane, propylcyclohexane and 1,2- and 1,4-dimethylcyclohexanes, indicate a similar, relatively small decrease (5—25%) in the yields of the alkene molecules too. On addition of radical scavengers, the G values for the C_nH_{2n+2} and C_nH_{2n+1}-*cyclo*-C_nH_{2n-1} alkanes decrease by ~70—90%.

Table V

Skeletal isomeric products of dimethylcyclohexanes

1,1-dimethylcyclohexane [23]	
product	G
6-methyl-1-heptene	0.35
2-methyl-2-heptene	0.50
2-methyl-1-heptene	0.40
other open-chain C_8H_{16}	0.10
Total	1.35

1,2-dimethylcyclohexanes [22]		
product	G_{cis}	G_{trans}
cis-2-octene	0.25	0.12
trans-2-octene	0.80	0.63
1-octene	0.13	0.40
5-methyl-1-heptene	0.1	0.07
Total	1.28	1.22

1,3-dimethylcyclohexane (*cis-trans* ratio 72 : 28)	
product	G
2-methy-1-heptene	0.14
cis-6-methyl-2-heptene	~0.07
trans-6-methyl-2-heptene	~0.24
6-methyl-1-heptene	~0.03
4-methyl-1-heptene	~0.20
cis-4-methyl-2-heptene	0.05
trans-4-methyl-2-heptene	~0.14
Total	0.87

1,4-dimethylcyclohexanes [22]		
product	G_{cis}	G_{trans}
3-methyl-1-heptene	0.20	0.18
cis-5-methyl-2-heptene	0.12	0.09
trans-5-methyl-2-heptene	0.24	0.30
5-methyl-1-heptene	0.08	0.10
Total	0.64	0.67

Table VI

Irradiation products of decalins **[22]**

Product	G_{cis}	G_{tran}
4-cyclohexyl-1-butene	0.08	0.08
1-butylcyclohexene	0.05	0.04
other butylcyclohexenes	~0.03	~0.03
Total	0.16	0.15

5. Discussion

5.1. *Split-off and decomposition of the side-chain*

On irradiation of methylcyclopentane, the most important products of removal of the methyl group are methane ($G = 0.12$), cyclopentane and cyclopentene ($G = 0.19$). The low methane yield shows that a considerable pro-

portion of the split-off methyl group is transformed not to methane, but to some other product; it may be assumed that the methyl radicals couple with methylcyclopentyl radicals to yield dimethylcyclopentane isomers. In the present experiments all the five possible isomers were shown to be formed, but the yields were very low, their overall G-value being ~ 0.1. Products of combination of the cyclopentyl radicals with the methylcyclopentyl radicals were found only in traces. The total yield for methyl group removal is therefore $G \sim 0.20$—0.25.

The frequency of splitting-off of the alkyl group was also estimated for the other alkylcycloalkanes; the relevant values are listed in column 6 of Table V. While the extent of detachment decreases somewhat with increasing length of the alkyl side chain on irradiation of both alkylcyclopentanes and alkylcyclohexanes, on irradiation of isopropyl- and *tert*-butylcyclohexane the side chain splits off with a frequency larger by about one order of magnitude than from alkylcycloalkanes with straight side chains. The frequency of splitting-off is the higher, the lower the energy of the given bond. At the same time, however, the frequency of rupture of a bond with a given dissociation energy decreases with the size of the molecule. A similar finding was made earlier [17] in connection with the radiolysis of non-cyclic alkanes.

In accordance with what was mentioned as regards the experimental findings, the rupture of other C–C bonds of the side chain proceeds with comparatively low yield. A more significant decomposition arises only for alkylcycloalkanes with branched side chains, and primarily in the case of isobutylcyclopentane, where the C–C bonds linked to the tertiary carbon atom of the branched side chain dissociate with a yield of $G \approx 0.6$ (*cf.* Section 4).

5.2. *Isomerization of rings to open-chain alkenes*

It can be seen from Tables I and II that the combined G value for the isomeric products with open-chain skeletons $(G(\Sigma$ skeletal isomer$))$ increases strongly (by ~ 60 and 90%, respectively) on progressing from the unbranched cycloalkane to the methylcycloalkane in both the cyclopentane and the cyclohexane series; with the increase of the length of the n-alkyl chain, it then gradually diminishes (Figs 1 and 2).

The Figures also give the $g(\Sigma$ skeletal isomer) values, which were calculated on the basis of energy absorbed primarily by the rings only, assuming that the energy absorption is proportional to the electron fractions. For the n-alkylcyclopentanes and the n-alkylcyclohexanes, the value of $g(\Sigma$ skeletal isomer) varies in the ranges 1.7—1.3 and 0.9—0.7, respectively. Similarly to $G(\Sigma$ skeletal isomer), beginning from the ethylcycloalkanes the g values decrease a little with the carbon atom number in both series.

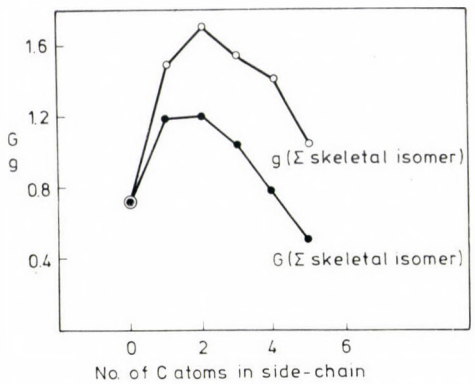

Fig. 1. $G(\Sigma$ skeletal isomer) and $g(\Sigma$ skeletal isomer) values of *n*-alkylcyclopentanes

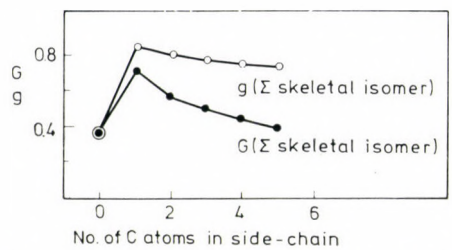

Fig. 2. $G(\Sigma$ skeletal isomer) and $g(\Sigma$ skeletal isomer) values of *n*-alkylcyclohexanes

According to the $G(\Sigma$ skeletal isomer) values, the yields of the products formed from the rings of the alkylcycloalkanes are twice those of the products formed from cyclopentane and cyclohexane, which are 0.72 and 0.37. This phenomenon is analogous with that observed in the radiolysis of branched-chain aliphatic compounds [17]: in both cases the alkyl branchings lead to a decrease in the energy of the weakest bond in the molecule, and therefore the frequency of C–C bond rupture increases.

The course of the $g(\Sigma$ isomer) values in Figs 1 and 2 also shows that isomeric products do not reveal the energy transfer from the side chain towards the ring, as observed for the aromatic hydrocarbons [21], but the decrease of the $g(\Sigma$ skeletal isomer) values for the higher carbon atom numbers is indicative of even a slight 'protective effect' of the alkyl chain. This can be seen even more clearly if the $G(\Sigma$ skeletal isomer) values for the pairs *n*-propylcyclohexane and isopropylcyclohexane, and *n*-butylcyclohexane and *tert*-butylcyclohexane, which contain the same numbers of carbon atoms, are compared: the $G(\Sigma$ skeletal isomer) values of the isopropyl and *tert*-butyl compounds are only 40% and 18%, respectively, of the values for the corresponding *n*-alkyl cyclohexanes, while the same numerical value is 85% for isobutyl- and *n*-butylcyclopentane. In these cases, in accordance with the discussion in

the foregoing section, splitting-off of the alkyl group from the ring and dissociation of the bonds of the side chain are very frequent. It follows from the competition of the bond ruptures, therefore, that as a result of the more probable splitting of the weaker C–C bonds between the tertiary–tertiary (isopropylcyclohexane), the quaternary–tertiary (*tert*-butylcyclohexane) or the tertiary–secondary and the tertiary–primary (isobutylcyclopentane) carbon atoms, the frequency of ring splitting is suppressed.

It can be seen from Tables II and V that the overall yield of the isomeric products is greater from every dimethylcyclohexane, than from ethylcyclohexane which contains the same number of carbon atoms [22, 23]. This phenomenon is analogous with what has already been observed in the radiation chemistry of open-chain alkanes [17]: the yield of the C–C bond-splitting products rises with the increase of the number of chain branchings. The highest $G(\Sigma$ skeletal isomer) values are exhibited by 1,1- and 1,2-dimethylcyclohexanes: in these, as a consequence of the quaternary, or the two linking tertiary carbon atoms, the C–C bond splittings are again strongly favoured for energetic reasons.

Tables I and II show that the skeletal isomeric products permit conclusions as to the very selective opening of the ring. The alkenes C_nH_{2n} predominantly have straight chains, and can thus be attributed to splitting at the tertiary carbon atom of the ring. Analogously as for the methyl and ethyl compounds [1], the straight-chain products suggest the following scheme for the mechanism of decomposition of *n*-propylcyclopentane:

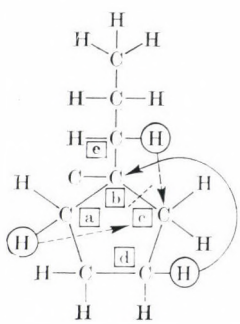

$$CH_3-CH_2-\boxed{e}CH_2-\boxed{b}CH_2-\boxed{a}CH_2-CH_2-\boxed{d}CH=\boxed{e}CH_2 \qquad (5a)$$

$$CH_3-CH_2-\boxed{e}CH_2-\boxed{b}CH=\boxed{a}CH-CH_2-\boxed{d}CH_2-\boxed{e}CH_3 \qquad (5b)$$

$$CH_3-CH_2-\boxed{e}CH=\boxed{b}CH-\boxed{a}CH_2-CH_2-\boxed{d}CH_2-\boxed{e}CH_3 \qquad (5c)$$

Transformation (5c) did not feature in our earlier work. Its assumption was necessitated by the fact that, on irradiation of *n*-propylcyclopentane, for example, in addition to the 1-octene and *cis*- and *trans*-4-octenes corresponding to processes (5a) and (5b), the 3-octenes also have a significant G value, and the formation of these can be interpreted formally only by a rearrangement of such a type. For the unbranched cyclopentane and cyclohexane, reactions (5a) and (5b) lead to formation of the same product, the 1-alkene, while naturally (5c) is not possible in this case. In the reaction of methylcyclopentane

and methylcyclohexane, process (5c) leads to the same result as (5a) the formation of 1-hexene or 1-heptene, while in the reaction of *n*-butylcyclopentane and *n*-pentylcyclohexane the same products, 4-nonenes or 5-undecenes, are formed in processes (5b) and (5c).

The main products of isopropylcyclohexane are 7-methyl-1-octene and 2-methyl-3-octenes, while those of *tert*-butylcyclohexane are 7,7-dimethyl-1-octene and 2,2-dimethyl-3-octenes, the formation of which may be interpreted on the basis of reactions of type (5a) and (5b). On irradiation of isopropylcyclohexane, 2-methyl-2-octene is formed in reaction (5c), whereas a reaction of this type is not possible for *tert*-butylcyclohexane.

6-Methyl-1-heptene and 2-methyl-2-heptene, the isomeric products obtained in highest yield on radiolysis of 1,1-dimethylcyclohexane, are formed by rupture of some ring C–C bond linked to the quaternary carbon atom, essentially analogously to reactions (5a) and (5b). 2-methyl-1-heptene is to be found in appreciable yield among the products; this may be interpreted by opening of the ring at the quaternary carbon atom and incorporation of the double bond between the quaternary carbon atom and one of the methyl groups, *i.e.* by a process analogous to reaction (5c) [23].

Irradiation of the 1,2-dimethylcyclohexanes leads mainly to formation of 1-octene and 2-octenes, indicating C–C bond rupture between the two tertiary carbon atoms. Following this bond rupture, the double bond is situated so as to yield 2-octene products, *via* either reaction (5a) or reaction (5b). Formation of 1-octene may be explained by incorporation of the double bond between one of the tertiary carbon atoms of the starting molecule and the carbon atom of the methyl group connected to it, *i.e.* by a process analogous to reaction (5c).

The product spectrum of the 1,2-dimethylcyclohexanes includes products indicative of rupture not only of the C–C bond between the two tertiary carbon atoms, but also of the C–C bond between one of the tertiary carbon atoms and the secondary carbon atom of the ring attached to it. Among these products, only 5-methyl-1-heptene was observed in a well-measurable yield.

The product spectrum of 1,3-dimethylcyclohexane is fairly complicated as a consequence of the relatively large number of products formed. Ring opening between 1 ring carbon atom (tertiary) and 2 (secondary), followed by formation of the products 2-methyl-1-heptene, *cis*- and *trans*-6-methyl-2-heptene, and 6-methyl-1-heptene, can be interpreted by reactions analogous to Eqs (5a), (5b) and (5c).

Ring opening between 1 ring carbon atom (tertiary) and 6 leads to 4-methyl-1-heptene in a rearrangement analogous to (5a) and (5c), and to *cis*- and *trans*-4-methyl-2-heptene in a transformation corresponding to (5b).

Formation of 3-methyl-1-heptene and *cis*- and *trans*-5-methyl-2-heptene, the most important open-chain isomeric products of irradiation of the 1,4-

dimethylcyclohexanes, can be explained by rearrangement processes analogous to (5a) and (5b) following C–C bond rupture at the tertiary carbon atom, while the lower-yield formation of 5-methyl-1-heptene is interpretable *via* a process similar to reaction (5c).

5.3. *Mechanism of skeletal isomerization*

As reported in section 4, radical scavengers in a concentration of 0.01—0.1 M in general decrease the yield of skeletal isomer products by 5—40%. Based on this finding alone, however, it is not possible to draw quantitative conclusions, for irradiation gives rise to many types of interactions between the scavengers and the intermediates of radiolysis; generally, for example, these interactions include not only radical capture, but also electron capture, and thus the yield decrease may be the result of both radical and electron capture. The comparatively low (5—40%) yield decrease, however, quite clearly shows that the skeletal isomer products are mainly formed in monomolecular reactions, and not in bimolecular processes.

Let us consider the same question from a different aspect. On irradiation of cyclopentane and cyclohexane in the presence of I_2 as scavenger, the open-chain alkyl radicals found in greatest yield were the 1-pentyl and 1-hexyl radicals, respectively [12, 13]. It is probable that analogous radicals are also formed from the cycloalkane derivatives. These radicals either abstract a hydrogen atom from neighbouring cycloalkane molecules [16], or undergo disproportionation reactions (7a) and (7b) or combination reaction (7c) with the cycloalkyl radicals, which are produced in very much larger amounts:

$$C_nH^{\cdot}_{2n+1} + \textit{cyclo}\text{-}C_nH_{2n} \rightarrow C_nH_{2n+2} + \textit{cyclo}\text{-}C_nH^{\cdot}_{2n-1} \qquad (6)$$

$$C_nH^{\cdot}_{2n+1} + \textit{cyclo}\text{-}C_nH^{\cdot}_{2n-1} \begin{cases} \longrightarrow C_nH_{2n+2} + \textit{cyclo}\text{-}C_nH_{2n-2} & (7a) \\ \longrightarrow C_nH_{2n} + \textit{cyclo}\text{-}C_nH_{2n} & (7b) \\ \longrightarrow C_nH_{2n+1}\text{-}\textit{cyclo}\text{-}C_nH_{2n-1} & (7c) \end{cases}$$

Formation of the products C_nH_{2n+2} and C_nH_{2n+1}-*cyclo*-C_nH_{2n-1} in radical reactions is supported by our observation that their yield decreases sharply in the presence of radical scavengers. In process (7b) a proportion of the cycloalkyl radicals are converted to cycloalkane again, while in addition an open-chain alkene is formed. On the basis of data relating to analogous radicals, the ratio for the disporportionation and combination reactions between the open-chain alkyl and cycloalkyl radicals can be estimated as $(k_{7a} + k_{7b})/k_{7c} = 0.2—0.6$ [24—26]. The low yield of the products C_nH_{2n+1}-*cyclo*-C_nH_{2n-1} ($G = 0.05—0.12$) demonstrates that only a few hundredths of a G unit of open-chain alkene can be produced in reaction (7b).

In summary, therefore, it may be stated that the skeletal isomer products are predominantly formed *via* a monomolecular path, but the question remains as to whether this is a 'biradical' or a 'concerted' process. Our considerations with regard to this are given below.

5.4. *Are biradicals necessary for interpretation of the reactions?*

In the presence of radical scavengers the product originating from capture of the biradical formed may be produced in accordance with Eq. (3). For example, if the radical scavenger in the radiolysis of cyclopentane is I_2, then 1,5-diiodopentane may be formed, whereas if it is ethylene then the scavenging products will be cycloheptane and 1-heptene. On gas chromatographic analysis of the irradiated cyclopentane–ethylene and cyclopentane–iodine systems, peaks were found which probably correspond to cycloheptane and 1-heptene and to 1,5-diiodopentane, but their yields were very low, not exceeding 0.01—0.03. This further means that if bifunctional biradicals are formed at all during the reaction, then their half-life must be less than a few times 10^{-10} s. At the same time the lower limit to the life-time of hypothetical biradicals is controlled by the time of rotation around the C–C bond, the frequency of which is $\sim 10^{13}$, and thus the time for one rotation is $\sim 10^{-13}$ s.

Despite the limited results of the biradical scavenging experiments, several factors point to the biradical mechanism:

(a) the composition of the products;

(b) stereochemical considerations and the phase effect;

(c) analogy with the photolysis of cycloalkanones.

Composition of the products

Rearrangement of the biradical formed on opening, to give an open-chain alkene end-product, can be explained by internal hydrogen atom migration: for example, on irradiation of *n*-propylcyclopentane octene is formed by transfer of one hydrogen atom in a strongly exothermic process (50—60 kcal mol^{-1}) from carbon atom 2 to carbon atom 5, or from carbon atoms 4 or 6 to carbon atom 1, in the biradical

$$\underset{1}{\dot{C}H_2}-\underset{2}{CH_2}-\underset{3}{CH_2}-\underset{4}{CH_2}-\underset{5}{\dot{C}H}-\underset{6}{CH_2}-\underset{7}{CH_2}-\underset{8}{CH_3}$$

The hydrogen transitions from C 2 to C 5, from C 4 to C 1 and from C 6 to C 1 yield 1-octene, 4-octene and 3-octene respectively.

As Table I shows, these products are actually formed in the irradiation (reactions (5a), (5b) and (5c)).

This finding can be generalized for the other cycloalkanes examined too: in the course of the reactions every open-chain alkene is formed in which the double bond is linked to a carbon atom a C–C bond of which breaks during the ring opening. Other C_n alkene products could be detected only in the decomposition of some cycloalkanes and only in traces. Reactions leading to formation of alkenes other than 1-alkenes are not stereospecific, for both *cis* and *trans* isomers are produced. The findings therefore strongly suggest biradical intermediates: since the 'concerted' mechanism is very selective [27, 28], if the process were to take place in that way, then only the formation of some of the products, possibly in very low numbers, might be expected.

Our cyclic isomerization experiments also permit conclucions as to biradical intermediates [22]. When pure *cis*- or *trans*-1,2- or 1,4-dimethylcyclohexane or decalin was irradiated in the presence of a radical scavenger, it was observed that the opposite cyclic isomer is generally formed in significant yield. The monomolecular reaction could be explained only by opening of the ring to give a biradical, followed by reclosure of the latter.

Stereochemical considerations and the phase effect

The possibilities of skeletal isomerization and the further reactions of the biradicals, *e.g.* hydrogen shift, are influenced by the steric characteristics of the intermediate and end-product. Accordingly, a study was made of the question of what product ratios are preferred in the event of possible hindered rotations of the alkyl groups (non-bonded interactions), primarily in the activated complexes, and whether the yield ratios to be expected on the basis of these agree with those actually observed (Table VII).

On rearrangement according to (5a) and (5b) of the 1,5-biradicals formed from cyclopentane and its derivatives, in the activated state corresponding to the 1,4-hydrogen shift the ring may be either planar or a little twisted [29, 30]. Formulas **I**—**III** show the activated complexes in configurations close to planar, but the following discussion is virtually unaffected if the ring is a little twisted.

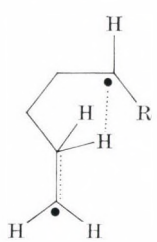

I

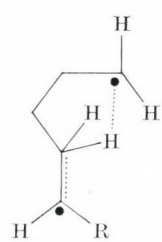

II

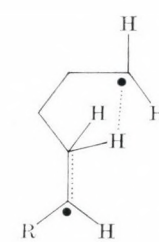

III

Table VII

Some characteristic yield ratios for open-chain isomeric products

	Ratio of yields of reactions (5c) and (5a) + (5b)	Ratio of yields of reactions (5a) and (5b)	Ratio of yields of *cis* and *trans* isomers of reaction (5b)
Methylcyclopentane			0.43
Ethylcyclopentane	0.25	0.80	0.35
Propylcyclopentane	0.24	0.65	0.31
Butylcyclopentane	0.17	0.54	0.26
Methylcyclohexane			0.40
Ethylcyclohexane	0.06	0.85	0.30
Propylcyclohexane	0.07	0.64	0.27
Butylcyclohexane	0.05	0.75	0.25
Isopropylcyclohexane	0.15	0.59	0.13
tert-butylcyclohexane	—	0.36	~0.12
1,1-dimethylcyclohexane	0.47	0.70	
cis-1,2-dimethylcyclohexane	0.12	—	0.31
trans-1,2-dimethylcyclohexane	0.53	—	0.19
1,3-dimethylcyclohexane (C1–C2 bond rupture)	0.07	0.45	0.29
1,3-dimethylcyclohexane (C1–C6 bond rupture)	—	—	0.36
cis-1,4-dimethylcyclohexane	0.14	0.56	0.50
trans-1,4-dimethylcyclohexane	0.17	0.46	0.30
cis-decalin		~1.6	
trans-decalin		~2.0	

From models relating to the transition state it is difficult to decide whether activated state **I**, leading to the terminal alkene, or activated states **II** + **III**, resulting in some other alkene, is the more favoured. The essential difference between the transition states **I**, leading to reaction (5a), and **II** + **III**, leading to (5b), is that in **I** the alkyl group R is linked to the ring and not to the side chain. Since the R group connected to the ring directly to the radical position, shields the radical position to a slight extent (**I**), it may increase non-bonded repulsive interactions; it is to be expected, therefore, that **I** is less favourable for end-product formation than is **II** + **III**. This is in agreement with the experimental findings (Table VII, numerical column 2).

Let us now compare transition states **III** and **II**, leading to formation of the *cis* and *trans* isomers. In **II** the alkyl group R lies away from the ring, and hence does not inhibit formation of the cyclic transition complex; its rotation

is free. In contrast, in **III** the R group overlaps the ring and thus its rotation may be partially hindered. This explains why the *cis* : *trans* ratio (Table VII, numerical column 3) is less than 1, and why its value decreases with the increasing size of R.

The activated states **I**, **II** and **III** may be produced relatively easily from the starting cyclopentanes, by rotation around one C–C bond, with subsequent slight distortions of the bond angle. For the 1,6-hydrogen shift corresponding to reaction (5c), formation of a 7-membered cyclic transition complex is necessary. Although the strain in 7-membered rings is practically the same as that in 5-membered rings (the strain energies of cyclopentane and cycloheptane are 6.3 and 6.4 kcal mol^{-1}, respectively [31]), the 7-membered cyclic complex demands a very considerable rearrangement of the original carbon skeleton, which at the same time may be the reason for the comparatively low yields in reactions of type (5c) (Table VII, column 1).

The activated state for the 1,5-hydrogen shift of the 1,6-biradicals formed from cyclohexanes is probably more reminiscent of the envelope than of the chair conformation [29, 30]. This is justified by the fact that the C–H bond is shorter than the C–C bond, and that hence the radical center may approach the shifting hydrogen atom more closely. Development of the near envelope conformation is also promoted by the fact that the unpaired electron is predominantly *p* in character, and is therefore directed at 90° compared to the other bonds of the carbon atom.

In connection with reactions of types (5a) and (5b), the same factor, *i.e.* the growing distance of R from the ring, again seems to favour reactions of type (5b), in agreement with the experimental findings (Table VII, column 2). With the exception of the decalin isomers, the ratio of the reactions of types (5a) and (5b) is less than 1. For the C_2—C_4 *n*-alkylcyclohexanes containing straight side chains, the ratio varies between 0.85 and 0.64; as examples where the side chain is branched, in isopropylcyclohexane the ratio is 0.59, while in *tert*-butylcyclohexane it is as low as 0.36. The cause of the decrease may be that the radical position is shielded more strongly by the branched alkyl groups than by the *n*-alkyl groups.

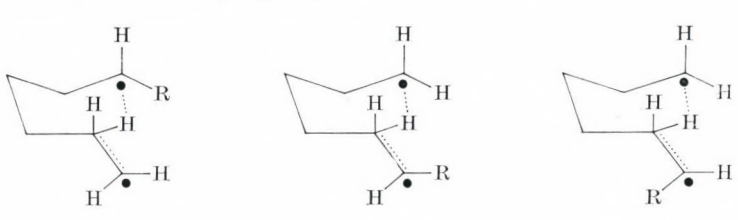

IV **V** **VI**

In the activated complex **IV** of 1,1-dimethylcyclohexane the radical position involved in the transfer of hydrogen may similarly be strongly shielded

by the two methyl groups attached to the radical position, but for the same hydrocarbon, formation of the activated states **V** and **VI** is also inhibited, as both may be regarded as '*cis*' reactions. These effects by and large cancel each other out, and the ratio of the reactions of types (5a) and (5b) is 0.7 *i.e.* the same as for monoalkyl compounds containing *n*-alkyl branching.

The products of the 1,2-dimethylcyclohexanes do not give a possibility for differentiating between reactions (5a) and (5b).

On rupture of the bond between carbon atoms 1 and 2 in the ring of 1,3-dimethylcyclohexane, only one hydrogen atom on carbon atom 5 is available for migration in **IV**: this justifies the relatively low (5a) : (5b) reaction ratio of 0.45. On rupture of the bond between carbon atoms 1 and 6 in the ring this reaction ratio cannot be calculated, for the transformations analogous to (5a) and to (5c) lead to formation of the same product, 4-methyl-1-heptene.

The 4-methyl group in the 1,4-dimethylcyclohexane isomers inhibits formation of the activated state **IV** (*cis* effect), this explaining the comparatively low (5a) : (5b) reaction ratios of 0.56 and 0.46.

In the decalin isomers, only one hydrogen atom is available for formation of transition states **V** and **VI**, and thus this promotes formation of **IV** and hence the higher relative rate of the reaction analogous to (5a). At the same time, in the case of **V** and **VI** a significant change is also necessary in the conformation of the 'intact' ring, but this is a more hindered process than the change in the carbon skeleton of the alkyl chain associated with formation of **IV**. These effects together lead to a higher proportion for the reaction of type (5a) than for that of type (5b).

As regards the yields of the *cis* and *trans* isomers in reactions of type (5b), analogous considerations hold as for the reactions of 5-membered rings.

For methylcyclohexane the *cis* : *trans* ratio is 0.4; with the increase of the number of carbon atoms in the *n*-alkyl side chain, this ratio gradually decreases to 0.25 (Table VII, column 3). If the side chain is not straight, but branched, then even lower values arise; *e.g.* on irradiation of isopropyl- and *tert*-butylcyclohexane the ratios are 0.13 and $\sim$0.12, respectively. This is in agreement with the consideration that the cause of the decrease is the increasing hindrance of free rotation as R becomes larger or more branched.

In the case of 1,1-dimethylcyclohexane and the decalin isomers, the same products are formed *via* transition states **V** and **VI**. On rupture of the bond between carbon atoms 1 and 2 in 1,3-dimethylcyclohexane, and on the reaction of the 1,2- and 1,4-dimethylcyclohexanes, the same aspects must be taken into consideration in the assessment of the product ratios as in the case of methyl- and ethylcyclohexanes, and the measured data too are close to the corresponding ratios for the *n*-alkylcycloalkanes. On rupture of the bond between carbon atoms 5 and 6 in 1,3-dimethylcyclohexane, **V** is singly inhibited because of the 3-methyl group, while **VI** is doubly hindered because

of the *cis* arrangement of the 1- and 3-methyl groups. Accordingly, the *cis* : *trans* ratio does not differ substantially from those for the *n*-alkylcyclohexanes.

For the 1,6-biradicals formed from the alkylcycloalkanes to undergo a rearrangement analogous to reaction (5c), a 1,7-hydrogen shift is necessary, *i.e.* 8-membered cyclic complexes must be formed. However, rings containing 8 atoms are fairly strained (the strain energy of cyclooctane is 9.9 kcal mol^{-1} [31]), while the 6-membered rings required for the 1,5-shift are practically strain-free. This may explain why the ratio of the reactions of type (5c) and (5a) + (5b) is very small, in fact even smaller than on the reaction of the cyclopentanes.

An exception is 1,1-dimethylcyclohexane, where, as a consequence of the two methyl groups attached to the carbon atom containing the radical site, the total number of hydrogen atoms that may be attacked is 6, in contrast with 2 such hydrogen atoms in ethyl- and propylcycloalkanes, for instance. The high rate of the reaction of type (5c) may also be due to the fact that, in accordance with what was reported in connection with 1,1-dimethylcyclohexane, formation of the activated complexes **IV**, **V** and **VI** is hindered.

The 1,2-dimethylcyclohexane isomers are similarly exceptions. Here methyl groups are linked to both radical positions, and therefore the number of hydrogen atoms that can be attacked in reaction (5c) is again 6; at the same time, there are also significant inhibitory effects in the formation of the activated complexes **IV**—**VI**. Experiments show that the product corresponding to (5c) is formed in a higher proportion only from *trans*-1,2-dimethylcyclohexane. The cause of this is unknown as yet.

The relative yields of the skeletal isomer products formed from the *cis* and *trans* isomers of the 1,2- and 1,4-dimethylcyclohexanes differ slightly (Table V). It appears that to a certain extent the activated complex 'remembers' its formation route. It is probable that in the intermediate state prior to transfer of the hydrogen atom the molecule does not 'straighten out' completely, but partially retains its original conformation. The possibility for this is provided by the fact, that with the exception of reactions of type (5c), movement of only a part of the molecule is sufficient for development of the transition states. This considerably promotes formation of the activated complexes, ensuring that these reactions have a pre-exponential factor larger by several orders of magnitude than in 'normal' (stereochemically not favoured) monomolecular radical isomerization, *e.g.* the conversion of the 3-heptyl radical to the 2-heptyl radical [32] (an A value of $\geqslant 10^{11}$ s^{-1} instead of 10^5—10^9 s^{-1}).

The biradical mechanism is also supported by the phase effect to be observed in open-chain alkene formation. POLAK *et al.* [9] found the yield of 1-hexene from cyclohexane to increase very significantly on melting, although the *G* value is otherwise only slightly influenced by temperature. This phase effect can only be interpreted *via* the biradical mechanism: because of the

higher density and the more defined internal structure, the solid phase favours not rearrangement of the biradical to aliphatic alkene having somewhat larger molar volume, but reclosure.

Analogy with the photolysis of cycloalkanones

In essence the analogy is twofold:

(a) on opening of the cycloalkanones at the carbonyl group, open-chain isomers are formed, *e.g.*:

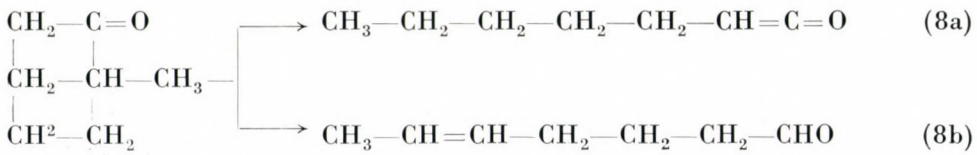

(8a)

(8b)

(b) mainly in the gas phase, some of the reacting molecules undergo decarboxylation, and the residual carbon chain either rearranges to an open-chain alkene, or is transformed to a cycloalkane [33, 34].

Some of the earlier publications proposed a 'concerted' mechanism [33—36] for reactions of type (8), whereas others [37—39] preferred a biradical mechanism; more recent papers, however, clearly highlight the biradical mechanism [40—44]. The following evidence, for example, supports the biradical mechanism:

(i) reaction (8b) is not stereospecific, and thus both *trans* and *cis*-enol are formed in it [40, 42, 45];

(ii) *cis*- and *trans*-2-methylheptanol are formed in identical proportions in the gas-phase photolysis of *cis*- and *trans*-2,6-dimethylcyclohexanone [45];

(iii) CIDNP (chemically induced dynamic nuclear polarization) studies have been used, for instance, to determine the proportions of reclosure of the biradicals and their further reaction to enol [46, 47].

On decarboxylation, the loss of CO leads to a biradical, which, if the deactivation is relatively low and the energy of the intermediate is relatively high, decomposes, while in the event of a more significant deactivation it either undergoes ring-closure or is transformed to an open-chain alkene [34, 43, 44].

As regards ring cleavage, the analogy between the radiolysis of cycloalkanes and the photolysis of cycloalkanones is otherwise obvious. Reaction (8a) for methylcyclohexanone corresponds to (5a) for propylcyclopentane, and similarly (8b) corresponds to (5b), and indeed in both cases the rates of the b-type reactions are the higher. Both *cis* and *trans* isomers are formed in (8b) and (5b). In the photolysis of methylcyclohexanone the *cis* : *trans* ratio was found to be ~ 0.3 [42], while in the radiolysis of the cycloalkane it varies generally between 0.2 and 0.4.

The 1,5- or 1,6-biradical originating from decarboxylation on photolysis of cyclohexanone [44] or cycloheptanone [48] is further transformed to the open-chain alkene, 1-pentene or 1-hexene (in addition to ring-closure to cyclopentane or cyclohexane), and these are also the main decyclization products of the radiolysis of cyclopentane or cyclohexane, where 1,5- or 1,6-biradicals may similarly be formed. The 2,6-heptyl biradical formed on decarboxylation of *cis*- and *trans*-2,6-dimethylcyclohexanones [45] rearranges to 2-heptenes (and also 1,2-dimethylcyclopentanes), while 2-alkenes (2-octanes) are similarly the main products of radiolysis of 1,2-dimethylcyclohexanes. The *cis* : *trans* ratio on photolysis of the cycloalkanones is 0.5, whereas on the radiolysis of the cycloalkanes it is 0.31 and 0.19 for the *cis* and *trans* modifications, respectively.

Since the existence of biradical intermediates in the transformations of cycloalkanones appears to be generally accepted, the analogy of the radiolysis products of cycloalkane ring cleavage with those of the reactions of the cycloalkanone permits conclusions as to analogous intermediates of the radiolysis process, *i.e.* biradicals.

On the above basis, therefore, not only can the experimental findings be explained *via* the biradical mechanism, but in certain cases they do not appear to be interpretable without biradicals. The assumption of biradical intermediates is therefore justified, although at present little information is available regarding their nature.

REFERENCES

[1] WOJNÁROVITS, L., FÖLDIÁK, G.: Acta Chim. (Budapest) **82,** 285 (1974)
[2] FÖLDIÁK, G., WOJNÁROVITS, L.: Acta Chim. (Budapest) **82,** 269 (1974)
[3] HARDWICK, T.: J. Phys. Chem., **66,** 1611 (1962)
[4] FREEMAN, G. R.: J. Chem. Phys., **36,** 1534 (1962)
[5] DAUPHIN, J.: J. Chim. Phys., **53,** 1207 (1962)
[6] DOEPKER, R. D., LIAS, S. G., AUSLOOS, P.: J. Chem. Phys., **46,** 4340 (1967)
[7] AUSLOOS, A., SCALA, A. A., LIAS, S. G.: J. Amer. Chem. Soc., **89,** 3677 (1967)
[8] EBERHARD, M. K.: J. Phys. Chem., **72,** 4509 (1968)
[9] GRACHOVA, T. A., MAKAROV, V. I., POLAK, L. S., AVDOVINA, E. N.: Radiation Effects, **10,** 157 (1971)
[10] SALEM, L., ROWLAND, C.: Angew. Chem. Internat. Edn., **11,** 92 (1972)
[11] FREEMAN, G. R.: Can. J. Chem., **44,** 245 (1966)
[12] KESZEI, CS., WOJNÁROVITS L., FÖLDIÁK, G.: Acta Chim. (Budapest) **92,** 331 (1977)
[13] ZAJTSEV, V. M., SEROVA, V. A., TIKHONOV, V. I.: Khim. Vysok. Energ. **7,** 174 (1973)
[14] FÖLDIÁK, G., WOJNÁROVITS, L.: Acta Chim. (Budapest) **82,** 305 (1974)
[15] HUGHES, B. M., HANRAHAN, R. J.: J. Phys. Chem., **69,** 2707 (1965)
[16] HO, S. K., FREEMAN, G. R.: J. Phys. Chem., **68,** 2189 (1964)
[17] FÖLDIÁK, G., CSERÉP, GY., GYÖRGY, I., HORVÁTH, ZS., WOJNÁROVITS, L.: Hung. J. Ind. Chem. Veszprém, **2,** Suppl., 277 (1974)
[18] KERR, J. A.: Chem. Rev., **66,** 465 (1966)
[19] WHYTOCH, D. A., CLARKE, J. D., GRAY, P.: J. Chem. Soc. Faraday Trans. I, **70,** 411 (1974)
[20] STULL, D. R., WESTRUM, E. F., SINKE, G. C.: The Chemical Thermodynamics of Organic Compounds, Wiley, New York 1969
[21] ZEMAN, A., HEUSIGNER, H.: Radiochim. Acta, **8,** 149 (1967)
[22] WOJNÁROVITS, L., FÖLDIÁK, G.: Radiochem. Radioanal. Lett., **23,** 343 (1975)
[23] WOJNÁROVITS, L., FÖLDIÁK, G.: Radiochem. Radioanal. Lett., **23,** 257 (1975)

[24] LARSON, C. W., RABINOVITCH, B. S., TARDY, D. C.: J. Chem. Phys., **47,** 4570 (1967)
[25] GEORGAKAKOS, H. H., RABINOVITCH, B. S., LARSON, C. W.: Int. J. Chem. Kinet., **3,** 535 (1971)
[26] GIBIAN, M., CORLEY, C.: Chem. Rev., **73,** 441 (1973)
[27] WOODWARD, R. B. and HOFFMANN, R.: The Conservation of Orbital Symmetry. Verlag Chemie Academic Press, Weinheim 1970
[28] FREY, H. M., WALSH, R.: Chem. Rev., **69,** 103 (1969)
[29] ELIEL, E. L., ALLINGER, N. L., ANGYAL, S. J., MORRISON, G. A.: Conformational Analysis. Interscience, New York 1965
[30] COYLE, J. D.: J. Chem. Soc. (B), **1971,** 1736
[31] BENSON, S. W.: Thermochemical Kinetics. Wiley, New York 1968
[32] MINTZ, K. J., LEROY, D. J.: Can. J. Chem., **51,** 3534 (1973)
[33] CALVERT, J. G., PITTS, J. N.: Photochemistry. Wiley, New York 1966
[34] BÉRCZES, T.: The decomposition of aldehydes and ketones. In: Comprehensive Chemical Kinetics, Vol. 5. Ed. BAMFORD, C. H. and TIPPER, C. F. H., Elsevier, Amsterdam 1972
[35] SRINAVASAN, R.: Advan. Photochem., **1,** 83 (1963)
[36] BENSON, S. W., KISTIAKOWSKY, C. B.: J. Amer. Chem. Soc., **64,** 80 (1942)
[37] BLACET, F. E., MILLER, A.: J. Amer. Chem. Soc., **79,** 4327 (1957)
[38] FLOWERS, M. C., FREY, H. M.: J. Chem. Soc., **1960,** 2758
[39] FREY, H. M.: Chem. Ind., **1961,** 1367
[40] BEDCOCK, C. C., PERONA, M. S., PITCHARD, G. O., RICHBORN, B.: J. Amer. Chem. Soc., **91,** 543 (1969)
[41] DALTON, J. C., DAWES, K., TURRO, N. J., WEISS, D. S., BURATROP, J. A., COYLE, J. D.: J. Amer. Chem. Soc., **93,** 7212 (1971)
[42] COYLE, J. D.: J. Chem. Soc. Perkin Trans. II, 683 (1972)
[43] SCALA, A. A., BALLAN, D. G.: Can. J. Chem., **50,** 3938 (1972)
[44] SCALA, A. A., BALLAN, D. G.: J. Phys. Chem., **76,** 615 (1972)
[45] ALUMBAUGH, R. L., PITCHARD, G. O., RICHBORN, B.: J. Phys. Chem., **69,** 3225 (1965)
[46] CLOSS, G. L., DOUBLEDAY, C. E.: J. Amer. Chem. Soc., **94,** 9248 (1972)
[47] CLOSS, G. L., DOUBLEDAY, C. E.: J. Amer. Chem. Soc., **95,** 2736 (1973)
[48] SRINAVASAN, R.: J. Amer. Chem. Soc., **81,** 5541 (1959)

László WOJNÁROVITS
Gábor FÖLDIÁK
H-1525 Budapest, P.O.B. 77

Acta Chimica Academiae Scientiarum Hungaricae, Tomus 93 (1), pp. 23—32 (1977)

KINETIC EQUATIONS OF MULTISTEP ELECTRODE PROCESSES, IV

EFFECT OF ADSORPTION OF THE INTERMEDIATE

L. KISS and J. FARKAS

(Departement of Physical Chemistry and Radiology, L. Eötvös University, Budapest)

Received April 26, 1976

The equation of the polarization curve for metal ionization and metal ion neutralization *via* a multistep mechanism is given for two and three reaction steps, for the case when the intermediates of the consecutive reaction are adsorbed on the electrode, and Langmuir's conditions are fulfilled. Conditions under linear Tafel sections are obtained, and the kinetic parameters belonging to these conditions have been established.

In earlier communications [1—3], the kinetics of electrode processes involving a series of reaction steps have been discussed. In each case, it has been assumed that the adsorption on the electrode of the components participating in the reaction or of those in the solution does not influence the kinetics of the process. Generally, this is to be expected if the adsorbed components cover only a very small part of the electrode surface.

In the discussion of the effect of adsorption on electrode processes two cases should be distinguished.

(a) All the components in the solution are bound by specific adsorption to the surface. Owing to this, the structure of the electric double layer and thereby the rate of the electrode process are changed. However, in this case the adsorbed particle is not (or not definitely) an intermediate of the electrode processes.

(b) The intermediates of the electrode process occurring in a series of reaction steps are adsorbed on the electrode and they cover an appreciable fraction of the surface.

In the following, a few problems in conjunction with case (b) will be discussed more extensively. In this case, the first step of metal dissolution is generally the chemisorption on the metal surface of one of the components of the solution. Intermediates formed in further reaction steps may also be adsorbed on the electrode. Thus, it must be taken into consideration that the uncovered electrode surface participates in the first step of the anodic process, and the rates of the steps in the series will be proportional to the ratio of the electrode surface (Θ_i) covered by the respective component if the Langmuir condition is fulfilled. On the other hand, if the electrode surface is energetically not homogeneous (Temkin's condition), or if a possible electric interaction of

the adsorbed particles with one another and with the electrode surface is taken into consideration (conditions of Frumkin's isotherm), the simple proportionality between Θ_i and the reaction rate is not valid [4, 5].

Temkin's condition, taking into consideration the dependence of the adsorption energy of the intermediates on the degree of coverage, at medium coverages gives rate equations which are in better agreement with experimental findings than the Langmuir condition. However, on the basis of the Temkin condition, only relatively simple processes can be discussed mathematically [4, 6, 7, 8]. During multistep processes several components (intermediates) may be adsorbed on the surface; a discussion of the kinetic relationships on the basis of Temkin's conditions is very complicated in this case and leads to results which are difficult to survey. Therefore, in the following, conditions will be analyzed on the basis of Langmuir's condition, because results obtained on this basis indicate also the effects to be expected on account of adsorption and in many cases are in good agreement with experimental data [8—10].

The following two-step process will be discussed:

$$\begin{aligned} &(1)\quad \mathrm{M} + \nu'\mathrm{K}^{n-} \underset{k_{k_1}}{\overset{k_{a_1}}{\rightleftharpoons}} (\mathrm{MK}_{\nu'}^{(z_1-\nu' n)+})_{\mathrm{ads}} + z_1 e \\ &(2)\quad (\mathrm{MK}_{\nu'}^{(z_1-\nu' n)+})_{\mathrm{ads}} + (\nu - \nu')\mathrm{K}^{n-} \underset{k_{k_2}}{\overset{k_{a_2}}{\rightleftharpoons}} \mathrm{MK}_{\nu}^{(z_2-\nu n)} + n_2 e \end{aligned} \qquad (\mathrm{I})$$

k_{a_i} and k_{k_i} $(i = 1, 2)$ are the rate constants of the respective reaction steps, which depend in the following way on the electrode potential:

$$k_{a_i} = k'_{a_i} \exp\left(\frac{\alpha_i n_i \mathrm{F}\varepsilon}{\mathrm{RT}}\right) \qquad (1)$$

$$k_{k_i} = k'_{k_i} \exp\left(-\frac{(1-\alpha_i) n_i \mathrm{F}\varepsilon}{\mathrm{RT}}\right) \qquad (2)$$

where k'_{a_i} and k'_{k_i} are the values of the rate constants when $\varepsilon = 0$, α_i is the transfer coefficient of the i-th step, and the other symbols are as usual.

In contrast to processes discussed earlier [1, 2], here it is permissible for the intermediate to cover an appreciable fraction of the surface, and desorption occurs only in the 2nd step (electrochemical desorption). As will be shown in the following, the kinetic relationships discussed are valid also if $z_1 = 0$ and $n_2 \neq 0$ (so called chemical-electrochemical or *ce* mechanism), or if $z_1 \neq 0$ and $n_2 = 0$ (*ec* mechanism), *i.e.* when step 2 is not an electrochemical but a chemical process.

In the description of the kinetic relationships the following simplifying assumptions are made.

(a) The transport of the components participating in the reaction to and from the electrode surface is not a hindered processes. (Diffusion does not affect the processes).

(b) The change in the structure of the electrical double layer can be neglected. (A high foreign ion concentration is used.)

(c) The intermediates are adsorbed on the surface of the electrodes and can depart from the surface only by the route given in equation (I).

(d) The Langmuir condition is valid, *i.e.* the adsorption energy does not change with the coverage of the electrode.

(e) The concentrations of the components in the solution and of those participating in the reaction practically do not change with time. (Volume and concentrations are relatively high.)

Under steady-state conditions, the following equations can be written [1] for process (I):

$$j = \frac{z_2}{z_1}\left[k_{a_1} c_{\mathrm{K}}^{\nu'} (1 - \Theta) - k_{k_1}\Theta\right] \tag{3}$$

$$j = \frac{z_2}{n_2}\left[k_{a_2}\Theta c_{\mathrm{K}}^{(\nu - \nu')} - k_{k_2}(1 - \Theta)\, c_{\mathrm{MK}}\right], \tag{4}$$

where Θ is the fraction of the surface covered by the intermediate of process (I), j is the current density passing through the electrode, c_{K} is the concentration of the complexing agent K^{n-} in the solution, and c_{MK} is the concentration of the metal complex $\mathrm{MK}_{\nu}^{(z_2 - \nu n)+}$ in the solution.

The system of equations (3)—(4) can be solved for unknowns j and Θ. When all the rate constants are of the same order of magnitude, the following expression can be written for the equation of the polarization curve:

$$j = z_2 \frac{k_{a_1} k_{a_2} c_{\mathrm{K}}^{\nu} - k_{k_1} k_{k_2} c_{\mathrm{MK}}}{n_2 k_{a_1} c_{\mathrm{K}}^{\nu'} + n_2 k_{k_1} + z_1 k_{a_2} c_{\mathrm{K}}^{\nu - \nu'} + z_1 k_{k_2} c_{\mathrm{MK}}} \tag{5}$$

and for the coverage of the electrode, under similar conditions:

$$\Theta = \frac{n_2 k_{a_1} c_{\mathrm{K}}^{\nu'} + z_1 k_{k_2} c_{\mathrm{MK}}}{n_2 k_{a_1} c_{\mathrm{K}}^{\nu'} + n_2 k_{k_1} + z_1 k_{a_2} c_{\mathrm{K}}^{\nu - \nu'} + z_1 k_{k_2} c_{\mathrm{MK}}} \tag{6}$$

As shown for multistep processes without adsorption [2], it is a sufficient condition for the linearizability of the polarization curves in the form ε *vs.* lg j that the rate constants of one step be considerably smaller than the other rate constants. According to Eq. (5), when adsorption occurs, this condition is insufficient for linearizability.

Table I

Kinetic parameters obtained when relationship (5) can be linearized

No.	k_{max}		$z_1 \neq 0$, $n_2 \neq 0$				$z_1 = 0$ $n_2 \neq 0$				$z_1 \neq 0$, $n_2 = 0$			
			$\alpha'(\beta')$	Θ	ν_K	ν_{MK}	$\alpha'(\beta')$	Θ	ν_K	ν_{MK}	$\alpha'(\beta')$	Θ	ν_K	ν_{MK}
Anodic polarization														
1	k_{k_1}	$(z_1 + \alpha_2 n_2)$	0	ν	0	$\alpha_2 n_2$	0	ν	0	z_1	0	ν	0
2	k_{a_1}	$\alpha_2 n_2$	1	$\nu - \nu'$	0	$\alpha_2 n_2$	1	$\nu - \nu'$	0	0	1	$\nu - \nu'$	0
3	k_{a_2}	$z_1 \alpha_1$	0	ν'	0	0	0	ν'	0	$\alpha_1 z_1$	0	ν'	0
4	k_{k_2}	$(z_1 \alpha_1 + n_2)$	1	ν	-1	n_2	1	ν	-1	$\alpha_1 z_1$	1	ν	-1
Cathodic polarization														
5	k_{k_1}	$-n_2(1-\alpha_2)$	0	0	1	$-n_2(1-\alpha_2)$	0	0	1	0	0	0	1
6	k_{a_1}	$-[z_1 + (1-\alpha_2)n_2]$	1	$-\nu'$	1	$-n_2(1-\alpha_2)$	1	$-\nu'$	1	$-z_1$	1	$-\nu'$	1
7	k_{a_2}	$-[(1-\alpha_1)z_1 + n_2]$	0	$-(\nu - \nu')$	1	$-n_2$	0	$-(\nu - \nu')$	1	$-(1-\alpha_1)z_1$	0	$-(\nu - \nu')$	1
8	k_{k_2}	$-(1-\alpha_1)z_1$	1	0	0	0	1	0	0	$-(1-\alpha_1)z_1$	1	0	0

Equation (5) can be linearized in the form ε *vs.* lg j only if one of the four terms in the denominator is considerably larger than the other three. Hence, in the case of adsorption, a straight section on the anodic and cathodic curves can be obtained under four conditions. Table I contains the apparent anodic (α') and cathodic (β') transfer coefficients, relevant to the four straight sections mentioned, as a function of the maximal rate constant ($k_{\max}$).

Table I contains also the coverage Θ belonging to the given conditions, further the order of reaction with respect to the complexing agent (ν_K) and to complex $MK_\nu^{(z_2-\nu n)+}$ in the solution (ν_{MK}).

The above kinetic parameters are given for the cases of both steps are electrochemical ($z_1 \neq 0$; $n_2 \neq 0$; *ee* mechanism), when the first step is a chemical and the second an electrochemical reaction ($z_1 = 0$, $n_2 \neq 0$, *ce* mechanism), and if the first is electrochemical and the second chemical ($z_1 \neq 0$, $n_2 = 0$, *ec* mechanism).

By way of an example in Figs 1—3 are shown at arbitrarily chosen parameters the ε *vs.* lg j polarization curves calculated on the basis of Eqs (5) and (6), and the dependence of the coverage Θ on the electrode potential for two different concentrations of the solution components participating in the reaction. With the parameters chosen, there are two linear sections the anodic polarization curve in Fig. 1. For section *a*, $\alpha' = 1{,}5$, for section *b*, $\alpha' = 0.5$. (Cases 1 and 2 of Table I.) In the potential range corresponding to section *a*, $\Theta = 0$, and in that corresponding to section *b*, $\Theta = 1$. (See Table I).

In cathodic polarization and with the parameters selected, case 5 of Table I is realized in any potential and current density range and, as can be

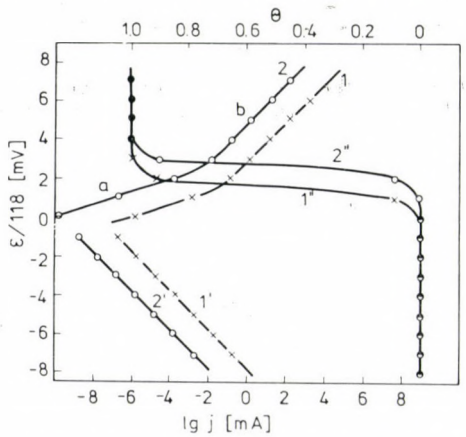

Fig. 1. Relationships between the electrode potential (ε), the logarithm of current density (j) and the degree of coverage of the electrode (Θ) for two-step processes under the following conditions: $k'_{a_1} = 10^6$ mA cm mol^{-1}; $k'_{k_1} = 10^6$ mA cm^{-2}; $k'_{a_2} = 1$ mA cm mol^{-1}, $k'_{k_2} = 10^{-5}$ mA cm mol^{-1}; $z_1 = 1$; $n_2 = 1$; $\nu = 2$, $\nu' = 1$; $T = 297$ K; $\alpha_1 = \alpha_2 = 0{,}5$. For curves 1, 1′ and 1″, $c_K = 1$ mol/dm^3, $c_{MK} = 1$ mol/dm^3; for curves 2, 2′ and 2″ $c_K = 10^{-2}$ mol/dm^3; $c_{MK} = 10^{-2}$ mol/dm^3; 1 and 2 anodic, 1′ and 2′ cathodic polarization curves, 1″ and 2″ the change of Θ with ε

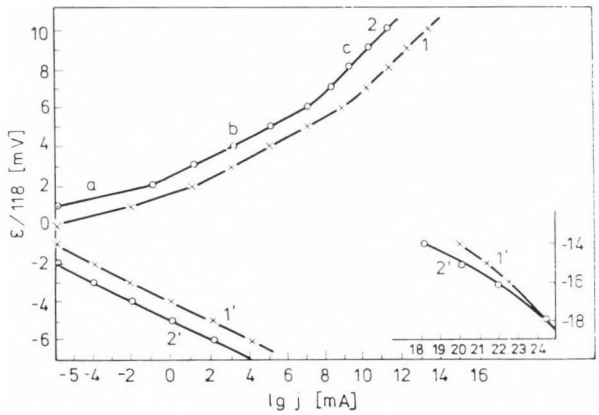

Fig. 2. The relationship ε *vs.* $\lg j$ for the parameters given in Fig. 1, with $n_2 = 2$. Symbols are identical with those used in Fig. 1

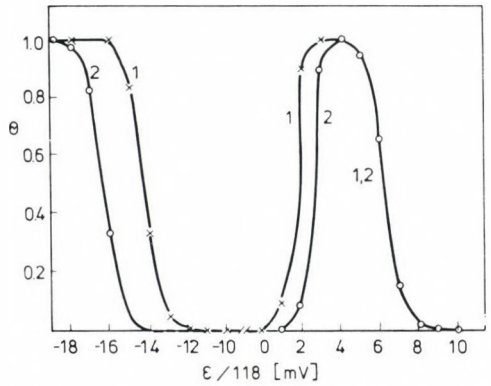

Fig. 3. The relationship Θ *vs.* ε for the parameters used in the calculation of the curves in Fig. 2. 1 — $c_K = 1$ mol/dm³; $c_{MK} = 1$ mol/dm³; 2 — $c_K = 10^{-2}$ mol/dm³; $c_{MK} = 10^{-2}$ mol/dm³

seen from Fig. 1, the cathodic apparent transfer coefficient $\beta' = -0.5$ and $\Theta = 0$.

Figure 1 illustrates the dependence of the rate of the process on the concentration of the ions K^{n-} and $MK_\nu^{(z_2-\nu n)+}$.

The parameters chosen for the calculation of the curves in Figs 2 and 3 are the same as those of the curves in Fig. 1, with the sole exception that here $n_2 = 2$ and hence $z_2 = 3$.

In this case, three linear sections appear on the anodic polarization curve shown in Fig. 2. For section *a*, $\alpha' = 2$, for section *b*, $\alpha' = 1$, and for section *c*, $\alpha' = 0.5$. Cases 1, 2 and 3 of Table I are realized. Accordingly (see Fig. 3), in the potential range corresponding to section *a*, $\Theta = 0$, in that of section *b*, $\Theta = 1$, and in that referring to *c*, $\Theta = 0$.

In cathodic polarization, at not too large negative potentials, case 5 of Table I is realized, and $\beta' = -1$. On the other hand, at very high cathodic polarization, the rate-determining role is taken over by step 1 of reaction scheme (I), which makes the rate of the process independent of the concentration of the complex ion in the solution, and $\beta' = -0.5$. (Case 8 of Table I.)

It should be mentioned that no measurements can be carried out over the very broad potential and current density ranges shown in Figs 1—3. In the experiments, only one section of the polarization curves shown in the figures, involving a few orders of magnitude of current density, is measured.

The kinetics of the three-step process can be discussed similarly as above. Let the following process take place:

$$\begin{aligned}
&(1)\quad \mathrm{M} + \nu'\mathrm{K}^{n-} \underset{k_{k_1}}{\overset{k_{a_1}}{\rightleftharpoons}} (\mathrm{MK}_{\nu'}^{(z_1-\nu' n)+})_{\mathrm{ads}} + z_1 e \\
&(2)\quad (\mathrm{MK}_{\nu'}^{(z_1-\nu' n)+})_{\mathrm{ads}} \underset{k_{k_2}}{\overset{k_{a_2}}{\rightleftharpoons}} (\mathrm{MK}_{\nu'}^{(z_2-\nu' n)+})_{\mathrm{ads}} + n_2 e \qquad \text{(II)} \\
&(3)\quad (\mathrm{MK}_{\nu'}^{(z_2-\nu' n)+})_{\mathrm{ads}} + (\nu-\nu')\mathrm{K}^{n-} \underset{k_{k_3}}{\overset{k_{a_3}}{\rightleftharpoons}} \mathrm{MK}_{\nu}^{(z_3-\nu n)+} + n_3 e
\end{aligned}$$

In this case, two intermediates can be adsorbed on the eletrode surface. If the conditions introduced for the two-step process are valid, the equation of the polarization curve and the surface coverages (Θ_1 and Θ_2) for the intermediates formed in steps 1 and 2 of (II) can be calculated by the method used earlier [1] as well as in the discussion of the two-step processes.

For process (II), under steady-state conditions, the following equations can be written:

$$j = \frac{z_3}{z_1}\left[k_{a_1} c_{\mathrm{K}}^{\nu'}(1 - \Theta_1 - \Theta_2) - k_{k_1}\Theta_1\right] \tag{7}$$

$$j = \frac{z_3}{n_2}\left[k_{a_2}\Theta_1 - k_{k_2}\Theta_2\right] \tag{8}$$

$$j = \frac{z_3}{n_3}\left[k_{a_3} c_{\mathrm{K}}^{\nu-\nu'}\Theta_2 - k_{k_3}(1 - \Theta_1 - \Theta_2)\, c_{\mathrm{MK}}\right] \tag{9}$$

The solving of the system of Eqs (7)—(9) for the unknows j, Θ_1 and Θ_2 gives the following expressions, when all the rate constants are of the same order of magnitude:

$$j = \frac{z_3\,(k_{a_1} k_{a_2} k_{a_3} c_{\mathrm{K}}^{\nu} - k_{k_1} k_{k_2} k_{k_3} c_{\mathrm{MK}})}{\mathrm{A}} \tag{10}$$

The surface coverage of the first intermediate is:

$$\Theta_1 = \frac{n_3 k_{a_1} k_{k_2} c_{\mathrm{K}}^{\nu'} + n_2 k_{a_1} k_{a_3} c_{\mathrm{K}}^{\nu} + z_1 k_{k_2} k_{k_3} c_{\mathrm{MK}}}{\mathrm{A}} \tag{11}$$

The coverage of the second intermediate:

$$\Theta_2 = \frac{n_3 k_{a_1} k_{a_2} c_{\mathrm{K}}^{\nu'} + z_1 k_{a_2} k_{k_3} c_{\mathrm{MK}} + n_2 k_{k_3} k_{k_1} c_{\mathrm{MK}}}{\mathrm{A}} \tag{12}$$

where:

$$\begin{aligned} \mathrm{A} = {} & z_1 (k_{a_2} k_{a_3} c_{\mathrm{K}}^{\nu - \nu'} + k_{a_2} k_{k_3} c_{\mathrm{MK}} + k_{k_3} k_{k_2} c_{\mathrm{MK}}) + \\ & + n_2 (k_{a_1} k_{a_3} c_{\mathrm{K}}^{\nu} + k_{k_1} k_{a_3} c_{\mathrm{K}}^{\nu - \nu'} + n_2 k_{k_1} k_{k_3} c_{\mathrm{MK}}) + \\ & + n_3 (k_{a_1} k_{k_2} c_{\mathrm{K}}^{\nu'} + k_{k_1} k_{k_2} + k_{a_1} k_{a_2} c_{\mathrm{K}}^{\nu'}) \end{aligned} \tag{13}$$

In an analogous way, are can calculate the polarization curve of multistep processes occurring in m consecutive steps in the course of which $m - 1$ intermediates can be adsorbed on the electrode surface.

As can be seen from relationships (10) and (13), the condition of the linearizability of the polarization curve in ε *vs.* $\lg j$ co-ordinates is that the values of two of the rate constants in Eq. (13) be considerably higher than those of the others. Table II contains those kinetic parameters, which are obtained when the conditions of linearization are fulfilled.

Relationships (10)—(12) can be used also when one or two reactions in process (II) are chemical steps. The kinetic parameters of such processes, proceeding according to a mixed mechanism (in the given case *cee*, *cce*, *ece*, *eec*, *cec* and *ecc* mechanisms are possible), can also be read from Table II, when taking into consideration that the number of transferred charges in the respective chemical process, z_1, n_2 or n_3 is zero. (Indeed, this can be observed also in Table I relevant to two-step processes.)

Similarly to the case of two-step processes, the ε *vs.* $\lg j$ curve has a linear section only if Θ_1 and Θ_2 are 1 or 0, or if both are zero. It can be established on the basis of the table that in electrode processes proceeding according to scheme (II), the anodic and cathodic polarization curves may exhibit Tafel lines with 9 different slopes.

As has been indicated, the measurements generally involve a relatively narrow range of current density. Thus, even in the case of an identical mechanism, Tafel lines with different slopes may be observed. If not Langmuir's but Temkin's condition is valid for processes (I) and (II), further linear sections may occur on the ε *vs.* $\lg j$ curve [6]. This again calls attention to the fact that on the basis of Tafel's straight line a conclusion on the process mechanism can be drawn only after due circumspection.

Table II

Kinetic parameters obtained when relationship (10) can be linearized

No.	k_{max1}	k_{max2}	Anodic polarization					Cathodic polarization				
			α'	Θ_1	Θ_2	ν_K	ν_{MK}	β'	Θ_1	Θ_2	ν_K	ν_{MK}
1	k_{k_1}	k_{k_2}	$z_1+n_2+\alpha_3 n_3$	0	0	ν	0	$-(1-\alpha_3)n_3$	0	0	0	1
2	k_{k_1}	k_{a_3}	$z_1+\alpha_2 n_2$	0	0	ν'	0	$-[(1-\alpha_2)n_2+n_3]$	0	0	$-(\nu-\nu')$	1
3	k_{a_1}	k_{k_2}	$n_2+\alpha_3 n_3$	1	0	$\nu-\nu'$	0	$-[z_1+(1-\alpha_3)n_3]$	1	0	$-\nu'$	1
4	k_{a_1}	k_{a_2}	$\alpha_3 n_3$	0	1	$\nu-\nu'$	0	$-[z_1+n_2+(1-\alpha_3)n_3]$	0	1	$-\nu'$	1
5	k_{a_1}	k_{a_3}	$\alpha_2 n_2$	1	0	0	0	$-[z_1+(1-\alpha_2)n_2+n_3]$	1	0	$-\nu$	1
6	k_{a_2}	k_{a_3}	$\alpha_1 z_1$	0	0	ν'	0	$-[(1-\alpha_1)z_1+n_2+n_3)$	0	0	$-(\nu-\nu')$	1
7	k_{k_1}	k_{k_3}	$z_1+n_3+\alpha_2 n_2$	0	1	ν	-1	$-(1-\alpha_2)n_2$	0	1	0	0
8	k_{k_2}	k_{k_3}	$z_1\alpha_1+n_2+n_3$	1	0	ν	-1	$-(1-\alpha_1)z_1$	1	0	0	0
9	k_{a_2}	k_{k_3}	$z_1\alpha_1+n_3$	0	1	ν	-1	$-[(1-\alpha_1)z_1+n_2]$	0	1	0	0

It should be noted that the steady-state method has been used for the calculation of the above relationships. This means that no assumptions were made concerning the rate constants of the individual steps the magnitudes of the rates relative to each other. However, when applying the quasi-equilibrium method often reported in the literature, it must be assumed that one of the steps involved in the process is rate-determining, while reactions preceding this step are practically at equilibrium. If there are several quasi-equilibrium steps before the rate-determining step, the exchange current of a given quasi-equilibrium step must always be considerably smaller than the exchange current of the preceding step. Hence, in the quasi-equilibrium method following must be included among the initial conditions:

$$j_{1,0} \gg j_{2,0} \gg \ldots \gg j_{i,0} \gg \ldots j_{(m-1)_0} \gg j_{m,0} \tag{14}$$

where $j_{i,0}$ is the exchange current of the i-th step, and $j_{m,0}$ is the exchange current of the rate-determining step.

If the quasi-equilibrium method is used for process (II) investigated by us, and step 3 is rate-determining in the anodic reaction, the following initial conditions should be used in the calculations:

$$k_{a_1} c_{\mathrm{K}}^{\nu'} (1 - \Theta_1 - \Theta_2) \simeq k_{k_1} \Theta_1 \gg k_{a_2} \Theta_1 \simeq k_{k_2} \Theta_2 \gg k_{a_3} c_{\mathrm{K}}^{\nu - \nu'} \Theta_2 \tag{15}$$

When the conditions of the quasi-equilibrium method are realized, the polarization curve does not exhibit *e.g.* section *c* of 118 mV slope, present on the anodic polarization curve in Fig. 2.

REFERENCES

[1] Kiss, L., Farkas, J.: Magy. Kém. Folyóirat, **80,** 542 (1974); Acta Chim. (Budapest) **84,** 161 (1975)
[2] Kiss, L., Varsányi, L.: Magy. Kém. Folyóirat, **81,** 446 (1975); Acta Chim. (Budapest) **88,** 259 (1976)
[3] Kiss, L.: Magy. Kém. Folyóirat **82,** 133 (1976)
[4] Conway, B. E.: Theory and principles of electrode processes. Ronald, New York 1965
[5] Б. Б. Дамаскин, О. А. Петрий: Введение в электрохимическую кинетику, Высшая школа, 1975, стр. 82, 134
[6] Я. Д. Зытнер: Электрохимия, **7,** 1265 (1971)
[7] Darwish, N. A., Hilbert, F., Lorenz, W. J., Rosswag, H.: Electrochim. Acta, **18,** 421 (1973)
[8] Horányi, Gy.: J. Electroanal. Chem., **51,** 163 (1974)
[9] Geana, D., El Miligy, A. A., Lorenz, W. J.: Corr. Sci., **13,** 505 (1973); Electrochim. Acta, **20,** 273 (1975)
[10] В. И. Кичигин, И. Н. Шерстобитова, В. В. Кузнецов: Электрохимия, **12,** 249 (1976)

László Kiss
József Farkas
} H-1088 Budapest, Puskin u. 11—13.

Acta Chimica Academiae Scientiarum Hungaricae, Tomus 93 (1), pp. 33—42 (1977)

PROCESS FOR THE PREPARATION OF PLATINUM CATALYSTS MODIFIED BY ADSORBED METALS

S. Szabó, F. Nagy and D. Móger

(Central Research Institute for Chemistry, Hungarian Academy of Sciences, Budapest)

Received May 31, 1976

A method has been developed for the preparation of platinum catalysts modified by adsorbed metals, suitable for the purposes of gas phase heterogeneous catalytic investigations.

Similarly, a method has been elaborated, for investigating the effect of adsorption of atmospheric oxygen and of heat treatment on air-dry, modified catalyst.

The methods have been illustrated on the example of Pt catalysts covered by copper; it has been established that neither oxygen adsorption nor heat treatment up to 100 °C does change the properties of a Pt catalyst covered with adsorbed copper. In the case of a platinum catalyst covered with gold, the original properties are retained up to 350 °C.

It is well known that various metals are adsorbed on platinum at potentials more positive than their reversible Nernst potential [1—22]. The metal adsorbed changes the adsorptive and catalytic properties of platinum [21—27].

Metal adsorption proceeding on the platinum surface can be precisely measured by electrochemical methods and, under suitable experimental conditions, a coverage of the desired degree can be attained. This permits to change reproducibly the adsorptive and catalytic properties by metal adsorption to the desired extent.

According to our knowledge, this possibility has been utilized so far only in the field of electrocatalysis, because the similarity of electrochemical and electrocatalytic methods simplifies the experimental conditions [21—27]. Since in gas phase heterogeneous catalysis the kinetic investigations cannot be performed in an electrochemical cell with metal adsorption, the 'damage-free' transfer of the catalyst into the reactor should be ensured. The adsorbed metal may be reoxidized in the presence of water by atmospheric oxygen according to the following equation:

$$Me_{ads} + \frac{n}{4} O_2 + \frac{n}{2} H_2O \rightleftharpoons Me^{n+} + n\,OH^- \qquad (1)$$

Therefore, the damage-free transfer of the catalyst can be ensured only with the exclusion of either oxygen or water. As the maintenance of oxygen-free conditions during the transfer of the catalyst into the catalytic reactor is difficult, the exclusion of water was chosen. An electrochemical cell has

been designed for this purpose in which not only the formation of the adsorbed metal layer, but the washing and drying of the catalyst can be carried out under oxygen-free conditions.

The catalyst came into contact with oxygen only in an air-dry state (free of adhering water). It has been experimentally checked whether the properties of the adsorbed metal are not permanently changed by oxygen adsorption during this process. Moreover, it has been investigated to what temperatures the catalyst prepared in this way can be heated without changing the original properties of the adsorbed metal.

I. Cell for catalyst preparation

As can be seen in Fig. 1, the cell differs only in its main electrode space from the three-vessel cells well known in electrochemical methodics. The space of the main electrode is closed at the bottom by a sealed-in glass filter (F),

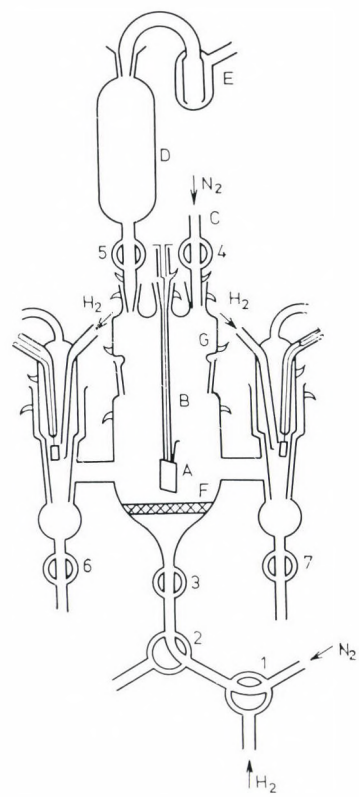

Fig. 1. Cell used for the preparation of the modified catalyst

and at the top by a ground stopper (G). The upper gas inlet cock (C), the main electrode (A, B) and the de-oxygenating vessel (D), together with the bubbling vessel (E) closing the latter, are connected with the main electrode space through ground joints sealed to stopper 'G'. (Ground joints are held together by clamping springs coated with cadmium.)

The liquid drain (2) and the gas inlet Y-cock (1) are joined through cock (3) to the bottom of the main electrode space.

After the closing of cocks 4, 6 and 7, the apparatus operates as a cell divided into three electrode spaces, as used in electrochemical methodics, with the difference that the flushing gas is introduced through glass filter 'F' into the main electrode space, and departs through de-oxigenating vessel 'D' into the atmosphere.

Only cocks 1, 2, 3, 4, 6 and 7 need lubrication during operation, the other cocks and ground joints do not.

1. *Exchange of solutions under oxygen-free conditions*

The exchange of solutions is performed in the following way: through cocks 1, 2 and 3, oxygen-free N_2 is bubbled into the main electrode space, while the new solution is poured into de-oxygenating vessel 'D' and the opening of cock 5 is adjusted so as to prevent the flow of liquid into the cell. After de-oxygenation for an adequate period, cock 5 is closed, the draining Y-cock is set to outflow, and the flushing gas is introduced through upper branch 'C', through the opening of cock 4, from the top into the cell. The solution can be removed in this way from the cell. Next, cock 2 is reset, and the flushing gas is introduced again through glass filter 'F' to the electrode, while cock 4 is closed and cock 5 is adjusted so that the new solution, which has been previously de-oxygenated in vessel 'D', flows slowly, under passing of flushing gas, into the space of the main electrode.

The exchange of solutions under oxygen-free conditions makes the cell suitable, in addition to preparative procedures, also for the electrochemical and electrocatalytic investigation of catalysts modified by adsorbed metals.

2. *Drying under oxygen-free conditions*

As mentioned in the introduction, in the presence of water, atmospheric oxygen destroys the adsorbed metal layer according to Eq. (1). Therefore, after the formation of the adsorbed metal layer and the washing of the catalyst with triply distilled (oxygen-free) water, drying can also be performed under oxygen-free conditions. For this purpose, after draining of the washing liquid through the main electrode space, dry, oxygen-free N_2 is passed until adhering water is also removed. Drying can be accelerated by the heating of the apparatus

with an infrared lamp. However, when a drying lamp is used, care must be excercised that the catalyst should not be exposed to thermal effects, which change the structure of the adsorbed metal layer.

After the termination of drying, the catalyst modified with adsorbed metal can be removed from the cell in an air-dry state and transferred into the catalytic reactor.

3. *Design of the electrodes*

Electrodes of two kinds were used in the cell. If further operations (heat treatment, chemical reaction) were to be carried out with the catalyst modified by adsorbed metal, the electrode shown in Fig. 1 was chosen. In this case, the electrode is a platinum plate of 99.99% purity and $\sim$2 cm^2 apparent surface ('A'), suspended on a Pt wire ('B'), bent to a hook, and sealed into a glass tube. During the various operations, the Pt electrode was handled only with teflon pincers.

For electrochemical investigations (10—12), the platinum plate, similarly of $\sim$2 cm^2 apparent surface and 99.99% purity, has been fixed by point-welding on the platinum wire sealed into glass.

The electrodes were washed with aqua regia until the appearance of the crystal texture and platinized in the way described in our earlier communication [10]. The hook electrode proper ('B') was not subjected to pretreatment other than washing with aqua regia.

The reference and auxiliary electrodes were also made of platinized platinum, according to a design employed in electrochemical practice.

II. Effect of oxygen adsorption on the adsorbed metal

Since the catalyst is transferred in air into the catalytic reactor, we have investigated whether or not oxygen adsorption during this process affects the properties of the adsorbed metal. For this purpose, the following series of experiments were carried out.

a) The charging curve of the platinized platinum catalyst in 1 *M* HCl was recorded (Fig. 2, curve 1). After this, an adsorbed copper layer was formed in the way described earlier [11], and the charging curve of this catalyst, covered with copper, was also recorded (Fig. 2, curve 2).

b) After recording of the charging curve, an adsorbed copper layer was again produced on the surface and the electrode washed and dried as described above.

c) The air-dry catalyst was taken out of the cell and kept for about 5 min in air, then placed back into the cell.

d) Next, dry H_2 gas was passed for 5 min through the main electrode space to reduce the oxygen adsorbed on the catalyst and to prevent thereby the oxidation of the adsorbed metal according to Eq. (1). After stopping of the hydrogen stream, 1 *M* HCl was again introduced under oxygen-free conditions and the charging curve of the catalyst pretreated in this way was recorded (Fig. 2, curve 3).

A comparison of curves 2 and 3 shows that, on applying the above process, the properties of the copper layer adsorbed on the platinized platinum catalyst do not change on contact with the atmosphere.

Similar experiments with platinized platinum catalysts covered by other metals (Au, Bi, Pd) gave the same results. However, in the case of platinum covered by adsorbed gold [28] and adsorbed palladium [29], adsorbed oxygen does not cause structural changes even in the presence of adhering water indeed or even perchloric acid, which considerably simplifies and extends the applicability of such catalysts.

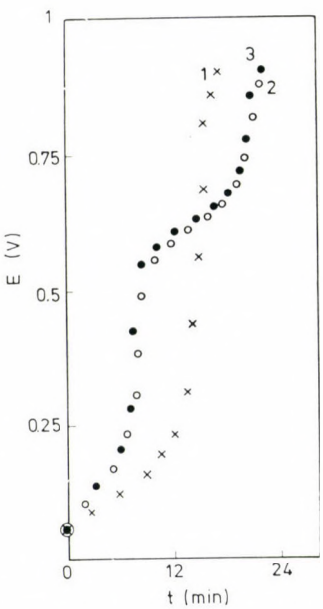

Fig. 2. 1. Charging curve in 1 *M* HCl; 2. charging curve of the catalyst covered by copper; 3. charging curve of the catalyst covered by copper after contact with atmospheric oxygen

III. Effect of thermal treatment on the modified catalysts

From the viewpoint of the applicability of catalysts modified with adsorbed metals, it is very important to know the highest temperature up to which they preserve their original structure. For the study of this problem,

operations described in part II have been complemented, after section c), by heat treatment performed under hydrogen.

Naturally, before the investigation of the modified catalysts, the platinized platinum plate proper has been subjected to thermal treatment under the same conditions as those used with the catalyst covered by adsorbed metal. During thermal treatment, the roughness factor of the catalyst decreased by about an order of magnitude and did not change any more after heat treatment of 15 min. In the further operations, a platinized platinum plate pretreated in this way was used.

For the heat treatment of air-dry catalysts covered by the metal, section c) of the previous paragraph was complemented by the following operations, presented specifically for copper covered catalysts.

c/1. The catalyst was placed into a reactor, air was removed with dry N_2, then dry H_2 gas was passed through the vessel.

c/2. The reactor was placed onto a thermostat of the desired temperature (accuracy ± 1 °C) and kept there for 20 min.

c/3. After thermostating, hydrogen was flushed with N_2 gas from the reactor, which was then allowed to cool. The heat-treated catalyst of room temperature was put back into the cell and its charging curve was recorded as described in section d) of the preceding paragraph.

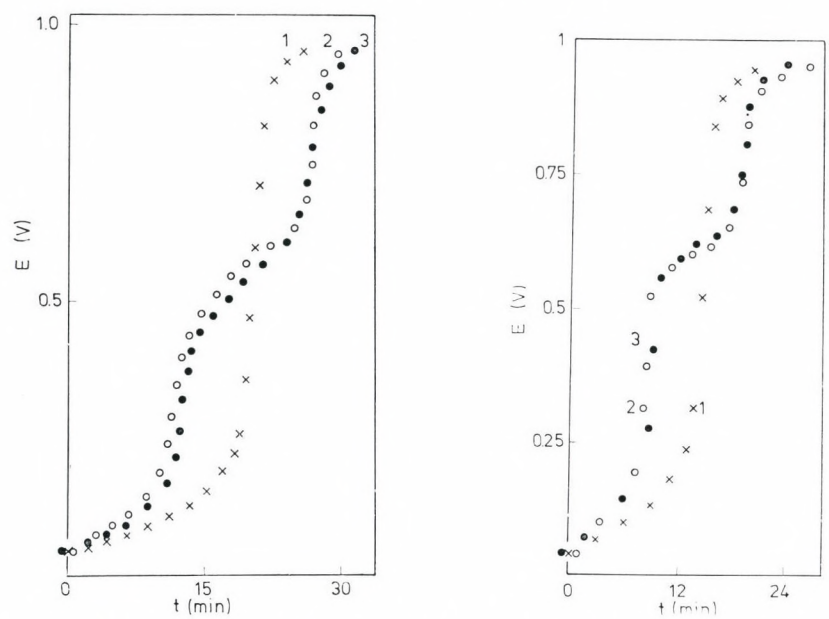

Fig. 3. 1. Charging curve in 1 *M* HCl; 2. charging curve of the catalyst covered by copper; 3. charging curve of the catalyst covered by copper after heat treatment at 100 °C

Fig. 4. 1. Charging curve in 1 *M* HCl; 2. charging curve of the catalyst covered by copper; 3. charging curve of the catalyst covered by copper after heat treatment at 150 °C

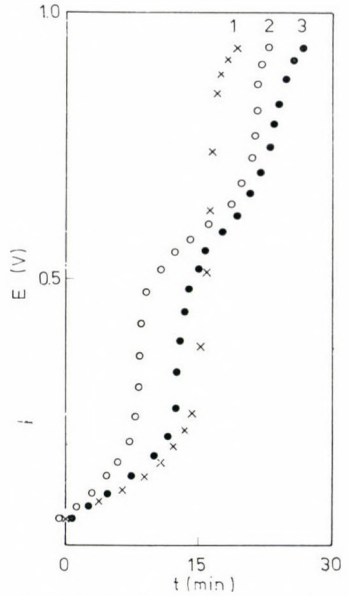

Fig. 5. 1. Charging curve in 1 *M* HCl; 2. charging curve of the catalyst covered by copper; 3. charging curve of the catalyst covered by copper after heat treatment at 200 °C

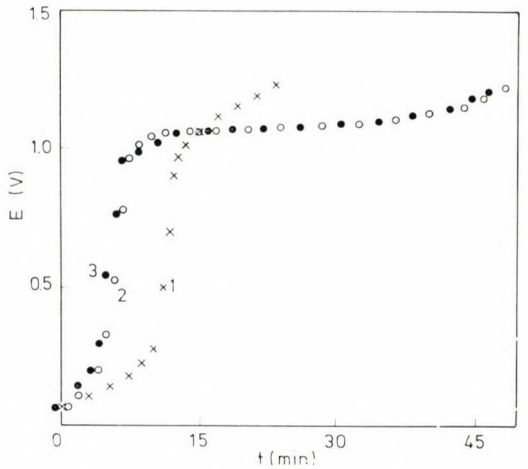

Fig. 6. 1. Charging curve in 0.2 *M* HCl; 2. charging curve of the catalyst covered by gold; 3. charging curve of the catalyst covered by gold after heat treatment at 350 °C

In the case of the copper-covered catalyst, heat treatment was performed at 100, 150 and 200 °C. As shown by Fig. 3, heat-treatment at 100 °C does not change the structure of the adsorbed metal since the charging curves of the treated and untreated catalysts coincide. However, on heat treatment at 150 °C (Fig. 4), and particularly at 200 °C (Fig. 5), there is a considerable

difference between the two charging curves, indicating alloy formation with the adsorbed metal layer. This is supported also by the observation that on cutting off the current after recording the charging curve, the potential of the catalyst returns to the range corresponding to the copper section. After washing and exchange of the solution under oxygen-free conditions, the charging curve was recorded again. At the potential corresponding to the copper section, a small wave actually appears on the charging curve, which may be due only to the oxidation of copper alloyed into the surface; no such wave has been observed in other measurements [11].

The heat treatment of the Pt catalyst covered with adsorbed gold deposited from a hydrochloric acid medium has also been performed [28]. As shown also by the comparison of Figs 6 and 7, up to 350 °C, gold does not form an alloy with the platinum base metal.

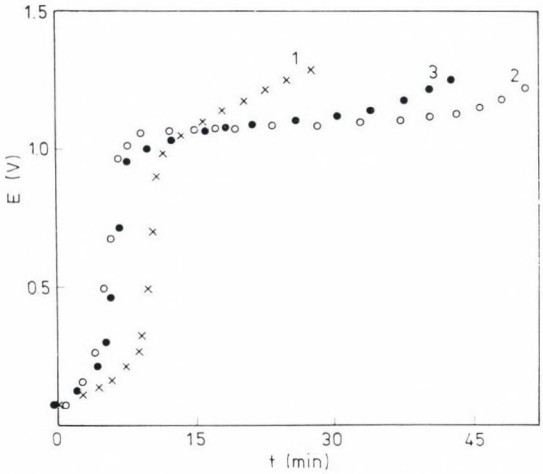

Fig. 7. 1. Charging curve in 0.2 *M* HCl; 2. charging curve of the catalyst covered by gold; 3. charging curve of the catalyst covered by gold after heat treatment at 400 °C

IV. Preparation of supported platinum catalysts modified by adsorbed metal

Since the adsorbed metal layer can be produced also by the ionization of hydrogen adsorbed on platinum [7], [10—12], [16—18], in principle, supported catalysts modified by adsorbed metals can also be prepared.

We started our work on the basis of data published in the literature [7], [16—18], however, it soon became evident that the available results are insufficient for the interpretation of the experimental phenomena. Using a type AP-56 Pt catalyst on Al_2O_3 support (USSR) in perchloric acid medium as model substance, we have found that its colour becomes a darker grey

after metal deposition (Ag, Cu, Bi). The conclusions of this study are reported in a previous publication [10, 12]: the adsorption process involves two steps. In the first step, a metal crystal is deposited on each platinum site. If, for some reason, this metal crystal cannot be transformed onto adsorbed metal in the next step, the colour of the catalyst will be changed by the finely dispersed metal, as has indeed been found in perchloric acid.

If in the case of a supported catalyst no conditions are found under which the metal coating is transformed into adsorbed coating, an alloy catalyst can be obtained by the heat treatment of the catalyst at the appropriate temperature in hydrogen atmosphere. This means that platinum deposited previously on the carrier is alloyed with an amount of the alloying substance equivalent to its original hydrogen capacity.

Metal deposition in hydrochloric acid medium does not change the colour of the AP-56 catalyst, thus in this case adsorbed metal has actually been formed. However, in the case of copper, the loss in charge due to redox system Cu^{2+}/Cu^{+} must also be taken into consideration in estimating the coverage; this loss is presumably strongly dependent on the pore structure of the catalyst [11].

The preparation itself can also be carried out in the cell shown in Fig. 1. However, when a perchloric acid medium is used, chloride ions leached from the supported catalyst must also be taken into account. In other words, in the preparation of supported catalysts involves the same considerations as that of pure metals.

REFERENCES

[1] Breiter, M. W.: J. Electrochem. Soc., **114,** 1125 (1967)
[2] Breiter, M. W.: Trans. Faraday Soc., **65,** 2179 (1969)
[3] Yoshida, T., Matsuda, I., Takeshita, T., Yoshioka, O.: Denki Kagaku, **40,** 853 (1972)
[4] Mikuni, F., Takamura, T.: Denki Kagaku, **38,** 113 (1970)
[5] Bowles, B. J.: Electrochim. Acta, **15,** 589 (1970)
[6] Bowles, B. J.: Electrochim. Acta **15,** 737 (1970)
[7] Cadle, S. H., Bruckenstein, S.: Anal. Chem., **43,** 1858 (1971)
[8] Cadle, S. H., Bruckenstein, S.: Anal. Chem., **44,** 1993 (1972)
[9] Furuya, N., Motoo, S.: Denki Kagaku, **41,** 307 (1973)
[10] Szabó, S., Nagy, F.: Magy. Kém. Folyóirat, **81,** 239 (1975)
[11] Szabó, S., Nagy, F.: Magy. Kém. Folyóirat, **81,** 365 (1975)
[12] Szabó, S., Nagy, F.: J. Electroanal. Chem. (In press)
[13] Schultze, W.: Ber. Bunsenges. Phys. Chem., **74,** 705 (1970)
[14] Tindall, G. W., Bruckenstein, S.: Electrochim. Acta, **16,** 245 (1971)
[15] Mikuni, F., Takamura, T.: Denki Kagaku, **39,** 579 (1971)
[16] Miller, J., Tóth, G.: Magy. Kém. Folyóirat, **78,** 265 (1971)
[17] Tóth, G.: Magy. Kém. Folyóirat, **70,** 361 (1964)
[18] Miller, J., Tóth, G.: Isotopenpraxis, **3,** 19 (1967)
[19] Kolb, D. M., Przasnyski, M., Gerisher, H.: J. Electroanal. Chem., **54,** 25 (1974)
[20] Lorenz, W. J., Hermann, H. D., Wüthrich, N., Hilbert, F.: J. Electrochem. Soc., **121,** 1167 (1974)
[21] Taylor, A. H., Kirkland, S., Brummer, S. B.: Trans. Faraday Soc., **67,** 809 (1971)
[22] Taylor, A. H., Kirkland, S., Brummer, S. B.: Trans. Faraday Soc., **67,** 819 (1971)
[23] Watanabe, M., Motoo, S.: J. Electroanal. Chem., **60,** 259 (1975)
[24] Watanabe, M., Motoo, S.: J. Electroanal. Chem., **60,** 267 (1975)

[25] WATANABE, M., MOTOO, S.: J. Electroanal. Chem., **60,** 275 (1975)
[26] ADZIC, R. R., SIMIC, D. N., DRAZIC, D. M., DESPIC, A. R.: J. Electroanal. Chem., **61,** 117 (1975)
[27] ADZIC, R. R., SIMIC, D. N., DRAZIC, D. M., DESPIC, A. R.: J. Electroanal. Chem., **65,** 587 (1975)
[28] SZABÓ, S., NAGY, F.: Magy. Kém. Folyóirat (In press).
[29] SZABÓ, S.: unpublished results

Sándor SZABÓ
Ferenc NAGY
Dezső MÓGER
H-1025 Budapest, Pusztaszeri út 59—67.

Acta Chimica Academiae Scientiarum Hungaricae, Tomus 93 (1), pp. 43—46 (1977)

COBALT(II) COMPLEXES OF N-BENZOYLPHENYL-HYDROXYLAMINE AND BENZOHYDROXAMIC ACID

A. SYAMAL and V. D. GHANEKAR

(Department of Chemical Technology, The University of Bombay, Matunga Road, Bombay 400019, India

and

Department of Chemistry, Regional Engineering College, Kurukshetra 132119, Haryana, India)

Received July 6, 1976

The cobalt(II) complexes of N-benzoylphenylhydroxylamine and benzohydroxamic acid have been synthesized and characterized by infrared and electronic spectra and magnetic susceptibility measurements. The complexes are pink in colour and have a tetrahedral structure. The complexes are very stable and do not undergo oxidation even on heating at 110 °C for several hours.

Introduction

N-Benzoylphenylhydroxylamine (N-phenylbenzohydroxamic acid) is extensively used as an analytical reagent [1, 2]. However, very little has been reported on the magnetic and spectral properties of the metal complexes of N-benzoylphenylhydroxylamine. We have recently reported the magnetic and spectral properties of tris (N-benzoylphenylhydroxylamine)chromium(III) [3] and the kinetics of substitution reactions of tris(N-benzoylphenylhydroxylamine)oxoniobium(V) [4]. Although several metal complexes of benzohydroxamic acid have been described [5], there is no report on the synthesis of cobalt(II and III) complexes of benzohydroxamic acid. In this communication we report the synthesis and characterization of cobalt(II) complexes of N-benzoylphenylhydroxylamine and benzohydroxamic acid. The complexes have been characterized by elemental analyses, infrared and electronic spectra, and magnetic measurements.

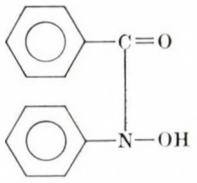

N-benzoylphenyl-hydroxylamine

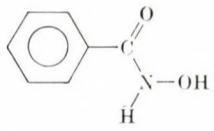

benzohydroxamic acid

Experimental

Cobalt(II) sulfate heptahydrate and sodium acetate trihydrate were the products of Sarabhai M. and Co. N-Benzoylphenylhydroxylamine and benzohydroxamic acid were purchased from Eastman Kodak Co.

Cobalt was determined gravimetrically by igniting the complexes to cobalt oxide and converting the oxide to anhydrous $CoSO_4$. Nitrogen was determined by the semimicro combustion technique. The magnetic susceptibility measurements were performed at room temperature by the Gouy method using $Hg[Co(NCS)_4]$ as standard. Diamagnetic corrections were computed using a standard source [6]. Infrared spectra were recorded on a Perkin Elmer Model 21 infrared spectrophotometer. Each spectrum was calibrated with a polystyrene film. Reflectance spectra were recorded on a Beckman DU recording spectrophotometer equipped with a reflectance attachment.

General method of synthesis

Cobalt(II) sulfate heptahydrate (0.28 g, 1 mmol) was dissolved in 200 ml water. To this bath. The appropriate ligand (3 mmd) was dissolved in a minimum amount of hot 95% alcohol. The ligand solution was added to the hot metal salt solution under stirring. The pH of the mixture was increased to 6.5 with 10% aqueous sodium acetate and the mixture was digested on a water bath for 30 min. The separated pink precipitate was suction filtered, washed with hot water and 95% ethanol. These were dried first under vacuum and then at 110 °C till constant weight. Yield = 50%. The complexes are insoluble in common solvents.

The analytical, magnetic and electronic spectral data of the complexes are presented in Table I. The infrared data are given in Table II.

Table I

Analytical, magnetic and electronic spectral data of cobalt(II) complexes[a]

Complex	Stoichiometry	Co %		N (%)	μ_{eff} (B.M.) (Temp.)	ν_{max} (cm^{-1})
[Co(benzoylphenylhydroxylamine)$_2$]	$CoC_{26}H_{20}O_4N_2$	Found Calcd.	12.3 12.21	5.5 5.79	4.62 (299)	8400, 18230, 20000 sh
[Co(benzohydroxamic acid)$_2$]	$CoC_{14}H_{12}N_2$	Found Calcd.	17.4 17.93	8.2 8.51	4.59 (298)	9000, 18930, 21100

[a] The magnetic moment was calculated using the Curie equation: $\mu_{eff} = 2.84(\chi_M^{corr} \times T)^{1/2}$ B. M.

Table II

Infrared spectral data of ligands and cobalt(II) complexes[a]

Compound	ν (C=O) (cm^{-1})	$\Delta\nu$ (C=O) (cm^{-1})
N-Benzoylphenylhydroxylamine	1630 s	
[Co(benzoylphenylhydroxylamine)$_2$]	1600 s	30
Benzohydroxamic acid	1642 s	
[Co(benzohydroxamic acid)$_2$]	1580 s	62

[a] s = strong

Results and discussion

The complexes were synthesized in the presence of hydroxylamine hydrochloride in order to avoid possible oxidation to cobalt(III) complexes. However, the cobalt(II) complexes of these hydroxamic acids are very stable and do not undergo oxidation even on heating at 110 °C. As cobalt(III) complexes of these ligands are not known, we tried to synthesize the cobalt(III) complexes by hydrogen peroxide oxidation of cobalt(II) acetate and the ligands. This led to the isolation of products which are paramagnetic. Oxidation of pure cobalt(II) complexes of these ligands with hydrogen peroxide also produced paramagnetic products. This resistance to hydrogen peroxide oxidation indicates the stable nature of the cobalt(II) complexes.

The analytical data indicate that the complexes are four-coordinate. The magnetic moment is quite diagnostic for the structure of cobalt(II) complexes. Considering the orbital contributions to the spin-only moment, a magnetic moment lying between 4.4—4.8 B.M. is regarded as associated with a tetrahedral structure [7]. Values in the range of 2.4—2.8 B.M. are regarded to indicate a probable square-planar structure. Octahedral cobalt(II) complexes exhibit magnetic moments in the range of 4.7—5.2 B.M. [7] The measured magnetic moments of our complexes (4.59—4.62 B.M.) indicate a tetrahedral structure.

In a field of tetrahedral symmetry the ^4F ground state of cobalt(II) is split into $^4A_2$, $^4T_2$ and $^4T_1(F)$, and three spin allowed transitions $^4A_2 \rightarrow {}^4T_2(\nu_1)$, $^4A_2 \rightarrow {}^4T_1(F)(\nu_2)$ and $^4A_2 \rightarrow {}^4T_1(P)$ (ν_3) are expected [8]. The electronic spectra of the present complexes exhibit bands at about 8500, 18500 and 20500 cm^{-1}. Since the ν_1 band is not usually observed due to the weak character of the $^4A_2 \rightarrow {}^4T_2$ transition, the observed bands should be assigned among ν_2 and ν_3 bands, one having probably a double peak due to the effect of spin-orbit coupling. In conformity with other tetrahedral cobalt(II) complexes [9] the band at 8500 cm^{-1} is assigned to the ν_2 transition. The doublet in the visible region with maxima at around 18500 and 20500 cm^{-1} should then be assigned to the components of the ν_3 transition [8, 9].

The infrared spectral data in the carbonyl stretching region indicate that the carbonyl absorptions occur at lower frequencies than those of the free ligands. This negative shift indicates coordination through the carbonyl group of the ligands. The absence of a ν(OH) stretch in the complexes indicates deprotonation of the ligands on complex formation. Owing to the complexity of the spectra other regions were not analyzed.

*

The authors are grateful to the University Grants Commission, New Delhi-1 for the award of a Junior Research Fellowship to V. D. G. This work was also supported in part by the faculty research fund of the University of Bombay.

REFERENCES

[1] MAJUMDAR, A. K.: N-benzoylphenylhydroxylamine and its analogues, Pergamon Press, New York 1972
[2] SINHA, S. K., SOHME, S. C.: Anal. Chim. Acta, **21,** 459 (1959)
[3] SYAMAL, A.: J. Prakt. Chem., **312,** 954 (1970)
[4] JOHNSON, R. C., SYAMAL, A.: J. Inorg. Nucl. Chem., **33,** 2547 (1971)
[5] BHADURI, S., RAY, P.: Science and Culture (Calcutta), **16,** 97 (1952); DUTTA, R. L., CHATTERJEE, B.: J. Indian Chem. Soc., **44,** 780 (1967)
[6] FIGGIS, B. N., LEWIS, J.: cited in Modern Coordination Chemistry, LEWIS, J., WILKINS, R. G., p. 403. Interscience, New York 1960
[7] COTTON, F. A., WILKINSON, G.: Advanced Inorganic Chemistry, Wiley Eastern Private Ltd., New Delhi p. 869. Second Edition 1966
[8] BALLHAUSEN, C. J.: Introduction to Ligand Field Theory, p. 258 McGraw Hill Book Co., New York 1962
[9] HOLM, R. H., CHAKRAVARTY, A., THERIOT, L. J.: Inorg. Chem., **5,** 625 (1966)

A. SYAMAL
V. D. GHANEKAR
Department of Chemistry, Regional Engineering College, Kurukshetra 132119, Haryana, India

Acta Chimica Academiae Scientiarum Hungaricae, Tomus 93 (1), pp. 47—49 (1977)

CARTESIAN CO-ORDINATES AND RING CLOSURE IN MOLECULAR MODELS

B. Rozsondai

(Central Research Institute for Chemistry, Hungarian Academy of Sciences, Budapest)

Received July 26, 1976

An automatic procedure for calculating Cartesian co-ordinates of atoms from geometrical parameters of molecular models has been developed. It allows attachment of groups to the skeleton and closing of asymmetric rings. Principles of the method are outlined.

When studying molecular structures and properties, we often need Cartesian co-ordinates of the atoms, while the geometry of the molecule is defined in terms of bond lengths, bond angles and dihedral (torsional) angles. The present method of calculating co-ordinates has been developed for use in gas electron diffraction studies. In addition to features of similar procedures, (see *e.g.* [1]), it includes (i) attachment of groups to the skeleton of the molecule in one step of calculation and (ii) ring closure, first of all for asymmetric rings.

General principles of the procedure will be summarized here. Expressions for the co-ordinates and their transformation can be derived for the different cases by using simple geometry.

General procedure

The model of the molecule is constructed step by step. The molecule is fixed in a primary (main) co-ordinate system and co-ordinates of some atoms are expressed directly. Further atoms or groups are attached by standardized procedures. Three noncollinear atoms with known main co-ordinates specify a secondary (local) co-ordinate system [2] for the positioning of a new atom or group. Local co-ordinates of new atoms are then transformed into main co-ordinates. At each stage we utilize the geometrical parameters given.

Each different mode of positioning an atom or a group in a local system is accomplished by a special computer subprogram (subroutine). Transformation is separated from the calculation of local co-ordinates. Therefore, a group (*e.g.* a methyl group) may conveniently be attached to different parts of the framework already existing, and computing time can be saved. A set of such subroutines may be included in a library for convenient use.

Ring closure

Closing a ring with given bond lengths and bond angles requires special consideration. A stepwise construction of the model fails for cyclic molecules: values of some dependent (*i.e.* unknown) parameters would be needed to fix consecutive atoms of the ring one by one. The whole ring, or at least a part of it, must be considered at the same time and nonlinear equations in several unknowns must be solved. The solution may be simple for some symmetric rings but other cases may prove very difficult.

Let us consider a ring with some (at least three) consecutive atoms already fixed in a co-ordinate system. The positions of the remaining k consecutive atoms are sought. Which is the minimum number of equations to be solved? When the new atoms are joined to complete the ring, $k + 1$ new bonds, $k + 2$ bond angles and $k + 3$ dihedral angles are formed. $3k$ of these parameters are independent and must be given to define the unknown co-ordinates, *six* of them are dependent.* (We assume here that no symmetry is required for the unknown parameters.) Now let us use known or unknown quantities to fix new atoms one by one, and let the chain grow at one end or both until it is terminated by two adjacent atoms. The position of atom N4 *e.g.*, in the local system of A1, A2 and A3 (Fig. 1), will be given through distance A3—N4, angle A2—A3—N4 and torsional angle ω_1. *Six* of the above $(k + 1) + (k + 2) + (k + 3)$ parameters will not be used in this process. If, say, N6 and A7 are the terminals — A7 being already fixed — N6 may be located without

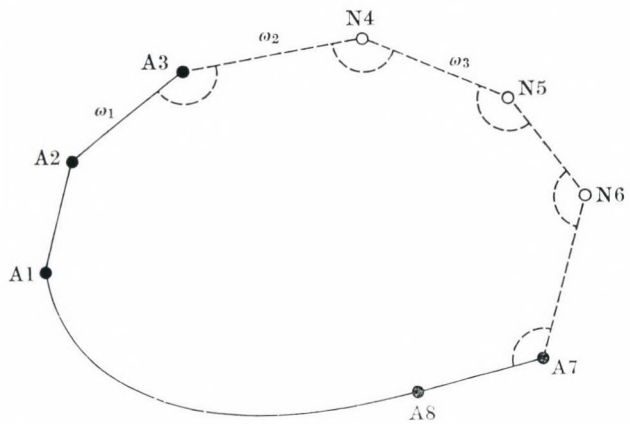

Fig. 1. Ring closure. A are atoms with known positions; N new atoms, ω torsional angles about bonds; — — — bonds and angles formed in the ring closing step. A8 may coincide with A1; or A7 and A8 with A1 and A2, respectively

* It should be noted that not *any* set of $3k$ parameters can be given. In Fig. 1, *e.g.*, the new bond lengths, the angles at N4, N5, N6 and angles of torsion about N4—N5 and N5—N6, although nine in number, are not all independent because they must reproduce the already fixed distance A3 . . .A7.

using distance N6—A7, angles N5—N6—A7 and N6—A7—A8 and angles of torsion around N5—N6, N6—A7 and A7—A8. The number of unknown parameters involved in locating the new atoms is equal to the number of known parameters nonutilized. The latter can be expressed in terms of the co-ordinates of atoms. Thus we get the necessary number of equations which can be solved numerically for the unknown parameters.

Thus, the natural conclusion follows that ring closure should be completed at the site where the largest number of dependent (unknown) parameters is concentrated.

These principles of ring closure have been realized so far for the case in Fig. 1: all bond distances and bond angles are independent and the three equations for ω_1, ω_2 and ω_3 are solved numerically [3]. Different solutions, if they exist, may be obtained from different initial values and conditions for the numerical procedure.

If $k = 2$ or 1 (a five- or four-membered ring or a part in some bridged ring systems), some of the bond lengths or angles are inevitably dependent, and the number of equations to be solved is two or one, respectively.

The required symmetry of the ring usually imposes additional constraints upon the dependent parameters and the number and kind of unknown variables must be considered in each individual case.

When closing a ring, we usually prefer all bond lengths and bond angles to be independent parameters. Besides, the required number of dihedral angles must be given. Other dihedral angles can be chosen as auxiliary unknown variables, like ω_1, ω_2 and ω_3 in the example above. The choice of other than the named parameters may be more convenient, depending on the actual problem.

For a given type of molecular model, one has to write a program that positions at least three noncollinear atoms in the main co-ordinate system, calls the necessary subroutines, performs symmetry operations and data input/output, etc. The memory requirements of this program and the subroutines will be small and will depend on the complexity of the model.

*

The author gratefully thanks Dr. I. HARGITTAI for interest and encouragement, GY. SCHULTZ for helpful discussions and Dr. R. L. HILDERBRANDT for valuable comments.

REFERENCES

[1] HILDERBRANDT, R. L.: J. Chem. Phys., **51,** 1654 (1969)
[2] EYRING, H.: Phys. Rev., **39,** 746 (1932)
[3] In the treatment by GŌ, N. and SCHERAGA, H. A.: Macromolecules, **3,** 178 (1970), the six torsional angles about bonds A2-A3 through A7-A8 are unknown variables, then the problem is reduced to the solution of an equation with a single unknown.

Béla ROZSONDAI, H-1088 Budapest, Puskin utca 11—13.

Acta Chimica Academiae Scientiarum Hungaricae, Tomus 93 (1), pp. 51—65 (1977)

REACTIONS OF MONO- AND DIARYLIDENECYCLOALKANONES WITH THIOUREA AND AMMONIUM THIOCYANATE

T. LÓRÁND, D. SZABÓ and A. NESZMÉLYI*

(Chemical Department of the Medical University, Pécs, and
**Central Research Institute for Chemistry of the Hungarian Academy of Sciences, Budapest)*

Received February 15, 1975; in revised form April 10, 1976

2-Arylidenecyclohexanones react with ammonium thiocyanate or thiourea to yield 4-aryl-3,4,5,6,7,8-hexahydro-2(1H)-quinazolinethiones (**Ia—f**). In the reaction of 2-arylidenecyclopentanones with ammonium thiocyanate, N,N'-bis[(2-arylidene)-cyclopentylidene]-thioureas (**IIa—b**) were obtained, while the reaction products with thiourea were 7H-4-aryl-3,4,5,6-tetrahydro-2(1H)-cyclopentapyrimidinethiones (**IIIa—b**). 2,6-Diarylidenecyclohexanones did not react with ammonium thiocyanate, but gave 4-aryl-8-arylidene-3,4,5,6,7,8-hexahydro-2(1H)-quinazolinethiones (**IVa—f**) with thiourea. When 2,5-dibenzylidenecyclopentanone was allowed to react with thiourea, the product was 7H-7-benzylidene-4-phenyl-3,4,5,6-tetrahydro-2(1H)-cyclopentapyrimidinethione (**V**). Mechanisms are suggested for the above reactions. Oxidation of **Ia** and **IVa** gave the corresponding 2-oxo-hexahydroquinazoline derivatives, **VI** and **VII** respectively.

α, β-Unsaturated ketones may react with thiourea in two different ways depending on the conditions of the reaction. In an acidic medium the ketone is protonated [1], the S atom of thiourea assumes nucleophilic character, and the reaction product will be mainly 1,3-thiazine derivative [2,3]. In base-catalyzed reaction deprotonation of the reagent occurs, the nitrogen atom will be nucleophilic, and 2-thionopyrimidine derivatives are obtained.

ZIGEUNER *et al.* [4,5] studied the reactions of α, β-unsaturated ketones with ammonium thiocyanate and thiourea, and similar conversions of chalcones have been reported by Egyptian authors [6]. In this case the reaction products were 2-thionopyrimidine derivatives.

In the present work 2-arylidenecyclohexanones and 2-arylidenecyclopentanones were allowed to react with thiourea and with ammonium thiocyanate. In the case of 2-arylidenecyclohexanones, the products were 4-aryl-3,4,5,6,7,8-hexahydro-2(1H)-quinazolinethiones (**Ia-f**) (Table I) with both reagents.

The main product in the reaction of 2-arylidenecyclopentanones with ammonium thiocyanate was N,N'-bis[(2-arylidene)-cyclopentylidene]-thiourea (**IIa, b**) (Table II), the by-product being 7H-4-aryl-3,4,5,6-tetrahydro-2(1H)-cyclopentapyrimidinethione (**IIIa**) (Table II). The same ketones yielded exclusively **IIIa** and **IIIb** in the reaction with thiourea.

The spectral properties of the compounds are as follows. In the IR

Table I

Compound Ar	M.p., °C	Formula M. W. Yield, %	Analysis, % Calcd.	Found
Ia C_6H_5	216 (d.)	$C_{14}H_{16}N_2S$ 244.36 60[d] 36[e]	C: 68.82 H: 6.60 N: 11.47 S: 13.12	68.75 6.71 11.62 13.29
Ib 4-Cl-C_6H_4	241 (d.)	$C_{14}H_{15}ClN_2S$ 278.81 31[d]	C: 60.31 H: 5.42 N: 10.05 S: 11.50 Cl: 12.72	60.19 5.62 9.93 11.26 12.62
Ic 4-CH_3-C_6H_4	240 (d.)	$C_{15}H_{18}N_2S$ 258.40 71[d]	C: 69.72 H: 7.02 N: 10.84 S: 12.42	69.69 7.03 10.97 12.24
Id 4-CH_3O-C_6H_4	223 (d.)	$C_{15}H_{18}N_2OS$ 274.40 45[d]	C: 65.66 H: 6.61 N: 10.21 S: 11.69	65.44 6.84 10.06 11.81
Ie 4-$N(CH_3)_2$-C_6H_4	238 (d.)	$C_{16}H_{21}N_3S$ 287.44 42[d]	C: 66.86 H: 7.36 N: 14.62 S: 11.16	66.77 7.43 14.68 11.06
If 2-furyl	202 (d.)	C_{12} $H_{14}N_2OS$ 234.32 13[e]	C: 61.51 H: 6.02 N: 11.96 S: 13.69	61.52 6.11 11.74 13.80

[a] Disappear on the effect of D_2O
[b] Recorded in $(CD_3)_2SO$
[c] Disappears on the effect of D_2O; the other NH proton is overlapped by the aromatic quartet, whose integrated value decreased on the addition of D_2O
[d] With NH_4SCN
[e] With thiourea

spectra of **Ia-f** and **IIIa, b** the $\nu C{=}O$ band of the starting ketones (1690—1719 cm^{-1}) disappeared and a sharp band of medium intensity due to the isolated $\nu C{=}C$ vibration appeared in the range 1710—1722 cm^{-1}. The cyclic thiourea structure was supported by the appearance of the νNH band between 3190 and 3300 cm^{-1} and of a sharp $\nu C{=}S$ band between 1180 and 1220 cm^{-1}.

UV (ethanol) λ_{max}, nm (log ε)	IR, cm^{-1} (KBr)	PMR, δ ppm ($CDCl_3$)
207 (4.36) 258 (4.26) 279 (4.14)	νNH: 3220 νC=C: 1718 νC=S: 1215	1.3—2.5 m 8H CH_2 4.8 s 1H CH 7.4 s 5H Ar 8.0; 6.9 s 2H NH[a]
223 (4.17) 259 (4.15) 277 (4.04)	νNH: 3200 νC=C: 1712 νC=S: 1215	1.0—2.2 m 8H CH_2 4.7 s 1H CH 7.2; 7.4 q 4H Ar J = 8.4 Hz 8.7; 9.5 s 2H NH[a,b]
219 (3.96) 258 (3.98) 274 (3.90)	νNH: 3200, 3320 νasCH_3: 2980 (sh.) νsCH_3: 2865 νC=C: 1712 νC=S: 1218	1.4—2.3 m 8H CH_2 2.3 s 3H CH_3 4.8 s 1H CH 7.3 d 4H Ar J = 6H z 6.8; 7.8 s 2H NH[a]
215 (3.92) 230 (4.05) 259 (4.07) 277 (4.05) 283 (4.03)	νNH: 3200 νasCH_3: 2960 (sh.) νsCH_3: 2862 νC=C: 1710 νC=S: 1210 νasC—O—C: 1255 νsC—O—C: 1040	1.2—2.3 m 8H CH_2 3.8 s 3H CH_3 4.8 s 1H CH 6.9; 7.3 q 4H Ar J = 10.8 Hz 7.7 s 1H NH[c]
214 (4.28) 251 (4.32) 274 (4.48)	νNH: 3190 νC=C: 1710 νC=S: 1220	1.4—2.3 m 8H CH_2 3.0 s 6H CH_3 4.7 s 1H CH 6.7; 7.2 q 4H Ar J = 9.6 Hz 7.7 s 1H NH[c]
219 (4.07) 259 4.09 280 (4.15)	νNH: 3200 νC=C: 1713 νC=C(furyl): 1560 1510 1370 νC=S: 1220	1.4—2.4 m 8H CH_2 5.0 1H CH 6.2—6.6; 7.2—7.5 m 3H (furan ring) 7.1; 8.1 s 2H NH[a]

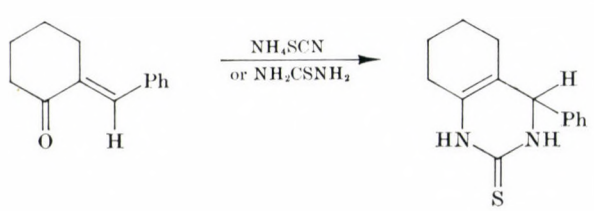

Ia

Fig. 1

Table II

Compound Ar	M.p., °C	Formula M. W. Yield, %	Analysis, % Calcd.	Found
IIa C_6H_5	192 (d.)	$C_{25}H_{24}N_2S$ 384.56 11[a]	C: 78.08 H: 6.29 N: 7.29 S: 8.34	78.06 6.14 7.28 8.33
IIb 4-CH_3O-C_6H_4	156 (d.)	$C_{27}H_{28}N_2O_2S$ 444.61 8[a]	C: 72.94 H: 6.35 N: 6.30 S: 7.21	73.01 6.24 6.21 7.20
IIIa C_6H_5	220 (d.)	$C_{13}H_{14}N_2S$ 230.34 2[a] 9[b]	C: 67.79 H: 6.13 N: 12.16 S: 13.92	67.63 6.03 12.01 13.89
IIIb 4-CH_3O—C_6H_4	190 (d.)	$C_{14}H_{16}N_2OS$ 260.37 11[b]	C: 64.60 H: 6.19 N: 10.76 S: 12.32	64.63 6.24 10.65 12.24
VI	184—186	$C_{14}H_{16}N_2O$ 228.30 43[g] 4[h]	C: 73.66 H: 7.07 N: 12.27	73.52 7.23 12.46
VII	209—211	$C_{21}H_{20}N_2O$ 316.41 40	C: 79.22 H: 6.37 N: 8.85	79.50 6.26 8.72

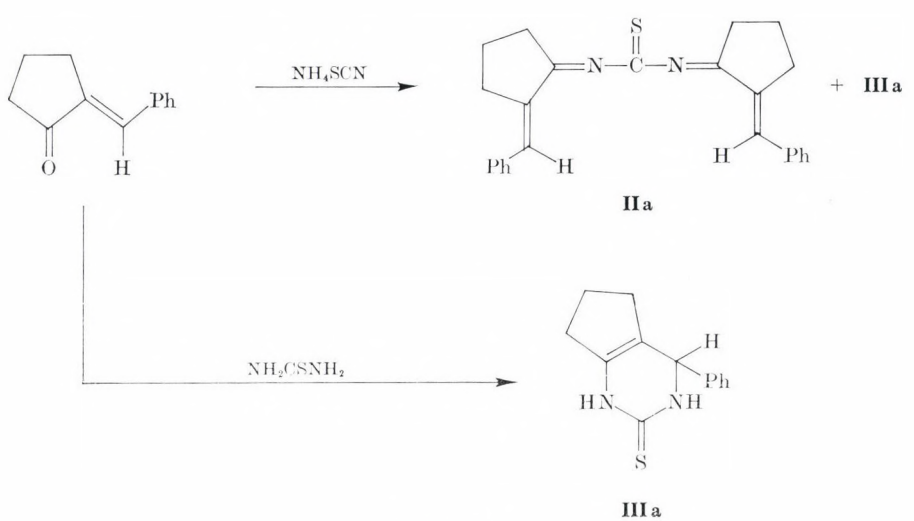

Fig. 2

λ_{max}, nm (log ε)	IR, cm^{-1} (KBr)	PMR, δ ppm (TFA)
212 (4.38) 273 (4.38) 347 (4.36)	ν=N—C=S: 2050 2000 (sh.) νC=N: 1630	2.1—3.6 m 12H CH_2 7.2—7.8 m 12H Ar and =CH—
212 (4.38) 284 (4.45) 354 (4.29)	ν=N—C=S: 2054 2000 (sh.) νC=N: 1630 νasC—O—C: 1258 νsC—O—C: 1030	1.7—3.2 m 12H CH_2 3.6; 3.63 s 6H CH_3 6.5—7.4 m 10H Ar and =CH—
210 (4.15) 258 (4.13) 286 (4.00)	νNH: 3190 νC=C: 1722 νC=S: 1195	1.0—2.3 m 6H CH_2 5.0 s 1H CH 7.3 s 5H Ar 8.7; 9.9 s 2H NH[d,e]
208 (4.10) 229 (4.05) 259 (4.07) 277 (4.01) 283 (4.00)	νNH: 3190 νC=C: 1720 νC=S: 1180 νasC—O—C: 1255 νsC—O—C: 1040	1.6—2.8 m 6H CH_2 3.8 s 6H CH_3 5.1 s 1H CH 6.9; 7.3 q 5H Ar and NH J = 9 Hz 8.5 s 1H NH[e,f]
213 (3.89) 257 (3.29)	νNH: 3245 3100 νC=C: 1712 (sh.) νC=O: 1695	1.0—2.5 m 8H CH_2 4.8 s 1H CH 7.3 s 5H Ar 5.7; 7.8 s 2H NH[e,d]
213 (4.21) 156 (4.14) 298 (4.19)	νNH: 3050—3370 (3 bands) νC=O: 1680	1.4—2.9 m 6H CH_2 4.9 s 1H CH 6.7 s 1H =CH— 7.2—7.7 m 10H Ar 5.8; 7.1 s 2H NH[e,d]

[a] With NH_4SCN
[b] With thiourea
[c] Recorded in $(CD_3)_2SO$
[d] Disappear with D_2O
[e] Recorded in $CDCl_3$
[f] Disappears on the effect of D_2O; the other NH proton is overlapped by the aromatic quartet, whose integrated value decreased on the addition of D_2O
[g] In oxidation
[h] In the reaction of 2-benzylidenecyclohexanone and urea
TFA = trifluoroacetic acid

The presence of the νC=S band excluded the possibility of the isomeric 1,3-thiazine structure.

In the PMR spectra of compounds **Ia-f** and **IIIa, b**, the signal of the olefinic proton of the starting compounds was absent and the signal of the C-4 methine proton appeared between δ = 4.7 and 5.0 ppm. At lower field

Table III

Compound Ar	M.p., °C	Formula M. W. Yield, %	Analysis, %	
			Calcd.	Found
IVa C_6H_5	196—198	$C_{21}H_{20}N_2S$ 332.48 50	C: 75.87 H: 6.06 N: 8.43 S: 9.64	76.05 6.19 8.36 9.66
IVb 4-Cl—C_6H_4	248—250	$C_{21}H_{18}ClN_2S$ 401.37 59	C: 62.84 H: 4.52 N: 6.98 S: 7.99 Cl: 17.67	62.60 4.80 6.93 7.98 17.44
IVc 4-CH_3—C_6H_4	228—229	$C_{23}H_{24}N_2S$ 360.52 46	C: 76.63 H: 6.71 N: 7.77 S: 8.89	76.46 7.00 7.78 8.83
IVd 4-CH_3O—C_6H_4	186—188	$C_{23}H_{24}N_2O_2S$ 392.52 80	C: 70.38 H: 6.16 N: 7.14 S: 8.17	70.24 6.40 7.18 8.10
IVe 4-$N(CH_3)_2$—C_6H_4	158 (d.)	$C_{25}H_{30}N_4S$ 418.62 77	C: 71.73 H: 7.22 N: 13.39 S: 7.66	71.64 7.44 13.38 7.72
IVf 2-furyl	150 (d.)	$C_{17}H_{16}N_2O_2S$ 312.40 29	C: 65.36 H: 5.16 N: 8.97 S: 10.26	65.59 5.42 8.88 10.23
V C_6H_5	245 (d.)	$C_{20}H_{18}N_2S$ 318.39 57	C: 75.45 H: 5.70 N: 8.80 S: 10.07	75.40 5.98 8.76 9.93

[a] Disappear on the effect of D_2O

[b] Recorded in $(CD_3)_2SO$

[c] Disappears on the effect of D_2O; the second NH proton is overlapped by the aromatic signal, whose integrated value decreased on the addition of D_2O

UV (ethanol) λ_{max}, nm (log ε)	IR, cm^{-1} (KBr)	PMR, δ ppm ($CDCl_3$)
210 (4.39)	νNH: 3185	1.4—1.8 m 2H CH_2
276 (4.43)	3100	1.8—2.1 m 2H CH_2
315 (4.14)	νC=C: 1619	2.3—2.8 m 2H CH_2
	νC=S: 1192	4.9 s 1H CH
		6.6 s 1H =CH—
		7.3 s 10H Ar
		7.2; 7.7 s 2H NH[a,g]
221 (4.26)	νNH: 3180	1.0—2.3 m 6H CH_2
280 (4.42)	3110	5.0 s 1H CH
320 (4.12)	νC=C: 1619	7.2 s 1H =CH—
	νC=S: 1198	7.5 s 8H Ar
		9.2; 9.4 s 2H NH[a,b]
210 (4.36)	νNH: 3200	1.4—2.9 s 6H CH_2
278 (4.44)	νasCH_3: 2949	2.3 s 6H CH_3
318 (4.14)	νsCH_3: 2870	4.9 s 1H CH
	νC=C: 1610	6.6 s 1H =CH—
	νC=S: 1192	7.2 s 8H Ar
		7.7 s 1H NH[c]
209 (4.47)	νNH: 3200	1.4—2.8 m 6H CH_2
286 (4.53)	3100	3.8 d 6H CH_3
319 (4.29)	νC=C: 1620 (sh.)	4.9 s 1H CH
	νasC—O—C: 1254	6.6—7.5 m 9HAr and =CH—
	νsC—O—C: 1030	7.7 s 1H NH[c]
210 (4.48)	νNH: 3200	1.3—2.2 m 6H CH_2
261 (4.41)	3100	2.9 d 12H CH_3
333 (4.46)	νC=C: 1610	4.7 s 1H CH
	νC=S: 1185	6.6—7.5 m 9H Ar and =CH—
		9.0 s 2H NH[b,d,e]
216 (3.99)	νNH: 3150	
288 (4.12)	3090	
324 (3.96)	νC=C: 1625 (sh.)	
394 (3.24)	νC=C: (furyl): 1585	
	1570	
	1477	
	1445	
	νC=S: 1190	
218 (4.19)	νNH: 3210	1.9—3.0 m 4H CH_2
285 (4.43)	νC=C: 1630	5.2 s 1H CH
313 (4.24)	νC=S: 1190	6.9 s 1H =CH—
		7.4 s 10H Ar
		9.0; 10.2 s 2H NH[a]

[d] Broad band
[e] Disappears on the effect of D_2O
[f] PMR spectrum could not be recorded because of the poor solubility of the substance
[g] PMR data obtained with a 100 MHz instrument

strength the signals of the two NH protons appeared either separately, or one was overlapped by the aromatic signal. These protons were exchangeable with D_2O. In the analysis of **IIa, b** the high C and H contents indicated that two ketone molecules had been involved in the reaction. The IR spectra had neither $\nu C{=}O$ nor νNH bands.

The question is why the reaction of 2-arylidenecyclohexanones differ from that of 2-arylidenecyclopentanones. In the vinylogous carbonyl compounds both the vinylogous carbon atom and the carbonyl carbon atom may behave as electrophilic centres, *i.e.* nucleophilic agents can attack at these two sites. In the IR spectra of 2-arylidenecyclohexanones and the respective cyclopentanones the frequency values of the $\nu C{=}O$ bands are different from each other (1690 and 1719 cm^{-1}, respectively). The deviation of 30 cm^{-1} is, according to literature data [7,8], due to the different extents of ring strain and of conjugation. The lower carbonyl frequency of 2-arylidenecyclohexanones indicates a larger extent of conjugation. On this basis it is reasonable to suppose that in 2-arylidenecyclohexanones the more effective electrophilic centre will be the vinylogous carbon atom. However, in 2-arylidenecyclopentanones a lower degree of conjugation should be assumed. Here, in the reaction with ammonium thiocyanate the carbonyl C-atom will be the more active electrophilic centre, however, its role is taken over by the vinylogous carbon atom when the reagent is thiourea. The mechanism proposed for the reaction of 2-arylidenecyclopentanones with ammonium thiocyanate is shown below.

In the base-catalyzed reaction of 2-arylidenecyclopentanones with thiourea the deprotonated form of the reagent is considered to be active.

An analogous mechanism is assumed for 2-arylidenecyclohexanones. In their reaction with ammonium thiocyanate the vinylogous carbon atom is attacked by the thiocyanate ion, and the final step of cyclization is the elimination of water.

Divinyl ketones readily form spiro compounds with bifunctional nucleophilic agents [9,10]. ZIGEUNER *et al.* obtained spiro-bis-hexahydropyrimidinethione derivatives in the reaction of phorone with ammonium thiocyanate and thiourea [11].

Under the reaction conditions applied by us, 2,6-diarylidenecyclohexanones failed to react with ammonium thiocyanate. Their base-catalyzed reaction with two moles of thiourea did not yield spiro-bis-pyrimidinethione but the products were 4-aryl-8-arylidene-3,4,5,6,7,8-hexahydro-2(1H)-quinazolinethiones (**IVa-f**) (Table III); similarly, 7H-7-benzylidene-4-phenyl-3,4,5,6-tetrahydro-2(1H)-cyclopentapyrimidinethione (**V**) (Table III) was obtained from 2,5-dibenzylidenecyclopentanone. The substitution pattern of the aromatic nucleus did not influence the course of the reaction.

The structures of the compounds formed were confirmed by elemental analysis, IR and PMR spectroscopic methods. The CMR spectrum of **IVa**

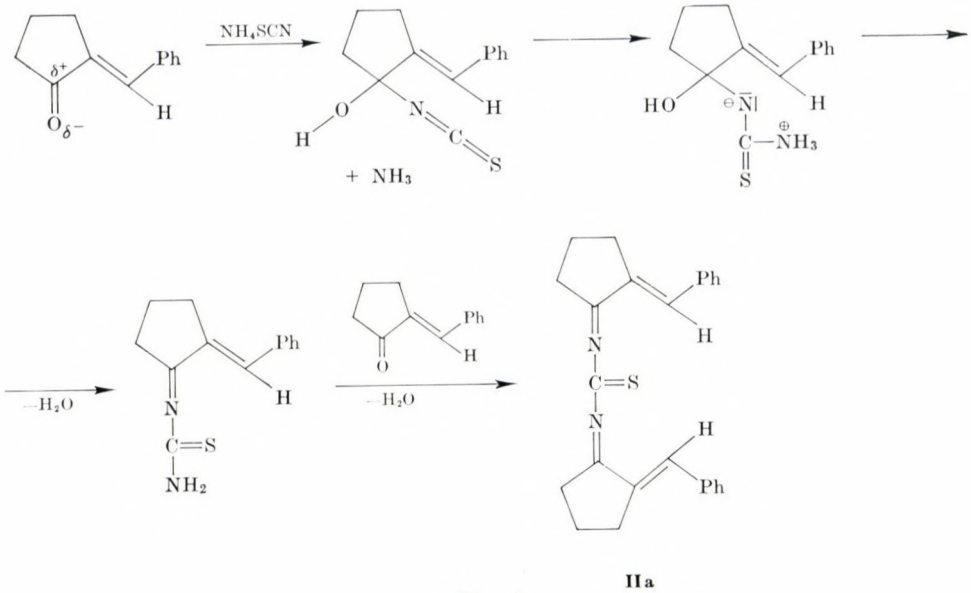

IIa

Fig. 3

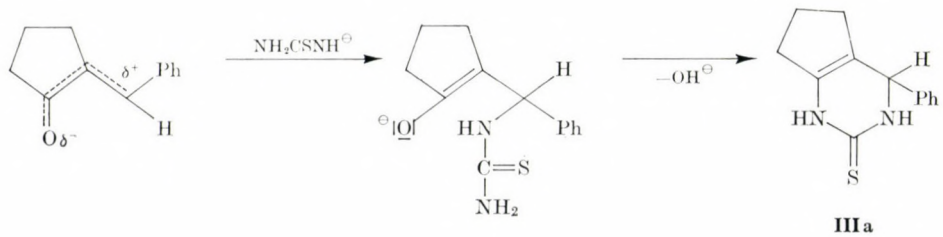

IIIa

Fig. 4

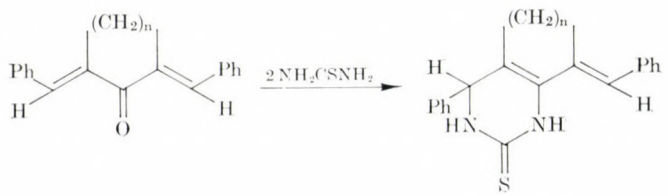

IVa (n = 3)
V (n = 2)

Fig. 5

was consistent with the suggested structure and at the same time excluded an *m*-thiazine structure also for compounds **Ia** and **IIIa**.

^{13}C spectrum of **IVa** recorded with wide range proton decoupling at 25.16 MHz (solvent: DMSO-d_6, temperature: 30 °C).

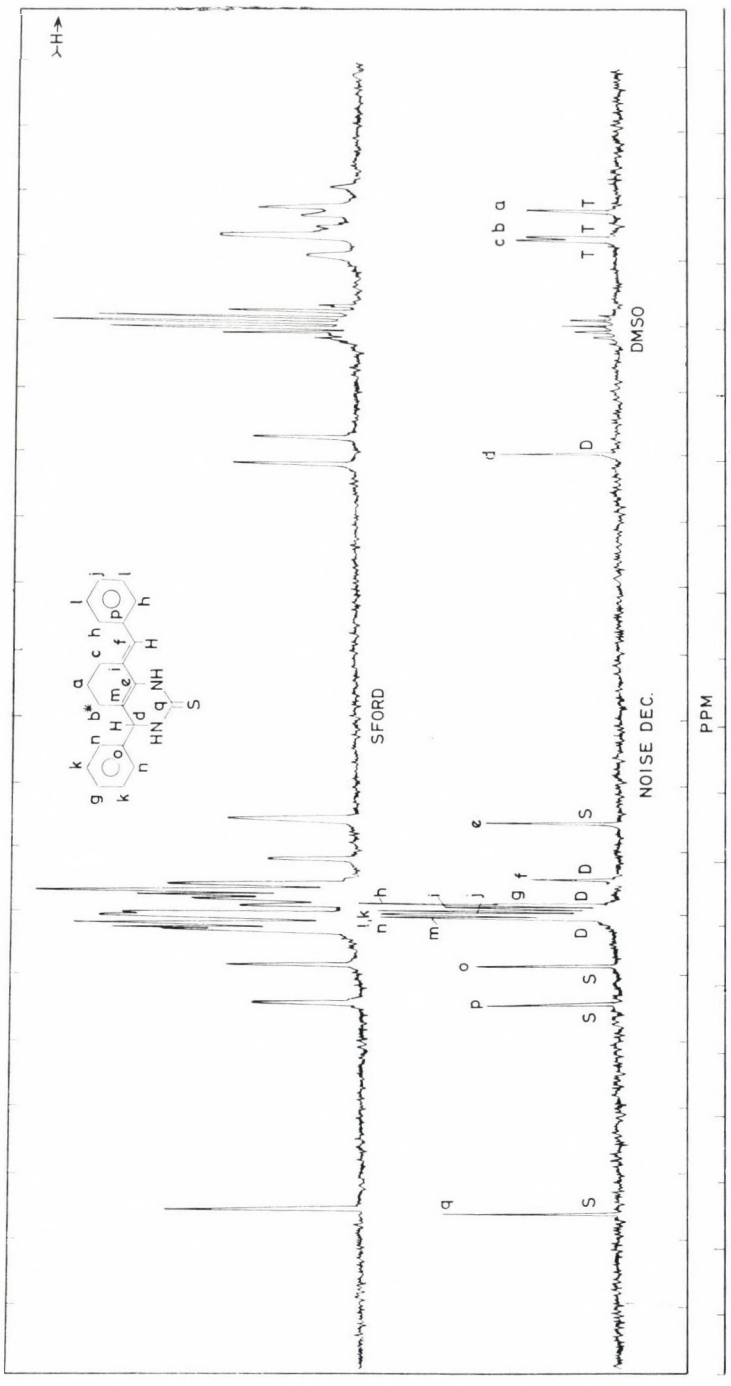
SFORD
NOISE DEC.
DMSO
PPM
^{13}C
0
20
40
60
80
100
120
140
160
180
200

Fig. 6

Fig. 7

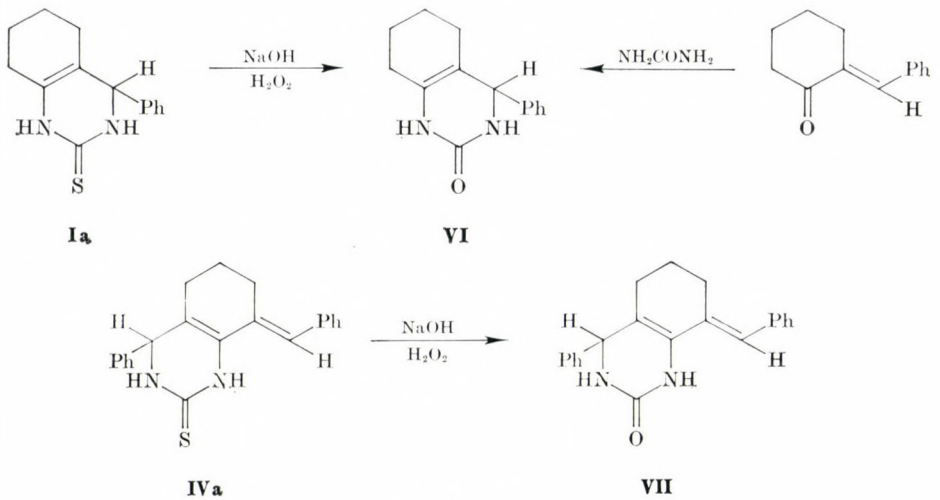

Fig. 8

Assignment of the lines in the noise decoupled ^{13}C resonance spectrum recorded at 25.16 MHz (Fig. 6 and Table IV) was carried out on the basis of the off-resonance spectrum (SFORD) with selective proton decoupling $^{13}C\{^{1}H\}$, and also using the natural, undecoupled spectrum. Each carbon atom in the molecule gives rise to a separate resonance line, and this also holds in the presence of two aromatic rings. Assignment of the carbon atoms in *para* and *meta* position was possible on the basis of their coupling of type $^{3}J_{CH}$ (multiplicity) in the undecoupled spectrum. The C=S bond appeared at 174.5 ppm. The signals of the quaternary carbon atoms at the condensation points could also be distinguished in the SFORD spectrum in the group of aromatic carbon atoms; although there was partial overlapping, the multiplicity of the lines gave unambiguous information. A crucial point in the determination of the structure was the signal of the tertiary carbon atom appearing at 59 ppm. Its $^{3}J_{CH}$ coupling (4.3 Hz) was observed with the carbon atom participating in the C=S bond. Similarly, two 'large' coupling effects of the $^{3}J_{CH}$ type were observed on the line assigned to the non-protonated carbon atom denoted by "e", appearing at 114.5 ppm. In view of these facts, the ^{13}CMR spectrum is in agreement with, and supports the structure **IVa** proposed in Fig. 5.

Table IV

Chemical shift, ppm	Assignment		Multiplicity	Intensity
174.5	2	q	s	62
142.8	1″	p	s	46
137.3	1′	o	s	50
129.4	2′, 6′	n	d	83
129.1	4a	m	s	64
128.9	3″, 5″	l	d	84
128.3	3′, 5′	k	d	84
128.0	4″	j	d	39
127.7	8	i	s	60
127.0	2″, 6″	h	d	90
123.0	8α	f	d	30
114.5	8a	e	s	46
59.0	4	d	d	40
26.4	7	c	t	37
26.0	5	b	t	31
21.9	6	a	t	33

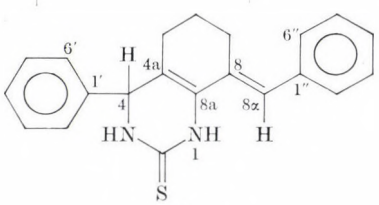

Fig. 9

The mass spectrum of **IVa** (see Experimental) also confirms the suggested structure.

The urea analogues of the cyclic thiourea compounds prepared were supposed to be obtainable by oxidation. The oxidation reaction may also afford evidence for the structures suggested for compounds **Ia** and **IVa**, since 2-thionohexahydroquinazolines are oxidized to 2-oxo-hexahydroquinazolines containing no sulfur, whereas the oxidation of the isomeric 2-imino-1,3-thiazine derivatives ('Y') would yield 2-oxo-1,3-thiazines ('Z').

The oxidation of **Ia** and **IVa** was attempted with various oxidizing agents (CrO_3, MnO_2, HgO, H_2O_2). Of these, only the treatment with alkaline H_2O_2 was effective; the results are in agreement with the observation of other workers [11].

The formation of 4-phenyl-3,4,5,6,7,8-hexahydro-2(1H)-quinazoline (**IV**) (Table II) and 8-benzylidene-4-phenyl-3,4,5,6,7,8-hexahydro-2(1H)-quinazo-

linone (**VII**) (Table II) also confirms the structures **Ia** and **IVa**. Structures of **VI** and **VII** were verified by their IR and PMR spectra; the sharp $\nu C{=}S$ band at about 1200 cm^{-1} was absent and an intense $\nu C{=}O$ band appeared at 1695 cm^{-1} (**VI**) and 1680 cm^{-1} (**VII**). The PMR spectrum of **VI** and **VII** showed the presence of two exchangeable protons (NH). The structure of **VI** was also proved by synthesis: the reaction product obtained from 2-benzylidenecyclohexanone and urea was identical with **VI**.

Experimental

The majority of the IR spectra was recorded with a Zeiss UR-10 spectrophotometer; the PMR spectra were obtained with a Perkin-Elmer R-12 spectrometer. Some of the PMR spectra and the ^{13}C measurements were taken with a Varian XL-100-15 FT instrument. The UV spectra were recorded with a Perkin-Elmer 402 spectrophotometer. The mass spectrum of **IVa** was obtained with an MS 902 mass spectrometer.

The 2-arylidenecycloalkanones were prepared by aldol condensation catalyzed by sodium hydroxide [12]. All the starting ketones were the *trans* isomers [13].

4-Phenyl-3,4,5,6,7,8-hexahydro-2(1H)-quinazolinethione (Ia)

(A) Reaction with ammonium thiocyanate

2-Benzylidenecyclohexanone (9.3 g; 0.05 mole) was dissolved in a mixture of benzene (40 ml) and cyclohexanol (4 ml). Ammonium thiocyanate (4.57 g; 0.06 mole) was added to the reaction mixture and it was refluxed for 8 hrs, using a water separator. The reaction mixture was then cooled, the white precipitate was filtered off, rinsed with benzene and washed with water until free from ammonium thiocyanate. The product was recrystallized from methanol.

Compounds **Ib**, **a**, **d**, **e**, were prepared in a similar way. **If** could not be obtained with ammonium thiocyanate, since the ketone decomposed during the long reaction time.

(B) Reaction with thiourea

Metallic sodium (1 g; 0.04 g-atom) was dissolved in anhydrous ethanol (50 ml). A solution of 2-benzylidenecyclohexanone (3.72 g; 0.02 mole) in anhydrous ethanol (50 ml) and thiourea (2.28 g; 0.03 mole) were added to it. The reaction mixture was refluxed for one and a half hours. The hot solution was then poured into water and acidified with conc. hydrochloric acid. The yellow precipitate was allowed to stand for a short time, then filtered off and the excess reagent was removed. **Ib**, **c**, **d** were crystallized from methanol, and **Ie**, **f** from ethanol. **Ia**—**f**: colourless crystals.

Other data are given in Table I.

Reaction of 2-arylidenecyclopentanones with ammonium thiocyanate

N,N'-bis[(2-Benzylidene)-cyclopentylidene]-thiourea (IIa) and 7H-4-phenyl-3,4,5,6-tetrahydro-2(1H)-cyclopentapyrimidinethione (IIIa)

In the preparation of **IIa** and **IIIa** the reaction conditions were the same as for **Ia** using ammonium thiocyanate. The yellow crystalline substance which separated was shown to be a mixture of **IIa** and **IIIa**. Compound **IIIa** could be extracted from the mixture with hot benzene, and **IIa**, insoluble in benzene, was crystallized from glacial acetic acid. In the reaction of 2-(4'-methoxybenzylidene) cyclopentanone no **IIIb** was obtained; the product was **IIb** with orange yellow colour, crystallized from a mixture of ethyl acetate and methanol.

Reaction of 2-arylidenecyclopentanones with thiourea

7H-4-Phenyl-3,4,5,6-tetrahydro-2(1H)-cyclopentapyrimidinethione (IIIa) and 7H-H-(4'-methoxyphenyl)-3,4,5,6-tetrahydro-2(1H)-cyclopentapyrimidinethione (IIIb)

These two compounds were prepared in a manner similar to the synthesis of **Ia**. Compounds **IIIa, b** were colourless substances; they were crystallized from benzene.

Other data regarding **IIa, b** and **IIIa, b** are shown in Table II.

Reaction of 2,6-diarylidenecyclohexanones with thiourea

The reaction of 2,6-dibenzylidenecyclohexanone and thiourea is presented as a characteristic example.

4-Phenyl-8-benzylidene-3,4,5,6,7,8-hexahydro-2(1H)-quinazolinethione (IVa)

Metallic sodium (1.40 g; 0.06 g-atom) was dissolved in anhydrous ethanol (100 ml). A suspension consisting of 2,6-dibenzylidenecyclohexanone (5.48 g; 0.02 mole) and thiourea (3.80 g; 0.06 mole) in anhydrous ethanol (100 ml) was added, and the reaction mixture was refluxed for 1.5 hr. During this time the starting material dissolved. The hot solution was poured into water and acidified with conc. acetic acid. After a short standing the precipitate was filtered off and washed with water until neutral. The product was crystallized from ethanol or from a mixture of ethanol and ethyl acetate.

IVa, b, c, d were colourless crystals. **IVe** and **IVf** are yellow and red crystalline substances, respectively.

In the mass spectrum of the product the following main lines appear: $m/e = 332$(M) 100%; $m/e = 304$ (M — 28) 11%; $m/e = 272$ (M—60) 4%; $m/e = 255$ (M—77) 78%.

Reaction of 2,5-dibenzylidenecyclopentanone with thiourea

7H-7-Benzylidene-4-phenyl-3,4,5,6-tetrahydro-2(1H)-cyclopentapyrimidinethione (V)

Metallic sodium (0.7 g; 0.03 g-atom) was dissolved in anhydrous ethanol (50 ml). A suspension of 2,5-dibenzylidenecyclopentanone (5.20 g; 0.02 mole) and thiourea (3.80 g; 0.05 mole) in anhydrous ethanol (50 ml) was added, and the reaction mixture was refluxed for 1.5 hr. A homogeneous solution was obtained. It was cooled, the crystals which separated were filtered off, washed with cold ethanol, and then with water until neutral, and recrystallized from a mixture of ethanol and ethyl acetate. The mother liquor was poured into water. An orange-yellow precipitate was obtained which was filtered off after a short period of standing, and washed until neutral. The substance obtained after crystallization was identical with the product from the first stage of the procedure.

V was a colourless crystalline substance.

Other data for **IVa, b, c, d, e, f** and **V** are shown in Table III.

Reaction of 4-phenyl-3,4,5,6,7,8-hexahydro-2(1H)-quinazolinethione (Ia) and 4-phenyl-8-benzylidene-3,4,5,6,7,8-hexahydro-2(1H)-quinazolinethione (IVa) with H_2O_2

4-Phenyl-3,4,5,6,7,8-hexahydro-2(1H)-quinazolinone (VI) and 8-benzylidene-4-phenyl-3,4,5,6,7,8-hexahydro-2(1H)-quinazolinone (VII)

Ia (1.06 g; 0.0044 mole) was dissolved in hot 0.5*N* methanolic solution of NaOH (100 ml) and 30% H_2O_2 (3 ml; 0,025 mole) was added dropwise while boiling the solution. The reaction mixture was refluxed for 1 hr. then poured into water while hot. It was allowed to stand for a short time; the white precipitate was then filtered off and washed with water until neutral. The product was crystallized from a mixture of ethanol and water to obtain **VI** as a colourless crystalline substance. The preparation of 8-benzylidene-4-phenyl-3,4,5,6,7,8-hexahydro-2(1H)-quinazolinone (**VII**) was effected in a similar manner. **VII** was a colourless crystalline substance, crystallized from ethanol.

Preparation of 4-phenyl-3,4,5,6,7,8-hexahydro-2(1H)-quinazolinone (VI) by the reaction of 2-benzylidenecyclohexanone and urea

A solution of 2-benzylidenecyclohexanone (3.72 g; 0.02 mole) and urea (4.80 g; 0.08 mole) in dimethyl sulfoxide (20 ml) was refluxed on a water bath for 1 hr. The hot solution was poured into water. A yellow precipitate separated which was allowed to stand for 1 hr, then filtered off, washed with water and recrystallized from a mixture of water and ethanol. The product was in all respects identical with that obtained in the oxidation reaction.

Other data for **VI** and **VII** are shown in Table II.

*

The authors' thanks are due to Dr. J. TAMÁS for the mass spectra, to Mr. L. SZALAI for the PMR spectra, to Dr. R. OHMACHT for the IR spectra and the analyses, to Dr. P. MOLNÁR for the UV spectra and to Mrs. L. ZUBOR and Miss Cs. SZEGVÁRI for their technical assistance.

REFERENCES

[1] SZÁNTAY, Cs.: Elméleti szerves kémia, p. 272. Műszaki Kiadó, Budapest 1971
[2] ZIMMERMANN, R.: Angew. Chem. **75,** 1025 (1963)
[3] CHASE, B. H., WALKER, J.: J. Chem. Soc., **1955,** 4443
[4] ZIGEUNER, G., ADAM, W., WEICHSEL, H.: Monath. Chem. **97,** 55 (1966)
[5] ZIGEUNER, G., BAYER, M., PALTAUF, F., FUCHS, E.: Monath. Chem. **98,** 23 (1967)
[6] SAMMOUR, A., SELIM, M. I. B., EL-DEEN, N., ABD-EL-HALIM, M.: J. Chem. U.A.R. **13,** 7 (1970)
[7] HOLLY, S., SOHÁR, P.: Infravörös spektroszkópia, p. 83, Műszaki Könyvkiadó, Budapest 1968
[8] BELLAMY, L. J.: The Infrared Spectra of Complex Molecules, 2nd ed. pp. 147—8. Methuen et Co. Ltd., Wiley & Sons Inc., London, New York 1966
[9] WENDELIN, W., HARLER, H.: Monath. Chem. **105,** 563 (1974)
[10] OSZBACH, GY., SZABÓ, D.: Acta Chim. (Budapest) **86,** 449 (1975)
[11] ZIGEUNER, G., FUCHS, E., BRUNETTI, H., STERK, H.: Monath. Chem. **97,** 36 (1966)
[12] NIELSEN, A. T., HOULIHAN, W. J.: The Aldol Condensation in Org. Reactions, Vol. 16. Wiley & Sons Inc., New York, London, Sidney 1968
[13] GEORGE, A., ROTH, H. J.: Tetrahedron Letters, **1971,** 4057

Tamás LÓRÁND, Dezső SZABÓ — H-7643 Pécs, Szigeti út 12
András NESZMÉLYI — H-1525 Budapest, Pusztaszeri út 57—69

Acta Chimica Academiae Scientiarum Hungaricae, Tomus 93 (1), pp. 67—75 (1977)

SULFENYLCHLORIDE, X

SULFENYLIERUNG EINIGER THIOAMIDE MIT TRICHLORMETHAN-SULFENYLCHLORID

G. STÁJER*, D. KORBONITS**, A. E. SZABÓ*, F. KLIVÉNYI* und E. VINKLER*

*(*Pharmazeutisch-Chemisches Institut der Medizinischen Universität, Szeged; **Fabrik Chemisch-Pharmazeutischer Produkte »Chinoin« AG, Budapest)*

Eingegangen am 5. September, 1975

1,3,4-Oxa- und Thiadiazol-5-thione sowie das Dinatrium-äthylenbisdithiokarbamat liefern mit Trichlormethansulfenylchlorid — im Gegensatz zu den Literaturangaben — Disulfide. Die zweifache Sulfenylierung von Alkyl- und Aryldithiokarbamaten ergibt neuartige Bisdithio-iminomethan-Derivate.

Nach unseren früheren Untersuchungen erfolgt der elektrophile Angriff des *p*-Toluolsulfenylchlorides (**1**) bei verschiedenen die *NH*—C=S-Gruppe enthaltenden ambidenten Nukleophilen an dem gut polarisierbaren Schwe-

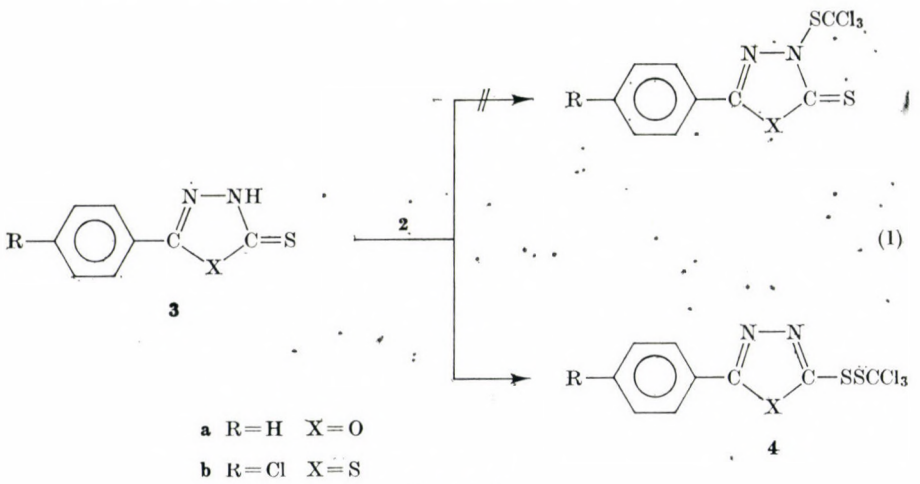

Formel 1

felatom und stets enstehen Disulfide. Im Gegensatz hierzu berichten METIVIER und BOESCH bei der Sulfenylierung von 1,3,4-Oxa- und Thiadiazol-5-thionen (z. B. **3a**, **b**) mit Trichlormethansulfenylchlorid (**2**) über die Bildung von Sulfenamid-Derivaten [1]. Es fragt sich, ob die Sulfenylierung ein und desselben Substrats überhaupt einmal eine *S*—*S*- und ein anderes Mal eine *N*—*S*-Bindung enthaltende Verbindung entstehen lassen kann. Um die Struktur

* IX. Mitteil.: G. STÁJER *et al.*, Chem. Ber, **107**, 299 (1974).

der nach den französischen Autoren hergestellten Sulfenamide mit der Struktur unserer Disulfide [2] vergleichen zu können, haben wir die Verbindungen **3a, b** mit **2** sulfenyliert und die gewonnenen Produkte **4a, b** IR-Untersuchungen unterzogen. Im Spektrum von **4a, b** treten die für den aromatischen Oxadiazolring charakteristischen Banden bei höheren Frequenzen auf als die Thioamid-Banden der Ausgangsverbindungen **3a, b** und dies deutet darauf hin, daß der Doppelbindungscharakter der sulfenylierten Verbindungen erhöht ist, d.h. auch die Verbindungen **4a, b** keine Sulfenamide, sondern Disulfide sind. Die Struktur **4** ist weiterhin dadurch bestätigt, daß die analogen Banden des Heteroringes von **4a** auch im Spektrum des 2-Äthylthio-5-phenyl-1,3,4-oxa-

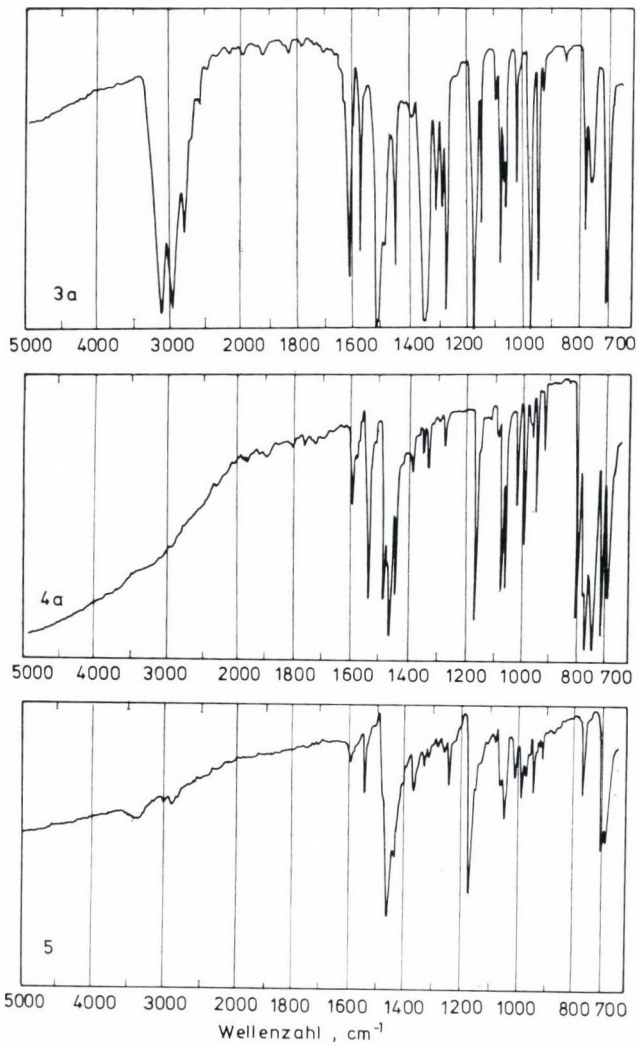

Abb. 1

Tabelle I

Wichtigere IR-Daten der untersuchten Verbindungen in KBr (cm^{-1})

Verbindung	ν NH	ν NH—C=S-Banden	ν N=C—S-Banden	νC—Cl	$\gamma C_{Ar}H$ $\gamma C_{Ar}C_{Ar}$
2	—	—	—	780 760 740	—
3a	3300—2600	1510 1340	—	—	700
4a	—	—	1540△ 1460	780 760 740	710 690
3b	3250—2600	1480 1270	—	—	810
4b	—	—	1500△ 1440	780 760 740	810
5	—	—	1540△ 1450	—	700 680
7	3150	1495 (1290)	—	790 770 740	—
10	—	—	1610 1350	790 760 740	—
11a	3280	1500 1360	—	790 750	710
12a	—	—	1600□	790 780—710	710 690
11b	3300	1540 1410	—	790 760 740	830
12b	—	—	1615□	790 760 740	840
11c	3280	1480 1370	—	790 760 740	830
12c	—	—	1610□	790 760 740	830

△ aromatische Oxadiazol-, bzw. Thiadiazolbanden
□ $\nu C{=}N + \nu C_{Ar}C_{Ar}$ gekoppelt

diazols (**5**) [3] erscheinen und daß die νC—Cl Banden zu finden sind (Formel 1, Tab. I, Abb. 1.).

Einer anderen Literaturangabe nach hat KLOPPING durch mehrfache Sulfenylierung des Bisdithiokarbamats **6** die Derivate **7**, **8** und **9** hergestellt [4] (Formel 2).

Es muß jedoch erwähnt werden, daß die Struktur der Verbindungen **8** und **9** nicht erwiesen ist, da der Autor für diese zersetzlichen Derivate — abweichend von Verbindung **7** — keine spektralen Daten angibt. Bei der Wiederholung der Versuche von KLOPPING ist es uns nicht gelungen, die *N*-sulfenylierten Derivate **8** und **9** herzustellen, während wir aus dem Disulfid **7** in wasserfreiem Äther ein vierfach *S*-sulfenyliertes Produkt, das neuartige Iminomethan **10** erhielten, dessen Schmelzpunkt sich von dem der vom Autor angegebenen Sulfenamide **8** und **9** unterscheidet.

Für die Struktur **10** spricht, daß im IR-Spektrum der Verbindung νC=N Banden erscheinen (Tab. I, Abb. 2). Die für die *NH*-Gruppen charakteristischen Banden erscheinen dagegen nicht und auch im PMR-Spektrum ist lediglich ein einziges, den Methylenprotonen entsprechendes Signal assignierbar. Die Verbindung ist zersetzlich, bei Raumtemperatur ist sie nur einige Stunden lang stabil. Im IR-Spektrum des 24-stündigen Präparates erscheinen intensive, der —*N*=*C*=*S*-Gruppe zuzuordnende Banden, und dies weist darauf hin, daß die Verbindung **10** während des Stehens zu Isothiocyanat zerfällt.

Aus Aryldithiokarbamaten entstehen mit **2** die Trithioperkarbamate vom Typ **11**, die in Gegenwart von *tert.*-Amin zu den mit der Verbindung **10**

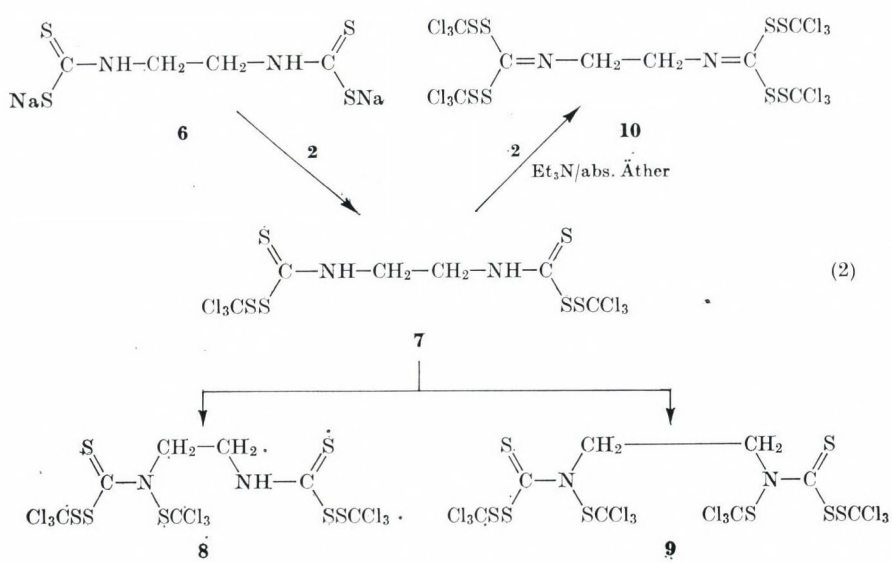

(2)

Formel 2

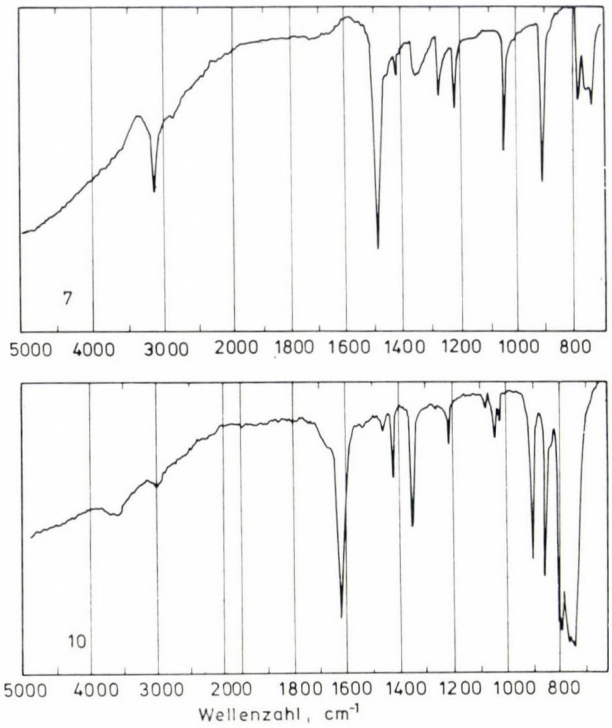

Abb. 2

verwandten Bisdithio-iminomethan-Derivaten **12** weitersulfenyliert werden; ihre Struktur haben wir ebenfalls mit IR-Untersuchungen erwiesen (Formel 3). Im Spektrum von **12a** erscheinen die gekoppelten $\nu C{=}N + \nu C_{Ar}C_{Ar}$ Banden im Vergleich zu **11a** bei höheren Frequenzen und dies deutet auf die Struktur **12** hin. Die größere Intensität zeigt gleichzeitig die Konjugation des aromatischen Ringes mit der C=N Bindung an, was ein weiterer Beweis dieser Struktur ist (Tab. I, Abb. 3).

Es sei bemerkt, daß die Verbindungen **12a**, **b**, **c** bei Raumtemperatur etwa 30 Tage stabil bleiben, also weitaus haltbarer sind als das Alkylderivat **10**.

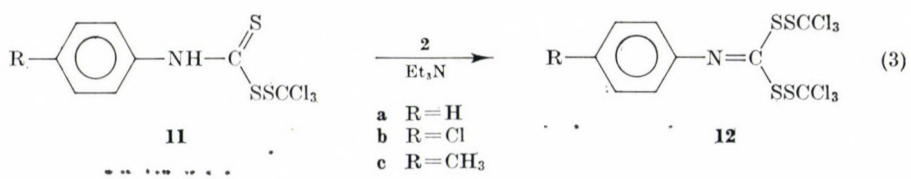

Formel 3

Früher hatten wir gefunden, daß die *p*-Toluolsulfenylierung von Ammonium-dithiokarbanylidaten zu Trithioverbindungen führt [5]. Die Verbindung **13** hingegen liefert — unter ähnlichen Bedingungen wie oben — unter Weiterreagieren mit **1** nicht das mit den Verbindungen **10** und **12** verwandte Bisdithio-Derivat, sondern *p*-Tolyltrisulfid (**15**) und Phenylisothiocyanat (**16**) (Formel 4).

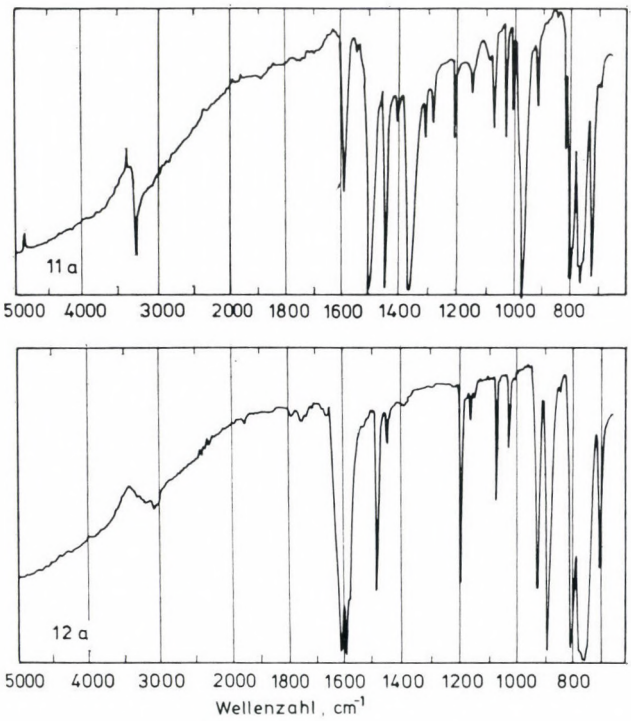

Abb. 3

Das von den vorhergehenden abweichende Ergebnis der Arylsulfenylierung läßt sich auf folgende Weise erklären: bei der Weitersulfenylierung von **13** ist die Entstehung des instabilen Produktes **14** anzunehmen. Aus diesem Zwischenprodukt wird das 'good leaving group' Molekül **15** abgespalten und das zurückbleibende protonierte Isothiocyanat wird unter Deprotonierung als **16** stabil.

Zum Studium dieser Erscheinung haben wir — mit Variation der Sulfenylchloride **1** und **2** — auch eine weitere 'gemischte' Sulfenylierung der Trithiokarbamate **11a** und **13** versucht. Während von **11a** und **1** das Ausgangsmaterial zurückgewonnen werden kann, lieferte die Reaktion des Trithioderivates

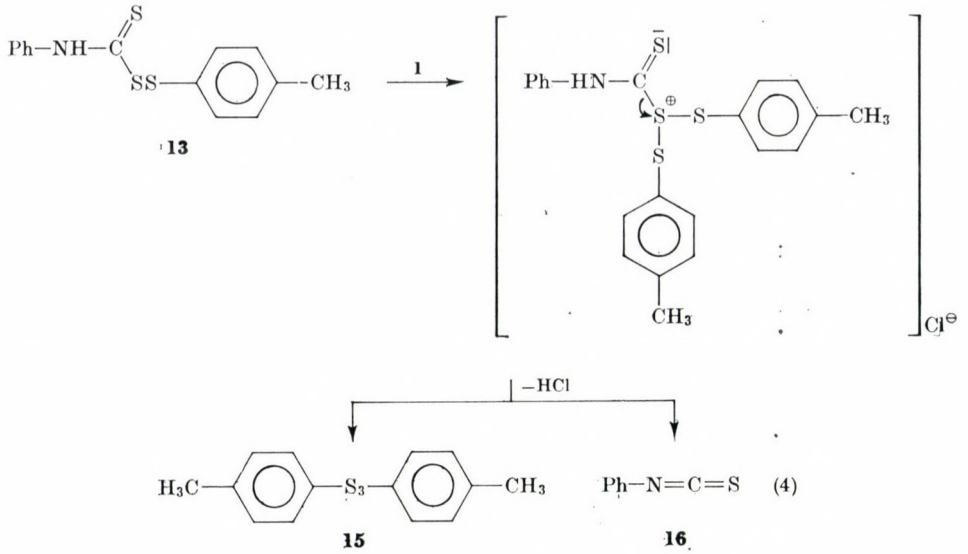

Formel 4

13 mit **2** das Hauptprodukt **12a**. Daneben sind auch **11a** und **13** im Reaktionsgemisch vorhanden. Die trichlormethan-sulfenylierte Verbindung kann also weiter alkylsulfenyliert, nicht aber arylsulfenyliert werden. Die monoarylsulfenylierte Verbindung **13** kann auch alkylsulfenyliert werden, aber so, daß ein Arylsulfenium-Ion aus dem entstandenen gemischten Disulfenyl-Derivat abgespaltet wird, wobei die Monoalkylsulfenyl-Verbindung **11a** entsteht. Diese ist entweder das Endprodukt oder sie nimmt noch eine Trichlormethansulfenyl-Gruppe auf und wird in **12** umgewandelt.

Mikrobiologische Untersuchungen haben gezeigt, daß die Derivate **11a** und **12a** auf Mikroben in einer Größenordnung wie daß *p*-Tolylderivat **13** wirken [6]. Die Trichlormethyl-Derivate hemmen von den neun Microorganismen: Bac. cereus var. mycoides, Staphylococcus aureus, Escherichia coli, Serratia marcescens, Saccharomyces cerevisiae, Candida albicans, Aspergillus niger, Syncephalastrum racemosum und Sarcia lutea nur das Wachstum des Hefepilzes Saccharomyces cerevisiae R_{12}, und zwar **11a** in 3 μg/ml und **12a** in 25 μg/ml Konzentration.

Experimenteller Teil

(Die Schmelzpunkte sind nicht korrigiert.)

Die IR-Spektren wurden in KBr-Pastillen bzw. in $CHCl_3$ mit den Geräten Spektromom 2000 bzw. Unicam SP 200, die PMR-Spektren mit dem Spektrometer JEOL HL-60 in $CDCl_3$, unter Verwendung von TMS als innerer Standard aufgenommen.

1. Herstellung der Verbindung 10: 5,11 g (0,01 Mol) **7** [4, 7] und 2 g (0,02 Mol) Triäthylamin wurden in 100 ml wasserfreiem Äther unter Kühlen und Rühren mit 3,7 g (0.02 Mol) **2** zur Reaktion gebracht, das Reaktionsgemisch wurde mit Wasser gewaschen, mit Na_2SO_4 getrocknet und der Äther verdunsten gelassen. Der ölige Rückstand wurde in trockenem Benzol gelöst, mit 3 Vol. Petroläther im Kühlschrank aufbewahrt, wobei nach 24 Stunden Kristallisierung erfolgte. Weiße, lockere Nadeln, Ausbeute 2,20 g (27%), Schmp.: 88—90 °C.

Analyse: $C_8H_4N_2Cl_{12}S_8 = 810{,}07$

Ber.: C 11,86 H 0,50 N 3,46 S 31,67%

Gef.: C 11,60 H 0,81 N 3,69 S 31,50%

PMR: δ CH_2(4H) = 4,18 ppm (*s*)

2. Sulfenylierung von Ammonium-N-Aryldithiokarbamaten (allgemeine Vorschrift): 0,02 Mol Ammonium-*N*-aryldithiokarbamat [8] werden in 100 ml wasserfreiem Äther mit 3,7 g (0,02 Mol) **2** zur Reaktion gebracht, das Reaktionsgemisch wird mit Wasser gewaschen, dann der Äther mit Na_2SO_4 getrocknet und im Vakuum bei Raumtemperatur verdampft.

2.1. Herstellung von S-Trichlormethyl-N-phenyltrithioperkarbamat (11a): 3,7 g Ammonium-dithiokarbanylidat wird nach 2. sulfenyliert und das gewonnene Produkt aus Benzol–Äthanol (1 : 1) kristallisiert. Gelbe Nadeln, Schmp. 101—102 °C. Ausbeute: 3,30 g (52%).

Analyse: $C_3H_6NCl_3S_3 = 318{,}69$
Ber.: C 30,15 H 1,90 N 4,40%
Gef.: C 30,40 H 1,94 N 4,22%

2.2. Herstellung von S-Trichlormethyl-N-p-chlorphenyl-trithioperkarbamat (11b): 4,4 g Ammonium-*N*-(*p*-chlorphenyl)-dithiokarbamat werden nach 2. sulfenyliert, mit der Abweichung, daß das Reaktionsgemisch nach Filtration — ohne Waschen — verarbeitet wird. Der Rückstand wird in Benzol kalt gelöst und nach Zugabe des gleichen Volumens Petroläther im Kühlschrank stehen gelassen. Gelbe Nadeln, Schmp. 71—72 °C. Ausbeute: 2,10 g (30%).

Analyse: $C_8H_5NCl_4S_3 = 353{,}1$
Ber.: C 27,21 H 1,43 N 3,97%
Gef.: C 27,07 H 1,60 N 3,70%

PMR: δ(NH) = 9,68 ppm, δArH (4H) = 7,62 ppm (Zentrum des AA'BB'-Multipletts)

2.3. Herstellung von S-Trichlormethyl-N-(p-tolyl)-trithioperkarbamat (11c): 4 g Ammonium-*N*-(*p*-tolyl)-dithiokarbamat werden nach 2.2. sulfenyliert und aufgearbeitet. Gelbe Prismen. Schmp. 60—61 °C, Ausbeute: 3,1 g (47%)

Analyse: $C_9H_8NCl_3S_3 = 332{,}72$
Ber.: C 32,49 H 2,42 N 4,21%
Gef.: C 32,20 H 2,50 N 4,01%

3. Herstellung von 12a,b,c (allgemeine Vorschrift): Zu 0,02 Mol Ammonium-Aryldithiokarbamat und 2 g Triäthylamin in 100 ml trockenem Äther werden unter Kühlung und Rühren 7,4 g (0,04 Mol) **2** zugetropft; das Reaktionsgemisch wird filtriert und der Äther bei Raumtemperatur unter verminderten Druck abgedampft.

3.1. Herstellung von Bis(Trichlormethyldithio)-N-Phenyliminomethan (12a): 3,8 g Ammoniumdithiokarbanylidat werden nach 3.) sulfenyliert und aufgearbeitet. Nach Versetzen des Rückstandes mit 10 ml Petroläther scheiden sich im Kühlschrank farblose Prismen aus. Schmp. 87—89 °C [aus Benzol–Äther (1 : 1)], Ausbeute: 3,60 g (38%).

Analyse: $C_9H_5NCl_6S_4 = 468{,}12$
Ber.: C 23,09 H 1,08 N 2,99%
Gef.: C 23,29 H 1,28 N 2,93%

3.2. Herstellung von Bis(Trichlormethyldithio)-N-(p-chlorphenyl)-iminomethan (12b): 4,4 g Ammonium-*N*-(*p*-chlorphenyl)-dithiokarbamat werden nach 3. sulfenyliert, das Reaktionsprodukt wird in Benzol kalt gelöst, auf eine Kieselgel-Säule aufgetragen und mit Petroläther eluiert. Nach Verdampfen des Lösungsmittels bei Raumtemperatur werden die Mittelfraktionen vereinigt und in Benzol kalt gelöst. Nach Versetzen der Lösung mit dem gleichen Volumen Petroläther scheiden sich beim Stehen im Kühlschrank blaßgelbe Kristalle aus. Schmp. 89—90 °C.

Analyse: $C_9H_4NCl_7S_4 = 502{,}55$
Ber.: C 21,51 H 0,80 N 2,79%
Gef.: C 21,34 H 1,15 N 2,90%

PMR: δArH (4H) = 7,10 ppm (Zentrum des AA'BB'-Multipletts)

3.3. Herstellung von Bis(Trichlormethyldithio)-N-(p-tolyl)-iminomethan (12c): 4 g Ammonium-*N*-(*p*-tolyl)-dithiokarbamat werden nach 3.2. sulfenyliert, der Rückstand des Petrolätherextrakts wird in Benzol gelöst und nach Zugabe von 2 Vol. Petroläther im Kühlschrank stehen gelassen. Blaßgelbe Nadeln, Schmp. 70—71 °C.

Analyse: $C_{10}H_7NCl_6S_4 = 482{,}14$
Ber.: C 24,91 H 1,46 N 2,91%
Gef.: C 24,75 H 1,67 N 3,12%

4. p-Toluolsulfenylierung des S-(p-Tolyl)-N-phenyltrithioperkarbamats (13): Zu 100 ml Ätherlösung von 5,8 g (0,02 Mol) **13** [5] und 2 g Triäthylamin werden unter Kühlen 3,20 g (0,02 Mol) **1** gegeben, das Reaktionsgemisch wird filtriert, mit Wasser gewaschen, mit Na_2SO_4 getrocknet und der Äther dann verdampfen gelassen. Der Rückstand wird in zwei Teile geteilt. Der eine Teil liefert — nach Wasserdampfdestillation — 1,10 g (81%) rohes **16**, das nach dem Trocknen mittels Destillation gereinigt und dann IR-spektroskopisch sowie aufgrund des Brechungsindexes identifiziert wird. Der zweite Teil wird auf eine Kieselgel-Säule aufgetragen, zuerst mit Petroläther und nachher mit Benzol eluiert. Nach Abdampfen des Lösungsmittels

werden der Rückstand des Endes der Petrolätherfraktionen und jener der ersten Benzolfraktionen vereinigt und dabei 1,7 g (61%) farblose Kristalle gewonnen. Nach Umkristallisieren aus Benzol–Petroläther (1 : 2) Schmp. 81—82 °C; mit autentischer Substanz [9] wird aufgrund IR und des Mischschmelzpunktes als **15** identifiziert.

5. p-Toluolsulfenylierung von 11a: 3,2 g (0,01 Mol) **11a** und 1,60 g (0,01 Mol) **1** werden in 30 ml trockenem Äther bei Raumtemperatur eine Stunde lang stehen gelassen. Nach Abdampfen des Äthers bei Raumtemperatur werden aus dem Rückstand 2,6 g **11a** zurückgewonnen. Nach Wiederholung der Sulfenylierung in Gegenwart von 1 g Triäthylamin wird aus dem Filtrat des Reaktionsgemisches 1 g **11a** erhalten.

6. Trichlormethansulfenylierung von 13: Zu der Lösung von 2,90 g (0,01 Mol) **13**, 1 g Triäthylamin und 50 ml Äther wird unter Kühlen 1,9 g (0,01 Mol) **2** zugetropft, aus dem Filtrat des Reaktionsgemisches der Äther bei Raumtemperatur verdampft, der Rückstand dann auf eine Kieselgel-Säule aufgegeben und zuerst mit Petroläther und dann mit Benzol eluiert. Nach Vereinigung der entsprechenden Fraktionen der Benzol-Eluate resultieren 1,5 g **12a**, das aus Benzol—Petroläther (1 : 1) umkristallisiert wird. Schmp. 87—89 °C.

Mit DC können im Reaktionsgemisch gleichzeitig auch **13** und **11a** identifiziert werden. — Adsorbent: Kieselgel G (Merck); Laufmittel: Benzol–Petroläther–Äthanol (5 + 90 + 5) bzw. Benzol–Petroläther–Cyclohexan (3 + 47 + 50). Detektion mit Na_2CO_3-alkalischem 1%igem $KMnO_4$.

LITERATUR

[1] Metivier, J., Boesch, R.: Fr. P. 1 337, 286 (1963); Brit. P. 988, 974; Fr. Addn. 82, 869; Fr. Addn. 84 014; ref. C. A. **62**, 7769e (1965)
[2] Klivényi, F., Stájer, G., Szabó, A. E., Pintye, J., Vinkler, E.: Acta Chim. (Budapest) **73**, 73 (1972)
[3] Hoggarth, E.: J. chem. Soc. (London) **1952**, 4814
[4] Klopping, H. L.: J. Org. Chem. **26**, 1146 (1961)
[5] Klivényi, F., Stájer, G., Szabó, A. E., Pintye, J.: Acta Chim. (Budapest) **73**, 63 (1972)
[6] Ferenczy, L., Kevei, F., Stájer, G., Klivényi, F., Pintye, J., Szabó, A. E.: Acta Pharm. Hung. **45**, 177 (1975)
[7] Klopping, H. L., Kerk, G. J.: Rec. Trav. Chim. Pays-Bas. **70**, 949 (1951)
[8] Heller, G., Bauer, W.: J. prakt. Chem. **65**, 369 (1902)
[9] Holmberg, B.: Ber. **43**, 226 (1910)

Géza Stájer
A. E. Szabó
Ferenc Klivényi
Elemér Vinkler
H-6701 Szeged, Pf. 121

Dezső Korbonits H-1325 Budapest, Újpest 1. Pf. 110

Acta Chimica Academiae Scientiarum Hungaricae, Tomus 93 (1), pp. 77—83 (1977)

ACYLATION REACTIONS OF DIETHYL IMINOCARBONATE, I

ACYLATION BY MEANS OF MONOFUNCTIONAL ACID CHLORIDES AND CHLOROFORMATES

Z. BENDE, I. BITTER and Z. CSŰRÖS

(Department of Organic Chemical Technology, Technical University, Budapest)

Received February 14, 1974; in revised form April 1, 1976

The reactions of diethyl iminocarbonate with carboxylic acid chlorides as well as chloroformates give the N-acyl derivatives of the starting material as the main products; the by-product of the acylation with chloroformate is ethyl carbamate, whereas with acid chlorides ethyl carbamate and ethyl N-acylcarbamate derivatives are also formed. In accordance with the suggested mechanism of the acylation it has been shown that when a tertiary amine for trapping the acid formed in the course of the reaction is also used, the only products of the acylations are new diethyl N-acyliminocarbonate derivatives.

Only a few of the publications dealing with the N-acylation of azomethines refer to acylation reactions of iminocarbonic acid esters offering a number of possible reactions (substitution, addition, isomerization, elimination).

FUJISAWA *et al.* [1] reported the acylation of diethyl N-phenyliminocarbonate with benzoyl chloride. In the course of the reaction ethyl N-phenyl-N-benzoylcarbamate and ethyl chloride, as by-product, were obtained; the reaction was described as an electrophilic addition followed by elimination of ethyl chloride.

It was to be expected that in the reactions of diethyl iminocarbonate containing a non-substituted imino group, acylating agents will give rise mostly to electrophilic substitution reactions, resulting in the formation of new N-acyl derivatives of the iminocarbonic ester. The acylating agents used were monofunctional carboxylic acid chlorides (acetyl chloride and benzoyl chloride) and methyl-, ethyl- or isopropyl chloroformates. The reaction with each acylating agent was examined in the presence and absence of triethylamine acting as an agent trapping the hydrochloric acid formed in the course of the reaction.

In every reaction (*c*) where triethylamine was used, exclusively the appropriate diethyl N-acyliminocarbonate derive (**II**) was obtained, in almost quantitative yield.

These products, except for the N-bezoyl derivative, are new compounds. In the acylation reactions (*a*) using acid chlorides, the product (**II**) was accompanied by ethyl N-acylcarbamate (**III**), ethyl carbamate (**IV**) and ethyl chloride (**V**); in the reactions with chloroformates (*b*) the by-products were compounds **IV** and **V**.

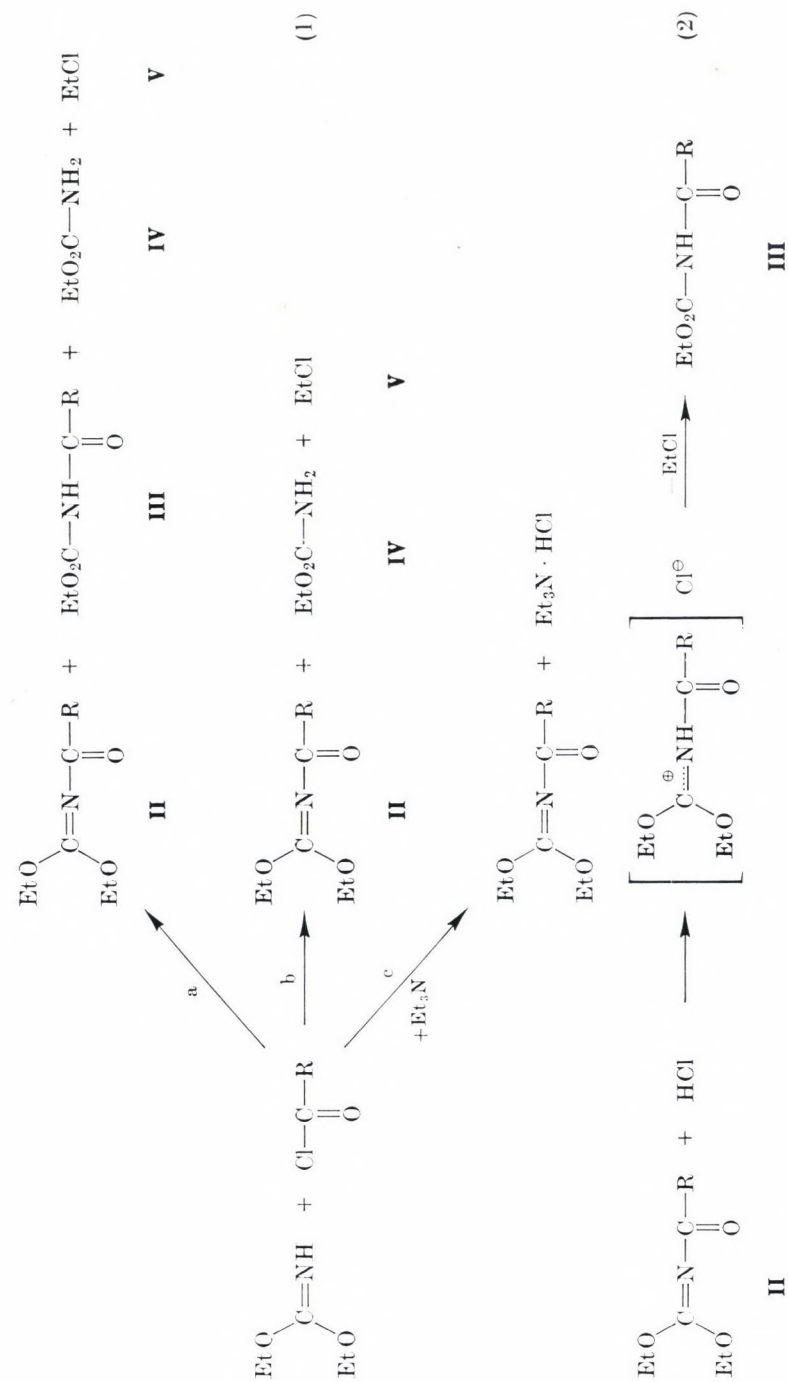

Investigation of the acylation reactions has established the following facts.

(1) The reactions in the presence of triethylamine took place below 10 °C to give product **II** in quantitative yield, and the result did not depend on the condition whether the triethylamine or the acylating agent was added first to the reaction mixture.

(2) Of the diethyl N-acyliminocarbonate derivatives prepared in the presence of triethylamine and identified as pure compounds (**II**), the N-acetyl and benzoyl derivatives were converted by hydrochloric acid at 30—45 °C, and the N-carbalkoxy derivatives at 40—55 °C, under anhydrous conditions, to give quantitatively the appropriate ethyl N-acylcarbamate derivatives (**III**).

At the same time, this reaction allowed the preparative identification of the new diethyl N-acyliminocarbonate derivatives (**II**).

(3) The acylations in the absence of triethylamine gave the best yields if the reagents were added at 0—10 °C, and the reaction mixture was heated to 40—50 °C before work-up. The acylations made without triethylamine can be characterized, on the basis of the isolated reaction products and the experiences described above, as shown below.

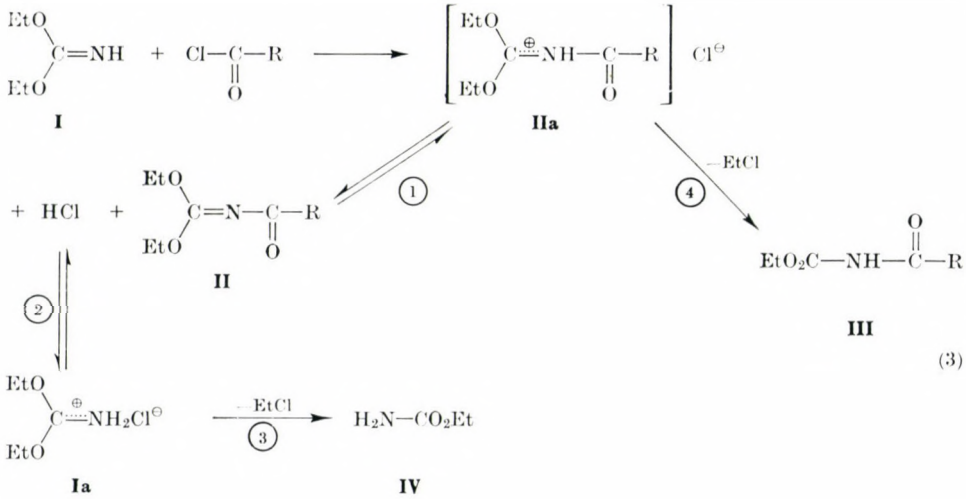

(3)

The part-processes of the reaction can be divided into two groups.

At the temperature of adding the reactants (0—10 °C), when elimination of ethyl chloride does not yet occur, the intermediate **IIa** is formed, which loses hydrogen chloride in an equilibrium reaction (1) to yield the end-product **II**. The released hydrogen chloride is bound by the starting compound **I** in equilibrium reaction (2), affording compound **Ia**. On completion of adding

Table I

R	Acylating agent R—COCl (g)	Product II				Elementary analysis II						
		g	%	b.p. °C/torr	Mol. wt.	Molecular formula	Calcd., %			Found %		
							C	H	N	C	H	N
CH_3	7.8	13.8	87	10 —111/15	159	$C_7H_{13}NO_3$	52.80	8.18	8.82	52.56	8.34	8.96
C_6H_5	14.05	15.5	70	134—4/2	known compound, lit. [3] b.p. 134—135°/2 torr							
CH_3O	9.45	12.4	71	115—8/10	175	$C_7H_{13}NO_4$	48.10	7.43	8.00	47.95	7.51	8.12
C_2H_5O	10.85	15.5	82	120—5/14	189	$C_8H_{15}NO_4$	50.80	7.94	7.42	50.48	8.00	7.52
$(CH_3)_2CHO$	12.25	14.6	72	115—8/8	203	$C_9H_{17}NO_4$	53.25	8.38	6.90	52.60	8.52	7.05

IR (film) [**II**; R=CH_3] : νCH: 2980—2900 (s—m), νC=O : 1720 (vs), νC=N: 1660 (vs), $\delta CH_2/CH_3$: 1480—1360 (s—m) ν_{as} O—C—O: 1307 (vs), ν C—N: 1265 (vs), ν_{as} C—O—C:1070 (vs), ν_s C—O—C: 1020 cm^{-1} (m)
[**II**; R=CH_3O, C_2H_5O, $(CH_3)_2CHO$]: ν C=O: 1735 cm^{-1} (vs), ν C=N: 1675 cm^{-1} (vs) otherwise the same as above

NMR($CDCl_3$) [**II**; R=CH_3]: δ = 4.52 ppm $(CH_2)_q$[4H]; 2.20 ppm $(CH_3)_s$ [3H]; 1.30 ppm $(CH_3)_t$ [6H]
[**II**; R=C_2H_5O]: δ = 4.30 ppm $(CH_2)_q$[6H]; 1.35 ppm $(CH_3)_t$ [9H]

the reagents, the amount of compounds **Ia**, **II** and **IIa** present in the reaction mixture are determined by the equilibria (1) and (2).

In the acylation reactions using acid chlorides, all the three products **II**, **III**, **IV** are obtained in about equal amounts; the rates of eliminations (3) and (4) are commensurable.

In the acylation reactions with chloroformates ethyl N-carbalkoxy-carbamate derivatives (**III**) were not formed. This reaction in the absence of a competing reaction partner — occurs quantitively. The fact that reaction (4) does not take place under the conditions of acylation with chloroformates is due to the facts that the equilibria (1) and (2) are shifted towards the side of **Ia**, and the rate of the elimination reaction (3) is much higher.

Experimental

(1) Acylation in the presence of triethylamine

General procedure. Compound **I*** (11.7 g; 0.1 mole) and triethylamine (10.1 g; 0.1 mole) were dissolved in dry toluene (40 ml) and a solution of the acylating agent (0.1 mole) in dry toluene (20 ml) was added at 0—10 °C. The mixture was then stirred at 15—20 °C for 30 min. The precipitated triethylamine hydrochloride was filtered off and washed with toluene (10 ml). The filtrates were combined and distilled in vacuum. The results of the experiments are summarized in Table I.

(2) The reaction of diethyl N-acyliminocarbonate derivatives (II) with hydrochloric acid

To a solution of diethyl N-acyliminocarbonate (**II**) (0,05 mole) in abs. dioxan (10 ml), a solution of HCl in abs. dioxan (33 ml; 59 mg HCl/ml) was added by drops, with stirring and cooling at 20 °C. After the addition of HCl had been completed, the reaction mixture was stirred (in the case of the N-acetyl and N-benzoyl derivatives for 1.5 hr. at 35 °C, and with N-carbalkoxy derivatives for 2.5 hrs. at 45 °C). The solution was then evaporated in vacuum to dryness, and the residual ethyl N-acylcarbamate derivatives were crystallized.
These reactions are summarized in Table II.

Table II

R	Starting materials		Products **III**				
	II, g	HCl, g	g	%	M.p., °C	lit. m.p., °C	lit. b.p., °C/torr
CH_3	7.95	1.95	5.83	89	76—7[1]	76—8 [4]	205—16/760
C_6H_5	11.05	1.95	8.10	83	109—110[1]	110—11 [5, 8]	—
CH_3O	8.75	1.95	6.47	87	72—3[2]	73 [7]	117—24/10 [7]
C_2H_5O	9.45	1.95	7.40	92	48—50[2]	49—40 [6]	215/715 133/12 [6]

1. from ethanol–water (2 : 1)
2. from petroleum ether–ethanol (3 : 1)

* The diethyliminocarbonate (**I**) was prepared according to SANDMEYER's method [2].

(3) Acylation in the absence of triethylamine

3.1. *Acylation with acetyl chloride*

Compound **I** (11.7 g; 0.1 mole) was dissolved in abs. toluene (40 ml) and a solution of acetyl chloride (7.8 g; 0.1 mole) in abs. toluene (10 ml) was added dropwise at 0—10 °C.

The reaction mixture was stirred at 35—40 °C for 1 hr, then fractionated in vacuum. The fraction boiling between 80 and 120 °C/10 torr was suspended in warm petroleum ether (50 ml); the undissolved solid was filtered off (4.9 g) and recrystallized from 60% aqueous ethanol, to obtain 3.8 g (29%) of ethyl N-acetylcarbamate (**III**; R = CH_3); m.p. 74—75 °C (identical with the product prepared as described in (2)).

The petroleum ethereal filtrate was evaporated in vacuum at 15—20 °C until turbidity appeared, the solution was then cooled to —20 °C, and the crystals which precipitated were filtered off, to obtain 2.05 g (23%) of ethyl carbamate (**IV**), m. p. 48—50 °C.

The filtrate of ethyl carbamate was evaporated and fractionated in vacuum to yield 4.5 g (28%) of diethyl N-acetyliminocarbonate (**II**; R = CH_3), identical with the product obtained in the presence of triethylamine as described in (1.)

3.2. *Acylation with benzoyl chloride*

To a solution of **I** (11.7 g; 0.1 mole) in dry toulene (40 ml) at 10 °C, a solution of benzoyl chloride (14.05 g; 0.1 mole) in abs. toulene (10 ml) was added, and after stirring at 35—45 °C for 2 hrs the reaction mixture was fractionated in vacuum.

The products were 2.9 g (33%) of ethyl carbamate (**IV**), b.p. 95—99 °C/15 torr, and 7.8 g (31%) of diethyl N-benzoyl-iminocarbamate (**II**; R = C_6H_5), identical with the product synthesized as described above (1).

The residue of the distillation was dissolved in ethanol (15 ml), filtered and the third product was precipitated from the filtrate with water and crystallized from a 2 : 1 mixture of water and ethanol. This product was 3.1 g (16%) of ethyl N-benzoylcarbamate (**III**; R = C_6H_5), m.p. 107—109 °C. The product proved to be identical with the compound obtained according to (2).

3.3 *Acylation with chloroformates*

General procedure. Compound **I** (11.7 g; 0.1 mole) was dissolved in abs. toluene (40 ml) and a solution of the chloroformate (0.1 mole) in toulene (10 ml) was added at 10 °C. The reaction mixture was then stirred for 2 hrs at 45—50 °C. The solvent was evaporated in vacuum and the residue was fractionated. The products were ethyl carbamate (**IV**) and the diethyl N-carbalkoxy-minocarbonate derivative (**II**) corresponding to the acylating agent used in the reaction; they were identical with the products prepared as described in (1). The data of the reactions are given in Table III.

Table III

R	RCOCl, g	II		IV	
		g	%	g	%
CH_3O	9.45	6.1	35	3.6	41
C_2H_5O	10.85	7.2	38	3.7	42
$(CH_3)_2CHO$—	12.25	6.1	30	3.2	36

REFERENCES

[1] FUJISAWA, T., NOHIRA, M., MUKAIYAMA, T.: Bull. Chem. Soc. Japan **40,** 337 (1967)
[2] SANDMEYER, T.: Chem. Ber. **19,** 862 (1886)
[3] IVANOVA, Zs. M., KIRSANOVA, N. A., STUKALO, E. A., DERKATCH, G. I.: Zhurn. Org. Him. **3,** (3) 480 (1967)
[4] DIELS, O. P. H.: Chem. Ber. **41,** 2396 (1908)
[5] BILLETER, J.: Chem. Ber. **36,** 3220 (1903)
[6] DIELS, O. P. H.: Chem. Ber. **36,** 743 (1903)
[7] DIELS, O. P. H.: Chem. Ber. **37,** 3673 (1904)
[8] VANINO, L.: Chem. Ber. **28,** 2383 (1895)

Zoltán BENDE
István BITTER
Zoltán CSŰRÖS
H-1111 Budapest Műegyetem rkp. 3.

Acta Chimica Academiae Scientiarum Hungaricae, Tomus 93 (1), pp. 85—93 (1977)

ACYLATION REACTIONS OF DIETHYL IMINOCARBONATE, II

ACYLATION WITH PHOSGENE AND OXALYL CHLORIDE

Z. BENDE, I. BITTER and Z. CSŰRÖS

(Department of Organic Chemical Technology, Technical University, Budapest)

Received April 1, 1976

Investigation of the reaction of diethyliminocarbonate with phosgene or with oxalyl chloride showed that, depending on the conditions, various products: carbethoxy isocyanate, diethoxymethylene or carbethoxy urea, isourea or oxamide derivatives were formed. On the basis of the reaction conditions, the intermediate and final products formed, the mechanism of the reactions has been investigated.

In our first communication [1] the characteristics of the reaction of diethyl-iminocarbonate with monofunctional acylating agents (carbonic acid chlorides, chloroformates) has been discussed. SAMARAI *et al.* [2, 3, 4] studied the acylation of imino esters with phosgene and oxalyl chloride, and established that in the case of both acylation agents the N-chlorocarbonyl derivatives of the starting material were formed, which were converted after isomerization and subsequent alkyl chloride elimination to the respective isocyanates.

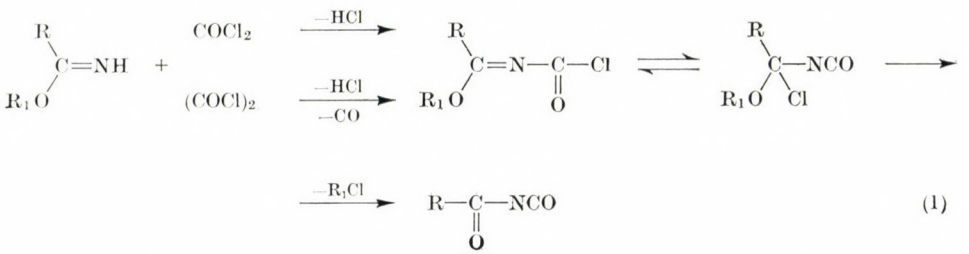

(1)

According to our results, on the acylation of diethyl-iminocarbonate under various conditions, analogous (or identical) reaction products corresponding to the analogous acid chlorides are formed. However, this analogy does not include reaction conditions, because the electrophility of the acylation agents and that of the primary intemediate products are rather different. The course and mechanism of the reactions (confined mainly to reaction steps which can be proved) are outlined in the reaction scheme. The primary intermediate products of acylation reaction (1, 1a) are diethoxymethylene carbamoyl chloride (**III**) and the respective oxamoyl chloride (**IIIa**). The final result and the course of the acylation depend on the reaction conditions and on the electrophility of the primary products (**III**, **IIIa**).

Mole ratios:
2 acid chloride: I: Et3N = 1:2:2,2
2a
3 II:I: Et3N = 5:1:1,1
3a IIa:I = 5:1
5 II:I = 10:1
5a IIa:I = 1:2
+ COCl2
+ (COCl)2
II
IIa
III
IIIa
IV
IVa
V
VI
VII
VIII
IX
+1. HCl, −2 EtCl
+1. HCl, −EtCl
−CO
−EtCl
−CO, −EtCl
+2 HCl
−2 EtCl

1.*O-ethyl-N-diethoxymethylene-N'-carbethoxy isourea* (**V**) *and N,N'-bis-diethoxymethylene oxamide* (**IVa**) (*reactions* 2, 2*a*)

In the reaction carried out at a 2 : 1 mole ratio of diethyl-iminocarbonate (**I**): acid chloride, and using for the binding of hydrochloric acid a molar quantity of triethylamine identical with **I**, the primary products (**III** and **IIIa**) react in unchanged form with the excess of **I**:

$$\mathbf{III} + \mathbf{I} + Et_3N \xrightarrow{2} \mathbf{IV} + Et_3N.HCl \qquad (2)$$

$$\mathbf{IIIa} + \mathbf{I} + Et_3N \xrightarrow{2a} \mathbf{IVa} + Et_3N.HCl \qquad (3)$$

The end product of the reaction with oxalyl chloride (2a), the oxamide product (**IVa**), not yet described in the literature, has been identified on the basis of its IR spectrum, elementary analysis and reactions:

$$\mathbf{IVa} + 2HCl \rightarrow$$

$$\xrightarrow{\text{abs. toluene}} \underset{\mathbf{IX}\ (61\%)}{\begin{matrix} O{=}C{-}NH{-}COOEt \\ | \\ O{=}C{-}NH{-}COOEt \end{matrix}} + \underset{\mathbf{VIII}\ (26\%)}{O{=}C\begin{matrix} \diagup NH{-}COOEt \\ \diagdown NH{-}COOEt \end{matrix}} + EtCl + CO \qquad (4)$$

$$\mathbf{IVa} + 2H_2O \xrightarrow{H^{\oplus}} H_2N{-}\underset{\underset{O}{\|}}{C}{-}\underset{\underset{O}{\|}}{C}{-}NH_2 + 2O{=}C\begin{matrix} \diagup OEt \\ \diagdown OEt \end{matrix} \qquad (5)$$

The product of acylation with phosgene (2) is not the symmetric urea product (**IV**) corresponding to **IVa**, but the isomer (**V**) containing conjugated C=N bonds, the structure of which has been proved by its IR and NMR spectra, hydrolysis and reaction with hydrochloric acid:

$$\mathbf{V} + 2HCl \xrightarrow[\text{abs. dioxane}]{} \mathbf{VIII} + 2EtCl \qquad (6)$$

$$\mathbf{V} + 2H_2O \xrightarrow{H^{\oplus}} \mathbf{XI} + \underset{\mathbf{XII}}{H_2N{-}\underset{\underset{O}{\|}}{C}{-}NH{-}COOEt} + EtOH \qquad (7)$$

2. *Carbethoxy isocyanate* (**VII**) *(3,—4, 3a—4a reactions)*

In the reaction with oxalyl chloride (3a—4a), carbethoxy isocyanate (**VII**) is formed in increasing quantities as end product on increasing the acylating agent — substrate ratio. In the reaction carried out at a **IIa** : **I** ratio of 1 : 1,

VII is formed with a yield of 42%, while in that of 5 : 1 mole ratio with a yield of 83%, because oxalyl chloride acylates besides base **I** also **I. HCl**, formed during acylation. Thus, **I** is converted virtually completely into diethoxymethylene oxamoyl chloride (**IIIa**), from which **VII** is formed by isomerization, carbon monoxide, then ethyl chloride elimination.

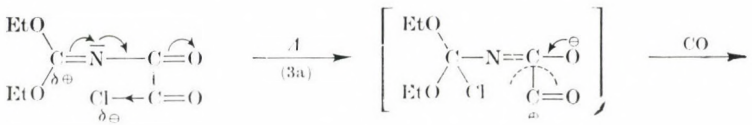

III a

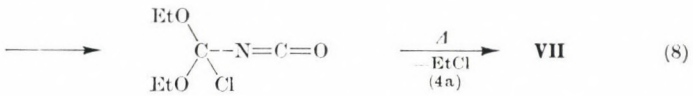

VI

According to our interpretation, the stable —N=C=O cumulated system is formed simultaneously with CO elimination, so that no N-chlorocarbonyl compound is formed as intermediate product, as contrary to the reaction scheme published in the literature, given in the introductory part (1). In the reaction with phosgene, the condition of the preparation of **VII** as end product is the complete conversion of **I** into diethyoxymethylene carbamoyl chloride (**III**). Since the electrophility of phosgene (as contrary to that of oxalyl chloride) is insufficient for the acylation of **I.HCl**, the isocyanate (**VII**) can be prepared as end product only when triethylamine is used in the reaction (for the elimination of the formation of **I.HCl**). When the equimolecular mixture of **I** and triethylamine is added to a solution containing tenfold quantity of phosgene, **III** is formed with an almost quantitative yield. From this, diethoxychloromethyl isocyanate (**VI**) is formed by isomerization (reaction 3), and **VII** is formed as end product by subsequent ethyl chloride elimination (reaction 4).

3. *N,N'-dicarbethoxy urea* (**VIII**) *and N,N'-dicarbethoxy oxamide* (**IX**) *(reactions 5, 5a)*

Changing the ratio of the reagents within a wide range in phosgenation reactions without trapping the hydrochloric acid, in each case N,N'-dicarbethoxy urea (**VIII**) is formed as main product. The yield of **VIII** is 66% at a **II** : **I** reagent ratio of 0.5 : 1, while 94% in the reaction at a mole ratio of 5 : 1. IR spectra taken during the reaction showed that the isocyanates **VI** and **VII** are formed as intermediate products, but only exclusively **VIII** or **VIII** and ethyl carbamate, formed by the eliminations of ethyl chloride, could be isolated as end products. On the basis of this, phosgenation of **I** without triethylamine can be interpreted as follows:

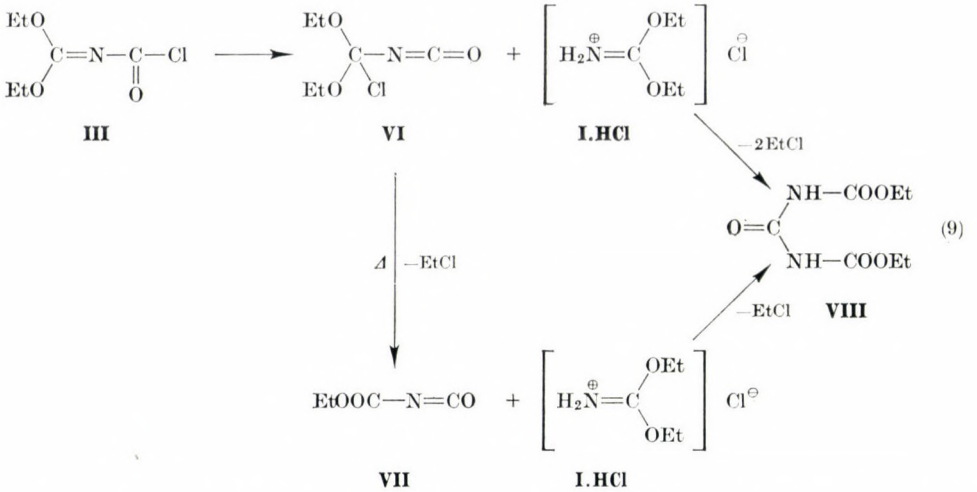

(9)

In the reaction of **I** and **II**, half of **I** is converted into N-chlorocarbonyl compound (**III**), the other half into **I.HCl**, which is not acylated by phosgene (**II**) even when present in a large excess. The possibility of a direct reaction of **I.HCl** with **III** of a substantially smaller electrophility than that of phosgene present in excess can be excluded. Isocyanates (**VI** and **VII**), formed from **III** on heating, and **I.HCl** present in equimolecular quantity, are converted quantitatively in the addition–elimination process into N,N'-dicarbethoxy urea (**VIII**) (9). (The addition–elimination reaction of **I.HCl** with **VII** has been proved in a separate experiment.)

In the reaction with oxalyl chloride (as contrary to that with phosgene), compounds of diurethane type (**VIII**, **IX**) are formed at an **I** : oxalyl chloride mole ratio of 2 : 1. Adding the substrate under these conditions to the solution

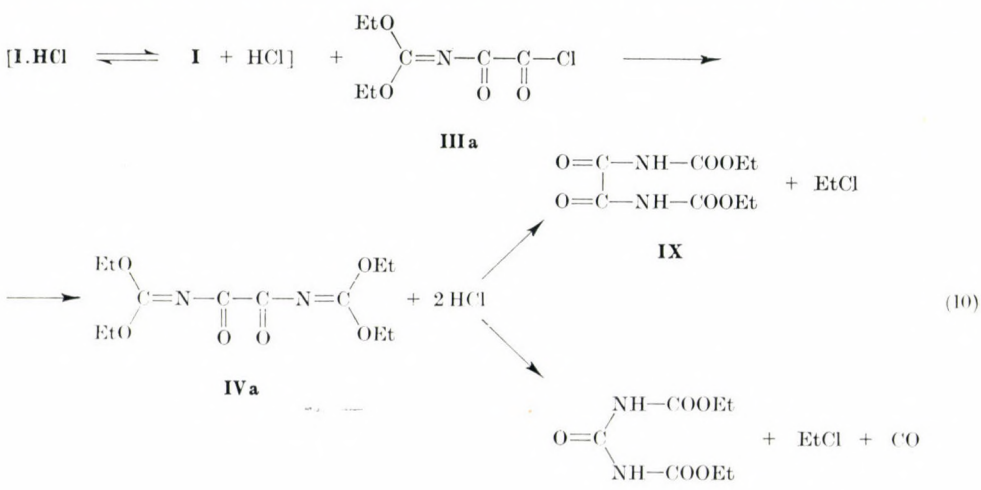

(10)

of the acylating agent, diethoxymethylene oxamoyl chloride (**IIIa**), from the half of **I** and **I.HCl** from the other half **I** are formed. The formation of **IX** presumes the reaction of **IIIa** with **I.HCl**, as a result of which N,N'-bis-diethoxymethylene oxamide (**IVa**) and twice the amount of hydrochloric acid is formed.

The reaction of **IVa** with the double amount of hydrochloric acid results on heating (see (4)) the formation of **VIII** and **IX**. It has been proved by the IR analysis of the reaction mixture that from a part of **IIIa** isocyanates **VI** and **VII** are formed as intermediates (see (8)), which react with the unconsumed **I.HCl**, and give in an addition–elimination process **VIII** (see (9)). In addition to the spectroscopic detection of the isocyanates (**VI**, **VII**), it is supported also by the quantitative ratio of **VIII** and **IX** formed in the acylation with oxalyl chloride that **VIII** is formed besides in the process indicated by reaction scheme (10) also in another reaction (9). From pure **IVa**, **IX** has been formed namely with a yield of 61%, **VIII** with a yield of 26% by reaction with hydrochloric acid (see (4)), while in the acylation of **I** with oxalyl chloride the yield of **IX** is 36%, and that of **VIII** 48%.

Experimental part

1. O-ethyl-N-diethoxymethylene-N'-carbethoxy isourea (V) and N,N'-bis-diethoxymethylene oxamide (IVa)

To a mixture of 100 ml of abs. toluene, 11.7 g (0.1 mole) of I and 11.1 g (0.11 mole) of triethylamine, 0.05 mole of acylating agent, dissolved in 50 ml of abs. toluene was added at 0—5 °C. The mixture was stirred at 25—30 °C for 90 minutes, and triethylamine hydrochloride separated was filtered off. The solvent was removed in vacuum from the filtrate, 25 ml of carbon tetrachloride was added, and after evaporation in vacuum, the residue was kept standing for one day in a vacuum desiccator over phosphorus pentoxide and paraffin chips.

Table I

	V ($C_{11}H_{20}N_2O_5$; M.w.: 260)			**IVa** ($C_{12}H_{20}N_2O_5$; M.w.: 288)		
Acylating agent	$COCl_2$: 5.0 g			$(COCl)_2$: 6.35 g		
Product	11.0 g (84.5%) decomposes during distillation			12.80 g (88.7%) b.p.: 120—6/0.5 mm Hg decomposition		
Elementary analysis	C	H	N	C	H	N
Calc. %	50.75	7.68	10.78	50.00	6.94	9.71
Found %	50.47	7.36	11.12	49.43	7.10	10.03

V: IR(CCl_4): νC=O: 1730, νC=N: 1660—80, ν_{as}OCO: 1300, ν_{as}C—O—C: 1075, ν_sCOC: 1025 cm^{-1}
NMR($CDCl_3$): δ = 4.25 ppm $(CH_2)q$ [8H] (two quartets)
δ = 1.30 ppm $(CH_3)t$ [12H] (two triplets).
IVa: IR(film): νC=O and νC=N: 1760, 1730, 1680; ν_{as}OCO: 1350, ν_{as}COC: 1060, ν_sCOC: 1020, (νC—N + νC=O); 1270 cm^{-1}
NMR($CDCl_3$): δ = 4.30 ppm (CH_2)q [8H], δ = 1.32 ppm (CH_3)t [12H].

Identification

V + anhydrous hydrochloric acid: 5.2 g (0.02 mole) of **V** was dissolved in abs. dioxane, and up to pH = 2, dry gaseous hydrochloric acid was introduced into the solution at 25—30 °C. The mixture was stirred at 40—45 °C for 90 minutes and evaporated to dryness in vacuum. The raw product (4.0 g; 98%) was recrystallized from water, to give 3.4 g (83.5%) of **VIII**. M.p.: 105—6 °C (m.p. in the literature [5]: 107 °C).

Acid hydrolysis of **V**: to a mixture of 10.4 g (0.04 mole) of **V**, 10 ml of ethanol and 6 ml of water, 3 ml of 1 *N* hydrochloric acid was added dropwise at 5—10 °C, the mixture was kept then for 30 minutes at 30—35 °C, 40 ml of water was added, and allophanic acid ethyl ester (**XII**) separated was filtered off. (3.7 g; 71.5%, m.p.: 192—4 °C, in the literature [6]:194—5 °C.) The organic phase of the filtrate was separated, and the aqueous phase was extracted with 2×15 ml of ether. The combined organic phases were dried over $MgSO_4$ and fractionated to give 3.2 g (68%) of diethyl carbonate (**XI**).

IVa + anhydrous hydrochloric acid: dry HCl gas was introduced at 25—30 °C into a mixture of 2.88 g (0.01 mole) of **IVa** and 30 ml of abs. toluene (pH ~ 2), stirred for 90 minutes at 30—35 °C, and **IX** separated was filtered off (1.45 g; 61%). M.p.: 169—171 °C (m.p. in the literature [7]: 172 °C). The filtrate was evaporated to dryness in vacuum, the residue recrystallized from a water–ethanol mixture, to yield 0.53 g (26%) of **VIII**. Acid hydrolysis of **IVa**: to a mixture of 7.65 g (0.02 mole) of **IVa**, 10 ml of ethanol and 5 ml of water, first 2 ml of 1*N* hydrochloric acid then 30 ml of water was added dropwise at 30—35 °C. After 30 minutes of stirring, oxamide (**X**), precipitating on cooling with ice, was filtered off. (1.48 g; 84%; m.p.: > 320 °C, decomp. [6]).

VIII IR (KBr) νNH_{mon}: 3230, $\nu NH_{assoc.}$: 3140, νC=O (coupled): 1810, 1740, Amide II: 1500—1560 cm^{-1} (broad)

IX IR (KBr) νNH: 3200, νC=O (coupled): 1790, 1750, 1700, Amide II: 1480 cm^{-1} (broad)

2. Carbethoxy isocyanate (VII)

2.1 To a solution of 19.8 g (0.2 mole) of phosgene in 100 ml of abs. benzene a mixture of 2.34 g (0.02 mole) of **I** and 2.22 g (0.022 mole) of triethylamine was added, the mixture was stirred for 1 hour at 30 °C, phosgene was removed at 15 Torr, triethylamine hydrochloride separated (2.56 g; 93%) was filtered off, and the IR spectrum[1] of the mixture was recorded. The filtrate was boiled for 2 hours, its IR spectrum was taken[2], and the **VII** content was determined preparatively[3] on a sample, and the product (**VII**) was separated by distillation[4] (b.p.: 111—114 °C/760 mm [8]).

2.2. To oxalyl chloride (Table II) or to a solution of oxalyl chloride in 60 ml of abs. toluene, 4.68 g (0.04 mole) of **I** was added dropwise at —5 to 0 °C, the mixture was stirred at 30 °C for 90 minutes, the IR spectrum was taken,[1] and the mixture was then boiled for 2 hours. The IR spectrum was recorded[2] again, and the product (**VII**) was isolated from the reaction mixture of the experiment without solvent by fractionation repeated three times. From the reaction mixture containing toluene, oxalyl chloride was distilled off, the product was recovered

[1] In the IR spectrum, the νN=C=O vibration of **VI** at 2310 cm^{-1} was assigned as a strong band, that of **VII** at 2250 cm^{-1} as a band of medium strength.

[2] In the IR spectra taken on samples of identical dilution as above, the characteristic absorption band of **VI** is very weak, that of **VII** very strong.

[3] Under stirring, saturated *p*-chloroaniline solution in toluene was added at 25—35 °C to the solution containing **VII** until the ceasing of the heat effect. One part of N-(4-chlorophenyl)-N'-carbethoxy urea (**XIII**) formed in this way precipitated immediately, the supernatant was evaporated to 1/3 of its volume, petroleum ether was added, and on salt ice cooling the other part of **XIII** precipitated. M. p.: 158—161 °C (m.p. in the literature [9]: 162 °C)

[4] **VII** can be recovered owing to the close boiling points from the solution in benzene only with a yield of 58%.

as toluene distillate, the carbethoxy isocyanate (**VII**) content of which was determined by derivative forming.[3] (See Table II)

Phosgene reaction (2.1)

Product: **VII** isolated by distillation: 1.35 g[5] (58%) N-(4-chlorophenyl)-N'-carbethoxy urea (**XIII**): 4.12 g[5] corresponding to 85% of **VII**.

VII IR ν_{as}NCO: 2250, νCO: 1745, ν_{s}NCO: 1430 cm^{-1}.

Oxalyl chloride reaction (2.2)

Table II

Mole ratio I : IIa	IIa (g)	Product		Yield (VII %)	Remark*
		VII (g)	XIII (g)		
1 : 1	7.6	—	4.10	42.0	1, 3
1 : 3	15.2		4.97	51.0	1, 3
1 : 5	25.4		8.55	87.5	1
1 : 5	25.4	3.8	—	81.7	2

* Remark: 1. Experiment in the presence of a solvent
2. Experiment in the absence of a solvent
3. In addition to carbethoxy isocyanate (**VII**), **IX** with a yield of 12% and **VIII** with a yield of 5% were also formed.

3. N,N'-Dicarbethoxy urea (VIII) and N,N' dicarbethoxy oxamide (IX)

3.1 Phosgene (**II**) was absorbed in 60 ml of abs. toluene at —5 °C, and a solution of **I** in 20 ml of toluene was added dropwise at —5 to 0 °C. The mixture was stirred at 25—30 °C for 3 hours, evaporated to dryness in vacuum, and the residue recrystallized from water.

Mole ratio (I : II)	I (g)	II (g)	Product (VIII) (g)	
1 : 0.5	11.70	4.9	6.7 (67%)	m.p.: 105—6 °C
1 : 5	2.34	9.90	1.92 (94%)	

3.2 To a solution of 2.54 g (0.02 mole) of oxalyl chloride (**IIa**) in 40 ml of abs. toluene a solution of 4.68 g (0.04 mole) **I** in 20 ml of toluene was added at —5 °C. The mixture was stirred for 90 minutes at 30—35 °C, and allowed to stand for 1 day. After cooling with ice N,N'-dicarbethoxy oxamide (**IX**) was filtered off, and recrystallized from an alcohol–water mixture (1.64 g; 36%, m.p. 169—171 °C). The filtrate was evaporated to dryness in vacuum, the residue recrystallized from petroleum ether — alcohol, to obtain N,N'-dicarbethoxy urea (**VIII**). (1.95 g; 48%, m.p.: 106—7 °C).

3.3 Reaction of **I.HCl** with isocyanates **VI**, **VII.** Into a solution of 2.34 g (0.02 mole) of **I** in 25 ml of abs. toluene dry gaseous hydrogen chloride was introduced (pH ~ 2) at —5 °C. To this mixture

a) 2.3 g (0.02 mole) of **VIII** dissolved in 40 ml of abs. toluene, or

b) **VI**—**VII** isocyanate mixture in toluene, prepared as described in 2.1 and used after filtering off the triethylamine hydrochloride (without boiling) was added at —5 to 0 °C.

The mixture was stirred first at 15—20 °C for 1 hour, then at 35—40 °C for a further hour, and evaporated to dryness in vacuum. The residue was washed with petroleum ether, dried and recrystallized from water.

Quantity of **VIII** formed: a) 3.7 g (91%)
b) 3.4 g (83%).

[5] Referred to the total reaction mixture

REFERENCES

[1] BENDE, Z., BITTER, I., CSŰRÖS, Z.: Acta Chim. (Budapest) in the press
[2] SAMARAI, L. J., VISHNEVSKII, O. V., DERKATCH, G. I.: Chem. Ber. **102,** 2972–6 (1969)
[3] SAMARAI, L. I., BONDAR, V. A., DERKATCH, G. I.: Angew. Chem. **80,** 620 (1968)
[4] SAMARAI, L. I., BELAYA, V. P., VISHNEVSKII, O. V.: Zsurn. Org. Him. **4,** 720 (1968)
[5] DAINS, F. B.: J. Am. Chem. Soc. **21,** 136–92 (1898)
[6] Dictionary of Org. Compounds. Eyre and Spottiswoode, London 1946
[7] BASTERFIELD, S., WOODS, E. L., WHELEN, D.: J. Am. Chem. Soc. **49,** 2945 (1927)
[8] OSTROGOVICH, G., BACALOGU, R., CATALINA, E.: Stud. Cerc. Stiint. Chim. **10,** 143–6 (1963); CA: 61, 2939b.
[9] CURD, F. H. S., DAVEY, D. G., RICHARDSON, D. N.: J. Chem. Soc. **1949,** 1732–38

Zoltán BENDE
István BITTER
Zoltán CSŰRÖS
H-1111 Budapest, Műegyetem rkp. 3.

Acta Chimica Academiae Scientiarum Hungaricae, Tomus 93 (1), pp. 95—98 (1977)

NEUE SYNTHESE VON 3,4-DIHYDRO- UND 1,2,3,4-TETRAHYDROCHINAZOLINEN UND IHRE STEREOCHEMISCHE UNTERSUCHUNG

J. FISCHER, G. TÓTH* und P. VÁGÓ

(Pharmakochemische Werke EGYT, Forschungslaboratorium, Budapest)

Eingegangen am 1. April 1976

3,4-Dihydro-chinazoline entstehen in der Reaktion von 4-substituierten Anilinen mit α-Halogen-äthern (R_2=H) in Tetrahydrofuran; wenn der α-Halogen-äther aber eine elektronenanziehende Gruppe ($R_2 = COOC_2H_5$) enthält, werden 1,2,3,4-Tetrahydro-chinazoline gebildet. Diese letztere Reaktion spielt stereoselektiv ab, wobei das *cis*-Isomer das Hauptprodukt ist. Das *cis/trans* Isomerengemisch bildet ein protonenkatalysiertes Gleichgewicht. Die Isomeren wurden mit Hilfe der NMR-Spektren identifiziert.

Die strukturbeweisende Synthese des 6-Methyl-3-(4-tolyl)-3,4-dihydrochinazolins wurde von WALTHER und BAMBERG [1] durch die Reaktion von *o*-Amino-*m*-xylyl-*p*-toluidin und Orthoameisenester verwirklicht. Die Reaktion von *p*-Toluidin und Formaldehyd lieferte ein Gemisch, aus dem EISNER und WAGNER [2] dieselbe Verbindung isolieren konnten.

Wir haben gefunden, daß 3,4-Dihydro- oder 1,2,3,4-Tetrahydro-chinazoline entstehen, wenn 4-substituierte Aniline mit α-Halogen-äthern in Tetrahydrofuran reagieren, wobei die Struktur der α-Halogen-äther entscheidend ist (Tabelle I.). In unserer früheren Arbeit [3] haben wir ein Dimerizationsprodukt der 4-Chlor-anil-glyoxylsäure angenommen, welches aber auf Grund der ausführlicheren physikalisch-chemischen Untersuchungen modifiziert werden mußte. Die 3,4-Dihydro-chinazoline (*A*) konnten wir mit Hilfe der schon früher beschriebenen Methoden hergestellten Verbindungen identifizieren. Die 1,2,3,4-Tetrahydro-chinazoline (*B*) entstehen in einer stereoselektiven Reaktion, wobei das reine und stabile *cis*-Isomer in einer Ausbeute von ca. 50% erhalten werden kann. Zur Identifizierung der Isomeren mit Hilfe der NMR-Spektroskopie haben wir auch das *trans*-Isomer hergestellt, wobei wir zwei Methoden gefunden haben. Unter protonenkatalysierten Umständen entsteht aus dem reinen *cis*-Isomer ein Isomerengemisch, in dem die Isomeren ein Gleichgewicht bilden.** Aus dem Gleichgewichtsgemisch konnte das reine *trans*-Isomer durch wiederholtes Umkristallisieren abgetrennt werden. Die Abbildung I zeigt das Gleichgewicht des Isomerengemisches am Beispiel von *cis/trans*-6-Methyl-3-*p*-tolyl-2,4-diäthoxycarbonyl-1,2,3,4-tetrahydro-chinazo-

* Institut für Organische Chemie der Med. Univ. Semmelweis NMR-Laboratorium, Budapest.

** Gleichgewichtskonstanten (*K*) auf Grund der NMR-Spektra bestimmt.

Tabelle I

Synthese von 3,4-Dihydro- und 1,2,3,4-Tetrahydro-chinazolinen

R	Hal	R_1	R_2	Produkt	F
4-Cl	Cl	CH_3	H	*A*	187—9° [2]
4-Br	Cl	CH_3	H	*A*	195—200° [2]
4-$COOC_2H_5$	Cl	CH_3	H	*A*	185—8° [5]
4-CH_3	Cl	CH_3	H	*A*	158—60° [1]
4-Cl	Cl	C_2H_5	$COOC_2H_5$	*B*	187—9°
4-Br	Cl	C_2H_5	$COOC_2H_5$	*B*	193—5°
4-$COOC_2H_5$	Cl	C_2H_5	$COOC_2H_5$	*B*	150—2°
4-CH_3	Cl	C_2H_5	$COOC_2H_5$	*B*	173—4°
4-COOH	Br	Cl–C$_6$H$_4$–	$COOC_2H_5$	*B*	200—5°

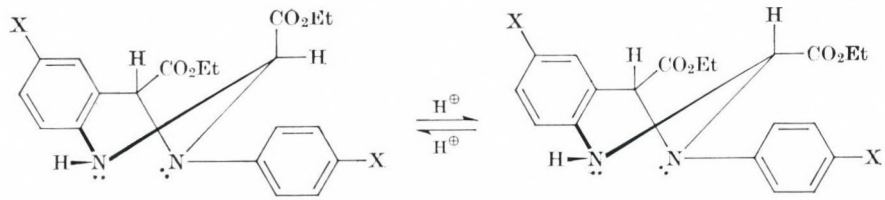

	Trans-Isomer NMR (δ)			Cis-Isomer NMR (δ)			
X	C(2)H	C(4)H		C(2)H	C(4)H		K(25 °C)
CH_3	5.44 d	5.27 s	12%	5.72 d	5.26 s	88%	7.3
Cl	5.38 d	5.18 s	16%	5.62 d	5.10 s	84%	5.3

linen und bei den Chlor-Analogen. Von den NMR-Signalen konnten wir feststellen, daß die Isomerisierung am C(2)-Atom vor sich geht, und für die kleinere chemische Verschiebung des C(2)-Atoms beim *trans*-Isomer die diamagnetische Wirkung der 3-Phenyl-Gruppe verantwortlich ist. Analoge Isomerisierungen sind aus der Literatur bekannt [4].

Die zweite Methode besteht aus einer oxidativ-reduktiven Umwandlung des *cis*-Isomers, wobei die Oxydation zum 3,4-Dihydro-chinazolin mit DDQ (2,3-Dichlor-5,6-dicyano-1,4-benzochinon) verwirklicht wurde. Das 3,4-Dihydro-Produkt wurde mit Hilfe von Platinoxid-Katalysator zu einem *cis*/*trans*-1,2,3,4-Tetrahydro-chinazolin-Gemisch hydriert, welches am *trans*-Isomer reicher ist als das Gleichgewichtsgemisch.

Über die NMR-Untersuchungen wird an anderer Stelle ausführlicher berichtet.

Beschreibung der Versuche

Allgemeine Herstellungsvorschrift der 3,4-Dihydro-chinazoline (A):

In wasserfreiem Tetrahydrofuran (20 ml) wird *p*-substituertes Anilin-Derivat (0.1 mol) gelöst, sodann wird Chlormethyl-methyläther (0.05 mol) in wasserfreiem Tetrahydrofuran (10 ml) zugetropft. Das Reaktionsgemisch wird 5 Stunden bei 50 °C gerührt, dann abgekühlt und Petroläther (Kp: 40—70°, 30 ml) zugegeben. Das abgeschiedene Produkt wird filtriert, mit Petroläther gewaschen und getrocknet. Das Rohprodukt wird in 1 : 1 NH_4OH-Lösung suspendiert, wieder filtriert und aus einem Gemisch von Aceton/Wasser umkristallisiert. Die Ausbeute beträgt 25—30%.

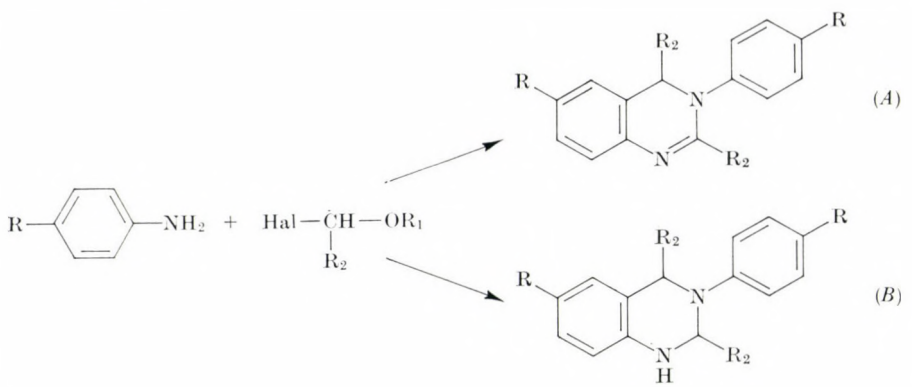

Allgemeine Herstellungsvorschrift der 1,2,3,4-Tetrahydrochinazoline (B) am Beispiel von cis-6-Chlor-3-(4-chlorphenyl)-2,4-diäthoxycarbonyl-1,2,3,4-tetrahydrochinazolin:

In wasserfreiem Tetrahydrofuran (30 ml) werden Äthyl 2-brom-2-(4-chlor-phenoxy)-acetat (14,6 g; 0.05 mol) und 4-Chlor-anilin (12,7 g; 0,10 mol) gelöst und das Reaktionsgemisch wird 5 Stunden bei 50 °C gehalten, dann abgekühlt und Petroläther (Kp: 40—70°) zugegeben, worauf sich ein kristallines Produkt abscheidet, das filtriert, mit Wasser gewaschen und dann aus Methanol umkristallisiert wird. Gewicht: 5,1 g (48,6%), weißes Produkt, Schmelzpunkt: 187—9°.

$C_{20}H_{20}Cl_2N_2O_4$ (423,3)
ber. C 56,75 H 4,76 Cl 16,75 N 6,52
gef. 56,88, 5,17 17,01 6,43
M.S.: m/e = 422 (M^+).
I.R. (KBr): ν_{max} = 3325 (NH), 1740, 1720 cm^{-1} (CO).
^{1}H-N.M.R. ($CDCl_3$): δ = 1,12t (3H); 1,30t(3H); 4,16q (2H); 4,27q (2H): CH_3CH_2OCO; 5,62d (1H), J_{CHNH} = 2,8 Hz: H-2; 4,95d (1H): NH; 5,10s (1H): H-4; 6,85 (2H), 7,5 (2H): AA'BB'-Typ: H-2', 6' und H-3', 5'; 7,0—7,2m (2H): H-5,7; 6,64d (1H), $J_{7,8}$ = 8,0 Hz: H-8.

Acetyl-Derivat: F: 90—2° (Äthanol–Wasser).

I.R. (KBr): ν_{max} = 1740, 1730 (CO-Ester), 1680 cm^{-1} (CO-Amid).
^{1}H-N.M.R. ($CDCl_3$): δ = 1,09t (3H); 1,18 (3H); 4,06q (2H); 4,14q (2H): CH_3CH_2OCO; 7,08s (1H): H-2; 5,31s (1H): H-4; 2 ,30s (3H): H_3CO; 6,70d (2H): H-2',6'; 7,1—7,4m (4H): H-3',5' und H-7,8; 7,45d (1H), $J_{5,7}$ = 2Hz: H-5.

trans-6-Chlor-3-(4-chlor-phenyl)-2,4-diäthoxycarbonyl-1,2,3,4-tetrahydro-chinazolin:

In einem Gemisch von Tetrachlorkohlenstoff (180 ml), Dichlormethan (40 ml) und Essigsäure (5 ml) wurde *cis*-6-Chlor-3-(4-chlor-phenyl)-2,4-diäthoxycarbonyl-1,2,3,4-tetrahydro-chinazolin (10,0 g; 0,024 mol) gelöst und für einen Tag bei Zimmertemperatur gehalten. Sodann wurde ein Teil des Lösungsmittels abgedampft und das reine *cis*-Isomer durch eine wiederholte fraktionierte Kristallisation abgetrennt, wobei das *trans*-Isomer in der Mutter-

lauge bleibt, aus der es mit Petroläther abgeschieden und durch Umkristallisieren aus Äthanol rein erhalten wurde. Schmelzpunkt: 133—6 C°, Ausbeute: 0,6 g (6%).

I.R. (KBr): ν_{max} = 3355 (NH), 1740, 1727 cm^{-1} (CO).
^{1}H-N.M.R. ($CDCl_3$): δ = 1,27t (3H); 1.35t (3H); 4 18q (2H); 4,26q (2H): CH_3CH_2OCO; 5,38d (1H), J_{CHNH} = 2,8 Hz: H-2; 4,63d (1H): NH; 5,18s (1H): H-4; 7,0 (2H); 7,2 (2H): AA'BB'-Typ: H-2',6' und H-3',5'; 7,15—7,25m (2H): H-5,7; 6,64d (1H), $J_{7,8}$ = 8,0 Hz: H-8.

trans-6-Methyl-3-(4-tolyl)—2,4-diäthoxycarbonyl-1,2,3,4-tetrahydro-chinazolin:

In wasserfreiem Dioxan (500 ml) wurde das *cis*-Isomer (23,8 g; 0,062 mol) bei 40° unter Rühren gelöst, sodann während 2 Stunden DDQ (14,3 g; 0,063 mol) in Dioxan (180 ml) zugetropft und das abgeschiedene 2,3-Dichlor-5,6-dicyano-hydrochinon abgetrennt. Das Filtrat wurde abgedampft, der Rückstand (39 g Öl) in Dichlormethan gelöst und mit 5%iger Na_2CO_3-Lösung gewaschen, bis die Waschlösung farblos wurde. Die Lösung wurde getrocknet und abgedampft. Der Rückstand betrug 18,6 g Öl, größtenteils 6-Methyl-3-(4-tolyl)-2,4-diäthoxycarbonyl-3,4-dihydro-chinazolin. Ohne Isolierung wurde der Rückstand in Tetrahydrofuran (200 ml) gelöst und in Gegenwart von Platinoxid (0,5 g) hydriert. Nach Filtrieren des Katalysators wurde das Filtrat abgedampft, der Rückstand in Dichlormethan gelöst und mit 5%iger Na_2CO_3-Lösung gewaschen; die organische Phase wurde abgedampft, wobei ein gelbes Öl (13,2 g) zurückbleibt. Diese wurde in Petroläther–Äthanol (1 : 3) gelöst und das *cis*-Produkt fraktioniert abgetrennt. Ein Isomerengemisch (4.2 g; F: 105—150 °C; *cis*/*trans* Verhältnis = 1 : 2) und reines *trans*-Isomer (0.6 g; F: 108—110 C°) wurden erhalten.

I.R. (KBr): ν_{max} = 3330 (NH), 1735, 1702 cm^{-1} (CO).
^{1}H-N.M.R. ($CDCl_3$): δ = 1,26t (3H); 1,33t (3H); 4,22q (2H); 4,31q (2H): CH_3CH_2OCO; 5,44d (1H), J_{CHNH} = 2,8 Hz: H-2; 5,27s (1H): H-4; 2,35s (6H): Ar-Me.

LITERATUR

[1] Walther, R., Bamberg, R.: J. prakt. Chem., **73,** 209 (1906)
[2] Wagner, E. C., Eisner, A.: J. Am. Chem. Soc., **59,** 879 (1937)
[3] Fischer, J., Tóth, G., Fodor, T., Rákóczi, J.: Acta Chim. (Budapest), **79,** 419 (1973)
[4] Bender, C. O., Bonnett, R.: J. Chem. Soc., (**1968**) 2186
[5] Cairncross, S. E., Bogert, M. T.: Collection, **8,** 57 (1936)

János Fischer
Pál Vágó
H-1475 Budapest, Pf. 100.

Gábor Tóth
H-1092 Budapest, Hőgyes E. u. 7.

Acta Chimica Academiae Scientiarum Hungaricae, Tomus 93 (1), pp. 99—102 (1977)

DIE DARSTELLUNG VON 1,3,4,6-TETRA-O-ACETYL-β-D-GLUCO- UND GALACTOPYRANOSE UND IHRER α-GLYKOSYLBROMID-DERIVATE

V. M. CHARI, M. JORDAN und H. WAGNER

(Institut für Pharmazeutische Arzneimittellehre der Universität München)

Eingegangen am 16. Juni 1976

Als Ausgangsverbindungen für die Synthese von Sambubiose und 2-O-Acylglucosiden und -galactosiden wurden 1,3,4,6-Tetra-O-acetyl-β-D-gluco- und galactopyranose und ihre α-Glykosylbromidderivate nach einem vereinfachten Verfahren in hohen Ausbeuten dargestellt.

Zur Synthese von Disacchariden nach Königs-Knorr werden im allgemeinen die Monosaccharid-β-tetra-O-acetate bevorzugt, da die dabei entstehenden β-Per-O-acetate besser kristallisieren als die Anomeren [1—5]. Über eine verbesserte Synthese von 1,2,3,6- und 1,2,4,6-Tetra-O-acetyl-β-D-glucopyranosen ist bereits berichtet worden [6]. Zur Synthese des 2-O-(2,3,4-tri-O-acetyl-α-D-xylopyranosyl)-3,4,6-tri-O-acetyl-α-D-glucopyranosylbromids [7] und natürlich vorkommender 2-O-Acylglucoside und Galactoside benötigten wir die 1,3,4,6-Tetra-O-acetyl-β-D-glucopyranose (**1**) als Zwischenstufe. Während wir die 1,3,4,6-Tetra-O-acetyl-α-D-glucopyranose (**2**) direkt aus Glucose leicht darstellen können [2], verläuft die von LEMIEUX und HUBER [3] ausgearbeitete und von D-Glucose ausgehende Synthese der anomeren Verbindung **1** über fünf Stufen — β-Penta-O-acetat, 3,4,6-Tri-O-acetyl-2-O-trichloracetyl-β-D-glucopyranosylchlorid, 3,4,6-Tri-O-acetyl-β-D-glucopyranosylchlorid, 3,4,6-Tri-O-acetyl-α-D-glucopyranosylchlorid — mit nachfolgender Substitution des Chlors durch eine Acetylgruppe. Außerdem verlangt die Synthese eine Arbeitszeit von mehreren Tagen.

Wir haben deshalb eine einfachere Darstellung des 1,3,4,6-Tetra-O-acetyl-β-D-glucopyranosids (**1**) ausgearbeitet. Als Kaschierungsmittel benutzten wir die selektive und leicht abspaltbare Monochloracetylgruppe [8]. Mit Pyridin und Chloracetylchlorid wurde 1,3,4,6-Tetra-O-acetyl-α-D-glucopyranose [2] (**2**) in das entsprechende 2-O-Chloracetat (**3**) in 43%iger Ausbeute überführt. Bei Verwendung von Chloracetanhydrid an Stelle von Acychlorid konnte die Ausbeute des Rohproduktes (**3**) sogar auf 85—90% erhöht werden. Über das α-Glykosylbromid (**4**) ließ sich **3** zur 1,3,4,6-Tetra-O-acetyl-2-O-chloracetyl-β-D-glucopyranose (**5**) in 58%iger Ausbeute umsetzen. Die Umwandlung von **3** in **5** konnte auch ohne Isolierung und Reinigung von **4** durchgeführt werden. Selektive Abspaltung der Chloracetylgruppe [8] erfolgte durch 45-minutiges Erhitzen in Methanol mit molaren Mengen Thioharn-

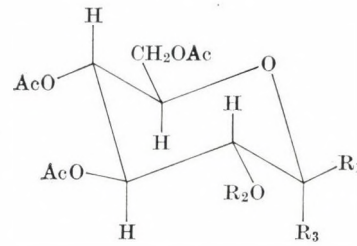

1 $R_1 = CH_3COO-$, $R_2 = R_3 = H$
2 $R_1 = R_2 = H$, $R_3 = CH_3COO-$
3 $R_1 = H$, $R_2 = ClCH_2CO-$, $R_3 = CH_3COO-$
4 $R_1 = H$, $R_2 = ClCH_2CO-$, $R_3 = Br$
5 $R_1 = CH_3COO-$, $R_2 = ClCH_2CO-$, $R_3 = H$

stoff. Das hierbei entstandene Pseudothiohydantoin wurde durch Auswaschen entfernt. Diese Reaktion ergab eine 50%ige Ausbeute. Die gesamte Reaktionsdauer von D-Glucose bis **1** konnte gegenüber der früheren Synthese auf mehr als die Hälfte der Zeit abgekürzt werden.

Auf die gleiche Weise wurde ausgehend von D-Galactose die 1,3,4,6-Tetra-O-acetyl-β-D-galactopyranose (**6**) synthetisiert. Die beiden bisher nicht bekannten α-Glykosylbromide **4** und **9** wurden rein erhalten, wobei **4** kristallisierte.

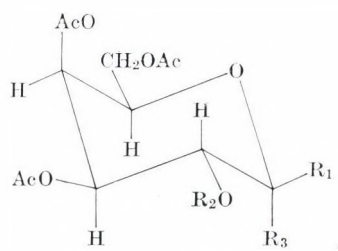

6 $R_1 = CH_3COO-$, $R_2 = R_3 = H$
7 $R_1 = R_2 = H$, $R_3 = CH_3COO-$
8 $R_1 = H$, $R_2 = ClCH_2CO-$, $R_3 = CH_3COO-$
9 $R_1 = H$, $R_2 = ClCH_2CO-$, $R_3 = Br$
10 $R_1 = CH_3COO-$, $R_2 = ClCH_2CO-$, $R_3 = H$

Experimenteller Teil

Alle Schmelzpunkte sind unkorrigiert. NMR: Varian 60 MHz mit TMS als inneren Standard, wenn nicht anders angegeben. DC: Kieselgel F_{254}-Fertigplatten (Merck), Schichtdicke 0,25 mm, Lösungsmittelsystem: Toluol–Äthylacetat 1 : 1.

1,3,4,6-Tetra-O-acetyl-2-O-chloracetyl-α-D-Glucopyranose (3)

Acylchlorid Methode:

Eine eisgekühlte Lösung von 10 g (28,7 mmol) **2** [2] in einem Gemisch von 10 ml Dichlormethan, 150 ml Äther und 5 ml absolutem Pyridin wurde tropfenweise mit einer Lösung von 5 ml Chloracetylchlorid in 10 ml Dichlormethan behandelt. Nach vollständiger Zugabe des Chloracetylchlorids wurde die Lösung 1 Std. stehen gelassen. Die Vollständigkeit der Reaktion wurde durch DC verfolgt. Die mit 150 ml Chloroform verdünnte Lösung wurde zweimal mit 150 ml Wasser mit 50ml kalter wässriger Salzsäure (0,5 N, 5 °C) und 150 ml wässeriger $NaHCO_3$-Lösung gewaschen, mit Na_2SO_4 getrocknet und mit Kohle geklärt. Die filtrierte Lösung wurde zu einem Sirup eingeengt, der durch Kristallisation aus Äthanol **3** als farblose Nadeln (5.2 g, 42,6%) lieferte. Schmp. 141—2 °C, $[\alpha]_D^{25}$ + 91,6° (c = 0,94 in $CHCl_3$). Lit. [3] Schmp. 143—4 °C, $[\alpha]_D^{25}$ + 98° ($CHCl_3$). NMR ($CDCl_3$): δ = 2,0 — 2,25 ppm (12H, 4 CH_3CO), 4,0 (s, 2H, $ClCH_2CO$—), 4,1—5,7 (6H, Zuckerprotonen), 6,35 (d, 1H, J = 3Hz, 1-H).

Anhydrid Methode:

Zu einer eisgekühlten Lösung von 10 g (28,7 mmol) **2** in einem Gemisch von 10 ml Dichlormethan, 150 ml Äther und 10 ml absolutem Pyridin wurde tropfenweise eine Lösung von 15g Chloracetanhydrid in 15 ml Dichlormethan zugegeben. Nach vollständiger Zugabe der Anhydridlösung wurde 30 Min. stehen gelassen und wie oben aufgearbeitet. Ausbeute an rohem **3** betrug 11 g (90%).

1,3,4,6-Tetra-O-acetyl-2-O-chloracetyl-α-D-glucopyranosylbromid (4)

Eine Lösung von 5 g **3** in 50 ml trockenem Dichlormethan wurde bei 0 °C mit 40%igem HBr in 20 ml Eisessig versetzt und 1,5 Stdn. stehen gelassen. Die Lösung wurde dann mit 150 ml Dichlormethan verdünnt, 2mal mit 100 ml Eiswasser, anschließend mit gesättigter wässriger $NaHCO_3$-Lösung und schließlich mit Wasser gewaschen, mit $CaCl_2$ getrocknet und bei 50 °C zu einem Sirup eingeengt. Beim kurzen Aufkochen mit Äther kristallisierte der Bromzucker **4** in farblosen Nadeln aus (4,5 g, 86%). Umkristallisieren erfolgte aus Äther–Hexan. Schmp. 116—9 °C $[\alpha]_D^{24}$ + 167,3° (c = 0,9689 in $CHCl_3$). NMR ($CDCl_3$): δ = 2,0—2,15 ppm (9 H, 3 CH_3CO—), 4,05 (s, 2H, $ClCH_2CO$—), 4,2—5,8 (6H, Zuckerprotonen), 6,6 (d, 1H, J = = 4Hz, H-1).

$C_{14}H_{18}O_9BrCl$ (445,7) Ber. C 37,73 H 4,07
Gef. C 38,87 H 4,17

1,3,4,6-Tetra-O-acetyl-2-O-chloracetyl-β-D-glucopyranose (5)

Eine Lösung von 4,5 g (10,1 mmol) **4** in 20 ml Chloroform wurde mit einer Lösung von 3,2 g (10.1 mmol) Quecksilberacetat in 50 ml Essigsäure behandelt und 2 Stdn. bei Zimmertemperatur stehen gelassen. Die Lösung wurde mit 50 ml Chloroform verdünnt, mehrmals mit Wasser gewaschen und mit $CaCl_2$ getrocknet. Die Chloroformlösung wurde eingeengt und der Rückstand aus Äthanol kristallisiert. Feine Nädelchen von **5** vom Schmp. 103—4 °C (2,9 g, 67%) $[\alpha]_D^{24}$ + 5,3° (c = 1,036 in $CHCl_3$); Lit. [3] Schmp. 118 °C, $[\alpha]_D^{25}$ + 9,8° ($CHCl_3$). NMR ($CDCl_3$): δ = 2,05—2,2 ppm (12H, 4 CH_3CO—), 4,05 (s. 2H, $ClCH_2CO$—), 4,2—5,5 (6H, Zuckerprotonen), 5,83 (d, 1H, J = 8 Hz, H-1).

1,3,4,6-Tetra-O-acetyl-β-D-glucopyranose (1

Thioharnstoff (0,1 g) und 0,5 g Calciumcarbonat wurden zu einer Lösung von 0,4 g **3** in 30 ml Methanol gegeben. Das Gemisch wurde 30 Min. lang am Rückfluß erwärmt. Die Umsetzung von **3** wurde durch DC verfolgt. Nach Zugabe von 50 ml Chloroform wurde mit 100 ml wässriger Essigsäure (1%) gewaschen. Die Chloroformschicht wurde mit Na_2SO_4 getrocknet, eingeengt und der erhaltene Sirup aus Äther–Hexan kristallisiert. Es ergab farblose Nadeln von **1** vom Schmp. 135—6 °C (0.16 g, 50%) $[\alpha]_D^{23}$ = +25° (c = 0,82 in $CHCl_3$); Lit. [3], Schmp. 136—7 °C, $[\alpha]_D^{25}$ + 26° ($CHCl_3$). NMR ($CDCl_3$): δ = 2,05—2,2 ppm (12H, 4 CH_3CO—), 2,85 (1H, breit verschwindet bei Zusatz von D_2O, —*OH*), 3,6—5,2 (6H, Zuckerprotonen), 5,65 (d 1H, J = 8 Hz, H-1).

Diese Reaktion ist auch mit mehrfachen Mengen von **3** durchführbar.

1,3,4,6-Tetra-O-acetyl-2-O-chloracetyl-α-D-galactopyranose (8)

hergestellt analog wie **3** ausgehend vom **7** [2] in 86%iger Ausbeute. Farblose Nadeln vom Schmp. 115—8 °C, $[\alpha]_D^{25} = +134{,}9°$ (c = 1,1951 in $CHCl_3$). Rf 0,7
NMR ($CDCl_3$): δ = 2,0—2,2 ppm (12H, $4CH_3CO$—), 4,0—4,5 (5H, —CH_2—O—$COCH_3$— —$COCH_2Cl$, CH) 5,35—5,6 (3H, Zuckerprotonen), 6,4 (d, 1H, J = 4 Hz, H-1).
$C_{16}H_{21}O_{11}Cl$ (424,8) Ber. C 45,23 H 4,98
Gef. C 45,21 H 4,75.

3,4,6-Tri-O-acetyl-2-O-chloracetyl-α-D-galactopyranosylbromid (9)

hergestellt analog wie **4** ausgehend von **8** in 90%iger Ausbeute, konnte nicht zur Kristallisation gebracht werden. Rf 0,8,
NMR ($CDCl_3$) δ = 1,05—2,15 ppm (9H, 3 CH_3CO—), 4,0—5,45 (8H, $ClCH_2CO$— und Zuckerprotonen), 6,7 (d, 1H, J = 4 Hz, H-1).

1,3,4,6-Tetra-O-acetyl-2-O-chloracetyl-β-D-galactopyranose (10)

hergestellt analog wie **5** ausgehend von **9** in 62%iger Ausbeute. Farblose Nadeln vom Schmp. 123—4 °C, $[\alpha]_D^{25} = +17{,}3°$ (c = 0,8204 in $CHCl_3$). Rf 0,7.
NMR ($CDCl_3$): δ = 1,95—2,2 ppm (12H, 4 CH_3CO—), 4,05 (s, 2H, $COCH_2Cl$), 4,15 (s, 3H, CH, —CH_2O—), 5,15—5,6 (3H, Zuckerprotonen), 5,8 (d, 1H, J = 8 Hz, H-1).
$C_{16}H_{21}O_{11}Cl$ (428,8) Ber. C 45,23 H 4,97
Gef. C 45,19 H 4,85

1,3,4,6-Tetra-O-acetyl-β-D-galactopyranose (6)

hergestellt analog wie **1** ausgehend von **10** in 56%iger Ausbeute. Farblose Nadeln vom Schmp 125—7 °C, $[\alpha]_D^{25} = +35{,}5°$ (c = 1,0193 in $CHCl_3$) Rf 0,42.
NMR ($CDCl_3$): δ = 2,05—2,25 ppm (12H, 4 CH_3CO—), 2,95 (1H, verschwindet bei Zusatz von D_2O, —OH), 3,5—5,5 (6H, Zuckerprotonen), 5,7 (d, 1H, J = 8 Hz, H-1)
$C_{14}H_{20}O_{10}$ (348,3) Ber. C 48,27 H 5,79
Gef. C 48,48 H 5,61

LITERATUR

[1] Reynolds, D. D., Evans, W. L.: J. Am. Chem. Soc. **60,** 2559 (1938)
[2] Helferich, B., Zirner, J.: Chem. Ber. **95,** 2604 (1962)
[3] Lemieux, R., Huber, G.: Canad. J. Chem. **31,** 1040 (1953)
[4] Koeppen, B. H.: Carbohyd. Res. **7,** 410 (1968)
[5] Koeppen, B. H.: Tetrahedron **24,** 4963 (1968)
[6] Koeppen, B. H.: Carbohyd. Res. **24,** 154 (1972)
[7] Chari, V. M., Wagner, H.: Chem. Ber. **109,** 426 (1976)
[8] Bertolini, M., Glaudemans, C. P. J.: Carbohyd. Res. **15,** 263 (1970)

V. M. Chari
M. Jordan
H. Wagner
8 München 2, Karlstr. 29, BRD

RECENSIONES

Corrosion Inhibitors. Manufacture and Technology

By Maurice William RANNEY

Noyes Date Corp., Park Ridge, New Yersey, U.S.A.—London, U.K., 1976

Based on a systematic digest of the processes patented in the U.S.A. between 1972 and 1975 the inhibitors used for corrosion prevention, and the technologies of their application, are described.

This is a very useful, informative review that embraces a wide field of technology; both research and technical staff engaged in the field of corrosion prevention by inhibitors can be recommended to peruse it.

The chapters of the book review the most important domains of the application of inhibitors.

Cooling-water systems, warm-water facilities, water works.

Here inhibitors applied for the prevention of corrosion damages in pipeline — reservoir systems are dealt with, also inhibitors added to antifreeze mixtures, and specifics used for the diminution of corrosion damages in units for the delivery of hot water or of steam.

Acid pickling processes.

The reduction by inhibitors, of the etching effects of acids used in metal pickling and surface finishing processes, is discussed here. By these inhibitors over-etching to acid is prevented, in their presence only the surface layer oxide are removed.

Inhibitors in the oil- and gas industries

Included are the additives that work against the destruction of metal apparatus used for the acid treatment of gases, also the protection applied to underground piping and storage tanks.

Inhibitors used in the automotive and aviation industries

These are the additives to fuels and to lubricating oils as well as those used in the hydraulic system of aircraft.

A substantial part of this comprehensive study deals with the materials successfully used in the protective treatment of metal surfaces. Within this section we find the formation of inorganic nonmetallic coatings like chromates, oxides, phosphates for the protection of aluminium, zinc, and iron; also the organic lacquer coatings which contain inhibitors, the so-called inhibitor-pigmented preparations are mentioned as well as products and inhibitors for the de-greasing, cleaning of metal surfaces.

A complete chapter deals with the additives found suitable for the prevention of the deterioration by corrosion of the metals most extensively applied, *i.e.* of steel, copper, and aluminium.

A register alphabetically ordered according to patentees, and to inventors, enhances the usefulness of this very good review which certainly will help specialists in research or industrial practice or in patent affairs.

The concise information based upon the systematization and description of patents readily lends itself to perusal and engages the attention and interest of staff dealing with corrosion problems.

E. LICHTENBERGER-BAJZA

MARSHALL SITTIG: *Aromatic Hydrocarbons — Manufacture and Technology*
Chemical Technology Review No. 56

Noyes Data Corporation, Park Ridge, New Yersey, 1976. 357 pp., 116 figures

The importance of aromatic hydrocarbons among the petrochemical feedstocks has further increased in recent years. With the rise of the crude oil prices it is even more important than before to be acquainted with the latest refining and petrochemical technologies giving the greatest possible amounts and exactly the desired product distributions of aromatics and/or aromatic derivatives from a unit amount of crude oil. Thus, the publication of M. SITTIG's book is timely and welcome.

The book consists of 16 chapters, the first nine describing the manufacture and separation of the industrially important aromatics, the others dealing with the manufacture of their derivatives.

In the introductory chapter, the author describes the most important physical properties, actual and potential uses and market position of benzene and the C_7—C_{12} alkylbenzenes. The market survey is based on the latest commercial data, but the production and consumption data refer mainly to the U.S.

The second chapter deals with the production of BTX aromatics from different feedstocks. Thus, the manufacture of benzene, toluene and xylenes from pyrolysis gasoline, by catalytic reforming of naphtha, by aromatization of alcohols, from C_5 hydrocarbons, from coal tar and from coal hydrogenation products is described in this chapter.

Among the catalytic reforming processes only those are dealt with which do feature aromatics separation. The author also describes a few processes producing olefins, acetylene, etc. as co-products along with aromatics. A special value of the second chapter is the comparatively detailed discussion of such reforming technologies which use particular catalyst compositions besides, or instead of, the generally applied $Pt–Al_2O_3$ or $Pt–Re–Al_2O_3$ catalysts. Some of these processes use tungsten, tin, iridium, etc., instead of rhenium as a second metal in the catalyst compositions. The aim of these metal components is to increase the dehydrocyclization activity of the catalysts.

Several processes are also described where dehydrocyclization is accomplished with zeolite type catalysts.

The third chapter deals with the production of naphthalene, the fourth with the manufacture of diphenyl from benzene and with that of phenylnaphthalene from benzene and naphthalene.

From chemical engineering aspects, the next chapter is very valuable giving a good review on the separation of aromatics from paraffins. The sixth chapter deals with the purification of aromatics.

In the seventh chapter, the author discusses the production and mainly the transformation of alkylbenzenes. However, the transalkylation technology known under the name 'Tatoray' could not be found among the processes reviewed. This process gives benzene, xylenes and small quantities of C_{10} aromatics from toluene and a C_9 aromatics fraction.

The separation of individual alkylbenzenes is reviewed in the eighth chapter, where the most detailed discussion is given naturally to the separation of C_8 aromatics.

One short chapter describes the production and separation of alkylnaphthalenes, and then the autor proceeds to review the manufacturing technologies of aromatic derivatives.

Separate chapters deal with the hydrogenation, sulfonation, oxidation, halogenation and nitrogen derivatives of aromatics. The greatest volume is devoted to the oxidation of aromatics, quite rightly, because the manufacture of several synthetic fibers, plastics and resins is based on these reactions. The 15th chapter has the title "Dehydrogenation of Alkylaromatics", but it would be more correct to give the title "Dehydrogenation of Ethylbenzene" to this chapter, as it reviews exclusively the technologies converting ethylbenzene to styrene.

In the last chapter of the book a few estimations concerning future aromatics production and demand are very shortly reviewed.

The book — as its title also suggests — deals with the manufacturing technologies of aromatic hydrocarbons and their derivatives. The chemical, reaction kinetic, thermodynamic and catalytic issues forming the bases of these technologies are not at all, or just per tangentem discussed. This is not mentioned as a fault of the book, but for orientation of those persons who look for this type of information. In compiling this book, the author based his work almost entirely on the U.S. patent literature, other sources, data published in journals

were used only in the description of the market position of the individual aromatics and in reviewing their production data.

Thus, the book of Marshall SITTIG is restricted to the short description of about 300 processes patented recently in the U.S. The author deals only with U.S. patents, and this feature — although big British, French, German, Japanese, etc. companies have their significant processes patented also in the U.S. — resulted in a certain onesidedness.

A great advantage of the book is the freshness of the reviewed material. The patents described date almost entirely from the period after 1964 and most of them have been granted after 1970. The short time between the writing and publication of the book is remarkable and should be appreciated: several patents dating from the second half of 1975 are discussed.

Simplified flow sheets of the more important processes are also given in the book, and the respective technologies are described in accordance with the flow-sheet.

At the end of the book indexes of the described patents, the inventors and companies holding the patents can be found; these make the orientation much easier.

Volume 56 of the Chemical Technology Review gives a valuable survey of the recent and latest manufacturing technologies of aromatic hydrocarbons and their derivatives for technology experts and, at the same time, it is a well compiled guide to the U.S. patent literature in this field.

I. SZEBÉNYI

YALE L. MELTZER: *Water-soluble Resins and Polymers Technology and Applications Chemical Technology Review No. 57*

Noyes Data Corporation, Park Ridge, New Jersey—London, England, 1976. 371 pp., 43 figures, 47 tables

The book is based on U.S. patents issued since 1966, dealing with the technology and application of water-soluble resins and polymers. The book comprises the following chapters:

Introduction
Market survey
Acrylamide polymers
Acrylic acid and methacrylic acid polymers
Cellulose ethers and other cellulose derivatives
Sodium carboxymethylcellulose (CMC)
Hydroxyethylcellulose (HCE)
Hydroxypropylcellulose (HPC)
Methylcellulose (MC)
Ethylcellulose (EC)
Ethylene oxide polymers and related products
Polyamide resins
Polyethyleneimine (PEI) and related products
Polyvinyl alcohol (PVA)
Polyvinylpyrrolidone (PVP) and related products
Starch, modified starch and starch derivatives
Natural gums
Inorganic stannic oxide polymers

Water-soluble resins and polymers form a special group of the high-polymeric compounds. Over the past 25 years their dynamic growth has centered in the synthetic polymers such as the cellulose ethers, polyvinyl alcohol (PVA), acrylamide polymers, ethylene oxide polymers, polyethyleneimine (PEI) and polyvinylpyrrolidone (PVP). They have made inroads into the traditional starch and natural gum markets, and served to expand their market through the development of new applications. Some of the main uses of water-soluble resins and polymers are in adhesives, binders, cakes, candies, cements, chromatography, clarifiers, coatings, cosmetics, detergents, emulsifiers, explosives, flavor additives, granulating agents, hair sprays, hand lotions, ice-cream, inks, laxatives, lithography, oil-well drilling, ointment compositions,

packaging, paints, paper, pharmaceuticals, pollution control, salad dressing, sizing agents, suspending agents, thickeners, warp sizes and water loss agents.

Connected with the individual chapters the book discusses in detail the processing and applications of water-soluble polymers, comprising the most important results.

Owing to its content, the book will undoubtedly win high acclaim among macromolecular chemists for its close relation to subjects originating during the last decade. Perhaps the only thing which might be objected is that the last chapter is somewhat outside the subject-matter.

The edition of the book shows careful work; misprints and errors were not found, the typography of the figures, formulas and tables is excellent.

The book may be recommended to industrial specialists as well as chemical engineers, technologists and scientific researchers.

I. GÉCZY

INDEX

PHYSICAL AND INORGANIC CHEMISTRY

ORGANIC CHEMISTRY

Printed in Hungary

A kiadásért felel az Akadémiai Kiadó igazgatója — Műszaki szerkesztő: Zacsik Annamária

A kézirat nyomdába érkezett: 1977. I. 11. — Terjedelem: 9,8 (A/5) ív, 46 ábra

74.4034 Akadémiai Nyomda, Budapest — Felelős vezető: Bernát György

ACTA CHIMICA

ТОМ 93—ВЫП. 1

РЕЗЮМЕ

Эффект циклической структуры на радиолиз углеводородов, IV
Радиолиз алкилциклопентанов и алкилциклогексанов, II. О некотрых бирадикальных проблемах

Л. ВОЙНАРОВИЧ и Г. ФЕЛЬДИАК

Обобщая более ранние результаты, на основе радиолиза циклопентановых и циклогексановых соединений с нормальными и разветвленными боковыми цепочками, C_nH_{2n} было установлено, что алкены с открытой цепочкой C_nH_{2n}, получаемые в качестве основного продукта за счет разрыва связи С—С — в соотвествии с энергетическими условиями — в основном образуются за счет разрыва связей С—С, присоединяющихся к атому углерода, располагающемуся у ответвления от кольца. Среди продуктов были всегда получены такие алкены, в которых двойная связь находится у такого атома углерода.

Выход скелетно-изомерных продуктов уменьшается с увеличением длины боковой цепочки и ее разветвленностью. Боковые цепочки с их повышенной способностью к расщеплению, как-будто «внутримолекулярно» защищают кольцо от распада.

На основе результатов исследований с акцепторами радикалов было установлено, что некоторая часть скелетно-изомерных продуктов образуется в бимолекулярной реакции алкильных монорадикалов с открытой цепочкой. На оставшуюся, большую долю выхода, однако, акцепторы радикалов не оказывали никакого влияния. На основе экспериментальных результатов и различных аналогий вероятным кажется протекание «унимолекулярных» реакций через бирадикалы.

О кинетических уравнениях многоступенчатых электродных процессов, IV
Влияние адсорбции промежуточного продукта

Л. КИШ и Й. ФАРКАШ

Было выведено и обсуждено уравнение поляризационной кривой для многоступенчатой ионизации металлов и восстановления металлических ионов для такого случая, когда промежуточные продукты адсорбируются на поверхности электрода, и условия Лангмюра реализуются. Были определены те условия и кинетические параметры, при которых кривые $\varepsilon - \log j$ становятся прямыми (ε — потенциал электрода, j — плотность поляризующего тока).

Метод получения платиновых катализаторов, модифицированных адсорбированными металлами

Ш. САБО, Ф. НАДЬ и Д. МОГЕР

Был разработан метод получения платиновых катализаторов, модифицированных адсорбированными металлами, используемых при исследовании газофазных гетерогенных каталитических реакций.

Одновременно с этим был разработан метод, позволяющий определить, каким образом влияет адсорбция кислорода воздуха и термообработка на воздушно-сухие, модифицированные катализаторы.

Метод демонтрируется на примере платиновых катализаторов, покрытых медью. Было установлено, что ни адсорбция кислорода, ни термообработка вплоть до 100°C не вызывают изменений в свойствах платиновых катализаторов, покрытых адсорбированной медью. В случае платиновых катализаторов, покрытых золотом, исходные свойства сохраняются вплоть до 350°C.

Комплексы кобальта(II) с *N*-бензоилфенилгидроксиламином и бензгидроксамовой кислотой

А. СЯМАЛ и В. Д. ГАНЕКАР

Комплекс кобальта(II) с N-бензоилфенилгидроксиламином и бензгидроксамовой кислотой были синтезированы и охарактеризованы на основе их ИК и электронных спектров, а также измерений магнитной восприимчивости. Комплексы имеют розовый цвет и тетрагональную структуру. Комплексы очень стабильны и не окисляются даже при продолжительном нагреве (несколько часов) при 110°C.

Расчёт декартовых координат и замыкание циклов молекулярных моделей

Б. РОЖОНДАИ

Предложен метод расчёта декартовых координат из геометрических параметров молекулярных моделей. Метод позволяет простое определение координат групп, находящихся на разных местах молекулы, и вычисление координат атомов, замыкающих несимметричный цикл.

Взаимодействие моно- и диарилиденциклоалканонов с тиокарбамидом и роданидом аммония

Т. ЛОРАНД, Д. САБО и А. НЕСМЕИ

2-Арилиденциклогексаноны, взаимодействуя с роданидом аммония и тиокарбамидом, дают 4-арил-3,4,5,6,7,8 - гексагидро-2(1H)-хиназолинтионы (**Ia—f**). 2-Арилиденциклопентаноны с роданидом аммония дают N,N'-бис[(2-арилиден)-циклопентилиден]-тиокарбамид (**IIa—b**), а с тиокарбамидом 7H-4-арил-3,4,5,6-тетралидро-2(1H)-циклопентапиримидинтион (**IIIa—b**). 2,6-Диарилиденциклогексаноны не реагируют с роданидом аммония, а с тиокарбамидом дают 4-арил-8-арилиден-3,4,5,6,7,8-гексагидро-2(1H)-хиназолинтион(**IVa—f**). Взаимодействие 2,5-дибензилиденциклопентанона с тиокарбамидом приводит к образованию 7H-7-бензилиден-4-фенил-3,4,5,6-тетрагидро-2(1H)-циклопентапиримидинтиона (**V**). Обсуждается механизм вышеупомянутых реакций. Окисление **Ia** и **IVa** приводит к соответствующим производным 2-оксогексагидрохиназолина (**VI**, **VII**).

Сульфенхлориды, X
Сульфенирование некоторых тиоамидов трихлорметансульфенхлоридом

Г. ШТАЙЕР, Д. КОРБОНИЧ, А. Е. САБО, Ф. КЛИВЕНИ и Е. ЕИНКЛЕР

1,3,4-Окса- и -тиадиазол-5-тионы, а также динатрийэтилен-бис-дитиокарбаматы, взаимодействуя с трихлорметансульфенхлоридом, дают — в противоположность до сих пор распространенным в литературе представлениям — дисульфиды. Одновременно, двойное сульфенирование алкил- и арилдитиокарбаматов приводит к образованию бис-дитиопроизводных иминометана.

Исследование реакций ацилирования диэтил-(иминокарбоната), I
Ацилирование монофункциональными хлоридами кислот и хлорформиатами

З. БЕНДЕ, И. БИТТЕР и З. ЧЮРЁШ

В реакциях диэтил-(иминокарбоната) с хлоридами карбоновых кислот, а также с хлорформиатами, в качестве основных продуктов образуются N-ацилипроизводные исходного вещества, а в качестве побочного продукта при хлорформиатном ацилировании — этилкарбамат и при ацилировании хлоридами кислот — производные этилкарбамата и этил-(N-ацилкарбамата).

В согласии с механизмом ацилирования было доказано, что при использовании органического фиксатора кислоты могут быть получены новые диэтил-(N-ацилиминокарбонатные) производные.

Исследование реакции ацилирования диэтил-(иминокарбоната), II
Ацилирование фосгеном и хлористым оксалилом

З. БЕНДЕ, И. БИТТЕР и З. ЧЮРЁШ

При исследовании реакции диэтил-(иминокарбоната) с фосгеном или хлористым оксалилом было установлено, что в зависимости от условий реакции могут быть получены различные продукты: производные карбетокси-изокарбамида или оксамида. В зависимости от условий реакции и на основе образующисхя промежуточных и конечных продуктов был установлен механизм протекающих реакций.

Новый синтез 3,4-дигидро- и 1,2,3,4-тетрагидрохиназолинов и их стереохимические исследования

Й. ФИШЕР, Г. ТОТ и П. ВАГО

3,4-Дигидрохиназолины образуются при взаимодействии α-галогенэфиров ($R_2 = H$) с 4-замещенными анилинами в тетрагидрофуране; 1.2,3,4-тетрагидрохиназолины образуются из таких α-галогенэфиров, которые содержат электроноакцепторную группу ($R_2 = COOC_2H_5$). Последняя реакция является стереоселективной, цис-изомер представляет собой главный продукт реакции. Смесь цис/транс дает протоннокатализированное равновесие. Изомеры были идентифицированы методом ЯМР.

Получение 1,3,4,6-тетра-O-ацетил-β-D-глюко- и галактопираноз и их α-гликозилбромидных производных

В. М. ЧАРИ, М. ЙОРДАН и Х. ВАГНЕР

По упрощенной методике и с высоким выходом были получены 1,3,4,6-тетра-O-ацетил-β-D-глюко- и галактопиранозы и их α-гликозилбромидные производные, которые служат исходными соединениями в синтезе самбубиозы и 2-O-ацил-глюкозида и -галактозида.

ANALYSIS OF STEROID HORMONE DRUGS

By **S. GÖRÖG** and **GY. SZÁSZ**

The early chapters of this book deal with fundamentals of structure, chemical reactions and therapeutic use of steroid hormones and summarize the development of techniques for their analysis. Various spectroscopic and other physical techniques for analysis are dealt with in the following chapters, but special emphasis is placed on chromatographic methods, particularly gas chromatography. The final chapters deal with analysis of functional groups, and provide practical details for analysing steroid hormones and the raw materials used in their semi-synthesis.

In English – Approx. 353 pages – Cloth

A co-edition – distributed in the socialist countries by KULTURA, Budapest, ISBN 963 05 1223 8; in all other countries by ELSEVIER PUBLISHING CO., Amsterdam

AKADÉMIAI KIADÓ
Budapest

ELSEVIER PUBLISHING CO.
Amsterdam

Simul — Ein Programm für die mathematische Simulation von verfahrenstechnischen Systemen

Herausgegeben von P. Benedek

Autorenkollektiv: G. Almásy, P. Benedek, M. Farkas,
I. Pallai, F. Simon, P. Szepesváry,
T. Sztanó

Das Buch gibt dem Leser eine Vorstellung über die Möglichkeiten, die für die chemische Technologie durch den Einsatz von Digitalrechnern geboten werden. Es vermittelt die von den Autoren angewendeten Methoden zur Errechnung physikalisch-chemischer Größen, beschreibt die zur Simulation der einzelnen Operationen ausgearbeiteten Modelle, und führt vor Augen, wie immer ein kompletter chemisch-technologischer Verfahrenszug in seinem stationänen Ablauf von dem SIMUL-System simuliert werden kann. Die mit speziellen Problemen einhergehenden Regelungs-, Rezirkulations- und Optimalisierungsfälle werden auch im besonderen auseinandergesetzt. Das letzte Kapitel demonstriert am Beispiel einer Anlage für Essigsäureanhydriderzeugung die Anwendung des SIMUL-Systems.

In deutscher Sprache · Etwa 320 Seiten · Ganzleinen
ISBN 963 05 1111 8

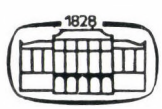

AKADÉMIAI KIADÓ
Verlag der Ungarischen Akademie der Wissenschaften
Budapest

Allgemeine und anorganische Chemie in Frage und Antwort

Von Dr. Dr. h. c. ERICH THILO, Berlin,
und Dr. GERT BLUMENTHAL, Berlin
15., neubearbeitete Auflage 1976
286 Seiten, 30 Abbildungen
Plasteinband 10,40 M; Ausland 12,— M. Bestell-Nr. 793 419 3

Der Band enthält eine Fülle auf dem neuesten Wissensstand basierenden Stoffes der allgemeinen und anorganischen Chemie. Auch wichtige chemische Details und Reaktionen werden aufgeführt. Um eine bessere Übersicht zu erreichen sind die Hauptabschnitte in Form der Dezimalklassifikation untergliedert, die einzelnen, Fragen dagegen durchnumeriert. Das Werk vermittelt als Repetitorium wie bisher die Fakten, die theoretischen Zusammenhänge und die Probleme.

Bestellungen an den Buchhandel erbeten

JOHANN AMBROSIUS BARTH LEIPZIG

Les Acta Chimica paraissent en français, allemand, anglais et russe et publient des mémoires du domaine des sciences chimiques.

Les Acta Chimica sont publiés sous forme de fascicules. Quatre fascicules seront réunis en un volume (4 volumes par an).

On est prié d'envoyer les manuscrits destinés à la rédaction à l'adresse suivante:

Acta Chimica
H-1521 Budapest, Hongrie

Toute correspondance doit être envoyée à cette même adresse.

La rédaction ne rend pas de manuscript.

Le prix de l'abonnement est de $ 32,00 par;volume.

Abonnement — en Hongrie à l'Akadémiai Kiadó (1363 Budapest, P.O.B, 24. C.C.B. Bankszámla) 215 11488 à l'étranger à l'Enterprise pour le Commerce Extérieur «Kultúra» (1389 H-Budapest 62, P.O.B. 149 Compte-courant No. 218 10990) ou l'étranger chez tous les représentants ou dépositaires.

Die Acta Chimica veröffentlichen Abhandlungen aus dem Bereich der chemischen Wissenschaften in deutscher, englischer, französischer und russischer Sprache.

Die Acta Chimica erscheinen in Heften wechselnden Umfanges. Vier Hefte bilden einen Band. Jährlich erscheinen 4 Bände.

Die zur Veröffentlichung bestimmten Manuskripte sind an folgende Adresse zu senden:

Acta Chimica
H-1521 Budapest, Ungarn

An die gleiche Anschrift ist auch jede für die Redaktion bestimmte Korrespondenz zu richten.

Manuskripte werden nicht zurückerstattet.

Abonnementspreis pro Band: $ 32,00.

Bestellbar für das Inland bei Akadémiai Kiadó (1363 Budapest, Postfach 24, Bankkonto Nr. 215 11488), für das Ausland bei dem Außenhandelsunternehmen „Kultúra" (1389 Budapest 62, P.O.B. 149. Bankkonto Nr. 218 10990) oder bei seinen Auslandsvertretungen und Kommissionären.

«Acta Chimica» издает статьи по химии на русском, французском, английском и немецком языках.

«Acta Chimica» выходит отдельными выпусками разного объема, 4 выпуска составляют один том и за год выходит 4 тома.

Предназначенные для публикации рукописи следует направлять по адресу:

Acta Chimica
H-1521 Budapest, ВНР

Всякую корреспонденцию в редакцию направляйте по этому же адресу.

Редакция рукописей не возвращает.

Подписная цена — $ 32,00 за том.

Отечественные подписчики направляйте свои заявки по адресу Издательства Академии Наук (1363 Budapest, P.O.B. 24, Текущий счет 215 11488), а иностранные подписчики через организацию по внешней торговле «Kultúra» (1389 H-Budapest 62, P.O.B. 149. Текущий счет 218 10990 или через ее заграничные представительства и уполномоченных.

Reviews of the Hungarian Academy of Sciences are obtainable at the following addresses:

AUSTRALIA
C.B.D. LIBRARY AND SUBSCRIPTION SERVICE, Box 4886, G.P.O., *Sydney N.S.W. 2001*
COSMOS BOOKSHOP, 145 Ackland Street, *St. Kilda (Melbourne), Victoria 3182*

AUSTRIA
GLOBUS, Höchstädtplatz 3, *1200 Wien XX*

BELGIUM
OFFICE INTERNATIONAL DE LIBRAIRIE, 30 Avenue Marnix, *1050 Bruxelles*
LIBRAIRIE DU MONDE ENTIER, 162 Rue du Midi, *1000 Bruxelles*

BULGARIA
HEMUS, Bulvar Ruszki 6, *Sofia*

CANADA
PANNONIA BOOKS, P.O.Box 1017, Postal Station "B", *Toronto, Ontario M5T 2T8*

CHINA
CNPICOR, Periodical Department, P.O.Box 50, *Peking*

CZECHOSLOVAKIA
MAD'ARSKÁ KULTURA, Národní třida 22, *115 66 Praha*
PNS DOVOZ TISKU, Vinohradská 46, *Praha 2*
PNS DOVOZ TLAČE, *Bratislava 2*

DENMARK
EJNAR MUNKSGAARD, Norregade 6, *1165 Copenhagen*

FINLAND
AKATEEMINEN KIRJAKAUPPA, P.O.Box 128, *SF-00101 Helsinki 10*

FRANCE
EUROPÉRIODIQUES S. A., 31 Avenue de Versailles, *78170 La Celle St.-Cloud*
LIBRAIRIE LAVOISIER, 11 rue Lavoisier, *75008 Paris*
OFFICE INTERNATIONAL DE DOCUMENTATION ET LIBRAIRIE, 48 rue Gay-Lussac, *75240 Paris Cedex 05*

GERMAN DEMOCRATIC REPUBLIC
HAUS DER UNGARISCHEN KULTUR, Karl-Liebknecht-Strasse 9, *DDR-102 Berlin*
DEUTSCHE POST, ZEITUNGSVERTRIEBSAMT, Strasse der Pariser Kommüne 3—4, *DDR-104 Berlin*

GERMAN FEDERAL REPUBLIC
KUNST UND WISSEN, ERICH BIEBER, Postfach 46, *7000 Stuttgart 1*

GREAT BRITAIN
BLACKWELL'S PERIODICALS DIVISION, Hythe Bridge Street, *Oxford OX1 2ET*
BUMPUS, HALDANE AND MAXWELL LTD., Cowper Works, *Olney, Bucks MK46 4BN*
COLLET'S HOLDINGS LTD., Denington Estate, *Wellingborough, Northants NN8 2QT*
WM. DAWSON AND SONS LTD., Cannon House, *Folkestone, Kent CT19 5EE*
H. K. LEWIS AND CO., 136 Gower Street, *London WC1E 6BS*

GREECE
KOSTARAKIS BROTHERS, International Booksellers, 2 Hippokratous Street, *Athens-143*

HOLLAND
MEULENHOFF-BRUNA B.V., Beulingstraat 2, *Amsterdam*
MARTINUS NIJHOFF B.V., Lange Voorhout 9—11, *Den Haag*
SWETS SUBSCRIPTION SERVICE, 347b Heereweg, *Lisse*

INDIA
ALLIED PUBLISHING PRIVATE LTD., 13/14 Asaf Ali Road, *New Delhi 110001*
150 B-6 Mount Road, *Madras 600002*
INTERNATIONAL BOOK HOUSE PVT. LTD., Madame Cama Road, *Bombay 400039*
THE STATE TRADING CORPORATION OF INDIA LTS., Books Import Division, Chandralok, 36 Janpath, *New Delhi 110001*

ITALY
EUGENIO CARLUCCI, P.O.Box 252, *70100 Bari*
INTERSCIENTIA, Via Mazzé 28, *10149 Torino*
LIBRERIA COMMISSIONARIA SANSONI, Via Lamarmora 45, *50121 Firenze*
SANTO VANASIA, Via M. Macchi 58, *20124 Milano*
D. E. A., Via Lima 28, *00198 Roma*

JAPAN
KINOKUNIYA BOOK-STORE CO. LTD., 17-7 Shinjuku 3 chome, Shinjuku-ku, *Tokyo 160-91*
MARUZEN COMPANY LTD., Book Department, P.O.Box 5050 Tokyo International, *Tokyo 100-31*
NAUKA LTD. IMPORT DEPARTMENT, 2-30-19 Minami Ikebukuro, Toshima-ku, *Tokyo 171*

KOREA
CHULPANMUL, *Phenjan*

NORWAY
TANUM-CAMMERMEYER, Karl Johansgatan 41—43, *1000 Oslo*

POLAND
WĘGIERSKI INSTYTUT KULTURY, Marszałkowska 80, *Warszawa*
CKP I W ul. Towarowa 28 *00-958 Warsaw*

ROUMANIA
D. E. P., *Bucureşti*
ROMLIBRI, Str. Biserica Amzei 7, *Bucureşti*

SOVIET UNION
SOJUZPETCHATJ — IMPORT, *Moscow*
and the post offices in each town
MEZHDUNARODNAYA KNIGA, *Moscow G-200*

SPAIN
DIAZ DE SANTOS, Lagasca 95, *Madrid 6*

SWEDEN
ALMQVIST AND WIKSELL, Gamla Brogatan 26, *101 20 Stockholm*
GUMPERTS UNIVERSITETSBOKHANDEL AB, Box 346, *401 25 Göteborg 1*

SWITZERLAND
KARGER LIBRI AG, Petersgraben 31, *4011 Base*

USA
EBSCO SUBSCRIPTION SERVICES, P.O.Box 1943, *Birmingham, Alabama 35201*
F. W. FAXON COMPANY, INC., 15 Southwest Park, *Westwood, Mass, 02090*
THE MOORE-COTTRELL SUBSCRIPTION AGENCIES, *North Cohocton, N. Y. 14868*
READ-MORE PUBLICATIONS, INC., 140 Cedar Street, *New York, N. Y. 10006*
STECHERT-MACMILLAN, INC., 7250 Westfield Avenue, *Pennsauken N. J. 08110*

VIETNAM
XUNHASABA, 32, Hai Ba Trung, *Hanoi*

YUGOSLAVIA
JUGOSLAVENSKA KNJIGA, Terazije 27, *Beograd*
FORUM, Vojvode Mišiča 1, *21000 Novi Sad*

ACTA CHIMICA

ACADEMIAE SCIENTIARUM HUNGARICAE

TOMUS 93 FASCICULUS 2

AKADÉMIAI KIADÓ, BUDAPEST

1977

ACTA CHIM. (BUDAPEST) ACASA2 93 (2) 107–214 (1977)

ACTA CHIMICA

A MAGYAR TUDOMÁNYOS AKADÉMIA KÉMIAI TUDOMÁNYOK OSZTÁLYÁNAK IDEGEN NYELVŰ KÖZLEMÉNYEI

Acta Chimica is a journal for the publication of papers on all aspects of chemistry in English, German, French and Russian languages.

Acta Chimica is published in 4 volumes per year. Each volume consists of 4 issues of varying size.

Manuscripts should be sent to

Acta Chimica
H-1521 Budapest, Hungary

Correspondence with the Editors should be sent to the same address. Manuscripts are not returned to the Authors.

Subscription rate $ 32.00 per volume.

Hungarian subscribers should order from Akadémiai Kiadó, 1363 Budapest, P.O. Box 24. Account No. 215 11488.

Orders from other countries are to be sent to "Kultúra" Foreign Trade Company (H-1389 Budapest 62, P.O. Box 149. Account No. 218 10990) or to its representatives abroad.

Acta Chimica Academiae Scientiarum Hungaricae, Tomus 93 (2), pp. 107—116 (1977)

APPLICABILITY OF THE PPP AND CNDO/2 METHODS FOR THE STRUCTURAL INVESTIGATION OF ORGANOSILICON COMPOUNDS I

J. RÉFFY, T. VESZPRÉMI, P. HENCSEI and J. NAGY

(Department of Inorganic Chemistry, Technical University of Budapest)

Received May 20, 1976

Quantumchemical calculations related to the molecular structure of phenylhalogenosilanes, phenoxysilanes and vinyl, allyl, phenyl, benzyl derivatives of IV./1. group elements were carried out by PPP, iterativ PPP and CNDO/2 methods. Among other things the charge distribution, dipole moment, electron transition energies, ionization energies of the molecules were calculated. Based on the comparison of the calculated and experimental data conclusions on the bond structures were drawn.

Introduction

Study on organometallic compounds has been in progress in the Department of Inorganic Chemistry of Budapest Technical University for more than twenty years. Our interest has been focussed particularly on the organic compounds of silicon, germanium and tin. The research work has included the preparation of a number of compounds, study of their industrial application, carrying out physico-chemical measurements, the interpretation of the experimental results and by the help of these results the structural investigation of these compounds. This way the application of quantumchemical methods is closely related to the research work in the Institute. Relatively few papers have been published on the quantumchemical interpretation of the structure of organosilicon compounds. The main difficulty of the calculations for these molecules as compared with organic molecules is caused by the presence of the silicon d orbitals. From among the quantumchemical methods first of all the PPP, iterativ PPP and CNDO/2 methods have been applied in our work for the investigation of structural problems. In order to study the scope of application of these methods calculations have been carried out for numerous compounds. In this paper some results of our calculations are presented.

Parameters

The necessary input parameters of our PPP calculations [1, 2] were chosen as follows. The valence state ionization energies and electron affinities were taken mainly on the basis of the work of HINZE and JAFFE [3, 4]. The

ionization energy and electronic repulsion integral of silicon $3d$ orbital were chosen −1.10 eV and 3.762 eV, respectively according to LEVISON and PERKINS [5]. For the calculation of the two-center electronic repulsion integrals the MATAGA—NISHIMOTO equation [6] was used. The resonance integrals were calculated by the WOLFSBERG—HELMHOLZ formula [7]. The value of proportionality factor k was determined from the resonance and overlap integrals of carbon–carbon bond in benzene [8]. The configuration interaction (CI) was taken into account in our calculations, and for larger molecules partial CI was applied.

The most important PPP parameters are summarized in Table I. In the

Table I

PPP parameters (in eV)

i	$-U_i$	γ_{ii}	i—j	$-\beta^0_{ij}$
C	11.16	11.13	C—C	2.39
N^+	28.733	16.776	C—N	1.73—2.07
O	17.693	15.217	C—O	2.15
O^+	32.9	21.53	N—O	2.41
F^+	39.964	21.713	C—F	1.92
Cl^+	26.675	12.949	C—Cl	1.76
Si	1.10	3.762	Si—C	1.02—1.32
Ge	0.984	3.762	Si—N	0.97—1.10
Sn	0.786	3.762	Si—O	1.26
			Si—F	2.36
			Si—Cl	0.65
			Ge—C	0.86
			Sn—C	0.88

Table II

The values of constants in the equation for calculating the ionization energy ($U_i = -a_i \exp(b_i Z_i^*)$)

i	a_i	b_i
C	0.6133	1.0362
N^+	0.9702	0.8723
O	0.7093	0.8144
O^+	0.8660	0.8459
F^+	0.7093	0.8144
Si	0.2066	0.9555
Cl^+	0.4348	0.7417

case of iterativ PPP method [9, 10] only the ionization energies were varied, the rest of the input parameters was taken as constant. The ionization energies were calculated from the BURNS effective nuclear charges [11] on the basis of exponential relations. The relations were determined from the data of isoelectronic series belonging to the same electronic state. The values of the constants in the used relations are represented in Table II.

The CNDO/2 calculations [12, 13, 14] were carried out with *s*, *p* and *d* basis by the original POPLE—BEVERIDGE program [15].

Results

We studied the molecular structure of *phenylhalogenosilanes* by PPP and iterativ PPP methods. The aim was to reproduce the ultraviolet spectra of the compounds investigated. The calculated and measured ultraviolet transitions are presented in Table III. It is worthy of mentioning that proper results were obtained for not only the position of the peaks but also for the intensities. The iterativ PPP results were somewhat worse.

The dipole moments of the compounds were calculated, too. The dipole moments were given as the vectorial addition of the μ_π dipole moments obtained by PPP method and dipole moments of the σ systems. For the latter purpose we modified the DEL RE method [17] and extended it for organosilicon compounds. As it can be seen in Table IV the experimental and calculated data agreed with a difference of 0.1—0.2 D. The only exception was the phenyltrifluorosilane, where the difference was rather large: 0.5 D. It can be accepted that the parameters used in the calculations are appropriate, and some molecular factor which has not been taken into consideration is responsible for the mentioned anomaly. For this reason it was supposed that the F–Si–F bond angles were less than tetrahedral and the total energy of the molecule was calculated in the function of the F–Si–F angle. By this method the value of the bond angle can be predicted. Since the DEL RE and PPP calculations are generally not used for the estimation of bond angles, we carried out CNDO/2 calculations as well. The results are shown in Fig. 1.

It can be seen that at about 107.5° *i.e.* at the minimum of the total energy the CNDO method results in a calculated dipole moment which is nearly the same as the experimental one. At the same time the DEL RE and PPP method provides a correct value for the dipole moment at about 103°. Although the value around 107° appears to be more probable, both methods indicated identical trend. In the methyltrifluorosilane with similar structure the F–Si–F angle is 106.5° (as it was determined by microwave spectroscopy [19]), and based on electron diffraction measurement ALEKSEJEV found this bond angle in phenyltrifluorosilane to be 106° [20].

Table III

Calculated and experimental ultraviolet transition energies of phenylhalogenosilanes (in eV)

Compound	PPP		IPPP		Exp. data [16]	
	$^1E_{CI}$	f	$^1E_{CI}$	f	ΔE	f
$C_6H_5SiF_3$	4.706 A''	0.0008	4.829 A''	0.0008	4.705	0.0041
	5.937 A'	0.0338	5.943 A'	0.0648	5.904	0.0954
$(C_6H_5)_2SiF_2$	4.695 A_2	0.0000	4.714 B_1	0.0006	4.687	0.0073
	4.696 B_1	0.0020	4.714 A_2	0.0000		
	5.809 B_2	0.1719	5.734 B_2	0.2595	5.740	0.1707
$CH_3(C_6H_5)SiF_2$	4.697 A''	0.0110	4.724 A''	0.0001	4.696	0.0033
	5.898 A'	0.0528	5.878 A'	0.0955	5.876	0.0927
$C_6H_5SiCl_3$	4.675 A''	0.0022	4.663 A''	0.0240	4.661	0.0041
	5.751 A'	0.1403	5.551 A'	0.2352	5.700	0.0909
$(C_6H_5)_2SiCl_2$	4.668 A_2	0.0000	4.656 A_2	0.0000		
	4.669 B_1	0.0041	4.657 B_1	0.0042	4.661	0.0076
	5.588 B_2	0.2896	5.323 B_2	0.3725	5.635	0.2267
$CH_3(C_6H_5)SiCl_2$	4.672 A''	0.0022	4.664 A''	0.0022	4.678	0.0029
	5.745 A'	0.1337	5.544 A'	0.2248	5.740	0.0846
$(C_6H_5)_3SiCl$	4.808 E	0.0003	4.711 A	0.0003		
	4.814 A	0.0004	4.711 E	0.0004	4.714	0.0056
	4.814 E	0.0004	4.712 E	0.0004		
	5.704 E	0.1809	5.467 E	0.2189		
	5.707 E	0.1748	5.472 E	0.2154	5.635	0.2946

Table IV

Calculated and experimental dipole moments of phenylhalogenosilanes (in Debye)

Compound	DEL RE + PPP	DEL RE + IPPP	Exper. data [18]
$C_6H_5SiF_3$	2.238	1.958	2.77
$(C_6H_5)_2SiF_2$	2.615	2.235	2.59
$(C_6H_5)_3SiF$	2.063	1.693	1.85
$C_6H_5SiCl_3$	2.246	2.296	2.21
$(C_6H_5)_2SiCl_2$	2.626	2.636	2.58
$(C_6H_5)_3SiCl$	2.123	2.023	2.16

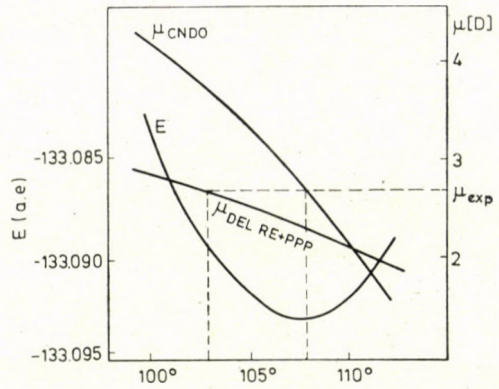

Fig. 1. Total energy and dipole moment of $C_6H_5SiF_3$ in the function of F–Si–F bond angle

Fig. 2 illustrates the charge distribution of phenyltrifluorosilane calculated by CNDO/2 and PPP + DEL RE methods. The nearly complete agreement of the silicon and fluor charges by the two methods is surprising. The charge distribution for phenyltrichlorosilane can be seen in Fig. 3. The trend

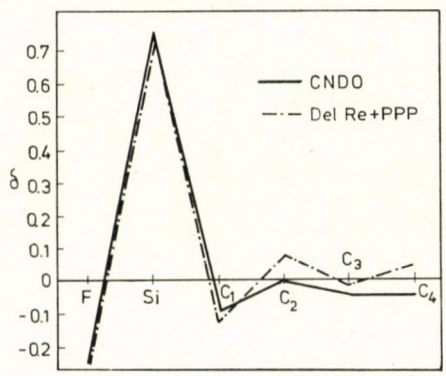

Fig. 2. Partial charges in $C_6H_5SiF_3$ by DEL RE + PPP and CNDO/2 methods

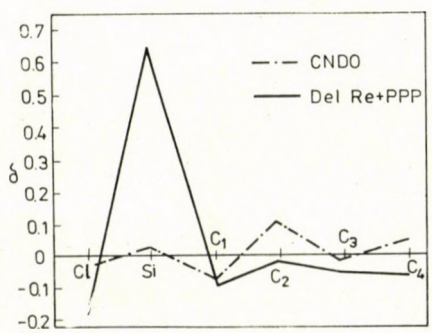

Fig. 3. Partial charges in $C_6H_5SiCl_3$ by DEL RE + PPP and CNDO/2 methods

of the atomic charges obtained by the two methods is also the same, but the CNDO/2 method strongly underestimates the charge of chlorine and silicon atoms, the chemical experience supports the results of PPP + DEL RE calculations.

In the following part we would like to report about our investigations on *compounds of similar type containing silicon, germanium and tin.*

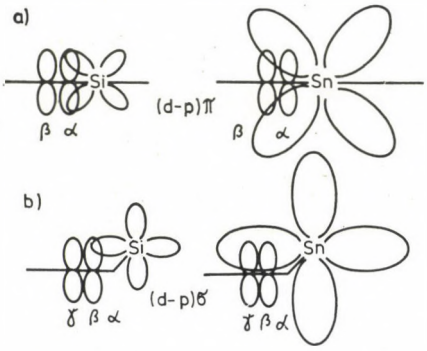

Fig. 4. Overlap of the d orbitals with the *p* orbitals of carbon atoms. *a)* for vinyl and phenyl derivatives; *b)* for allyl and benzyl derivatives

It is known that the vacant *d* orbitals of silicon participate in chemical bonds. For germanium and tin compounds, however, this interaction has not been made clear. According to various experimental data the role of *d* orbitals is negligible, on the other hand ultraviolet spectroscopical measurements — in the case of unsaturated hydrocarbons — show the interactions with *d* orbitals being considerable. Namely the spectra of germanium and tin compounds in comparison with those of the corresponding carbon and silicon analogons indicate important shifts which cannot be simply explained by inductive effect. To study the effect of *d* orbitals PPP calculations were carried out. First only an interaction of the heteroatom with carbon atom in α position (*i.e.* the corresponding resonance integral β_{ij}) was taken into account, then the interaction with carbon atom in β and even in γ position was considered. Calculations were also performed when the interaction of the heteroatom with the π system was entirely neglected. The calculated and experimental results are summarized in Table V. As it can be seen the best results were obtained for compounds of various type with the assumption of different interactions, and the explanation of the results can be given on the basis of a model shown in Fig. 4.

In the case of vinyl and phenyl derivatives the heteroatom is placed in the plane of the π system, and only a bond of π character can be formed. On going from silicon to tin the *d* orbital becomes more diffuse and larger in diameter. Hereby the overlap and the interaction with the *p* orbital of the

Table V

Calculated and experimental ultraviolet transition energies for compounds of type $RM(CH_3)_3$ (in eV)

R	M	Without heteroatom	Interaction in α position	Interaction in β position	Interaction in γ position	ΔE_{exp} [21]
C_6H_5-	C	4.719	—	—	—	4.714
		5.983				5.949
	Si	4.730	4.668	4.810	—	4.687
		6.006	5.687	6.079		5.766
	Ge	4.731	4.693	4.787	—	4.798
		6.010	5.816	6.060		5.792
	Sn	4.734	4.707	4.803	—	4.793
		6.014	5.905	6.087		5.955
$CH_2=CH-$	C	7.447	—	—	—	7.424 (ethylene)
	Si	7.302	6.102	6.932	—	6.964
	Ge	7.304	6.262	6.876	—	6.792
	Sn	7.336	6.530	7.298	—	6.635
$C_6H_5CH_2-$	C	4.696	—	—	—	4.779
		5.940				5.866
	Si	4.696	4.695	4.648	—	4.635
		5.940	5.926	5.688		5.609
	Ge	4.696	4.695	4.664	4.583	4.604
		5.940	5.931	5.773	5.512	5.509
	Sn	4.696	4.695	4.657	4.568	4.544
		5.940	5.935	5.778	5.526	5.248
$CH_2=CH-CH_2-$	C	7.029	—	—	—	—
	Si	7.029	6.428	6.230	—	6.456
	Ge	7.029	6.484	6.313	5.922	6.325
	Sn	7.029	6.743	6.439	5.930	6.901

neighbouring and farer carbon atoms weakens. On the contrary for the allyl and benzyl derivatives the heteroatom is rotated out of the plane of the π system and there is a possibility of forming a σ interaction between the *d* orbital and the corresponding carbon atom in β position. This interaction can be extended for farer carbon atoms if the size of the *d* orbital is increasing. In these terms all the results shown can be explained.

To study the structure of substituted *phenoxytrimethylsilanes* ($XC_6H_4OSi(CH_3)_3$, where X = CH_3, Cl, NO_2, $OSi(CH_3)_3$, F in *orto*, *meta* and

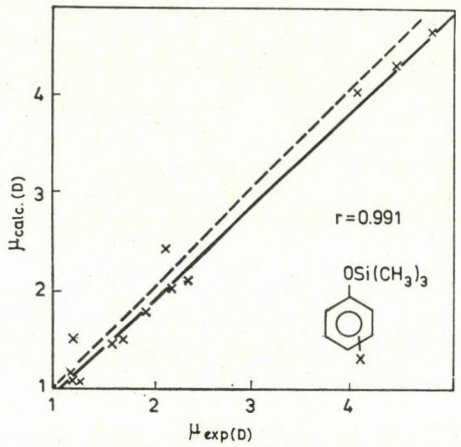

Fig. 5. Plot of the calculated dipole moments of phenoxysilanes against the experimental values

para positions) iterativ PPP calculations were carried out, in which a planar model was assumed and confirmed by the agreement of the experimental and calculated electronic transition energies demonstrated later. Based on the π charge distribution and the σ charges obtained by DEL RE method we calculated the dipole moment of the compounds with the assumption of free rotation. It was supposed that the trimethylsiloxy group rotates freely around the oxygen–aromatic carbon axis, meanwhile the charge distribution does not change, and all the spatial arrangements are of same energy and of same possibility. In most cases the dipole moment calculated this way shows a good agreement with the experimental value as it is illustrated in Fig. 5.

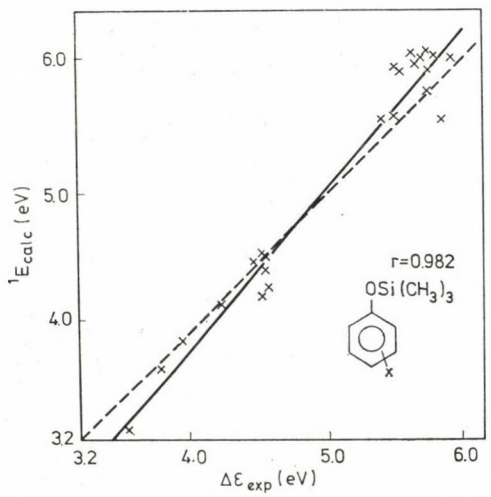

Fig. 6. Plot of the calculated $^1E_{CI}$ values of phenoxysilanes against experimental electron transition (ΔE)

The greatest difference for the *orto*-bis-(trimethylsiloxy)-benzene can be unambigously explained by the size of the trimethylsiloxy group hindering the rotation. The good agreement of the calculated and experimental data supports the assumed geometrical model, for example the value of the Si–O–C_{ar} bond angle to be 121°. The electronic transition energies of phenoxysilanes calculated by IPPP method are presented in Fig. 6 in the function of the experimental electronic transitions. The value of the correlation coefficient is 0.982.

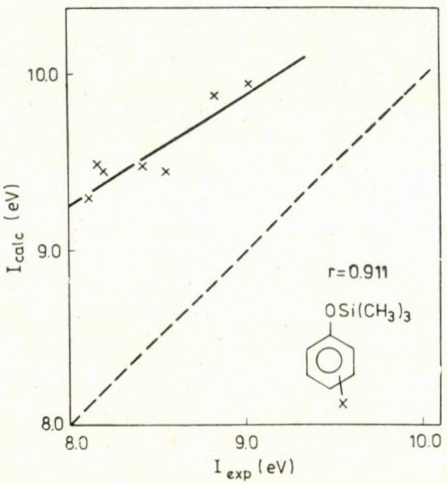

Fig. 7. Plot of the calculated ionization energies of phenoxysilanes against the experimental values

Fig. 7 illustrates the correlation between the experimental and calculated ionization energies of phenoxysilanes. Although the calculated values are about 1 eV higher than the experimental ones, the correlation coefficient (r) is 0.911.

REFERENCES

[1] PARISER, R., PARR, R. G.: J. Chem. Phys. **21,** 466, 767 (1953)
[2] POPLE, J. A.: Trans. Faraday Soc. **49,** 1375 (1953)
[3] HINZE, J., JAFFE, H. H.: J. Am. Chem. Soc. **84,** 540 (1962).
[4] HINZE, J.: Ph. D. Dissertation. Univ. of Cincinnati, 1962
[5] LEVISON, K. A., PERKINS, P. G.: Theor. Chim. Acta **14,** 206 (1969)
[6] MATAGA, N., NISHIMOTO, K.: Z. Phys. Chem. (Frankfurt) **13,** 140 (1957)
[7] WOLFSBERG, M., HELMHOLZ, L.: J. Chem. Phys. **20,** 837 (1952)
[8] NAGY, J., HENCSEI, P.: J. Organometal. Chem. **32,** 39 (1971)
[9] BROWN, R. D., HEFFERNAN, M. L.: Trans. Faraday Soc. **54,** 757 (1958)
[10] BROWN, R. D., HEFFERNAN, M. L.: Aust. J. Chem. **12,** 319 (1959)
[11] BURNS, G.: J. Chem. Phys. **41,** 1521 (1964)
[12] POPLE, J. A., SANTRY, D. P., SEGAL, G. A.: J. Chem. Phys. **43,** S 129 (1965)
[13] POPLE, J. A., SEGAL, G. A.: J. Chem. Phys. **43,** S 136 (1965); **44,** 3289 (1966)
[14] POPLE, J. A., BEVERIDGE, D. L., DOBOSH, P. A.: J. Chem. Phys. **47,** 2026 (1967)

[15] POPLE, J. A., BEVERIDGE, D. L.: Approximate Molecular Orbital Theory. McGraw-Hill Book Co., New York, 1970. Appendix A. p. 163
[16] HENCSEI, P., RÉFFY, J., MESTYANEK, Ö., VESZPRÉMI, T., NAGY, J.: Periodica Polytech. **16,** 101 (1972)
[17] NAGY, J., HENCSEI, P., RÉFFY, J.: Acta Chim. Acad. Sci. Hung. **65,** 51 (1970)
[18] MCCELLAN, A. L.: Tables of Experimental Dipole Moments. Freeman and Co., London, 1963
[19] DURIG, Y. R., LI, Y. S., TONG, C. C.: J. Mol. Struct. **14,** 225 (1972)
[20] ALEKSZEJEV, N. V.: private communication
[21] NAGY, J., RÉFFY, J.: J. Organometal. Chem. **22,** 565 (1970)

József RÉFFY
Tamás VESZPRÉMI
Pál HENCSEI
József NAGY
H-1521 Budapest.

Acta Chimica Academiae Scientiarum Hungaricae, Tomus 93 (2), pp. 117—122 (1977)

STUDY OF THE HYDRATION OF MACROMOLECULES, III*

MEASUREMENT OF THE SELF-DIFFUSION OF WATER IN POLY(ACRYLIC ACID) SOLUTIONS

Gy. INZELT and P. GRÓF

(Department of Physical Chemistry and Radiology, Eötvös Loránd University, Budapest)

Received June 16, 1976

The self-diffusion coefficient of water was determined at 25 and 35°C in aqueous solutions of poly(acrylic acid) (PAA) in the concentration range of 3—10 wt.%. The open-end capillary method without stirring was used to measure the self-diffusion coefficient. ^{18}O was employed as a tracer in water, and the samples were analyzed with a mass spectrometer. The specific volumes and viscosities of the solutions, and the average degree of dissociation of the PAA were determined.

In the concentration range examined, the self-diffusion coefficient of water decreases linearly with increasing PAA concentration at both temperatures. The activation energy of self-diffusion was found to be 4.9 ± 1.2 kcal mol^{-1}. The hydration number of the PAA carboxy group was calculated: depending on the form factor, this was 4.9—5.4 and 5.6—6.0 water molecules per COOH group at 25 and 35 °C, respectively.

As a continuation of our previous work [1, 2], in the present study it was desired to determine the hydration number of the carboxy groups of poly(acrylic acid) (in the following PAA).

The selection of PAA was justified by the fact that it is the simplest model substance for the determination of the hydration of the carboxyl group. PAA is a macromolecule which is readily dissolved in water, and which behaves as a non-electrolyte in the concentration range employed in this work.

Numerous estimates of the extent of hydration of the carboxy group are to be found in the literature [3—9]. These values must be treated with a certain degree of reserve, however. Firstly, the systems investigated were multicomponent solutions of polypeptides or proteins with complicated structures [3, 5, 6], in which it was problematical to assign the bound water to one functional group. Further, the possibilities given by the methods did not provide a satisfactory basis for reliable quantitative conclusions [5, 7—9].

Accordingly, the different authors obtained hydration numbers varying within wide limits (1—7.5 water molecular per COOH group).

Thus, it is not surprising if the differences in the numerical values were accompanied by other contradictions: for example, certain authors [5, 7, 8] considered that hydration of the ionized form is the significant reaction,

* For Part II, see Ref. [2].

whereas others [6] drew the conclusion that the carboxy group interacts strongly with water only in the uncharged state.

In the present paper an account is given of our results obtained on the measurement of the self-diffusion coefficient of water. The variations in the self-diffusion coefficient of water were investigated in the PAA concentration range of 3–10 wt.%, at 25 and 35°. The densities and viscosities of the solutions were measured at 25, 30 and 35 °C. The average degree of dissociation of the PAA at the concentration examined was also determined.

The hydration number of the carboxy group and the activation energy of the transport processes were calculated.

Experimental

The PAA used was a commercial product of Polysciences. The mass average molecular weight of the sample was 150,000.

The determinations of the self-diffusion coefficient of water, and the viscosities and specific volumes of the solutions, were reported earlier [1]. The degree of dissociation and the dissociation equilibrium constant were determined by pH-measurement and by potentiometric titration, as described in the literature [10].

Results and discussion

The results of the self-diffusion measurements are listed in Table I. At both temperatures the relative self-diffusion coefficient of water, and the value of this corrected in accordance with the WANG relation [1], decrease linearly as a function of the PAA concentration in the interval examined. The average activation energy for the self-diffusion of water ($\Delta H_D^{\pm}$) was found to be 4.9 ± 1.2 kcal mol^{-1}, which, within the experimental error, does not differ from the value observed for the process in pure water. This is in accord-

Table I

Self-diffusion coefficient of water in PAA solutions at 25 and 35 °C

PAA concentration (%)	$D_{25} \times 10^5$ (cm^2 s^{-1})	$D_{35} \times 10^5$ (cm^2 s^{-1})	$\Delta H_D^{\pm}$ (kcal mol^{-1})
0.00	2.57 ± 0.02	3.49 ± 0.15	4.9 ± 0.8
3.06	2.22 ± 0.08	2.81 ± 0.12	4.4 ± 1.3
5.10	1.98 ± 0.10	2.64 ± 0.08	5.1 ± 1.3
7.17	1.77 ± 0.12	2.29 ± 0.16	4.6 ± 1.3
10.26	1.41 ± 0.07	1.91 ± 0.08	5.3 ± 1.1

The scatter of the measurement is given by the average error of the mean value.

ance with the idea that the initial step in the process of self-diffusion is the breakage of 2 hydrogen-bonds per activated molecule. For determination of the hydration number it is necessary to know the specific volume of the macromolecule. The value of this was calculated from the specific volumes measured for the solutions, these data being given in Table II. Values of 1.500

Table II

Specific volumes of aqueous solutions of PAA at various temperatures

PAA concentration (%)	V_t		
	at 25 °C ($cm^3\ g^{-1}$)	at 30 °C ($cm^3\ g^{-1}$)	at 35 °C ($cm^3\ g^{-1}$)
0.00	1.0029	1.0044	1.0060*
3.06	0.9931	0.9947	0.9967
5.10	0.9865	0.9881	0.9890
7.17	0.9795	0.9802	0.9815
10.26	0.9686	0.9707	0.9713

* [11].
Relative error of the specific volumes: $\pm 0.6\%$.

and 1.667, ascribable to spherical and rod shapes, were used as the form factor ($\bar{\alpha}$), assuming that in the case of the random coil formed by the PAA molecules it is probably necessary to calculate with values intermediate between the two extreme forms, but not exactly determined. It should be noted that the PAA molecules exhibit a spherical form on an electron-microscopic photograph of the film obtained by evaporation of the solvent from a dilute solution, in contrast with the picture similarly prepared for the alkali metal salts of PAA, where the extended form of the macromolecules can be well seen [12]. Our measurements indicate that the specific volumes of PAA at 25 and 35° are 0.653 and 0.645 $cm^3\ g^{-1}$, respectively. When calculations were made with these apparent specific volumes, the WANG relation [1] led to the hydration numbers given in Table III. In the present case too the diffusion of the macromolecule was neglected, and it was assumed that all of the carboxy groups are accessible as regards hydration.

For PAA it is particularly justified to examine what group the hydration numbers obtained is to be assigned to, since the polyelectrolyte macromolecule can be conceived of as the copolymer of monomers which contain COOH or COO^- groups. It is obvious that the hydrations of the two groups to be considered with regard to the effect under investigation may differ (in the present case too hydration of the vinyl base-chain may be disregarded). From the dissociation degree data, listed in Table IV, it can be seen that

Table III

Hydration numbers of the carboxy group of PAA at 25 and 35 °C for two values of $\bar{\alpha}$

Temperature (°C)	H No. of H_2O molecules per COOH group	
	at $\bar{\alpha} = 1.500$	at $\bar{\alpha} = 1.667$
25	5.4 ± 0.6	4.9 ± 0.6
35	6.0 ± 1.2	5.6 ± 1.2

Table IV

Average degree of dissociation and dissociation equilibrium constant (K_d) *of PAA at 25 °C*

PAA concentration (%)	Degree of dissociation
3.06	0.016
5.10	0.011
7.17	0.009
10.26	0.006

$\overline{K}_d = 4.2 \times 10^{-5}$

there is roughly one COO^- group for every 100 COOH groups. This ratio varies as a function of the concentration: in the range examined here the maximum deviation from the above value can be expressed with a factor of 1.6. It appears reasonable, therefore, taking into account the above numerical ratio, to assign the hydration numbers to the non-ionic COOH group. In the concentration interval in question the structure-breaking effect of the ionic groups does not seem significant either, as this should be reflected in the concentration dependence of the self-diffusion coefficient and in the activation energy of self-diffusion. Nor is it justified to draw such a conclusion from the temperature dependence of the hydration numbers, because of the greater uncertainty of the determination. The hydration numbers obtained in the present work are in good agreement with the value of 4—5 water molecules per COOH group calculated theoretically by SPONSLER *et al.* [3], and with the results of X-ray diffraction and infrared absorption measurements by the same authors, which led to a hydration number of 4 water molecules per COOH group in proteins.

The same conclusion was reached by other authors [4] from compressibility measurements. The agreement is less good with the results of NMR studies [5], according to which the hydration numbers of the non-dissociated and the dissociated forms are 2 and 6—7.5 water molecules per carboxy

group, respectively. The latter conclusions were obtained from examinations relating to frozen protein solutions, and thus, just as in the case of the result obtained from water-binding measurements on the solid macromolecule as sorbent (1 water molecule per carboxy group), it appears justified to use the values judiciously.

The results of our viscosity measurements are to be found in Table V. In agreement with our earlier conclusions, it may be stated on the basis of

Table V

Viscosities of PAA solutions at 25, 30 *and* 35 °C

PAA concentration (%)	η_{25} (cP)	η_{30} (cP)	η_{35} (cP)	$\Delta H^{\neq}$ (kcal mol^{-1})
0.00	0.8903	0.7975	0.7193*	—
3.06	3.176	2.909	2.660	3.2±0.2
5.10	5.764	5.369	4.946	2.8±0.4
7.17	11.60	—	9.940	2.8±0.5
10.26	27.22	24.86	22.46	3.5±0.3

* [13].
Relative error of the viscosities: ±1%.

the concentration dependence that there is no correlation between the macroviscosity of the solution and the self-diffusion of the solvent. The latter can be brought into correlation only with the microviscosity of the environment of the solvent molecules. According to our investigations [14], the increase of the microviscosities with the concentration, which can be calculated from the variation of the dielectric relaxation time of water, is in good agreement with the decrease of the self-diffusion coefficient in the case of the PAA solutions too. This will be analyzed in greater detail in the following paper of this series.

*

The authors wish to express their thanks to Olivér KAPOSI and József TAMÁS for the mass-spectrometric measurements in their laboratories, and Kálmán UJSZÁSZY, Péter BRUCK and Mrs. Zs. BALTHAZÁR for their help in mass-spectrometric analysis.

REFERENCES

[1] INZELT, Gy., GRÓF, P.: Acta Chim. (Budapest), **88,** 13 (1976)
[2] MASSZI, Gy., INZELT, Gy., GRÓF, P.: Acta Biochim. Biophys. Acad. Sci. Hung. **11,** 45 (1976)
[3] SPONSLER, O. L., BATH, J. D., ELLIS, J. W.: J. Phys. Chem., **44,** 996 (1940)
[4] PAZINSKII, A. G.: Zh. Fiz. Khim., **20,** 981 (1946); Koll. Zh., **8,** 53 (1946)
[5] KUNTZ, I. D.: J. Amer. Chem. Soc. **93,** 514, 516 (1971)
[6] GLASEL, J. A.: J. Amer. Chem. Soc., **92,** 375 (1970)
[7] IKEGAMI, A.: Biopolymers, **6,** 431 (1968)
[8] ASAI, H.: J. Phys. Soc. Japan, **16,** 761 (1961)
[9] KATCHMAN, B., MCLAREN, A. D.: J. Amer. Chem. Soc., **73,** 2124 (1951)

[10] See *e.g.* F. OOSAWA: Polyelectrolytes, pp. 73—75. Dekker, New York 1971
[11] KELL, G. S.: J. Chem. Eng. Data, **12**, 66 (1967)
[12] TAGER, A. A.: Fiziko-khimiya polimerov, p. 127, GNTI, Moskow 1963
[13] WEBER, W.: Z. ang. Phys., **7**, 96 (1955); **15**, 342 (1963)
[14] GRÓF, P.: Dissertation, Budapest 1975

György INZELT
Pál GRÓF
H-1088 Budapest, Puskin u. 11—13.

Acta Chimica Academiae Scientiarum Hungaricae, Tomus 93 (2), pp. 123—133 (1977)

STUDIES WITH PARCHMENT SUPPORTED MEMBRANES, XIII

DETERMINATION OF THE THERMODYNAMICALLY EFFECTIVE FIXED CHARGE DENSITY AND PERMSELECTIVITY

FASIH A. SIDDIQI, M. NASEEM BEG, SURENDRA P. SINGH and ABDUL HAQ

(Physical Chemistry Division, Department of Chemistry Aligarh Muslim University, Aligarh 202001 *INDIA)*

Received July 26, 1976

The membrane potentials arising across two parchment supported hexacyanoferrate(II) membranes of silver and cadmium are used to evaluate the thermodynamically effective fixed charge densities of KOBATAKE. KOBATAKE's theory is based on the thermodynamics of irreversible processes. KOBATAKE's equation was used under two limiting conditions, namely in the concentration range and in the dilute range. The two limiting forms of KOBATAKE's equation gave identical values of Θ for both membranes. The theoretical predictions for membrane potentials by KOBATAKE's equation are borne out quite satisfactorily by the experimental results obtained with the silver and cadmium hexacyanoferrate(II) membranes investigated.

The theories of transport of charged or uncharged particles through membranes have been treated under the following headings; (a) the idealized theory of TMS [1—2] and its refinement [3], (b) pseudo thermodynamic approach due to SCATCHARD [4] and the treatment based on the thermodynamics of irreversible processes [5—8] and (c) a kinetic approach based on the theory of absolute reaction rates [9—10]. NAGASAWA and KOBATAKE [10] have taken the structure of the membrane into account and by the application of the Poisson—Boltzmann equation computed ionic concentrations in the membrane phase. In order to substantiate our earlier findings [11—19] extensive investigations have been made for the determination of membrane charge density and are reported in this paper on the basis of the thermodynamics of irreversible processes given by KOBATAKE *et al.* [20—25].

Experimental

Preparation of membranes

The membranes of silver and cadmium hexacyanoferrate(II) were prepared by the method of interaction suggested by WEISER [26]. First parchment paper was soaked in distilled water for two hours and then tied carefully to the flat mouth of a beaker which contains 0.2 *M* silver nitrate. This was suspended for about 72 hours in a 0.2 *M* solution of potassium hexacyanoferrate(II). The two solutions were interchanged and kept for another 72 hours. The silver hexacyanoferrate(II) membrane thus prepared was washed with deionized water

for the removal of free electrolyte. A similar procedure was adopted for the preparation of cadmium hexacyanoferrate(II) membrane by taking a 0.2 *M* solution of cadmium chloride and potassium hexacyanoferrate.

Measurement of membrane potential

The potential developed by setting up a concentration cell of the following type described by MICHAELIS [27], SOLLNER and GREGOR [28] and MARSHALL and AYERS [29]

S.C.E.	Solution C_1	Membrane	Solution C_2	S.C.E.

was taken as a measure of membrane potential. The measurements were carried out at 25 °C using a Pye precision potentiometer (No. 7568).

Result and discussion

The membrane potential data obtained with the silver and cadmium hexacyanoferrate(II) in various 1 : 1 electrolytes were plotted as a function of $\log \frac{C_1 + C_2}{2}$ with the ratio $v = C_2/C_1$ fixed at 10. These plots are shown in Fig. 1.

KOBATAKE *et al.* [21] derived the following equation for the electric current density $(I)_c$, relative to the frame of reference fixed to the membrane, using the basic flow equation provided by the thermodynamics of irreversible processes,

$$(I)_c = -F(l_+C_+ + l_-C_-)\frac{d\Phi}{dx} - RT\left(l_+C_+\frac{d\ln a_+}{dx} - l_-C_-\frac{d\ln a_-}{dx}\right) + F(C_+ - C_-)U_m . \quad (1)$$

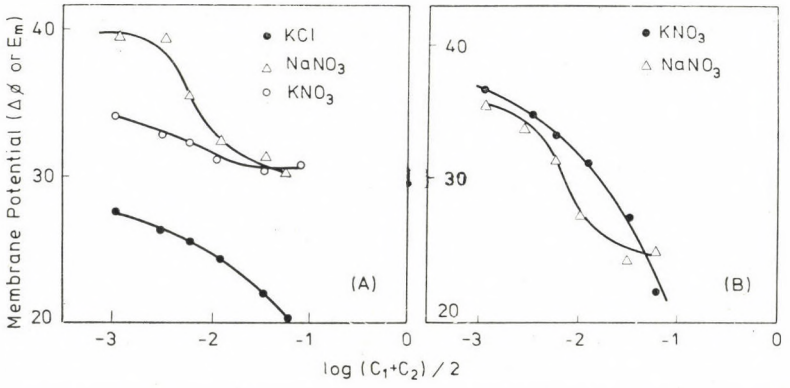

Fig. 1. Plots of observed potential $\Delta\Phi$ against log $(C_1 + C_2)/2$ for various electrolytes with (A) Cadmium Hexacyanoferrate(II) and (B) Silver Hexacyanoferrate(II) membranes

Here l_+ and l_- are molar mobilities of $+ve$ and $-ve$ ions defined in terms of the mass fixed frame of reference, U_m is the velocity of the local centre of mass, Φ is the electric potential, C_+ and C_- are concentrations of $+ve$ and $-ve$ ions in moles per cubic centimeter of solution, a_+ and a_- are activities of positive and negative ions in moles per cubic centimeter of solution, R is the gas constant, T the absolute temperature of the system and F the Faraday constant.

For the evaluation of U_m, the viscous force acting on 1c.c. of solution in the membrane is represented by $-\left(\frac{1}{K}\right) U_m$, where K is a constant which is considered to depend on the viscosity of the solution and the structural details of the polymer network of which the membrane is composed. The same volume of solution undergoes an electric force which is represented by

$$-F(C_+ - C_-)\left(\frac{\mathrm{d}\Phi}{\mathrm{d}x}\right). \tag{2}$$

In the steady state, the sum of these two forces is zero, so that

$$U_m = -KF(C_+ - C_-)\left(\frac{\mathrm{d}\Phi}{\mathrm{d}x}\right). \tag{3}$$

For convenience, KOBATAKE *et al.* have considered a membrane which is ionized negatively with a charge density Θ (in moles/c.c.). Then the requirement that the electric neutrality must be realized in any element of the membrane gives the relation

$$C_+ - C_- = 0\,. \tag{4}$$

Since in the system considered here no electric field is applied externally across the membrane, no net charge is transported from one side of the membrane to the other. This means that $(I)_c$ must be zero at a cross-section of the membrane. Substituting Eqs 3 and 4 into Eq. 1, putting $(I)_c$ equal to zero, and solving for $\frac{\mathrm{d}\Phi}{\mathrm{d}x}$, the following expression is obtained

$$\frac{\mathrm{d}\Phi}{\mathrm{d}x} = \frac{-\left(\frac{RT}{F}\right)\left[l_+(C_- + \Theta)\left(\frac{\mathrm{d}\ln a_+}{\mathrm{d}x}\right) - l_-C_-\left(\frac{\mathrm{d}\ln a_-}{\mathrm{d}x}\right)\right]}{(l_+ + l_-)\,C_- + l_+\Theta + KF\Theta^2}. \tag{5}$$

To proceed further, the activities a_+ and a_- must be known as function of C_-.

Assumption for a_+ and a_-:

KOBATAKE *et al.* have assumed the following relations

$$a_+ = C_-; \text{ and } a_- = C_- \tag{6}$$

$$\nu_+ = C_-/(C_- + \Theta); \quad \nu_- = 1 \, . \tag{7}$$

Here ν_+ and ν_- are the activity coefficients of $+ve$ and $-ve$ ions in the membrane.

Equation for membrane potential

With Eqs 6, 7 assumed for a_+ and a_- Eq. 5 becomes

$$\frac{\mathrm{d}\Phi}{\mathrm{d}x} = -\frac{RT}{F}\left[\frac{(l_+ - l_-)C_- + l_+\Theta}{[(l_+ + l_-)C_- + l_+\Theta + KF\Theta^2]C_-}\right]\frac{\mathrm{d}C_-}{\mathrm{d}x} \tag{8}$$

when the bulk solution on both sides of the membrane are vigorously stirred, no potential gradient is set up in them, so that the desired membrane potential $\Delta\Phi$ is obtained by integrating $\dfrac{\mathrm{d}\Phi}{\mathrm{d}x}$ over the thickness of the membrane. The final expression for the membrane potential is given by

$$\Delta\Phi = -\left(\frac{RT}{F}\right)\left[\frac{1}{\beta}\ln\frac{C_2}{C_1} - \left(1 + \frac{1}{\beta} - 2\alpha\right)\ln\left(\frac{C_2 + \alpha\beta\Theta}{C_1 + \alpha\beta\Theta}\right)\right] \tag{9}$$

$$\text{where } \alpha = \frac{l_+}{l_+ + l_-} \quad \text{and} \quad \beta = 1 + \left(\frac{KF\Theta}{l_+}\right) \tag{10, 11}$$

and the parameters have been assumed to be independent of salt concentration.

KOBATAKE *et al.* [21] have derived two useful limiting forms of Eq. 9. These are (a) when C_2 becomes sufficiently small with ν fixed; Eq. 9 may be expanded to give

$$|\Delta\Phi_\gamma| = \frac{1}{\beta}\ln\nu - \frac{\nu - 1}{\alpha\beta\nu}\left(1 + \frac{1}{\beta} - 2\alpha\right)\left(\frac{C_2}{\Theta}\right) + \cdots \tag{12}$$

where $|\Delta\Phi_\gamma|$ is the absolute value of a reduced membrane potential defined by

$$\Delta\Phi_\gamma = F\Delta\Phi/RT \tag{13}$$

(b) It has also been shown by KOBATAKE *et al.* that at a fixed ν the inverse of an apparent transference number t^-_{app} for the Co-ion species in a negatively

charged membrane is proportional to the inverse of the concentration C_2 in the region of high salt concentration. Here t^-_{app} is defined by the relation

$$|\Delta\Phi_\gamma| = (1 - 2\,t^-_{app}) \ln \nu \tag{14}$$

substituting for $\Delta\Phi$ from Eq. 9 and expanding the resulting expression for t^-_{app} in powers of $1/C_2$ gives

$$\frac{1}{t^-_{app}} = \frac{1}{(1-\alpha)} + \frac{(1+\beta-2\alpha\beta)(\nu-1)\alpha}{2(1-\alpha)^2 \ln \nu}\left(\frac{\Theta}{C_2}\right) + \ldots \tag{15}$$

For the evaluation of the thermodynamic effective fixed charge density by the method of KOBATAKE *et al.* the following procedure was adopted.

Equation 12 indicates that a value of β and a relation between α and Θ can be obtained by evaluating the intercept and the initial slope of a plot of $|\Delta\Phi_\gamma|$ against C_2. Figure 2 illustrates plots of $|\Delta\Phi_\gamma|$ *versus* C_2 in the region of low concentration that were determined for electrolyte with both membranes. The value of intercept is equal to $1/\beta \ln \nu$, by which β may be evaluated. Values are given in Table I.

Table I

Values of parameters α, β, Θ *and* ΦX *for various electrolyte system at* $\nu = 10$

Membrane	Silver hexacyanoferrate(II)				Cadmium hexacyanoferrate(II)			
Electrolyte	α	β	Θ	ΦX	α	β	Θ	ΦX
KNO_3	0.68	1.69	0.0061	0.00215	0.75	1.81	0.0011	0.0083
KCl	—	—	—	—	0.68	2.27	0.0008	0.0063
$NaNO_3$	0.68	1.64	0.0035	0.00418	0.75	1.48	0.0011	0.0054

Θ are evaluated from the slope $= \dfrac{(1+\beta-2\alpha\beta)(\nu-1)\alpha\Theta}{2(1-\alpha)^2 \ln \nu}$

ΦX from graph 5.

Eq. 15 indicates that the intercept of a plot of $\dfrac{1}{t^-_{app}}$ against $1/C_2$ at fixed ν allows the values of α to be determined, which are shown in Fig. 3 for both membranes with the electrolyte. The value of the intercept is equal to $\dfrac{1}{(1-\alpha)}$, from which α may be evaluated. Values are given in Table I.

For the evaluation of Θ, there are two limiting cases

(i) in the dilute range the slope, of Eq. 12 is given by

$$\frac{\nu-1}{\alpha\beta\nu}\left(1+\frac{1}{\beta}-2\alpha\right)\frac{1}{\Theta}.$$

The graphical value of the slope determined from Fig. 2 is equated with the above expression after substituting the value of α and β, Θ may thus be determined.

(ii) in the concentration range using Eq. 15. The slope is given by

$$\frac{(1+\beta-2\alpha\beta)(\nu-1)\alpha}{2(1-\alpha)^2 \ln \nu}\,\Theta$$

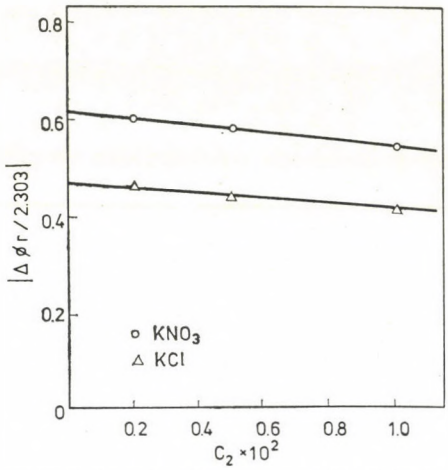

Fig. 2. $|\Delta\Phi_\gamma|/2.303$ *vs.* $C_2 \times 10^2$ plots for electrolyte with (Δ) Cadmium Hexacyanoferrate(II) and (o) Silver Hexacyanoferrate(II) membranes

The graphical value of the slope determined from Fig. 3 is equated with the above expression. The values of α and β are substituted and thus the value of Θ is evaluated. KOBATAKE has suggested that, provided his equation for the membrane potential is correct, then the two values of Θ (in the two limiting cases) thus determined from the opposite limits should agree. In the present

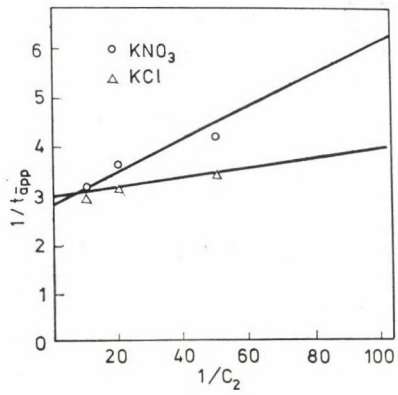

Fig. 3. $1/\bar{t}_{app}$ *vs.* $1/C_2$ plots for electrolyte with (Δ) Cadmium Hexacyanoferrate(II) and (o) Silver Hexacyanoferrate(II) membranes

investigation with parchment supported membranes, the two values obtained from opposite limits agree with one another thereby confirming the applicability of KOBATAKE *et al.* equation to these systems also.

Once the values of the parameters α, β and Θ for a given membrane electrolyte system have been determined, one can calculate the theoretical $\Delta\Phi$ *versus* C_2 curve for the value of ν and then compare it with the corresponding experimental data. For this comparison Eq. 9 may be rewritten in the following form as suggested by KOBATAKE

$$\frac{(\nu - e^q)}{(e^q - 1)} = X$$

with q and X defined by

$$q = \frac{\left[|\Delta\Phi_\gamma| + (1 - 2\alpha)\ln\nu\right]}{\left[\frac{1}{\beta} + (1 - 2\alpha)\right]}$$

and

$$X = \frac{C_2}{\alpha\beta\Theta}.$$

If this equation is valid the values of $\frac{\nu - e^q}{e^q - 1}$ together with the predetermined α, β and Θ (from Table I) must fall on a straight line which has a unit slope and passes through the coordinate origin, when plotted against X. This behaviour should be observed irrespective of the value of ν and the kind of membrane electrolyte (1 : 1 system) used. Figure 4 demonstrates that the theoretical predictions, based on KOBATAKE's membrane potential expression is borne out quite satisfactorily by our experimental results on parchment supported membranes.

KOBATAKE *et al.* developed another theory for the evaluation of charge density of membranes [25]. This theory is based on the expression of permselectivity, which they derived by taking some assumption. Both the activity coefficients and mobilities of small ions in charged membranes can be expressed by the following expression

$$\nu_+ = \nu_+^0(C_- + \Phi X)/(C_- + X), \quad \nu_- = \nu_-^0 \tag{16}$$

$$u_+ = u_+^0(C_- + \Phi X)/(C_- + X), \quad u_- = u_-^0. \tag{17}$$

Here ν_i, u_i, ν_i^0 and u_i^0 ($i = +, -$) stand for the activity coefficient and mobility of ionic species i in the membrane and in the bulk solution, respectively C_- and X are the concentration of anion adsorbed on the membrane

(in moles per litre of water in the membrane), and the stoichiometric concentration of charges fixed in the membrane. According to the convention suggested by GUGGENHEIM [30] ν_+^0 can be equated with ν_-^0 for 1 : 1 electrolyte, and they are replaced by the mean activity coefficient $\nu_\pm^0$ of the electrolyte component. In Eq. 16, Φ represents the fraction of counter ions in the unbounded form, *i.e.* excluding those tightly bound to the polymer skeleton constituting the membrane. ΦX may be referred to as the thermodynamically effective fixed charge density of the membrane.

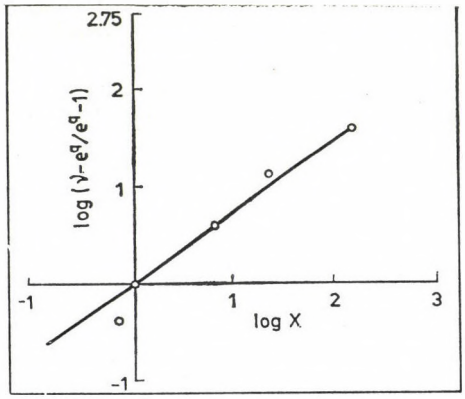

Fig. 4. Plots of $\log(\nu - e^q/e^q - 1)$ *vs.* $\log X$ for KNO_3 with Silver Hexacyanoferrate(II) membrane

Consider a system in which a negatively charged membrane is immersed in an electrolyte solution of concentration C. Under this condition the Donnan equilibrium for small ions holds between the membrane phase and the solution then we have

$$(\nu_\pm^0)^2 C^2 = \nu_+ C_+ \nu_- C_- \,. \tag{18}$$

The mass fixed transference number of the anion in the membrane, is defined by

$$\tau_- = u_- C_- / (u_+ C_+ + u_- C_-) \,. \tag{19}$$

Introducing Eqs 16, 17 and 18 into Eq. 19 together with the electrical neutrality condition, *i.e.* $C_+ = C_- + X$
we obtain

$$\tau_- = 1 - \alpha \frac{(4\zeta^2 + 1)^{1/2} + 1}{(4\zeta^2 + 1)^{1/2} + (2\alpha - 1)} \tag{20}$$

where

$$\zeta = C/\Phi X \tag{21a}$$

and

$$\alpha = \frac{u_+^0}{(u_+^0 + u_-^0)} \,. \tag{21b}$$

On the other hand, the apparent transference number of the anion in the membrane, t^-_{app} is defined from the observed membrane potential $\Delta\Phi$ by the following Nernst equation

$$\Delta\Phi = -\left(\frac{RT}{F}\right)(1 - 2t_{-app}) \ln \frac{C_2}{C_1}. \tag{22}$$

Here C_1 and C_2 are the concentration of the external solutions on the two sides of the membrane, and R, T, and F have their usual thermodynamics

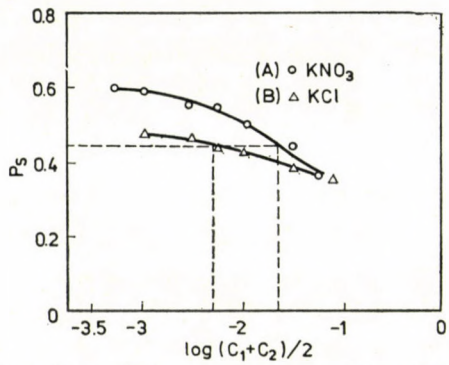

Fig. 5. Plots of P_s defined by equation 23 against log $(C_1 + C_2)/2$ for electrolyte with (Δ) Cadmium Hexacyanoferrate(II) and (o) Silver Hexacyanoferrate(II) membranes

meaning. It has been found by KOBATAKE *et al.* [18] that the difference between τ_- and t^-_{app} was less than 2% in the wide range of salt concentration, when the averaged concentration $\frac{C_1 + C_2}{2}$ was replaced by C. Therefore, if we replace τ_- by t^-_{app}, and C by $\frac{C_1 + C_2}{2}$ Eq. 20 is applicable even when the concentrations on the two sides of the membrane are different. Rearrangement of Eq. 20 leads to

$$\frac{1}{(4\zeta^2 + 1)^{1/2}} = \frac{1 - t^-_{app} - \alpha}{\alpha - (2\alpha - 1)(1 - t^-_{app})} \equiv P_s. \tag{23}$$

Here P_s is a measure of permselectivity of the membrane–electrolyte system.

For the evaluation of the thermodynamically effective fixed charge density ΦX, the various values of permselectivity P_s were calculated by substituting the values of α (bulk) and t^-_{app} in Eq. 23, and then plotted against $\log \frac{C_1 + C_2}{2}$. The results are shown in Fig. 5 (*vide* Table II). The term ζ has been defined as the ratio between the average concentration C and the

Table II

Values of permselectivity P_S for various electrolytes at different concentrations

Membrane	← Silver hexacyanoferrate(II)→						← Cadmium hexanocyanoferrate(II)→					
Electrolyte	Concentrations 'M'						Concentrations 'M'					
	0.1	0.05	0.02	0.01	0.005	0.002	0.1	0.05	0.02	0.01	0.005	0.002
KNO_3	0.35	0.44	0.50	0.54	0.56	0.59	0.49	0.50	0.52	0.52	0.54	0.56
KCl	—	—	—	—	—	—	0.36	0.39	0.43	0.44	0.46	0.48
$NaNO_3$	0.55	0.55	0.59	0.64	0.68	0.69	0.62	0.64	0.65	0.70	0.75	0.76

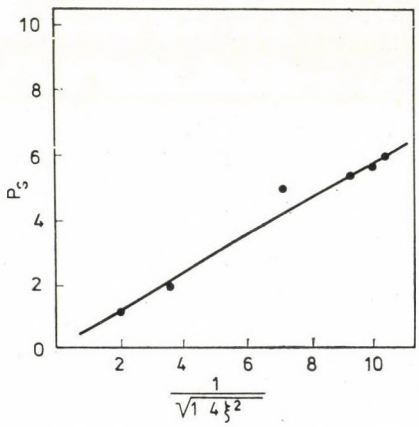

Fig. 6. Plots of P_S *vs.* $\frac{1}{\sqrt{1+4\xi^2}}$ for KNO_3 with Silver Hexacyanoferrate(II) membrane

effective fixed charge density ΦX *i.e.* $\zeta = \frac{C}{\Phi X}$ the units of both C and ΦX are expressed in terms of moles or equivalents/litre when the average concentration C is equal to the effective fixed charge density ΦX *i.e.* $C/\Phi X = \zeta = 1$, the value of P_s must give $\frac{1}{\sqrt{5}} = 0.447$ from left hand side of Eq. 23. The corresponding concentration is obtained from the plots of P_s *versus* long C as given in Fig. 5. The value of the concentration is equal to the fixed charge density, the ΦX values are given for electrolytes with both membranes in Table I. Further, the plots of P_s *versus* $(1 + 4\,\zeta^2)^{-\frac{1}{2}}$ were drawn for one membrane with KCl and shown in Fig. 6. It is evident that the line nearly passes through the origin with unit slope, thereby confirming the applicability of KOBATAKE's equation to these membranes.

*

The authors are grateful to Professor WASIUR RAHMAN, Head of the Department of Chemistry, for providing research facilities. The financial assistance from CSIR (New Delhi, India) to two of us S.P.S. and A.H. is gratefully acknowledged.

REFERENCES

[1] TEORELL, T.: Proc. Soc. Expt. Biol., **33,** 282 (1935); Proc. Natl. Acad. Sci., (U.S.A.), **21,** 152 (1935); Z. Elektrochem. **55,** 460 (1951)
[2] MEYER, K. H., SIEVERS, K. F.: Helv. Chim. Acta., **19,** 649, 665, 987 (1963)
[3] SCHLOGL, R.: Z. Elektrochem., **57,** 195 (1953); Z. Physik. Chem. (Frankfurt), **1,** 305 (1954)
[4] SCATCHARD, G.: J. Am. Chem. Soc., **75,** 2883 (1956)
[5] HILLS, G. J., JACOBES, P. W. N., LAKSHMINARAYANAIAH, N.: Proc. Roy. Soc. (London) A262, 246 (1961)
[6] KOBATAKE, Y.: J. Chem. Phys. **28,** 146 (1958)
[7] LORIMER, J. W., BOTERENBROOD, E. I., HERMANS, J. J.: Disc. Faraday Soc. **21,** 141 (1956)
[8] STAVERMAN, A. J.: Trans. Faraday Soc. **48,** 176 (1952)
[9] NAGASAWA, M., KAGAWA, I.: Disc. Faraday Soc., **21,** 52 (1956)
[10] NAGASAWA, M., KOBATAKE, Y.: J. Phys. Chem., **56,** 1017 (1952)
[11] SIDDIQI, F., A., PRATAP, S.: J. Electroanal. Chem. **23,** 137, 147 (1969)
[12] SIDIQI, F. A., LAKSHMINARAYANAIAH, SAKSENA, K.: Z. Physik Chem. (Frankfurt) **72,** 298, 307 (1970)
[13] SIDDIOI, F. A., LAKSHMINARAYANAIAH, NASIM, Beg, M.: J. Polym. Sci., **9,** 2853, 2869 (1971)
[14] LAKSHMINARAYANAIAH, SIDDIQI, A.: Biophys. J. **11,** 603, 617 (1971)
[15] LAKSHMINARAYANAIAH, SIDDIQI: Biophys. J. **12,** 540 (1972)
[16] LAKSHMINARAYANAIAH, N., SIDDIQI, F. A.: in "Membrane Processes in Industry and Biomedicine" Edited by M. Bier, Plenum Press, New York (1971)
[17] SIDDIQI, F. A., NASIM, Beg, M., SINGH, P., HAO, A.: Bull. Chem. Soc. Japan. **49,** 2864 (1976)
[18] SIDDIQI, F. A., BEG, M. N., HAO, A., SINGH, P.: Bull. Chem. Soc., Japan **49,** 2858 (1976)
[19] SIDDIQI, F. A., BEG, M. N., SINGH, S. P.: J. Polym. Sci. **15,** 959 (1977)
[20] KOBATAKE, Y., TAKEGUCHI, N., TOYOSHIMA, Y., FUJITA, H.: J. Phys. Chem. **69,** 3981 (1965)
[21] KAMO, N., TOYOSHIMA, Y., KOBATAKE, Y.: Kolloid-Z, Z-Polym. **249,** 1061 (1971)
[22] KAMO, N., TOYOSHIMA, Y., NOZAKI, H., KOBATAKE, Y.: Kolloid Z, Z-Polym. **248,** 914 (1971)
[23] TOYOSHIMA, Y., YUSSA, M., KOBATAKE, Y., FUJITA, H.: Trans. Faraday Soc., **63,** 2803, 2814 (1967)
[24] YUSSA, M., KOBATAKE, Y., FUJITA, H.: J. Phys. Chem. **72,** 2871 (1968)
[25] KAMO, N., OCKAWA, M., KOBATAKE, Y.: J. Phys. Chem., **77,** 92 (1973)
[26] WEISER, H. B.: J. Phys. Chem. **34,** 355, 1826 (1930)
[27] MICHAELIS, L.: Bull. Natl. Res. Council (U.S.A.), **69,** 119 (1929)
[28] SOLLNER, K., GREGORE, H. P.: J. Phys. Chem. **51,** 299 (1947)
[29] MARSHALL, C. E., AYERS, A. D.: J. Am. Chem. Soc. **70,** 1297 (1948)
[30] GUGGENHEIM, E. A.: Phil. Mag.: **19,** 588 (1935)

Fasih A. SIDDIQI
M. Naseem BEG
Surendra P. SINGH
Abdul HAQ

Aligarh 202001 India.

Acta Chimica Academiae Scientiarum Hungaricae, Tomus 93 (2), pp. 135—140 (1977)

MAGNETIC PROPERTIES OF COPPER(II) COMPLEXES OF ONO DONOR TRIDENTATE SCHIFF BASES DERIVED FROM 2-HYDROXY-1-NAPHTHALDEHYDE AND ALCOHOLAMINES

A. SYAMAL and K. S. KALE

(Department of Chemistry, Regional Engineering College, Kurukshetra 132119 Haryana India)

Received August 25, 1976

The synthesis of several new copper(II) complexes of Schiff bases derived from 2-hydroxy-1-naphthaldehyde and ethanolamine, propanolamine, isopropanolamine, 2-amino-2-methylpropanol are described. The Schiff bases coordinate through 0,0 and N as dibasic tridentate ligands. The complexes were characterized by elemental analysis, magnetic susceptibility measurements (83—297 °K), infrared and electronic spectra. The complex containing propanolamine, exhibits magnetic moment of 0.46 B.M. ($-J = 846$ cm^{-1}) indicating the presence of strong antiferromagnetic interaction. In this complex the spins of the interacting copper(II) ions are completely coupled having a sole population of the singlet state. The complexes containing ethanolamine and isopropanolamine are involved in ferromagnetic spin-spin exchange ($J = +28$ to $+67$ cm^{-1}). The copper(II) complex with the ligand 2-hydroxynaphthaldehyde-2-methylpropanol exhibits the behaviour of antiferromagnetic exchange ($-J = 91$ cm^{-1}). A comparison of the magnetic properties of the complexes with the corresponding oxovanadium(IV) complexes is presented.

Introduction

In recent years there has been considerable interest on the synthesis and magnetic studies of copper(II) complexes of Schiff bases derived from salicylaldehyde and alcoholamines [1—3]. In continuation of our work in this area [1] we report here the synthesis and magnetic properties of copper(II) complexes of Schiff bases (I) derived from 2-hydroxy-1-naphthaldehyde and ethanolamine, propanolamine, isopropanolamine, and 2-amino-2-methylpropanol. The complexes were characterized by elemental analysis, magnetic susceptibility measurements and electronic spectra.

Experimental

Materials and methods

Copper was determined iodometrically after igniting the complexes to copper oxide and dissolving the oxide in HCl. Nitrogen analyses were carried out by semimicro Dumma's method. Magnetic susceptibility measurements were performed at 83—297 °K by the Gouy method using $Hg[Co(NCS)_4]$ as a standard. The temperature variation was done using a modified cryostat similar in design to that described by FIGGIS and NYHOLM [4]. Diamagnetic corrections of the metal and ligand atoms were calculated using a standard source [5]. The

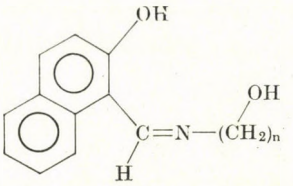

Ia n = 2,3

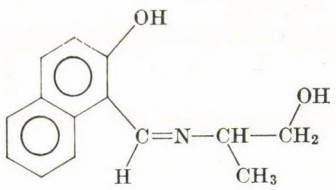

Ib

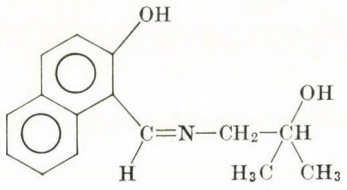

Ic

Fig. 1

reflectance spectra were recorded with the help of a Unicam SP8000 recording spectrophotometer equipped with a reflectance attachment. 2-Hydroxynaphthaldehyde and alcoholamines were purchased from Fluka AG (Switzerland).

General method of preparation of the complexes

2-Hydroxy-1-naphthaldehyde (0.86g, 0.005 mole) was dissolved in 30 ml of hot methanol. To this a methanolic solution of the appropriate alcoholamine (0.005 mole in 15 ml) was added and the mixture was refluxed on a steam bath for 30 min and a yellow solution of the Schiff base was obtained. Copper(II) acetate monohydrate (1.0 g, 0.005 mole) was dissolved in 60 ml hot methanol. The Schiff base solution was then added to the copper acetate solution slowly with stirring and the mixture was refluxed for two hours while stirring magnetically. The separated green precipitates were suction filtered, washed with methanol and dried under vacuum at room temperature. Yield = 80%. The complexes are insoluble in common non-coordinating organic solvents.

The analytical data are presented in Table I.

Table I

Analytical data of copper(II) complexes[a]

Complex	Stoichiometry	%Cu		%N	
		Found	Reqd.	Found	Reqd.
Cu(hydrox-ethanolamine)	$CuC_{13}H_{11}NO_2$	22.1	22.96	4.9	5.05
Cu(hydrox-isopropanolamine)	$CuC_{14}H_{13}NO_2$	21.0	21.86	4.9	4.82
Cu(hydrox-propanolamine)	$CuC_{14}H_{13}NO_2$	21.0	21.86	5.2	4.82
Cu(hydrox-2-amino-2-methylpropanol)	$CuC_{15}H_{15}NO_2$	19.9	20.85	4.8	4.60

[a] Abbreviation: hydrox = 2-hydroxy-1-naphthaldehyde.

Results and discussion

The new complexes reported in this paper have been prepared by the chelation reaction of copper(II) acetate and the Schiff bases derived from 2-hydroxynaphthaldehyde and ethanolamine, propanolamine, isopropanolamine and 2-amino-2-methylpropanol. The absence of the ν(OH) stretching frequency in the infrared spectra of the complexes indicates deprotonation of the Schiff bases on complex formation and dibasic behaviour of the ligands. The analytical data of the complexes indicate 1 : 1 copper : ligand ratio and the complexes are apparently tricoordinated. The ligands are behaving as tridentate dibasic ligands as is evident from infrared and analytical data. The tridentate dibasic character of these ligands allows the complexes to dimerise or polymerise. The insolubility of the complexes in non-coordinating solvents indicates polymeric nature of the complexes. The molecular

Table II

Magnetic susceptibility data of copper(II) complexes from 83 to 297 °K[a] [b]

Cu(hydrox-ethanolamine)				Cu(hydrox-isopropanolamine)			
Temp. (°K)	χ_M^{corr} (10^{-6} cgs. unit)	μ_{eff} (B.M.)	J cm^{-1}	Temp. (°K)	χ_M^{corr} (10^{-6} cgs. unit)	μ_{eff} (B.M.)	J cm^{-1}
297	1489	1.89		297	1352	1.84	
210	2184	1.92		206	2069	1.85	
177	2608	1.93	+67	151	2828	1.86	+28
155	2998	1.94		118	3702	1.88	
124	3865	1.97		107	4258	1.92	
101	4883	1.99		83	6048	2.01	
85	5805	2.01					
Cu(hydrox-2-amino-2-methalpropanolamine)				Cu(hydrox-propanolamine)			
Temp. (°K)	χ_M^{corr} (10^{-6} cgs. unit)	μ_{eff} (B.M.)	J cm^{-1}	Temp. (°K)	χ_M^{corr} (10^{-6} cgs. unit)	μ_{eff} (B.M.)	J cm^{-1}
297	1177	1.68		297	88	0.46	−846
202	1616	1.62					
170	1843	1.59	−91				
147	2032	1.55					
115	2480	1.52					
98	2752	1.47					
85	3022	1.44					

[a] The magnetic moment was calculated using the Curie equation: $\mu_{eff} = 2.84\,(\chi_M^{corr} \times T)^{1/2}$ B.M.

[b] TIP $= 60 \times 10^{-6}$ cgs unit; g $= 2.1$.

weights cannot be determined due to the insolubility of the complexes in common solvents. But magnetic susceptibility data of the complexes indicate magnetically condensed nature of the complexes. The magnetic moments (see Table II) of the complexes copper(hydroxynaphthaldehyde–ethanolamine) and copper(hydroxynaphthaldehyde–isopropanolamine) increase as the temperature is lowered. The exchange integral, J of the complexes was calculated using Bleaney—Bowers equation [7]:

$$\chi_M^{corr} + \frac{g^2 N\beta^2}{3kT}[1 - 1/3 \exp(J/kT)]^{-1} + N\alpha$$

where N_α = the temperature-independent paramagnetism term, χ_M^{corr} = magnetic susceptibility per g — atom of copper corrected for diamagnetism, and g = gyromagnetic ratio. J of the complexes copper(hydroxynaphthaldehyde–ethanolamine) and copper(hydroxynaphthaldehyde–isopropanolamine) is positive (see Table II). These informations indicate the presence of ferromagnetic exchange in these complexes [7, 8]. The complex copper(hydroxynaphthaldehyde–propanolamine) has only a small temperature-independent paramagnetism term (μ_{eff} = 0.46 BM at 297 °K) and the complex is involved in strong antiferromagnetic exchange. This compound is novel in the sense that the spins are completely coupled with sole population being the diamagnetic singlet state. J of the complex copper(hydroxynaphthaldehyde–propanolamine) is estimated to be —846 cm^{-1}. The strong antiferromagnetic exchange requires a Cu(II) environment very close to a planar structure and hence the entire molecule is probably flat. There exists a correlation between J values and Cu—O—Cu bond angles. The crossover bond angle (Cu—O—Cu) from ferromagnetic to antiferromagnetic exchange is ~98° [9]. The strong antiferromagnetic interaction (J = —846 cm^{-1}) in copper(hydroxynaphthaldehyde–propanolamine) indicates Cu—O—Cu bond angle is appreciably higher than 98°. It is of interest to know that the complexes copper (salicylaldehyde–propanolamine) and copper (acetylacetone–propanolamine) complexes exhibit also small temperature-independent paramagnetism term (μ_{eff} at room temperature = 0.49 B.M. and 0.41 B.M. respectively) [2, 10]. The single crystal X-ray structure of copper(acetylacetone-propanolamine) indicates the dimeric nature of the complex with alcoholic oxygen atoms as the bridging atoms [10]. We suggest a similar dimeric structure for the copper(hydroxynaphthaldehyde–propanolamine) complex. The magnetic data of the copper-(hydroxynaphthaldehyde-2-amino-2-methylpropanol) complex indicate that the magnetic moment of the complex decreases as the temperature is lowered and this is characteristic of the presence of antiferromagnetic exchange (—J = 91 cm^{-1}) [11]. As the complex is antiferromagnetic a structure similar to copper(acetylacetone–propanolamine) may be proposed for this complex.

The magnetic properties of copper(hydroxynaphthaldehyde–ethanolamine) and copper(hydroxynaphthaldehyde–isopropanolamine) are comparable with the magnetic properties of copper(acetylacetone–ethanolamine) [10] and copper(salicylaldehyde–ethanolamine) [1]. The single crystal X-ray structure of copper(acetylacetone–ethanolamine) indicates the tetrameric nature of the complex [10]. A similar tetrameric structure has been proposed for copper-(salicylaldehyde–ethanolamine) [1]. As the magnetic properties of our complexes, copper(hydroxynaphthaldehyde–ethanolamine) and copper(hydroxynaphthaldehyde–isopropanolamine) are similar to these complexes a tetrameric structure may be proposed to our ferromagnetic complexes [1, 10].

The reflectance spectra of the complexes exhibit one asymmetric band centered at around 16000—17000 cm^{-1} (see Table III). This band is assigned

Table III

Electronic spectral data of copper(II) Schiff base complexes

Complex	Medium	ν_{max} cm^{-1}
Cu(hydrox-ethanolamine)	reflectance	15 970
Cu(hydrox-isopropanolamine)	reflectance	15 870
Cu(hydrox-propanolamine)	reflectance	17 990
Cu(hydrox-2-amino-2-methyl-propanol)	reflectance	16 950

to the *d–d* transitions. It is interesting to note that the complexes with antiferromagnetic properties exhibit this band at higher energy in comparison to the complexes with ferromagnetic properties. This difference in band position may be attributed to the presence of different structure in antiferromagnetic and ferromagnetic complexes [10, 12].

It is of interest to compare the magnetic properties of these complexes with the corresponding oxovanadium(IV) complexes as both copper(II) oxovanadium(IV) ions belong to $s = 1/2$ system. The oxovanadium(IV) complexes of the present ligands are all involved in antiferromagnetic exchange [13, 14]. The mechanism of antiferromagnetic exchange in these oxovanadium(IV) complexes is believed to be through the direct σ overlap of d_{xy} orbitals of adjacent vanadium atoms [13]. In copper(II) complexes the unpaired electron is in the $d_{x^2-y^2}$ orbital and electronic spin–spin exchange takes place by superexchange through the bridging atoms in tridentate ligands. As the copper(II) and oxovanadium(IV) complexes with the ligands hydroxynaphthaldehyde–propanolamine, hydroxynaphthaldehyde-2-amino-2-methylpropanol are all involved in antiferromagnetic exchange, probably the structures of these copper(II) and oxovanadium(IV) complexes are similar and presumably

they are dimeric. The requirement for the complexes to possess triplet ground state (ferromagnetic spin–spin exchange) is that the adjacent metal ions should have their unpaired electrons in orthogonal interacting orbitals. To have such an orthogonal overlap through out-of-plane interaction involving d_{z^2} orbital is quite favourable in copper(II) complexes. In oxovanadium(IV) complexes the d_{z^2} orbital is in the direction of V = 0 axis and direct interaction of this orbital with the d_{xy} orbital of another V atom at 90° does not seem to be feasible. However, the coupling of the unpaired spins at 90° in the orbitals *e.g.* $V_1 d_{z^2}$ — suitable orbital of the ligand atom (coordinated to another V atom) in the square plane $-V_2 d_{x^2-y^2}$ may lead to ferromagnetism which would be sufficiently weak because the unpaired electron in oxovanadium(IV) complexes is in the d_{xy} orbital and $d_{xy} - d_{x^2-y^2}$ or $d_{xy} - d_{z^2}$ mixing will occur only in the excited state. The magnetic properties of copper(II) and oxovanadium(IV) complexes of the ligands hydroxynaphthaldehyde–ethanolamine and hydroxynaphthaldehyde–isopropanolamine indicate that the structures of the complexes are different in these two metal ions. The oxovanadium(IV) complexes with these ligands are believed to be dimeric and in case of copper(II) complexes we have proposed a tetrameric structure with out-of-plane interaction.

*

The authors are indebted to the Department of Atomic Energy (Govt. of India) for support of this work. This work is also supported in part by the faculty research fund of the University of Bombay.

REFERENCES

[1] Syamal, A., Theriot, L. J.: J. Coord. Chem. **2** (1973) 241
[2] Kato, M., Muto, Y., Jonassen, H. B., Imai, K., Harano, A.: Bull. Chem. Soc., Japan, **41** (1968) 1864
[3] Tokii, T., Muto, Y., Kato, M., Imai, K., Jonassen, H. B.: J. Inorg. Nucl. Chem. **34** (1972) 3377
[4] Figgis, B. N., Nyholm, R. S.: J. Chem. Soc. **1959,** 331
[5] Figgis, B. N., Lewis, J.: cited in Modern Coordination Chemistry, Edited by Lewis, J. and Wilkins, R. G., (Interscience Publishers, Inc., New York), (1960) 403
[6] Bleany, B., Bowers, K. D.: Proc. Roy. Soc. A**214** (1952) 451
[7] Casey, A. T., Hoskins, B. F., Williams, F. D.: Chem. Comm. 904 (1970)
[8] Barnes, J. A., Hodgson, D. J., Hatfield, W. E.: Inorg. Chem. **11** (1972) 144
[9] McGregor, K. T., Watkins, N. T., Lewis, D. L., Drake, R. F., Hodgson, D. J., Hatfield, W. E.: Inorg. Nucl. Chem. Lett., **9,** (1973) 423
[10] Bertrand, J. A., Kelley, J. A.: Inorg. Chim. Acta, **4** (1970) 203
[11] Syamal, A.: Coord. Chem. Rev. **16** (1975) 309
[12] Bertrand, J. A., Kirkwood, C. E.: Inorg. Chim. Acta., **6** (1972) 248
[13] Syamal, A.: Indian J. Chem. **11** (1973) 363
[14] Syamal, A., Kale, K. S.: Indian J. Chem. (in press)

A. Syamal
K. S. Kale
Kurukshetra 132119, Haryana, India.

Acta Chimica Academiae Scientiarum Hungaricae, Tomus 93 (2), pp. 141–148 (1977)

ELEKTROCHEMISCHE UND ESR-SPEKTROSKOPISCHE UNTERSUCHUNGEN AM RADIKALANION DES OKTACYAN-CHINODIMETHANS

L. Bucsis und H. Kiesele

(Chemisches Laboratorium der Universität Freiburg i. Br.)

Eingegangen am 29. August 1976

Das Dianion des 1,4-Bis(dicyanmethyl)-2,3,5,6-tetracyanbenzols **3** und des Tetracyan-hydrochinons **6** wurden chemisch und elektrochemisch oxidiert. Als Reaktionsprodukt erwies sich das Radikalanion des Oktacyan-chinodimethans **4** und das Oktacyanchinodimethan (OCNQ) **5**, bzw. das Radikalanion Tetracyan-benzosemichinon **7** und das Tetracyan-benzochinon **8**. Die Halbstufenpotentiale der Übergänge Dianion/Radikalanion und Radikalanion/Chinoid wurden gemessen. Die Werte genügen der Hammett-Gleichung und passen gut in die Reihe der 7,7′,8,8′-Tetracyan-chinodimethane, bzw. Chinone. Die chemische Oxidation führt zum Radikalanion **4** bzw. **7**. Aus den ESR-Spektren von **4** und **7** wurden die N-Kopplungskonstanten entnommen. Ergebnisse von HMO-Berechnungen stimmen mit diesen Kopplungskonstanten gut überein.

Die Charge Transfer (CT)-Salze des Tetracyan-chinodimethans (TCNQ) **1** mit Tetrathio-fulvalen **2** und anderen Donoren wurde wegen ihrer außergewöhnlichen elektrischen Eigenschaften in den letzten Jahren intensiv untersucht [1, 2].

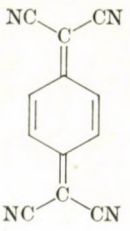

1

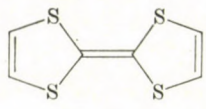

2

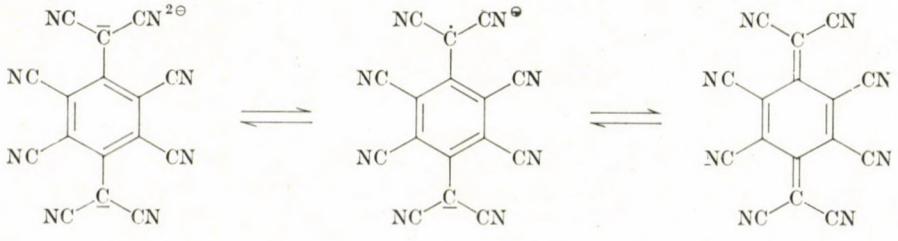

3 **4** **5**

Da Oktacyan-chinodimethan (OCNQ) **5** ähnliche Eigenschaften aufweisen sollte, schien es von Interesse, Oxidationsversuche am Dianion des 1,4-Bis(-dicyanmethyl)-2,3,5,6-tetracyanbenzols **3** [3] durchzuführen. Hierzu haben wir das Redoxsystem **3** $\rightleftharpoons$ **4** $\rightleftharpoons$ **5** zunächst mit Hilfe von Gleichstrom- und Cyclischer Voltammetrie untersucht und die paramagnetische Spezies **4** ESR-spektroskopisch charakterisiert.

Frühere Untersuchungen [4] haben gezeigt, daß das TCNQ ein analoges Verhalten zum Benzochinon aufweist. Daher wurde das Tetracyan-benzochinon **8** [5, 6] bzw. dessen Dianion **6** mit in die Untersuchungen einbezogen.

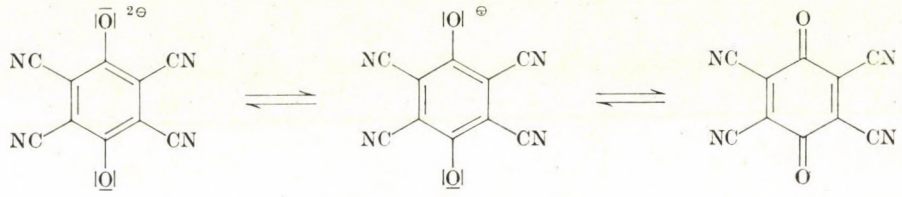

6 **7** **8**

Um eine quantitative Einordnung der beiden Verbindungen **5** und **8** in die Reihe der Tetracyan-chinodimethane bzw. Chinone zu ermöglichen, wurde ihr Redoxverhalten mit dem der Grundkörper sowie einiger Derivate verglichen.

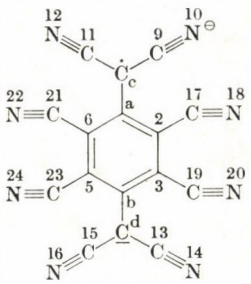

Im folgenden soll über die elektrochemischen und ESR-spektroskopischen Untersuchungen berichtet werden.

Elektrochemische Untersuchungen

Das Polarogramm des Dianions **3** zeigt bei der anodischen Oxidation zwei reversible Einelektronenübergänge. Abbildung 1. Dieser Befund wird durch das Cyclische Voltammogramm bestätigt, das in Abbildung 2 dargestellt ist. Das gleiche Redoxverhalten ist auch bei den anderen Verbindungen dieser Serie zu beobachten.

Erwartungsgemäß besitzt das percyanierte OCNQ-System die positiv-

sten Potentiale innerhalb der Tetracyan-chinodimethan-Reihe [7]. Wählt man das erste Reduktionshalbstufenpotential von TCNQ **1** als Bezugspunkt und bildet $\Delta E^1_{1/2}$, d. h. die Potentialdifferenzen zu den jeweils ersten Halbstufenpotentialen der anderen Verbindungen dieser Serie, so fügen sich die bestimmten Potentialwerte zwanglos in eine Lineare Freie Energie Beziehung (LFE) nach Hammett ein. Abbildung 3. Tabelle I. Aus dem Diagramm ergibt sich eine Reaktionskonstante $\varrho_Q = 340$; die potentialerhöhende Wirkung einer Cyangruppe beträgt +230 mV.

In der Chinonreihe erfolgt die anodische Oxidation des Dianions **6** in

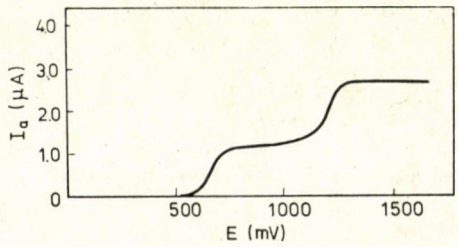

Abb. 1. Gleichstrom-Voltammogramm des Natriumsalzes von **3** in Benzonitril/0,1 m TBAP

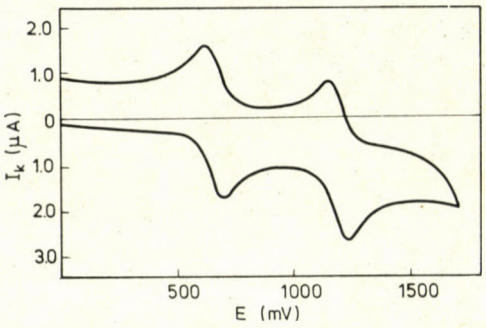

Abb. 2. Cyclisches Voltammogramm des Natriumsalzes von **3** in Benzonitril TBAP, v = = 0,297 V/sec

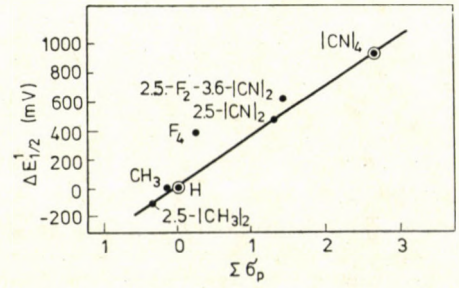

Abb. 3. LFE-Beziehung für die Redoxpotentiale $\Delta E^1_{1/2}$ der Tetracyan-chinodimethanreihe. Die Punkte entstammen Literaturzitat [7]

Tabelle I

Halbstufenpotentiale des Oktacyan-chinodimethans, des Tetracyanbenzochinons und einiger verwandten Verbindungen

Verbindung	Chinoid/Radikalanion			Radikalanion/Dianion		$\Delta E_{1/2}$ mV
	$E^1_{1/2}$ mV	s mV	$\Delta E^1_{1/2}$ mV	$E^2_{1/2}$ mV	s mV	
TCNQ	303	63		— 348	82	651
OCNQ	1209	53	906	661	63	548
Benzochinon	— 400			—1340		940
Durochinon	— 760		— 360	— 1635		875
Tetracyanchinon	995	68	1395	174	69	821

$E_{1/2}$: Halbstufenpotentiale in Benzonitril/0,1 m TBAP gegen Ag/AgCl-Bezugselektrode,
s: Aus der logarithmischen Analyse [12] ermittelte Geradensteigungen.

zwei reversiblen Einelektronenübergängen. Auch hier erhöht eine zunehmende Zahl elektronenanziehender Cyangruppen das Redoxpotential und so besitzt das Tetracyan-benzochinon **8** unter den Chinonen das höchste Redoxpotential. Ähnlicherweise erlaubt die $\Delta E^1_{1/2}$-Bildung den Vergleich mit anderen Chinonen [8]. Die Reaktionskonstante ist jedoch mit $\varrho_{Ch} = 530$ um 190 größer als bei den Tetracyan-chinodimethanen. Abbildung 4. Die potentialerhöhende Wirkung einer Cyangruppe vergrößert sich; sie beträgt 350 mV und ist damit um 120 mV größer, als bei den Tetracyan-chinodimethanen.

Aus den Quotienten der Reaktionskonstanten $\varrho_{Ch}/\varrho_Q = 1{,}6$ wird ein stärkerer Substituenteneinfluß auf das Benzochinon gegenüber dem TCNQ-System ersichtlich.

Vergleicht man die Differenzen $\Delta E_{1/2}$ zwischen dem ersten und zweiten Halbstufenpotential innerhalb der beiden Reihen, so findet man, daß die Dif-

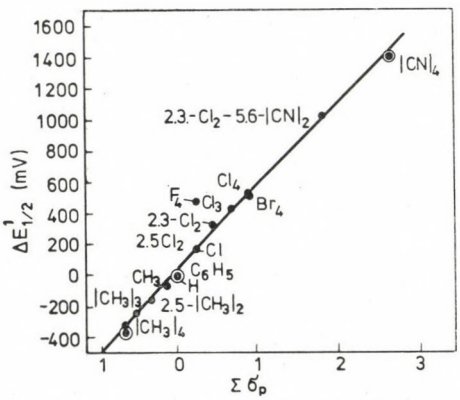

Abb. 4. LFE-Beziehung für die Redoxpotentiale $\Delta E^1_{1/2}$ der Chinonreihe. Die Punkte entstammen Literaturzitat [8]

ferenz beim OCNQ-System von allen aufgeführten Verbindungen am kleinsten ist. Dieser Befund verdient besondere Beachtung, da nach [1] die elektrische Leitfähigkeit eng mit $\Delta E_{1/2}$ korreliert ist. Da OCNQ weiterhin das positivste Reduktionspotential aufweist — Lage des Redoxpotentials ist ein weiteres Kriterium zur Beurteilung der elektrischen Leitfähigkeit [1] — erscheint **5** zur Herstellung von leitenden CT-Salzen besonders geeignet.

ESR-spektroskopische Untersuchungen

Das ESR-Spektrum des OCNQ-Radikalanions ($OCNQ^{\cdot-}$) **4** ist in Abbildung 5 dargestellt. Es besteht aus zwei Nonetts, die auf zwei Paare von je vier äquivalenten Stickstoffatomen zurückzuführen sind. Daneben ist eine Reihe intensitätsschwacher Linien zu erkennen, die von ^{13}C-Aufspaltungen herrühren. Die Stickstoffkopplungskonstanten betragen $a_{N'} = 1{,}09$ G und $a_{N''} = 0{,}125$ G. Das mit diesen Werten simulierte ESR-Spektrum ist in Abbildung 6 wiedergegeben. Für die Simulation wurden Lorentz-Kurven und eine Halbwertsbreite von 99 mG zugrunde gelegt.

Die Zuordnung der Kopplungskonstanten geht aus der theoretisch berechneten Spindichteverteilung hervor. Danach ist die Aufspaltung von $a_{N'} = 1{,}09$ G auf exocyclische Nitrilgruppen zurückzuführen, während die kleine Kopplungskonstante $a_{N''} = 0{,}125$ G den kernständigen Nitrilgruppen zugeschrieben werden muß. Diese Interpretation wird auch durch einen Vergleich mit dem Radikalanion des TCNQ gestützt. Bei diesem Radikal wur-

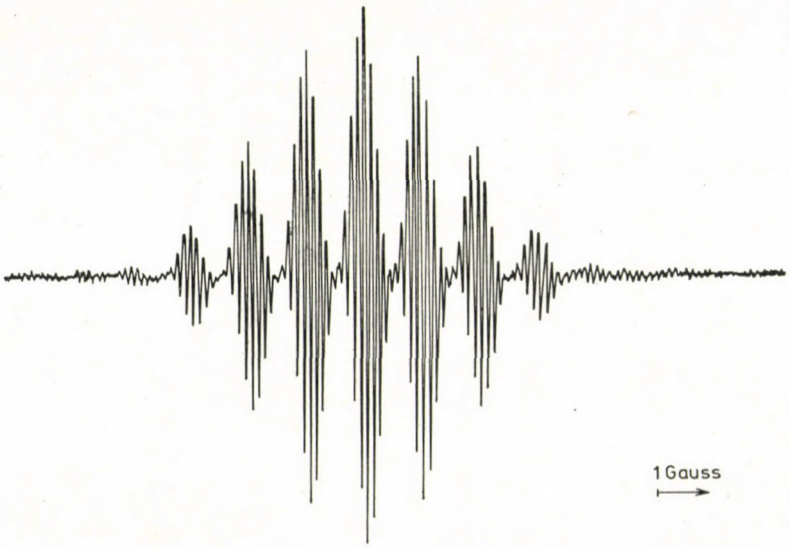

Abb. 5. Experimentelles ESR-Spektrum des Pyridiniumsalzes von **4** in DME bei 25 °C

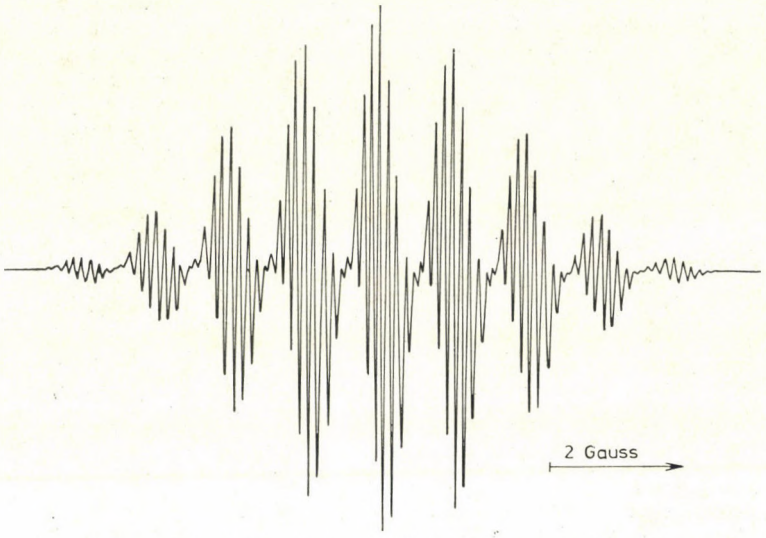

Abb. 6. Simuliertes ESR-Spektrum von **4**

den die Stickstoffkopplungskonstanten der exocyclischen Nitrilgruppen zu 1,02 bzw. 1,01 G bestimmt [9, 10].

Die Spindichteverteilung haben wir nach dem HMO-Verfahren berechnet, wobei die in Tabelle II angeführten Parameter verwendet wurden, die sich eng an Literaturwerte [9] anlehnen.

Die Umrechnung der Spindichten in Kopplungskonstanten erfolgte über die einfache Relation [11]:

$$a_N = K_N^N \cdot \varrho_N$$

Für K_N^N wurde ein Wert von 25 G eingesetzt. Die theoretisch berechneten Spindichten und Kopplungskonstanten sind zusammen mit den experimentell ermittelten Werten in Tabelle II aufgeführt.

Die relativ gute Übereinstimmung zwischen experimentellen und berechneten Kopplungskonstanten läßt darauf schliessen, daß die $C(CN)_2$-Gruppierung koplanar zum übrigen Molekülgerüst angeordnet ist. Eine solche Anordnung wäre eine weitere notwendige Voraussetzung für die Ausbildung leitender CT-Kristalle [1].

Es erscheint bemerkenswert, daß die Aufenthaltswahrscheinlichkeit des ungepaarten Elektrons an den C(CN)-Gruppierungen des $OCNQ^{\cdot-}$-Radikals sehr viel größer ist als im Ring, obwohl man qualitativ erwarten würde, daß die vier kernständigen CN-Gruppen zu einer gleichmäßigeren Spindichteverteilung führen.

Demgegenüber weist das Radikalanion **7** eine wesentlich größere Kopplungskonstante an den kernständigen CN-Gruppen auf. Sie beträgt 0,3 G. Das sehr einfache ESR-Spektrum des Radikals ist in Abbildung 7 dargestellt.

Tabelle II

Berechnete Spindichten, Kopplungskonstanten und experimentelle ^{14}N-Kopplungskonstanten des Oktacyan-chinodimethan-Radikalanions

Position	ber. Spindichte ϱ	$a_{ber.}$ [G]	$a_{exp.}$ [G]
a, b	0,0346	0,86	
c, d	0,2315	5,79	
2, 3, 5, 6	0,0484	1,21	
9, 11, 13, 15	0,0107	0,27	
10, 12, 14, 16	0,0460	1,15	1,09
17, 18, 21, 23	0,0022	0,06	
18, 20, 22, 24	0,0096	0,24	0,125

HMO-Parameter: alle $\alpha_C = \alpha_0$
alle $\alpha_N = \alpha_C + 1{,}0\,\beta_0$
alle $\beta_{C=N} = 2{,}0\,\beta_0$
alle $\beta_{C-C\equiv N} = 0{,}9\,\beta_0$
$\beta_{a-c} = \beta_{b-d} = 0{,}9\,\beta_0$
alle übrigen $\beta = \beta_0$

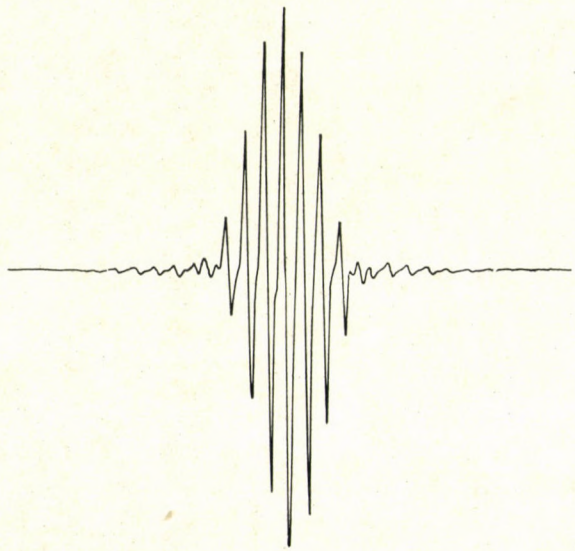

Abb. 7. Experimentelles ESR-Spektrum von 7 bei 25 °C

Experimentelles

Elektrochemische Untersuchungen

Die elektrochemischen Untersuchungen wurden in einer 0,1 molaren Lösung von Tetrabutylammonium-perchlorat (TBAP) in wasserfreiem Benzonitril in einem Dreielektrodenverfahren durchgeführt. Als Arbeitselektrode wurde eine Pt-Scheibenelektrode verwendet, deren Umdrehungsgeschwindigkeit bei den DC-Messungen 750 U/min betrug. Als Bezugselektrode diente eine Ag/AgCl-Elektrode in Benzonitril/Tetramethylammoniumchlorid. **3** wurde als Natriumsalz [3] und **6** als Di-tetraäthylammonium **6a** eingesetzt.

Di-tetraäthylammonium-salz des Tetracyan-hydrochinons **6a**: 0,5 g Tetracyan-hydrochinon-Dioxan-Komplex [5, 6] werden in 20 ml Wasser/Aceton (1 : 1) gelöst und so lange mit Tetraäthylammonium-hydroxyd versetzt bis die entstehende tiefrote Farbe nicht mehr dunkler wird. Dann läßt man das Lösungsmittel an der Luft verdunsten, bis nur noch überschüßige Base und dunkelrote Kristalle übrig bleiben. Nach dem Abpressen auf einer Tonplatte wird getrocknet und unter Feuchtigkeitsausschluß aufbewahrt.

ESR-spektroskopische Untersuchungen

Das Radikalanion **4** wurde aus **3**, das als Dipyridiniumsalz [3] vorlag, durch Oxidation mit Brom in Dimethoxiäthan (DME) hergestellt. Das Radikalanion **7** erhielten wir durch Oxidation von **6a** mit Jod in DME. Die Radikallösungen wurden durch mehrmaliges Einfrieren unter Reinststickstoff, Abpumpen und Auftauen von Sauerstoff befreit und bei 25 °C in abgeschmolzenen Proberöhrchen mit einem Varian E9 ESR-Spektrometer gemessen.

Radikalanion des Oktacyan-chinodimethans **4**: 0,116 g (0,25 mMol) Dipyridiniumsalz des 1,4-Bis(-dicyanmethyl)-2,3,5,6-tetracyan-benzols **3a** werden in 30 ml abs. DME suspendiert und mit 0,02 g (0,25 mMol) Brom versetzt. Es wird 30 sec geschüttelt, wobei das Radikal in Lösung geht. Die grüne Radikallösung wird in das ESR-Röhrchen abfiltriert und entgast.

Radikalanion des Tetracyan-benzochinons **7**: 0,02 g Di-tetraäthylammoniumsalz des Tetracyan-hydrochinons **6a** werden in 2 ml Acetonitril gelöst und ein Körnchen Jod zugegeben. Die Radikalbildung ist an der grünen Farbe der Lösung erkenntlich. Die Lösung wird in ein ESR-Röhrchen agbefüllt, das Acetonitril im Hochvakuum entfernt und durch DME ersetzt.

LITERATUR

[1] GARITO, A. F., HEEGER, A. J.: Accounts Chem. Res. **7**, 232 (1974)
[2] METZ, W. D.: Science **190**, 450 (1975)
[3] BUCSIS, L., FRIEDRICH, K.: im Druck
[4] MELBY, L. R., HARDER, R. J., HERTLER, W. R., MAHLER, W., BENSON, R. E., MOCHEL, W. E.: J. Am. Chem. Soc., **84**, 3374 (1962)
[5] WALLENFELS, K., BACHMANN, G., HOFMANN, D., KERN, R.: Tetrahedron **21**, 2239 (1965)
[6] BUCSIS, L., FRIEDRICH, K.: im Druck
[7] MARTIN, E. L.: US Patent 3.558,621
[8] PEOVER, M. E.: J. Chem. Soc. **1962**, 4540
[9] FISCHER, P. H., MCDOWELL, C. A.: J. Am. Chem. Soc. **85**, 2694 (1963)
[10] JONES, M. T., HERTLER, W. R.: J. Am. Chem. Soc. **86**, 1881 (1964)
[11] SCHEFFLER, K., STEDMANN, H. B.: Elektronenspinresonanz Springer, Berlin—Heidelberg—New York 1970
[12] TOMES, J., Coll. Czech. Chem. Commun. **7**, 198 (1935)

Lóránt BUCSIS
Herbert KIESELE
D-7888 Rheinfelden, Hertenerstr. 9a, BRD.

Acta Chimica Academiae Scientiarum Hungaricae, Tomus 93 (2), pp. 149–155 (1977)

UNTERSUCHUNGEN AN METALLCHELATEN MIT LIGANDEN VOM CUPROIN- UND FERROINTYP, XXV[1]

ÜBER DIE STRUKTUR VON CHLORO(CUPROIN)KUPFER(II)-CHELATEN

D. REHOREK und Ph. THOMAS

(Sektion Chemie der Karl-Marx-Universität Leipzig, DDR)

Eingegangen am 29. September, 1976

Kupfer(II)-Chelate des Typs $Cu(cuproin)Cl_2$ und $Cu(cuproin)_2Cl_2$ (cuproin = dmp, dmch, dpch und bich)[2] wurden mittels ESR-, UV/Vis- und Leitfähigkeitsmessungen untersucht. Die Ergebnisse der Messungen stehen in Übereinstimmung mit einer verzerrt-tetraedrischen Struktur des $Cu(bich)Cl_2$ sowie mit verzerrten trigonal-bipyramidalen bzw. quadratisch-pyramidalen Struktur der übrigen Chelate.

Für die Chelate $Cu(phen)Cl_2$ und $Cu(bipy)Cl_2$ konnten anhand von UV/Vis- und ESR-Spektren [1, 2, 3], in neuerer Zeit auch durch FIR- und RAMAN-Untersuchungen [4] quasioktaedrische Strukturen mit brückenbildenden Chloridionen nachgewiesen werden.

Eine von STEPHENS *et al.* [5] durchgeführte Röntgenstrukturanalyse ergab eine verzerrte trigonal-bipyramidale Struktur für das Chelat $Cu(bipy)_2Cl_2 \cdot 6\,H_2O$, womit früher publizierte Ergebnisse von ESR-Messungen [6] bestätigt werden konnten. Über die Struktur der analogen Cuproin-Chelate ist mit Ausnahme des Chelats $Cu(bich)Cl_2$, für das auf der Basis der optischen Spektren sich einander widersprechende Strukturen angegeben wurden [7, 8], und des hydratisierten $Cu(dmp)Cl_2 \cdot H_2O$, über das sowohl Daten von Röntgenstrukturuntersuchungen als auch Einkristall-ESR-Messungen vorliegen [9, 10, 11], nichts bekannt.

Wir haben mit Hilfe von ESR-, reflexionsspektroskopischen und Leitfähigkeitsmessungen Kupfer(II)-Chelate des allgemeinen Typs $Cu(cuproin)Cl_2$ bzw. $Cu(cuproin)_2Cl_2$ (cuproin = dmp, dmch, dpch und bich)[2] untersucht, um daraus Aussagen über die Struktur der ersten Koordinationssphäre zu gewinnen, worüber in dieser Arbeit berichtet werden soll.

[1] XXIV. Mitteilung: REHOREK, D., THOMAS, PH.: Z. anorg. allg. Chem. **429**, 237 (1977).

[2] Für die verwendeten Liganden wurden in dieser Arbeit folgende Abkürzungen benutzt:

phen — 1,10-Phenanthrolin, bipy — 2,2′-Bipyridin, dmp — 2,9-Dimethyl-1,10-phenanthrolin, dmch — 3,3′-Dimethylen-4,4′-dimethyl-2,2′-bichinolin, dpch — 3,3′-Dimethylen-4,4′-diphenyl-2,2′-bichinolin, bich — 2,2′-Bichinolin.

Experimentelles

Die Darstellung der Chelate $Cu(bich)Cl_2$, $Cu(dmp)Cl_2$, $Cu(dmp)Cl_2 \cdot H_2O$, $Cu(dmp)_2Cl_2$ und $Cu(dmch)Cl_2$ ist bereits in der Literatur [11—14] beschrieben wurden. $Cu(dpch)Cl_2$ wurde als rotes Chelat nach einer der Darstellung des $Cu(dmch)Cl_2$ [12] analogen Vorschrift erhalten.

Zur Darstellung der Chelate $Cu(dpch)_2Cl_2$ und $Cu(dmch)_2Cl_2$ wurde eine Lösung von 340 mg $CuCl_2 \cdot 2H_2O$ (2mMol) in 30 ml Methanol langsam unter intensivem Rühren zu einer Lösung von 4 mMol des organischen Liganden in Chloroform gegeben. Die dunkelgrüne Lösung wurde 15 Minuten gerührt und anschließend im Vakuum eingeengt. Die sich dabei abscheidenden Kristalle wurden abgesaugt und aus Methanol umkristallisiert. Die Trocknung erfolgte im Vakuum über P_4O_{10}. Die Elementaranalyse entspricht der oben angegebenen Zusammensetzung.

Versuche zur Darstellung von $Cu(bich)_2Cl_2$ verliefen ohne das gewünschte Ergebnis.

Die verwendeten Liganden waren entweder käufliche Produkte (FERAK, VEB Laborchemie Apolda) oder wurden im Falle des dpch nach [15] dargestellt.

Die ESR-Spektren der polykristallinen Chelate wurden bei 295 K mit Hilfe eines Spektrometers vom Typ JES-3BQ der Fa. JEOL (Japan) im X-Band mit DPPH als Vergleichsprobe ($g = 2{,}0036$) aufgenommen.

Die Auswertung der ESR-Spektren erfolgt nach SEARL *et al.* [16] bzw. KNEUBÜHL [17]. Sämtliche ESR-Parameter sind in Tab. I zusammengefaßt. Zusätzlich wurden noch die Parameter des von BILLING *et al.* [11] am Einkristall und von uns im Pulver vermessenen $Cu(dmp)Cl_2 \cdot H_2O$ sowie die Werte für die entsprechenden Komplexe des 1,10-Phenanthrolins und des 2,2′-Bipyridins mit in die Tabelle aufgenommen.

Die Reflexionsspektren der pulverförmigen Proben wurden im Bereich von 1200—400 nm bei Raumtemperatur mit Hilfe eines Einstrahlphotometers vom Typs VSU-2 der Fa.

Tabelle I

Meßergebnisse

Chelat	ESR-Parameter[a]			Banden im Reflexionsspektrum[b]	R[c]
	$g_1 = g_\perp$	g_2	$g_3 = g_{II}$		
$Cu(dmch)_2Cl_2$	2,008	2,142	2,227	640(CT), 870(dd), 990(dd)	1.57
$Cu(dpch)_2Cl_2$		2,14[d]		650(CT), 850(dd), 960(dd)	—
$Cu(dmp)_2Cl_2$	2,096	2,122	2,164	670(CT), 780(dd), 940(dd), 1050(dd)	0.62
$Cu(phen)_2Cl_2$	2,008	2,132	2,190	780(dd), 900(dd)	2,14
$Cu(bipy)_2Cl_2$[e]	2,19		2,02	790(dd), 890(dd)	∞
$Cu(dmch)Cl_2$	2,053	2,122	2,264	520(CT), 890(dd), 1020(dd)	0,49
$Cu(dpch)Cl_2$	2,036	2,128	2,342[f]	500(CT), 860(dd), 1000(dd)	0,43
$Cu(bich)Cl_2$	2,071		2,343	480(CT), 1020(dd)	0
$Cu(dmp)Cl_2$	2,032	2,175	2,275	500 (CT), 850(dd), 1000(dd)	1,43
$Cu(dmp)Cl_2 \cdot H_2O$	2,028	2,127	2,277	790(dd), 1100(dd)	0,67
$Cu(dmp)Cl_2 \cdot H_2O$[g]	2,0299	2,1325	2,2752		
$Cu(phen)Cl_2$	2,056		2,258	690(dd)	0
$Cu(bipy)Cl_2$[h]	2,055		2,252	690(dd)	0

a) Meßgenauigkeit $\pm 0{,}008$
b) Meßgenauigkeit ± 20 nm, im Klammern Zuordnungen
c) Definition s. Text
d) starke Austauschwechselwirkungen, s. Text
e) Meßdaten [6] entnommen
f) schwach aufgelöste Cu-Hyperfeinstruktur: $a_3 = 62 \pm 10$ G
g) Meßdaten [11] entnommen
h) Meßdaten [3] entnommen

VEB CARL ZEISS Jena aufgenommen. Die Lage der *d–d*-Banden ist in Tab. I angegeben. Die Leitfähigkeitsmessungen wurden an 10^{-4} molaren Lösungen in Nitromethan an einem Meßgerät des Typs LM 301 der Fa. VEB Hydromat Bannewitz durchgeführt. Die erhaltenen Werte sprechen im Falle der Mono-Chelate für Nichtelektrolyte und im Falle der Bis-Chelate für 1 : 1-Elektrolyte [18].

Diskussion der Meßergebnisse

Mit Ausnahme der Chelate $Cu(dpch)_2Cl_2$ und $Cu(bipy)_2Cl_2$ lieferten alle Bis-Chelate ESR-Spektren mit ausgeprägter rhombischer Symmetrie. Das im Falle des $Cu(dpch)_2Cl_2$ beobachtete annähernd isotrope ESR-Spektrum ist mit hoher Wahrscheinlichkeit auf Austauschwechselwirkungen zwischen kristallographisch nichtäquivalenten paramagnetischen Zentren zurückzuführen [19].

Aus diesem Grunde sind Aussagen über die Struktur der ersten Koordinationssphäre des $Cu(dpch)_2Cl_2$ anhand des ESR-Spektrums nicht möglich. Da jedoch das Reflexionsspektrum des $Cu(dmch)_2Cl_2$ eine große Ähnlichkeit mit dem des $Cu(dpch)_2Cl_2$ aufweist, kann angenommen werden, daß beide Chelate eine ähnliche Struktur besitzen.

Das ESR-Spektrum des $Cu(bipy)_2Cl_2$ läßt sich durch einen Spin-HAMILTON-Operator axialer Symmetrie beschreiben. Wegen $g_{II} < g_{\perp}$ kann auf einen d_{z^2}-Grundzustand geschlossen werden. Das Abweichen des Wertes für g_{II} von 2,0023, dem *g*-Wert des freien Elektrons, ist auf Austauschwechselwirkungen zurückzuführen. Die ausgeprägt rhombische Symmetrie der ESR-Spektren der übrigen Bis-Chelate spricht für einen Grundzustand der Form (1).

$$| 0 \rangle = \alpha[\cos \Phi \, d_{z^2} + \sin \Phi \, d_{x^2-y^2}] - \alpha' \psi_L(0) \qquad (1)$$

$'\psi_L(0)$ stellt hierbei eine symmetrieadaptierte Linearkombination von Atomorbitalen der Liganden dar.)

Bei Kenntnis der optischen Übergänge und der entsprechenden Kovalenzparameter ist der Mischungskoeffizient Φ aus den *g*-Werten berechenbar. Allerdings setzt dies voraus, daß die experimentell ermittelten *g*-Werte nicht durch Austauschwechselwirkungen verfälscht worden sind. Wie aber das Beispiel der Chelate $Cu(dpch)_2Cl_2$ und $Cu(bipy)_2Cl_2$ zeigt, können Austauschwechselwirkungen nicht generell vernachlässigt werden. Möglicherweise sind sie bei den übrigen Chelaten von geringerer Größe, aber da ein Vergleich mit diamagnetisch verdünnten Proben fehlt, können keine Angaben über die Stärke dieser Wechselwirkungen gemacht werden. Wir können uns deshalb lediglich auf Trendaussagen beschränken, wobei wir annehmen, daß für die einzelnen Chelate etwa gleich große Meßfehler auftreten.

Nach DUDLEY und HATHAWAY [20] stellt die Größe $R = \dfrac{g_2 - g_1}{g_3 - g_2}$

($g_1 < g_2 < g_3$ für rhombische Symmetrie, $g_1 = g_2 = g_\perp$ bzw. $g_2 = g_3 = g_\perp$ für axiale Symmetrie) ein gutes Maß für die Mischung von d_{z^2}- und $d_{x^2-y^2}$-Wellenfunktionen dar. R kann von 0 (reine $d_{x^2-y^2}$-Funktion) bis ∞ (reine d_{z^2}-Funktion) variieren. Für $R = 1$ gehen die d_{z^2}- und die $d_{x^2-y^2}$-Funktion etwa zu gleichen Teilen in den Grundzustand ein.

Tab. I enthält die berechneten R-Werte.

Im Falle der Koordinationszahl 5 — diese kann auf der Basis der Leitfähigkeitsmessungen für die Bis-Chelate angenommen werden — ergeben sich als mögliche Strukturen die quadratische Pyramide und die trigonale Bipyramide, die jeweils durch Verzerrung ineinander übergehen können. Beide Grenzstrukturen sind durch einen unterschiedlichen Grundzustand gekennzeichnet: d_{z^2} für die trigonale Bipyramide und $d_{x^2-y^2}$ für die quadratische Pyramide [21]. Da durch Verzerrung die d_{z^2}- und die $d_{x^2-y^2}$-Funktion im Grundzustand miteinander mischen, kann umgekehrt bei Kenntnis des Ausmaßes der Mischung ausgesagt werden, ob die Struktur mehr der quadratischen Pyramide ($R < 1$) oder der trigonalen Bipyramide ($R > 1$) entspricht (vgl. Abb. 1).

Demnach liegt das Chelat $Cu(dmp)_2Cl_2$ in einer verzerrten quadratisch-pyramidalen Anordnung, bei der sich die beiden heterocyclischen Liganden aus sterischen Gründen in *cis*-Stellung befinden, vor, wogegen die übrigen Bis-Chelate stärker in Richtung einer trigonalen Bipyramide verzerrt sind. Neben den ESR-Daten weist auch das Reflexionsspektrum des $Cu(dmp)_2Cl_2$,

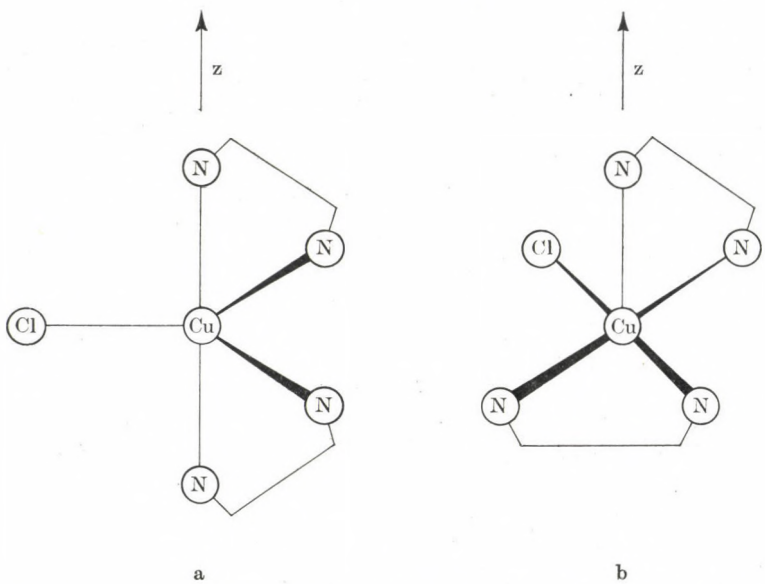

a b

Abb. 1. a: trigonal-bipyramidale Struktur (d_{z^2}-Grundzustand); b: quadratische Pyramide ($d_{x^2-y^2}$-Grundzustand)

insbesondere die hypsochrome Verschiebung der kurzwelligen *d–d*-Bande, auf das abweichende strukturelle Verhalten hin.

$Cu(phen)_2Cl_2$ besitzt wie auch das $Cu(bipy)_2Cl_2$ eine im wesentlichen trigonal-bipyramidale Struktur. Allerdings ist im Falle des $Cu(phen)_2Cl_2$ der Grad der Verzerrung etwas größer als beim bipy-Chelat, was vermutlich auf die gegenüber dem 2,2′-Bipyridin verringerte Drehbarkeit des Phenanthrolingerüsts zurückzuführen ist.

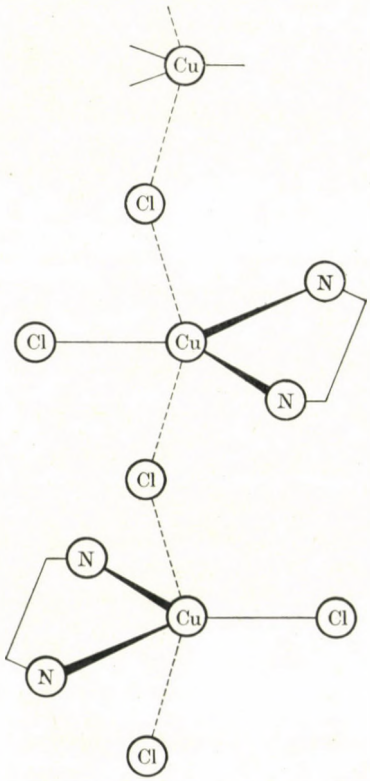

Abb. 2. Chloroverbrückte trigonal-bipyramidale Struktur

Ein Teil der Mono-Chelate weist überraschenderweise ein ähnliches ESR-spektroskopisches Verhalten wie die Bis-Chelate auf. Mit Ausnahme des $Cu(bich)Cl_2$ liefern die Mono(cuproin)-kupfer(II)-Chelate ESR-Spektren rhombischer Symmetrie. $Cu(bich)Cl_2$ sowie die beiden Ferroin-Chelate $Cu(bipy)Cl_2$ $Cu(phen)_2Cl_2$ zeigen dagegen ESR-Spektren axialer Symmetrie mit $g_\perp < g_{II}$, was auf einen $d_{x^2-y^2}$- bzw. d_{xy}-Grundzustand hinweist. Wie die Leitfähigkeitsmessungen zeigen, liegen alle hier untersuchten Mono-Chelate als Nichtelektrolyte vor, woraus sich eine Koordinationszahl von mindestens 4 ergibt.

Für $Cu(phen)Cl_2$ und $Cu(bipy)Cl_2$ konnten IR-spektroskopisch Chlorobrücken nachgewiesen werden [4] und in Übereinstimmung mit ESR- und

optischen Spektren [1, 2, 3] quasioktaedrische Strukturen abgeleitet werden. Der für Cu(bich)Cl ESR-spektroskopisch ermittelte g_{II}-Wert ist mit $g_{II} = 2{,}343$ bedeutend größer als bei den oktaedrischen Komplexen $Cu(phen)Cl_2$ und $Cu(bipy)Cl_2$. KOKOSZKA *et al.* [22] ermittelten für $Cu(phen)Cl_2$ in verzerrt-tetraedrischer Umgebung, das durch Dotierung von $Zn(phen)Cl_2$ mit Cu^{2+} erhalten wurde, einen g_{II}-Wert von 2,297, der damit beträchtlich über dem für oktaedrische Koordination erhaltenen Wert liegt. Wir nehmen an, daß auch im $Cu(bich)Cl_2$ eine verzerrt-tetraedrische Koordination vorliegt,

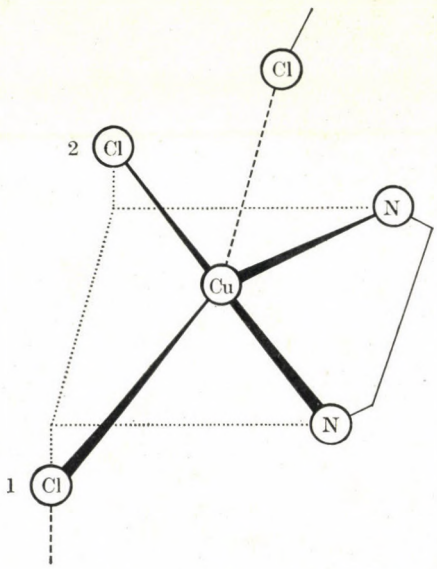

Abb. 3. Quadratisch-pyramidale Struktur mit Chlorobrücken (Die beiden Chloratome 1 u. 2 befinden sich außerhalb der durch Kupferatom und die beiden Stickstoffatome gebildeten Chelatebene.)

was auch mit der gegenüber den oktaedrisch koordinierten Chelaten $Cu(bipy)Cl_2$ und $Cu(phen)Cl_2$ beobachteten bathochromen Verschiebung der *d–d*-Banden in Übereinstimmung steht.

$Cu(dmp)Cl_2 \cdot H_2O$ hat nach Untersuchung von BILLING *et al.* [11] eine Struktur, die am besten als verzerrte quadratische Pyramide beschrieben werden kann. Die von uns an einer polykristallinen Probe ermittelten *g*-Werte stimmen gut mit den von BILLING *et al.* erhaltenen Einkristalldaten überein.

Trotz auffallender äußerlicher Unterschiede — das wasserfreie $Cu(dmp)Cl_2$ ist wie die anderen Dichloro-mono(cuproin)-Chelate rot, die hydratisierte Form dagegen grün — haben die ESR- und auch die Reflexionsspektren beider Chelate, bei letzteren v. a. im Bereich der *d–d*-Banden, eine große Ähnlichkeit miteinander, was auf strukturelle Gemeinsamkeiten hinweist.

Die unterschiedliche Farbe der Chelate ist in erster Linie auf den bei einer Wellenlänge von etwa 500 nm auftretenden Charge-Transfer-Übergang im $Cu(dmp)Cl_2$ zurückzuführen. Eine der des $Cu(dmp)Cl_2 \cdot H_2O$ ähnliche Struktur des $Cu(dmp)Cl_2$ bedingt, daß bei letzterem jeweils ein Chloratom als Brückenligand fungiert (vgl. Abb. 2). Der *R*-Wert des wasserfreien $Cu(dmp)Cl_2$ beträgt 1,43 und ist damit größer als für die hydratisierte Form. Die Struktur des $Cu(dmp)Cl_2$ ähnelt deshalb mehr einer trigonalen Bipyramide. Bei den beiden anderen Mono-cuproin-Chelaten sind die *R*-Werte kleiner als 1. Wegen der ausgeprägten rhombischen Symmetrie der ESR-Spektren sind jedoch auch hier zusätzliche Wechselwirkungen mit benachbarten Chelaten über Chlorobrücken anzunehmen, was mit der schlechten Löslichkeit der Chelate im Einklang steht. Auf Grund der *R*-Werte ergibt sich eine verzerrte quadratisch pyramidale Struktur, wobei wahrscheinlich die beiden unmittelbar koordinierten Chloratome (vgl. Abb. 3) zusammen mit den Stickstoffatomen des Heterocyclus ein verzerrtes Tetraeder bilden, was die gegenüber dem $Cu(dmp)Cl_2$ beobachtete bathochrome Verschiebung der kurzwelligen *d–d*-Bande erklären würde und aus sterischen Gründen plausibel erscheint.

LITERATUR

[1] Hyde, K., Kokoszka, G. F., Gordon, G.: J. Inorg. Nucl. Chem. **31,** 1993 (1969)
[2] Reimann, C., Gordon, G.: Nature **205,** 902 (1965)
[3] Procter, I. M., Hathaway, B. J., Hodgson, P. G.: J. Inorg. Nucl. Chem. **34,** 3689 (1972)
[4] Wilde, R. E., Srinivasan, T. K. K.: J. Inorg. Nucl. Chem. **36,** 328 (1974)
[5] Stephens, F. S., Tucker, P. A.: J. Chem. Soc. Dalton Trans. **1973,** 2293
[6] Elliott, H., Hathaway, B. J., Slade, R. C.: J. Chem. Soc. A **1966,** 1443
[7] Harris, C. M., Patil, H. R. H., Sinn, E.: Inorg. Chem. **6,** 1102 (1967)
[8] Faye, G. H.: Can. J. Chem. **44,** 2729 (1966)
[9] Preston, H. S., Kennard, C. H. L.: Chem. Commun. **1967,** 1167
[10] Preston, H. S., Kennard, C. H. L.: J. Chem. Soc. **A 1969,** 2955
[11] Billing, D. E., Dudley, R. J., Hathaway, B. J., Tomlinson, A. A. G.: J. Chem. Soc. A **1971,** 691
[12] Uhlemann, E., Thomas, PH., Kempter, G.: J. prakt. Chem. **30,** 273 (1965)
[13] Breckenridge, J. G., Lewis, R. W. J., Quick, L. A.: Can. J. Res. **17** B, 258 (1939)
[14] Hall, J. R., Marchant, N. K., Plowman, R. A.: Austral. J. Chem. **15,** 480 (1962)
[15] Uhlemann, E., Thomas, PH., Kempter, G.: Z. anorg. allg. Chem. **341,** 11 (1965)
[16] Searl, J. W., Smith, R. C., Wyard, S. J.: Proc. Roy. Soc. **78,** 1174 (1961)
[17] Kneubühl, F. K.: J. Chem. Phys. **33,** 1074 (1960)
[18] Geary, W. J.: Coord. Chem. Rev. **7,** 811 (1971)
[19] Procter, I. M., Hathaway, B. J., Nicholls, P.: J. Chem. Soc. **A 1968,** 1678
[20] Dudley, R. J., Hathaway, B. J.: J. Chem. Soc. **A 1970,** 2799
[21] Pal, A. K., Pal, D.: Proc. Nucl. Phys., Solid State Physical Symp., 14th, **1969,** 381
[22] Kokoszka, G. F., Reimann, C. W., Allen, H. C.: J. Phys. Chem. **71,** 121 (1967)

Detlef Rehorek, Philipp Thomas | Sektion Chemie der Karl-Marx-Universität, DDR-701 Leipzig, Liebigstr. 18.

Acta Chimica Academiae Scientiarum Hungaricae, Tomus 93 (2), pp. 157—163 (1977)

SOME CHEMICAL ASPECTS OF 3-THIONO-1,2-DITHIOLES, VI

Mohamed A.-F. ELKASCHEF, Farouk M. E. ABDEL-MEGEID and Ahmad A. ELBARBARY

(National Research Centre, Dokki, Cairo, Egypt)

Received September 28, 1975;
in revised form August 15, 1976

Compound **I** reacted with amines to give N-substituted-3-thionoisothiazole derivatives (**IVa, b**), while compounds **II** and **III** gave 1,3-di-(substituted amino)-3-thiono-1-propene derivatives (**VIa—c** and **VIIa—d**). Compounds **I**, **II** and **III** gave with diphenyldiazomethane the benzhydrylidene derivatives **IX**, **X** and **XI**, respectively. Compounds **II** and **III** with diazofluorene yielded the respective 3-fluorenylidene-1,2-dithiole derivatives **XII** and **XIII**, while compound **I** gave the spiro [fluorenethiophene] derivatives **XIV**. The product from compound **I** with copper-bronze was the dibenz-thiophenothiophene **XVII**, whereas compound **III** afforded 2,5-di-(*p*-methoxyphenyl)thiophene (**XX**).

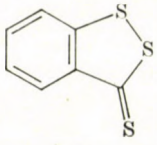

I

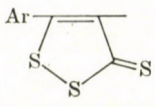

II and **III**

II: Ar = Ph;
III: Ar = $C_6H_4OCH_3$ (*p*-)

Although many reactions of 3-thiono-1,2-dithioles are known [2] and, their reactions with amines were not clarified, and their reactions with diazoalkanes and copper bronze were not studied at all.

We found that the reaction of compound **I** with hydrazine hydrate and phenylhydrazine gave the N-amino (**IVa**) and N-phenylamino-4,5-benzo-3-thiono(2*H*)-isothiazole (**IVb**), respectively, thus confirming the result obtained by MCCLELLAND *et al.* [3].

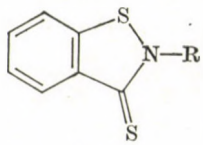

IV

a: R = NH_2;
b: R = NHPh

* Part V: s. [1].

Treatment of compound **IVa** with nitrous acid did not give the expected hydroxy derivative (**IVa**, R = OH instead of NH_2), but yielded 2,2'-di-(N-hydroxybenzamide) disulfide (**V**). The structure of this compound was supported by its IR spectrum and molecular weight determination (*cf.* Experimental).

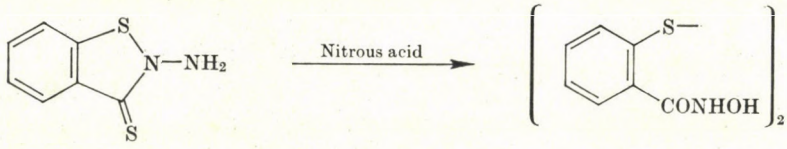

IVa **V**

Compound **II** reacted with methylamine, ethylamine, or hydrazine hydrate to give 1,3-di-(N-methylamino)-1-phenyl-3-thiono-1-propene (**VIa**), 1,3-di-(N-ethylamino)-1-phenyl-3-thiono-1-propene (**VIb**), and 1,3-dihydrazo-1-phenyl-3-thiono-1-propene (**VIc**), respectively. Similarly, compound **III** gave 1,3-di-(N-methylamino)-1-(*p*-methoxyphenyl)-3-thiono-1-propene (**VIIa**), 1,3-di-(N-ethylamino)-1-(*p*-methoxyphenyl)-3-thiono-1-propene (**VIIb**), 1,3-dihydrazo-1-(*p*-methoxyphenyl)-3-thiono-1-propene (**VIIc**), and 1,3-di-(N-benzylamino)-1-(*p*-methoxyphenyl)-3-thiono-1-propene (**VIId**) with methylamine, ethylamine, hydrazine hydrate, and benzylamine, respectively. The reaction sequence may be explained as follows:

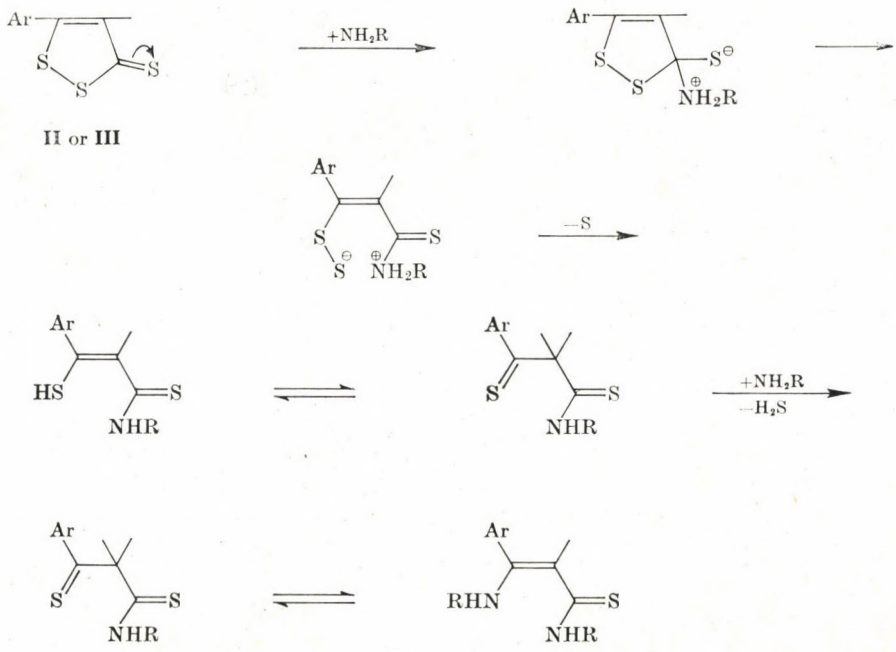

II or **III**

VI and **VII**

VI: Ar = Ph; **VII**: Ar = $C_6H_4OCH_3(p)$
a: R = CH_3; *b*: R = C_2H_5; *c*: R = BH_2; *d*: R = CH_2Ph

The IR spectra of compounds **IVa**, **IVb**, **VIa**, **VIc**, **VIIb** and **VIIc** supported the structures given. The A, B, C, . . . marking assignation for thioamides according to JENSEN and NIELSEN [4] is given for these compounds as shown in Table I.

Compound **I** reacted with diazomethane to give the normal reaction of thioketones, thus affording 3,3'-[3,3'-bis(4,5-benzo-1,2-dithiole)] sulfide (**VIII**)

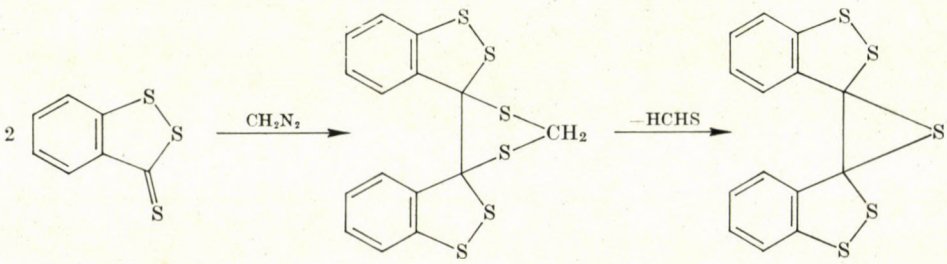

I **VIII**

With diphenyldiazomethane, compounds **I**, **II**, and **III** behaved normally, yielding 3-benzhydrylidene-4,5-benzo-1,2-dithiole (**IX**), 3-benzhydrylidene-5-phenyl-1,2-dithiole (**X**), and 3-benzhydrylidene-5-(*p*-methoxyphenyl)-1,2-dithiole (**XI**), respectively. Compounds **II** and **III** also behaved normally with diazofluorene to give 3-(9'-fluorenylidene)-5-phenyl-1,2-dithiole (**XII**) and 3-(9'-fluorenylidene)-5-(*p*-methoxyphenyl)1,2-dithiole (**XIII**), respectively, whereas compound **I** yielded spiro [(9*H*-fluorene)-9,2'-(3'-oxo-4',5'-benzo-2'*H*-thiophene)] (**XIV**).

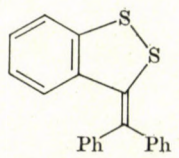

IX

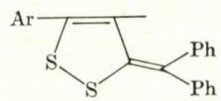

X and **XI**

X: Ar = Ph;
XI: Ar = $C_6H_4OCH_3$ (*p*-)

With copper-bronze compound **I** afforded 4,5-4',5-dibenzothiophene(2,3-3',2')thiophene (**XVII**).

Intermediate **XV**, formed through free radical cleavage, reacted to give **XVI** which, in turn, was converted by treatment with copper + bronze to **XVII**. Actually, BAKER *et al.* [5] obtained the dithiobenzoate **XV** (C=O, instead of C=S) together with compound **XVII** by boiling thiosalicylic acid

with phosphorus pentoxide. Compound **XV** (C=O, instead of C=S) was also isolated as a product from the reaction of the oxo-analogue of compound **I** with copper bronze [1].

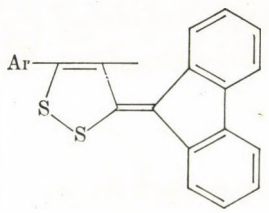

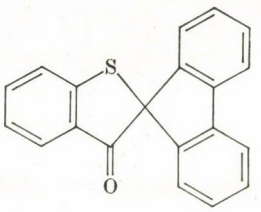

XIV

XII: Ar = Ph;
XIII: Ar = $C_6H_4OCH_3$ (*p*-)

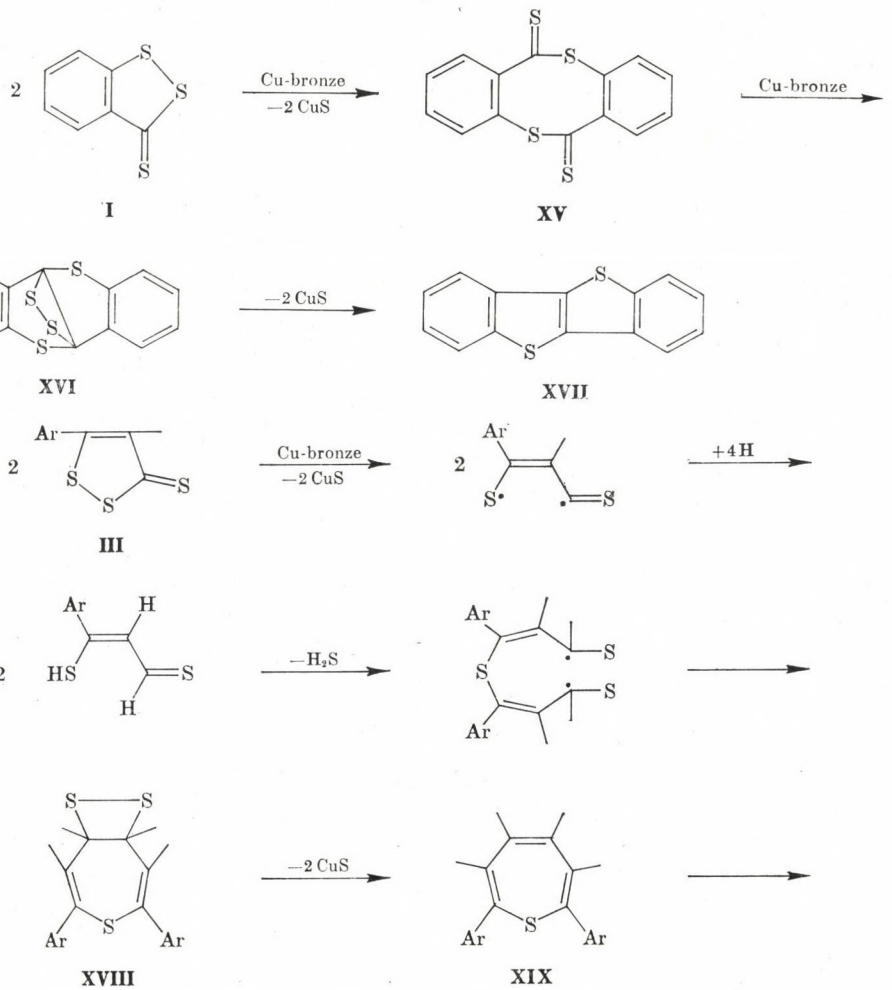

XVIII **XIX**

Compound **II** did not react with copper bronze, while compound **III** gave 2,5-di-(*p*-methoxyphenyl)thiophene (**XVIII**). The sequence of this reaction can be explained as follows:

In support of the given mechanism is the postulation of a peroxide formation [1] similar to the persulfide **XVIII** in the reaction of the oxo-analogue of compound **II** with copper bronze where compounds **XIX** and **XX** Ar=Ph, instead of *p*-methoxyphenyl were actually isolated.

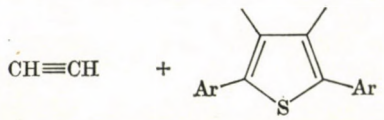

XX

Ar = $C_6H_4OCH_3$ (*p*-)

Experimental

M.p'.s are uncorrected and have been measured on a Kofler microscope. Microanalyses were performed by the Micro-analytical Laboratory, N.R.C., Egypt. Molecular weights were determined by electro-thermal method (New-Mayer) at the Micro-analytical Unit, Faculty of Science, Cairo University. IR spectra were measured in KBr using a UR 10 spectrophotometer (Carl Zeiss, Jena).

Action of amines and hydrazines on compounds I, II and III

A mixture of compound **I**, **II** or **III** in ethanol and excess of the amine (methylamine 33% aqueous soln., ethylamine 33% aqueous soln., or benzylamine) or the hydrazine (hydrazine hydrate 99% soln., or phenylhydrazine) was refluxed for 5 hrs till no evolution of hydrogen sulfide gas was detected. On concentration, yellow crystals of sulfur separated and were removed by filtration. The filtrate was evaporated and the residue was recrystallized from the proper solvent (*cf.* Table II).

Table I

Selected bands in the IR region (cm^{-1}) for compounds **IVa,b VIa—c,** *and* **VIIb, c**

Compound	A band	B band	C band	D band	E band	F band	G band	NH_2 or NH Stret.	C=C
IVa	1620 s	1480 s	1260 m	1135 m	850 vs	750 vs	650 m	3370 s	—
IVb	—	1485 s	1260 w	1125 w	—	725 m	680 s	3250 w	—
VIa	—	1490 m	1260 s	1115 m	—	725 m	700 s	3230 s	1610 s
VIb	—	1495 s	1280 s	1116 s	—	722 m	700 m	3250 vs	1620 s
VIc	1615 w	1495 vs	1295 vs	1110 s	880 m	725 m	680 m	3100—3150 s	1600 m
VIIb	—	1490 vs	1255 vs	1110 s	—	735 s	680 w	3240 vs	1615 vs
VIIc	1620 s	1485 vs	1270 s	1115 m	850 s	725 m	700 m	3100 w	1620 s

vs = very strong, s = strong, m = medium, w = weak.

Table II

Action of amines and hydrazines ($R-NH_2$) on compounds **I**, **II** *and* **III**

Starting compound	R	Product and yield, %	M. p., °C	Molecular formula (Mol. wt.)	Analysis, % Calcd./Found			
					C	H	N	S
I	NH_2	**IVa**[1] (85)	128	$C_7H_6N_2S_2$ (182)	46.15 46.21	3.30 3.28	15.38 15.24	
					Mol. wt. Found: 175			
I	NHPh	**IVb**[1] (68)	103—105	$C_{13}H_{10}N_2S_2$ (258)	60.47 60.33	3.88 3.85	10.85 10.33	24.81 24.26
II	CH_3	**VIa**[1] (77)	99—100	$C_{11}H_{14}N_2S$ (206)			13.59 12.75	
II	C_2H_5	**VIb**[1] (74)	67—68	$C_{13}H_{18}N_2S$ (234)			11.97 11.04	13.68 13.60
II	NH_2	**VIc**[2] (58)	1999	$C_9H_{12}N_4S$ (208)				15.38 15.07
III	CH_3	**VIIa**[1] (86)	117	$C_{12}H_{16}ON_2S$ (236)	61.02 60.86	6.78 6.67	11.86 11.76	13.57 13.77
III	C_2H_5	**VIIb**[3] (68)	122	$C_{14}H_{20}N_2OS$ (264)	63.64 63.46	7.58 7.75	10.61 10.13	12.12 12.10
III	NH_2	**VIIc**[4] (75)	124—125	$C_{10}H_{14}N_4OS$ (238)				13.44 12.60
III	CH_2Ph	**VIId**[5] (35)	179—180	$C_{24}H_{24}N_2OS$ (388)			7.21 7.00	8.25 8.27

Solvent of crystallization: [1] *n*-hexane; [2] benzene; [3] methanol–H_2O; [4] methanol; [5] ethanol.

Action of nitrous acid on compound IVa

A cold solution of sodium nitrite (1 g) in a minimum amount of water was added to a cold solution of compound **IVa** (0.5 g; 0.0027 mole) in hydrochloric acid (50 ml). The reaction mixture was kept at room temperature for 24 hrs. The resulting solid, 2,2[3]-di-(N-hydroxybenzamide) disulfide (**V**) (0.6 g; 75%) was filtered off and recrystallized from light petroleum (b.p. 40—60 °C); m.p. 110 °C.

$C_{14}H_{12}N_2O_4S_2$ (336). Calcd. N 8.33. Found N 7.65%. IR: 1720 cm^{-1} and 1760 cm^{-1} (C=O), 3280 cm^{-1} (NH—OH).

Action of diazoalkanes on compounds I, II and III

A mixture of compound **I**, **II**, or **III** in dry benzene and an excess of the diazoalkane [diazomethane (prepared from nitrosomethylures, diphenyldiazomethane prepared from benzophenone hydrazone), or 9,9-diazofluorene (prepared from 9-fluorene hydrazone)] was refluxed for 6 hrs. The solvent was evaporated and the residue was either chromatographed using an alumina column and the proper eluent, or solidified and recrystallized from the proper solvent (*cf.* Table III).

A mixture of copper bronze (1.9 g) and compound **I** (2 g; 0.0108 mole) dissolved in dry xylene (100 ml) was refluxed for 10 hrs. and filtered while hot. The oily residue, after distillation of the solvent under reduced pressure, was chromatographed on an alumina column. Using *n*-hexane as eluent, 4,5[3],5[3]-dibenzothiopheno(2,3-3[3],2[3])-thiophene (**XVII**) (0.9 g; 69%) was separated and recrystallized from *n*-hexane. M.p. and mixed m.p. with an authentic sample of **XVII** [5]: 216 °C.

Table III

Action of diazoalkanes (N_2CR_2) on compounds **I**, **II**, *and* **III**

Starting compound	R	Product and yield, %	M.p., °C	Molecular formula (Mol. wt.)	Analysis, % Calcd./Found		
					C	H	S
I	H	**VIII**[1] (21)	147	$C_{14}H_8S_5$ (336)			47.61 47.20
I	Ph	**IX**[1] (44)	168	$C_{20}H_{14}S_2$ (318)	75.47 75.69	4.40 4.65	20.13 20.18
II	Ph	**X**[2] (43)	143—144	$C_{22}H_{16}S_2$ (344)	76.73 76.40	4.68 4.90	18.58 18.14
III	Ph	**XI**[2, a] (32)	145	$C_{23}H_{18}OS_2$ (374)	73.78 74.18	4.92 4.92	17.11 16.87
II	R_2=biphenylene	**XII**[2] (15)	211	$C_{22}H_{14}S_2$ (342)	77.19 77.11	4.09 4.05	18.71 18.84
III	R_2=biphenylene	**XIII**[2, a] (32)	188	$C_{23}H_{16}OS_2$ (372)	73.19 73.92	4.30 4.70	
					Mol. wt. Found: 350		
I	R_2=biphenylene	**XIV**[1, b] (19)	222—224	$C_{20}H_{12}OS$ (300)	80.00 80.38	4.00 4.42	10.67 10.64

Solvent of crystallization: [1] *n*-hexane; [2] ethanol.
Eluent: [a] *n*-hexane–benzene (50 : 50); [b] light pet.–benzene (30 : 70).
IR spectra: Compound **IX**, 1590 cm^{-1} (C=C and Ph). Compound **XIV**, 1595 cm^{-1} (Ph), 1700 cm^{-1} (C=O).

Action of copper bronze on compound I

A mixture of copper bronze (3 g) and compound **III** (2 g; 0.102 mole) dissolved in dry xylene (100 ml) was refluxed for 10 hrs and filtered while hot. The oily residue, after evaporation of the solvent under reduced pressure, was chromatographed on an alumina column. Using a cyclohexane-benzene mixture (50 : 50) as eluent, 2,5-di-(*p*-methoxyphenyl)thiophene (**XX**) (0.4 g; 33%) was separated and recrystallized from *n*-hexane. M.p. and mixed m.p. with authentic sample of **XX** [6]: 215—216 °C.

REFERENCES

[1] Part V: ELKASCHEF, M. A.-F., ABDEL-MEGEID, F. M. E., ELBARBARY, A. A.: Tetrahedron **30,** 4113 (1974)
[2] LANDIS, P. S.: Chem. Rev. **65,** 238 (1965)
[3] MCCLELLAND, E. W., WARREN, L. A., JAKSON, J. H.: J. Chem. Soc. **1929,** 1582
[4] JENSEN, K., NIELSEN, P. H.: Acta Chem. Scand **20,** 597 (1966)
[5] BAKER, W., ELNAWAWY, A. S., OLLIS, W. D.: J. Chem. Soc. **1952,** 3163
[6] CAMPAIGNE, E., FOYE, W. O.: J. Org. Chem. **17,** 1405 (1952)

Mohamed A.-F. ELKASCHEF
Farouk M. E. ABDEL-MEGEID
Ahmad A. ELBARBARY

National Research Centre,
Dokki, Cairo, Egypt.

Acta Chimica Academiae Scientiarum Hungaricae, Tomus 93 (2), pp. 165—168 (1977)

CONVERSIONS OF TOSYL AND MESYL DERIVATIVES OF THE MORPHINE GROUP, XVII*

"AZIDOMORPHINE" DERIVATIVES, I

S. MAKLEIT, J. KNOLL,** R. BOGNÁR, S. BERÉNYI and G. KISS

*(Institute of Organic Chemistry, Kossuth Lajos University Debrecen, and **Institute of Pharmacology, Semmelweis Medical University, Budapest)*

Received Januar 30, 1976

In view of the very favourable pharmocological properties of "azidomorphine", the investigation of further derivatives appeared to be promising for both theoretical and practical reasons. The synthesis of "14-hydroxyazidomorphine" (3,14β-dihydroxy-4,5α-epoxy-6β-azido-17-methylmorphinan) is reported.

The pharmacological investigation of "azidomorphine" (3-hydroxy-4,5α-epoxy-6β-azido-17-methylmorphinan) [**1**a—d] gave surprising results, according to which [**2**a—h] this compound is "the most potent analgesic known so far among the semisynthetic morphine derivatives, and its tolerance and dependence capacity is strikingly low in respect to its analgesic effect", further, in man, "azidomorphine proved to be an analgesic 40—50 times as potent as morphine"; taking into account the relationships which have been between the action and chemical structure of semisynthetic morphine derivatives [3], the preparation of some derivatives of "azidomorphine" appeared to be promising [4a, b].

In the present communication we described in detail the preparation of "14-hydroxyazidomorphine" (3,14β-dihydroxy-4,5α-epoxy-6β-azido-17-methylmorphinan).

Starting from thebaine (**1**), 14-hydroxycodeinone (**2**) can be obtained according to SEKI [3]; on catalytic hydrogenation [5] this affords 14-hydroxydihydrocodeinone (**3**). 14-Hydroxydihydromorphinone (**4**) was prepared according to WEISS [6]. Compound **4** can be reduced with sodium borohydride [7] to give 14-hydroxydihydromorphine (**5**) in a surprisingly stereospecific reaction. This trihydroxy derivative can be partially acetylated in a special way [8a, b] to obtain the 3-0-acetyl derivative (**6**) which, on treatment with tosyl or mesyl chloride, gives the 6-0-tosyl or mesyl derivative (**7**) Azidolysis affords then the desired compound (**8**).

The detailed pharmacological investigation of this derivative [**2**f, g, h, **9**a, b] confirmed our presumptions. "14-Hydroxyazidomorphine" proved to

* Part XVI: S. MAKLEIT, T. MILE, R. BOGNÁR: Acta Chim. Budapest **89**, 275 (1976) and Magyar Kém. Folyóirat **81**, 564 (1975).

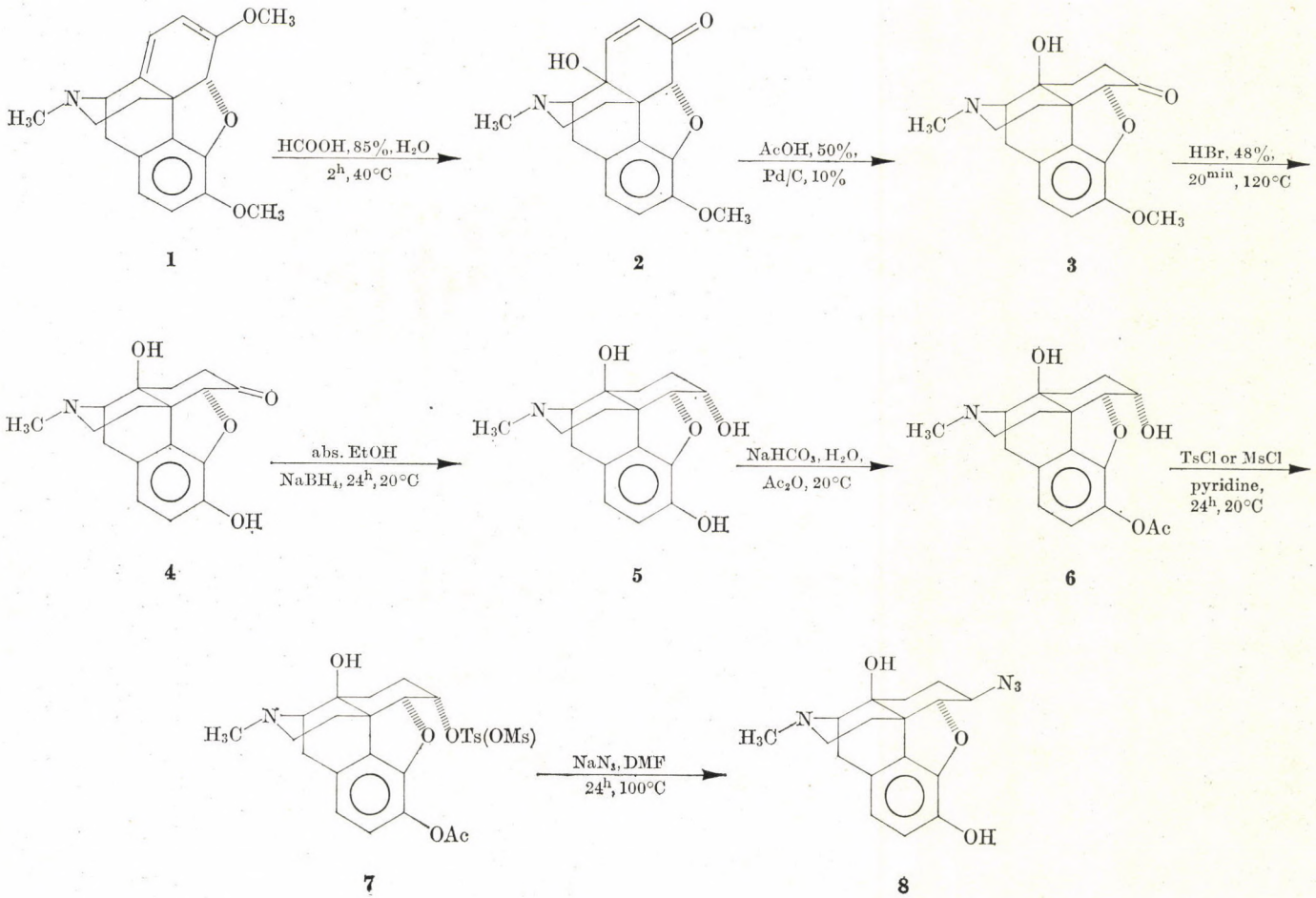
OCH3
H3C
N
O
OCH3
HCOOH, 85%, H2O
2h, 40°C
HO
O
AcOH, 50%,
Pd/C, 10%
OH
HBr, 48%,
20min, 120°C
abs. EtOH
NaBH4, 24h, 20°C
NaHCO3, H2O,
Ac2O, 20°C
TsCl or MsCl
pyridine,
24h, 20°C
OAc
OTs(OMs)
NaN3, DMF
24h, 100°C
N3

1 2 3

4 5 6

7 8

be an analgesic of the same efficiency as "azidomorphine", its toxicity being 11. 6 and 6.5 times lower in mice and rats, respectively; it is a more potent antitussive agent than azidomorphine; tolerance and the dependence capacities are identical.

Experimental

3-O-Acetyl-14-hydroxydihydromorphine (6)

To a suspension of 3 g (9.9 mmoles) 14-hydroxydihydromorphine and 30 g sodium hydrogen carbonate in 300 ml water, a total of 15 ml acetic anhydride was added in three equal portions, with stirring. After the termination of gas evolution, stirring was continued for 5 min. After extraction with 5×60 ml of chloroform, the combined chloroform solutions were washed 2×10 ml of a 5% aqueous solution of sodium hydroxide and with 2×20 ml of water, the solution was dried over magnesium sulfate and evaporated to dryness. The residual gum (3 g) was suitable for further processing.

3-O-Acetyl-6-O-tosyl-14-hydroxydihydromorphine (7)

A solution of 2.18 g (11 mmoles) *p*-toluenesulfonyl chloride in 12 ml anhydrous pyridine was added dropwise to a solution of 3 g 8.65 mmoles 3-O-acetyl-14-hydroxydihydromorphine in 12 ml anhydrous pyridine, with stirring, at a temperature between 0 °C and −5 °C. The mixture was stirred for further 2 hrs at this temperature, and it was allowed to stand 24 hrs at room temperature. The reaction mixture was then poured into 300 ml of water satured with sodium hydrogen carbonate and extracted with 3×60 ml of chloroform. The combined chloroform solutions were washed with 2×20 ml of water, dried over magnesium sulfate and evaporated. The residue was then dissolved in 50 ml ethyl acetate and washed with 3×10 ml of water, dried over magnesium sulfate and evaporated. After rubbing the residue with anhydrous ether, the solidified crystalline substance was filtered off to obtain 2.6 g 69.5% of the product, m.p. 193—194 °C, $[\alpha]_D$ −166.6° (c = 0.9; chloroform).

$C_{26}H_{29}O_7NS$ (500.981). Calc. N 2.8; S 6.4. Found N 2.77, S 6.49, 6.34%.

IR: $\nu_{OAC} = 1770$ cm^{-1}.

6-Deoxy-6-azido-14-hydroxydihydroisomorphine ("14-hydroxyazidomorphine") (8)

A solution of 2.5 g 35 mmoles sodium azide in 8.4 ml water was added to solution of 1.8 (3.5 mmoles) 3-O-acetyl-6-O-tosyl-14-hydroxydihydromorphine in 56 ml anhydrous dimethylformamide. The reaction mixture was heated for 24 hrs. at 100 °C, cooled, poured into 220 ml of water and extracted with 3×60 ml of chloroform. The combined chloroform solution was washed with 2×15 ml of a saturated aqueous solution of sodium chloride. The solution was then dried over magnesium sulfate and evaporated. After the removal of chloroform, the residual amount of dimethylformamide was evaporated at 60 °C at a pressure of 0.1 torr. The residue was rubbed with acetone to obtain a crystalline substance 0.86 g; 73.1%, m.p. 222—223 °C, $[\alpha]_D$ −185.9° (c = 0.53; anhydrous ethanol).

$C_{17}H_{20}O_3N_4$ (328.356). Calc. N 17.1. Found N 18.0, 18.37%.

IR: $\nu_{N_3} = 2100$ cm^{-1}.

*

The authors' thanks are expressed to Main Department I of Natural Sciences of the Hungarian Academy of Sciences and to Alkaloida Chemical Works Tiszavasvári for supporting this research.

REFERENCES

[1] a. MAKLEIT, S., BOGNÁR, R.: Kém. Közl. **30,** 289 (1968)
b. BOGNÁR, R., MAKLEIT, S.: Acta Chim. Acad. Sci. Hung. **58,** 203 (1968)
c. BOGNÁR, R., MAKLEIT, S., MILE, T.: Magyar Kém. Folyóirat **74,** 525 (1968)
d. BOGNÁR, R., MAKLEIT, S., MILE, T.: Acta Chim. Acad. Sci. Hung. **59,** 379 (1969)
[2] a. KNOLL, J., FÜRST, Zs., KELEMEN, K.: Orvostudomány **22,** 266 (1971)
b. KNOLL, J.: Pharmacol. Res. Commun. **5,** 175 (1973)
b. KNOLL, J.: Pharmacol. Res. Commun. **5,** 175 (1973)
c. KNOLL, J., FÜRST, Zs., KELEMEN, K.: J. Pharm. Pharmac. **25,** 929 (1973)
d. KNOLL, J., FÜRST, Zs., VIZI, E. S.: Pharmacology **10,** 354 (1973)
e. RÉTSÁGI, G., SCHWARTZMANN, E.: Orvostudomány **24,** 359 (1973)
f. KNOLL, J., MAKLEIT, S., FRIEDMANN, T., HÁRSING, L. G., Jr., HADHÁZY, P.: Arch. Internat. Pharmacodyn. et Thér. **210,** 241 (1974)
g. KNOLL, J., MAKLEIT, S., FRIEDMANN, T., HÁRSING, L. G. Jr., HADHÁZY, P.: Orvostudomány **26,** 89 (1975)
h. KNOLL, J., MAGYAR, K., MAKLEIT, S., ZÓLYOMI, G., ZSILLA, G.: Orvostudomány **26,** 111 (1975)
[3] SEKI, I.: Ann. Sankyo Res. Lab. **17,** 1 (1965)
[4] a. BOGNÁR, R., MAKLEIT, S., KNOLL, J., BERÉNYI, S., HORVÁTH, G.: Commun. Dept. Chem. Bulgarian Acad. Sci. **8/1,** 203 (1975)
b. BOGNÁR, R., MAKLEIT, S., KNOLL, J., BERÉNYI, S., HORVÁTH, G.: Kém. Közl. **44,** 1 (1975)
[5] FREUND, M., SPEYER, L.: J. prakt. Chem. **94,** 135 (1916)
[6] WEISS, U.: J. Am. Chem. Soc. **77,** 5891 (1955)
[7] WEISS, U., DAUM, S. J.: J. Med. Chem. **8,** 123 (1965)
[8] a. WELS, L. H.: J. Org. Chem. **19,** 1409 (1954)
b. WELS, L. H.: J. Am. Chem. Soc. **74,** 4967 (1952)
[9] a. KNOLL, J., FÜRST, Zs., MAKLEIT, S.: J. Pharm. Pharmac. **27,** 99 (1975)
b. KNOLL, J., FÜRST, Zs., MAKLEIT, S.: Orvostudomány **26,** 103 (1975)

Sándor MAKLEIT
Rezső BOGNÁR
Sándor BERÉNYI
Géza KISS

KLTE Szerves Kémiai Intézet
H-4010, Debrecen

József KNOLL

SOTE Gyógyszertani Intézet
H-1085, Budapest

Acta Chimica Academiae Scientiarum Hungaricae, Tomus 93 (2), pp. 169—174 (1977)

CONVERSIONS OF TOSYL AND MESYL DERIVATIVES OF THE MORPHINE GROUP, XVIII*

"AZIDOMORPHINE" DERIVATIVES, II

S. MAKLEIT, J. KNOLL,** R. BOGNÁR, S. BERÉNYI, G. SOMOGYI and G. KISS

*(Institute of Organic Chemistry, Kossuth Lajos University, Debrecen, and **Institute of Pharmacology, Semmelweis Medical University, Budapest)*

Received Januar 30, 1976

In the course of investigations of "azidomorphine" derivatives, 3-deoxy-, 3-0-ethyl and 3-0-morpholinylethyl-"azidomorphines" were prepared. Of these compounds "3-0-ethylazidomorphine" ("Azidodionin") proved to be the most efficient antitussive agent known so far, according to tests on experimental animals.

Owing to reasons mentioned in our preceding communication, we continued our investigations concerning the modification of "azidomorphine", with the primary purpose of the chemical modelling of our new theoretical research concepts about the mechanism of action of morphine (J. KNOLL).

The modification of the C-3 phenolic hydroxyl group of morphine, in the simultaneous presence of a C-6 azido group, was considered by us to be a route necessary and possibly leading to new practical results [1a, b].

In the present communication the details of these investigations are described.

3-Deoxydihydromorphine (**1**) [2a, b] was prepared in the known way, whose tosyloxy derivative (**2**) afforded on azidolysis 3-deoxyazidomorphine (4,5α-epoxy-6β-azido-17-methylmorphinan) (**3**). According to the results of pharmacological investigations carried out so far, compound **3** appears to have no practical significance.

When ethylmorphine (**4**) was hydrogenated (**5**) and the product converted into the tosyl and mesyl derivatives (**6a**, **6b**), subsequent azidolysis, carried out in the way developed by us for the morphine alkaloids, gave "Azidodionin" (**7**) (3-ethoxy-4,5α-epoxy-6β-azido-17-methylmorphinan). The pharmacological investigation of this compound afforded another new result of prominent importance [3a, b, c]. "Azidoethylmorphine was found to be in the rat 60 times more potent orally than codeine, *i.e.* it is the hitherto known most potent oral antitussive in this test".

* Part XVII: S. MAKLEIT, J. KNOLL, R. BOGNÁR, S. BERÉNYI, G. KISS: Acta Chim., Budapest **93,** 165 (1977) and Magyar Kém. Folyóirat **82,** 430 (1976).

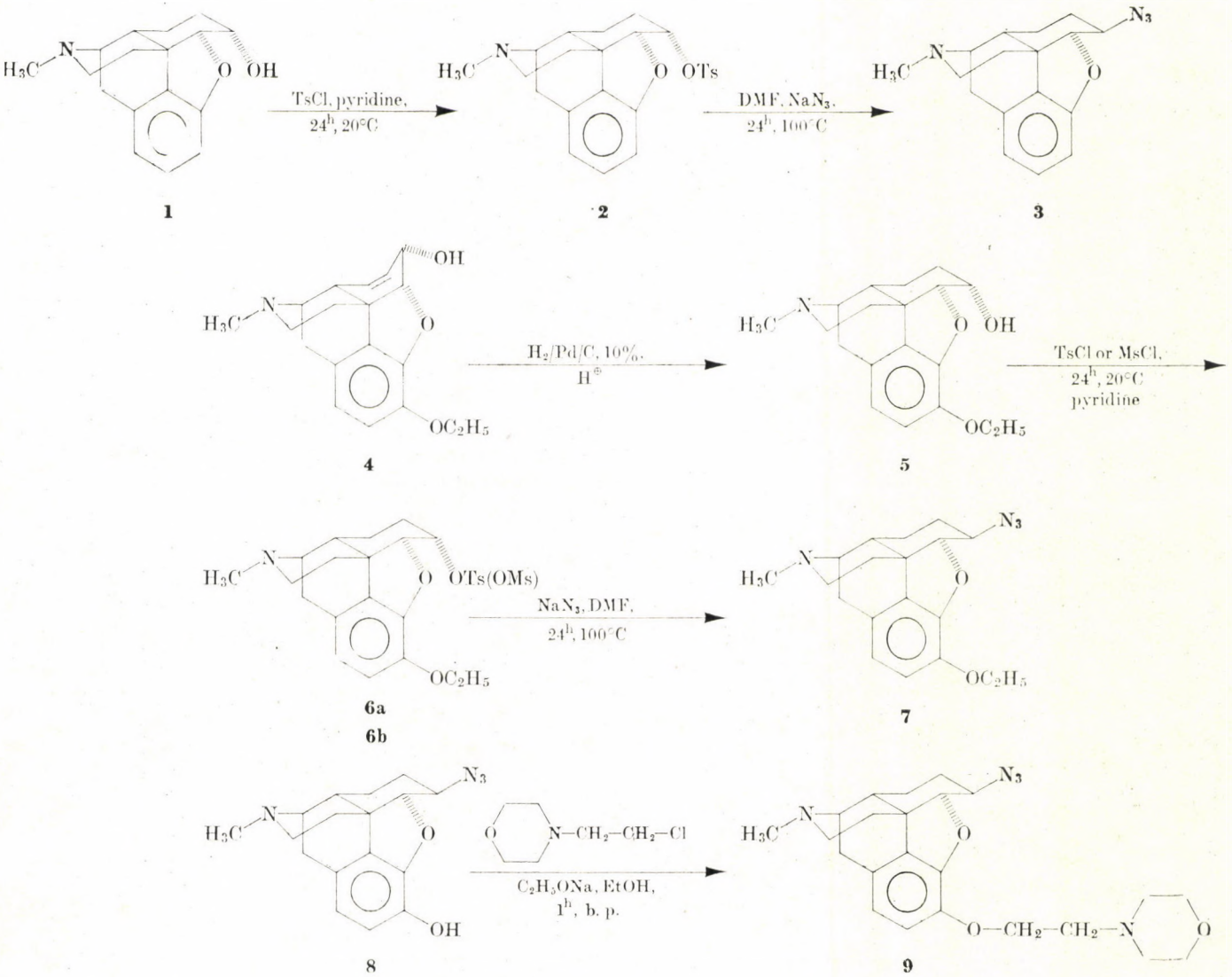
TsCl, pyridine,
24h, 20°C
DMF, NaN3,
24h, 100°C
1
2
3
H2/Pd/C, 10%,
H⊕
TsCl or MsCl,
24h, 20°C
pyridine
4
5
NaN3, DMF,
24h, 100°C
6a
6b
7
C2H5ONa, EtOH,
1h, b. p.
8
9

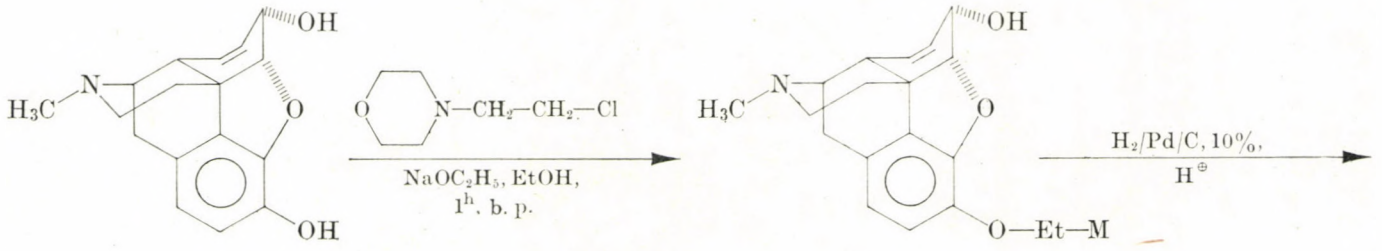

10 **11**

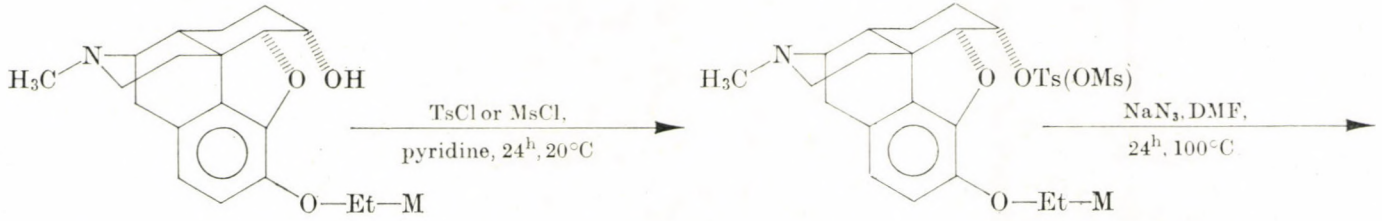

12 **13a** **13b**

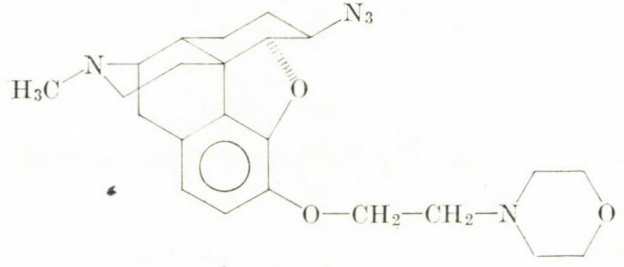

9

It is known that 3-O-morpholinylethylmorphine (**11**) [4] has favourable pharmacological properties. Taking this into account, we prepared 3-O-morpholinylethylazidomorphine (3-morpholinylethoxy-4,5α-epoxy-6β-azido-17-methylmorphinan) (**9**). This compound can be synthesized either by the alkylation of azidomorphine (**8**), which can be carried out since the azido group is rather stable in alkaline medium, or directly, starting from morphine (**10**). The pharmacological properties of the compound have been published earlier [3a, b].

Experimental

3-Deoxy-6-O-tosyldihydromorphine (2)

3-Deoxydihydromorphine (**1**) (4.1 g; 0.015 mole), prepared in the known way [2a, b], was dissolved in anhydrous pyridine, and a solution of 2.95 g (0.015 mole) p-toluensulfonyl chloride in 15 ml anhydrous pyridine was added by drops. Stirring was continued for 2 hrs at 0 °C and the mixture was allowed to stand 24 hrs. at room temperature. It was then poured into 400 ml of a saturated aqueous solution of sodium hydrogen carbonate and extracted with 3×100 ml of chloroform. The combined chloroform solution was washed with 2×25 ml of water, dried over magnesium sulfate and evaporated to dryness. The residue was dissolved in 50 ml ethyl acetate, washed with 3×20 ml of water, dried and evaporated. The residue was a gum weighing 3.25 g which was processed further in this form.

$C_{26}H_{29}O_4NS$ (451.564).

3-Deoxyazidomorphine (3)

A solution of 6.5 g sodium azide (0.1 mole) in 16 ml water was added to a solution of 3.35 g of compound **2** (0.0074 mole) in 100 ml anhydrous dimethylformamide, and the mixture was heated 24 hrs. at 100 °C. The mixture was poured into 500 ml of water, and extracted with 4×100 ml of chloroform. The combined chloroform solutions were washed with 2×50 ml of a saturated aqueous solution of sodium chloride, dried over magnesium sulfate and evaporated. The residue crystallized from anhydrous ether to give 1.17 g (20%) of the product; $[\alpha]_D$ −238° (c = 0.5; chloroform).

$C_{17}H_{20}ON_4$ (296.36). Calc. N 18.98. Found N 17.94%.

The product was chromatographically homogeneous (Silica gel G Merck; solvent system benzene-methanol (8 : 2); detection with Dragendorff reagent).

$\nu_{N_3} = 2100\ cm^{-1}$.

6-O-Tosyldihydroethylmorphine (6a)

A solution of 50 g (159 mmoles) dihydroethylmorphine in 200 ml anhydrous pyridine was cooled to a temperature between 0 °C and −5 °C, and a solution of 37 g (190 mmoles) tosyl chloride in 200 ml anhydrous pyridine was added dropwise, with stirring. After further stirring for 2 hrs. under cooling in ice-water, the mixture was allowed to stand 24 hrs at room temperature, and poured into 5000 ml of a saturated aqueous solution of sodium hydrogen carbonate; the mixture was extracted with 4×250 ml of chloroform. The combined chloroform extracts were then washed with 2×100 ml of a saturated aqueous solution of sodium chloride, dried over magnesium sulfate and evaporated to dryness to remove all pyridine. The remaining gum was dissolved in 500 ml ethyl acetate and washed with 3×70 ml of water. The ethyl acetate solution was dried over magnesium sulfate and evaporated to obtain 58.5 g of residual gum.

$C_{26}H_{31}O_5NS$ (469.584).

6-O-Mesyldihydroethylmorphine (6b)

A solution of 14.85 g (47 mmoles) dihydroethylmorphine in 60 ml anhydrous pyridine was cooled to a temperature between 0 °C and −5 °C, and the solution of 4.06 ml (6.014 g; 53.5 mmoles) methanesulfonyl chloride in 60 ml anhydrous pyridine was added dropwise, with stirring, during about 20 minutes. Stirring was continued for further 2 hrs under cooling in ice-water, the mixture was allowed to stand 24 hrs at room temperature, poured into 1500 ml of a saturated aqueous solution of sodium hydrogen carbonate, extracted with 3 × 200 ml of chloroform, and the combined chloroform extracts were washed with 2 × 70 ml of a saturated aqueous solution of sodium chloride. The chloroform solution was dried over magnesium sulfate and evaporated to dryness to remove all pyridine. The remaining gum was dissolved in hot anhydrous ether (about 40—50 ml). Crystallisation started instantaneously to yield 11.86 g (64%) of the product, m.p. 135—136 °C; $[\alpha]_D$ 96.1° (= 0.52; chloroform).

$C_{20}H_{27}O_5NS$ (393.430). Calc. N 3.56; S 8.14%. Found N 3.43; S 8.22%.

Azidodionine bitartarate (7)

A solution of 58.5 g (124 mmoles) 6-O-tosyldihydroethylmorphine was prepared in 1700 ml of anhydrous dimethylformamide, and 81 g (1240 mmoles) of sodium azide dissolved in 200 ml water was added. The homogeneous reaction mixture was poured into 5500 ml water and extracted with 4 × 400 ml of benzene. The combined benzene solutions were washed with 3 × 100 ml of a saturated aqueous solution of sodium chloride, dried over magnesium sulfate and evaporated (20 torr, 50 °C). The residue was 40 g of a gum which was dissolved in 200 ml of anhydrous ethanol. To this hot solution, the solution of 17.5 g of *d*-tartaric acid in 150 ml of hot anhydrous ethanol was added. On cooling the salt precipitated as yellow crystal plates (51 g; 65% calculated for the starting material), m.p. 193 °C, base content ~67%. The base precipitated from the crude product was only slightly contaminated. Recrystallization of the salt from 200 ml of water gave 44.3 g of the product, m.p. 197 °C.

$C_{23}H_{30}O_8N_4 \cdot H_2O$ (508.556). Calc. N 11.05. Found N 11.35, 11.18%.

IR: $\nu_{N_3} = 2100$ cm^{-1}, $[\alpha]_D$ −84° (c = 0.5; water).

3-O-Morpholinylethylazidomorphine (9)

0.17 g (7.4 mmoles) sodium metal was dissolved in 10 ml anhydrous ethanol, and 1 g (3.12 mmoles) azidomorphine (**8**) was dissolved in this solution. After the addition of 0.85 g (4.56 mmoles) finely powdered morpholinylethylchloride hydrochloride, the mixture was refluxed on a water bath for 1 hr. After cooling, sodium chloride was removed by filtration, the pH of the solution was adjusted to 5—6 with 10% aqueous hydrochloric acid, and the solution evaporated to dryness in vacuum. The residue was dissolved in 20—25 ml of water, transferred into a shaking funnel and made alkaline (pH = 9) with 50% aqueous sodium hydroxide solution, then extracted with 3 × 30 ml of chloroform. The combined chloroform extracts were washed with 2 × 15 ml of water and dried over magnesium sulfate. Evaporation to dryness left a gum which rapidly converted on standing into well developed crystals; washing with *n*-hexane or anhydrous ether gave 0.55 g (40%) of the product, m.p. 80—81 °C; $[\alpha]_D$ −138.8° (c = 0.72; chloroform).

$C_{23}H_{31}O_3N_5$ (425.512). Calc. N 16.46. Found N 16.38, 16.14%.

IR: $\nu_{N_3} = 2100$ cm^{-1}.

3-O-Morpholinylethyl-6-O-mesyldihydromorphine (13b)

A solution of 6.4 g (15.8 mmoles) 3-O-morpholinylethyldihydromorphine in 25.6 ml anhydrous pyridine was mixed at 0°, by dropwise addition, with a solution of 1.18 ml (1.75 g; 15.2 mmoles) methanesulfonyl chloride in 25.6 ml anhydrous pyridine. After stirring for 2 hrs at 0 °C, the mixture was allowed to stand 24 hrs at room temperature, then poured into 250 ml of a saturated aqueous solution of sodium hydrogen carbonate. The mixture was extracted with 3 × 50 ml of chloroform and the combined chloroform extracts washed with 2 × 10 ml of saturated aqueous solution of sodium chloride. After drying over magnesium sulfate, the solution was evaporated to leave a residual gum (5.8 g; 76%) suitable for further processing.

$C_{24}H_{34}O_6N_2S$ (474.536).

3-O-Morpholinylethylazidomorphine (9)

To a solution of 5.8 g (8.8 mmoles) of compound **13b** in 186 ml dimethylformamide, a solution of 7.56 g (85 mmoles) sodium azide in 22.4 ml water was added at once; the mixture was then maintained at 100 °C for 24 hrs. After cooling, the reaction mixture was poured into 700 ml of water and extracted with 3×100 ml of chloroform. The combined chloroform extracts were washed with 2×40 ml of a saturated aqueous solution of sodium chloride and dried over magnesium sulfate. The residue obtained on evaporation was crystallized from n-hexane to yield 2.1 g (40%) of the product, m.p. 80—81 °C, $[\alpha]_D$ −138.8° (c = 0.72; chloroform).

$C_{23}H_{31}O_3N_5$ (425.512). Calc. N 16.46. Found N 16.38, 16.53%.

IR: $\nu_{N_3} = 2100$ cm^{-1}.

*

The author's thanks are expressed to Main Department I of Natural Sciences of the Hungarian Academy of Sciences and to Alkaloida Chemical Works (Tiszavasvári) for supporting this research.

REFERENCES

[1] a. Bognár, R., Makleit, S., Knoll, J., Berényi, S., Horváth, G.: Commun. Dept. Chem. Bulgarian Acad. Sci. **8/1,** 203 (1975)
b. Bognár, R., Makleit, S., Knoll, J., Berényi, S., Horváth, G.: Kémiai Közl. **44,** 1 (1975)
[2] a. Bognár, R., Gaál, Gy., Kerekes, P., Horváth, G., T-Kovács, M.: Magyar Kém. Folyóirat **81,** 51 (1975)
b. Bognár, R., Gaál, Gy., Kerekes, P., Horváth, G., T-Kovács, M.: Org. Prep. Proc. Int. **6/6,** 305 (1974)
[3] a. Knoll, J., Makleit, S., Friedmann, T., Hársing, L. G., Jr., Hadházy, P.: Arch. Internat. Pharmacodyn. et Thér. **210,** 241 (1974)
b. Knoll, J., Makleit, S., Friedmann, T., Hársing, L. G., Hadházy, P.: Orvostudomány **26,** 89 (1975)
c. Knoll, J., Magyar, K., Makleit, S., Zólyomi, G., Zsilla, G.: Orvostudomány **26,** 111 (1975)
[4] Gyöngy, I., Makleit, S., Mészáros, Z., Szlávik, L.: Hungarian Pat. Appl., No. 1456 April 5, (1956)

Sándor Makleit
Rezső Bognár
Sándor Berényi
Gábor Somogyi
Géza Kiss

KLTE Szerves Kémiai Intézet
H-4010, Debrecen

József Knoll

SOTE Gyógyszertani Intézet
H-1085, Budapest.

Acta Chimica Academiae Scientiarum Hungaricae, Tomus 93 (2), pp. 175—181 (1977)

CONVERSIONS OF TOSYL AND MESYL DERIVATIVES OF THE MORPHINE GROUP, XIX**

"AZIDOMORPHINE" DERIVATIVES, III

S. MAKLEIT, J. KNOLL,* R. BOGNÁR, S. BERÉNYI, G. SOMOGYI and G. KISS

*(Organic Chemical Department, Kossuth Lajos University, Debrecen, and *Pharmacological Institute, Semmelweis Medical University, Budapest)*

Received January 30, 1976

To find new derivatives with morphineantagonistic properties and to prepare model compounds for morphine-receptor studies, several new N-substituted nor–"azidomorphine"-derivatives, including N-allyl-nor-"azidomorphine" (**5**), N-allyl-nor-"azidocodeine" (**6**), 14-hydroxy-N-allyl-nor-"azidomorphine" (**19**), 14-hydroxy-N-allyl-nor-"azidocodeine" (**24**), N-cyclopropylmethyl-nor-"azidomorphine" (**25**) and 14-hydroxy-N-cyclopropilmethyl-nor-"azidomorphine" (**26**) have been synthesized.

Owing to reasons mentioned in our previous papers, and in view of the morphine-antagonistic action of N-substituted morphine derivatives (N-allyl-normorphine = nalorphine, 14-hydroxy-N-allyldihydronormorphinone = naloxone, 14-hydroxy-N-cyclopropylmethyldihydronormorphinone = naltrexone), it seemed rewarding to attempt the synthesis of N-substituted derivatives of "azidomorphine".

In the present paper our studies in this field [1a, b] will be discussed in detail.

The following derivatives have been prepared:

N-allyl-nor-"azidomorphine" (3-hydroxy-4,5α-epoxy-6β-azido-17-allylmorphinan) (**5**),
N-allyl-nor-"azidocodeine" (**6**),
14-hydroxy-N-allyl-nor-"azidomorphine" (**19**).
14-hydroxy-N-allyl-nor-"azidocodeine" (**24**),
N-cyclopropylmethyl-nor-"azidomorphine" (**25**), and
14-hydroxy-N-cyclopropylmethyl-nor-"azidomorphine" (**26**).

The synthesis of compound **5** has been accomplished in two different ways. When starting from azidomorphine (**7**), partial acetylation of the phenolic hydroxyl group yielded 3-0-acetylazidomorphine (**8**), which was converted into the 3-0-acetyl-N-cyano-nor-derivative (**9**), by Braun's method.

** Part XVIII: S. MAKLEIT, J. KNOLL, R. BOGNÁR, S. BERÉNYI, G. SOMOGYI, G. KISS: Acta Chim. (Budapest) **93**, 169 (1977) and Magyar Kém. Folyóirat **82**, 432 (1976)

Alkaline hydrolysis and subsequent acid hydrolysis resulted in **11** *via* the intermediate **10**; this product can be further converted in different ways. Treatment with allyl bromide yields compound **5**, while the reaction product with cyclopropylmethyl bromide is compound **25**. Another possibility for the preparation of **5** involves the use of the well-known N-allyl-nor-dihydromorphine. Partial acetylation of this compound results in **1**, and the 6-0-tosyl and 6-0-mesyl derivative (**3**) can be obtained by treatment with tosyl and mesyl chloride, respectively. Compound **5** is formed by the azidolysis of this compound. This method is also described in a U.S. patent [2] published in 1975 (May 6, 1975). It is considered important to emphasize that this synthesis path had been reported earlier by us in our comprehensive papers [1a, b] (dates of arrival to press: 1a: August 21, 1974; 1b: August 15, 1974).

One of the synthetic routes to N-cyclopropylmethyl-nor-azidomorphine (**25**) has already been mentioned. The starting material in the other procedure, described in the literature [3] is N-cyclopropylmethyl-nor-morphine. Compound **2** was obtained by hydrogenation and partial acetylation of the phenolic hydroxyl group of this compound, and the product was then converted further into the 6-0-tosyl and 6-0-mesyl derivatives (**4**), respectively. The desired compound **25** was obtained in the azidolysis step. This synthetic route has been published in another U.S. patent [4] (April 29, 1975). Our comments concerning this patent are the same as for the previous one.

On the basis of our important observation that the Braun reaction can readily be accomplished in the presence of the azido group, the simple conversion of the azido compounds, prepared earlier, to the desired products seemed to be possible.

The Braun reaction of "azidocodeine" (3-methoxy-4,5α-epoxy-6-β-azido-17-methylmorphinan) (**12**) [5a—d] proceeds through **13** yielding **14**, and allylation of the reaction product gives compound **6**.

When subjecting the 3,14-diacetoxy derivative (**16**) of "14-hydroxyazidomorphine" (3,14β-dihydroxy-4,5α-epoxy-6β-azido-17-methylmorphinan) (**15**) [6] to the Braun reaction, the corresponding *nor* derivative (**18**) is obtained through the intermediate **17**. Allylation of **18** yields N-allyl-nor-"14-hydroxyazidomorphine" (**19**), while its reaction with cyclopropylmethyl bromide is suitable for the preparation of the N-cyclopropylmethyl derivative (**26**).

The Braun reaction of "14-hydroxyazidocodeine" (3-methoxy-4,5α-epoxy-6β-azido-14β-hydroxy-17-methylmorphinan) (**20**) [7a, b] or its 14-acetoxy derivative (**21**) takes place through compound **22** resulting in the *nor* derivative (**23**) which can then be converted into **24** in an allylation reaction.

Detailed data of the pharmacological tests of compounds **5** and **19** have already been published earlier [10].

Table I

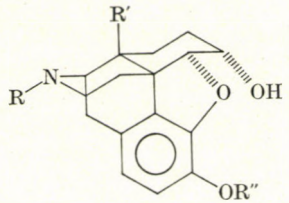

No	R	R'	R"	M.p., °C	Yield, %	$[\alpha]_D$	Formula, M.W.	Calcd.	Found	IR, cm^{-1}
1	allyl	H	CH_3CO	gum	—	—	—	—	—	allyl 933, OAc 1750
2	cyclopropylmethyl	H	CH_3CO	gum	—	—	—	—	—	cyclopropylmethyl 1040, 3070, OAc 1756

Table II

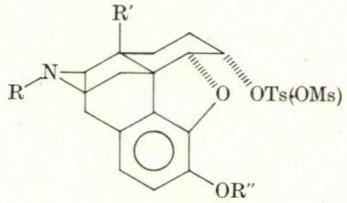

No	R	R'	R"	M.p., °C	Yield, %	$[\alpha]_D$	Formula,[6] M.W.	Calcd.	Found	IR cm^{-1}
3	allyl	H	$COCH_3$	gum	—	—	—	—	—	SO_2 1370, 1190, 1220
4	cyclopropylmethyl	H	$COCH_3$	129—130	49	—150	$C_{29}H_{33}O_6NS$ 523.9	N 2.68 S 6.13	2.53 5.97	SO_2 1360, 1178, 1190

Table III

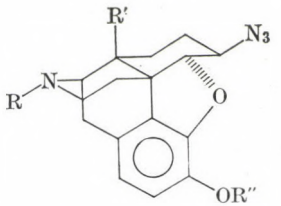

No	R	R'	R''	M.P., °C	Yield, %	$[\alpha]_D$	Formula, M.W.	Calcd.	Found	IR cm^{-1}
5	allyl	H	H	128—130	77.5	—190	$C_{19}H_{22}O_2N_4$ 338.3	N 16.5	N 15.83	N_3 2100, allyl 930
6	allyl	H	CH_3	96—97	26.2	—210.2	$C_{20}H_{24}O_2N$ 352.4	N 16.0	N 16.1	N_3 2100, allyl 930, 940, 3000
7	CH_3	H	H	azidomorphine; (3-hydroxy-4,5α-epoxy-6β-azido-N-methylmorphinan)						
8	CH_3	H	$COCH_3$	gum	—	—	—	—	—	N_3 2100, OAc 1770
9	CN	H	$COCH_3$	191	90.3	—308.4	$C_{19}H_{19}O_3N_5$ 365.3	N 19.16	N 19.33	OAc 1774, N_3 2108 N-CN 2214
10	CN	H	H	202	96.5	—225.5	$C_{17}H_{17}O_2N_5$ 323.3	N 21.66	N 21.68	N_3 2082, N—CN 2192
11	H	H	H	245	47	—181 ($CHCl_3$: EtOH = 2 : 1)	$C_{16}H_{18}O_2N_4$ 297.3	N 18.84	N 19.08	N_3 2080—2105, NH 3298
12	CH_3	H	CH_3	azidocodeine; (3-methoxy-4,5α-epoxy-6β-azido-N-methylmorphinan)						
13	CN	H	CH_3	158—159	96.5	—273.6	$C_{18}H_{19}O_2N_5$ 337.4	N 20.76	N 20.6	N_3 2110, N—CN 2211
14	H	H	CH_3	gum	—	—	—	—	—	N_3 2100, NH 3320
15	CH_3	OH	H	14-hydroxyazidomorphine; (3,14β-dihydroxy-4,5α-epoxy-6β-azido-17-methylmorphinan)						
16	CH_3	$OCOCH_3$	$COCH_3$	169—170	93	—266.5	$C_{21}H_{23}O_5N_4$ 411.4	N 13.6 OAc 20.8	N 13.2 19.2	N_3 2100, OAc 1746, 1773

Table III (continued)

17	CN	$OCOCH_3$	$COCH_3$	184—185	74	—284.1	$C_{21}H_{20}O_5N_5$ 422.4	N 16.5	N 16.68	N_3 2100, OAc 1746, 1773 N—CN 2210
18	H	OH	H	higher than 360	54	—159.3 (1N HCl)	$C_{16}H_{17}O_3N_4$ 313.3	N 17.7	N 17.52	N_3 2100, NH 3320
19	allyl	OH	H	148—150	89.5	—200 (0.25)	$C_{20}H_{21}O_3N_4$ 365.4	N 15.8	N 15.75	N_3 2100, allyl 927 3078
20	CH_3	OH	CH_3	14-hydroxyazidocodeine; (3-methoxy-4,5α-epoxy-6β-azido-14β-hydroxy-17-methylmorphinan)						
21	CH_3	$OCOCH_3$	CH_3	158—159	96.5	—225	$C_{20}H_{24}O_4N_4$ 384.4	N 14.57	N 13.93	N_3 2103, OAc 1725, 1250 1280
22	CN	$OCOCH_3$	CH_3	164—166	83.5	—246.8	$C_{20}H_{21}O_4N_5$ 395.4	N 17.71	N 17.81	N_3 2103, OAc 1740, N—CN 2219
23	H	OH	CH_3	178—180	63.6	—202.8	$C_{17}H_{21}O_3N_4$ 329.4	N 17.06	N 16.6	N_3 2101, NH 3300, C-14-OH 3420
24	allyl	OH	CH_3	78—81	76	—219.8	$C_{20}H_{25}O_3N_4$ 369.4	N 15.2	N 14.98	N_3 2100, allyl 927
25	cyclopropylmethyl	H	H	143	53	—174	$C_{20}H_{24}O_2N_4$ 352.7	N 15.9	N 15.9	N_3 2102, cyclopropylmethyl 1045, 3080
26	cyclopropylmethyl	OH	H	201	37	—188 (0.25)	$C_{20}H_{24}O_3N_4$ 368.7	N 15.2	N 15.1	N_3 2100, cyclopropylmethyl 1038, 3080

Experimental

M.p.'s, given in the Tables, are uncorrected and were measured in open capillaries The homogeneity of the substances was checked by thin-layer chromatography in all cases [Silicagel G, Merck; benzene–methanol (8 : 2), Dragendorff]. Optical rotation data were obtained in chloroform solution in 0.5 concentration, unless indicated otherwise.

The reactions are grouped and described in classes according to types.

(1) **Preparation of 3-O-acetyl derivatives** was based on Wels' [8a, b] method. Compounds synthesized in this way were **1**, **2** and **8**.

(2) **Preparation of tosyl and mesyl esters** was accomplished according to our usual method: the compound was allowed to react with 0.2 mole excess of tosyl chloride or mesyl chloride in pyridine 2 hrs at 0 °C and then 24 hrs at 20 °C. Compounds prepared in this way were **3** and **4**.

(3) **Azidolysis of sulfonic acid esters** was carried out according to the method developed by us, using 9 mole excess of sodium azide in dimethylformamide medium, 24 hrs, 100 °C. The method was employed in the preparation of compounds **5** and **25**.

(4) **The Braun reaction of azido compounds** was effected in chloroform solution with one mole excess of cyanogen bromide at 60 °C for 2.5—6 hrs. Compounds obtained in this way were **9**, **13**, **17** and **22**.

(5) **Deacetylation to remove the 3-O-acetyl group** was accomplished in slightly alkaline medium (2.5% alkali in aqueous ethanol) in the course of the preparation of **10**.

(6) Deacetylation of 3,14-diacetyl and 14-acetyl derivatives and hydrolysis of the cyano group were done simultaneously (5—10% aqueous hydrochloric acid, boiling for 5—10 hrs). This method was employed with substances **11**, **14**, **18** and **23**.

(7) **N-alkylation of nor-azido compounds** (allyl, cyclopropylmethyl) could be achieved best in absolute ethanol with an equivalent molar quantity of allyl bromide and cyclopropylmethyl bromide, respectively, in the presence hydrogen carbonate, refluxing the mixture for 10 hrs. Compounds obtained in this way were **5**, **6**, **19**, **24**, **25** and **26**.

*

The authors' thanks are due to Department I of the Hungarian Academy of Sciences and to the Alkaloida Chemical Works (Tiszavasvári) for supporting this research.

REFERENCES

[1a] Bognár, R., Makleit, S., Knoll, J., Berényi, S., Horváth, G.: Commun. Dept. Chem. Bulgarian Acad. Sci. **8**, 203 (1975)
[1b] Bognár, R., Makleit, S., Knoll, J., Berényi, S., Horváth, G.: Kém. Közl. **44**, 1 (1975)
[2] Meltzer, R. I. (to Warner-Lambert Co.) U.S. Pat. 3,882,127 (06 May, 1975); C.A. **83/13**, 590 (1975)
[3] Gates, M., Montzka, T. A.: J. Med. Chem. **7**, 127 (1964)
[4] Meltzer, R. I. (to Warner-Lambert Co.) U.S. Pat. 3,880,862 (29 April, 1975); C.A. **83/9**, 687 (1975)
[5a] Makleit, S., Bognár, R.: Kémiai Közl. **30**, 289 (1968)
[5b] Bognár, R., Makleit, S.: Acta Chim. Acad. Sci. Hung. **58**, 203 (1968)
[5c] Bognár, R., Makleit, S.: Magyar Kém. Folyóirat **74**, 523 (1968)
[5d] Bognár, R., Makleit, S.: Acta Chim. Acad. Sci. Hung. **59**, 373 (1969)
[6] Makleit, S., Knoll, J., Bognár, R., Berényi, S., Kiss, G.: Acta Chim (Budapest) and Magyar Kém. Folyóirat **82**, 430 (1976)
[7a] Makleit, S., Radics, L., Bognár, R., Mile, T., Oláh, É.: Magyar Kém. Folyóirat **78**, 223 (1972)
[7b] Makleit, S., Radics, L., Bognár, R., Mile, T., Oláh, É.: Acta Chim. Budapest **74**, 99 (1972)
[8a] Wels, L. H.: J. Org. Chem. **19**, 1409 (1954)
[8b] Wels, L. H.: J. Am. Chem. Soc. **74**, 4967 (1952)

[9] CURRIE, A. C., GILLON, J., NEWBOLDS, G. T., SPRING, F. S.: J. Chem. Soc. **1960,** 773
[10] KNOLL, J.: Problems of Drug Dependence, 1975. Proceedings of the Thirty-seventh Annual Scientific Meeting of the Committee on Problems of Drug Dependence, Washington, D. C. May 19—21, 1975, 892

Sándor MAKLEIT
Rezső BOGNÁR
Sándor BERÉNYI
Gábor SOMOGYI
Géza KISS

KLTE Szerves Kémiai Intézet
H-4010, Debrecen

József KNOLL

SOTE Gyógyszertani Intézet
H-1085, Budapest

Acta Chimica Academiae Scientiarum Hungaricae, Tomus 93 (2), pp. 183—191 (1977)

REACTIONS ACCOMPANIED BY ACYL SPLITTING IN N-CARBAMOYLSUCCINIMIDE DERIVATIVES

K. HARSÁNYI, K. TAKÁCS and A. SIMAY

(Pharmaceutical and Chemical Works Chinoin, Budapest)

Received March 26, 1976

The acyl splitting reactions of N-carbamoylsuccinimide (**III**) and its derivatives of formula **IV** with nucleophilic agents and by thermal treatment have been investigated. It has been found that **III** undergoes endo- or exocyclic acyl splitting when acted upon by nucleophilic agents, whereas in compounds **IV** only an exocyclic C–N bond rupture occurs. Thermal effect produces in compounds **III** and **IV** exocyclic acyl splitting, which can be accelerated with free radical initiators or with organic bases.

It is well known that triply acylated ammonia derivatives can be readily induced by nucleophilic agents to undergo reactions accompanied by the splitting of acyl groups. Open-chain triacylammonia derivatives have particularly strong acylating properties [1].

Derivatives of the general formula **I**, containing the triacylated nitrogen atom as the member of a pyrrole ring, can be considered special representatives of this group. The reactions of these compounds with nucleophilic agents can proceed in two directions, by rupture of endocyclic or exocyclic acyl-N bond (reaction path A and B, respectively) (Fig. 1).

Within the group of **Ia** compounds, only acyl splitting of type A has been observed [2]. This is probably due to the stable, conjugated 10π electron structure of the compounds, a conjugation which remains unchanged in a reaction of type A. Both the decrease and the increase of conjugation (**Ib** and **Ic**, respectively) as compared with **Ia**, brings about reaction B. In the case of compounds **Ib** [3—6] and **Ic** [7—12] either process A or process B will occur, depending on the nature of the R group [6, 8], on the character of the nucleophilic agent [5], and on the reaction conditions [4]. In a few cases, simultaneous occurrence of both processes, A and B, has been observed [4, 12].

The acyl splitting reaction of type B can be brought about also thermally in certain cases. Thus, e.g., from N-carbamoylmaleinimide (**II**) maleinimide can be prepared at 100—110 °C [2].

In the present work, reactions of some new **Ib** and **Id** derivatives (**III** and **IV**), effected by nucleophilic agents or by thermal influence have been studied.

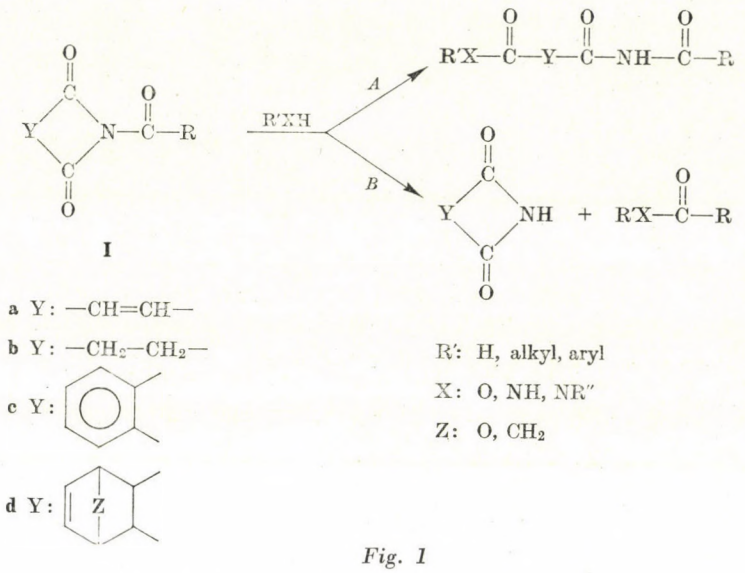

Fig. 1

Compound **III** was prepared by the catalytic hydrogenation of **II**, while compounds **IVa** and **b** by the Diels—Alder reaction of II with cyclopentadiene (**Va**) and furan (**Vb**), respectively (Fig 2).

In the reaction of **II** and **Va**, the known endo-**IVa** [14] was formed, in

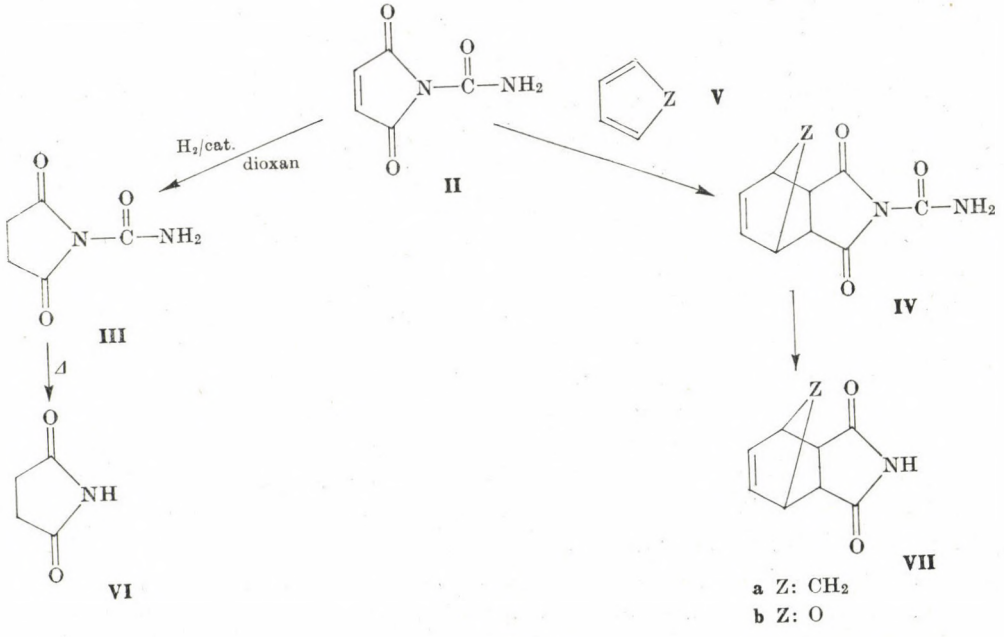

Fig. 2

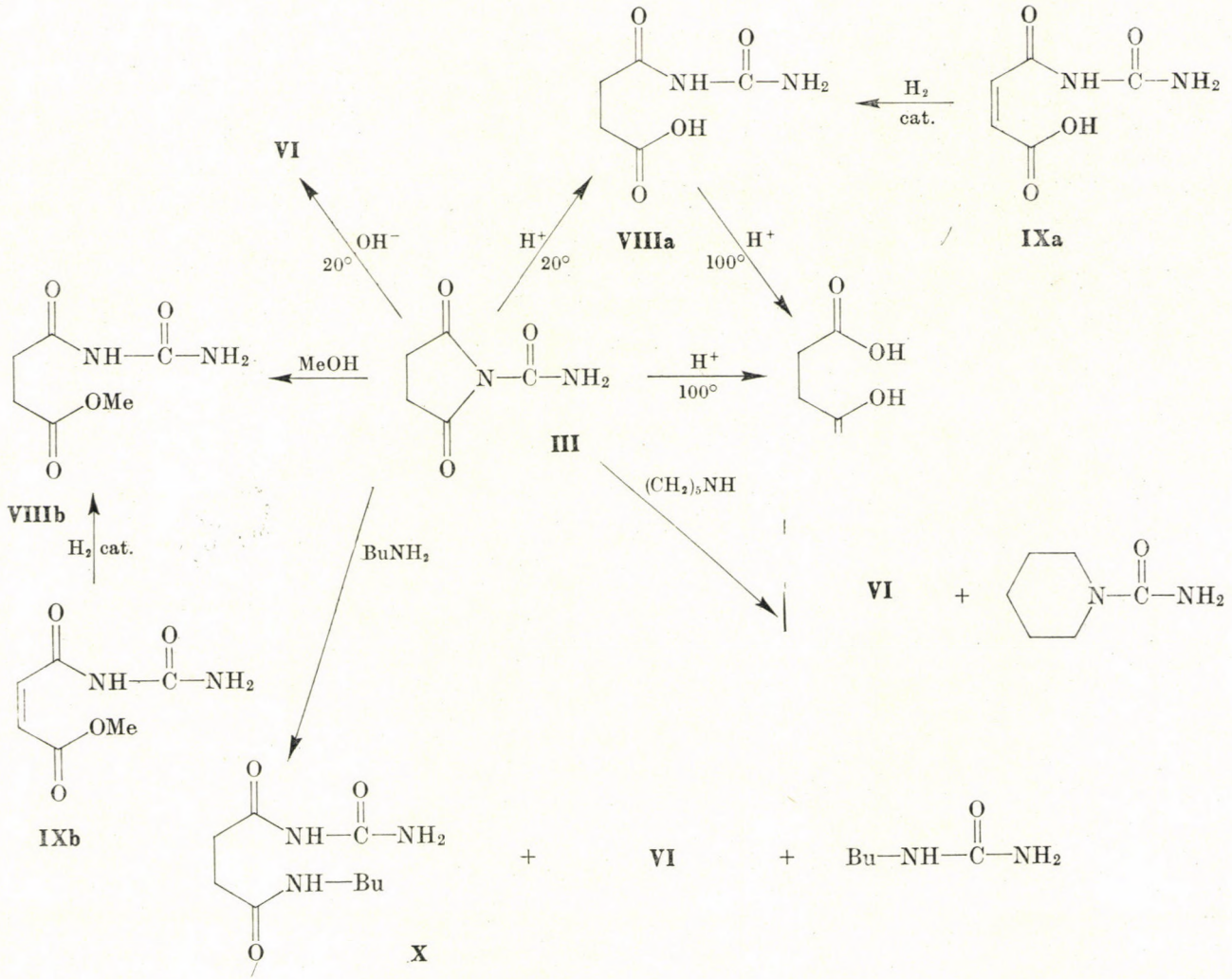
VI
OH⁻
20°
H⁺
20°
VIIIa
H₂
cat.
IXa
H⁺
100°
MeOH
III
H⁺
100°
VIIIb
H₂ cat.
(CH₂)₅NH
BuNH₂
VI
IXb
X
VI
Bu—NH—C—NH₂

accordance with general stereochemical principles [13]. However, in the addition reaction of **II** and **Vb**, exo-**IVb** was obtained both at 60 °C and at 20 °C, as contrary to the results of the reaction of furan and maleinimide [15].

Acyl splitting by nucleophilic agents

In accordance with analogous cases published in the literature [3—6], compound **III** showed an alternative reactivity towards nucleophilic agents.

In the course of its hydrolysis, bond rupture of type A was found in acidic medium, and bond rupture of type B in basic medium. Alcoholysis (methanol) also was a reaction of type A. In aminolysis effected with an aliphatic primary amine (butylamine), concurrent A and B reactions were observed, whereas with a secondary amine (piperidine) exclusively acyl splitting of type B occurred. The scheme of the reactions is shown in Fig. 3.

Compounds **VIIIa** and **b** have also been prepared in an authentic way, by the catalytic hydrogenation of the known compounds [2] **IXa** and **b**.

In contrast to **III**, in the reactions of compounds **IVa** and **b** with various nucleophilic agents, uniformly an acyl splitting process of type B was found, independently of the nature of the reagent and the reaction conditions (temperature, pH). In acid or alkaline hydrolysis, methanolysis, and in aminolysis with a primary or secondary amine, both at 55 and 20 °C, exclusively the known endo-**VIIa** [16] and exo-**VIIb** [15, 17] were obtained from endo-**IVa** and exo-**IVb**, respectively. The reactions took place generally under very mild conditions, thus *e.g.* the alkaline hydrolysis of **IVb** gave exo-**VIIb** even at 0 °C. This also proves the exo configuration of the compound **IVb**, as isomerization is unlikely to take place at 0 °C [15, 16].

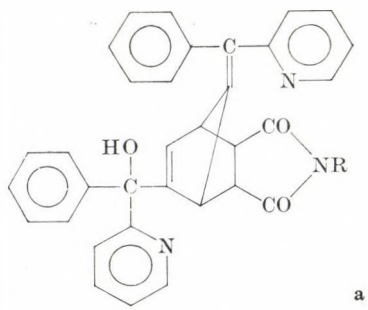

XI

a R: H

b R: CO—NH_2

Fig. 4

Acyl splitting by thermal influence

In the course of the thermolysis of **III**, similarly to the case of **II** [2], a process of type B occurred at 100—110 °C and succinimide (**VI**) was formed. It was shown that the reaction can be catalyzed with free radical initiators (*e.g.* benzoyl peroxide), or organic bases (pyridine, triethylamine), in the presence of which the reaction proceeds already at 60—80 °C giving good yields.

Similarly, in the course of the thermolysis of compounds **IV** a reaction of type B took place (Fig. 2), and at a considerably higher rate than in the case of **III**. In these cases too, the reaction could be considerably accelerated with benzoyl peroxide or with organic bases. (See Table II in Experimental.) The "thermolysis" of **IVa** proceeded in the presence of triethylamine already at room temperature.

No isomerization took place in the course of the reaction, uniformly endo-**VIIa** [16] and exo-**VIIb** [15, 17] were formed. Neither could isomerization be effected in the melt of endo-**IVa** by thermolysis at 180 or 220 °C [18]; homogeneous endo-**VIIa** was formed under these conditions too.

Thus, in the course of our investigations, compounds **IV** were found to undergo exclusively an acyl splitting of type B in reactions, effected both with nucleophilic agents and by thermal influence. In view of this result, a new synthesis [20], more convenient than those known so far, has been developed for the production of compound **XIa** [19], having selective rodenticidal activity and known under generic name Norbormide.

Experimental

M.p.-s are uncorrected. The IR spectra were recorded in KBr pellets with a Zeiss UR-20 spectrophotometer.

Preparation of N-carbamoylsuccinimide (III)

To 7.0 g (0.05 mole) of **II**, dissolved in 250 ml of dioxan, 3 g of a dioxan-wet 8% Pd/C catalyst was added, and hydrogenation was carried out at room temperature and atmospheric pressure. After hydrogen absorption had ceased, the solution was filtered from the catalyst and concentrated in vacuum to 40 ml, to obtain 4.2 (59%) of crystalline **III**, m.p. 158—160 °C (from ethylacetate).

IR: νNH_2 3420 ms, 3300 ms, 3265 ms; $\nu C{=}O$ 1795 s, 1750 s, br, 1710 sh.

$C_5H_6N_2O_3$ (142.12). Calcd. C 42.25; H 4.22; N 19.71. Found C 42.46; H 4.23; N 19.56%

Synthesis of compounds IV

(1) 7.0 g (0.05 mole) of **II** was allowed to react as described in the literature [14] with 8.3 ml (0.1 mole) of **Va**, to yield 7.85 g (76%) of endo-**IVa**, m.p. 151—153 °C (from methyl ethyl ketone).

IR: νNH_2 3415 s, 3350 sh, 3269 m, 3200 m; $\nu C{=}O$ 1775 s, 1755 s, 1701 s.

In the same way as above, 8.4 g (78%) of exo-**IVb** was obtained by the reaction of 7.0 g (0.05 mole) of **II** with 17.5 ml (0.24 mole) of **Vb**; m.p. 132—134 °C (d.) (from dioxan).

IR: νNH_2 3415 s, 3300 s, 3270 sh; $\nu C{=}O$ 1790 s, 1760 s, 1710 s.

$C_9H_8N_2O_4$ (208.17). Calcd. C 51.93; H 3.87; N 13.46. Found C 51.67; H 3.82; N 13.38%.

(2) 7.0 g (0.05 mole) of **II** was suspended in 25 ml of dry chloroform. Under cooling and stirring, 4.5 ml (0.055 mole) of **Va** was added dropwise at room temperature, and the reaction mixture was stirred at 20—25 °C for 16 hrs to obtain 9.25 g (90%) of endo-**IVa** m.p. 154—156 °C (acetone).

In an identical way, 2.0 g (68%) of exo-**IVb** was obtained by reacting 2.0 g (0.014 mole) of **II** with 3 ml (0.042 mole) of **Vb** for 36 hrs; exo-**IVb** melts at 132—135 °C with decomposition and is identical with **IVb** prepared as described above.

Reactions of III with nucleophilic agents

1. Acid hydrolysis

(a) 0.50 g (0.0035 mole) of **III** was mixed with 3 ml of 5*N* HCl, and the mixture was shaken at room temperature for 4 hrs. The solid substance was filtered off to obtain 0.50 g (89%) of **VIIIa**, m.p. 217—218 °C (d.)

$C_5H_8N_2O_4$ (160.13). Calcd. C 37.50; H. 5.04; N 17.50; Found C 37.47; H 5.11; N 16.90%.

(b) 1.0 g (0.007 mole) of **III** was boiled in 3 ml of 5 *N* HCl for 10 min. On cooling, 0.55 g (67%) of succinic acid (m.p. 186—188 °C) crystallized from the clear solution.

Under identical conditions, 0.20 g (55%) of succinic acid (m.p. 186—187 °C) was obtained from 0.50 g (0.0031 mole) of **VIIIa**.

Preparation of VIIIa by the hydrogenation of IXa

3.2 g (0.023 mole) of **IXa** [2] was mixed with 200 ml of 96% alcohol, and 1 g of an alcohol-wet 8% Pd/C catalyst was added; the mixture was hydrogenated at room temperature and atmospheric pressure. After the hydrogen absorption had ceased, the reaction mixture was heated to the boiling point, and the hot solution was filtered from the catalyst. On cooling 2.3 g (63%) of **VIIIa** crystallized, m. p. 216—217° (d.); this product was indentical with **VIIIa** prepared as described above.

2. Alkaline hydrolysis

To 0.5 g (0.0035 mole) of **III** there was added 10 ml of water and then, at room temperature, 10% NaOH solution, until the solid substance had dissolved. After a short standing, the clear solution was acidified with hydrochloric acid and evaporated to dryness in vacuum. The residue was recrystallized from 2 ml of 96% alcohol to give 0.30 g (79%) of **VI**, m.p. 124—125 °C.

3. Methanolysis

0.5 g (0.0035 mole) of **III** was refluxed with 5 ml of methanol for 4 hrs. After cooling 0.35 g (58%) of **VIIIb** crystallized, m.p. 180—181 °C (dioxan.)

$C_6H_{10}N_2O_4$ (174.16).

Calcd. C 41.37; H 5.79; N 16.08. Found C 41.70; H 5.98; N 16.18%.

Preparation of VIIIb by the hydrogenation of IXb

2.38 g (0.0155 mole) of **IXb** [2] was dissolved in 100 ml of methanol, 1 g of methanol-wet 8% Pd/C catalyst was added, and hydrogenation was carried out at room temperature and atmospheric pressure. After the hydrogen absorption had ceased, the reaction mixture was heated to the boiling point and the hot solution was filtered to remove the catalyst. On cooling, 1.8 g (67%) of **VIIIb** crystallized from the filtrate, m.p. 180—181 °C; this product was identical with **VIIIb**, prepared as described above.

4. Aminolysis

(a) To 0.5 g (0.0035 mole) of **III**, 7 ml of acetone and 0.35 ml (0.0035 mole) of butylamine were added, and the mixture was boiled for 4 hrs. After cooling, the substance which precipitated was filtered by suction to obtain 0.08 g (10.5 %) of **X**, m.p. 237—238 °C (from ethanol).

IR: νNH_2 3390 mw, 3335 mw; νNH: 3230 mw, br.; $\nu C{=}O$ + amide I 1700 sh, 1670 s; amide II 1555 s.

$C_9H_{17}N_3O_3$ (215.25). Calcd. C 50.22; H 7.96; N 19.52. Found C 50.00; H 8.03; N 19.40%.

Evaporation of the acetonic mother liquor in vacuum and recrystallization of the residue from benzene gave 0.20 g (53%) of **VI**, m.p. 123—125 °C.

Evaporation of the benzene mother liquor in vacuum and recrystallization of the residue from petroleum ether yielded 0.06 g (15%) of butylurea, m.p. 95—96 °C.

(b) 1.0 g (0.007 mole) of **III** was dissolved in 10 ml of acetone and 0.7 ml (0.007 mole) of piperidine was added; the mixture was boiled for 4 hrs, and then evaporated to about 5 ml. After cooling, the substance which separated was filtered off, and recrystallized from alcohol to obtain 0.60 g (67%) of carbamoylpiperidine, m.p. 102—104 °C.

The evaporation of the acetonic mother liquor in vacuum and recrystallization of the residue from benzene gave 0.30 g (39%) of **VI**, m.p. 123—125 °C.

Reactions of compounds IV with nucleophilic agents

1. Acid hydrolysis

0.52 g (0.0025 mole) of endo-**IVa** was mixed with 10 ml of water, 0.5 ml of conc. HCl and 2 ml of dioxan were added, and the reaction mixture was shaken at room temperature for 2 hrs. The solid substance which separated was filtered off and recrystallized from water to give 0.34 g (84%) of endo-**VIIa**, m.p. 184—187 °C (lit. [16] m.p. 187 °C).

In an identical way, during a reaction time of 7 hrs, 0.15 g (37%) of exo-**VIIb** was formed from 0.52 g (0.0025 mole) of exo-**IVb**; m.p. 160—163 °C (lit. [17] m.p. 159—161 °C).

2. Alkaline hydrolysis

0.52 g (0.0025 mole) of endo-**IVa** was mixed with 5 ml of water and at room temperature, 40% NaOH solution was added dropwise, until the solid substance had dissolved. The solution was allowed to stand for 10 min., then acidified with hydrochloric acid, and the substance which separated was filtered off to obtain 0.40 g (98%) of endo-**VIIa** m.p. 185—187 °C.

The reaction of 0.52 g (0.0025 mole) of exo-**IVb** according to the preceding process gave 0.25 g (61%) of exo-**VIIb**, m.p. 161—163 °C.

In an identical way, in a reaction carried out at 0 °C, 0.52 g (0.0025 mole) of exo-**IVb** yielded 0.22 g (54%) of exo-**VIIb**, m.p. 161—163 °C.

3. Methanolysis

0.52 g (0.0025 mole) of endo-**IVa** was mixed with 5 ml of methanol, and the mixture was refluxed for 4 hrs. After cooling, the solid which separated was filtered off, and recrystallized from alcohol to obtain 0.22 g (54%) of endo-**VIIa**, m.p. 185 °C.

In an identical way, 0.20 g (49%) of exo-**VIIb** (m.p. 157—160 °C) was obtained from 0.52 g (0.0025 mole) of exo-**IVb**.

4. Aminolysis

0.52 g (0.0025 mole) of compound **IV** in 5 ml of acetone was mixed with 0.003 mole of the amine compound and the reaction mixture was boiled for 2 hrs. After the evaporation of the solution, the residue was triturated under toluene, and the solid substance was recrystallized from water. Yields are given in Table I.

Thermolytic investigation of compounds III and IV

0.0035 mole of **III** or 0.0025 mole of **IV** was heated in 5 ml of solvent, or without solvent, at the temperature and for the time given in Table II. When using a catalyst, 0.3 ml of pyridine or 0.3 ml of triethylamine, or 0.3 g of benzoyl peroxide was added to the reaction mixture before heating.

After cooling, the solvent was distilled off in vacuum and the residue recrystallized from alcohol. In all the experiments **VI** (m. p. 124—125 °C) was obtained from **III**, endo-**VIIa** (m.p. 185—187 °C) from endo-**IVa**, and exo-**VIIb** (m.p. 160—163 °C) from exo-**IVb**.

Yields and thermolysis conditions are summarized in Table II.

Table I

Aminolysis data of compounds **IV**

Starting material	Reagent amine	Product	Yield, %
endo-**IVa**	butylamine	endo-**VIIa**	74
endo-**IVa**	piperidine	endo-**VIIa**	61
exo-**IVb**	butylamine	exo-**VIIb**	61
exo-**IVb**	piperidine	exo-**VIIb**	56

Table II

Thermolytic investigation of compounds **III** *and* **IV**

Solvent	Catalyst	Temperature, °C	Reaction time, hr.	Yield, %		
				III ↓ **VI**	**IVa** ↓ **VIIa**	**IVb** ↓ **VIIb**
—	—	210—220	3	—	86	—
—	—	180—190	3	—	74	—
dimethylformamide	—	b.p.	1	81	—	—
methyl ethyl ketone	—	b.p.	2	0	61	65
methyl ethyl ketone	pyridine	b.p.	4	20	86*	—
methyl ethyl ketone	triethylamine	b.p.	4	57	—	—
methyl ethyl ketone	benzoyl peroxide	b.p.	4	52	—	—
acetone	—	b.p.	2	—	0	0
acetone	pyridine	b.p.	2	—	49	24
acetone	triethylamine	b.p.	2	39**	79	73
acetone	benzoylperoxide	b.p.	2	—	69	48
acetone	triethylamine	20	5	—	74	—

* After a reaction time of 2 hours.
** After a reaction time of 4 hours.

Preparation of XIa

5.22 g (0.0095 mole) of the **XIb** geometrical isomeric mixture was mixed with 60 ml of water and 6 ml of conc. HCl. After the dissolution of the solid, the solution was clarified with charcoal and 20% NaOH solution was added dropwise to the filtrate to adjust pH 7; 4.65 g (95%) of the **XIa** hemihydrate geometrical isomeric mixture was obtained.

2 $C_{33}H_{25}N_3O_3 \cdot H_2O$ (1041.12). Calcd. C 76.13; H 5.03; N 8.07. Found C 75.99; H 5.02; N 7.76%.

*

The authors wish to thank István Remport for the microanalyses, Károly Horváth for the IR spectroscopic investigations, and László Tóth for his help in the experimental work.

REFERENCES

[1] ALLENSTEIN, E., BEYL, V., EITEL, W.: Chem. Ber. **102,** 4089 (1969) and references given therein
[2] TAWNEY, P. O. *et al.:* J. Org. Chem. **25,** 56 (1960)
[3] PEARSON, D. E., SIGAL, M. V. Jr.: J. Org. Chem. **15,** 1055 (1950)
[4] BOYD, H. *et al.:* Int. J. Peptide Protein Res. **4,** 109 (1972)
[5] GOERDELER, J., HORSTMANN, H.: Chem. Ber. **93,** 671 (1960)
[6] LEHMANN, G., ARACKAL, T. J.: Ann. **754,** 154 (1971)
BOYD, H., LEACH, S. J., MILLIGAN, B.: Int. J. Peptide Protein Res. **4,** 117 (1972)
[7] HELLER, G., JACOBSON, P.: Chem. Ber. **54,** 1107 (1921)
[8] STELLA, V., HIGUCHI, T.: J. Pharm. Sci. **62,** 968 (1973)
[9] BORISAVLJEVIC, R., MAMUZICA, R. I., MIHAILOVIC, M. L.: Glasnik Khem. Drustva, Beograd, **27,** 201 (1962); C.A. **59,** 6306 h (1963)
RABJOHN, N., DRUMM, M. F., ELLIOTT, R. L.: J. Am. Chem. Soc. **78,** 1631 (1956)
[10] US. Pat. 3,337,505; C.A. **67,** 82718 k (1967)
[11] IMAI, Y., ABE, T.: Nippon Kagaku Kaishi **1972,** 1872; C.A. **78,** 28736 d (1973); CLARKE, S., HIDER, R. C., JOHN, D. I.: J. Chem. Soc., Perkin Trans. 1. **1973,** 230
[12] HURD, C. D., DULL, M. F.: J. Am. Chem. Soc. **54,** 2432 (1932); **57,** 774 (1935)
[13] SAUER, E.: Angew. Chem. **79,** 76 (1967)
[14] BOEHME, W. R. *et al.:* J. Med. Pharm. Chem. **5,** 769 (1962)
[15] KWART, H., BURCHUK, J.: J. Am. Chem. Soc. **74,** 3094 (1952)
[16] CULBERSON, C. F., WILDER, P., Jr.: J. Org. Chem. **25,** 1358 (1960)
NAGASE, T.: Bull. Chem. Soc. Japan, **37,** 1175 (1964)
[17] BERSON, J. A., SWIDLER, R.: J. Am. Chem. Soc. **76,** 4060 (1954)
[18] GANTER, C., SCHEIDEGGER, V., ROBERTS, J. D.: J. Am. Chem. Soc. **87,** 2771 (1965) and references therein
[19] French Pat. 1,386,735; C.A. **63,** 3006d (1965)
POOS, G. I. *et al.:* J. Med. Chem. **9,** 537 (1966)
[20] Hung. Pat. 153,974; C.A. **70,** 3841f (1969) Hung. Pat 153,988; C.A. **69,** 26864j (1968)

Kálmán HARSÁNYI
Kálmán TAKÁCS
Antal SIMAY
H-1325 Budapest-Ujpest 1. Pf. 110.

Acta Chimica Academiae Scientiarum Hungaricae, Tomus 93 (2), pp. 193—200 (1977)

ALKALOIDS CONTAINING THE INDOLO[2,3-c]QUINAZOLINO[3,2-a]PYRIDINE SKELETON, V*

3,4-SECORUTECARPAN

K. HORVÁTH-DÓRA, G. TÓTH, J. TAMÁS** and O. CLAUDER

(Institute of Organic Chemistry, Faculty of Pharmaceutical Sciences, Semmelweis Medical University, Budapest and

***Central Research Institute for Chemistry of the Hungarian Academy of Sciences, Budapest)*

Received March 26, 1976

The reduction of a rutacarpine (**12**) with lithium aluminium hydride gave, in addition to rutecarpene (**13**) and 3α-rutecarpan (**14**), a product arising by further ring cleavage. This compound proved to be 3,4-secorutecarpan (**15**). The structure of each compound was confirmed by the analysis of their IR, NMR and MS spectra.

The chemical behaviour of hortiamine (**1**) [1], a representative of alkaloids with indolo[2,3-c] quinazolino[3,2-a]pyridine skeleton, was studied by PACHTER *et al.* [2]. By treatment with water, hortiamine was converted into 6-methoxyhetsinine (**2**). Reaction of the latter with acetic anhydride gave, in addition to the mono- and diacetyl derivatives the compound called isohortiamine (**3**).

On hydrogenating isohortiamine (**3**) in the presence of Adams catalyst, four hydrogen atoms were taken up, and tetrahydroisohortiamine (**4**) was obtained which is in fact 3,4-secodihydrohortiamine.

Interestingly, this tape of ring cleavage has not been observed with hortiamine (**1**) or dihydrohortiamine (**5**) (Fig. 1).

A similar ring opening combined with the uptake of hydrogen was reported by TŐKE *et al.* [3], who observed the formation of 3,4-secoyohimbine (**7**) in the reduction of the 3,4-dehydro product (**6**) obtained from natural α-yohimbine (Fig. 2).

BANERJI *et al.* [4] prepared the 3,4-secolactams of some yohimbine alkaloids by means of anhydrous sodium acetate in acetic anhydride. They found, however, that a secolactam was formed only from alkaloids with rings D/E fused *cis*. Thus *e.g.* the secolactam of structure **9** was obtained from venenatic acid (**8**) [5] (Fig. 3).

The fission of the C(3)-N_b bond of some yohimbine alkaloids was effected with cyanogen bromide by ALBRIGHT and GOLDMAN [6], to obtain the corresponding 3,4-secocyanamide in a fair yield (**10** → **11**) (Fig. 4).

On investigating the reduction of rutecarpine (**12**), we reported in an

* Part IV: Acta Chimica (Budapest), **89**, 85 (1976).

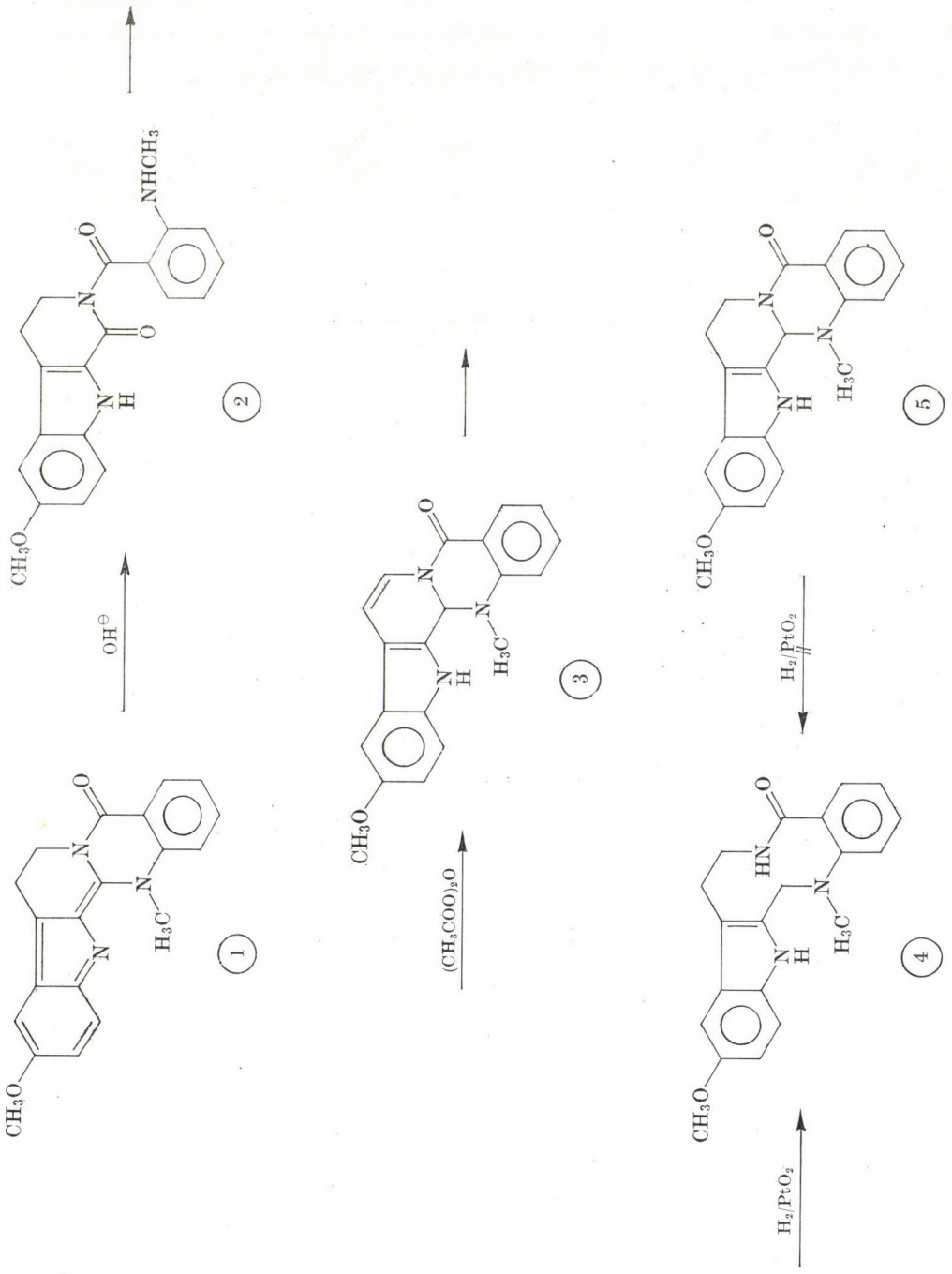

Fig. 1

earlier communication [7] that the reduction with lithium aluminium hydride gave two products, rutecarpene (**13**) and rutecarpan (**14**), depending on the solvent applied (Fig. 5).

Later mass spectrometric investigation of the product suspected to be rutecarpan (**14**) revealed that it was not a homogeneous substance, but it contained besides the compound of molecular weight 275, corresponding to 3α-rutecarpan (**14**), large amounts of a substance of molecular weight 277 (**15**).

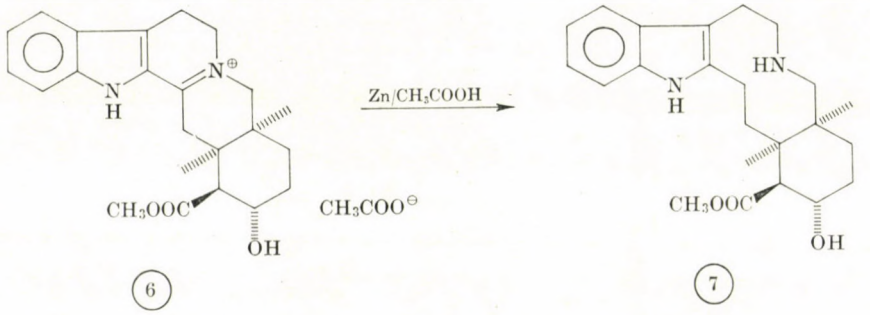

6 7

Fig. 2

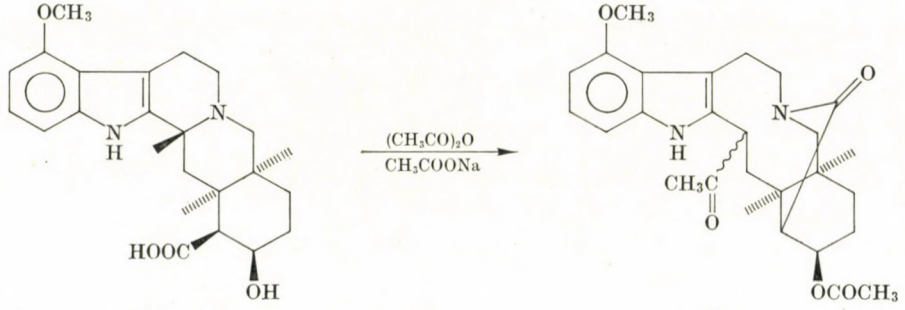

8 9

Fig. 3

10 11

Fig. 4

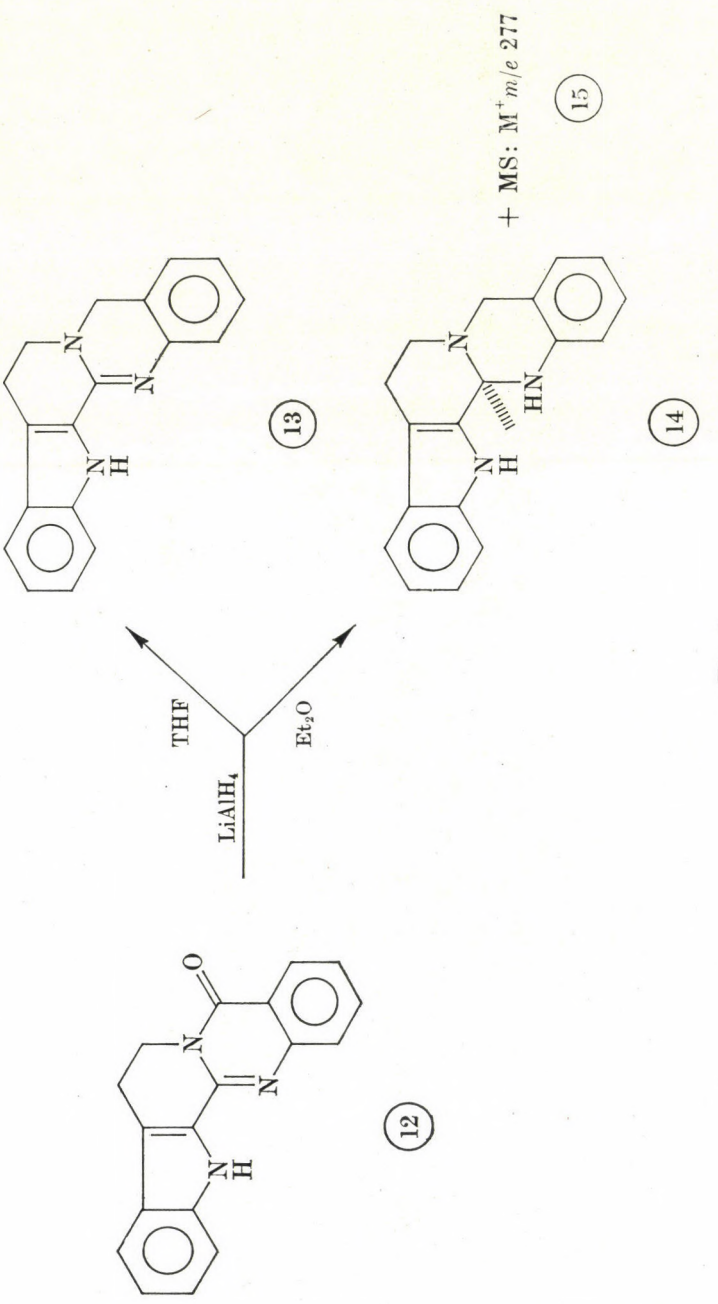

Fig. 5

These two substances were separated by preparative thin-layer chromatography (Kieselgel H; benzene : acetone 1 : 1). Accordingly, the earlier data concerning the physical and spectroscopic properties of 3α-rutecarpan (**14**) [7, 8] require some correction: M.p. 123—125 °C; UV (EtOH): max. (log ε): 282 (3.96), 290 (3.93). IR (KBr): 3400 cm^{-1} (ν NH, indole), 3250 cm^{-1} (ν NH, sec.), 2850, 2815, 2750 cm^{-1} (Bohlmann band).

The characteristic data of the substance of molecular weight 277 (**15**) are as follows: M.p. 192—193 °C; UV (EtOH): max. (log ε): 283 (3.89), 290 (3.82). IR (KBr): 3440 cm^{-1} (ν NH, indole), 3400, 3360 cm^{-1} (ν NH, sec.), 750, 735 cm^{-1} (γ CH, *o*-disubst.).

Since the UV spectrum of substance **15** was characteristic of a regular

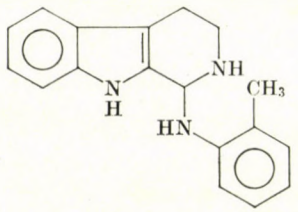

a

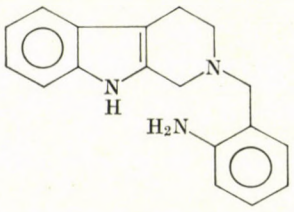

b

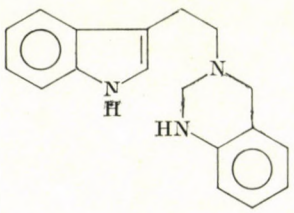

c

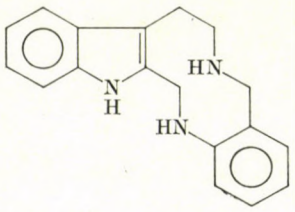

d

(15)

MS: M^+ *m/e* 277

IR ($CHCl_3$): νNH 3470 (indole), 3300 cm^{-1}

NMR:	$C(6)H_2$	$C(5)H_2$	$C(21)H_2$	$C(3)H_2$	NH	indole NH
$CDCl_3$	2.85s(A_4)		3.51s	3.72s	3.9 (2H)	7.45 (1H)
CF_3COOH	3.45 (2H)	4.10 (2H)	4.74 (2H)	5.01 (2H)		

Fig. 6

indole chromophore, we presumed that the two additional hydrogen atoms were used up in the splitting of the following C–N or C–C linkages:

(*a*) N_b—C(21); (*b*) C(3)—N(14); (*c*) C(2)—C(3); (*d*) C(3)—N_b.

On this basis we had to consider four alternative structures. Of these, it was possible to choose the right one on the basis of the IR, NMR and MS spectra (Fig. 6).

Since the pair of bands characteristic of the primary amino group was absent in the IR spectrum of the dilute solution of compound **15** in chloroform, structure (*b*) could at once be excluded.

According to the mass spectrum of compound **15**, the molecular ion of the compound had low stability, in agreement with the four possible alternative structures. The main decomposition process of this compound is the formation of the trihydro-β-carboline cation with *m/e* 171, which can be derived from the molecular ion by the elimination of an *o*-aminobenzyl radical; the latter also appears as a fragment with positive charge (*m/e* 106). This main decomposition process can be interpreted by any of the hypothetical structures (*a*), (*b*) and (*d*), but definitely excludes the alternative (*c*). In case of structure (*c*) the formation of ions with *m/e* 130 and 145 would predominante, just as in the fragmentation of 3,14-dihydrorutecarpine [9].

In the NMR spectrum of the compound, in turn, three NH protons were identified. On this basis the variant (*c*) can be similarly excluded. Further, since the singlet δ characteristic of the methyl groups on the aromatic skeleton did not appear at around 2.2, also structure (*a*) had to be excluded, leaving (*d*) as the only possible structure for compound **15**, which was consistent with all observed spectroscopic data.

At the same time an interesting effect was observed in the NMR spectrum of **15** recorded in $CDCl_3$ solution: the chemical shift of the methylene protons of the carbon atoms C(5)—C(6) was identical. Accordingly, a band of type A_4 appeared at δ 2.85. On the effect of salt formation this isochronism disappeared in CF_3COOH solution, and the triplets corresponding to the individual methylene protons could be readily identified at 3.45 and 4.10, respectively.

It follows that as a by-product of the reduction, a 10-membered ring was formed with fission of the C(3)—N_b linkage, and the product was 3,4-secorutecarpan (**15**).

Experimental

M.p.'s were determined by a Boetius M. instrument, UV spectra were recorded with a UNICAM SP-500 instrument, and IR spectra were obtain with a UNICAM SP-1200 spectrophotometer. The NMR spectra were recorded on a Jeol PS-100 equipment at 100 MHz, using TMS as internal standard; the chemical shifts are given on the basis of the convention $\delta_{TMS} = 0$ ppm. Mass spectra were recorded by an instrument AEI MS-902 (70 eV).

Rutecarpine (12)

This compound was prepared as described in our earlier communication [7], from 1.86 g of 1,2,3,4-tetrahydro-1-oxo-β-carboline (0.01 mole), 1.37 g of anthranilic acid (0.01 mole), and 10 ml of phosphorus oxychloride in 25 ml of anhydrous benzene. M.p. 256—258 °C.
UV (EtOH): max (log ε): 278 (3.88), 290 (3.92), 332 (4.48), 345 (4.54), 364 (4.44).
IR (KBr): 3350 cm^{-1} (ν NH, indole), 1660 cm^{-1} (ν C=O, lactam), 765, 725 cm^{-1} (γCH, *o*-disubst.).
NMR ($CDCl_3$): δH_2—C(5) 4.51 t (2 H); H_2—C(6) 3.20 t (2 H); H—C(19) 8.13 d (1 H); $J_0 = 7$ Hz; NH 9.35 s (1 H).
MS: the mass spectrum is given in another paper [9].

Rutecarpene (13)

Rutecarpene was prepared as earlier [7], by reducing 0.28 g of rutecarpine (**12**) (0.001 mole) in 20 ml of anhydrous tetrahydrofuran with 0.12 g of lithium aluminium hydride (0.003 mole). M.p. 205—207 °C.
UV (EtOH): max (log ε): 336 (4.28).
IR (KBr): 3430 cm^{-1} (ν indole, NH), 760 and 740 cm^{-1} (γCH, *o*-disubst.).
NMR ($CDCl_3$): H_2—C(5) 3.44 t (2 H); H_2—C(6) 3.03 t (2.H); H_2—C(21) 4.50 s (2.H).
MS: *m/e* (I%): 273.1268 (75%), $C_{18}H_{15}N_3$; 272 (100%); 243 (3%); 169 (1.1%); 155 (1.5%).

3α-Rutacarpan (14)

0.28 g of rutacarpine (**13**) (0.001 mole) was reduced in 40 ml of anhydrous ether with 0.23 g of lithium aluminium hydride (0.006 mole) as described in our earlier communication [7]. Processing of the reaction mixture gave 0.20 g of the product, which was separated on a Kieselgel H preparative layer. The developing solvent system was a 1 : 1 mixture of benzene and acetone. The fraction with R_f 0.66 was eluted with anhydrous ethanol and recrystallized from the same solvent to obtain 0.05 g of **14**, m.p. 123—125 °C.
UV (EtOH): max (log ε): 282 (3.96), 290 (3.93).
IR (KBr): 3400 cm^{-1} νNH indole, 3250 cm^{-1} (νNH, sec.), 2850, 2815, 2750 cm^{-1} (Bohlmann bands), 745 cm^{-1} (γCH, *o*-disubst.).
($CHCl_3$): 3480 cm^{-1} (νNH indole), 3350 cm^{-1} (νNH, sec.), 2750, 2810, 2840 cm^{-1} (Bohlmann bands).
NMR ($CDCl_3$): H_a—C(5) 3.15 m (1 H); H_e—C(5) 3.65 m (1 H); H_2—C(6) 2.78 m (2 H): H_2—C(21) 3.68 d (1 H); 3.92 d (1 H); $^2J_{AB} = 16.0$ Hz, H—C(3) 4.39 s (1 H).
MS: *m/e* (I%): 275.1426 (68%), $C_{18}H_{17}N_3$; 274 (75%); 169 (100%); 144 (13%); 143 (25%).

3,4-Secorutecarpan (15)

(a) The fraction with R_f 0.75 adsorbed in the separation of rutacarpan (**14**) on the Kieselgel H preparative layer (solvent system 1 : 1 mixture of benzene and acetone), was eluted with anhydrous ethanol. The solvent was evaporated and the residue crystallized from acetone to yield: 0.05 g of **15**, m.p. 195—198 °C.
UV (EtOH): max (log ε): 283 (3.89), 292 (3.83).
IR (KBr): 3440 cm^{-1} (νNH, indole), 3400, 3360 cm^{-1} (νNH, sec.), 750, 735 cm^{-1} (γCH, *o*-disubst.).
($CHCl_3$): 3470 cm^{-1} (νNH, indole), 3300 cm^{-1} (νNH, sec.).
NMR ($CDCl_3$): H_2—C(5) and H_2—C(6) 2.85 s (4 H, type A_4); H_2—C(21) and H_2—C(3) 3.50 s (2 H) and 3.74 s (2 H); N_b—H and N(14)—H 3.9 s (2.H); indole NH 7.45 s (1 H).
(CF_3COOH): H_2—C(5) 4.10 m (2 H); H_2—C(6) 3.45 t (2 H); H_2—C(21) and H_2—C(3) 4.74 (2 H) and 5.01 (2 H), respectively.
MS: *m/e* (I%): 277.1584 (2.8%), $C_{15}H_{19}N_3$; 171 (100%); 144 (15%); 143 (39%); 106 (18%).
(b) 0.13 g of rutecarpan (**14**) (0.0005 mole) was dissolved in 20 ml of methanol, and 0.09 g of sodium borohydride (0.0025 mole) was added into the solution under cooling with ice. The mixture was stirred 3 hrs at room temperature. It was then evaporated on a water bath, the residue dissolved in 20 ml of water and shaken with 1 × 30 ml and 2 × 20 ml portions of chloroform. The solution was dried and the solvent evaporated to leave a colourless oily residue which was crystallized from acetone. Yield 0.08 g (60%), m.p. 195—198 °C.

REFERENCES

[1] PACHTER, I. J., RAFFAUF, R. F., ULLYOT, G. E., RIBEIRO, O.: J. Am. Chem. Soc. **82,** 5187 (1960)
[2] PACHTER, I. J., MOHRBACHER, R. J., ZACHARIAS, D. E.: J. Am. Chem. Soc. **83,** 635 (1961)
[3] TŐKE, L., HONTY, K., SZABÓ, L., SZÁNTAY, Cs.: J. Org. Chem. **38,** 2496 (1973)
[4] BANERJI, A., MAJUMDER, P. L., Mrs. CHATTERJEE, A.: Indian J. Chem. **11,** 1057 (1973)
[5] RAY, A. B., Mrs. CHATTERJEE, A.: J. Indian Chem. Soc. **41,** 638 (1964)
[6] ALBRIGHT, J. D., GOLDMAN, L.: J. Am. Chem. Soc. **91,** 4313 (1969)
[7] CLAUDER, O., HORVÁTH-DÓRA, K.: Acta Chim. (Budapest) **72,** 221 (1972)
[8] TERZIAN, A. G., SAFRAZBEKYAN, R. R., KHAZNAKYAN, L. V., TATEVOSYAN, G. T.: Izv. Akad. Nauk Arm. SSR., Khim. Nauki **14,** 393 (1961)
[9] TAMÁS, J., BUJTÁS, Gy., HORVÁTH-DÓRA, K., CLAUDER, O.: Acta Chim. (Budapest), **89,** 85 (1976)

Klára HORVÁTH-DÓRA
Gábor TÓTH
Ottó CLAUDER
H-1092 Budapest, Hőgyes E. u. 7.

József TAMÁS
H-1025 Budapest, Pusztaszeri út 57—69.

Acta Chimica Academiae Scientiarum Hungaricae, Tomus 93 (2), pp. 201—203 (1977)

PREPARATION AND INVESTIGATION OF LEWIS ACID COMPLEXES, XII*

INVESTIGATIONS ON THE CYCLIZATION OF 1,2,3,4-TETRA-ACETYL-ß-D-GLUCOPYRANOSE INTO 2,3,4-TRIACETYL-LEVOGLUCOSANE**

(PRELIMINARY COMMUNICATION)

E. ZÁRA-KACZIÁN and GY. DEÁK

(Institute of Experimental Medicine, Hungarian Academy of Sciences, Budapest)

Received June 3, 1977

Recently we published [1, 2] our investigations on the mechanism of the reaction of $TiCl_4$ with pentaacetyl-β-D-glucopyranose and 2,3,4-triacetyl-levoglucosane, respectively. Our working hypothesis in the investigation of the reaction mechanism was that a study of the structure of the so-called initial complexes formed from the starting materials, and that of the complexes isolated at a later point of time of the reaction, will yield information permitting a deeper insight into the reactions.

The substrates of the reactions to be studied, triacetyl-levoglucosane and pentaacetyl-β-D-glucopyranose, are polyfunctional from the point of view of electron pair donation. Since no data were available in the literature, at first we studied on model compounds the relationship between the structure of the compounds, their tendency for complex formation and the structure of the complexes.

In the investigation of the complexes, the analysis of their IR spectra played a decisive role. These were recorded under conditions which eliminated the possibility of decomposition of the complexes.

In the course of the investigation of the ring splitting reaction the idea presented itself to study with the methods, used so far with good results, the conversion of 1,2,3,4-tetraacetyl-β-D-glucopyranose, catalyzed with $SnCl_4$ and yielding 2,3,4-triacetyl-levoglucosane (Fig. 1), which can be considered rather as a mirror reaction of the ring cleavage.

This reaction was first reported by LEMIEUX [3], who supposed that the primary step was the formation of a 1,2-α-cyclic ion, which then transformed into the end product by the intramolecular attack of the free OH group in position 6. Lemieux described this reaction as an extreme "pull" form of the "push-pull" mechanism, characteristic of some S_N2 type reactions.

* Part XI: FENICHEL, L., DEÁK, GY., BAKÓ, P., HOLLY, S. and CSŰRÖS, Z.: Acta Chim. (Budapest) **85**, 313 (1975).

** Presented at the 173rd National Meeting (Friedel-Crafts Centennial Symposium) of the American Chemical Society, New Orleans, Louisiana, March 23, 1977.

By TLC, IR spectroscopy and in preparative experiments we established that — in contrast with LEMIEUX's statement — at room temperature the reaction is completed within 15 minutes and only one kind of product can be detected (besides the unchanged tetraacetyl-glucose). This means that the reaction is rather fast and highly selective. Therefore, kinetic measurements were performed in diluted and cooled solutions; in this case the reaction time was 70 minutes. At −20 °C the reaction can be frozen out; thus sometimes even the recording of the IR spectra was performed in specially cooled cells.

The spectrum of the chloroform solution of tetraacetyl-glucose shows that, in an equilibrium system, a species containing an intramolecular hydrogen bond is also present. On the basis of our earlier results we assumed that under the conditions of the reaction a complex is formed from the substrate and the catalyst. Indeed, we succeeded in preparing an isolable complex containing

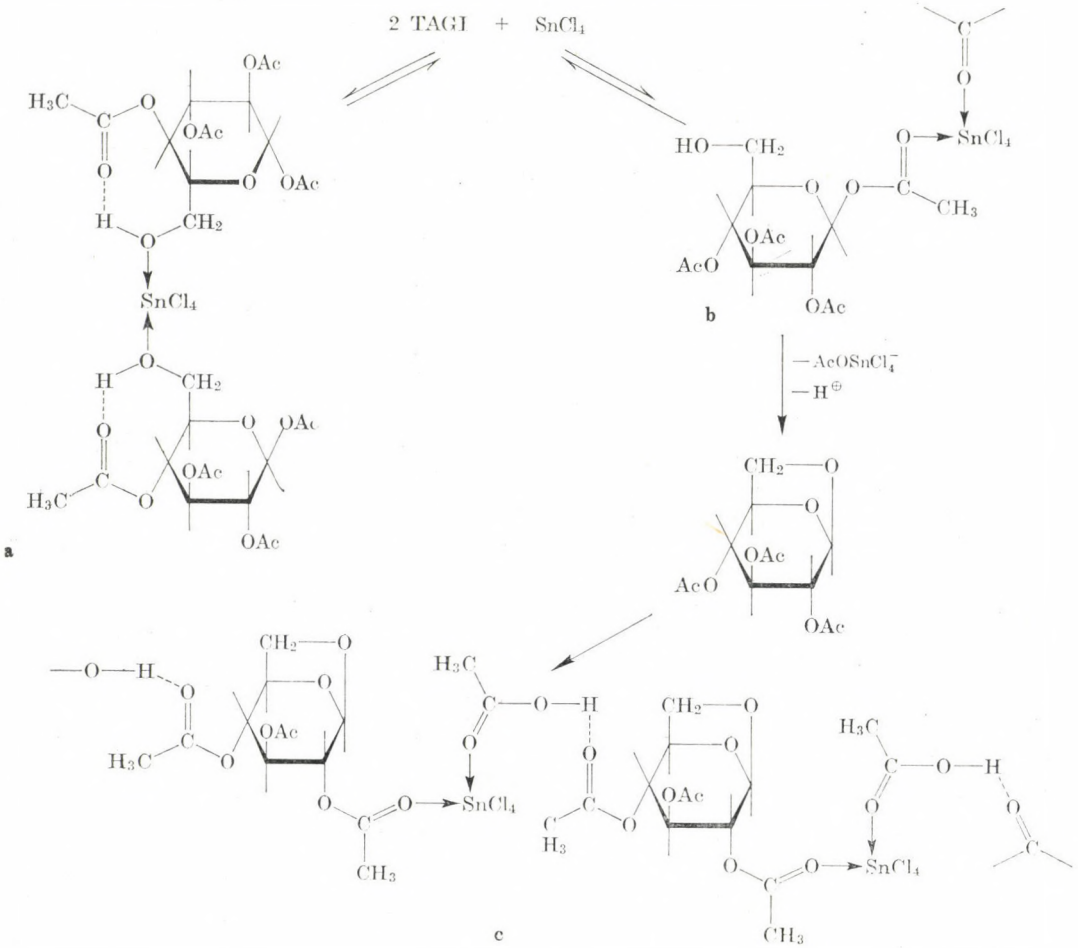

Fig. 1

2 moles of tetraacetyl-glucose and 1 mole of $SnCl_4$. Surprisingly, however, the spectrum of this complex does not reveal a shifted carbonyl band. On investigating the changes in the spectra we came to the conclusion that $SnCl_4$, as a Lewis acid, is linked in the complex to the hydroxyl group (Fig. 1, **a**). This assumption was proved by experiments performed on model compounds.

While investigating the transformation of tetraacetyl-glucose into triacetyl-levoglucosane in chloroform solution at room temperature, we observed that the band characteristic of the ν OH stretching vibration diappears immediately after the mixing of the tetraacetyl-glucose and $SnCl_4$ solutions. By assuming the formation of a 2 : 1 complex, as mentioned earlier, this change in the spectrum can be explained.

From the IR spectra we concluded, that in an equilibrium reaction also a small quantity of such a complex is formed in which $SnCl_4$ is presumably linked to the carbonyl oxygen of the C-1 acetyl group (Fig. 1, **b**), but this complex rapidly undergoes further reactions. In this complex the carbon–oxygen bond of the carbon atom in position 1 is weakened by the electron attraction of $SnCl_4$ and by the effect of the adjacent acetoxy group; the acetoxy group is split off in the form of $AcOSnCl_4^-$ anion, while the oxygen of the hydroxyl group in position 6 becomes linked by nucleophilic substitution to carbon atom C-1, with the loss of a proton.

When the reaction is completed, a new band appears in the spectrum at 1660 cm^{-1}, which is a shifted carbonyl band belonging to the acetyl group in complex linkage.

Surprisingly, however, a new strong band is exhibited at 1720 cm^{-1}, which can be detected at an earlier stage of the reaction as an inflexion and is continuously increasing in intensity. According to our assumption the primary product of the reaction is a complex containing triacetyl-levoglucosane, $SnCl_4$ and acetic acid in 1 : 1 : 1 proportion (Fig. 1, **c**). Depending on the conditions of the reaction, this complex dissociates into its constituents and thus we obtain a complex spectrum.

REFERENCES

[1] Fenichel, L., Deák, Gy., Holly, S., Bakó, P., Csűrös, Z.: Acta Chim. (Budapest) **85,** 299 (1975)
[2] Fenichel, L., Deák, Gy., Bakó, P., Holly, S., Csűrös, Z.: Acta Chim. (Budapest) **85,** 313 (1975)
[3] Lemieux, R. U., Brice, C.: Can. J. Chem. **30,** 295 (1952)

Erzsébet Zára-Kaczián
Gyula Deák
H-1450 Budapest, P.O. Box. 67.

RECENSIONES

B. KAKÁC und Z. J. VEJDELEK:

Handbuch der photometrischen Analyse organischer Verbindungen

Verlag Chemie, 1974

Das zweibändige Werk »Handbuch der photometrischen Analyse organischer Verbindungen« wurde 1974 vom Verlag Chemie herausgegeben. Auf dem Gebiet der instrumentalen chemischen Analyse sind jene Reaktionen von großer Wichtigkeit, mit deren Hilfe irgendein stabiles, farbiges Derivat der zu untersuchenden Substanz hergestellt werden kann, um eine quantitative Bestimmung durch Photometrierung zu ermöglichen.

Die Verfasser sammelten und systematisierten ein riesiges Material und achteten dabei sorgfältig darauf, jeden Faktor in Betracht zu ziehen, welcher auf den Reaktionsgang und auf die Bildung des farbigen Endprodukts einen Einfluß ausübt. Bei Messungen dieses Typs ist die Angabe von Meßvorschriften, welche die Selektivität und Reproduzierbarkeit der Methoden gewährleisten, von großer Wichtigkeit.

Diese Aufgabe, das Erreichen des gesetzten Ziels, wurde von den Verfassern sehr interessant gelöst. Das Beilstein-System wurde als Grundlage gewählt und die zu analysierenden Verbindungen wurden nach ihren funktionellen Gruppen in 18 Hauptgruppen und diese in 212 Nebengruppen unterteilt. Diese Gruppierung erfolgte nach jenen funktionellen Gruppen, die in der Farbreaktion teilnehmen.

Die einzelnen Hauptgruppen wurden im allgemeinen folgendermaßen bearbeitet:

Die Grundprinzipien, d.M. das Wesen der einen oder mehreren zur photometrischen Bestimmung führenden Reaktionen, werden dargelegt, sodann werden im Rahmen der Nebengruppen die wichtigsten Reaktionstypen eingehend besprochen. Es wird besonders darauf geachtet, bei jeder Reaktion Aufschluß über die Spezifizität der Reaktion und über eventuelle Störfaktoren zu geben. Schließlich werden die benötigten Reagenzien angeführt und eine kurze, sehr gut zusammengefaßte Beschreibung der Reaktion gegeben. Dies wird im allgemeinen aufgrund je eines Fachartikels zusammengestellt, doch wird am Ende einer Jeden Nebengruppe die ganze dies bezügliche Literatur angegeben. Innerhalb der Nebengruppen werden als Abschluß der Beschreibung der einzelnen Reaktionstypen jene Verbindungen in Tabellen zusammengefaßt, deren Bestimmung noch der erörterten Literatur erfolgt. Das Buch enthält 672 Tabellen dieser Art.

Einige weitere Daten über das Buch:

Das Schrifttum der Nebengruppen enthält die bibliographischen Daten von rund 7,500 Fachmitteilungen. Diese Zahl umfaßt auch jene Fachmitteilungen, die nicht eingehend aufgearbeitet, nur aufgrund einer Referatenzeitschrift angeführt wurden. Die Zahl der in den Tabellen angeführten Verbindungen übertrifft 6000!

Diese Daten zeugen von der eine unglaublich große Energie erfordernden Arbeit, die die Verfasser bei der Zusammenstellung des Buches leisteten. Es muß noch erwähnt werden, daß die Verfasser über die Systematisierung der gesammelten Literatur hinaus noch die einzelnen Verfahren auszuwerten hatten, um das von ihnen als beste beurteilte auszuwählen, wobei sicher die beschriebenen Verfahren in mehreren Fällen kontrolliert, d.h. die angegebenen Methoden geprüft werden mußten.

Der Rezensent hält das gut Konzipierte, auf hohem Niveau stehende Werk in der Bibliothek eines jeden Laboratoriums, in dem man sich mit der Analyse von organischen Präparaten befaßt, als unentbehrlich.

L. LÁNG

BILTZ—KLEMM—FISCHER:

Experimentelle Einführung in die Anorganische Chemie, 71. Auflage

de Gruyter Lehrbuch; Berlin—New York 1975

In der Chemie werden Ergebnisse im allgemeinen auf induktivem Wege durch eine eingehende Analyse und Systematisierung der Erfahrungen erreicht. Diese Methode zielt eine immer tiefere Einbettung der einzelnen Kenntnisse in das sich allmählich erweiternde System der Zusammenhänge. Die deduktive Methode führt ebenfalls zu bedeutenden Erfolgen, doch kann man diese Ergebnisse ebenfalls als einen Teil dieser Einbettung betrachten.

Aus diesem Grund liegt die Folgerung auf der Hand, daß der Anfänger auf diesem induktiven Wege in die Chemie eingeführt werden muß. Dieser Weg ist geeignetum, die Freude an den Erscheinungen zu wecken und die Beobachtungsgabe zu schulen. Mit solchem Ziele gibt das vorliegende Buch dem Anfänger ein mit äußerst einfachen Mitteln zu verwirklichendes Programm, in welchem die Theorien nicht als das Primäre behandelt werden, sondern als Mittel zur Erkennung der Zusammenhänge dienen.

Zu Beginn wird eine äußerst einfache Ausrüstung und Manipulationstechnik dargelegt, welche auch in der Mittelschule zur Verfügung stehen. Diese Einführung wird mit einer Zusammenfassung der wichtigsten Arbeits- und Vorsichtsmaßregeln des chemischen Laboratoriums beendet.

Danach werden die typischen Nichtmetalle und Nichtmetallverbindungen behandelt. Chlor, Schwefel, Stickstoff, Kohle und Phosphor gehören diesem Abschnitten, in dem auch die experimentelle Begründung wichtiger chemischen Begriffe erfolgt. So werden die Begriffe von Säuren und Basen, der chemischen Umsetzung, der Konzentration, der elektrolytischen Dissoziation, der chemischen Bindung sowie Oxidation und Reduktion besprochen und in der Interpretation angewandt. Einen wichtigen Teil dieses Abschnittes bildet die Besprechung der IUPAC Nomenklatur.

Bei der Behandlung der Metallverbindungen werden die wichtigeren Repräsentanten der Alkali- und Erdmetallealkali (einschließlich Ammonium bzw. Magnesium), Aluminium, Elemente der Gruppen IB und IIB und schließlich Repräsentanten der Übergangselemente und der Gruppen IVB und VB besprochen. Die Kentnisse, die das chemische Verhalten dieser Repräsentanten betreffen, werden ebenfalls in einem System geordnet, wobei die Zusammenhänge im Rahmen des chemischen Gleichgewichtes aufgezeigt und erklärt werden. In dieser Beziehung das Massenwirkunggesetz und seine Anwendungen auf verschiedene Erscheinungen dienen für die Erweiterung und Vertiefung der Anschauungsweise des Lesers.

Ein kleinere Abschnitt ist den weniger wichtigen Nichtmetallverbindungen sowie einigen weiteren Metallverbindungen gewidmet. Besonders die erstgenannte Verbindungsgruppe ist geeignet, die Variabilität der Bindung der anorganischen Moleküle zu veranschaulichen.

Das Buch ist sehr lehrreich und dazu geeignet, den Anfänger in das chemische Denken einzuführen. Das ist besonders durch das Bestreben der Verfasser bedingt, das Periodensystem der Elemente zugrunde zu legen und dessen Nutzen bei allen Vergleichen und Orientierungen aufzuzeigen.

Der Inhalt des Buches kann nach dem Verfasser auch einer Reduktion unterworfen werden. Nach dem Durcharbeiten des Buches hat man auch den entgegengesetzten Eindruck. Das Buch ist auch einer Erweiterung fähig, und der Leser hat auch in dieser Hinsicht eine ausgezeichnete Initiative bekommen. Diese 71. Auflage und auch die folgenden werden mit Interesse erwartet.

P. HUHN

G. WÜNSCH: *Optische Analysenmethoden zur Bestimmung anorganischer Stoffe*

Sammlung Göschen 2606
Walter de Gruyter et Co.

Berlin, New York 1975. 316 Seiten. DM 19,80

Der die optischen analytischen Methoden behandelnde, in der in weiten Kreisen bekannten und beliebten Serie »Sammlung Göschen« erschienene Band wird sowohl hinsichtlich des Umfangs als auch des Gehaltes der ursprünglichen Zielsetzung der Serie gerecht: Förderung

des allgemeinen Lernens. Er gibt eine klare, moderne, kurzgefaßte, doch für das Verständnis und die Praxis ausreichende Orientierung über die wichtigsten, in den optischen Laboratorien üblichen analytischen Methoden: über Spektrophotometrie, Turbidimetrie, Fluorometrie, Flammenspektrometrie und Atomabsorption. Der Verfasser befaßt sich nicht mit den Geräten und der Praxis der Emissionsspektrographie, vermutlich deshalb, weil diese in einem separaten Band behandelt werden.

Das Buch behandelt die Themen auf mittlerem Niveau, so daß es für Oberschüler sowie für andere Leser ohne Hochschulausbildung in Chemie oder Physik leicht verständlich ist. Gleichzeitig ist es auf dem neuesten Stand und liefert auch zur sachgemäßen und sorgfältigen Ausführung der beschriebenen Methoden ausreichende Informationen.

Ein großes Verdienst des Buches ist, daß im ersten Teil eine ausführliche Beschreibung der Grundprinzipien der einzelnen Methoden der Atom- und Molekularspektroskopie, der einzelnen Baueinheiten der verwendeten Geräte (Lichtquelle, Monochromator, Detektor usw.), des prinzipiellen Aufbaus der Geräte und der verschiedenen Methoden des Messens und der Auswertung erfolgt. Ein wesentlicher Teil ist der Fehlerberechnung, den die Genauigkeit erhöhenden Methoden, den Signal-Geräusch-Verhältnissen, der Empfindlichkeit und dem Begriff der Nachweisbarkeitsgrenze gewidmet.

Der zweite Teil des Bandes ist spezieller Natur. Es enthält die eingehende Beschreibung der photometrischen, turbidimetrischen, fluorometrischen, flammenphotometrischen und mittels Atomabsorption ausgeführten Bestimmung von etwa 30 Elementen. Die Beschreibungen erstrecken sich auf das Grundprinzip die Versuchsausführung und darüber hinaus auf die Bereitung der Reagenzien, die Aufnahme der Vergleichskurven, die Angabe der Störelemente, die Vorbereitung der Probe und die Behandlung des Gerätes. Heutzutage, wo oft nachlässig zusammengestellte Mitteilungen und Lehrbücher erscheinen, kann die Zusammenstellung und Abfassung des speziellen Teiles vom didaktischen Gesichtspunkt wahrhaftig als einwandfrei und musterhaft bezeichnet werden. Das Buch gibt dem Leser vieles, was sonst nur von sehr erfahrenen und guten Pädagogen vermittelt wird.

Der dritte Teil des Buches befaßt sich mit der Beschreibung grundlegender Übungen, unter anderem mit der Bestimmung der Löslichkeit, mit der Untersuchung der Zusammensetzung von Komplexverbindungen und mit der Ausarbeitung neuer Photometrischer Methoden.

Jeder Abschnitt des Buches gibt dem Leser nützliche Hinweise auf Bücher, in denen die einzelnen Teilthemen zu finden sind und die nachzuschlagen sich bei weiteren Problemen lohnt.

Am Ende des Buches befindet sich ein nützliches Sachregister.

Ich glaube, die kleinformatige Broschüre wird für jeden eine nützliche Hilfe oder ein Lehrbuch sein, der sich die Praxis der optischen analytischen Methoden anzueignen wünscht oder sich in den Methoden auskennen möchte. Außerdem kann das Buch jenen Fachleuten als Beispiel empfohlen werden die Analytik zu unterrichten.

J. INCZÉDY

T. ERDEY-GRÚZ: *Kinetik der Elektrodenprozesse*

Akadémiai Kiadó, Budapest 1975. 581 Seiten

Der Erfolg eines wissenschaftlichen Buches, welches das Interesse eines weiten fachlichen Kreises beansprucht, wird neben der guten Brauchbarkeit und dem hohen Niveau der Behandlung des Gegenstands durch den leichtverständlichen Stil und durch die klare und logische Ausführung des Stoffen bestimmt. All diese vorteilhaften Eigenschaften konnten bereits bei der ersten — in ungarischer Sprache erschienenen — Ausgabe des vorliegenden Buches, dessen Verfasser als Klassiker dieses Wissenschaftsgebiets gilt, eindeutig festgestellt werden. Diese Bewertung wird auch durch die Tatsache unterstützt, daß der Rezensent — nach der englischen Ausgabe — nunmehr die zweite fremdsprachige Ausgabe begrüßen darf und dies mit Freude tut. Die Kinetik der Elektrodenprozesse ist heute ein hochwichtiger, grundlegender Zweig der Elektrochemie und der elektrochemischen Technologie; seine Bedeutung nimmt stets zu. Folglich ist eine Behandlung des Stoffes in der Art und in dem Umfang des vorliegenden Werks, worin die Vorteile eines Lehrbuchs mit einer auf hohem Niveau und auf dem neuesten Stand stehenden Darlegung des gesamten Wissenschaftsgebiets oder zumindest eines überwiegenden Teiles davon mit einem sachkundigen Ausblick nach vorwärts verbunden sind unzweifelhaft sehr nützlich und sogar — ich möchte die Behauptung wagen —

in einer deutschsprachigen Ausgabe äußerst notwendig, da ja diese Sprache — zumindest in einem großen Teil des europäischen wissenschaftlichen Lebens — trotz der zunehmenden Verbreitung der englischen Sprache auch heute noch ein lebendiges und sich stets weiter entwickelndes Medium der wissenschaftlichen Kommunikation geblieben ist und auch in Zukunft bleiben wird.

Das Buch ist in acht große Abschnitte gegliedert, wovon Abschnitt 8 als Anhang betrachtet werden kann und eine hervorragende Zusammenfassung der Grundbegriffe darstellt (Elektrodenpotentiale, galvanische Elemente, Transportvorgänge, anodische und kathodische Ströme, Theorie der Doppelschicht, Grundlagen der Theorie der absoluten Reaktionsgeschwindigkeit und ihre Anwendungsmöglichkeiten auf die Geschwindigkeit von Elektrodenprozessen, elektrokinetische Versuchsverfahren usw.).

In den sieben Hauptabschnitten werden folgende Fragen behandelt: 1. Grundlagen der Kinetik von Elektrodenprozessen; Elektrodenprozesse, bei denen der Ladungsübergang geschwindigkeitsbestimmend ist. 2. Elektrodenprozesse mit durch die chemische Reaktion bestimmter Geschwindigkeit. 3. Elektrodenprozesse mit diffusionsbestimmter Geschwindigkeit. 4. Kinetik einiger wichtiger Elektrodenprozesse (H_2-, Cl_2-, O_2-Gaselektroden, Redoxelektrode, elektrolytische Metallabscheidung, Elektrokristallisation). 5. Elektrodenprozesse in Salzschmelzen. 6. Elektrodenprozesse an Leitergrenzflächen. 7. Kinetik der anodischen Filmbildung.

Einer großer Vorteil des Buches ist, daß jedes Kapitel mit einem ausführlichen Literaturverzeichnis (bearbeitet im allgemeinen bis Mitte 1974) abgeschlossen wird und ein Namensregister sowie ein sehr ausführliches Sachverzeichnis am Ende des Buches die Orientierung erleichtert.

Zusammenfassend kann eindeutig festgestellt werden, daß das Buch ein äußerst wertvolles Hilfsmittel für die große Zahl deutschsprechender Forscher, Technologen und Hochschullehrer im deutschen Sprachgebiet und auch darüber hinaus darstellt.

E. BERECZ

Topics in Current Chemistry. 63. Bonding and Structure

Springer Verlag, Berlin, 1976. 202 pp.

This well established series, concerned mainly with the theoretical aspects of chemistry, offers under this title three reviews on widely differing topics by authors active in the respective fields. The first one "*Discriminating Interactions Between Chiral Molecules*" by David P. CRAIG and P. MELLOR (48 pp.) deals with the chemical physics of what one used to call diastereomeric interactions, but for which the authors now coined the term 'chirodiastaltic interactions'. After shortly reviewing all kinds of such interactions so far observed, from the well known m.p. phenomena through complex stability to chiral discrimination in physiological reactions, the authors take account of the microscopic physical interactions which may be the primary factors in chiral discrimination. Of all this so far only the very short range interactions denoted usually as van der Waals forces have been considered (also this only qualitatively) as the reason for different packing in diastereomeric (*l-l vs. l-d*, or *l-L vs. l-D*, etc.) crystal structures. Now in a systematic and quantitative way chiral discrimination by all other possible interactions have been evaluated and probable ranges in energy terms predicted for various kinds of dipole-dipole, dipole-multipole, magnetic moment, dispersion and resonance interactions. The possibility of this last one for pairs differing only in their chirality (*l*, *d*) has been first recognized by the authors and is essentially a postulated difference in the resonance interaction of ground state and excited state between species of like (*d-d* or *l-l*) and unlike (*d-l*) chirality. Most of the effects, apart from packing forces, are too small to be observed with present day techniques, though multipole interactions in oriented helical polymers may be considerable.

The review by Rolf GLEITER and Ruedi GYGAX "*No-Bond-Resonance Compounds, Structure, Bonding and Properties*" (40 pp.) is a critical discussion of the problem, whether trithiapentalene and its congeners should be considered as equilibrium or resonance species:

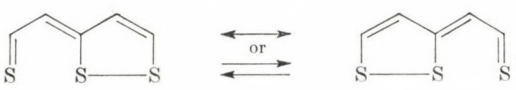

As it should be these days, almost exclusively physical techniques and theoretical calculations are invoked. If there is an equilibrium, the energy barrier of this must be under NMR detection level. The authors show that other spectroscopic techniques and various quantum chemical approaches also fail to provide an unambiguous answer except for photoelectron spectroscopy, which gives results in favour of the resonance alternative. The predicted resonance energy is, however, rather low.

Electron rich linear three-center bonds may be encountered in several other systems; the oldest and most trivial one might be the triiodate anion.

The longest chapter in this volume (107 pp.) devoted to "*The Molecular Zeeman Effect*" was contributed by D. H. SUTTER and W. H. FLYGARE. The reviewer is only qualified to give but a descriptive report of this part. The review was prompted by a substantial development in microwave spectroscopy in the late sixties which enabled the study of the molecular Zeeman effect of small diamagnetic molecules. It is a powerful technique to provide information concerning the electronic structure, in particular about molecular electric quadrupol moments and magnetic susceptibility anisotropies. The review is comprehensive; it covers both the theoretical aspects, as the quantum mechanical treatment of the effect and practical ones, such as instrumentation, measuring techniques, methods of evaluation, etc. All this is illustrated by several examples and also tables of experimental Zeeman effect values are presented.

The volume can be recommended to those interested in quantum chemistry, chemical physics and molecular spectroscopy.

M. NÓGRÁDI

Topics in Sulfur Chemistry. Vol. 1.

(Ed. A. SENNING)
Georg Thieme Publishers, Stuttgart, 1976. 223 pp.

The characteristic marks of tbe development of chemistry, can be recognized also in sulfur chemistry, this special field of chemical sciences. The number of newly prepared compounds increases rapidly, the compounds find more and more practical applications and, at the same time, important results are published in the field of theoretical research aimed at the elucidation of the structure and reactivity of sulfur compounds. This rapid development requires the publication of comprehensive works, facilitating survey and affording rapid information about the actual trends and fields of sulfur chemistry. As examples, "The Chemistry of Organic Sulfur Compounds," edited by N. KHARASH, of wich two volumes have appeared, or the series "Organic Compounds of Sulphur, Selenium and Tellurium" may be mentioned. The first contains reviews on single special topics of organic sulfur chemistry, and the latter, a continuously published work of several volumes, gives account on papers published during a given period. In view of the fact that survey works are needed, the publication of the new series "Topics in Sulfur Chemistry" is certainly welcome. The aim of the Editor and Publisher is to give reviews on the inorganic, organic, physical, analytical and biochemical sectors of sulfur chemistry, the intention being the publication of one volume a year.

The first volume, published in 1976, consists of three chapters of high level: J. P. MARINO gives an interesting survey on sulphur-containing cations; I. PHOTAKI on the role of sulfur compounds in the chemistry of amino acid protecting groups; and, finally, M. HAAKE on organic sulfodiimides, systematically covering the literature almost up to the present day.

Sulfur-containing cations play an important part in organic chemistry. Several such structures have been described as stable compounds or selective intermediates. In his paper "Sulfur-Containing Cations", J. P. MARINO discusses the relevant compounds grouped according to the coordination number of sulfur.

Of the mono-coordinated compounds, the chemistry of sulfenium ions and thiazyl cations is discussed. Among 2-coordinated sulfur cations, results obtained in the investigation of isothiuronium salts, thiocarbonium ions, sulfur–nitrogen cations and sulfur-containing radical cations are reported. In accordance with their importance, the author discusses sulfonium salts at a considerable length, dealing with their derivatives containing halogen, nitrogen, sulfur and oxygen substituents, and with the thiopyrylium cation. The up-to-date survey also treats problems in conjunction with the structures and the reactions of the compounds discussed, and research work on the problems of reaction mechanism is mentioned.

In the second chapter ("The Role of Sulphur in Amino Acid Protective Group Chemistry"), I. PHOTAKI discusses a theme from the field of peptide chemistry: the chemistry of sulfur-containing amino acids and the properties of sulfur-containing amino and carboxyl protective groups. The author describes the most important properties of sulfur-containing amino acids, processes used for the protection of the mercapto, amino and carboxyl groups of cysteine, and the incorporation of sulfur-containing amino acids into peptide chains. Of the N-protecting groups sulfenyl, sulfonyl and thiouretane types are discussed. The chapter, which will be a useful aid to peptide chemists, contains several prescriptions for the preparation of protected amino acids and peptides and for the removal of the protecting groups.

The third chapter ("The Chemistry of S,S-Diorgano-Sulfodiimides"), written by M. HAAKE, deals with research in conjunction with sulfodiimides, which have been known for about ten years. The author discusses the preparation, structure and physical properties of these particular sulfon analogues. Of the reactions characteristic of sulfodiimides, the substitution of imide hydrogen by metal or halogen, the formation of the N—Si, N—P and N—S bonds, conversions induced by alkylating and acylating agents are treated in detail, and finally, addition to the double bond is discussed. Sulfodiimides are important compounds from both the theoretical and practical points of view thus this modern survey on their research will be of interest in a rather wide sphere. In summary it can be concluded that the first volume of this new series publishing reviews in the field of sulfur chemistry, contains valuable papers written by specialists, which will be of aid not only to sulfur-organic chemists, but will command the interest of a wider circle. As a continuation of this useful initiative, we await the further volumes of the series, which, in view of the increasing importance of research in sulfur-chemistry, if possible, should also be larger, containing more reviews.

Á. KUCSMAN

Alkaloids

(Ed. K. Wiesner), Butterworths, London—Boston, 1976.
(International Review of Science, Organic Chemistry, Ser. 2., Ed. D. H. Hey.)

Under the general title "International Review of Science", Butterworts have tackled a great piece of work: the presentation to experts, in review form, of the most recent results in natural sciences, subdivided according to the several disciplines. First in sequence chemistry has been dealt with and within this domain organic chemistry has been published in ten volumes, up to 1973. This was the first series of this work. In order to bring it up-to-date and to maintain its usefulness, the publishers decided to re-publish, every second year, under unchanged titles but with ever progressive contents, the several volumes as parts of a second, third, etc., series.

This book on "Alkaloids" is the 9th volume of the 2nd series; it was completed in 1975, and contains 318 pages. In eight chapters the latest progress in the domain of eight families of alkaloids, arbitrarily selected, is excellently reviewed. The several authors of the chapters are well known and acknowledged experts, their names are to be found in the monograph "The Alkaloids" by R. F. MANSKE, occasionally at the head of the same chapter here as there, (*e.g.* S. W. PELLETIER, on diterpenoid alkaloids, in Vol. 12. p. 1, 1970). Yet, apart from the high level of expert knowledge shown as a common feature, the two works do overlap, firstly because the present book does not aim at nor does it claim completeness, and secondly, because it is written for the information of a wider circle of scientists interested in natural organic substances. This purpose is attained by the lucidity, the clear-cut arrangement of the text and, above all, by short, skilful introductions dealing with the previous literature, which severally precede the chapters.

The first chapter, by Z. VALENTA and H. J. LIU, is about Ormosia alkaloids, first reviewed in R. F. MANSKE's "The Alkaloids", Vol. 9, pp. 213. The present authors survey the progress of the nine years since. The diversity of the five- and six-membered rings with three nitrogen atoms is due to the high number of asymmetry centres in the ring. Several successful syntheses have been already reported.

A review on the Cephalotaxus alkaloids is given by J. A. FINDLAY. Since several anti-leukaemia compounds are to be found in this family, research has been intensified in this domain, too; there are several syntheses known of these four-membered groups of compounds which contain also a benzazepine moiety in their skeleton.

The two chapters on mono- and sesquiterpenoids (V. SNIECKUS) and on diterpenoid alkaloids (S. W. PELLETIER and S. W. PAGE), occupy prominent place both in importance and

in size. From the pharmacological point of view, this domain is very diverse and promising, thus several attempted and successful syntheses have been published.

Among the summaries special attention may be accorded also to that by M. HESSE and H. SCHMID, on the spermidine and spermine alkaloids containing macro-heterocycles. In this comparatively novel and not quite well known family of plant bases, there are macrocyclic lactam rings constructed of polyamine, mostly of spermidine or spermine and of a suitably substituted carbooxylic acid. The physiological importance of the polyamine component generally found in both animal and vegetable organisms has only recently become a matter of study; it is known that this component reacts with nucleic acids and, probably just thereby, it stimulates the growth of micro-organisms, plant and animal cell cultures. For some representatives of this family syntheses proving the structures have been reported.

In summing up: this book, in well chosen, concise and clear presentation acquaints the reader with some novel results in the field of alkaloid chemistry, in connexion with eight families of these compounds. In a library intended to serve research in the chemistry of natural organic substances, and in the field of pharmacology, this book certainly ought to be available.

L. TŐKE

M. SITTIG: *Detergent Manufacture*

Noyes Data Corporation, Park Ridge, New Jersey-London, England, 1976. 388 pages

This book, Volume 62 in the Chemical Technology Review series, will be useful and instructive to specialists producing and utilizing tensides, for it provides a satisfactorily comprehensive review of an extremely wide range of subjects, from the production of the starting materials to the transportation of the commercially distributed products.

The first chapters of the book provide a picture of the preparation of the starting materials for detergent syntheses. They describe first the production of straight-chain paraffins in the pure state, and then that of straight-chain olefins. This is followed by an account of the preparation and purification of trimeric and tetrameric compounds of propylene, the straight-chain alcohols, alkyl halides, alkylaromatic compounds and alkylphenols. After the synthesis of the tenside base materials, it deals with oxyethylation, sulphation and sulfonation, and with the processing and characterization of the products thus obtained. Separate accounts are given of active constituents of different types (containing nitrogen, phosphorus, etc.), shaping, investigation methods, "builders" of phosphate form and those not containing phosphorus, other constituents (enzymes, antimicrobial substances, etc.), shipment forms of the products, and their final utilization. Lastly, it describes the development tendencies to be expected in this branch of industry.

The above features are treated primarily from an industrial aspect, on the basis of U.S. patents. This is perhaps the greatest value of the book, for it discusses the patents in such depth and detail that the reader obtains a very good appraisal of the individual procedures. Information of similar thoroughness could be acquired from a literature search only at the expense of much time and trouble.

It is particularly worthwhile to draw attention to the large number of flowcharts to be found in the book. These provide a good supplement to the text, are illustrative, and greatly facilitate a rapid survey. The Figures of the apparatus and equipments are of a similarly high standard and easy to follow.

Other valuable features of the book are the "Company Index", the "Inventor Index" and the "US Patent Number Index". There is no "Subject Index", but, because of the nature of the book, this is fully made up for by the detailed list of contents.

The sequence of the individual chapters is logical, and the author's style is concise and readily understandable. This is a useful and valuable book of high standard.

J. MORGÓS

Andrew M. WELLS: *Printing Inks*

Recent Developments

(Chemical Technology Review No. 61)
Noyes Data Corporation, Park Ridge, New Jersey—London, England, 1976
328 pp., 8 figures, 280 tables

The book presents an advanced, technically oriented review of printing ink technology based on U.S. patents issued since 1965 and relating to the manufacture and application of printing inks.

It consists of the following chapters:

Introduction
Flexographic Inks
Lithographic Varnishes, Heat Set and Moisture Set Inks
Gravure Inks
Newspaper Inks
Specialty Inks and Applications
Additives for Printing Inks
Pigments and Dyestuffs
Radiation Curable Systems
Company Index
Inventor Index
U.S. Patent Number Index

The book gives detailed technical information and can be used as a guide to the U.S. patent literature in the field of printing inks.

Printing ink is a mixture of coloring matter dissolved or dispersed in a carrier to form a fluid or paste. The colorants are pigments and dyes, while the vehicles or carriers are light petroleum solvents up to heavy mineral oils.

Recently in the printing industry newer techniques and specialty applications are gaining a foothold. With the many types of printing methods currently in use, a variety of printing inks are required. The inks can be divided into those based on mineral oils and those using other vehicles. The latter group is based on a varnish technology similar to that used in the protective coatings field.

Mineral oil inks are used almost exclusively in newsprint. In the last years, there has been a proliferation of inks for rather specific end uses, such as porous tip pens, ball point pens, electrical microcircuitry, magnetic applications as in bank check processing and conductive coatings. Reactive pigment mixtures and fluorescent dyes have also been developed.

With the increasingly severe regulations for air pollution control, considerable research and development activity has been devoted to high solids systems and ultraviolet curable printing inks. Ultraviolet cured inks require only one-third the energy and one-fifth the capital cost when compared with conventional heat cured systems.

The book reviews over 250 descriptions, recipes and processes related to binder resin development, ink formulation and additives. Indexes by company, inventor and patent number help in providing easy access to the information contained in the book. The book can be recommended to professional workers in the printing industry as well as to chemical engineers and research chemists.

I. GÉCZY

H. G. HENNING, W. JUGELT und G. SAUER:

Praktische Chemie für Mediziner und Naturwissenschaftler

VEB Verlag Volk und Gesundheit. Berlin, DDR, 1976.
434 Seiten, 76 Abbildungen, 32 Tabellen

Das Buch, das seit seiner ersten Publikation im Jahre 1966 in der dritten Auflage erschien, ist für die chemische Grundausbildung von Studierenden der Medizin und anderen Universitäts- und Hochschulstudenten gedacht, deren Hauptfach nicht die Chemie ist. Dementsprechend gibt das Buch eine kurze Einleitung zur Aneignung der elementaren Laborato-

riumstechnik und anschließend eine bündige Zusammenfassung der Grundlagen der allgemeinen und anorganischen, der physikalischen, der organischen und der analytischen Chemie.

Wenn man bedenkt, daß diese Themenkreise ein riesiges Wissensmaterial umfassen und daß der Gesamtumfang des Buches nur 434 Seiten beträgt, so erkennt man, welch schwierige Aufgabe die Autoren übernommen haben. Bei der Auswahl und Zusammenstellung des im Buch vorzulegenden Materials konnte natürlich nicht nur hinsichtlich der Stoffkenntnisse, sondern auch in bezug auf grundlegende Gesetzmäßigkeiten keine Vollständigkeit angestrebt werden. Das Ziel der Autoren war, die moderne chemische Anschauungsweise und chemisches Denken zu vermitteln.

Dabei gelang es ihnen, den ziemlich allgemeinen Fehler von Werken dieser Art zu vermeiden, welcher darin besteht, daß man mittels sehr kurzer Zusammenfassung zu vieler Beispiele ein charakteristisches Bild von dem gesamten Wissenschaftszweig zu geben versucht. Dagegen behandeln die Autoren lieber wenigere Beispiele, die aber die allgemeine Gültigkeit chemischer Grundgesetze wiederspiegeln und mit einander in Verbindung gebracht werden können.

Verständnis und Aneignung des Materials werden durch die rezeptartig angegebenen einfachen Versuche und Berechnungsbeispiele sehr erleichtert. Kontrollfragen am Ende eines jeden Unterabschnittes dienen zur selbständigen Kontrolle des Verständnisses der wichtigeren Zusammenhänge.

Wie aus der bisherigen Rezension hervorgeht, ist das Buch ausgezeichnet geeignet, Universitätsstudenten, für die im Laufe ihrer weiteren Studien Chemie eine Hilfswissenschaft ist mit den Grundlagen dieser Wissenschaft vertraut zu machen. Das Gelernte ermöglicht es ihnen, später sich jene Teile der Chemie anzueignen, die sich eng an ihr Fachgebiet anschließen.

Wegen des beschränkten Umfanges des Werkes sowie wegen der verschiedenen Vorbildung und den verschiedenen Ansprüchen des angesprochenen Leserkreises (Studenten) verwendeten die Autoren in der Behandlung der einzelnen Zusammenhänge vernünftige Vereinfachungen, welche die Verwirklichung der obigen Zielsetzungen nicht gefährden. Das bringt jedoch mit sich, daß das Buch ungeeignet ist um Universitätsstudenten, die sich mit Chemie als Hauptdisziplin befassen (Chemiker, Pharmazisten) als Hilfsmittel zu dienen.

Das Buch ist vor allem für Medizinstudenten, Biologen und eventuell für Studenten, die sich dem chemischen Lehramt widmen, gedacht, doch kann es auch für Fachleute anderer Diszplinen von Interesse sein, die eine Kenntnis der grundlegenden Zusammenhänge der Chemie anstreben.

K. BURGER

B. CSÁKVÁRI: *Molecular geometry of inorganic compounds on the basis of the valence shell electron pair repulsion theory* (in Hungarian). Volume 30 of the series "Advances in chemistry"

Akadémiai Kiadó, Budapest, 1976 (196 pages, 140 Figures, 46 Tables)

In Volume 30 of this series, which enjoys great popularity among Hungarian chemists, the author and editor gives an account of the Valence Shell Electron Pair Repulsion Theory (VSEPR) and the related research field. This theory, or rather approach, to the propagation and development of which the author and his colleagues have made great contributions, began to become widespread in university chemical teaching from the end of the 1960's.

The molecular geometry of inorganic compounds can nowadays be regarded as clarified in principle on the basis of experiments, even if there are still some white spots in this field. The question is primarily one of *why* the combining electron shells of the given atoms lead to just that structure (internuclear distances, bond angles, symmetry) which can be calculated from the measured data. Today it seems that the combinational possibilities for the electron shells of the atoms are so varied, especially if the condensed phases too are taken into consideration, that a simple answer cannot be given to this *why*. CSÁKVÁRI's book has the great advantage that, insofar as possible, it gives the least complicated answer by the application of the VSEPR theory.

For this reason, his book will be very profitably used not only by students, but also by research workers dealing with inorganic chemistry and the structure of matter. This is facilitated by the large number of tabulated data, the many, well-prepared Figures, and the 52 references collected at the end of the book.

The book contains 5 chapters: 1. Introduction; 2. Fundamentals of the valence shell electron pair repulsion theory; 3. General questions of the stereochemistry of hydrogen and the elements of the second period; 4. Structures of compounds of hydrogen and the elements of the second period; 5. Stereochemistry of the elements of the third and higher periods. After clarifying the theoretical foundations, the book deals with the stereochemistry of the individual central atoms on the basis of the periodic system. In spite of the fact that for editorial reasons this series has no index, the sequence employed in the present volume makes it very easy to handle.

E. BODOR

INDEX

PHYSICAL AND INORGANIC CHEMISTRY

ORGANIC CHEMISTRY

Printed in Hungary

A kiadásért felel az Akadémiai Kiadó igazgatója — Műszaki szerkesztő: Zacsik Annamária

A kézirat nyomdába érkezett: 1977. II. 10. — Terjedelem: 9,8 (A/5) ív, 55 ábra

77.4146 Akadémiai Nyomda, Budapest — Felelős vezető: Bernát György

ACTA CHIMICA

ТОМ 93—ВЫП. 2

РЕЗЮМЕ

Применение методов ППП и ППДП/2 для структурных исследований кремнеогранических соединений, I

Й. РЕФФИ, Т. ВЕСПРЕМИ, П. ХЕНЧЕИ, Й. НАДЬ

Были проведены расчеты молекулярной структуры фенилгалогенсиланов, феноксисиланов, винил-, аллил-, фенил- и бензил-производных элементов группы IV/1 с помощью методов, ППП, итеративного ППП и ППДП/2. Среди прочего, были рассчитаны распределение заряда в некоторых молекулах, дипольные моменты, электронные переходы и энергии ионизации. Из сравнения расчетных и экспериментальных данных были сделаны заключения относительно структуры связей.

Исследование гидратации макромолекул, III

Коэффициент самодиффузии воды в водных растворах поли(акриловой кислоты)

ДЬ. ИНЗЕЛЬТ и П. ГРОФ

Коэффициент самодиффузии воды в водных растворах поли(акриловой кислоты) (ПАК) с концентрацией 3 ÷ 10 вес.% был измерен при 25 и 35°С, используя метод капилляра с открытым концом. Вода была мечена O^{18} и содержание изотопа определялось с помощью масс-спектрометрии. Измерения также включают определение специфических объемов, вязкостей растворов, а также их степени диссоциации.

Коэффициент самодиффузии воды линейно уменьшается с весовой долей ПАК в изученном интервале концентраций. Энергия активации самодиффузии воды равна 4,9 ± 1,2 ккал/моль. Число гидратации равно 4,9—5,4 и 5,6—6,0 молекул воды на группы COOH при 25 и 35°С, соответственно, в зависимости от фактора формы, использованного в расчете.

Исследование мембран с пергаментным носителем, XI

Определение термодинамически эффективной, фиксированной плотности заряда и селективной проницаемости

Ф. А. СИДИКИ, М. Н. АСЕЕМ БЕГ, С. П. СИНГ и А. НАК

Потенциалы, возникающие между двумя мембранами гексацианоферрата(II) серебра и кадмия на пергаментном носителе были использованы для определения термодинамически эффективной, фиксированной плотности заряда по Кобатаке. Теория Кобатаке основана на термодинамике необратимых процессов. Аравнение Кобатаке было использовано при двух граничных условиях, а именно в области концентрированных и в области разбавленных растворов. Две граничные формы уравнения Кобатаке дают идентичные величины Θ для обоих мембран. Теоретические предсказания потенциалов мембран, полученные из уравнения Кобатаке, вполне удовлетворительно совпадают с экспериментальными результатами, полученными из исследования мембран гексацианоферратов (II) серебра и кадмия.

Магнитные свойства комплексов меди(II) с ONO донорнотридентатными основаниями Шиффа, полученными из 2-гидрокси-1-нафтальдегида и аминоспиртов

А. СИАМАЛ и К. С. КАЛЕ

Описывается синтез некоторых новых комплексов меди(II) с шиффовыми основаниями, полученными из 2-гидрокси-1-нафтальдегида с этаноламином, пропаноламином, изопропаноламином, 2-амино-2-метилпропанолом. Основания Шиффа координируются через O,O и N как диосновные тридентатные лиганды. Комплексы были охарактеризованы данными элементарного анализа, измерений магнитной восприимчивости (83—297°K), а также их инфракрасными и электронными спектрами. Комплекс, содержащий пропаноламин, имеет магнитный момент 0,46 B. M. ($-\tau=846$ см$^{-1}$), указывая на наличие сильного антиферромагнитно взаимодействия. В этом комплексе спины взаимодействующих ионов меди(II) полностью спарены, имея единственную популяцию синглетного состояния. Комплексы, содержащие этаноламин и изопропаноламин, обладают ферромагнитным спин-спиновым взаимодействием ($\tau = +28$ до $+67$ см$^{-1}$). У комплекса меди(II) с лигандом 2-гидроксинафтальдегид-2-амино-2-метилпропанол было обнаружено антиферромагнитное взаимодействие ($-\tau = 91$ см$^{-1}$). Приводится сравнение магнитных свойств комплексов с соответствующими комплексами оксованадия(IV).

Электрохимические и ЭПР исследования анион-радикала октацианхинодиметана

Л. БУЧИШ и Х. КИСЕЛЕ

Дианионы 1,4-бис(дицианметил)-2,3,5,6-тетрацианбензола *3* и тетрациангидрохинона *6* были окислены электрохимическими и химическими путями. Продуктами были анион-радикал октацианхинодиметана *4* и октацианхинодиметан *5*, а также тетрацианбензосемихинон *7* и тетрацианбензохинон *8*, соответственно. Были измерены потенциалы полуволны ступеней дианион/анион-радикал и анион-радикал/хинон. Результаты согласуются с уравнением Гамметта, полученным как в серии 7,7', 8,8'-тетрацианхинодиметанов, так и в серии хинонов. Химическое окисление приводит к образованию продуктов *4* и *7*, соответственно. Были сняты их ЭПР спектры и полученные константы расщепления на азоте сравнивались с рассчитанными по ЛКАО—МО. Величины, предсказываемые расчетами хорошо согласуются с экспериментальными данными.

Исследование металлических хелатов с лигандами типа купроина и ферроина XXV

О структуре хелата хлоро(купроин)мед(II)

Д. РЕХОРЕК и Ф. ТОМАС

Способом ЭПР, УФ и видимой спектроскопии, а также измерением электропроводимости были изучены хелаты меди(II) типа Cu(купроин)Cl_2 и Cu(купроин)$_2Cl_2$ (где купроин = cmp, cmch, dpch и bich^2). Результаты измерений хорошо согласуются с искаженной тетраэдрической структурой для Cu(bich)Cl_2 и с искаженной тригональной-бипирамидальной и квадратно-пирамидальной структурами остальных хелатов.

Некоторые химические свойства 3-тионо-1,2-дитиолов, VI

М. А.-Ф. ЭЛЬКАШЕФ, Ф. М. Е. АБДЕЛЬ-МЕГЕЙД и А. А. ЭЛЬБАРБАРИ

Соединение *I*, взаимодействуя с аминами, дает N-замещенные производные 3-тионоизотиазола *(IVa, b)*, в то время как *II* и *III* дают 1,3-аминодизамещенные производные 3-тионо-1-пропена *(VIa-c* и *VIIa-d)*. Соединения *I*, *II* и *III* с дифенилдиазометаном

дают производные бензгидрилидена (*IX*,*X* и *XI*, соответственно. Соединения *II* и *III*с диазофлуореном дают соответствующие производные 3-флуоренилиден-1,2-дитиола *XII* и *XIII*, в то время как *I* дает производные спиро [флуорентиофена] *XIV*. Соединение I в присутствии медной бронзы дает дибензтиофенотиофен *XVII*, в то время как *III* дает 2,5-ди-(п-метоксифенил)тиофен (*XX*).

Превращения тозиловых и мезиловых производных морфиновой группы, XVIII

«Азидоморфиновые» производные, I

Ш. МАКЛЕЙТ, И. КНОЛЛ, Р. БОГНАР, Ш. БЕРЕНИ и Г. КИШ

Принимая во внимание очень ценные фармакологические свойства т. наз. «азидоморфина», казалось целесообразным исследование дальнейших новых производных как с теоретической, так и с практической точек зрения.

В настоящем сообщении описывается синтез т. наз. «14-гидроксиазидоморфина» (3,14 β-дигидрокси-4,5 α-эпокси-6β-азидо-17-метилморминана).

Превращения тозиловых и мезиловых производных морфиновой группы, XVIII

«Азидоморфиновые» производные, II

Ш. МАКЛЕЙТ, Й. КНОЛЛ, Р. БОГНАР, Ш. БЕРЕНИ, Г. ШОМОДИ и Г. КИШ

В ходе исследований были синтезированы т. наз. «азидоморфиновые» производные и соответствующие 3-деокси-, 3—0-этил- и 3—0-морфолинилэтил-аналоги.

Соответственно данным исследований с животными, оказалось, что 3—0-этил-«азидоморфин» («азидодионин») является эффективным средством против кашля.

Исследование тозиловых и мезиловых производных в морфиновом ряду, XIX

Азидопроизводные, III

Г. МАКЛЕЙТ, Й. КНОЛЛ, Р. БОГНАР, Ш. БЕРЕНИ, Г. ШОМОДИ и Г. КИШ

С целью получения соединений с антагонистическим влиянием к морфину и моделирования исследований рецептора морфина были получены многие новые N-замещенные нор-«азидоморфиновые» производные. Это следующие соединения: N-аллил-нор-«азидоморфин» (*5*), N-аллил-нор-«азидокодеин» (*6*), 14-гидрокси-N-аллил-нор-«азидоморфин» (*19*), 14-гидрокси-N-аллил-нор-«азидокодеин» (*24*), N-циклопропилметил-нор-«азидоморфин» (*25*) и 14-гидрокси-N-циклопропилметил-нор-«азидоморфин» (*26*).

Исследование реакций отщепления ацила от производных N-карбамоилсукцинимида

К. ХАРШАНИ, К. ТАКАЧ и А. ШИМАИ

Были исследованы реакции отщепления ацила от N-карбамоилсукцинимида (III) и его производных (IV) под влиянием нуклеофильных реагентов или тепла. Было установлено, что в то время как III под влиянием нуклеофильных реагентов претерпевает эндо- или экзоциклическое отщепление ацила, для IV наблюдалось лишь экзоциклическое расщепление С—N связи. Под влиянием тепла как для III, так и для IV наблюдалось экзоциклическое отщепление ацила, которое ускорялось под влиянием радикальных инициаторов или органических оснований.

Алкалоиды со скелетом индоло [2, 3-с]хиназолино[3,2-а]-пиридина, V

3,4-Секорутекарпан

К. ДОРА-ХОРВАТ, Г. ТОТ, Й. ТАМАШ и О. КЛАУДЕР

Восстановление рутекарпина (12) алюмогидридом лития приводит к образованию, наряду с рутекарпеном (13) и 3α-рутекарпаном (14), нового продукта — за счет дальнейшего раскрытия цикла — который, как было доказано, представляет собой 3,4-секорутекарпан (15). Строение отдельных соединений подтверждали на основе их ИК ЯМР и МС спектров.

INTRODUCTION TO RADIOANALYTICAL PHYSICS

(Nuclear Methods monograph series of the *Journal of Radioanalytical Chemistry* and *Radiochemical and Radioanalytical Letters*. Number 1. Editors of the series: T. Braun and E. Bujdosó.)

By G. Deconninck

Backscattering of charged particles, X-ray emission following charged particle bombardment, prompt X-rays and particles from nuclear reactions, radioactivity from charged particles and photon activation have given rise to new analytical techniques. This book provides a comprehensive study of the principles on which these analytical methods are founded. In spite of the complexity of nuclear physics, simple formulae are given for each typical application, with the analytical problem in view. A great number of figures, solved problems, as well as applications which illustrate each topic help in the use of the formulae.

In English · Approx. 200 pages · Cloth

A co-edition – distributed in the socialist countries by KULTURA, Budapest, ISBN 963 05 1249 1; in all other countries by ELSEVIER SCIENTIFIC PUBLISHING COMPANY, Amsterdam

---

Akadémia Kiadó

Budapest

Elsevier Scientific Publishing Company

Amsterdam

Les Acta Chimica paraissent en français, allemand, anglais et russe et publient des mémoires du domaine des sciences chimiques.

Les Acta Chimica sont publiés sous forme de fascicules. Quatre fascicules seront réunis en un volume (4 volumes par an).

On est prié d'envoyer les manuscrits destinés à la rédaction à l'adresse suivante:

Acta Chimica
H-1521 Budapest, Hongrie

Toute correspondance doit être envoyée à cette même adresse.

La rédaction ne rend pas de manuscript.

Le prix de l'abonnement est de $ 32,00 par volume.

Abonnement — en Hongrie à l'Akadémiai Kiadó (1363 Budapest, P.O.B. 24, C.C.B. 215 11488), à l'étranger à l'Entreprise pour le Commerce Extérieur «Kultúra» (H-1389 Budapest 62, P.O.B. 149 Compte-courant No. 218 10990) ou l'étranger chez tous les représentants ou dépositaires.

Die Acta Chimica veröffentlichen Abhandlungen aus dem Bereich der chemischen Wissenschaften in deutscher, englischer, französischer und russischer Sprache.

Die Acta Chimica erscheinen in Heften wechselnden Umfanges. Vier Hefte bilden einen Band. Jährlich erscheinen 4 Bände.

Die zur Veröffentlichung bestimmten Manuskripte sind an folgende Adresse zu senden:

Acta Chimica
H-1521 Budapest, Ungarn

An die gleiche Anschrift ist auch jede für die Redaktion bestimmte Korrespondenz zu richten.

Manuskripte werden nicht zurückerstattet.

Abonnementspreis pro Band: $ 32,00.

Bestellbar für das Inland bei Akadémiai Kiadó (1363 Budapest, Postfach 24, Bankkonto Nr. 215 11488), für das Ausland bei dem Außenhandelsunternehmen »Kultúra« (H-1389 Budapest 62, P.O.B. 149. Bankkonto Nr. 218 10990) oder bei seinen Auslandsvertretungen und Kommissionären.

«Acta Chimica» издают статьи по химии на русском, английском, французском и немецком языках.

«Acta Chimica» выходит отдельными выпусками разного объема, 4 выпуска составляют один том и за год выходят 4 тома.

Предназначенные для публикации рукописи следует направлять по адресу:

Acta Chimica
H-1521 Budapest, ВНР

Всякую корреспонденцию в редакцию направляйте по этому же адресу.

Редакция рукописей не возвращает.

Подписная цена — $ 32,00 за том.

Отечественные подписчики направляйте свои заявки по адресу Издательства Академии Наук (1363 Budapest, P.O.B. 24, Текущий счет 215 11488), а иностранные подписчики через организацию по внешней торговле «Kultúra» (H-1389 Budapest 62, P.O.B. 149. Текущий счет 218 10990) или через ее заграничные представительства и уполномоченных.

Reviews of the Hungarian Academy of Sciences are obtainable at the following addresses:

AUSTRALIA
C.B.D. LIBRARY AND SUBSCRIPTION SERVICE, Box 4886, G.P.O., *Sydney N.S.W. 2001*
COSMOS BOOKSHOP, 145 Ackland Street, *St. Kilda (Melbourne), Victoria 3182*

AUSTRIA
GLOBUS, Höchstädtplatz 3, *1200 Wien XX*

BELGIUM
OFFICE INTERNATIONAL DE LIBRAIRIE, 30 Avenue Marnix, *1050 Bruxelles*
LIBRAIRIE DU MONDE ENTIER, 162 Rue du Midi, *1000 Bruxelles*

BULGARIA
HEMUS, Bulvar Ruszki 6, *Sofia*

CANADA
PANNONIA BOOKS, P.O.Box 1017, Postal Station "B", *Toronto, Ontario M5T 2T8*

CHINA
CNPICOR, Periodical Department, P.O.Box 50, *Peking*

CZECHOSLOVAKIA
MAD'ARSKÁ KULTURA, Národní třida 22, *115 66 Praha*
PNS DOVOZ TISKU, Vinohradská 46, *Praha 2*
PNS DOVOZ TLAČE, *Bratislava 2*

DENMARK
EJNAR MUNKSGAARD, Norregade 6, *1165 Copenhagen*

FINLAND
AKATEEMINEN KIRJAKAUPPA, P.O.Box 128, *SF-00101 Helsinki 10*

FRANCE
EUROPÉRIODIQUES S. A., 31 Avenue de Versailles, *78170 La Celle St.-Cloud*
LIBRAIRIE LAVOISIER, 11 rue Lavoisier, *75008 Paris*
OFFICE INTERNATIONAL DE DOCUMENTATION ET LIBRAIRIE, 48 rue Gay-Lussac, *75240 Paris Cedex 05*

GERMAN DEMOCRATIC REPUBLIC
HAUS DER UNGARISCHEN KULTUR, Karl-Liebknecht-Strasse 9, *DDR-102 Berlin*
DEUTSCHE POST, ZEITUNGSVERTRIEBSAMT, Strasse der Pariser Kommüne 3—4, *DDR-104 Berlin*

GERMAN FEDERAL REPUBLIC
KUNST UND WISSEN, ERICH BIEBER, Postfach 46, *7000 Stuttgart 1*

GREAT BRITAIN
BLACKWELL'S PERIODICALS DIVISION, Hythe Bridge Street, *Oxford OX1 2ET*
BUMPUS, HALDANE AND MAXWELL LTD., Cowper Works, *Olney, Bucks MK46 4BN*
COLLET'S HOLDINGS LTD., Denington Estate, *Wellingborough, Northants NN8 2QT*
WM. DAWSON AND SONS LTD., Cannon House, *Folkestone, Kent CT19 5EE*
H. K. LEWIS AND CO., 136 Gower Street, *London WC1E 6BS*

GREECE
KOSTARAKIS BROTHERS, International Booksellers, 2 Hippokratous Street, *Athens-143*

HOLLAND
MEULENHOFF-BRUNA B.V., Beulingstraat 2, *Amsterdam*
MARTINUS NIJHOFF B.V., Lange Voorhout 9—11, *Den Haag*
SWETS SUBSCRIPTION SERVICE, 347b Heereweg, *Lisse*

INDIA
ALLIED PUBLISHING PRIVATE LTD., 13/14 Asaf Ali Road, *New Delhi 110001*
150 B-6 Mount Road, *Madras 600002*
INTERNATIONAL BOOK HOUSE PVT. LTD., Madame Cama Road, *Bombay 400039*
THE STATE TRADING CORPORATION OF INDIA LTS., Books Import Division, Chandralok, 36 Janpath, *New Delhi 110001*

ITALY
EUGENIO CARLUCCI, P.O.Box 252, *70100 Bari*
INTERSCIENTIA, Via Mazzé 28, *10149 Torino*
LIBRERIA COMMISSIONARIA SANSONI, Via Lamarmora 45, *50121 Firenze*
SANTO VANASIA, Via M. Macchi 58, *20124 Milano*
D. E. A., Via Lima 28, *00198 Roma*

JAPAN
KINOKUNIYA BOOK-STORE CO. LTD., 17-7 Shinjuku 3 chome, Shinjuku-ku, *Tokyo 160-91*
MARUZEN COMPANY LTD., Book Department, P.O.Box 5050 Tokyo International, *Tokyo 100-31*
NAUKA LTD. IMPORT DEPARTMENT, 2-30-19 Minami Ikebukuro, Toshima-ku, *Tokyo 171*

KOREA
CHULPANMUL, *Phenjan*

NORWAY
TANUM-CAMMERMEYER, Karl Johansgatan 41—43, *1000 Oslo*

POLAND
WĘGIERSKI INSTYTUT KULTURY, Marszałkowska 80, *Warszawa*
CKP I W ul. Towarowa 28 *00-958 Warsaw*

ROUMANIA
D. E. P., *Bucureşti*
ROMLIBRI, Str. Biserica Amzei 7, *Bucureşti*

SOVIET UNION
SOJUZPETCHATJ — IMPORT, *Moscow*
and the post offices in each town
MEZHDUNARODNAYA KNIGA, *Moscow G-200*

SPAIN
DIAZ DE SANTOS, Lagasca 95, *Madrid 6*

SWEDEN
ALMQVIST AND WIKSELL, Gamla Brogatan 26, *101 20 Stockholm*
GUMPERTS UNIVERSITETSBOKHANDEL AB, Box 346, *401 25 Göteborg 1*

SWITZERLAND
KARGER LIBRI AG, Petersgraben 31, *4011 Base*

USA
EBSCO SUBSCRIPTION SERVICES, P.O.Box 1943, *Birmingham, Alabama 35201*
F. W. FAXON COMPANY, INC., 15 Southwest Park, *Westwood, Mass, 02090*
THE MOORE-COTTRELL SUBSCRIPTION AGENCIES, *North Cohocton, N. Y. 14868*
READ-MORE PUBLICATIONS, INC., 140 Cedar Street, *New York, N. Y. 10006*
STECHERT-MACMILLAN, INC., 7250 Westfield Avenue, *Pennsauken N. J. 08110*

VIETNAM
XUNHASABA, 32, Hai Ba Trung, *Hanoi*

YUGOSLAVIA
JUGOSLAVENSKA KNJIGA, Terazije 27, *Beograd*
FORUM, Vojvode Mišiča 1, *21000 Novi Sad*

ACTA CHIMICA

ACADEMIAE SCIENTIARUM HUNGARICAE

TOMUS 93 FASCICULI 3—4

AKADÉMIAI KIADÓ, BUDAPEST

1977

ACTA CHIM. (BUDAPEST) ACASA2 93 (3—4) 215—426 (1977)

ACTA CHIMICA

A MAGYAR TUDOMÁNYOS AKADÉMIA KÉMIAI TUDOMÁNYOK OSZTÁLYÁNAK IDEGEN NYELVŰ KÖZLEMÉNYEI

Acta Chimica is a journal for the publication of papers on all aspects of chemistry in English, German, French and Russian.

Acta Chimica is published in 4 volumes per year. Each volume consists of 4 issues of varying size.

Manuscripts should be sent to

Acta Chimica
H-1521 Budapest, Hungary

Correspondence with the Editors should be sent to the same address. Manuscripts are not returned to the Authors.

Subscription rate $ 32.00 per volume.

Hungarian subscribers should order from Akadémiai Kiadó, 1363 Budapest, P.O.Box 24. Account No. 215 11488.

Orders from other countries are to be sent to "Kultúra" Foreign Trade Company (H-1389 Budapest 62, P.O. Box 149. Account No. 218 10990) or to its representatives abroad.

Acta Chimica Academiae Scientiarum Hungaricae, Tomus 93 (3—4), pp. 215—220 (1977)

CERTAIN CHARACTERISTICS OF HOLOGRAPHIC PLATES AND THEIR APPLICABILITY IN SPECTRAL ANALYSIS

Z. BURGUDJIEV,* K. ZIMMER** and E. BOBOLINA*

*(*Department of Atomic Physics, Faculty of Physics, Sofia University, Bulgaria*
***Institute of Inorganic and Analytical Chemistry, L. Eötvös University, Budapest)*

Received June 7, 1976

Authors have found that the values of the photometric (instrumental) fluctuation and total errors occurring in measuring the photographic blackening in case of holographic plates are equal to that of the ordinary plates, and the 1-transformation can be used to the blackening curve in this case just as well as in case of the ordinary spectral plates. The spectral properties of the two kinds of plates are practically identical. Better results may be expected with holographic spectral plates in the visible region on the spectral lines, but their sensitometric sensitivity is considerably less and therefore, in order to attain the optimal background value, the exposure time must be prolonged.

The applicability of a photomaterial in spectral analysis can be properly assessed if its basic characteristics, in particular the blackening curve shape and the signal-to-noise ratio, are known. As regards ordinary spectral plates with a resolving power of the order of 100 lines/mm, this question may be considered as sufficiently clarified. However, this does not apply to holographic plates, which greatly differ in resolving power. Their assessment, which is of practical interest, is the subject of this article.

Experimental

Holographic plates made at the Cinema and Radio Institute in Sofia [1] with a resolving power of approx. 2800 lines/mm were used in our investigation. By means of a mercury lamp, a three prism glass spectrograph C. Zeiss, Jena (slit width: 50 μm) and change of exposure time, certain photographic blackenings were obtained on them after developing. These were measured with a nonautomatic G-2 microphotometer, C. Zeiss, Jena, at a 10 mm fixing height of the slit and a 20-fold standard enlargement; the width of its slit was 0.20, 0.40, 0.60 and 0.80 for the determination of microphotometric error and 0.40 mm for the total and fluctuation errors and characteristic curve. Thirty measurements each were made of the respectively selected blackenings in order to determine the size of the standard deviations characterizing the errors of interest.

Results and discussion

a) *Microphotometric (instrumental) error in measuring photographic blackenings*

The experimental data on the size of the microphotometric error $\sigma_m(S)$ in measuring the blackenings S on the treated holographic plates for a 0.40 mm slit width of the microphotometer are shown in Fig. 1. The experimen-

tal points for blackenings less than approx. 1.7 lie well around the theoretical curve for this error, calculated by the formula $\sigma_m(S) = \sigma_{m_0} \cdot \sqrt{1 + 10^{2S}}$ [2, 3]. For the constant σ_{m_0} we have a value of $0.23 \cdot 10^{-3}$, which coincides with the value obtained in [3], for the same microphotometer and for ORWO (GDR) spectral plates.

The following specification was made in the region of very low blackenings. At a 0.40 mm slit width of the microphotometer for a slight spectral line with approx. 0.02 blackening a microphotometric error with a value of $0.36 \cdot 10^{-3}$ was measured by attuning zero on the blackening scale upon the plate's fog, as well as a microphotometric error with a value of $0.33 \cdot 10^{-3}$ by attuning zero on a clean substrate (glass). The microphotometric error found for a 0.01 blackening of the plate's fog was $0.34 \cdot 10^{-3}$. The practical coincidence of these three values, analogous as reported in [4], shows that in the region of the lowest blackenings no increase in the value of the microphotometric error should be expected above the one obtained by the above-mentioned formula which might be due to the fog on the photomaterial.

Figure 2 shows the dependence of the constant σ_{m_0} in our measurements on the slit width of the microphotometer. Just as with spectral plates, here too, the value of this constant does not depend on the slit width when the latter exceeds 0.40 mm, *i.e.* the size of the measured area on the photoplate is above 0.010 mm^2.

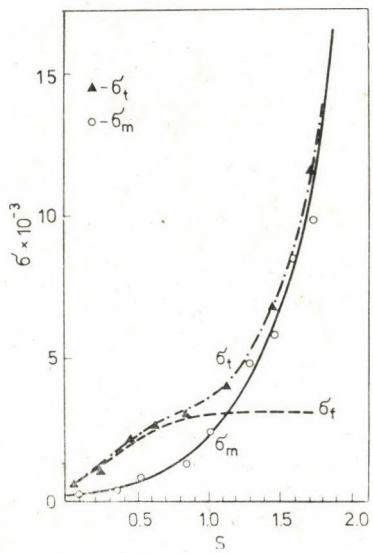

Fig. 1. Values of the photometric σ_m and fluctuation error σ_f and the calculated values of the total error σ_t in the function of the value of blackening S measured on holographic plates, in case of application of a densitometer (magnified 20 times with a slit of 10 mm height and 0.40 mm width)

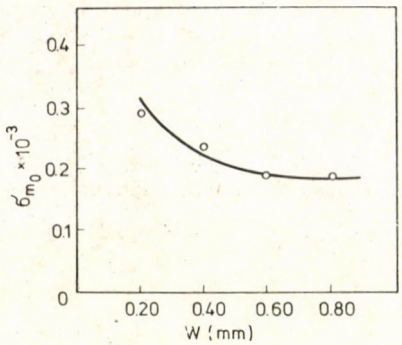

Fig. 2. Value of the constant σ_{m_0} in the function of the value of the slit width W of the densitometer (magnified 20 times with a slit of 10 mm height)

b) *Fluctuation and total errors in measuring photographic blackenings*

The fluctuation error $\sigma_f(S)$ in measuring photographic blackenings on holographic plates was determined by the method described in [5]. The size of the total error $\sigma_t(S)$ in measuring photographic blackenings was connected with the microphotometric and the fluctuation error by means of the formula $\sigma_t^2(S) = \sigma_f^2(S) + \sigma_m^2(S)$.

Fig. 1 shows the results of the determined size of the fluctuaton and total error at a 0.40 mm slit width of the microphotometer. It may be concluded that the value of the total error in holographic plates is determined chiefly by the value of the fluctuation error only in the blackening range of 0 to appr. 0.7, while above it the microphotometric error becomes determinant. The course of the fluctuation error curve in the indicated region of small blackenings can be approximated by the expression: $\sigma_f(S) = \sigma_{f_0} + a_f \cdot S$ where we have $\sigma_{f_0} = 0.35 \cdot 10^{-3}$ and $a_f = 3.75 \cdot 10^{-3}$. The value of the constant σ_{f_0} is practically equal to that of the fluctuation error of blackening on the plate's fog $S_w = 0.01$ for which we measured $\sigma_f = 0.37 \cdot 10^{-3}$.

These results are analogous to those obtained in [5] for ORWO spectral plates. There is, as might be expected, a certain difference in the value of the constant a_f.

c) *Application of l-transformation and Y_l-approximation to the blackening curve of holographic plates*

The equation of the *l*-transformation [6 – 9] of the underexposed part of the characteristic curve is given by

$$l = s + (k - s) \cdot \log (1 - 10^{-s}), \qquad (1)$$

where l is the transformed blackening $s = \frac{S}{\gamma}$ the reduced blackening, $k = \frac{S_L}{\gamma}$ the transformation constant, γ being the slope and S_L the blackening of the lowest point of the straight part.

The equation of the Y_l-approximation of the underexposed part of the characteristic curve, which is deduced by using Eq. (1) [10, 2] is given by:

$$\gamma Y = S + (S_L - S) \cdot \log \left(1 - 10^{-\frac{S}{\gamma}}\right) + (\gamma Y_L - S_L). \qquad (2)$$

Y being the log of the exposure, $Y = \log H$, and Y_L corresponding to blackening S_L.

The universality of the l-transformation with different types of spectral photomaterial was demonstrated in [6—11], so that it is worthwhile to check its applicability to holographic plates as well. Since the standard deviation $\sigma(l)$ of the l-transformation is equal to the standard deviation $\sigma(Y)$ of the Y-approximation [10], the result obtained will be valid also for the latter. At present there is no sense in looking for more exact equations for transforming or approximating the underexposed part of the characteristic curve as shown in [10].

The values experimentally determined for the parameters, forming parts of Eqs (1) and (2), as well as for the standard deviation $\sigma(l)$ of the l-transformation at different wave-lengths of the visible region and for the treated holographic plates are shown in Table I. These plates, as can be seen there,

Table I

λ(nm)	405	436	546	577 578	612
γ	2.25	2.60	4.16	4.16	1.50
S_L	0.52	0.44	0.68	0.78	0.40
k	0.23	0.18	0.16	0.19	0.26
H_L^*	1.0	3.7	2.2	1.5	6.2
R	400	463	585	543	321
S_R	0.20	0.20	0.20	0.20	0.20
Q	880	230	510	750	120
S_Q	0.09	0.10	0.10	0.10	0.05

* The values of H_L are in relative units

are distinguished by a relatively high contrast coefficient and small values of the transformation constant k. The values of $\sigma(l)$ are of the same order as in [9, 10]. It should be noted that $\sigma(l)$ is determined by finding the differ-

ences between the tabular value [12] for the transformed blackening l and its value of the prolongation of the straight part of the reduced blackening curve. These differences correspond to blackenings ranging in size between the values of 0.03 and S_L.

It may be concluded from the above that the l-transformation and the Y_l-approximation of the underexposed part of the characteristic curve are applicable to holographic plates treated in a manner analogous to that for ordinary spectral plates.

d) *Contrast and informational sensitivity of holographic plates*

The properties of the treated holographic plates reviewed so far show complete similarity to ordinary spectral plates. This makes it possible to determine the contrast R and the informational Q sensitivity in holographic plates by the method used in [5] for spectral plates, *i.e.* by means of the formulas:

$$R = \max. \left\{ 0.4343\gamma \Big/ \left[1 + \frac{S_L - S}{\gamma(10^{S/\gamma} - 1)} - \log(1 - 10^{-S/\gamma}) \right] \cdot \right.$$
$$\left. \cdot \left[0.35\, S_w \cdot 10^{-3} + 3.75\, S \cdot 10^{-3} \right] \right\} \tag{3}$$

$$Q = \max. \left\{ 0.4343\, \gamma \cdot 10^{\frac{S_L - S}{\gamma}} \Big/ H_L (1 - 10^{-S/\gamma})^{\frac{S_L - S}{\gamma}} \cdot \right.$$
$$\left. \cdot \left[1 + \frac{S_L - S}{\gamma(10^{S/\gamma} - 1)} - \log(1 - 10^{-S/\gamma}) \right] \cdot \left[0.35\, S_w \cdot 10^{-3} + 3.75\, S \cdot 10^{-3} \right] \right\} \tag{4}$$

The values obtained for the magnitudes R and Q, as well as the blackenings S_R and S_Q at which they are attained are given in Table I.

e) *Applicability of holographic plates in spectral analysis*

The sole criterion for the applicability of photomaterial in spectral analysis is, as shown in [13], their contrast sensitivity. Moreover, the higher the value of this indicator of a certain material, the greater the possibilities of improving the analysis by its use.

The values of the contrast sensitivity R of holographic plates, shown in Table I, are on the whole two or three times higher than those for ORWO spectral plates investigated in [5]. This is due primarily to the lower value of fog blackening in thin-layer holographic plates and partly to the low value of their transformation constant k.

It follows that, when making an analysis along spectral lines lying in the visible region, better results may be expected with holographic than with ordinary spectral plates. It should be borne in mind, though, that — owing the small sensitometric sensitivity of holographic plates (two or three orders lower than that of spectral plates) — the advantages obtained by the use of the latter will be at the expense of a considerable lengthening of the exposure time necessary to attain the optimal value S_R on the background of the spectra. This lengthening of exposure time can be obtained only in the analysis of samples which are not consumed during exposure time, say, of gases, or when their quality consecutively entering the electrode gap is practically unchangeable, as is the case with solid metal and alloy samples.

REFERENCES

[1] Patent No. 18055, Institute for Inventions, Sofia, Bulgaria
[2] BURGUDJIEV, Z.: Comm. Dep. Chem. Bulg. Acad. Sci. **3,** 279 (1970)
[3] BURGUDJIEV, Z., BELCHEV, St. NIKOVA, R., ALEXANDROV, A.: Bulg. J. Phys. II. 39 (1975)
[4] ZIMMER, K.: Lecture on the Symposium of the Working Committee for Spectrochemistry of the Hungarian Academy of Sciences, held in Debrecen, June 2, 1972
[5] BURGUDJIEV, Z., LYOCHKOVA, M., VOYKOVA, T.: Bulg. J. Phys. II. 492 (1975)
[6] TÖRÖK, T., ZIMMER, K., RÉTI, S.: Microchim. Acta **1962,** 611
[7] TÖRÖK, T., ZIMMER, K.: Acta Chim. Acad. Sci. Hung. **41,** 97 (1964)
[8] TÖRÖK, T., ZIMMER, K.: Ann. Univ. Sci. Budapest. **8,** 11 (1966)
[9] ZIMMER, K., TÖRÖK, T., ASZTALOS, I.: Chemia Analityczna **11,** 1065 (1966)
[10] BURGUDJIEV, Z.: Bulg. J. Phys. II. 122 (1975)
[11] ZIMMER, K., BASSA, Zs.: XIV. Coll. Spectr. Intern., Debrecen, 1967, 847
[12] ZÖRÖK, T., ZIMMER, K.: Quantitative Evaluation of Spectrograms by means of 1-Transformation, Heyden and Sons Budapest, 1972
[13] BURGUDJIEV, Z., LYOCHKOVA, M., STEFANOVA, D., KOLEVA, I.: Microchim. Acta, 1976, 141

Z. BURGUDJIEV
E. BOBOLINA
Sofia—26 5 "Anton Ivanov" Blvd, Bulgaria
Károly ZIMMER H-1443 Budapest, Pf. 123.

acta Chimica Academiae Scientiarum Hungaricae, Tomus 93 (3—4), pp. 221—235 (1977)

INVESTIGATION OF THE GAS PHASE THERMAL DECOMPOSITION OF BROMINATED METHANES

B. A. KISS, T. DEUTSCH, O. KAPOSI and L. LELIK

(Department of Physical Chemistry and Radiology, Eötvös L. University, Budapest)

Received October 15, 1975

The concentration changes of products obtained by the gas phase pyrolysis of methyl bromide, methylene bromide and bromoform have been determined in the temperature range of 720 — 1170 K.

First, the presumable direction of thermal decomposition was predicted by thermodynamic considerations and calculations, and then the most probable reaction steps were determined from experimental facts. By using the toluene carrier gas technique to investigate the decomposition of bromoform, the C–Br bond strength was determined from the temperature dependence of the rate constant of the bond dissociation reaction. The bond energy was found to be 51.0 kcal/mole.

The steps of chain reactions were confirmed by thermochemical data obtained from mass spectrometric measurements.

1. Introduction

This paper deals with the gas phase pyrolysis of mono-, di- and tribromomethane. These studies, using primarily infrared spectroscopic methods, were performed in parallel with our investigations on the heterogeneous thermal decomposition processes taking place on an incandescent tungsten wire [1–3], since the mass spectrometric technique applied in the latter ruled out the possibility of gas phase thermal decomposition in the reactor of given design.

The compounds studied are ingredients of the filling gases of bromine-cycle halogen lamps, and these compounds decompose at the working temperature of the lamps. This is the technical background of our previous [1–3] and recent pyrolytic investigations. From the aspects of the tungsten cycle, the distribution of hydrogen and bromine formed in thermal decomposition is of basic importance [4–6]. As an illustration, Figs 1a and 1b show the partial pressures of tungsten bromides as a function of temperature at hydrogen : bromine ratios of 1 and 0.5 [6].

By a comparison of the homogeneous and heterogeneous thermal decomposition processes of methyl and methylene bromide, we found [7] that the results obtained, apart from the inherent thermochemical information, may not be correlated, since the reaction mechanisms are basically different.

The pyrolysis of the fourth member of the series, tetrabromomethane, on an incandescent spiral has also been studied [8], but our present experimental apparatus cannot be used to study the corresponding gas phase thermal decomposition.

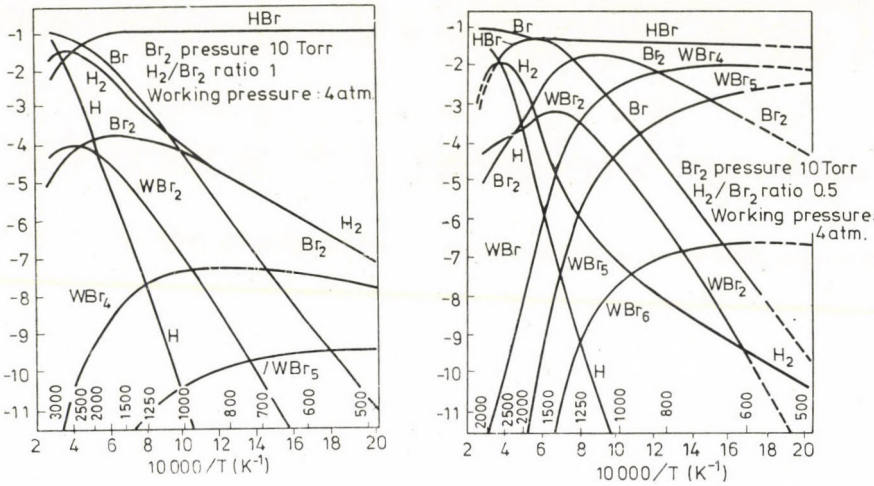

Fig. 1. Equilibrium of the tungsten–bromine–hydrogen system as a function of temperature and bromine to hydrogen ratio

The kinetics of the gas phase thermal decomposition of brominated methanes was investigated primarily to determine the C–Br bond strength [9—12]. For such purposes the toluene carrier gas technique has often been applied, which terminates the chain reaction after the first step with toluene as radical trap [9]. This method was used here in the investigation of bromoform. The literature of the corresponding chlorine derivatives contains complete reaction schemes [13—19]. The rate constants are generally determined from the experimental curves by using the principle of quasi-steady state radical concentration [16, 18].

2. Experimental

(a) Apparatus

The gas phase pyrolysis of the compounds was studied in a flow system. The samples were passed in argon stream through a quartz tube which was the lining of the oven of a Chevenard thermobalance with controlled heating. In measurements on bromoform toluene was also mixed into the stream. The gaseous reaction products were detected after cooling by infrared spectrophotometry [20] and supplementary chemical analysis. The scheme of the apparatus is shown in Fig. 2.

Since methyl bromide is a gas at room temperature, the most convenient method was to feed the system from a cylinder filled with argon containing methyl bromide in known

concentration. In this case the units between capillary manometer 3 and oven 7 were disconnected.

With methylene bromide and bromoform, the argon carrier was saturated with the vapour of the sample at a partial pressure corresponding to the temperature of the liquid to be studied. The temperature of methylene bromide was adjusted to 273 K and that of bromoform to 313 K, corresponding to vapour pressures of 12.8 and 17.3 Torr, respectively [21]. Bromoform vapour was prevented from condensation by heating line (22 in Fig 2.) between the vessel and the oven.

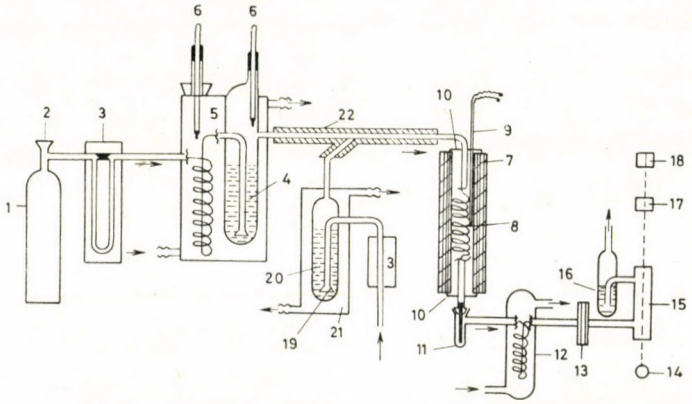

Fig. 2. Apparatus for gas phase pyrolytic investigations. (1) Argon gas cylinder, (2) precision reductor, (3) capillary manometer (calibrated), (4) liquid sample, (5) thermostating jacket, (6) thermometer, (7) oven, (8) quartz tube coil (reactor), (9) Pt—PtRh thermocouple, (10) closing lid, (11) condensation vessel, (12) thermostating jacket, (13) gas filter (G4), (14) IR light source, (15) IR cell, (16) organic liquid seal, (17) monochromator, (18) detector, (19) perforated gas inlet, (20) toluene, (21) thermostating jacket, (22) electric heating coil

When applying the carrier gas technique, toluene, mixed previously with bromoform arriving from the other line, was fed into the reactor in a similar way, through a thermostating vessel held at 293 K (partial pressure 22.0 Torr).

The flow rate was measured with a differential manometer, and it was maintained at a steady value during the measurements. The reactor was a quartz tube, 8 mm in internal diameter. The coil consisted of 7 turns with a spacing of 16—17 mm; the outer diameter of the coiled section was 38 mm. The temperature was measured near the mid-point of oven 7. The accuracy of the measurement was ± 5 K. According to our measurements, the difference in temperature between the mid-point and the ends of the coil was no greater than this accuracy. Vessel 11 in the figure was included to collect the condensation products with longer chains.

In cooler 12 the gaseous products leaving the reaction chamber are brought to room temperature, thereby ensuring measurement conditions identical to those of calibration. As the thermolysis also yields fine grains of solid carbon which, passed by the gas flow to the cell windows of the spectrometer, would reduce the measured transmission, the system also contains gas filter 13. Liquid seal 16 containing an organic substance prevents the back-diffusion of air, *i.e.* the formation of an oxidizing atmosphere.

To analyze the products, the gas leaving the thermal zone was passed through the gas cell of a UR 10 infrared spectrophotometer (length: 100 mm, volume: 129 cm^3, windows: KBr); in some instances the reaction products were absorbed in appropriate liquids and analyzed by chemical methods. The total volume of the gas was also checked by a gasometer. (Since the total pressure of the reaction components did not exceed 2% of the pressure of argon, the change in volume upon absorption of the reaction products was neglected.)

In the steady state at the temperature of investigation the flow rate was 4 l/h. The residence time of the reaction mixture, calculated by the method given below, was 15 s at 873 K.

b) Analytical methods

The following materials were used. Methyl bromide, Fluka purissimum (purified by repeated distillation); Methylene bromide, Fluka purissimum (purified by repeated distillation); Bromoform, Merck p. a. Since the compound decomposes relatively quickly upon the effect of light without the stabilizers acetone and ethanol mixed into the reagent, the stabilizers were distilled out immediately before the measurements. The purity was accepted as satisfactory when no CO_2 and CO could be detected by IR spectrophotometry in the reaction product.

The spectrophotometric measurement was calibrated for the IR active gases (all components except bromine and hydrogen) at a total argon pressure of 1 atm. The concentrations of the components were measured at the following wavenumbers:

methyl bromide	612	cm^{-1}
methylene bromide	647.5	cm^{-1}
methane	3011	cm^{-1}
hydrogen bromide	2484	cm^{-1}
acetylene	728	cm^{-1}

In the calibration measurements the brominated methane derivatives were determined by polarographic methods [22] after absorption in cooled dioxan. Acetylene was determined by the method of BARNES [23] after absorption in silver nitrate, hydrogen bromide was measured by alkalimetric and bromine by iodometric methods after absorption in alkali and carbon tetrachloride, respectively. To calibrate for methane, the cell was filled with methane of known partial pressure through a pump system. The transmittances of the samples were measured after adjusting the total pressure to 1 atm with argon gas. In some measurements the precipitated carbon was oxidized with air at 770 K, and measured in the form of carbon dioxide. The condensed products were determined by IR spectroscopy only qualitatively in carbon tetrachloride solution, and thus we did not attempt to set up an accurate material balance.

(c) Results

The compositions of the gas mixtures produced by the thermal decomposition of the compounds investigated are shown as a function of temperature in Figs 3 — 6. In Tables I and II the material balances of the pyrolysis of methyl and methylene bromide are given.

Table I

Material balance of the pyrolysis of CH_3Br as a function of temperature, in percentage of the atoms introduced

T (K)	O(%)		H(%)		Br(%)	
	identified	unidentified	identified	unidentified	identified	unidentified
700	100.0	0	100.0	0	100.0	0
800	98.9	1.1	99.7	0.3	98.4	1.6
900	98.4	1.6	94.4	5.6	98.1	1.9
1000	97.4	2.6	92.4	7.6	97.5	2.5
1100	95.2	4.6	91.4	8.6	97.2	2.8

as a function of temperature. The reason for the deviation from 100% is the formation of unidentified pyrolysis products with higher molecular weight.

As can be seen from Fig. 3, the decomposition of methyl bromide (original partial pressure 31 Torr) starts at 820 K. The main product of the reaction is hydrogen bromide accounting for the total bromine content at 1070 K. The curve of methane runs similarly passing a maximum at 1070 K. The maximum of methylene bromide at 920 K deserves

Table II

Material balance of the pyrolysis of CH_2Br_2 as a function of temperature, in percentage of the atoms introduced

T (K)	O(%)		H(%)		Br(%)	
	identified	unidentified	identified	unidentified	identified	unidentified
700	100.0	0	100.0	0	100.0	0
800	98.5	1.5	99.2	0.8	98.9	1.1
900	96.2	3.8	98.5	1.5	98.1	1.9
1000	94.6	5.4	97.7	2.3	96.9	3.1
1100	93.9	6.1	96.9	3.1	96.5	3.5

attention from the viewpoint of the reaction mechanism. The appearance of acetylene and carbon is similar to that observed with the thermal decomposition of methylene bromide.

Figure 4 shows that the thermal decomposition of methylene bromide (partial pressure 12.8 Torr) starts at about 720 K, as indicated by the appearance of hydrogen bromide. The concentration of the latter increases gradually up to 970 K, and hardly changes above that temperature. The curve of carbon (CO_2) shows similar properties. Acetylene appears at 770 K in amounts less by several orders, and it passes a maximum at 1070 K. The amount of bromine is a maximum at 770 K. The infrared spectrum of the oily product collected in vessel (11) is shown in Fig. 7; the assignment of the spectrum is given in Table III.

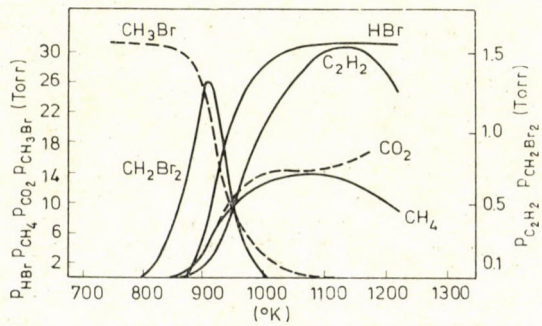

Fig. 3. Composition of the pyrolysis gas of methyl bromide as a function of the temperature

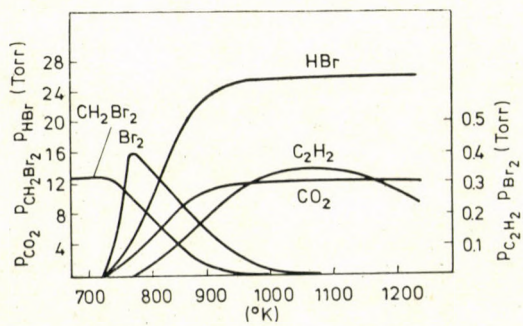

Fig. 4. Composition of the pyrolysis gas of methylene bromide as a function of the temperature

Table III

Assignment of the IR spectrum shown in Fig. 7

Band (cm^{-1})	Assignment
3075	$=CH_2$ ν_{as}
2960	$-CH_3$ ν_{as}
2925	$-CH_2-$ ν_{as}
2870	$-CH_3$ ν_s
2853	$-CH_2-$ ν_s
1725	C=O
1583	C=C (conjugated)
1465	$-CH_2-$ δ_s
1425	$-CH_3$ δ_{as}
1382	$-CH_3$ δ_s
1286	
1130	
1078	
1042	?
970	
874	
820	
740	
710	$(CH_2)_n$ δ_{as}

It is certain from the assigment that the product may not contain appreciable amounts of bromine, since there is no observable band in the C–Br stretching region (550—650 cm^{-1}). It can be stated that the main bulk of the substance consists of normal paraffins, irrespective of the non-assigned bands. It is also certain that the substance is a mixture of various hydrocarbons. (The presence of a ν C = O band at 1725 cm^{-1} is slightly surprising, since in the gaseous product not even traces of CO or CO_2 could be detected. This band suggests that some traces of oxygen in the argon might be responsible for the formation of carbonyl compounds which were enriched in the condensation vessel.)

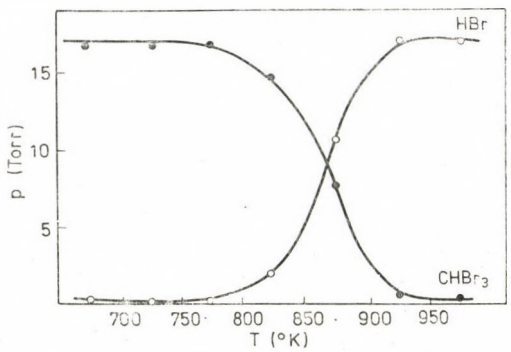

Fig. 5. Composition of the pyrolysis gas of bromoform as a function of the temperature.

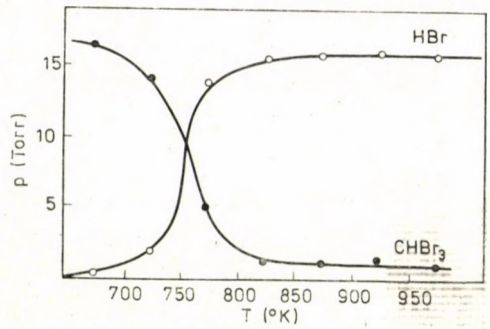

Fig. 6. Composition of the pyrolysis gas of bromoform as a function of the temperature (with toluene carrier gas)

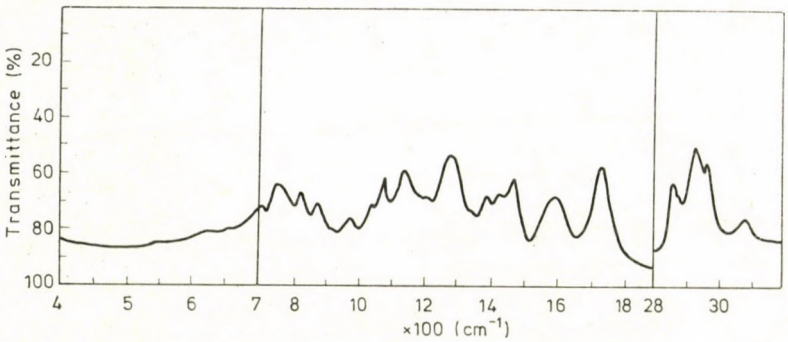

Fig. 7. IR spectrum of the oily product formed in the gas phase thermal decomposition of methylene bromide

Table IV

Partial pressures of methyl and methylene bromide during gas phase pyrolysis, as a function of the temperature

Temperature (K)	Reaction time (s)	Undecomposed		Conversion	
		Methyl bromide, p_i (Torr)	Methylene bromide, p_i (Torr)	Methyl bromide, p_i (Torr)	Methylene bromide, p_i (Torr)
298	38.6	31.0	12.8	0.00	0.00
673	17.1	31.0	12.8	0.00	0.00
773	14.9	31.0	10.2	0.00	0.20
823	13.9	30.8	6.1	0.01	0.52
873	13.2	29.8	2.0	0.04	0.85
923	12.5	16.3	0.6	0.48	0.95
973	11.8	5.4	0.2	0.83	0.99
1073	10.6	0.6	0.0	0.98	1.00
1173	9.8	0.0	0,0	1.00	1.00

In order to determine the dissociation energy of the C–Br bond, the thermal decomposition of bromoform was studied by the toluene carrier gas technique.

Table V

Partial pressures of bromoform during gas phase pyrolysis, as a function of the temperature

Temperature (K)	Reaction time (s)	Without toluene		With toluene		Rate constant, k (s^{-1})
		Undecomposed p_i (Torr)	Conversion	Undecomposed p_i (Torr)	Conversion	
298	23.2	17.3	0.00	17.3	0.00	0
673	10.3	16.3	0.05	—	—	—
723	9.5	14.1	0.18	—	—	—
773	8.9	5.0	0.71	16.7	0.03	0.0036
823	8.4	1.0	0.94	14.4	0.17	0.0229
873	8.0	0.9	0.95	7.7	0.55	0.1007
923	7.8	0.9	0.95	0.5	0.97	0.7760

It can be seen from Figs 5 and 6 that in the carrier gas the decomposition of bromoform starts by about 70 K higher than without toluene. The reason for this is that toluene forms benzyl bromide with the abstracted bromine atoms, thereby suppressing the chain reaction. It is worth noting that only hydrogen bromide could be observed in the gas phase, and thus the probable reaction scheme must account for the fact that no bromine is formed during the reaction, although it is stoichiometrically expected. The IR spectrum of the condensed products shows the presence of carbon tetrabromide.

The changes in pressure of starting substances as a function of temperature are given in Tables IV and V, together with the residence times calculated by the method given in section 3/b. Table V also contains the calculated rate constants, since the kinetics of the C–Br dissociation reaction could not be determined for bromoform by measuring hydrogen bromide.

3. Interpretation of the results

It is noted in advance that in the probable mechanism of thermal decomposition the dissociation of the C–Br bond is assumed to be the first step with all three compounds, similarly to the decomposition schemes found in the literature for chlorine, fluorine [14—19] and bromine derivatives [9—12]. This mechanism is proved indirectly by the bond dissociation energies (which are the activation energies of this reaction) obtained by radical trapping techniques. These energies are in good agreement with the data obtained by other methods (spectroscopic and mass spectrometric).

As to the probable direction of thermal decomposition, preliminary estimates can be made from thermodynamic data. For this reason, the thermodynamic data of the three compounds studied and their thermal decomposition products are given in Table IV. The data show that, with the exception of methyl bromide, the bromo derivatives are unstable with respect to their elements even at room temperature. Their liability to decomposition is further

enhanced by the fact that the elements may form hydrogen bromide with a negative free enthalpy of formation [24].

Although under the given experimental conditions equilibrium processes are out of consideration, it was worth investigating the possible equilibrium compositions. In order to calculate the equilibrium composition of pyrolytic mixtures a computer algorithm was developed [7, 24, 25], in which the free enthalpy of the complete system was minimized by the method of steepest descent. The results of the calculations are shown in Figs 8 and 9. On bromo-

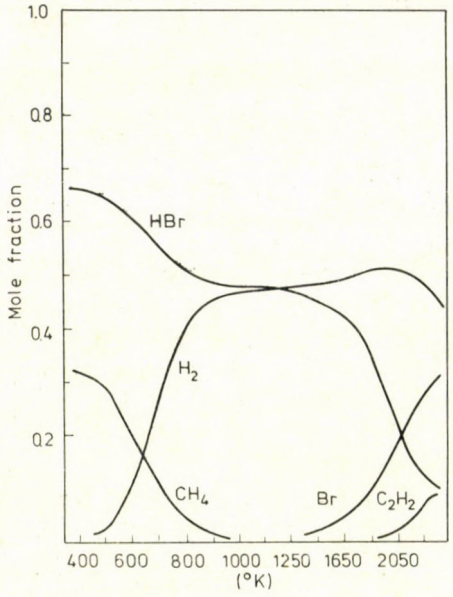

Fig. 8. Equilibrium composition of the pyrolysis gas of methyl bromide

form no calculation was performed, since of the presumable decomposition products only hydrogen bromide could be detected experimentally, and the computer program also requires as input the compounds assumed to be formed. For the other two derivatives the input consisted of the compounds detected experimentally. The diagrams do not show the curves of solid carbon

According to Fig. 8, if equilibrium is assumed, the decomposition of methyl bromide yields hydrogen and hydrogen bromide as main products, and some methane. From Fig. 9, the main products of the decomposition of methylene bromide are hydrogen bromide, hydrogen and bromine. The appearance of acetylene can be attributed to secondary processes. It is noted that the experimental results on methylene bromide, except for the small amount of acetylene and bromine, are in good agreement with these calcu-

lations. However, with methyl bromide the mechanism discussed below does not permit the formation of hydrogen, instead, as shown later, the formation of methylene bromide is a characteristic reaction step.

It is stressed that when comparing the results of thermodynamic calculations and kinetic investigations several factors must be taken into account, *e.g.* the presence of noble gases, the surface to volume ratio of the reactor, the coverage of the reactor walls with carbon, which play important roles in the reaction mechanism.

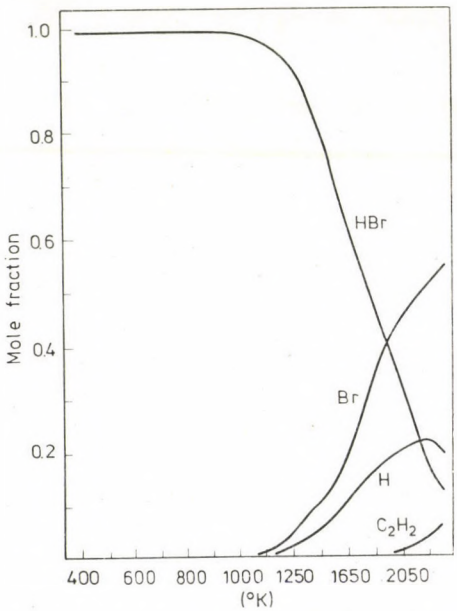

Fig. 9. Equilibrium composition of the pyrolysis gas of methylene bromide

Section 3/a deals with the mechanism of the thermal decomposition of the compounds, whereas section 3/b gives the calculations of the bond dissociation energy of bromoform obtained by the toluene carrier gas technique. The mechanism of the decomposition of methylene bromide is discussed before that of methyl bromide, because in the latter methylene bromide is also formed, and thus the two decomposition processes can be conceived to run in parallel.

It is noted that the various steps of the mechanisms are verified on the basis of the corresponding heats of reaction. The thermochemical data of radicals, required for these calculations, were determined by the mass spectrometric measurements [1–3] already mentioned.

3/*a*. *Probable mechanisms of the gas phase pyrolysis of brominated methane derivatives*

Consider first the thermal decomposition of methylene bromide. Its first step is a thermally activated dissociation process:

$$CH_2Br_2 \rightarrow \cdot CH_2Br + Br\cdot \qquad \Delta E = 62.5 \text{ kcal/mole} \qquad (1)$$

The chain carrier is the active bromine atom, which leads to the following processes:

$$CH_2Br_2 + Br\cdot \rightarrow \cdot CHBr_2 + HBr \qquad \Delta E = 14.6 \text{ kcal/mole} \qquad (2)$$

$$\cdot CHBr_2 \rightarrow C + HBr + Br\cdot \qquad \Delta E = -33.0 \text{ kcal/mole} \qquad (3)$$

Reaction (3), presumably the resultant of partial processes not discussed here, involves a great decrease in free enthalpy ($\Delta E = -33.0$ kcal/mole),

Table VI

Thermodynamic data of brominated methane derivatives and their decomposition products [24]

Compound	Enthalpy of formation (kcal/mole)	Standard entropy (cal/Kmole)
CH_3Br	−9.0	58.7
CH_2Br_2 (g)	−1.0	70.1
$CHBr_3$ (g)	6.0	79.0
CBr_4 (g)	12.0	85.5
C (s)	0.0	1.4
H_2	0.0	31.2
Br_2 (g)	7.3	58.6
Br	22.6	41.8
HBr	−8.7	47.4
CH_4	−17.9	44.5
C_2H_2	54.2	48.0

which justifies the assumption of this process. The radicals $\cdot CHBr_2$ formed in reaction (2) and $\cdot CH_2Br$ formed in reaction (1) take part mainly in recombinations, and the former may also react with the starting compound:

$$CH_2Br_2 + \cdot CHBr_2 \rightarrow C_2H_2Br_2 + HBr + Br\cdot \qquad (4)$$

The resulting dibromomethylene undergoes thermal decomposition in the process

$$C_2H_2Br_2 \rightarrow 2C + 2HBr \qquad (5)$$

Equation (6) shows the recombination of radical $\cdot CH_2Br$ and the elimination of dibromoethane:

$$2 \cdot CH_2Br \rightarrow C_2H_4Br_2 \rightarrow C_2H_2 + 2HBr \qquad (6)$$

Acetylene is formed presumably in reaction (6), whereas the double bonds formed in various elimination reactions are responsible for polymerization, *i.e.* for the formation of higher products. Although the assumption of reaction (6) is sufficient to explain the formation of acetylene, reactions (4) and (5) were also included into the decomposition scheme on analogy with the corresponding chlorine derivatives [14]. The combination of reactions (2, 3) and (4, 5) leads to a hydrogen bromide to carbon ratio 2 : 1. The maximum of bromine concentration can be interpreted by the fact that at higher temperatures reaction (2), being endothermic, becomes dominant, thereby suppressing the recombination of bromine atoms. The maximum of acetylene concentration is due presumably to self-decomposition.

The pyrolysis of methyl bromide proceeds, in agreement with the experimental results, presumably in the following manner.

The starting step is again the dissociation of the bromine-carbon bond:

$$CH_3Br \rightarrow \cdot CH_3 + Br\cdot \qquad \Delta E = 69.0 \text{ kcal/mole} \qquad (7)$$

By reacting with the starting substance, both radicals produce further radicals according to the reactions

$$CH_3Br + Br\cdot \rightarrow HBr + \cdot CH_2Br \qquad \Delta E = 13.3 \text{ kcal/mole}$$

$$CH_3Br + \cdot CH_3 \rightarrow CH_4 + \cdot CH_2Br \qquad \Delta E = 1.7 \text{ kcal/mole} \qquad (9)$$

The resulting radical $\cdot CH_2Br$ also reacts with the starting substance (unlike the analogous radical $\cdot CH_2Cl$, which is, for energetic reasons, stabilized by recombination only [16]):

$$CH_3Br + \cdot CH_2Br \rightarrow CH_2Br_2 + \cdot CH_3 \qquad \Delta E = 2.0 \text{ kcal/mole} \qquad (10)$$

The presence of methylene bromide is explained by reaction (10). Consequently, carbon and acetylene detected experimentally are formed, in part, during the decomposition of methylene bromide. The disappearance of

bromine can be attributed to the fact that the activation energy of bond dissociation is 7 kcal/mole higher for methyl bromide than for methylene bromide, and thus the decomposition starts by about 100 K higher . Accordingly, bromine already cannot be found in Fig. 4 at about 920 K. Since the methyl radicals are consumed in exothermic reaction (9), their recombination product, ethane, cannot be detected.

The thermal decomposition of bromoform also starts with the thermally activated dissociation of the C–Br bond:

$$CHBr_3 \rightarrow \cdot CHBr_2 + Br\cdot \qquad \Delta E = 55.5 \text{ kcal/mole} \tag{11}$$

The chain is started by the bromine atom:

$$CH_3Br + Br\cdot \rightleftharpoons \cdot CBr_3 + HBr \qquad \Delta E = 9.5 \text{ kcal/mole} \tag{12}$$

This reaction is reversible, causing the thermal decomposition to be a partly product-inhibited process.

The tribromomethyl radical either recombines with the bromine atoms:

$$\cdot CBr_3 + Br\cdot \rightarrow CBr_4 \tag{13}$$

or the chain propagates, on analogy with the corresponding chlorinated radical [19], in the following steps:

$$\cdot CBr_3 \rightarrow \cdot\cdot CBr_2 + Br\cdot \tag{14}$$

$$\cdot\cdot CBr_2 + CHBr_3 \rightarrow C_2Br_4 + HBr \tag{15}$$

Tetrabromomethane formed in reaction (13) was found in crystalline form in the condensation vessel (11) and in the cooler parts of the reactor tube. Consequently, the bromine content is represented by the solid products, and this is the reason why it could not be found in the gas phase. The experimental facts suggest that the recombination of Br· is also insignificant.

When the carrier gas contains toluene, the above reactions do not take place, since toluene in excess is brominated in the reaction

$$C_6H_5{-}CH_3 + 2Br\cdot \rightarrow C_6H_5{-}CH_2Br + HBr \tag{16}$$

According to this equation, the rate constant of reaction (11) can be determined by measuring the amount of hydrogen bromide formed. Furthermore, its temperature dependence permits the bond dissociation energy to be determined.

3/*b*. *Determination of the C–Br bond dissociation energy of bromoform*

In flow systems the reaction time is a function of the geometry and temperature distribution of the reactor. The situation is sometimes complicated by the fact that, as in our case, the reaction involves a change in volume, but due to the great dilution of the reactant (2 *v*/*v* %) this effect can be neglected here. As to the geometry, plug flow is assumed and mass transport by diffusion is neglected at the flow rates applied. As a further simplification, the reactor is regarded as isothermal, and it is assumed that the reaction mixture is heated instantaneously to the temperature of the reactor.

In a carrier gas containing toluene, bromoform decomposes in a first-order reaction instead of a chain reaction with complicated kinetics, and thus the integration of the rate equation yields

$$k = 1/t \ln (p_0/p) \tag{17}$$

where t is the residence time and
p and p_0 are the instantaneous and starting partial pressures of bromoform.

The value of p_0/p can be determined from infrared spectrophotometric measurements (through the measurement of hydrogen bromide), whereas the reaction time can be calculated from Eq. (18):

$$t = \frac{V_r \cdot T_0}{Q} \cdot \frac{1}{T} \tag{18}$$

where V_r is the volume of the reactor (52.3 cm^3),
Q is the volume rate measured at the inlet temperature (2.18 cm^3/s),
T_0 is the inlet temperature of the gas (298 K), and
T is the temperature of the reactor.

The rate constants given in Table V were calculated by means of Eq. (18).

According to the theory of thermal activation, the temperature dependence of rate constants can be described by the Arrhenius equation:

$$\ln k = \ln A - E/RT \tag{19}$$

where A is the frequency factor,
E is the activation energy, and
R is the universal gas constant.

The activation (dissociation) energy determined graphically from Eq. (19) is 51.0 kcal/mole, and frequency factor A equals 1.2×10^{13} (Fig. 10). The literature value of activation energy is 55.5 kcal/mole [24]; the difference of the two values is insignificant.

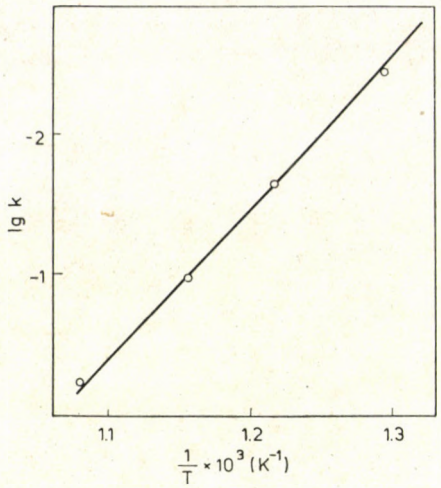

Fig. 10. Temperature dependence of the rate constant

REFERENCES

[1] KAPOSI, O., RIEDEL, M., DEUTSCH, T.: Magy. Kém. Folyóirat, **80,** 419 (1974)
[2] KAPOSI, O., RIEDEL, M., DEUTSCH, T.: Magy. Kém. Folyóirat, **79,** 505)1973)
[3] KAPOSI, O., RIEDEL, M., DEUTSCH, T.: Acta Chim. (Budapest), **81,** 43 (1974)
[4] RABENAU, A.: Angew. Chem. ,**79,** 1, 43 (1967)
[5] COVINGTON, E. J.: Illum. Eng., **63,** 134 (1968)
[6] KOPELMAN, B., WORMER, K. A.: Illum. Eng., **64,** 230 (1969)
[7] DEUTSCH, T.: Ph. D. Thesis Eötvös L. University, Budapest 1975
[8] LELIK, L.: Thesis, Eötvös L. University, Budapest 1975
[9] SZWARC, M.: Proc. Roy. Soc. Ser. A., **207,** 5 (1951)
[10] SEHON, A. H., SZWARC, M.: Proc. Roy. Soc. Ser. A, **209,** 110 (1951)
[11] SZWARC, M.: Chem. Rev., **47,** 175 (1950)
[12] KERR, J. A.: Chem. Rev., **66,** 5, 465 (1966)
[13] BAMFORD, C. H., TIPPER, C. F. J.: Comprehensive chemical kinetics; Vol. 5, E. S. Swinborne: The Decomposition of Halogen Compounds, p. 149. Elsevier Publ. Co., Amsterdam—London—New York 1972
[14] HOARE, M. R., NORVISH, R. G. W., WHITTGHAM, G.: Proc. Roy. Soc. Ser. A, **250,** 180 (1959)
[15] HOARE, M. R., NORVISH, R. G. W., WHITTIGHAM, G.: Proc. Roy. Soc. Ser. A, **250,** 197 (1959)
[16] VACHEROT, M., MARI, R., NICLAUSE, M.: Compt. Rend., **252,** 1945 (1961)
[17] LE MOAN, G.: Compt. Rend., **257,** 179 (1963)
[18] HOLBROOK, K. A.: Trans. Faraday Soc., **57,** 2151 (1961)
[19] SEMELUK, G. P., BERNSTEIN, R. B.: Proc. Roy. Soc. Ser. A., **207,** 46 (1951)
[20] KISS, B. A.: Acta Chim. Acad. Sci. Hung., **63,** 243 (1970)
[21] Handbook of Chemistry and Physics. The Chemical Rubber Co. D—103, Cleveland, Ohio 1964—1965
[22] STACKELBERG, M., STRACKE, W.: Z. Electrochem., **53,** 3, 118 (1949)
[23] BARNES, L., MOLININI, L. J.: Anal. Chem., **27,** 1025 (1955)
[24] STULL, D. R., WESTRUM, E. F., SINKE G. C.,: The Chemical Thermodynamics of Organic Compounds, p. 635—769. John Wiley 1969
[25] WHETI, W. B., JOHNSON, S. M., DANTZIG, G. B.: J. Chem. Phys., **28,** 751 (1958)

András B. KISS
Tibor DEUTSCH
Olivér KAPOSI
László LELIK

H-1088 Budapest, Puskin u. 11—13.

Acta Chimica Academiae Scientiarum Hungaricae, Tomus 93 (3—4), pp. 237—243 (1977)

CALCULATION OF THE REACTION FIELD FACTOR IN A SPHERICALLY-SYMMETRICALLY LAYERED DIELECTRIC

(REFINEMENT OF THE ONSAGER MODEL)

J. LISZI and L. MÉSZÁROS

(Electrochemistry Department Research Group of the Hungarian Academy of Sciences, Department of Physical Chemistry, Chemical Industrial University, Veszprém)

Received March 9, 1976

The ONSAGER model relating to the static relative permittivity of liquids was modified by replacing the homogeneous dielectric in the ONSAGER model by a heterogeneous dielectric. In the new model the cavity is surrounded by a spherical shell of relative permittivity ε_{loc}, which is situated in a dielectric of relative permittivity ε_0 of infinite extent. The reactive field factor corresponding to this new model was determined, and a study was made of what effect the immediate environment of the cavity has on the reactive field factor.

BEVERIDGE and SCHNUELLE [1] investigated the free energy of an arbitrary charge distribution in a spherical cavity, when the cavity is surrounded by a spherical shell of relative permittivity ε_{loc} which, in turn, is situated in a dielectric of relative permittivity ε_0 of infinite extent. The model regards these dielectrics as structureless continua.

We shall utilize the results of BEVERIDGE and SCHNUELLE to examine how the reaction field factor is affected by replacing the homogeneous dielectric in the ONSAGER theory [2] by a spherically-symmetrically layered heterogeneous dielectric.

The Onsager reaction field factor

The ONSAGER theory relating to the static relative permittivity of liquids [2] models a molecule possessing a permanent dipole moment as a point-like dipole situated in a spherical cavity. The substance surrounding the cavity is regarded as a homogeneous continuum, which is polarized by the inhomogeneous electric field of the permanent dipole. The environment polarized by the dipole gives rise to the reaction field, which, together with the cavity field, creates the local electric field acting on the dipole.

The reaction field strength R is proportional to the dipole moment μ giving rise to it:

$$R = f\mu \tag{1}$$

where f is the reaction field factor. The equation refers to a non-polarizable dipole. In the present paper we follow the original ONSAGER theory and deal with non-polarizable dipoles, but our results are also directly applicable to polarizable dipoles [3].

In a reaction field of strength R, the free energy F of the non-polarizable dipole [3] is

$$F = -\frac{1}{2}\mu R = -\frac{1}{2}f\mu^2 \tag{2}$$

For the ONSAGER model:

$$F = \frac{1-\varepsilon}{2\varepsilon+1} \cdot \frac{\mu^2}{a^3} \tag{3}$$

where ε is the static relative permittivity of the homogeneous dielectric surrounding the cavity. From Eqs (2) and (3) the ONSAGER reaction field factor is

$$f = f_{\mathrm{ONS}} = \frac{2(\varepsilon-1)}{(2\varepsilon+1)\,a^3} \tag{4}$$

The reaction field factor in a spherically-symmetrically layered dielectric

Let there be two charges creating a dipole in the interior of a sphere of radius a and of relative permittivity $\varepsilon_i = 1$. Let the sphere be surrounded by a spherical shell of external radius b (*i. e.* of thickness $b - a$) and of relative permittivity $\varepsilon_{\mathrm{loc}}$, which is situated in a dielectric of relative permittivity

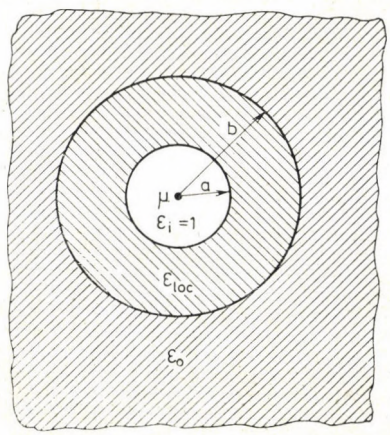

Fig. 1

ε_0 of infinite extent (Fig. 1). If dielectrics are regarded as structureless continua, then from [1] the free energy of the dipole is

$$F = \frac{1}{2}\left\{\frac{2(1-\varepsilon'_a)}{2\varepsilon'_a+1}\cdot\frac{\mu^2}{a^3}+\frac{2(1-\varepsilon_b)}{2\varepsilon_b+1}\left[1-\frac{1-\varepsilon'_a}{2\varepsilon'_a+1}\right]\frac{\mu^2}{b^3}\right\} \tag{5}$$

where

$$\varepsilon_b = \varepsilon_0/\varepsilon_{\mathrm{loc}} \tag{6}$$

$$\varepsilon'_a = \varepsilon_a\left[1+\frac{2(1-\varepsilon_a)(1-\varepsilon_b)}{2\varepsilon_b+1}\cdot\frac{a^3}{b^3}\right]^{-1} \tag{7}$$

$$\varepsilon_a = \varepsilon_{\mathrm{loc}}/\varepsilon_i \tag{8}$$

and the other notations are the same as previously. From a comparison of Eqs (2) and (5), the reaction field factor f of the new model is

$$f = \frac{2(\varepsilon'_a-1)}{(2\varepsilon'_a+1)a^3}+\frac{2(\varepsilon_b-1)}{(2\varepsilon_b+1)b^3}\left[1-\frac{1-\varepsilon'_a}{2\varepsilon'_a+1}\right] \tag{9}$$

where ε'_a is determined by Eq. (7).

The first term of Eq. (9):

$$f_1 = \frac{(2\varepsilon'_a-1)}{2(\varepsilon'_a+1)a^3} \tag{10}$$

depends primarily on the interaction of the dipole and the dielectric in the spherical shell, whereas the second term:

$$f_2 = \frac{2(\varepsilon_b-1)}{(2_b+1)b^3}\left[1-\frac{1-\varepsilon'_a}{2\varepsilon'_a+1}\right] \tag{11}$$

is determined primarily by the interaction of the dipole and the dielectric outside the spherical shell. If $\varepsilon_{\mathrm{loc}} = \varepsilon_0$, then $\varepsilon_b = 1$, $\varepsilon'_a = \varepsilon_a = \varepsilon_0$ and Eq. (9) sin plifies to the ONSAGER equation (4). If $\varepsilon_{\mathrm{loc}} = 1$, then $\varepsilon_a = 1$, $\varepsilon_b = \varepsilon_0$ and Eq. (9) is transformed to the ONSAGER equation relating to a sphere of radius b.

Eq. (9) therefore determines the reaction field factor in the case when the relative permittivity in the immediate environment of the dipole molecule is different from that in the interior of the phase.

Application of the new model

The BEVERIDGE—SCHNUELLE model consisting of a double-layer spherically-symmetric dielectric can be regarded as a refinement of the ONSAGER model. It is known that, on the directing action of the electric field of the ions, the static relative permittivity is generally smaller in the solvate sheath than in the main bulk of the solution [4]. A similar, but naturally smaller directing action can also be conceived in the case of dipole molecules. Accordingly, it is worthwhile examining what effects the thickness and relative permittivity of the spherical shell have on the reaction field factor. With the aid of some numerical examples, we shall discuss in what cases it is justified to calculate the reaction field factor with Eq. (9), and when the original ONSAGER theory gives a good approximation.

As a consequence of the directing action, the relative permittivity of the spherical shell can be expected to be smaller than the relative permittivity of the main bulk of the liquid, and in our calculations, therefore, $\varepsilon_{loc} \leq \varepsilon_0$. The static relative permittivity of apolar liquids generally has a value around 2, and thus the case $\varepsilon_{loc} < 2$ has not been examined. (Reference was made earlier to the limiting case $\varepsilon_{loc} = 1$.) Taking into account the static relative permittivities customary for organic liquids, we carried out or calculations with $\varepsilon_0 = 100$, 20 and 5.

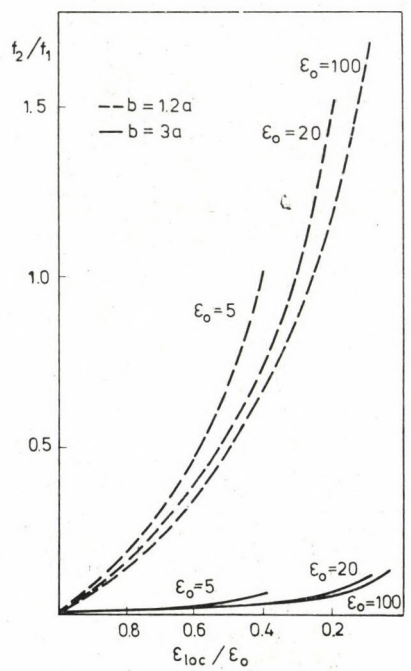

Fig. 2

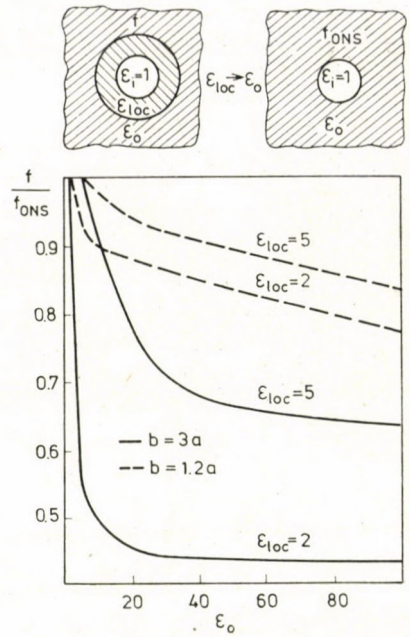

Fig. 3

Turning to a molecular viewpoint, the dielectric in the spherical shell can be identified with the neighbours of the molecule taken to be situated centrally. Our calculations were therefore made with two different spherical shell thicknesses.

(1) $b = 3a$. This may correspond to the case in which the liquid phase consists of spherical molecules of the same size, and the dielectric in the spherical shell is comprised of the nearest neighbours of the molecule regarded as the central one.

(2) $b = 1.2\ a$. This may be the case in which relatively large dipole molecules are surrounded by relatively small solvent molecules.

In Fig. 2, the quotient of f_2, calculated from Eq. (11), and f_1, calculated from Eq. (10), is depicted as a function of $\varepsilon_{loc}/\varepsilon_0$. The smaller the effect of the external dielectric compared to that of the dielectric in the spherical shell, the smaller the quotient f_2/f_1. The Figure reveals that for molecules of the same size (if $b = 3a$) the effect of the external dielectric is practically negligible, and the reaction field factor is determined by the dielectric in the spherical shell. If $b = 1.2\ a$, *i.e.* if relatively large dipole molecules are surrounded by small solvent molecules, then the effect of the external dielectric may also be appreciable; indeed, in some cases it is even conceivable that the latter effect becomes the determining one.

In Fig. 3 f is the reaction field factor corresponding to the new model, and f_{ONS} is the ONSAGER reaction field factor for the case when the cavity is surrounded by a homogeneous dielectric of relative permittivity ε_0. The dielectric in the spherical shell has a double effect.

(1) It keeps the external dielectric of relative permittivity ε_0 away from the cavity of radius a. The thicker the spherical shell, the stronger this

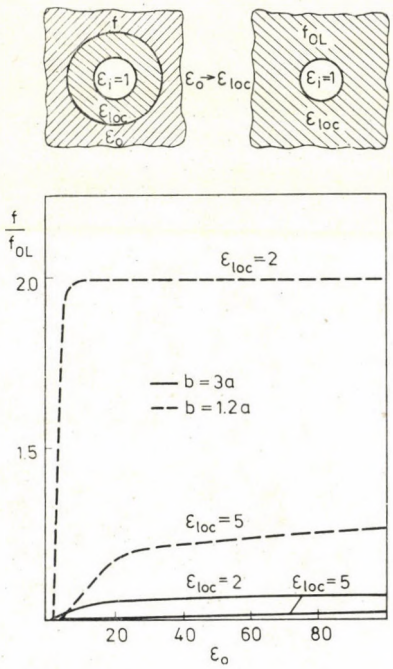

Fig. 4

effect. The curves relating to the case $b = 3a$ lie below the curves relating to the case $b = 1.2\ a$.

(2) The permanent dipole also polarizes the dielectric in the spherical shell, and this polarization, too, participates in the development of the reaction field factor. The larger ε_{loc}, the closer f approaches f_{ONS}. This can be seen in the Figure from the facts that the curves corresponding to $\varepsilon_{loc} = 5$ are found above these corresponding to $\varepsilon_{loc} = 2$, and that if $\varepsilon_{loc} \to \varepsilon_0$, then $f \to f_{ONS}$.

In Fig. 4 f is the reaction field factor corresponding to the new model, and f_{OL} is the ONSAGER reaction field factor in the case when the cavity is surrounded by a continuous dielectric of relative permittivity ε_{loc}. The double effect of the dielectric in the spherical shell can be observed in this Figure too.

(1) The thicker the spherical shell, the less $f f_{OL}$ differs from unity. The curves relating to the case $b = 3a$ are to be found below the curves relating to the case $b = 1.2\ a$.

(2) The larger the relative permittivity of the spherical shell, the closer f approaches f_{OL}. In the limiting case, if $\varepsilon_0 \to \varepsilon_{loc}$, then $f \to f_{OL}$.

To summarize, it may be stated that the immediate environment of the dipole molecule may have a considerable effect on the reaction field factor. The thicker the spherical shell in the heterogeneous model, and the closer ε_{loc} approaches ε_0, the more the reacti n field factor is determined by the dielectric in the spherical shell. If the thickness of the spherical shell is the same as or greater than the radius of the cavity, then the dielectric outside the spherical shell has practically no effect on the reaction field factor. From a molecular viewpoint, this result may be described in that, for molecules of the same size, only the closest neighbours of the molecules participate in the development of the reaction field factor. If relatively large dipole molecules are surrounded by relatively small solvent molecules, then the reaction field factor is affected by other molecules too, besides the closest neighbours. The effect of these is the greater, the smaller the solvent molecules compared to the dipole molecules.

REFERENCES

[1] BEVERIDGE, D. L., SCHNUELLE, G. W.: J. Phys. Chem., **79**, 2562 (1975)
[2] ONSAGER, L.: J. Amer. Chem. Soc., **58**, 1486 (1936)
[3] BÖTTCHER, C. J. F.: Theory of Electric Polarization, Vol. 1, Elsevier, Amsterdam, 1973
[4] HARNED, H. S., OWEN, B. B.: The Physical Chemistry of Electrolytic Solutions, 3rd Ed., Reinhold

Lajos MÉSZÁROS
János LISZI
H-8201 Veszprém.

Acta Chimica Academiae Scientiarum Hungaricae, Tomus 93 (3—4), pp. 245—256 (1977)

SORPTION OF SOLVENT–NON-SOLVENT MIXTURES ON PHENOL–RESITOL GELS

E. WOLFRAM, J. GYÖRGYI-EDELÉNYI and M. NAGY

(Department of Colloid Chemistry, Eötvös L. University, Budapest)

Received April 1, 1976

The degree of swelling, on a weight-per-weight basis, of resin platelets obtained from films by drying, in binary liquid mixtures containing various amounts of a solvent component (acetone, 1,4-dioxane, methanol or *n*-propanol) and a non-solvent one (water or *n*-heptane) was determined at swelling equilibrium. From the data, both the amount of solvent bound by the resin phase and the sorption parameter were calculated over the total range of composition.

As a rule, the non-solvent diminished the uptake of solvent by the polymer, except for aqueous mixtures of both acetone and dioxane, where a synergetic effect was observed. It was found that reverse sorption, *i.e.* the relative enrichment of the non-solvent in the sorption layer, as shown by negative values of the sorption parameter, occurred in systems in which the interaction of the two solvent components was not too weak.

The results were found to be in agreement with our earlier data for poly (vinyl alcohol), and could be explained in accordance with POUCHLÝ's theoretical interpretation.

Introduction

Molecular interactions of polymers and binary liquid mixtures are manifested in solvation in the case of dissolved polymers, and in sorption (accompanied by macroscopic swelling) on polymer networks. As a result of these two processes (widely termed collectively as sorption in the literature), the binding by the polymer of that component of the mixture which is a thermodynamically good solvent for the polymer is generally favoured in comparison to the binding of the other component. That is, the solvation–sorption layer becomes richer in the former component compared to the initial composition of the mixture, and poorer in the latter component. Thus, the interaction with the polymer results in a displacement, similarly to the adsorption of liquid mixtures on usal adsorbents, and in addition to the value of the total sorption, it is also necessary to know the extent of the enrichment, the preferential (or selective) sorption, in order to be able to describe the process. The latter factor is mostly given in the literature by γ, the sorption parameter; this is defined as the excess amount of the solvent component referred to unit amount of the polymer, both quantities being expressed in either volumes or masses. The sorption parameter is therefore a calculation value analogous to the Gibbs adsorption excess: $\gamma > 0$ means

an enrichment, and $\gamma < 0$ an impoverishment, while $\gamma = 0$ corresponds to the sorption azeotrope.

Former investigations, mainly relating to dissolved polymers, indicate that in general the first case occurs in non-polar polymer–solvent–non-solvent systems, over the total range of mixture compositions [1—3]. ŽIVNÝ *et al.* [4] first observed the second effect, which they termed inverse sorption, in the poly(methyl methacrylate)–benzene–methanol system. In investigations over the entire concentration range, a change in sign of the sorption parameter at a certain concentration has been described for a number of systems [5—8].

It was obvious to ascribe the phenomenon qualitatively to the competitive nature of the interactions, and to interconnect the change in selectivity with the association of the mixture components [5, 6] or the solubility of the polymer [7]. This connection was first expressed in an exact form by POUCHLÝ *et al.* [9]; on the basis of their formula, both the total and the selective sorption can be calculated in systems either dilute or concentrated as regards the polymer. It was also pointed out that the change in character results primarily from the association of the mixture components. If self-association of one of the components is predominant the azeotrope occurs in the vicinity of that mixture composition which correspond to the maximum of the total sorption, while if nterassociation is the predominant interaction, then γ changes in sign at the minimum.

Selective sorption on polymer networks (gels) has scarcely been dealt with, and even then it has primarily been used as a method of determining interaction constants [10, 11].

We earlier [12—14] made a detailed study of the sorption of various aliphatic alcohol–water mixtures on poly(vinyl alcohol) gels. It was found that the γ *vs.* c_{alcohol} curves exhibited several local extremes, which could be correlated with the characteristic viscosity changes of the poly(vinyl alcohol) solutions prepared with the above mixtures [15], and thus with the mixture structure. As a result of these investigations, we were the first to point out that what was found be true for the sorption on dissolved polymers is also valid for the sorption on gels of the same polymers with low cross-linking degrees. This finding was later confirmed by studies of different authors on other systems [16].

An account was given by us earlier [17] of the sorption from water–alcohol mixtures on phenol–formaldehyde gels in the resitol state; this was studied as one possibility of characterizing matrices prepared for GPC purposes. Since the γ *vs.* c curve shapes also indicated the predominant role of the mixture structure in the case of these gels, with their complicated chemical compositions and topographies [18], it appeared justified to examine the question more closely. In the present work, sorption on these gels was determined from solvent–non-solvent mixtures in which the non-solvent was water

or *n*-heptane, and the solvent was methanol, *n*-propanol, acetone or 1,4-dioxane. The reasons for these choices were that both the polar water and the non-polar heptane precipitate the resin, but it is only water that interacts with the solvent components of the mixture, heptane exhibits practically no interaction. It is therefore to be hoped that further information may be obtained on the role of the mixture structure in the competitive interactions.

Experimental

Preparation of gels

In order to attain as uniform a network density as possible, and to avoid the uncertainty arising from the fact that for gel pearls the degree of swelling can be given only in relation to standard centrifugation conditions, for the purposes of the present investigations the gels were prepared in platelet form in the following manner.

A solution with a resin concentration of 46 g/100 cm^3 was prepared from an unfractionated novolak-state resin ($\overline{M}_n \approx 1200$) with an 18 : 82 v/v water – ethanol mixture, and 56 mg paraformaldehyde and 1 mg sodium hydroxide were added per 1 g resin to yield the resitol state. Material 'precondensed' on a glycerine bath was pured out onto a siliconized glas plate possessing a rim, and further condensed in a drying oven, the temperature being progressively increased up to 90°C. On the completion of condensation, the gel was divided up while still hot, and extracted with the appropriate solvent component of the sorption studies. Depending on the degree of cross-linking of the gel, which may be regulated *via* the rate of increase of temperature, the quantity of the fraction leached out varied between 25 and 60%. The platelets used for the sorption studies had been extracted and then dried to a constant weight in air, in order to avoid the error arising with samples swollen in solvents of relatively high vapour pressure. The amount of the pure solvent bound by the air-dried samples was large enough for the swelling to be reversible. The decrease in swelling brought about by the drying was less than 10% (only 4% for dioxane and *n*-propanol). Two types of gel (I and II) were prepared, with different cross-linking degrees. Table I gives the degrees of swelling S_r and the polymer contents c_p of the gels at equilibrium in the solvents used.

Table I

Degree of swelling S_r and polymer concentration c_p of gels in the examined solvents

Solvent	S_r g solvent/g dry gel		c_p weight %	
	I	II	I	II
1,4-dioxane	8.3	3.8	10.8	20.8
n-propanol	7.7	2.9	11.5	25.4
Acetone	7.4	2.4	11.9	29.8
Methanol	6.3	1.7	13.8	37.1

Determination of swelling and sorption characteristics

About 0.1 g of the air-dried gels were measured with analytical accuracy into ground-glass stoppered test-tubes, and liquid mixtures of known composition were added in amounts corresponding to a dry gel : liquid ratio of 1 : 10 or 1 : 30, depending on the degree of swelling of the sample. The paraffin-sealed test tubes were kept at room temperature for one week during which they were shaken several times daily. Preliminary measurements had indicated

that this time was sufficient for equilibrium to be established, while the lack of any special thermostating did not affect the results to an extent in excess of the limits of error. Depending on the difference between the refractive indices of the components, the mixture compositions were determined at 25.0 ± 0.1° C, with a maximum error of 1.0%, using either an ITR-2 interferometer or a Zeiss refractometer.

For determination of the total sorption, that is the degree of swelling S_r corresponding to the swelling equilibrium, the liquid adhering to the surface of the gel sample was removed with filter paper and the weights of the sample were measured in this state and after drying to a constant weight in vacuum at 60° C. The relative error in the determination of S_r calculated from the weight difference is less than 5%.

In the knowledge of the masses m_p and m_0 of the air-dried gel and the initial mixture, respectively, of S_r, and of the initial and equilibrium weight fractions of the solvent, w_i and w_e respectively, in the mixture, it is possible to calculate the quantity of solvent actually bound:

$$A = \frac{m_0 w_i - (m_0 - m_p S_r) w_e}{m_p}$$

and also the sorption parameter:

$$\gamma = \frac{(w_i - w_e) m_0}{m_p}$$

Results

Some parameters of the solvent and non-solvent components of the mixtures examined are listed in Table II, mainly to illustrate why these components were selected. It can be seen that the value of the solubility

Table II

Some characteristic data on the mixture components at 25°

δ: Hildebrand solubility parameter ($\delta_{gel} \approx 10$)*
ε: dielectric constant ($\varepsilon_{gel} \approx 6$)**

Component	Symbol	ε	δ
Solvents			
1,4-dioxane	D	2.2	10.0
acetone	A	21.4	10.0
methanol	M	33.7	14.9
n-propanol	P	22.2	11.9
Non-solvents			
water	W	78.5	24.2
n-heptane	H	1.9	7.5

* Fom swelling-measurement data

** J. H. FERRY (Ed.): Chemical Engineers' Handbook, Mc Graw-Hill, New York 1941. p. 2644

parameter of the gel was a deciding factor: the solubility parameters of dioxane and acetone are the same as that of the polymer, while those of the alcohols are larger, that of water substantially larger, and that of the heptane smaller than that of the resin. Similar relations also exist with regard to the dielectric constants: while those of dioxane and heptane are smaller than that of the gel, those of the other compounds are larger, that of water by more than an order of magnitude. Since one of the non-solvent components is appreciably polar, while the other is non-polar, numerous combination possibilities were available.

Dependence of the total sorption (degree of swelling) and solvent-binding on the mixture composition

Mixtures over the whole concentration range can be prepared of the four solvent and two non-solvent components in the following six combinations: D—W, A—W, D—H, A—H, M—W and P—W. Such S_r *vs.* w_e, sol ent curves are shown in Fig. 1. The possibility of a classification into three groups is immediately apparent:

(a) a maximum occurs for the A–W and D–W systems;

(b) in the D–H, A–H and M–W cases the slopes of the curves progressively increase;

(c) the P–W mixture yields an *S*-shaped curve.

It is a common feature of all three types that up to a certain mixture composition (w_e at least 0.4) the swelling increases only slightly with the solvent concentration, its value barely exceeding 1 g liquid/1 g gel; a relatively sudden rise then follows. It is noteworthy that the slopes of the steeply-rising sections, which to a first approximation may be regarded as linear are almost identical for types (a) and (c) and for the D–H system of type

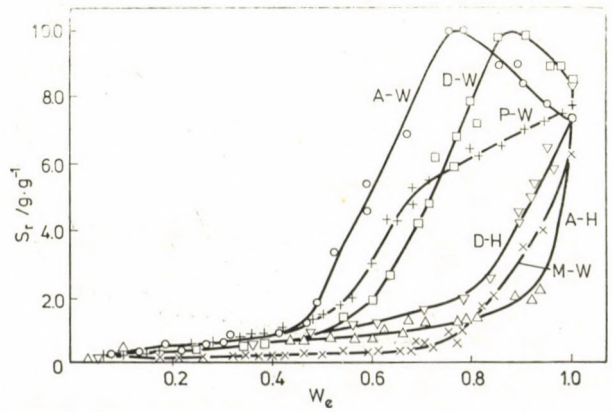

Fig. 1. Dependence of degree of swelling on the mixture composition

(b); as regards the other type (b) systems, the slope for the M–W system is smaller than this, and that for the A–H system substantially larger. The values corresponding to some characteristic points of the curves are given in Table III.

Table III

Some characteristic data on the S_r vs. w_e curves for gel I

Curve type*	Mixture	w_1**	w_2	dS_r/dw_e	$S_{r,1}$***	$S_{r,max}$	$S_r(w_e = 1)$
a	A—W	0.45	0.78	33	1.0	9.9	7.4
a	D—W	0.58	0.87	35	1.3	10.00	8.3
b	D—H	0.84	—	35	2.5	—	8.3
b	A—H	0.95	—	1	2.8	—	7.4
b	M—W	0.75	—	23	0.7	—	6.3
c	P—W	0.56	—	30	1.9	—	7.7

* *a:* maximum; *b:* convex to w_e axis; *c:* S-shaped
** w_1: value of w_e at beginning of steep section; w_2: value of w_e at $S_{r,\,max}$ (only for type a)
*** $S_{r,1}$: value of S_r at beginning of steep section

From the shape of the curves and the data in Table III, it is clear that the composition dependence of the total sorption is determined primarily by the nature of the non-solvent component of the mixture. This is particularly striking on comparison of the A–W and A–H, and the D–W and D–H mixture pairs: no matter whether the solvent component is acetone or dioxane, if it is combined with water instead of heptane, a synergetic effect is observed.

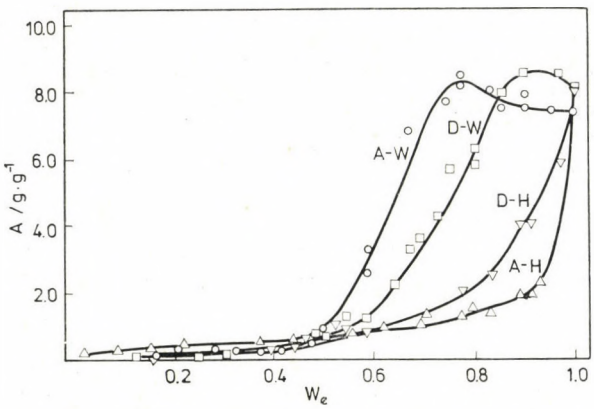

Fig. 2. Dependence of the solvent binding on the mixture composition for gel I

The extent of this is a little larger in the case of acetone than for dioxane (and at the same time the maximum occurs at a lower concentration for acetone), but the maximum degree of swelling is approximately the same for the two systems.

If the degree of swelling curves are compared with the solvent sorption *vs.* composition curves to be seen in Fig. 2, it is found that for the heptane systems containing acetone or dioxane as solvent (unlike to the aqueous systems containing the same solvents) the S_r and A curves almost overlap each other; that is, over the entire composition range it is practically only the solvent that is the active swelling component. A similar finding can be made for mixtures of alcohols and water too.

Dependence of the sorption parameter on the mixture composition

More information can be obtained from the curves of Figs 3 and 4, which show the changes in γ with composition. Here, two types can be distinguished:

(a) γ is positive over the entire composition range (A–H, D–H and P–W systems, see Fig. 3);

(b) γ is zero and changes in sign at given mixture compositions, *i.e.* at least one sorption azeotrope and inverse sorption are exhibited.

Otherwise, the two types of curves pass through at least one local extreme. The characteristic data on the curves are to be found in Table IV.

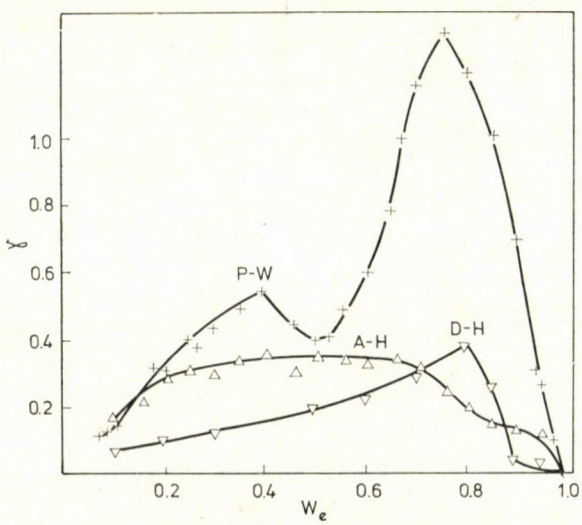

Fig. 3. Dependence of the sorption parameter on the mixture composition for gel I in the case of non-inverse sorption

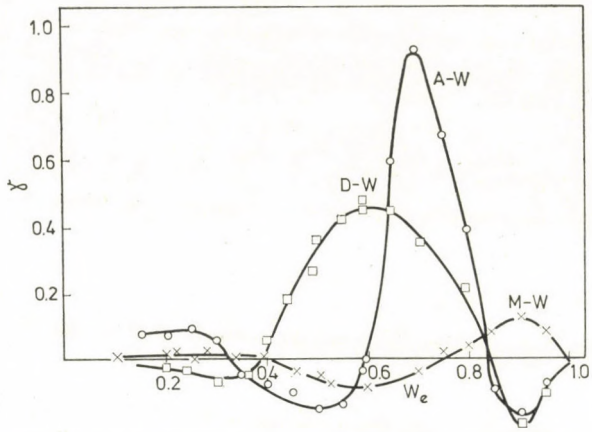

Fig. 4. Dependence of the sorption parameter on the mixture composition for gel I in the case of inverse sorption

Table IV

Some characteristic data on the γ vs. w_e curves for gel I

		w_e values relating to the indicated γ						
Curve type	Mixture	Max. 1	Azeotrope 1	Min. 1	Azeotrope 2	Max. 2	Azeotrope 3	Min. 2
*a**	P—W	0.4	—	0.5	—	0.75	—	—
a	A—H	0.5	—	—	—	—	—	—
a	D—H	0.8	—	—	—	—	—	—
*b***	D—W	—	0.38	—	—	0.6	0.85	0.9
b	M—W	0.35	0.42	0.6	0.73	0.9	—	—
b	A—W	0.25	0.33	0.5	0.6	0.7	0.84	0.9

* *a:* $\gamma > 0$ in the entire series of mixtures
** *b:* presence of sorption azeotropes and inverse sorption

Role of the cross-linking degree of the gel

As examples, Figs 5—7 show in turn the composition dependence of the degree of swelling, the solvent binding and the sorption parameter for the dioxane–water and dioxane–heptane mixture systems, in the case of two resins with different cross-linking degrees. In accordance with expectation, the absolute values of the total sorption, the selective binding of the solvent, and the sorption parameter decrease with an increase of the network density,

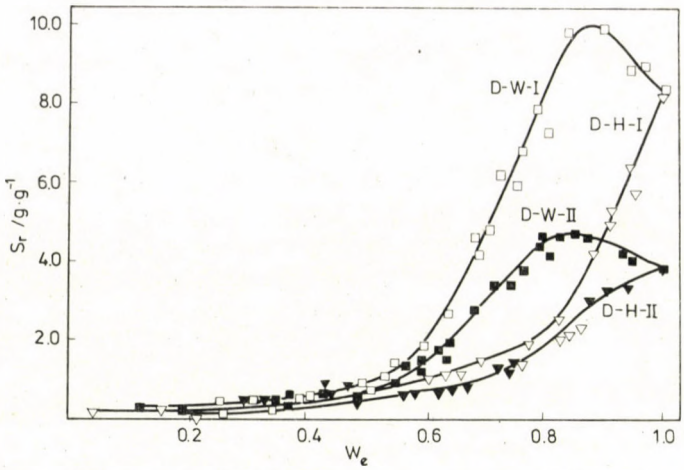

Fig. 5. Dependence of the degree of swelling on the mixture composition on gels with different cross-linking degrees

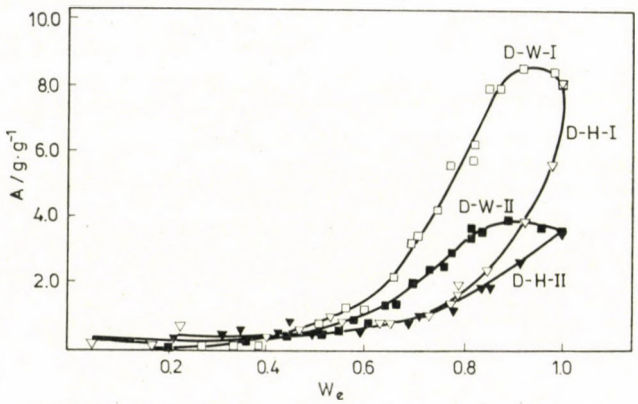

Fig. 6. Dependence of the solvent binding on the mixture composition on gels with different cross-linking degrees

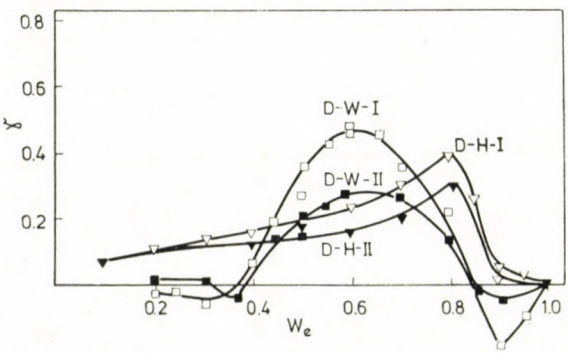

Fig. 7. Dependence of the sorption parameter on the mixture composition on gels with different cross-linking degrees

but without there being either a change in the nature of the curves or an appreciable shift in the composition corresponding to each specific point. It must also be noted that for dioxane–heptane mixtures the effect of the network density exceeds the limits of error only at mixture compositions close to the pure non-solvent, and at solvent mole fractions less than 0.9 the effect can barely be observed. On this basis, therefore, it may be stated that a change in the cross-linking degree (at least within the limits selected) does not affect the interaction qualitatively, nor quantitatively either except if the overall solvating effect of the liquid mixture is not too small.

Discussion

Analysis of the experimental data clearly reveals that the sorption on the resin gels of various mixtures which exhibit appreciable quantitative and qualitative differences, is primarily influenced by the interaction between the components of the mixture. This is demonstrated most markedly by the results obtained for mixtures containing acetone or dioxane as solvent. The solubility parameters of the two resin solvents agree with one another and with that of the resin. If the non-solvent component is water, which associates strongly with both of the above solvents (as proved by the maximum in the viscosities of the mixtures appearing at a given composition), then a pronounced synergetic effect occurs in the solvation, the sorption parameter and viscosity maxima being observed at practically the same mixture composition. However, if the mixture contains *n*-heptane as non-solvent, the interaction of this with the solvent component being virtually negligible, then the *n*-heptane only dilutes the solvent (the composition curve of the viscosity is monotonous), and thus the sorption decreases even at high solvent concentration. This can also be seen from the shapes of the A *vs.* w_e curves.

Supporting evidence is provided by the experimental finding that the sorption parameter varies according to a maximum–minimum curve for mixtures in which association occurs, while its change in sign lies at the maximum of the composition curve of the total sorption, and hence at the composition giving the greatest extent of synergism. At the same time, this result is in agreement with both earlier experimental results (relating to different systems), and the above-mentioned quantitative conclusions of POUCHLÝ: the maximum value of the sorption parameter is to be expected where the mutual association of the mixture components is the predominant interaction, that is on the steep section of the composition curve of the degree of swelling, at a composition preceding the local maximum in this curve.

It can be seen that the experimental results correspond qualitatively to the classical LUNDELIUS rule [19] regarding the correlation between the extent to which substances dissolved in various solvents are adsorbed on non-swelling adsorbents, such as active carbon, and the solubilities of these substances in the solvents in question: the higher the solubility (*i.e.* the interaction of the solution components), the less extensive the adsorption under otherwise identical conditions.

The conditions are somewhat different in the case of the alcohol–water mixtures, in which the Hildebrand parameter of the solvent component differs appreciably from that of the polymer, but the mixtures are known to be strongly structured, the interaction of methanol with water being greater than that of propanol. In accordance with this, in the case of propanol the sudden increase in the degree of swelling occurs at a much lower alcohol concentration ($w_e = 0.53$) than for methanol ($w_e = 0.77$). It must be pointed out that at these two mixture compositions the dielectric constants of the two types of mixture are the same ($\varepsilon = 47$); in addition to the structuring, this emphasizes the importance of the polarity too.

Of course, in connection with the given interpretation it must be borne in mind that the concentration of the polymer component of the ternary system also varies in parallel with the composition change of the sorption; under the conditions applied it fell from a value of more than 50% to values below 10% with the increase of the overall sorption. Thus, the relative weight of the competitive effects also changes with the mixture composition, in the sense that the higher the polymer content of the system, the more prominent the role of the structure of the medium, while in the strongly swollen systems (with comparatively low concentrations as regards the polymer) roles are played by the interactions of the mixture components, both with each other and with the polymer.

REFERENCES

[1] COWIE, J. M., BYWATER, S.: Makromol. Chem., **1**, 581 (1966)
[2] OKITA, K., TERAMOTO, A., KAWAHARA, K., FUJITA, F.: J. Phys. Chem. **72**, 278 (1968)
[3] HERT, M., STRAZIELLE, C.: Makromol. Chem. **175**, 2149 (1974)
[4] ŽIVNÝ, A., POUCHLÝ, J., ŠOLC, K.: Collect. Czech. Chem. Commun. **32**, 2753 (1967)
[5] TUZAR, Z., KRATOCHVIL, P.: Collect. Czech. Chem. Commun. **32**, 3358 (1967)
[6] TUZAR, Z., BOHDANECKY: Collect. Czech. Chem. Commun. **34**, 289 (1969)
[7] COWIE, J. M., MCCRINDLE, J. T.: Europ. Polym. J. **8**, 1325 (1972)
[8] DUŠEK, K., SEDLACEK, B.: IUPAC Internat. Symp. Macromolecules, Leiden, Sept. 1970, Book of Abstr., Vol. 1, p. 137
[9] POUCHLÝ, J., ŽIVNÝ, A., ŠOLC, K.: Collect. Czech. Chem. Commun. **37**, 988 (1972)
[10] KRIGBAUM, W. R., CARPENTER, D. K.: J. Polymer Sci. **14**, 241 (1954)
[11] SEIDL, J., DUŠEK, K.: Collect. Czech. Chem. Commun. **31**, 2695 (1966)
[12] NAGY, M., WOLFRAM, E., HORVÁTH, M.: Annales Univ. Sci. Budapest Sect. Chim. **11**, 63 (1969)

[13] NAGY, M., WOLFRAM, E., INZELT, GY., BEKE, GY.: Acta Chim. (Budapest) **74,** 233 (1972)
[14] NAGY, M., WOLFRAM, E., GYŐRFI-SZEMEREI, A.: J. Polymer Sci. Part C **39,** 169 (1972)
[15] NAGY, M., WOLFRAM, E.: Annales Univ. Sci. Budapest. Sect. Chim. **11,** 57 (1968)
[16] HERT, M., STRAZIELLE, C.: Makromol. Chem. 1976, 1849 (1975)
[17] UDVARHELYI, K., GYÖRGYI-EDELÉNYI, J., WOLFRAM, E.: Kémiai Közlemények **42,** 37 (1974)
[18] TROSTYANSKAYA, E. B., BABAYEVSKII, P. G.: Vysokomol. Soed. **10,** 288 (1968)
[19] See FREUNDLICH, H.: Kapillarchemie, 4. Aufl, Leipzig, 1930, Bd. 1, p. 260

Ervin WOLFRAM
Judit GYÖRGYI-EDELÉNYI
Miklós NAGY
H-1088 Budapest, Puskin u. 11—13.

Acta Chimica Academiae Scientiarum Hungaricae, Tomus 93 (3—4), pp. 257—265 (1977)

PROPERTIES OF ALCOHOL–AMINE MIXTURES, XII

ELECTRIC CONDUCTANCE OF TRI(*n*-BUTIL)AMINE–ALCOHOL MIXTURES

F. RATKOVICS and M. LÁSZLÓ

(Electrochemistry Department Research Group of the Hungarian Academy of Sciences, Department of Physical Chemistry, University of Chemical Industries, Veszprém)

Received April 29, 1976

A study was made of the specific conductance in mixtures of tri(*n*-butyl)amine with methanol, ethanol, 1-propanol or 1-butanol over the entire concentration range at 20 and 45° . The results were interpreted on the basis of a model assuming electrolytic dissociation of associates of the mixed type A_iB, consisting of one amine and several alcohol molecules. It was found that at a given amine concentration the concentration of the mixed associate is practically independent of the alcohol component in the mixture, and, in agreement with the Bjerrum ion-association theory, the maximum value of the specific conductance depends on the dielectric factor of the alcohol used as solvent. The number of alcohol molecules in the dissociated mixed associates was calculated, and from the temperature dependence of this conclusions were drawn regarding the cyclic or chain nature of the pure alcohol associates. It was found that in the temperature range examined methanol is characterized by chain association, and the higher homologues by increasing cyclic association. These results are in agreement with those of our earlier investigations.

In the study of the electric conductance of alcohol–amine mixtures we have shown that the phenomena connected with the electrolytic dissociation of mixed molecular associates containing alcohol and amine can be discussed on the basis of a model in which associates of type A_iB are assumed, containing a single amine and several alcohol molecules [1]. The question arises as to whether this assumption has a realistic basis, or whether the model was simply fortunately selected, but formation of mixed associates of type A_iB must be regarded as an assumption without any physical basis. In the present work it was attempted to answer this question and in addition to obtain further information relating to the association of alcohol–amine mixtures.

Experimental

The method reported earlier [1,2] was used to study the conductance of tri(*n*-butyl) amine–alcohol mixtures over the entire concentration range at 20 $\pm$ 0.1 and 45 $\pm$ 0.1° . The alcohols used were methanol, ethanol, 1-propanol and 1-butanol. These were Reanal products of analytically purest quality, while the amine was a Fluka product of analytically pure quality. Prior to use the amine was carefully freed from water. Measurements were made with a Radelkis OK-102/1 conductometer. The results are given in Tables I—IV.

Table I

Specific and molar specific conductances of methanol–tri(n-butyl)amine mixtures

c_{amine} mole · dm^{-3}	Specific conductance $\varkappa$, μS · cm^{-1}		Molar specific conductance 10^3 λ, Ω^{-1} · cm^2	
	20°	45°	20°	45°
0	2.02	11.34		
0.168	43.56	65.16	259.28	387.86
0.336	53.28	67.50	158.57	200.89
0.504	55.80	76.86	110.71	152.50
0.672	57.96	77.40	86.25	115.18
0.840	50.40	81.00	60.00	96.43
1.176	45.50	66.42	38.42	56.48
1.680	37.08	56.16	22.07	33.43
2.016	32.94	44.10	16.34	21.87
2.520	16.92	23.04	6.71	9.14
2.856	7.38	10.44	2.58	3.65
3.360	0.94	1.242	0.28	0.37
4.197	0	0.014	0	0

Table II

Specific and molar specific conductances of ethanol–tri(n-butyl)amine mixtures

c_{amine} mole · dm^{-3}	Specific conductance $\varkappa$, μS · cm^{-1}		Molar specific conductance 10^3 λ, Ω^{-1} · cmν	
	20°	45°	20°	45°
0	1.35	1.49		
0.168	5.81	7.61	34.58	45.33
0.336	7.16	8.15	21.31	24.27
0.504	7.33	9.36	14.54	18.57
0.672	8.80	9.54	13.09	14.20
0.840	8.70	9.36	10.36	11.14
1.176	7.33	8.26	6.23	7.02
1.680	5.47	5.42	3.25	3.22
2.016	3.55	3.42	1.76	1.70
2.520	1.39	1.22	0.55	0.48
2.856	0.50	0.46	0.17	0.16
3.360	0.05	0.05	0.02	0.01
4.197	0	0.02	0	0

Table III

Specific and molar specific conductances of 1-*propanol–tri(n-butyl)amine mixtures*

c_{amine} mole · dm^{-3}	Specific conductance $\varkappa$, μS · cm^{-1}		Molar specific conductance 10^3 λ, Ω^{-1} · cm^2	
	20°	45°	20°	45°
0	0.76	1.03		
0.168	2.38	2.88	14.17	17.14
0.336	2.75	3.22	8.18	9.59
0.504	2.77	3.51	5.50	6.96
0.672	2.92	3.29	4.34	4.90
0.840	2.63	3.11	3.13	3.70
1.176	2.14	2.47	1.82	2.10
1.680	1.28	1.33	0.76	0.79
2.016	0.75	0.75	0.37	0.37
2.520	0.22	0.23	0.09	0.09
2.856	0.08	0.08	0.03	0.03
3.360	0	0.02	0	0.01
4.197	0	0.01	0	0

Table IV

Specific and molar specific conductances of 1-*butanol–tri(n-butyl)amine mixtures*

c_{amine} mole · dm^{-3}	Specific conductance $\varkappa$, μS · cm^{-1}		Molar specific conductance 10^3 λ, Ω^{-1} · cm^2	
	20°	45°	20°	45°
0	0.31	0.41		
0.168	0.70	0.95	4.17	5.68
0.336	0.79	1.03	2.35	3.05
0.504	0.82	1.03	1.63	2.04
0.672	0.78	0.97	1.16	1.45
0.840	0.70	0.86	0.83	1.03
1.176	0.53	0.83	0.45	0.70
1.680	0.26	0.42	0.15	0.25
2.016	0.13	0.24	0.07	0.12
2.520	0.05	0.06	0.02	0.03
2.856	0	0.03	0	0.01
3.360	0	0	0	0
4.197	0	0	0	0

Discussion

Interpretation of the phenomena connected with association of the tert.-amine–alcohol mixtures is facilitated considerably by the fact that only a single amine molecule can take part in the mixed association. *Via* the free electron pair on its nitrogen atom, the amine may be linked by a single hydrogen bond to either one free monomeric alcohol molecule, or the chain-ending of a chain association of alcohol molecules. The mixed associates thus formed may therefore only be of A_iB type (where A denotes the alcohol, and B the tert.-amine molecule). Since an association of type A_iB was assumed in a model earlier [1] to interpret the electric conductance of alcohol–*n*-butylamine mixtures, this model was also used in an attempt to interpret our experimental data for the tri(*n*-butyl)amine–alcohol mixtures. As an example, Fig. 1 shows the specific conductance of the methanol–tri(*n*-butyl)amine system as a function of the amine concentration. In Fig. 2, $-\log(\lambda^2 \cdot c_{am})$ is plotted as a function of $\log c_{alc}$ for the same system. The latter plot permits calculation of the number n of alcohol molecules present in the electrolytically dissociated associations, assumed in the model to have an average composition A_nB, from the slope of the straight line (slope $= -n$). Accordingly, this was determined for every mixture examined, from the data measured at both 20 and 45°. Before turning to a quantitative evaluation on the basis of the model, it is to advantage to consider the results qualitatively.

It can be seen from the example presented that the specific conductance exhibits a maximum at an amine concentration of about 0.5 mole · dm^{-3}. The tabulated data reveal that neither the variation of the temperature nor a change in the alcohol component leads to a substantial alteration in the position of the maximum, which is practically constant in the systems under consideration.

It may also be stated that the specific conductance increases on the elevation of the temperature in every mixture, over the entire concentration interval. This is in contrast with what was observed for primary amine–alcohol mixtures, where the temperature coefficient of the specific conductance of mixtures containing several amine molecules turned out to be negative. The magnitude of the specific conductance at the concentration corresponding to the maximum conductance is characteristic for the alcohol component; it decreases monotonously from methanol to 1-butanol. This is illustrated in Fig. 3, where the logarithm of the maximum specific conductance ($\log \varkappa_{max}$) is plotted as a function of the reciprocal dielectric factor of the alcohol component. It may be concluded from the Figure that the decrease in the conductance with the change in the dielectric factor of the alcohol may be simply explained by the decrease in the electrolytic dissociation constant, *i.e.* in the number of ions participating in the conductance.

In the sense of the Bjerrum ion association theory, under comparable conditions the ion association is the more extensive, the smaller the dielectric factor of the solvent. It may be deduced from the theory how the equilibrium constant of the ion association, which is the reciprocal equilibrium constant of the ion dissociation, varies as a function of the dielectric factor of the solvent. ln K_d is an approximately linear function of $1/\varepsilon$, where K_d is the ion dissociation equilibrium constant, and ε is the dielectric factor [3].

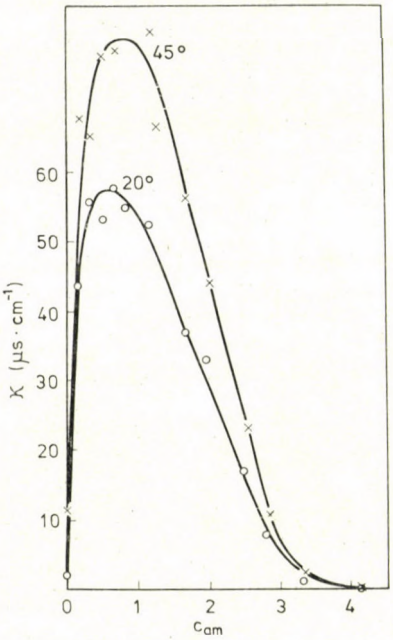

Fig. 1. Specific conductances of methanol–tri(*n*-butyl)amine mixtures at 20 and 45°

Since it may reasonably be assumed in the present case that the mixed associates are weak electrolytes and that their degree of electrolytic dissociation may be expressed using the molar specific conductance, it follows that, in the event of the validity of the correlation based on the Bjerrum theory, the logarithm of the molar specific conductance is also a linear function of $1/\varepsilon$. It has also been seen that the maximum in the specific conductance lies at the same amine concentration in every mixture examined; thus, ln $\varkappa_{max}$ may be plotted instead of log λ if a fixed mixed associate concentration relates to a given amine concentration. Reversing this sequence of ideas, it follows that a plot of log $\varkappa_{max}$ *vs.* $1/\varepsilon$ will yield a straight line if the concentration of mixed associates capable of dissociation is identical in every system examined at the amine concentration corresponding to the maximum conductivity. It can be seen from the Figure that, to a good approximation,

our results determine a straight line. This additionally means that at a given concentration there are approximately the same numbers of mixed associates in every system considered. This conclusion is well compatible with the experimental finding that the heats of mixing of tri(*n*-butyl)amine with the alcohols in question scarcely differ from one another at this concentration [4].

The applicability of the model derived with the assumption of association of type A_iB, *i.e.* the fact that the linearization derived from the model proved successful, is shown by the example presented in Fig. 2. The n values deter-

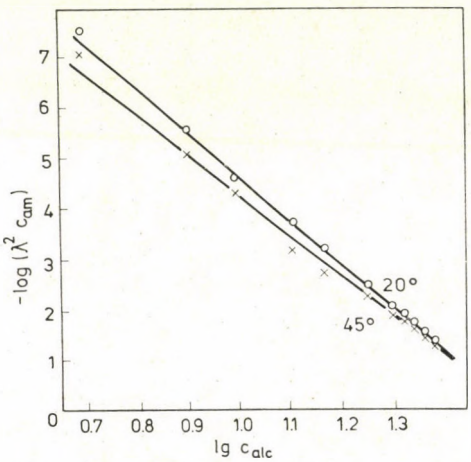

Fig. 2. Plot of $-\log(\lambda^2 \cdot c_{am})$ *vs.* $\log c_{alc}$ for methanol–tri(*n*-butyl)amine mixtures

mined from the experimental data, *i.e.* the average numbers of alcohol monomers in the electrolytically dissociated mixed associates, are given in Table V for every system examined, and for both temperatures.

The data in Table V lead to the following findings. At both temperatures the value of n increases on proceeding from methanol towards butanol. At

Table V

Average number n of alcohol monomers in electrolytically-dissociated mixed associations in tri(n-butyl)amine mixtures

Alcohol component	n	
	20°	45°
Methanol	5.5	5.1
Ethanol	7.1	7.1
1-propanol	7.6	8.5
1-butanol	9.4	10.1

the higher temperature, n decreases for methanol, is the same for ethanol, and increases for 1-propanol and 1-butanol.

Before any further discussion of our results, we wish to point out the earlier mentioned circumstance that the average association degree of the alcohol component and the determined value of n may be significantly different. This is explained in that the mixed associates containing several alcohol molecules of necessity dissociate to ions more easily than those in which there are few alcohol molecules, and thus n is not the same as the average i value for mixed associates of the type A_iB present in the system; further,

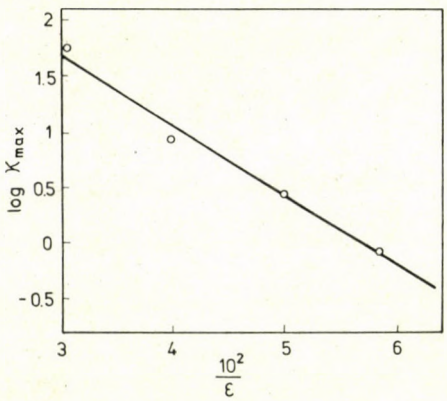

Fig. 3. Maximum specific conductance of alcohol–amine mixtures as a function of the dielectric factor of the alcohol component at 20°

it can not be excluded that the average association degree in the A_j-type associations of alcohol molecules is different from that in the mixed associates.

If all these factors are taken into account, far-reaching conclusions can not be drawn from the value of n, with regard to either the average association degree of the pure alcohol, or that of the mixed association. Nevertheless, information on the association conditions in the pure alcohols is provided by the variation in the value of n as a function of temperature. This can be interpreted *via* the following sequence of ideas.

(a) If chain associates are present to a predominant extent in the pure alcohol, than at all events an increase in the temperature is accompanied by a decrease in the average association degree. It follows from this that as the temperature of the mixture rises, of necessity the average association degree of the mixed associates also decreases, and together with it the value of n for the ionically dissociating associates. The methanol–tri(n-butyl)amine system was found to behave in this way.

(b) If cyclic associates consisting of a few molecules predominate in the pure alcohols, then as the temperature rises the average association degree may increase, for as the hydrogen bonds holding the rings together break, an increasing number of chain associates are formed, which may link together to yield long chains. Hence, in the certain temperature interval where the rings are progressively converted to chains, the average association degree of the pure alcohol may increase with the rise of temperature. This phenomenon may lead to the result that both the number of alcohol molecules

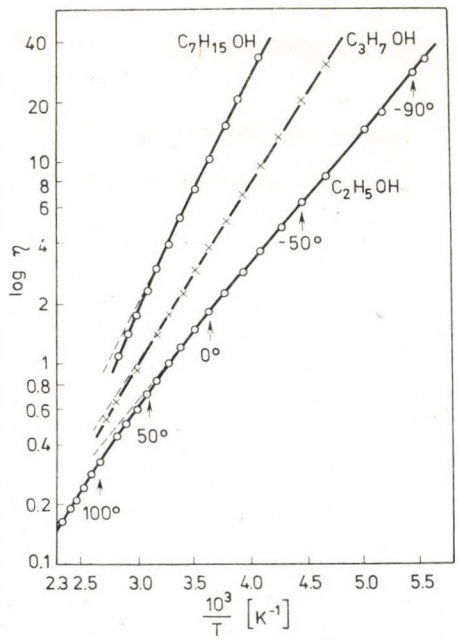

Fig. 4. Temperature dependence of the viscosities of some pure alcohols, in the plotting log η *vs.* $1/T$

in the mixed associates and the value of n may increase with rising temperature in alcohol–amine mixtures. This was observed for the mixtures of tri(*n*-butyl)amine with 1-propanol or 1-butanol.

It must be noted that the fact of an increasing average association degree with elevation of the temperature in pure alcohols is proved by the phenomenon that the activation enthalpies of viscous flow for the alcohols (to a good approximation a mesure of the average molar mass of the associates) begin to increase on proceeding to higher temperatures in just the temperature range under consideration. This is shown in Fig. 4, based on literature data [5].

The plotted data include those for ethanol, and it can be seen that the log η *vs.* $1/T$ curve is indicative of the rupture of the cyclic associates at higher

temperature for this alcohol too. At the same time, the value of n calculated from the electric conductance was found to be constant. This can probably be explained in that the conductance was examined over only a relatively narrow temperature range, and this was not sufficient to demonstrate the change in the n value in this case.

Reference should be made here to the fact that when the properties of alcohol–hydrocarbon mixtures were investigated, primarily cyclic associates were found to form in the cases of 1-pentanol and 1-heptanol [6]. This result is in agreement with the conclusion that may be drawn from the temperature -dependence of the n values. It may be seen that for the most part methanol in the pure state forms chain associates, whereas the higher homologues tend increasingly to form cyclic association polymers as the molecular weight increases. This result also explains the previously uninterpreted phenomenon that with every primary, secondary or tertiary amine examined methanol gives a considerably larger exothermic heat of mixing than the other alcohol homologues, since in methanol there is no need for the energy-consuming splitting of the rings of the alcohol associates as the mixed associates are being formed [7—9].

REFERENCES

[1] RATKOVICS, F., LÁSZLÓ, A., SALAMON, T.: Magyar Kém. Folyóirat **82,** 30 (1976)
[2] RATKOVICS, F., LÁSZLÓ-PARRAGI, M.: Acta Chim. (Budapest), **84,** 45 (1975)
[3] ERDEY-GRÚZ T.: Transzportfolyamatok vizes oldatokban (Transport processes in aqueous solutions)
[4] RATKOVICS, F., SALAMON, T.: Acta Chim. (Budapest), **88,** (in press)
[5] RAZNJEVIC, K.: Hőtechnikai táblázatok (Thermal Engineering Tables). Műszaki Könyvkiadó, Budapest, Zagreb, 1964
[6] SALAMON, T., LISZI, J., RATKOVICS, F.: Acta Chim. (Budapest), **87,** 137 (1975)
[7] RATKOVICS, F., LISZI, J., LÁSZLÓ, M.: Acta Chim. (Budapest), **79,** 387 (1973)
[8] RATKOVICS, F., LÁSZLÓ, M.: Acta Chim. (Budapest), **79,** 395 (1973)
[9] RATKOVICS, F., GUTI, ZS.: Acta Chim. (Budapest), **83,** 63 (1974)

Ferenc RATKOVICS
Mária LÁSZLÓ
H-8201 Veszprém.

Acta Chimica Academiae Scientiarum Hungaricae, Tomus 93 (3—4), pp. 267—277 (1977)

PROPERTIES OF ALCOHOL–AMINE MIXTURES, XIII

ELECTRIC CONDUCTANCE IN MIXTURES OF PRIMARY OR SECONDARY AMINES WITH ALCOHOLS

F. RATKOVICS and M. LÁSZLÓ

(Electrochemistry Department Research Group of the Hungarian Academy of Sciences, Department of Physical Chemistry, University of Chemical Industries Veszprém)

Received May 20, 1976

A study was made of the electric conductances of *n*-butylamine – alcohol and di(*n*-butyl)amine—alcohol mixtures at 0, 20 and 45°. The results were evaluated with the aid of a model based on the assumption of the elctrolytic dissociation of mixed associates of the type A_nB. The results reveal that di(*n*-butyl)amine primarily forms mixed associates of type A_nB, and to a lesser extent those of type A_iB_j. In *n*-butylamine–alcohol mixtures it is necessary to consider association not only of type A_nB, but also of type A_iB_j, especially in the range of medium alcohol concentrations. Investigation of the temperature dependence of the number of alcohol molecules found in the mixed associates confirmed the conclusion drawn previously from other results, that the cyclic structure is increasingly more characteristic for the self-association of the pure alcohols on proceeding from methanol towards 1-butanol.

It was earlier shown [1] that study of the electric conductance of tertiary amine–alcohol mixtures gives a possibility for the determination of some of the alcohol–amine associates. By means of examinations of the effect of temperature changes, conclusions could be drawn with regard to the association conditions in the pure alcohols too; it was found that on proceeding from methanol towards the higher homologues, the pure alcohols consist increasingly of cyclic associates. It was also found that the electric conductance of tertiary amine–alcohol mixtures could be attributed to the electrolytic dissociation of mixed associates of the type A_iB. The average numbers of alcohol molecules in the electrolytically dissociating mixed associates were determined at 20 and 45°.

The present paper deals with the electric conductance of primary and secondary amine–alcohol mixtures. Examinations were made by the method reported earlier [2]. The alcohols were Reanal products of analytically purest quality, while *n*-butylamine and di(*n*-butyl)amine were Fluka products of analytically pure quality. Before use, all compounds were carefully freed from water. The experimental results are given in Tables I—VIII.

Data measured at 0 and 20° on the conductance of *n*-butylamine–alcohol mixtures were published previously [3].

Table I

Specific and molar specific conductances of methanol–di(n-butyl)amine mixtures

c_{amine} mole · dm^{-3}	Specific conductance $\varkappa$, μS · cm^{-1}		Molar specific conductance 10^3 λ, Ω^{-1} · cm^2	
	20°	45°	20°	45°
0	2.02	11.34		
0.235	101.52	111.60	432.00	474.89
0.470	119.16	126.00	253.53	268.08
0.705	119.88	124.20	170.04	176.17
0.940	110.34	131.40	117.38	139.79
1.175	101.34	126.00	86.25	107.23
1.644	76.50	95.40	46.53	58.03
2.349	38.88	67.14	16.55	28.58
2.818	24.12	43.92	8.56	15.58
3.523	9.54	6.21	2.71	1.76
3.993	3.42	5.92	0.86	1.48
4.698	0.35	0.63	0.08	0.13
5.872	0	0.02	0	0.01

Table II

Specific and molar specific conductances of ethanol–di(n-butyl)amine mixtures

c_{amine} mole · dm^{-3}	Specific conductance $\varkappa$, μS · cm^{-1}		Molar specific conductance 10^3 λ, Ω^{-1} · cm^2	
	20°	45°	20°	45°
0	1.35	1.89		
0.235	7.88	18.36	33.55	58.98
0.470	11.16	14.22	23.74	30.25
0.705	10.80	15.84	15.32	22.47
0.940	9.36	13.14	9.96	13.98
1.175	9.00	11.88	7.66	10.11
1.644	7.02	9.36	4.38	5.69
2.349	3.60	5.00	1.53	2.13
2.818	2.16	2.84	0.77	.101
3.523	0.66	0.94	0.19	0.26
3.993	0.24	0.37	0.06	0.09
4.698	0	0.07	0	0.01
5.872	0	0.01	0	0

Table III

Specific and molar specific conductances of 1*-propanol–di(n-butyl)amine mixtures*

c_{amine} mole · dm^{-3}	Specific conductance $\varkappa$, μS · cm^{-1}		Molar specific conductance 10^3 λ, Ω^{-1} · cm^2	
	20°	45°	20°	45°
0	2.76	1.03		
0.235	2.79	4.66	11.87	19.84
0.470	2.68	3.87	5.70	8.23
0.705	2.56	3.74	3.63	5.31
0.940	2.29	3.33	2.44	3.54
1.175	2.07	2.95	1.76	2.51
1.644	1.37	2.05	0.83	1.25
2.349	0.69	0.94	0.29	0.40
2.818	0.37	0.48	0.13	0.17
3.523	0.11	0.12	0.03	0.04
3.993	0	0	0	0
4.698	0	0	0	0
5.872	0	0	0	0

Table IV

Specific and molar specific conductances of 1*-butanol–di(n-butyl)amine mixtures*

c_{amine} mole · dm^{-3}	Specific conductance $\varkappa$, μS · cm^{-1}		Molar specific conductance 10^3 λ, Ω^{-1} · cm^2	
	20°	s 45°	20°	45°
0	0.31	0.40		
0.235	0.90	1.15	3.83	4.90
0.470	0.81	1.12	1.72	2.39
0.705	0.70	0.97	0.99	1.38
0.940	0.66	0.85	0.70	0.91
1.175	0.57	0.80	0.48	0.68
1.644	0.36	0.49	0.22	0.30
2.349	0.16	0.20	0.07	0.09
2.818	0.10	0.10	0.03	0.03
3.523	0.01	0.03	0	0.01
3.993	0	0	0	0
4.698	0	0	0	0
5.872	0	0	0	0

Table V

Specific and molar specific conductances of methanol–n-butylamine mixtures at 45°

c_{amine} mole · dm^{-3}	Specific conductance $\varkappa$, μS · cm^{-1}	Molar specific conductance 10^3 λ, Ω^{-1} · cm^2
0	11.34	
0.404	149.40	369.80
0.808	181.80	225.00
1.212	192.60	158.91
1.616	196.20	121.41
2.021	183.60	90.85
2.829	131.40	46.45
4.042	93.60	23.16
4.850	65.16	13.43
6.062	29.70	4.90
6.871	18.18	2.64
8.083	4.19	0.52
10.104	0.03	0.01

Table VI

Specific and molar specific conductances of ethanol–n-butylamine mixtures at 45°

c_{amine} mole · dm^{-3}	Specific conductance $\varkappa$, μS · cm^{-1}	Molar specific conductance 10^3 λ, Ω^{-1} · cm^2
0	1.89	
0.404	17.64	43.66
0.808	19.62	24.28
1.212	21.96	18.12
1.616	21.96	13.59
2.021	19.80	9.80
2.829	17.64	6.23
4.042	14.22	3.52
4.850	11.16	2.30
6.062	6.48	1.07
6.871	3.53	0.51
8.083	0.95	0.12
10.104	0.03	0.01

Table VII

Specific and molar specific conductances of 1-*propanol–n-butylamine mixtures at* 45°

c_{amine} mole · dm^{-3}	Specific conductance $\varkappa$, μS · cm^{-1}	Molar specific conductance 10^3 λ, Ω^{-1} · cm^2
0	1.03	
0.404	4.69	11.61
0.808	6.05	7.48
1.212	6.43	5.30
1.616	6.77	4.19
2.021	6.08	3.01
2.829	5.00	1.77
4.042	2.97	0.73
4.850	2.12	0.44
6.062	1.03	0.17
6.871	0.52	0.08
8.083	0.17	0.02
10.104	0.02	0

Table VIII

Specific and molar specific conductances of 1-*butanol–n-butylamine mixtures at* 45°

c_{amine} mole · dm^{-3}	Specific conductance $\varkappa$, μS · cm^{-1}	Molar specific conductance 10^3 λ, Ω^{-1} · cm^2
0	0.41	
0.404	1.96	4.86
0.808	2.21	2.74
1.212	2.83	2.33
1.616	3.28	2.03
2.021	2.90	1.43
2.829	2.05	0.72
4.042	1.76	0.44
4.850	1.33	0.27
6.062	0.72	0.12
6.871	0	0
8.083	0	0
10.104	0	0

Discussion

Since the properties of the tertiary amine–alcohol mixtures (the simplest systems as regards association) are already known [1], it is reasonable to discuss the present results in comparison with these earlier ones. The systems containing the secondary amine will first be discussed in sequence: the secondary amine may form only two hydrogen bonds to one alcohol or one other amine molecule, its self-association is not extensive, and dielectric studies show that it forms chain-like association polymers in the pure state [4].

Di(n-butyl)amine–alcohol mixtures

Let us first examine the specific conductance in the di(*n*-butyl)amine–alcohol mixtures as functions of temperature and concentration. Figure 1 illustrates the results for the mixture with methanol. The shapes of the curves are similar for the mixtures with the other alcohols, but on proceeding from methanol to butanol the concentration relating to the maximum conductance is shifted from 0.5 to 0.25 mole. $\cdot$ dm^{-3}. On elevation of the temperature, the specific conductance increased in every secondary amine–alcohol mixture examined.

The compositions of the mixed associates participating in electrolytic dissociation were determined on the basis of the method developed earlier [2]. According to the model, a plot of log ($\lambda^2 \cdot c_{am}$) must be linear. This is shown in Fig. 2 on the data for the di(*n*-butyl)amine–methanol system. It can be

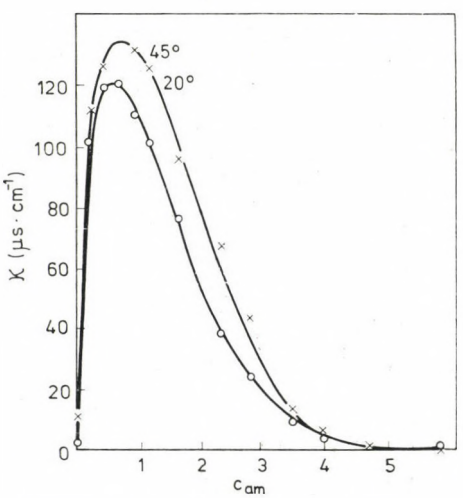

Fig. 1. Specific conductances of methanol–di(*n*-butyl)amine mixtures at 20 and 45°

seen that, in accordance with expectations, the results yield straight lines. The slopes of these give the number n of alcohol molecules in the electrolytically dissociating mixed associates of average composition A_nB. These results are listed in Table IX for every secondary amine–alcohol mixture examined, at 20 and 45°.

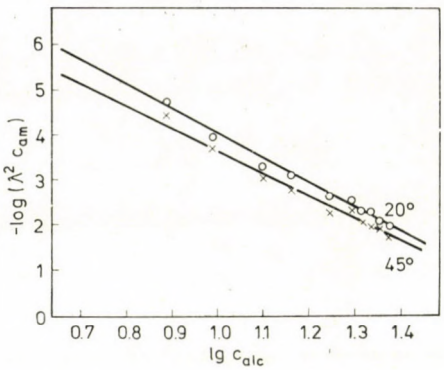

Fig. 2. Linearization of molar specific conductances of methanol–di(*n*-butyl)amine mixtures at 20 and 45°

Table IX

Average number n of alcohol molecules in the electrolytically-dissociating mixed associates

Mixture	n	
	20°	45°
di(*n*-butyl)amine–methanol	8.75 (5.5)*	8.00 (5.1)
di(*n*-butyl)amine–ethanol	9.0 (7.1)	9.00 (7.1)
di(*n*-butyl)amine–1-propanol	10.20 (7.6)	10.80 (8.5)
di(*n*-butyl)amine–1-butanol	10.75 (9.4)	11.75 (10.4)

* For comparison, the data relating to the corresponding tri(*n*-butyl)amine mixtures are given in brackets

It follows from the structure of the di(*n*-butyl)amine molecule that it may form two types of mixed associate.

(a) *Via* one hydrogen bond it may be linked to a chain-like alcohol associate:

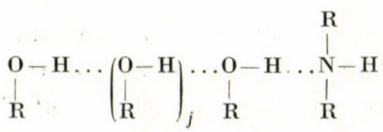

or A_nB where $n = j + 2$

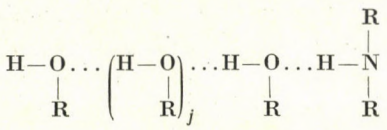

but as regards these two structures electrolytic dissociation is probable only in the former case, when $H_2NR_2^+$ and $(ROH)_{j+1}RO^-$ may be formed.

(b) *Via* two hydrogen bonds it may be linked to two chain-like alcohol associates:

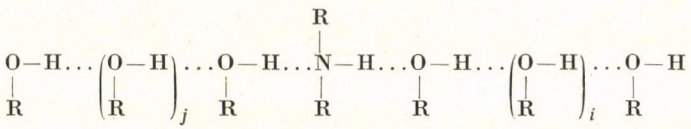

From this mixed association, which is similarly of type A_nB, where $n = j + 2 + i + 2 \sim 2\ (j + 2)$, ions may be formed without any difficulty: $(ROH)_{j+1}RO^-$ and $(ROH)_{i+1}RO \cdot H_2NR_2^+$.

The same result is reached if it is assumed that $R_2NH_2^+$ forms an associate with a chain-like alcohol associate.

Of the possibilities given here, only the first is analogous with the association process possible in tri(*n*-butyl)amine mixtures, and thus an explanation must be sought for why the *n* observed for the secondary amine are larger than the values measured for the tertiary amine. The reason is that the association process variant (b) also occurs. This process is particularly important in methanol, where chain formation has been shown to be characteristic of the associate of the pure alcohol. The *n* values for the higher alcohol analogues containing few chain associates are scarcely larger than the values determined with the tertiary amine, and hence the great majority of the mixed associates are formed as in variant (a).

The temperature dependence of *n* is the same as that observed for tertiary amines, and thus supports the conclusion [1] that pure methanol consists for the most part of chain associates, and the higher homologues to an ever increasing extent of cyclic associates.

The self-association of di(*n*-butyl)amine was not taken into account in the evaluation, for in the pure state this is quite low (the average association degree $\alpha = 1.26$), and it may be presumed that it is even less important in the presence of alcohol [5].

n-Butylamine–alcohol mixtures

From a qualitative aspect the results here differ from those reported above only insofar as the specific conductance of the *n*-butylamine–methanol mixture exhibits a slight decrease on elevation of the temperature.

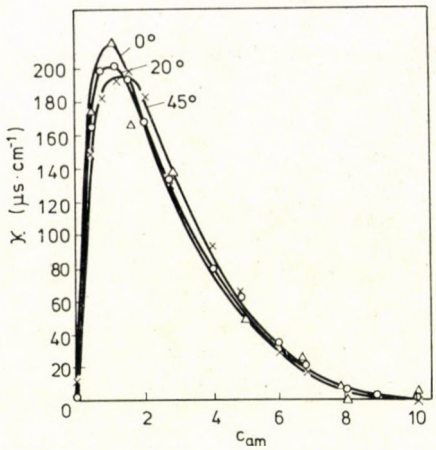

Fig. 3. Specific conductances of methanol–*n*-butylamine mixtures at 0, 20 and 45°

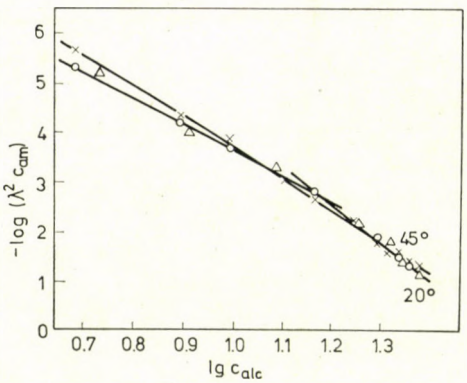

Fig. 4. Linearization of molar specific conductances of methanol–*n*-butylamine mixtures at 20 and 45°

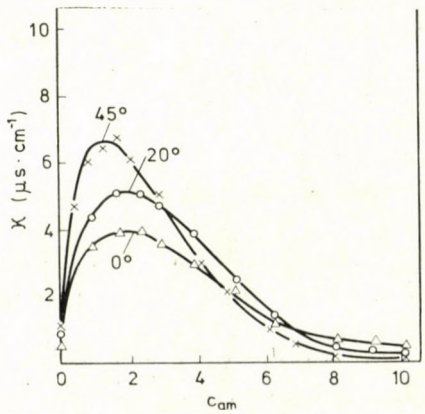

Fig. 5. Specific conductances of propanol–*n*-butylamine mixtures at 0, 20 and 45°

In these systems too linearization based on the association model is successful, but it is striking that in the methanol-containing system a steeper linear section was observed at log $c_{alc} > 1.15$ than at lower alcohol concentrations. The differences are illustrated in Figs 3–6.

The results obtained from the slopes of the straight lines regarding the numbers of alcohol molecules in the electrolytically dissociating mixed associates are given in Table X.

Table X

Number n of alcohol molecules in the electrolytically-dissociating mixed associations

Mixture	n*					
	0°		20°		45°	
n-butylamine–methanol	(7.85)	5.25	(7.85)	5.25	(7.6)	6.25
n-butylamine–ethanol		6.62		5.60		5.40
n-butylamine–1-propanol		4.54		5.34		6.72
n-butylamine–1-butanol		4.43		5.10		5.37

* The values in brackets relate to the initial high alcohol concentration. The results at 0 and 20° were obtained earlier [3]

The tabulated data show that in every mixture the value of n is much lower than in mixtures of the same alcohol with tertiary amines. It follows that associates of the type A_iB_j must also be present in significant amounts, for only in this way are there so few alcohol molecules per one amine molecule as assumed in the model.

The initial steep section observed for methanol shows that primarily associate of type A_iB occurs at high alcohol concentrations, particularly in methanol, where there is a favourable possibility for this because of the chain nature of the self-association of the alcohol.

As already referred to, the finding that the differential dn/dT is positive means that the cyclically associated structure of the alcohol changes with increasing temperature: every more and longer chain polymers are formed. These chain associates next interact with the amine present to form mixed associates capable of dissociation. This can be seen in comparison with our earlier results in the cases of 1-propanol and 1-butanol too, but in these systems the increase in the value of n may also result from the self-association of the primary amine decreasing, and the mixed associate, complexes of type A_iB_j being converted to be of type A_iB.

This phenomenon may be held responsible for the fact that in the case of methanol, where $dn\ dT$ was always negative in mixtures containing secondary or tertiary amines and it was thus concluded that the chain association

of methanol plays a dominant role, dn/dT is not clearly negative here. It appears probable that whereas the decrease of the chain length of the alcohol associates with the rise of temperature means a negative contribution to dn/dT, if the mixed associates of type A_iB_j containing several amine molecules are transformed to be of type A_iB then the value of n is increased. This conception is also supported by the fact that at high methanol concentrations, where the A_iB-type associate has been seen to predominate, the expected decrease occurs between 20 and 45° (from 7.85 to 7.60). At lower alcohol concentrations, where the association is presumably of type A_iB_j, in agreement with what has been said an increase in the value of n was observed.

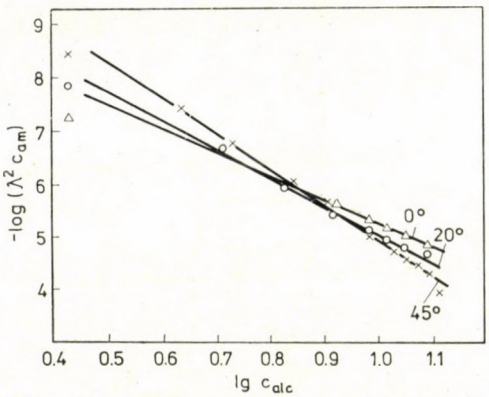

Fig. 6. Linearization of molar specific conductances of propanol–*n*-butylamine mixtures at 0, 20 and 45°

One sign of the inadequacy of the model is that the error in the determination of the n values depends on the concentration interval over which the measurements extend. In the range we employed the mean error was $\pm 2\sigma = 0.1$; together with the magnitude of the observed effects compared to one another, this does not permit further calculations to be carried out from our results with the necessary certainty, but in our view there can be no doubt as to the reliability of the qualitative conclusions.

REFERENCES

[1] RATKOVICS, F., LÁSZLÓ, M.: Magyar Kémiai Folyóirat (in press)
[2] RATKOVICS, F., LÁSZLÓ, M.: Magyar Kémiai Folyóirat **80,** 310 (1974)
[3] RATKOVICS, F., LÁSZLÓ, M., SALAMON, T.: Magyar Kémiai Folyóirat **82,** 30 (1976)
[4] RATKOVICS, F., DOMONKOS, L.: Magyar Kémiai Folyóirat **82,** 109 (1976)
[5] RATKOVICS, F., SALAMON, T.: Magyar Kémiai Folyóirat (in press)

Ferenc RATKOVICS
Mária LÁSZLÓ
H-8201 Veszprém.

Acta Chimica Academiae Scientiarum Hungaricae, Tomus 93 (3—4), pp. 279—288 (1977)

ON THE APPLICABILITY OF THE V. S. E. P. R. MODEL FOR THE MOLECULAR GEOMETRIES OF SOME TETRAHEDRAL AND RELATED MOLECULES*

I. HARGITTAI** and A. BARANYI***

*(**Central Research Institute of Chemistry, Hungarian Academy of Sciences and ***Research Institute for Telecommunication, Budapest)*

Received June 2, 1976

Most geometrical variations in tetrahedral and related systems are in agreement with the predictions of the V.S.E.P.R. model as is demonstrated by recent experimental data. It is not generally valid, however, that the bond angles decrease as the number of lone electron pairs increases. A simple point-charges-on-the-sphere model is not capable to predict the relationship of bond angles in molecule pairs of AX_3E and AX_2E_2.

The valence shell electron pair repulsion (V. S. E. P. R.) model [2] is successfully used for accounting for and explaining variations of molecular geometries in extensive classes of inorganic compounds. This model finds as well its application for tetrahedral and related molecules, such as AX_4, AX_3E and AX_2E_2, where A is the central atom. X is the ligand and E is the lone electron pair.

Each pair of molecules such as NX_3, OX_2, PX_3, SX_2, or SOX_2, SO_2X_2 with X = Cl and F ligands strictly follow the empirical rules of the V. S. E. P. R. model. This has been repeatedly demonstrated and recent experimental data lend further support to this observation (*cf.* Tables I and II).

Further examples are provided by the geometrical parameters of a series of XSO_2Y molecules, of which only the bond angles are presented in Table III to illustrate their relationship.

$$\sphericalangle X-S-Y < \sphericalangle O=S-X, \quad \sphericalangle O=S-Y < \sphericalangle O=S=O$$

Note that older data presented for a similar series in Ref. 2[+] were less conclusive for the relationship between the X–S–X and O=S–X bond angles.

The data in Tables I and II provide also a different kind of comparison, *viz.* the variations in the bond angles when bonding pairs are replaced by lone pairs of electrons. GILLESPIE noted [2] in his book (p. 40) that "...in the series CH_4, NH_3 and H_2O the bond angle decreases from 109.5° to 107.3° and to 104.5° as the number of non-bonding pairs increases."

* Reported to the Second European Crystallographic Meeting, Keszthely, 1974 [1].
[+] p. 155, Table 7. 11 [2].

Table I

*X—A—X bond angles in AX_3E and AX_2E_2 molecules**

AX_3E	X—A—X (°)	AX_2E_2	X—A—X (°)
NH_3	108.2 [3]	OH_2	107.2 [9]
NCl_3	107.1 [4]	OCl_2	111.2 [10]
NF_3	102.4 [5]	OF_2	103.2 [11]
PH_3	93.5 [6]	SH_2	92.2 [12]
PCl_3	100.3 [7]	SCl_2	103.0 [13]
PF_3	97.8 [8]	SF_2	98.2 [14]

* All data refer to vapour phase

Table II

*Halogen–sulphur–halogen bond angles in some simple molecules**

SO_2X_2	X—S—X (°)	SOX_2	X—S—X (°)	SX_2	X—S—X (°)
SO_2Cl_2	100.0 [15]	$SOCl_2$	96.1 [15]	SCl_2	103.0 [13]
SO_2F_2	96.1 [16]	SOF_2	92.2 [17]	SF_2	98.2 [14]

X = Cl or F

* All data refer to vapour phase

Table III

*Bond angles in some simple sulphone molecules**

XSO_2Y	X—S—Y (°)	O=S=O (°)	X—S=O (°)	O=S—Y (°)	References
FSO_2F	96.1	124.0	108.3		[16]
$ClSO_2Cl$	100.0	123.5	107.7		[15]
CH_3SO_2F	98.2	123.1	110.0	106.2	[18]
CH_3SO_2Cl	101.0	120.8	109.5	107.1	[19]
$CH_3SO_2CH_3$	102.6	119.7	108.2		[20]
$(CH_3)_2NSO_2Cl$	103.0	122.7	108.8	105.8	[21]
$C_6H_5SO_2Cl$	100.9	122.5	110.0	105.5	[22]

* All data refer to vapour phase

Going from the four ligand case to the three ligand plus one lone electron pair case is simple. The ligand bonding pair is replaced by a lone pair with larger space requirements around the central atom and thus exercising more repulsion toward the other bonding electron pairs. Consequently, the bond angles decrease. The data of Table I as illustrated also by Fig. 1 show complete agreement with the above statement.

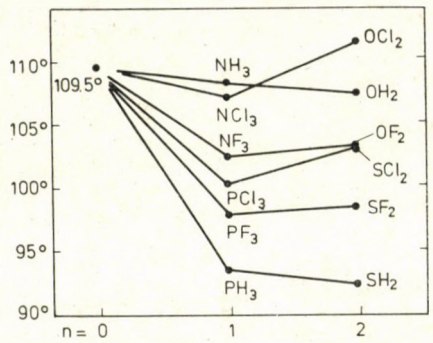

Fig. 1. Variations in the bond angles in tetrahedral systems with no, one, and two lone pairs of electrons (n) in the valence shell of the central atom

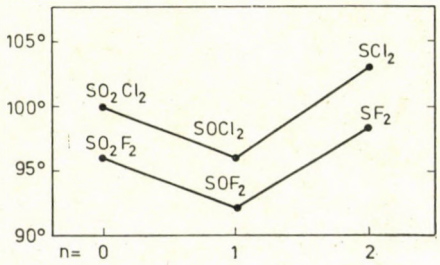

Fig. 2. Variations in the bond angles in SO_2X_2, SOX_2E, and SX_2E_2 (X = F or Cl) systems (n number of lone pairs of electrons in the valence shell of the sulphur atom)

As a second ligand of AX_3E is replaced by an other lone pair, a further decrease of the X–A–X bond angle would be expected according to GILLESPIE's original statement. This is observed, however, for NH_3, H_2O and PH_3, SH_2 pairs only, while for other compound pairs with chlorine or fluorine ligands the opposite trend is realized, as seen in Table I and Fig. 1.

For systems with double bonds, the application of the V. S. E. P. R. model is more difficult for similar comparisons, since this model does not decide whether or not a lone pair will be larger than a double bond. The data for SO_2X_2 and SOX_2 (Table II) may indicate that in case of sulphur as central atom the lone pair is larger than the double bond.

Following the decrease in the bond angle as one of the oxygen atoms is substituted by a lone pair, a further decrease of the X–S–X bond angle could be expected as the remaining oxygen of SOX_2 is replaced by an other lone pair. However, the opposite is observed (Table II, Fig. 2).

The interpretation of the changes of the bond angles as going from the three ligand plus one lone pair case to the two ligand plus two lone pair case is rather complicated since in addition to the bonding pair — bonding pair and bonding pair — lone pair repulsions, there are also lone pair — lone pair repulsions present. The resulting configuration depends, in the final account, on the relative magnitudes of the three different types of interactions.

To examine further the above changes, a simple point-charges-on-the--sphere model was constructed in which bonding electron pairs and lone

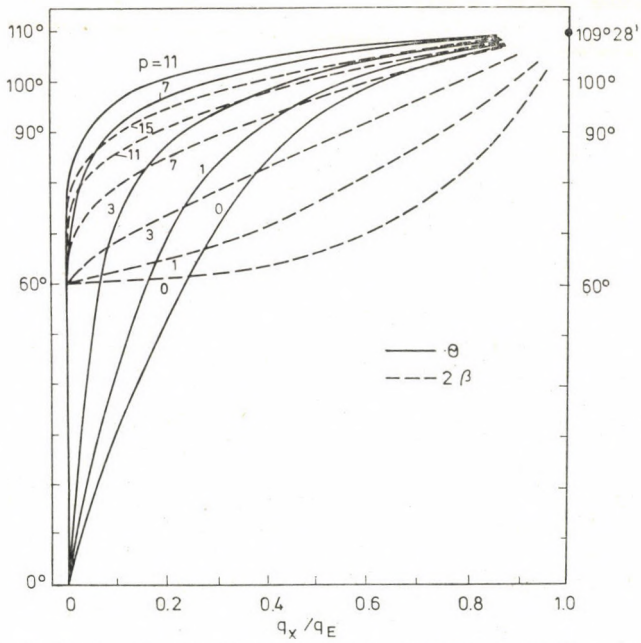

Fig. 3. Variations in the bond angles Θ and 2β for the AX_3E and AX_2E_2 systems, resp., plotted against the ratio of the charges q_X/q_E as calculated for different values of the repulsion exponent p

electron pairs are represented by a smaller charge (q_X) and a larger charge (q_E), respectively. The configuration is then determined in which only radial forces may act on the charges (see Appendix).At the same time it is strongly emphasized that using the charges q_X and q_E implies by no means that the origin of repulsions is simply electrostatic.

The results of the calculations are demonstrated by Fig. 3. showing the variations of the bond angles in the AX_3E (Θ) and AX_2E_2 (2β) systems

vs. the ratio of the two different charges. The calculations were performed for different values of the repulsion exponent p. It is seen that Θ is always smaller than 109°28′, while 2β may be larger or smaller than Θ depending on the values of p. Thus, the changes in bond angles as going from AX_4 to AX_3E are generally well understood* and are invariant to the choice of the repulsion exponent. On the other hand, the relationship between the bond angles of molecule pairs AX_3E and AX_2E_2 strongly depends on the choice of the repulsion exponents and, accordingly, the simple model loses its predictive power for these structural changes.

Summarizing, although many structural variations in tetrahedral and related molecules are in agreement with the predictions of the V. S. E. P .R. model, it is not generally valid that the bond angles decrease as the number of lone electron pairs increases. In this respect the molecules with hydrogen turn out to be rather the exceptions. It would be tempting to speculate on possibile explanations concerning this anomaly. The model, however, ignores too many important factors to make such speculations justified.

*

Useful discussions on the subject with numerous colleagues are acknowledged.

Appendix

In this section the relationship between the charge ratio q_X/q_E and the angles characterizing the configurations of the AX_3E and AX_2E_2 systems will be derived assuming a points-on-the-sphere model.

A Cartesian co-ordinate system with $\bar{i}$, $\bar{j}$ and $\bar{k}$ unit vectors will be considered. The point charges are located on the surface of a sphere with unity radius.

The AX_3E case

According to Fig. A1, $\sphericalangle$ E–A–X $= 90° + \varphi$ and $\sphericalangle$ X–A–X is labelled by Θ. Either of these angles determines the configuration of the system with C_{3v} symmetry;

$$\cos\Theta = 1 - \frac{3}{2}\cos^2\varphi\,. \tag{1}$$

* The larger than tetrahedral angle in OCl_2 may be a consequence of the relatively large size of the ligands.

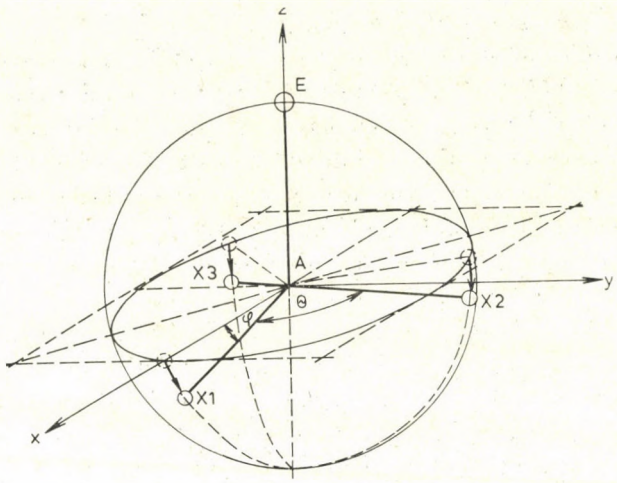

Fig. A1. Geometrical model for the AX_3E system

The position vectors of the points are

$$\begin{aligned}
\bar{r}_{\mathrm{E}} &= \bar{k} \\
\bar{r}_{\mathrm{X1}} &= \cos\varphi\ \bar{i} - \sin\varphi\,\bar{k} \\
\bar{r}_{\mathrm{X2}} &= -\frac{1}{2}\cos\varphi\,\bar{i} + \frac{\sqrt{3}}{2}\cos\varphi\,\bar{j} - \sin\varphi\,\bar{k} \\
\bar{r}_{\mathrm{X3}} &= -\frac{1}{2}\cos\varphi\,\bar{i} - \frac{\sqrt{3}}{2}\cos\varphi\,\bar{j} - \sin\varphi\,\bar{k}
\end{aligned} \tag{2}$$

The force between the charges q_1 and q_2 with position vectors $\bar{r}_1$ and $\bar{r}_2$, respectively, is expressed as follows:

$$\bar{F}_{1,2} = \frac{\bar{r}_1 - \bar{r}_2}{|\bar{r}_1 - \bar{r}_2|^{p+1}}\, q_1 q_2 ,$$

Thus the resultant force acting on the charge X_1

$$\bar{F}_{\mathrm{X1}} = \bar{F}_{\mathrm{X1,X2}} + \bar{F}_{\mathrm{X1,X3}} + \bar{F}_{\mathrm{X1,E}} =$$

$$= \frac{\bar{r}_{\mathrm{X1}} - \bar{r}_{\mathrm{X2}}}{|\bar{r}_{\mathrm{X1}} - \bar{r}_{\mathrm{X2}}|^{p+1}}\, q_{\mathrm{X}}^2 + \frac{\bar{r}_{\mathrm{X1}} - \bar{r}_{\mathrm{X3}}}{|\bar{r}_{\mathrm{X1}} - \bar{r}_{\mathrm{X3}}|^{p+1}}\, q_{\mathrm{X}}^2 + \frac{\bar{r}_{\mathrm{X1}} - \bar{r}_{\mathrm{E}}}{|\bar{r}_{\mathrm{X1}} - \bar{r}_{\mathrm{E}}|^{p+1}}\, q_{\mathrm{X}} q_{\mathrm{E}}$$

$$\bar{F}_{X1} = \frac{\frac{3}{2}\cos\varphi\,\bar{i} - \frac{\sqrt{3}}{2}\cos\varphi\,\bar{j}}{(\sqrt{3}\cos\varphi)^{p+1}} q_X^2 + \frac{\frac{3}{2}\cos\varphi\,\bar{i} + \frac{\sqrt{3}}{2}\cos\varphi\,\bar{j}}{(\sqrt{3}\cos\varphi)^{p+1}} q_X^2 +$$

$$+ \frac{\cos\varphi\,\bar{i} - (\sin\varphi + 1)\,\bar{k}}{(\sqrt{2 + 2\sin\varphi})^{p+1}} q_X q_E = \tag{3}$$

$$= \frac{3\cos\varphi\,\bar{i}}{(\sqrt{3}\cos\varphi)^{p+1}} q_X^2 + \frac{\cos\varphi\,\bar{i} - (\sin\varphi + 1)\,\bar{k}}{(\sqrt{2 + 2\sin\varphi})^{p+1}} q_X q_E$$

For the points-on-the-sphere model the force $\bar{F}_{X1}$ has the only nonzero component in the direction of the position vector $\bar{r}_{X1} = \cos\varphi\,\bar{i} - \sin\varphi\,\bar{k}$, therefore the vectorial product of $\bar{F}_{X1}$ and $\bar{r}_{X1}$ is zero:

$$\bar{F}_{X1}\, x\, \bar{r}_{X1} = 0 \tag{4}$$

Accordingly, we have

$$\frac{3q_X^2}{(\sqrt{3}\cos\varphi)^{p+1}} + \frac{q_X q_E}{(\sqrt{2 + 2\sin\varphi})^{p+1}} = \frac{(\sin\varphi + 1)\, q_X q_E}{\sin\varphi(\sqrt{2 + 2\sin\varphi})^{p+1}}$$

By rearranging the terms

$$\frac{q_X}{q_E} = \frac{1}{3\sin\varphi}\left(\frac{\sqrt{3}\cos\varphi}{\sqrt{2 + 2\sin\varphi}}\right)^{p+1} \tag{5}$$

Eqs (1) and (5) characterize the AX_3E configuration.

The AX_2E_2 case

According to Fig. A2, the bond angle $\sphericalangle$ X–A–X $= 2\beta$ and the angle $\sphericalangle$ E–A–E $= 2\alpha$. The configuration has C_{2v} symmetry.

The position vectors of the points are

$$\begin{aligned} \bar{r}_{E1} &= \sin\alpha\,\bar{i} + \cos\alpha\,\bar{j} \\ \bar{r}_{E2} &= -\sin\alpha\,\bar{i} + \cos\alpha\,\bar{j} \\ \bar{r}_{X1} &= -\cos\beta\,\bar{j} + \sin\beta\,\bar{k} \\ \bar{r}_{X2} &= -\cos\beta\,\bar{j} - \sin\beta\,\bar{k} \end{aligned} \tag{6}$$

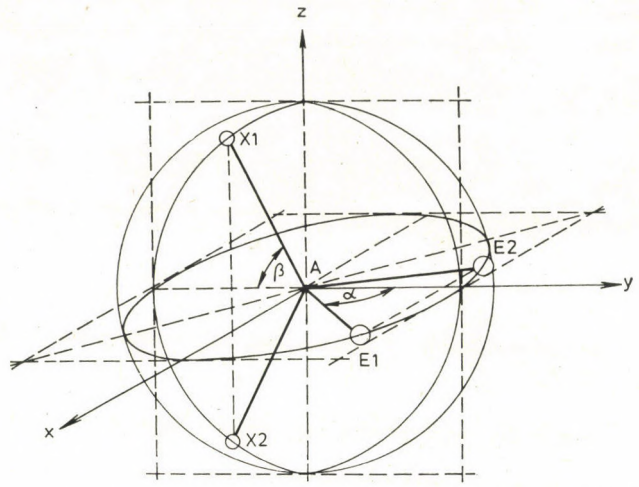

Fig. A2. Geometrical model for the AX_2E_2 system

The force acting on the charge E1 can be obtained as

$$\bar{F}_{E1} = \left[\frac{2 \sin \alpha}{(2 \sin \alpha)^{p+1}} q_E^2 + \frac{2 \sin \alpha}{(2 + 2 \cos \alpha \cos \beta)^{\frac{p+1}{2}}} q_E q_X \right] \bar{i} +$$

$$+ \frac{2(\cos \alpha + \cos \beta)}{(2 + 2 \cos \alpha \cos \beta)^{\frac{p+1}{2}}} q_E q_X \bar{j}$$

From the condition $\bar{F}_{E1} \, x \, \bar{r}_{E1} = 0$,

$$\frac{q_E}{q_X} \cdot \frac{\cos \alpha}{(2 \sin \alpha)^{p+1}} = \frac{\cos \beta}{(2 + 2 \cos \alpha \cos \beta)^{\frac{p+1}{2}}} \tag{7}$$

is obtained. As there are two unknowns in (7), another relation is derived for the force acting on the charge X1 as follows

$$\bar{F}_{X1} = \frac{2 \sin \beta \, \bar{k}}{(2 \sin \beta)^{p+1}} q_X^2 + \frac{- \sin \alpha \, \bar{i} - (\cos \alpha + \cos \beta) \, \bar{j} + \sin \beta \, \bar{k}}{(2 + 2 \cos \alpha \cos \beta)^{\frac{p+1}{2}}} q_E q_X +$$

$$+ \frac{\sin \alpha \, \bar{i} - (\cos \alpha + \cos \beta) \, \bar{j} + \sin \beta \, \bar{k}}{(2 + 2 \cos \alpha \cos \beta)^{\frac{p+1}{2}}} q_E q_X$$

Using the condition $\bar{F}_{X1}\, x\, \bar{r}_{X1} = 0$,

$$\frac{q_X}{q_E} \cdot \frac{\cos\beta}{(2\sin\beta)^{p+1}} = \frac{\cos\alpha}{(2+2\cos\alpha\cos\beta)^{\frac{p+1}{2}}} \tag{8}$$

From the equations (7) and (8) the angles α and β can be calculated. Multiplying equations (7) and (8),

$$2\sin\alpha\sin\beta = 1 + \cos\alpha\cos\beta\,, \tag{9}$$

is obtained and dividing equations (7) and (8) we have

$$\frac{q_X}{q_E} = \frac{\cos\alpha}{\cos\beta}\left(\frac{\sin\beta}{\sin\alpha}\right)^{\frac{p+1}{2}}. \tag{10}$$

Finally, by substituting

$$\sin\alpha\sin\beta = u \tag{11}$$

$$\frac{\sin\alpha}{\sin\beta} = v \tag{12}$$

we have

$$\frac{q_X}{q_E} = \frac{2-v}{2v-1}\, v\, v^{\frac{p}{2}} \tag{13}$$

and

$$u = \frac{4v - v^2 - 1}{3v} \tag{14}$$

$$\sin^2\alpha = \frac{4v - v^2 - 1}{3} \tag{15}$$

$$\sin^2\beta = \frac{\sin^2\alpha}{v^2} \tag{16}$$

By using Eqs (13)–(16) the characteristic angles α and β can now be determined from the charge ratio (q_X/q_E).

Note added in proof (August 2, 1977): New experimental data on XSO_2Y sulphones fully support the observation concerning the relationship between the bond angles around the sulphur atom. Table III can be supplemented by

the following data (in degrees, and corresponding to the format of Table III):

CH_3OSO_2F	96.8	124.4	109.5	106.8	[23]
CH_3OSO_2Cl	102.8	122.2	108.7	106.4	[24]
$CH_2{=}CHSO_2Cl$	100.2	122.0	109.8	106.4	[25]
$OCNSO_2Cl$	98.0	122.8	108.3	107.8	[26]
CCl_3SO_2Cl	97.8	121.5	108.3	109.2	[27]

Ab initio molecular orbital calculations were carried out [28] in order to gain more insight into the structural variations discussed in this paper. The experimental bond angle variations have been remarkably well reproduced and several interesting observations could be made. However, no interpretation of the bond angle variations could be provided.

REFERENCES

[1] HARGITTAI, I.: Second European Crystallographic Meeting, Collected Abstracts, pp. 441—443, Keszthely, 1974
[2] GILLESPIE, R. J.: Molecular Geometry, Van Nostrand Reinhold, London, 1972 and references cited therein
[3] KUCHITSU, K., GUILLORY, J. P., BARTELL, L. S.: J. Chem. Phys., **49,** 2488 (1968)
[4] BÜRGI, H. B., STEDMAN, D., BARTELL, L. S.: J. Mol. Struct., **10,** 31 (1971)
[5] OTAKE, M., MATSUMURA, C., MORINO, Y.: J. Mol. Spectroscopy, **28,** 316 (1968)
[6] BARTELL, L. S., HIRST, L. C.: J. Chem. Phys., **31,** 449 (1959)
[7] HEDBERG, K., IWASAKI, M.: J. Chem. Phys., **36,** 589 (1962)
[8] MORINO, Y., KUCHITSU, K., MORITANI, T.: Inorg. Chem., **8,** 867 (1969)
[9] SHIBATA, S., BARTELL, L. S.: J. Chem. Phys., **42,** 1147 (1965)
[10] BEAGLEY, B., CLARK, A. H., HEWITT, T. G.: J. Chem. Soc. (London), 658 (1968)
[11] MORINO, Y., SAITO, S.: J. Mol. Spectroscopy, **19,** 435 (1966)
[12] SUTTON, L. E. (Editor): Tables of Interatomic Distances and Configuration in Molecules and Ions, Spec. Publ. 18, Chem. Soc., London, 1965
[13] MORINO, Y., MURATA, Y., ITO, T., NAKAMURA, J.: J. Phys. Soc. Japan, **17,** BII 37 (1962)
[14] KIRCHHOFF, W. H. JOHNSON, D. R., POWELL, F. X.: J. Mol. Spectroscopy, **48,** 157 (1973)
[15] HARGITTAI, I.: Acta Chim. Acad. Sci. Hung., **60,** 231 (1969)
[16] LIDE, D. R., JR., MANN, D. E., FRISTROM, R. M.: J. Chem. Phys., **26,** 734 (1957)
[17] HARGITTAI, I., MIJLHOFF, F. C.: J. Mol. Struct., **16,** 69 (1973)
[18] HARGITTAI, I., HARGITTAI, M.: J. Mol. Struct., **15,** 399 (1973)
[19] HARGITTAI, M., HARGITTAI, I.: J. Chem. Phys., **59,** 2513 (1973)
[20] HARGITTAI, M., HARGITTAI, I.: J. Mol. Struct., **20,** 283 (1974)
[21] HARGITTAI, I., BRUNVOLL, J.: Acta Chem. Scand., A, **30,** 634 (1976)
[22] BRUNVOLL, J., HARGITTAI, I.: J. Mol. Struct., **30,** 361 (1976)
[23] HARGITTAI, I., SEIP, R., NAIR, K. P. R., BRITT, CH. O., BOGGS, J. E., CYVIN, B. N.: J. Mol. Struct., **39,** 1 (1977)
[24] HARGITTAI, I., SCHULTZ, GY., KOLONITS, M.: J. C. S. Dalton Trans., 1299 (1977)
[25] BRUNVOLL, J., HARGITTAI, I.: Acta Chim. (Budapest), in press
[26] BRUNVOLL, J., HARGITTAI, I., SEIP, R.: J. C. S. Dalton Trans., in press
[27] BRUNVOLL, J., HARGITTAI, I., SEIP, R.: To be published
[28] SCHMIEDEKAMP, A., SKAARUP, S., PULAY, P., HARGITTAI, I., CRUICKSHANK, D. W. J., BOGGS, J. E.: submitted to J. Amer. Chem. Soc.

István HARGITTAI H-1525 Budapest, Pf. 17.
András BARANYI H-1525 Budapest, Pf. 15.

Acta Chimica Academiae Scientiarum Hungaricae, Tomus 93 (3—4), pp. 289—306 (1977)

REACTION OF HYDROGEN CHEMISORBED ON UNSUPPORTED PT CATALYST WITH OXYGEN

D. MÓGER, M. HEGEDÜS, G. BESENYEI and F. NAGY

(Central Research Institute for Chemistry, Hungarian Academy of Sciences)

Received June 9, 1976

For a metallic Pt catalyst it has been shown that:
(1) In accordance with Langmuir's earlier study, the reaction

$$\left.\begin{matrix}(H_2)_g \\ + \\ (H)_a\end{matrix}\right\} + (O)_c \rightarrow H_2O\,;\ t \leq 20\ ^\circ C \qquad (I)$$

takes place already at room temperature, as verified experimentally.
($(H_2)_g$ is the gaseous, while $(H)_a$ is the chemisorbed hydrogen removable with an inert gas stream at room temperature. $(O)_c$ is the chemisorbed oxygen not removable with an inert gas stream at room temperature.)
(2) The three types (γ, ε, δ) of chemisorbed hydrogen ($(H)_c$)) do not react with either gaseous or chemisorbed oxygen at room temperature. That is,

$$\left.\begin{matrix}(O_2)_g \\ + \\ (O)_c\end{matrix}\right\} + (H)_c \not\rightarrow H_2O\,;\ t \leq 20\ ^\circ C \qquad (II)$$

(3) Any reaction between chemisorbed oxygen and hydrogen occurs only at temperatures where the desorption of hydrogen also takes place. Accordingly, the following reaction path is suggested:

$$(H)_c \xrightarrow{\text{warming}} [(H_2)_g + (H)_a + (H)_{c'}] \xrightarrow{+(O)_c} H_2O + (H)_{c'} \quad t > t_l \qquad (III)$$

where t_l is the lowest temperature where the desorption of a particular type of chemisorbed hydrogen (γ,ε, δ) already takes place at a finite rate. Subscript c' refers to chemisorbed hydrogen of the types γ, ε and δ.
(4) Chemisorbed oxygen is bonded more firmly than chemisorbed hydrogen (oxygen desorbs at a higher temperature than does hydrogen, as established by TPD). Consequently, since reaction (I) occurs at temperatures where reaction (II) does not take place, and this cannot be ascribed to thermodynamic reasons, a kinetic hindrance should be supposed.

Namely, the two possible pathways for reaction (I) are as follows:

$$(H_2)_g + (O)_c \rightarrow H_2O \qquad (Ia)$$

$$(H)_a + (O)_c \rightarrow (OH)_a \xrightarrow{(H)_a} H_2O \qquad (Ib)$$

Pathway (Ia) corresponds essentially to the so-called Rideal mechanism, whereas pathway (Ib) implies the mobility of H_a, which is supported by the rapidity of H/D exchange between H_2 and D_2 at room temperature.

For reaction (II), also two possible paths can be envisaged:

$$(O_2)_g \rightarrow (O)_c \xrightarrow{(H)_c} (OH)_a \xrightarrow{(H)_c} H_2O \qquad \text{(IIa)}$$

$$(H)_c + (O_2)_g \rightarrow (O_2H)_a \rightarrow \begin{cases} (OH)_a \xrightarrow{(H)_c} H_2O \\ + \\ (O)_c \xrightarrow{(H)_c} (OH)_a \xrightarrow{(H)_c} H_2O \end{cases} \qquad \text{(IIb)}$$

As described previously, if the adsorbent is covered simultaneously with chemisorbed hydrogen and oxygen, then the chemisorbed oxygen, without any decrease in the amount of $(H)_c$, can be removed with gaseous hydrogen already at room temperature. For this reason, it should be assumed that the second step of reaction path (IIa) as well as the first one of (IIb) are kinetically hindered. For reaction path (IIa) a kinetic hindrance may, for instance, result from the fact that the chemisorbed species $(O)_c$ and $(H)_c$) are localized. When only $(H)_c$ is considered to be localized, a steric hindrance should also be supposed. A similar steric hindrance should be assumed for reaction path (IIb). That is, the hydrogen is so 'deeply' in the crystal lattice that reaction

$$(O)_c + (H)_c \rightarrow (OH)_a$$

and

$$(O_2)_g + (H)_c \rightarrow (O_2H)_a$$

cannot take place.

(5) In view of the results described in the present paper, the usual interpretation of the results of 'oxygen–hydrogen' titrations [5, 6] in heterogeneous catalysis — at least for Pt — becomes doubtful. This is supported by the following facts.

(5.1) As shown in our previous paper [1], only an adequate treatment procedure (H_2 pressure, temperature, adsorption time) permits unequivocal saturation of Pt catalyst with hydrogen of the same quantity. If this procedure is not applied, the initial state with respect to chemisorbed hydrogen remains ill-defined.

(5.2) As the chemisorbed hydrogens desorbing above room temperature do not react with oxygen at room temperature, the oxygen consumption may not be considered as equal to the amount of oxygen consumed for oxidation of chemisorbed hydrogen plus the amount of oxygen chemisorbed. Therefore, the end-point of titration is also ill-defined.

(5.3) For exygen chemisorption on a Pt catalyst, it has not been verified whether a special procedure is required (as for hydrogen) to ensure saturation of the catalyst with oxygen of the same quantity. On account of this, if oxygen has been chemisorbed on the catalyst, the initial state also seems to be poorly defined.

(5.4) Although chemisorbed oxygen reacts with gaseous hydrogen already at room temperature, if the unequivocality of hydrogen chemisorption is not ensured, then even the end-point of such a titration is not well-defined.

In our previous paper [1] the temperature programmed desorption (TPD) study of the chemisorption of hydrogen on unsupported Pt powder has been described in detail. It has been shown that (i) in contrast to literature data [2, 3], not two but three maxima can be observed on the TPD curve recorded above room temperature and (ii) the chemisorption states of hydrogen assigned to these maxima are obtainable only under adequate sorption conditions (temperature, H_2-pressure, time, etc.). On the basis of thermodynamic considerations, the adsorption state of the highest bond energy (that is the hydrogen species corresponding to the maximum at higher temperatures) is expected to be more stable than those with lower bond

energies. The experimental results, however, have shown the establishment of equilibrium between the different hydrogen species to be subject to considerable kinetic hindrance, that is, the chemisorbed hydrogen species of lower bond energy does not transform to the more stable hydrogen species of higher bond energy, even on standing for several days at ambient temperature. Therefore, of particular interest is the question whether these chemisorbed hydrogens show different reactivities, and if so, whether this phenomenon may be attributed to kinetic or thermodynamic factors. LANGMUIR [4] first observed that chemisorbed hydrogen is much less reactive toward gaseous oxygen than is chemisorbed oxygen toward gaseous hydrogen. To obtain further insight into this problem, the different chemisorbed hydrogen species stable at room temperature were reacted with oxygen.

It is known that the oxygen and/or hydrogen adsorption capacity of a Pt catalyst can be determined by 'titration' of the catalyst with hydrogen and oxygen, respectively. This widespread use of this method [5, 6] provides an additional reason for undertaking these experiments.

Since several procedures have been employed in the experiments and these should often be referred to in discussion on the results, a brief summary of the most frequent procedures and of the results will be given in next section. For the sake of clarity, code numbers will be assigned to the procedures to be described, and the procedures as well as their results will be referred to by these code numbers.

A) Basic experimental procedures and results

Purification of the catalyst surface

The catalyst warmed up to 500 °C is treated alternately in a stream of H_2 and O_2. After the last treatment with hydrogen, hydrogen is replaced with an inert gas (N_2 or He), and the catalyst is cooled down to room temperature in a stream of N_2 or He. It is assumed that the catalyst thus pretreated does not contain any chemisorbed hydrogen or oxygen [1]. This catalyst will be regarded as starting material throughout the paper.

1.1 *The catalyst is treated with hydrogen at room temperature for* 1—2 *min*

According to the results reported earlier [1], no chemisorbed hydrogen can be detected by TPD after this pretreatment. It is, however, known that Pt catalyzes H/D exchange between H_2 and D_2 already at room temperature. Consequently, the formation of chemisorbed H atoms should also be supposed under the circumstances given. The rate of desorption of hydrogen thus

chemisorbed is, however, high so that it can be removed from the surface with inert gases already at room temperature. As a result of this procedure, the catalyst and the surrounding gas phase will contain the following hydrogen species

$$(H_2)_g + (H)_a \tag{1.1}$$

where $(H_2)_g$ is molecular hydrogen in the gas phase and $(H)_a$ denotes the atomic hydrogen adsorbed.

1.2 *Starting from a higher temperature, the catalyst, according to an adequate program, is cooled to room temperature in an atmosphere of* H_2

It has been shown [1] that under such conditions different chemisorption states of hydrogen can be observed by TPD above room temperature. Of course, the amounts of the chemisorbed hydrogen species depend on the program applied. If these chemisorbed hydrogens (hydrogens of the types γ, ε and δ) are denoted by $(H)_c$, the hydrogen species present in the system are

$$(H_2)_g + (H)_a + (H)_c \tag{1.2}$$

2.1 *The catalyst is treated with* O_2 *at room temperature for* 1–2 *min*

In this case, in contrast to the similar treatment with hydrogen (*cf.* 1.1), the adsorbed oxygen cannot be removed with an inert gas stream at room temperature. Thus, the system contains the following oxygen species

$$(O_2)_g + (O)_c \tag{2.1}$$

where $(O_2)_g$ is the oxygen present in the gas phase and $(O)_c$ is the chemisorbed oxygen removable from the catalyst surface above room temperature only.

3.1 *After the adsorption procedures outlined in previous paragraphs, the catalyst is exposed to a stream of an inert gas at room temperature*

By this procedure $(H)_c$ and $(O)_c$ cannot be removed but both the adsorptive present in the gas phase and the weakly bonded adsorbate can be removed [1, 7]. Thus, combining this procedure with Procedure 1.1 or 1.2 or 2.1, the result is

$$-(H_2)_g - (H)_a \text{ and/or } -(O_2)_g \tag{3.1}$$

3.2 *After the treatment described in the previous paragraph, the catalyst is warmed up to* 600 °C *(according to an adequate program) in an inert gas stream (TPD run)*

Upon this heat treatment, both chemisorbed hydrogen $(H)_c$ and chemisorbed oxygen $(O)_c$ desorb from the catalyst surface, that is, upon partial desorption of $(H)_c$ and $(O)_c$, the transient systems $[(H_2)_g + (H)_a + (H)_c]$ and $[(O_2)_g + (O)_c]$, respectively, are formed, from which $(H_2)_g$ and $(O_2)_g$ are removed with the inert gas stream. If the catalyst has originally contained $(H)_c$ and $(O)_c$, the result is

$$-(H)_c \text{ and } -(O)_c \tag{3.2}$$

respectively.

B) Combinations of the basic procedures and the information obtainable from the experiments

Procedure a: (2.1 + 3.1)

This combination is accomplished by injecting a certain number of O_2 pulses into the inert gas stream before the catalyst and measuring the amount of effluent oxygen in the gas stream. Thus, from the mass balance of O_2, the amount of $(O)_c$ denoted by $N^\circ\{(O)_c\}$ can be calculated

$$\Delta N^\circ\{O_2\} = \frac{1}{2} N^\circ\{(O)_c\} \tag{a—1}$$

where $\Delta N^\circ\{O_2\}$ is the amount of O_2 retained by the catalyst.

Procedure b: (1.2 + 3.1)

On combining *Procedures* 1.2 and 3.1, a catalyst is obtained which will contain firmly chemisorbed hydrogen only. The amount of hydrogen is dependent of the program employed in *Procedure* 1.2 and is denoted by

$$N^\circ\{(H)_c\} \tag{b—1}$$

Procedure c: (*b* + 3.2)

Thus, after *Procedure b* a TPD measurement is carried out. The peak area is proportional to the amount of hydrogen desorbed, therefore, its amount,

$N^\circ\{H_2\}$, written in the form

$$N^\circ\{H_2\} = \frac{1}{2} N^\circ\{(H)_c\} \qquad (c-1)$$

can be obtained by calibration.

Procedure d: $(b + 2.1 + 3.1)$

This procedure, which is analogous to *Procedure a*, can be performed as follows. Pulses of O_2 are introduced onto a catalyst that already contains chemisorbed hydrogen $(H)_c$. For oxygen present in the gas phase, a combination of Eqs (a–1) and (b–1) gives the following mass balance (formation of water is also considered)

$$\Delta N_d\{O_2\} = \frac{1}{2} y_1 N^\circ\{(O)_c\} + \frac{1}{4}(1 - x_1) N^\circ\{(H)_c\} \qquad (d-1)$$

x_1 and y_1 are defined by

$$\begin{aligned} x_1 &\equiv N_d\{(H)_c\}/N^\circ\{(H)_c\}; \quad 0 \leq x_1 \leq 1 \\ y_1 &\equiv N_d\{(O)_c\}/N^\circ\{(O)_c\}; \quad 0 \leq y_1 \leq 1 \end{aligned} \qquad (d-2)$$

where $\Delta N_d\{O_2\}$ is the amount of O_2 retained by the catalyst from the gas stream, $N_d\{(H)_c\}$ and $N_d\{(O)_c\}$ are the amounts of chemisorbed hydrogen and oxygen, respectively, after this procedure.

Procedure e: $(a + 1.1 + 3.1)$

This combination is accomplished by injecting pulses of H_2 onto a catalyst that contains $(O)_c$ (*Procedure a*) and is kept in an inert gas stream at room temperature. On considering the result of *Procedure* 1.1 and the possible formation of water, the mass balance for hydrogen can be written as

$$\Delta N_e\{H_2\} = (1 - y_2) N^\circ\{(O)_c\} \qquad (e-1)$$

where y_2 is given by

$$y_2 \equiv N_e\{(O)_c\}/N^\circ\{(O)_c\}; \quad 0 \leq y_2 \leq 1 \qquad (e-2)$$

here $\Delta N_e\{H_2\}$ is the amount of H_2 retained by the catalyst and $N_e\{(O)_c\}$ is the amount of chemisorbed oxygen remaining on the catalyst.

Procedure f: $(d + 1.1 + 3.1)$

In this case hydrogen is admitted to the catalyst-adsorbate system (implemented by *Procedure d*) at room temperature, then at the same temperature the hydrogen is flushed out with an inert gas stream. As in the course of *Procedure e*, water may be formed without affecting the amount of chemisorbed hydrogen.

Considering Eq. (d—2), the amount of water formed, $\Delta N_f\{H_2O\}$, can be written as

$$\Delta N_f\{H_2O\} = (1 - y_3)y_1 N^\circ\{(O)_c\} \qquad \text{(f—1)}$$

y_3 being defined by

$$y_3 \equiv N_f\{(O)_c\}/N_d\{(O)_c\} = N_f\{(O)_c\}/y_1 N^\circ\{(O)_c\}; \quad 0 \leq y_3 \leq 1 \qquad \text{(f—2)}$$

The amount of chemisorbed hydrogen remains unchanged, thus,

$$N_f\{(H)_c\} = N_d\{(H)_c\} = x_1 N^\circ\{(H)_c\} \qquad \text{(f—3)}$$

where $N_f\{(H)_c\}$ and $N_d\{(O)_c\}$ are the amounts of chemisorbed hydrogen and oxygen remaining on the catalyst surface.

Procedure g: $(d + 3.2)$

After Procedure *d* a TPD measurement is carried out, which permits to determine the amount of desorbed hydrogen, $N_g\{H_2\}$. Considering the possible formation of water, the mass balance for $N_g\{H_2\}$ can be obtained from Eqs (d—2) and (c—1)

$$N_g\{H_2\} = \frac{1}{2} N_d\{(H)_c\} - N_d\{(O)_c\} = \frac{1}{2} x_1 N^\circ\{(H)_c\} - y_1 N^\circ\{(O)_c\} \qquad \text{(g—1)}$$

$$\frac{1}{2} x_1 N^\circ\{(H)_c\} \geq y_1 N^\circ\{(O)_c\}$$

Procedure h: $(f + 3.2)$

In this experiment the TPD run is performed after *Procedure f*. Considering Eqs (f—2), (f—3) and (c—1) as well as the possible formation of water, the mass balance for the amount of desorbed hydrogen, $N_h\{H_2\}$, can

be given as

$$N_h\{H_2\} = \frac{1}{2} N_f\{(H)_c\} - N_f\{(O)_c\} = \frac{1}{2} x_1 N^\circ\{(H)_c\} - y_1 y_3 N^\circ\{(O)_c\} \qquad \text{(h—1)}$$

$$\frac{1}{2} x_1 N^\circ\{(H)_c\} \geq y_1 y_3 N^\circ\{(O)_c\}$$

The sorption characteristics to be expected for each procedure are summarized in Table I.

Table I

Summary of the characteristics for Procedures a–h

Procedure code	Before procedure		After procedure	
	$N\{(H)_c\}$	$N\{(O)_c\}$	$N\{(H)_c\}$	$N\{(O)_c\}$
(*a*) : 2.1 + 3.1	0	0	0	$N^\circ\{(O)_c\}$
(*b*) : 1.2 + 3.1	0	0	$N^\circ\{(H)_c\}$	0
(*c*) : (*b*) + 3.2	$N^\circ\{(H)_c\}$	0	0	0
(*d*) : (*b*) + 2.1 + 3.1	$N^\circ\{(H)_c\}$	0	$N_d\{(H)_c\}$	$N_d\{(O)_c\}$
(*e*) : (*a*) + 1.1 + 3.1	0	$N^\circ\{(O)_c\}$	0	$N_e\{(O)_c\}$
(*f*) : (*d*) + 1.1 + 3.1	$N_d\{(H)_c\}$	$N_d\{(O)_c\}$	$N_f\{(H)_c\}$	$N_f\{(O)_c\}$
(*g*) : (*d*) + 3.2	$N_d\{(H)_c\}$	$N_d\{(O)_c\}$	0	0
(*h*) : (*f*) + 3.2	$N_f\{(H)_c\}$	$N_f\{(O)_c\}$	0	0

(*a*) $\Delta N^\circ\{O_2\} = \frac{1}{2} N^\circ\{(O)_c\}$ (*c*) $N^\circ\{H_2\} = \frac{1}{2} N^\circ\{(H)_c\}$

(*d*)
$$\begin{cases} \Delta N_d\{O_2\} = \frac{1}{2} N_d\{(O)_c\} + \frac{1}{4} N^\circ\{(H)_c\} - N_d\{(H)_c\} \\ N_d\{(O)_c\} = y_1 N^\circ\{(O)_c\};\ 0 \leq y_1 \leq 1 \\ N_d\{(H)_c\} = x_1 N^\circ\{(H)_c\};\ 0 \leq x_1 \leq 1 \end{cases}$$

(*e*)
$$\begin{cases} \Delta N_e\{H_2\} = N^\circ\{(O)_c\} - N_e\{(O)_c\} \\ N_e\{(O)_c\} = y_2\ N^\circ\{(O)_c\};\ 0 \leq y_2 \leq 1 \end{cases}$$

(*f*)
$$\begin{cases} N_f\{(O)_c\} = y_1 y_3\ N^\circ\{(O)_c\};\ 0 \leq y_3 \leq 1 \\ N_f\{(H)_c\} = N_d\{(H)_c\} = x_1\ N^\circ\{(H)_c\} \end{cases}$$

(*g*) $N_g\{H_2\} = \frac{1}{2} N_d\{(H)_c\} - N_d\{(O)_c\} = \frac{1}{2} x_1 N^\circ\{(H)_c\} - y_1 N^\circ\{(O)_c\}$

(*h*) $N_h\{H_2\} = \frac{1}{2} N_f\{(H)_c\} - N_f\{(O)_c\} = \frac{1}{2} x_1\ N^\circ\{(H)_c\} - y_1 y_3\ N^\circ\{(O)_c\}$

Table IIa

Sorption characteristics and results of the different procedures

Procedure code	Before procedure		After procedure		
	10^{-5} mol				
	$N\{(H)_c\}$	$N\{(O)_c\}$	$N\{(H)_c\}$	$N\{(O)_c\}$	
(*a*) : 2.1 + 3.1	0	0	0	0.90	$\Delta N^{\circ}\{O_2\} = 0.45\times10^{-5}$ mol
(*b*) : 1.2 + 3.1	0	0	3.04	0	$N^{\circ}\{H_2\} = 1.52\times10^{-5}$ mol
(*c*) : (*b*) + 3.2	3.04	0	0	0	
(*d*) : (*b*) + 2.1 + 3.1	3.04	0	3.04 x_1	0.90 y_1	$\Delta N_d\{O_2\} = 0.45\times10^{-5}$ mol
(*dI*) : (*b*) + 2.1 + 3.1	3.04	0	3.04	0.90	$x_1 = y_1 = 1$
(*dII*) : (*b*) + 2.1 + 3.1	3.04	0	3.04 x_1	0.90 y_1	$0 \leq y_1 < 1$; $x_1 = 0.41 + 0.59\ y_1$
(*e*) : (*a*) + 1.1 + 3.1	0	0.90	0	0	$\Delta N_e\{H_2\} = 0.90\times10^{-5}$ mol; $y_2 = 0$
(*fI*) : (*dI*) + 1.1 + 3.1	3.04	0.90	3.04	0.90 y_3	$0 \leq y_3 \leq 1$
(*fII*) : (*dII*) + 1.1 + 3.1	3.04 x_1	0.90 y_1	3.04 x_1	0.90 y_1y_3	
(*gI*) : (*dI*) + 3.2	3.04	0.90	0	0	$N_g\{H_2\} = 0.62\times10^{-5}$ mol $= (1.52-0.90)\times10^{-5}$ mol
(*gII*) : (*dII*) + 3.2	3.04 x_1	0.90 y_1	0	0	$N_g\{H_2\} = 0.62\times10^{-5}$ mol $= 0.62\ x_1\times10^{-5}$ mol $0 \leq y_1 < 1$; $x_1 = 0.41 + 0.59\ y_1$

Table IIb

Sorption characteristics and results for Procedures d–h

Procedure code	Before procedure		After procedure		
	10^{-5} mol				
	$N\{(H)_c\}$	$N\{(O)_c\}$	$N\{(H)_c\}$	$N\{(O)_c\}$	
(*dI*) : (*b*) + 2.1 + 3.1	3.04	0	3.04	0.90	$\Delta N_d\{O_2\} = 0.45\times10^{-5}$ mol; $x_1 = y_1 = 1$
(*e*) : (*a*) + 1.1 + 3.1	0	0.90	0	0	$\Delta N_e\{H_2\} = 0.90\times10^{-5}$ mol; $y_2 = 0$
(*fI*) : (*dI*) + 1.1 + 3.1	3.04	0.90	3.04	0.90 y_3	$0 \leq y_3 \leq 1$
(*gI*) : (*dI*) + 3.2	3.04	0.90	0	0	$N_g\{H_2\} = 0.62\times10^{-5}$ mol
(*hI*) : (*fI*) + 3.2	3.04	0.90 y_3	0	0	$N_h\{H_2\} = 1.52\times10^{-5}$ mol $y_3 = 0$
(*fI*) : (*dI*) + 1.1 + 3.1	3.04	0.90	3.04	0	$y_3 = 0$
(*hI*) : (*fI*) + 3.2	3.04	0	0	0	$N_h\{H_2\} = 1.52\times10^{-5}$ mol

C) Results and discussion

The experimental results characteristic of the sorption properties of the catalyst before and after *Procedures a—c* are listed in Table IIa. If *Procedure d* is performed on a catalyst that has been pretreated by *Procedure b* (*cf.* Table IIa), then, within the limits of experimental error, the value $\Delta N_d\{(O)_2 = 0.45 \times 10^{-5}$ mol is obtained. Therefore, using the data in Table IIa, the following relationship can be deduced

$$0.45\,(1 - y_1) = 0.76\,(1 - x_1) \tag{4}$$

Trivial solutions of Eq. (4) are

$$x_1 = 1; \quad y_1 = 1 \tag{5.1}$$

This means that under the experimental conditions employed oxygen does not react with hydrogen ($x_1 = 1$), and the amount of oxygen adsorbed on a surface covered with hydrogen H_c is equal to that of oxygen adsorbed on a hydrogen-free surface ($y_1 = 1$), since it follows from Eqs (d—2) and (5—1) that

$$N_d\{(O)_c\} = N^\circ\{(O)_c\} = 0.90 \times 10^{-5} \text{ mol}$$
$$N_d\{(H)_c\} = N^\circ\{(H)_c\} = 3.40 \times 10^{-5} \text{ mol} \tag{5.2}$$

If Eq. (5.1) is not satisfied, that is, $x_1 = 1$ and $y_1 = 1$ are not adequate solutions of Eq. (4), then from Eq. (4)

$$x_1 = 0.41 + 0.59\, y_1 \tag{5.3}$$

That is, oxygen $[(O_2)_g + (O)_c]$ reacts only with a fraction of adsorbed hydrogen $(1 - x_1)$, and chemisorbed hydrogen decreases the adsorption of oxygen to such an extent that Eq. (4) should be fulfilled. The two subcases discussed above are denoted by dI and dII, respectively (*cf.* Table IIa).

When the catalyst is pretreated by *Procedure a* and then *Procedure e* is performed (the data characteristic of the chemisorption of the catalyst are shown in Table IIa), one obtains within the limits of experimental error

$$\Delta N_e\{H_2\} \approx 0.90 \times 10^{-5} \text{ mol} \tag{6}$$

Substitution of the value of $\Delta N_e\{H_2\}$ as well as that of $N^\circ\{(O)_c\}$ given in the table into Eqs (e—1) and (e—2) leads to

$$y_2 = 0 \tag{7.1}$$

$$N_e\{(O)_c\} = 0 \tag{7.2}$$

That is, the reaction of oxygen with hydrogen $[(H_2)_g + (H)_a]$ goes to completion.

On performing *Procedure f* on a catalyst pretreated by *Procedure d*, the sorption characteristics are modified as shown in Table 2a (Eqs (f—1), (f—2) and (f—3) are also taken into account).

In the case of *Procedure g*, a TPD measurement is carried out on a catalyst which has been pretreated by *Procedure d*. From Eq. (g—1)

$$N_g\{H_2\} = \frac{1}{2} x_1 N^\circ\{(H)_c\} - y_1 N^\circ\{(O)_c\} \geq 0 \tag{8.1}$$

As two subcases have been introduced for *Procedure d*, the sorption characteristics obtained after *Procedure g* should also be subdivided into two classes {*gI* and *gII*}. Using Eq. (8.1), the results can be given as shown in Table IIa. For the experiments of this type

$$N_g\{H_2\} = 0.62 \times 10^{-5} \text{ mol} \tag{8.2}$$

As can be seen from the Table, this result permits one to make a choice between alternatives *gI* and *gII* (and, of course, between *dI* and *dII*). The value of $N_g\{H_2\}$ (*cf.* Eq. (8.2)) is consistent with subcase *gI (dI)* only. For this reason, subcases *dII* and *fII* that contradict the experimental results, can be ruled out. Consequently,

$$x_1 = y_1 = 1 \tag{8.3}$$

On account of the results obtained, some of the data in Table IIa may be omitted. The concrete sorption characteristics of the catalyst before and after *Procedures d—g* are again listed in Table IIb.

For *Procedure h* the value of $N_h\{H_2\}$ obtained experimentally is

$$N_h\{H_2\} = 1.52 \times 10^{-5} \text{ mol} \tag{9.1}$$

Substitution of the values of x_1, y_1 (*cf.* Eq. (8.3)) and the corresponding data in Table IIb into Eq. (h—1) gives

$$1.52 = \frac{1}{2} 3.04 - 0.90\, y_3$$

whence

$$y_3 = 0 \tag{9.2}$$

That is, the reaction of chemisorbed oxygen $(O)_c$ with hydrogens $(H_2)_g$ and $(H)_a$, in accordance with the experimental results of *Procedure e*, goes to

completion during *Procedure f*. Accordingly, the results of *Procedures fI* and *hI* are repeated in Table IIb.

Concerning the reactivities of chemisorbed hydrogen and oxygen, the following conclusions have been drawn from the experimental results outlined in this section.

(i) Chemisorbed hydrogen $(H)_c$, which is stable even at room temperature, does not react with either gaseous or chemisorbed oxygen at room temperature (*cf.* Eq. (8.3), $x_1 = 1$):

$$[(O_2)_g + (O)_c] + (H)_c \not\rightarrow H_2O \qquad (10.1)$$

$$(T \sim 290\ K)$$

(ii) Chemisorbed oxygen $(O)_c$, which cannot be removed from the catalyst surface with an inert gas at room temperature, reacts with hydrogen (*i.e.* with $(H_2)_g$ and $(H)_a$) already at room temperature (*cf.* Eqs (7.1) and (9.2), $y_2 = y_3 = 0$):

$$[(H_2)_g + (H)_a] + (O)_c \rightarrow H_2O \qquad (10.2)$$

$$(T \sim 290\ K)$$

(iii) Chemisorbed hydrogen $(H)_c$ and oxygen $(O)_c$, which desorb above room temperature only, react with each other under TPD conditions (*cf.* result of *Procedure gI*).

D) Reaction of chemisorbed hydrogen species (γ, ϵ, δ) of different bond strengths with chemisorbed oxygen

Procedure g ($d + 3.2$) described in the previous section can be accomplished also by injecting different numbers of oxygen pulses (in *Procedure d*) onto the catalyst saturated with chemisorbed hydrogen ($\Delta N\{O_2\} < \Delta N^{\circ}\{O_2\}$), then performing a TPD measurement.

The TPD curves recorded after injection of various amounts of oxygen are shown in Fig. 1.

It is to be seen that under TPD conditions the three types of hydrogen (γ, ε, δ) show considerably different reactivities toward adsorbed hydrogen. If the equivalent amount of chemisorbed oxygen is less than or equal to the amount of chemisorbed hydrogen of type γ, then oxygen reacts practically only with this type of chemisorbed hydrogen. Chemisorbed hydrogen of type ε reacts with chemisorbed oxygen only if the amount of chemisorbed oxygen has exceeded the equivalent amount of chemisorbed hydrogen of type γ.

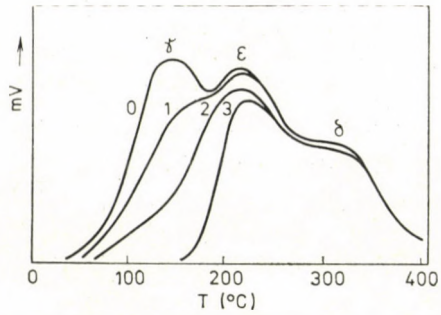

Fig. 1. TPD curves of a Pt catalyst saturated with chemisorbed hydrogens (γ, ε, δ) upon chemisorption of various amounts of oxygen

$$\Delta N_0\{O_2\} = 0; \quad \Delta N_1\{O_2\} < \Delta N_2O_2 < \Delta N_3O_2$$

The chemisorbed hydrogens, however, desorb during TPD, that is, depending on the temperature, the following reactions should also be considered:

$$(H)_c \rightleftharpoons (H)_a \rightleftharpoons (H_2)_g; \quad J_2' \tag{11.1}$$

Accordingly, three paths can be given for the reaction between chemisorbed hydrogen and oxygen, taking place under TPD conditions. These are as follows:

$$\begin{array}{lccccc} & [(H_2)_g + (H)_a + (H)_{c'}] & + & (O)_c & \xrightarrow{J_2''} & \\ & \uparrow J_2' & & & & \downarrow \\ \text{TPD;} & (H)_c & + & (O)_c & \xrightarrow{J_1} & H_2O + (H)_{c'} \\ & \downarrow J_3' & & & & \uparrow \\ & [(H_2)_g + (H)_a + (H)_{c'}] & + & [(O_2)_g + (O)_{c'}] & \xrightarrow{J_3''} & \end{array} \tag{11.2}$$

The path $J_3 = J_3' + J_3''$ can be excluded as a TPD study of oxygen [3] has shown that oxygen desorbs at a much higher temperature than hydrogen.

As described previously (*cf.* Eq. (10.1) in Section C), reaction J_1 does not take place at room temperature. This result, however, does not eliminate the possibilty of J_1 under TPD conditions since, on heating, the rate of this reaction may increase, provided the reaction is subject to kinetic hindrance only. Occurrence of desorption (11.1) during TPD and the result expressed by Eq. (10.2) strongly support the conclusion that path $J_2 = J_2' + J_2''$ is operative in the system under consideration.

In order to obtain additional evidence for path J_2, the following set of measurements was also performed which, however, does not eliminate the possibility of J_1. In these experiments we treated with oxygen (1.2 + 3.1)

a catalyst that did not contain chemisorbed hydrogen of type γ (*cf.* Fig. 2). (For details of the preparation, see Ref. [1]). After treatment with oxygen at 100 °C (hereinafter *Procedure* 2.2) the catalyst was cooled to room temperature and then the oxygen was flushed out (*Procedure* 3.1). Subsequently, a TPD curve was recorded (*Procedure* 3.2). This was done both (a) after treatment of the catalyst with H_2 at ambient temperature (*Procedure* 1.1 + + 3.1) and (b) without H_2-treatment (see Figs 3 and 4).

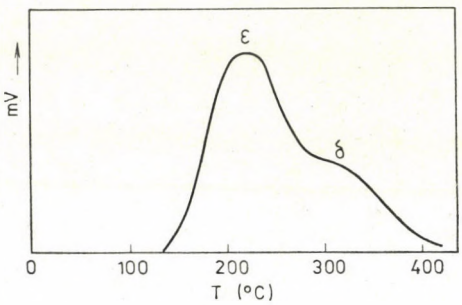

Fig. 2. TPD curve of a Pt catalyst not containing chemisorbed hydrogen of type γ

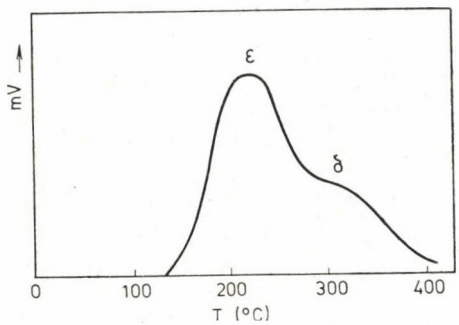

Fig. 3. TPD curve of a Pt catalyst not containing chemisorbed hydrogen of type γ, after pretreatment with oxygen at 100 °C and with hydrogen at room temperature

For *Procedure* 1.2 + 3.1 (initial state) the amount of hydrogen chemisorbed on the catalyst $\left(N_0^*\{(H)_c\}\right)$ can be calculated from the TPD curve in Fig. 2:

1.2 + 3.1:

$$N_0^*\{(H)_c\} = \frac{1}{2} N_0^*\{H_2\} \tag{12.1}$$

where $N_0^*\{H_2\}$ is the amount of desorbed hydrogen determined from the TPD curve shown in Fig. 2.

By applying *Procedures* 2.2 and 3.1, one obtains a set of procedures that can be regarded as analogous to *Procedure d* described in Section B:

1.2 + 3.1 + 2.2 + 3.1:

$$N_1^*\{(H)_c\} = \xi_1 N_0^*\{(H)_c\} \; ; \quad 0 \leq \xi_1 \leq 1 \quad N_1\{(O)_c\} = N_0^*\{(O)_c\} \qquad (12.2)$$

where $N_1\{(O)_c\}$ and $N_0^*\{(O)_c\}$ are the amounts of oxygen chemisorbed, and $N_1\{(H)_c\}$ is the amount of chemisorbed hydrogen remaining on the catalyst.

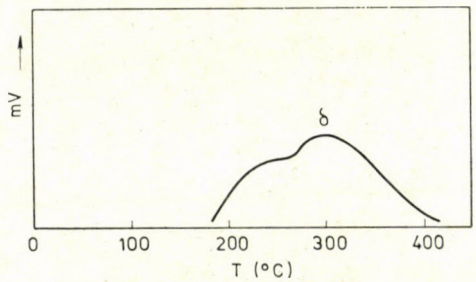

Fig. 4. TPD curve of a Pt catalyst not containing chemisorbed hydrogen of type γ, after pretreatment with oxygen at 100 °C

When the catalyst is treated also with hydrogen at room temperature (*cf.* Fig. 3), the resulting procedure will be analogous to *Procedure f* in Section B. Accordingly,

1.2 + 3.1 + 2.2 + 3.1 + 1.1 + 3.1:

$$N_2^*\{(H)_c\} = N_1^*\{(H)_c\} = \xi_1 N_0^*\{(H)_c\} \qquad (13.1)$$

$$N_2^*\{(O)_c\} = \eta N_0^*\{(O)_c\} \; ; \quad 0 \leq \eta_1 \leq 1$$

where $N_2^*\{(H)_c\}$ and $N_2^*\{(O)_c\}$ are the amounts of chemisorbed hydrogen and oxygen remaining on the catalyst after this procedure.

If a TPD measurement is then carried out (*Procedure* 3.2), the mass balance for the amount of hydrogen desorbed, $N_3^*\{H_2\}$, can be written by analogy of Eq. (h−1) (*cf. Procedure h* in Section B):

1.2 + 3.1 + 2.2 + 3.1 + 1.1 + 3.1 + 3.2:

$$N_3^*\{H_2\} = \frac{1}{2} N_2^*\{(H)_c\} - N_2^*\{(O)_c\} = \frac{1}{2} \xi_1 N_0^*\{(H)_c\} - \eta_1 N_0^*\{(O)_c\} \qquad (13.2)$$

A comparison of Figs 2 and 3 shows that the two curves are practically identical, that is

$$N_0^*\{H_2\} = N_3^*\{H_2\} \tag{13.3}$$

Thus, from Eqs 12.1, 13.2 and 13.3

$$\xi_1 = 1\ ;\ \eta_1 = 0 \tag{13.4}$$

The above relationship means that the chemisorbed hydrogen of type ε is not capable, at least within 10—20 min, to react with the system involving $(O_2)_g$ and $(O)_c$ even at 100 °C ($\xi_1 = 1$). It is also to be seen that oxygen chemisorbed at 100 °C reacts with the system $(H_2)_g + (H)_c$ already at room temperature ($\eta_1 = 0$).

However, a comparison of Figs 2 and 4 shows that if the chemisorbed oxygen is not removed, then, under TPD conditions, chemisorbed oxygen reacts mainly with chemisorbed hydrogen of type ε.

E) Experimental

Detailed description of the TPD measurements is given in our previous paper [8].

The Pt catalyst (adsorbent) was prepared by reduction of a 0.16 *M* aqueous solution of H_2PtCl_6 with hydrogen. To obtain an ion-free catalyst, the platinum powder was washed with deionized water several times and, after drying, it was pressed into tablets 0.8—1.0 mm in thickness. Since the specific surface area of the Pt catalyst decreases on thermal treatment the catalyst samples, prior to the measurements, were calcined in a stream of H_2 of atmospheric pressure at 650 °C for 1 hr and then kept at this temperature in a stream of air of atmospheric pressure for 1 hr. The specific surface area of the catalyst thus pretreated was cca. 0.1 m^2/g, as determined both electrochemically and by krypton adsorption. The TPD curves of these catalysts were reproducible to within a relative error of 3—5%.

For purification, the hydrogen used in the measurements was diffused throught a Pd membrane warmed to 500 °C. To remove oxygen, N_2 and He were passed through copper contacts at 200 °C, and then, for drying, through Linde 4A molecule sieve cooled with dry ice-acetone. O_2 and air were purified by passing through columns filled with clinoptilolite molecular sieve.

In the TPD and pulse runs, the flow rate and pressure of the inert gases were 16 cm^3/min and 1.05 atm, respectively. The reactor was heated at a rate of 15 °C/min. The amount of the catalyst employed was 3.3 g.

By the method described earlier [1], it can be achieved that the Pt should be covered maximally with chemisorbed hydrogens stable above room temperature. A TPD curve thus obtained is shown in Fig. 5. The TPD peak area corresponds to 1.55×10^{-5} mol of chemisorbed hydrogen, as determined by calibration of the H_2 detector.

The amount of O_2 (H_2) retained by the catalyst was determined by injecting 20μl pulses of oxygen (hydrogen) into the inert gas stream before the catalyst bed with a microsyringe and monitoring the amount of effluent oxygen (hydrogen) at constant temperature. (Runs with oxygen were made in a stream of He, whereas those with hydrogen were performed in a stream of N_2.) Two examples of the results obtained by utilizing the pulse technique are shown in Figs 6 and 7.

In order to check the validity of our results for the catalyst prepared by reduction with hydrogen, the experiments were repeated on two commercial catalysts of different types as well as on a catalyst prepared by reduction of aqueous H_2PtCl_6 with formaldehyde. Apart from the differences in the amount and in the ratio of the three types of chemisorbed hydrogen (γ, ε, δ), it has been found that the experimental results can be interpreted similarly as in the case of Pt powder prepared by ourselves and studied in detail.

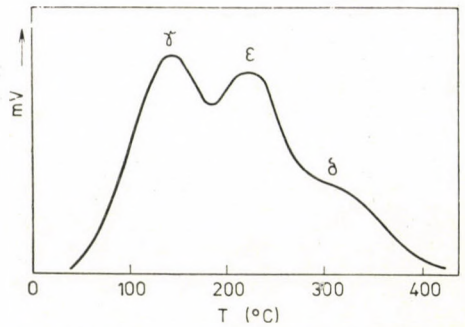

Fig. 5. TPD curve of a Pt catalyst saturated maximally with chemisorbed hydrogens stable at room temperature

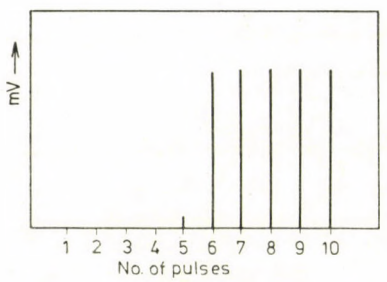

Fig. 6. Amount of oxygen retained by a Pt catalyst as determined at room temperature by a pulse technique

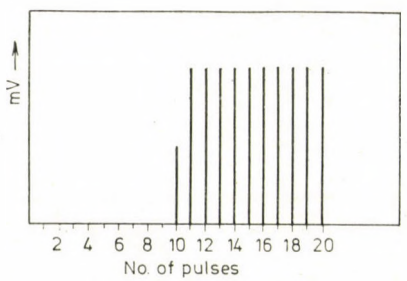

Fig. 7. Amount of hydrogen retained by a Pt catalyst containing adsorbed oxygen as determined at room temperature by a pulse technique

REFERENCES

[1] MÓGER, D., BESENYEI, G., NAGY, F.: Magy. Kém. Folyóirat, **81,** 284 (1975)
[2] TSUCHIYA, S., AMENOMIYA, Y., CVETANOVIC, R. I.: J. Catal., **19,** 245 (1970)
[3] SOKOLSKII, D. V., POPOVA, N. M., BABENTIOVA, L. V., SALNISKOVA, V. K.: Dokl. Akad. Nauk SSSR, **210,** 888 (1973)
[4] LANGMUIR, I.: Trans. Faraday Soc., **17,** 62 (1921)
[5] BENSON, J. E., BOUDART. M.: J. Catal., **4,** 704 (1965)
[6] MEARS, D. E., HANSFORD, R. C.: J. Catal., **9,** 125 (1967)
[7] KALLEN, W., CZANDERNA, A. W.: J. Coll. Interface Sci., **38,** 1, 152 (1972)
[8] MÓGER, D., KOVÁCS, G.: Magy. Kém. Folyóirat, **81,** 123 (1975)

Dezső MÓGER
Mihály HEGEDÜS
Gábor BESENYEI
Ferenc NAGY

H-1025 Budapest, Pusztaszeri út 59—67.

Acta Chimica Academiae Scientiarum Hungaricae, Tomus 93 (3—4), pp. 307—314 (1977)

ALUMINIUM-NICOTINE EXCHANGE EQUILIBRIA: PART III- ON KAOLINITE

J. P. SINGHAL and R. P. SINGH,

(Chemical Laboratories, Faculty of Engineering and Technology, Aligarh Muslim University, Aligarh, India)

Received July 16, 1976

A thermodynamic study of the exchange equilibria between nicotine and Al-kaolinite yielded isotherm, separation factors, selectivity coefficients and standard free energy changes which indicated a non-spontaneous reaction with a lower preference for nicotine. The reaction was exothermic. Its non-spontaneity found confirmation from entropy loss. A stronger binding of nicotine to fixed specific sites of kaolinite in the Stern layer was, however, revealed. The activity coefficients and the excess thermodynamic functions were indicative of the reaction behaving as a highly heterogeneous non-ideal system.

Introduction

In view of the encouraging results obtained during the course of our earlier work (SINGHAL *et al.*, 1975, 1976) on the exchange between aluminium and nicotine on illitic and montmorillonitic clays, it was considered desirable to extend the work to kaolinite in its aluminium form. Clays exhibit ion-exchange properties. They provide sites for cation exchange reactions and form clay organic complexes. In its aluminium saturated form kaolinite behaves as a Brönsted acid (LLOYD and CONLEY, 1970) to supply protons to nicotine in aqueous medium yielding the following exchange reaction

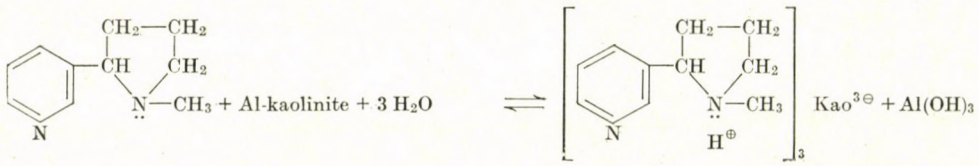

The above reaction was found to be reversible (SINGHAL and SINGH, 1970) in these laboratories.

The aim of the present investigation was therefore to obtain further informations from the thermodynamic approach of the earlier workers (GAINES and THOMAS, 1953; HOWERY and THOMAS, 1965; SINGHAL and SINGH, 1973)

for the exchange reaction between Al-kaolinite and nicotine. It was considered that such a study will prove useful in further understanding the nature of adsorption of complex pesticides such as nicotine on clays and soils.

Materials and methods

Kaolinite was a monomineralic A.P.I. sample from Bath, South Carolina. After suitable treatment its $<2\mu$ fraction was converted (SINGHAL *et. al.*, 1975) into Al-kaolinite of pH 4.5. The concentration of the suspension was 22.18 g per litre. Its Al-CEC as determined by the method of FRINK an PEECH (1963) was found to be 8.4 meq per 100 g kaolinite.

The exchange was carried out by taking 10 ml samples of Al-kaolinite suspension in a number of glass stoppered tubes and adding different amounts of standard 0.15N nicotine solution and adjusting the mixture to 25 ml in each case with distilled water. The mixtures were shaken at 30 $\pm$ 0.1°C in the first set of experiments and 60 $\pm$ 0.1 °C in the second set for 6 hours in each case. The suspensions were then centrifuged and aluminium and nicotine determined in the supernatant liquids (SINGHAL *et. al.*, 1975). The corresponding concentration of aluminium in the kaolinite phase was obtained by substracting its concentration in the supernatant liquids from the Al-CEC and that for nicotine from nicotine added minus the nicotine in the supernatants.

Results and discussion

The exchange equilibria between Al-kaolinite and nicotine can be described by the following equation

$\overline{C}_{Al} + C_{nicotine} \rightleftharpoons C_{Al} + \overline{C}_{nicotine}$ (1), where barred quantities represent the equivalent concentrations in the clay phase and unbarred, the con-

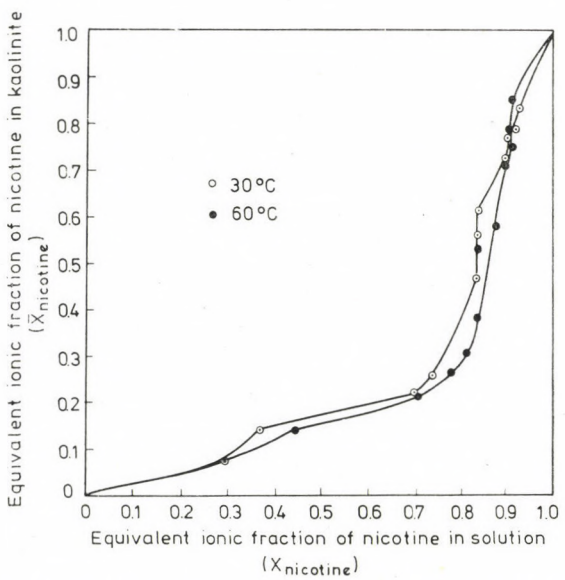

Fig. 1. Exchange isotherms for nicotinium-ion on aluminium kaolinite at 30° and 60°C

centrations in the solution. The ionic fractions of aluminium and nicotine in the solid and solution phases, the separation factors and the selectivity coefficients for various values of ionic fractions of nicotine were calculated by the usual methods as mentioned earlier (EL-SAYED, *et al.*, 1970; HELFFERICH, 1962; SINGHAL *et al.*, 1976). The values are given in Table I.

Table I

Values of equivalent ionic fractions of aluminium and nicotine and selectivity quotients at 30° and 60 °C for the nicotine exchange with Al-kaolinite

30 °C

S. N.	$\bar{X}_{Al}$	X_{Al}	$\bar{X}_{nicotine}$	$X_{nicotine}$	$\alpha_{Al}^{nicotine}$	K_C	log K_C
1.	1.000	1.000	0.000	0.000	0.000	0.0000	0.0000
2.	0.920	0.710	0.080	0.290	0.212	0.0018	−2.7447
3.	0.851	0.626	0.149	0.374	0.089	0.0032	−2.4949
4.	0.782	0.303	0.218	0.696	0.121	0.0119	−1.9245
5.	0.691	0.266	0.309	0.734	0.162	0.0287	−1.5421
6.	0.668	0.186	0.332	0.814	0.114	0.0189	−1.7235
7.	0.525	0.171	0.475	0.829	0.187	0.0613	−1.2125
8.	0.434	0.169	0.566	0.831	0.265	0.1320	−0.9101
9.	0.377	0.167	0.623	0.833	0.331	0.1853	−0.7321
10.	0.267	0.104	0.733	0.896	0.319	0.2133	−0.6710
11.	0.220	0.102	0.780	0.898	0.403	0.3428	−0.4650
12.	0.199	0.085	0.801	0.915	0.374	0.3200	−0.4949
13.	0.152	0.077	0.848	0.923	0.465	0.3928	−0.4069
				60 °C			
1.	1.000	1.000	0.000	0.000	0.000	0.0000	0.0000
2.	0.920	0.710	0.080	0.290	0.213	0.0018	−2.7447
3.	0.851	0.558	0.149	0.442	0.099	0.0046	−2.3376
4.	0.782	0.304	0.218	0.696	0.112	0.0119	−1.9245
5.	0.761	0.230	0.269	0.770	0.106	0.0129	−1.8894
6.	0.686	0.190	0.314	0.810	0.107	0.0161	−1.7932
7.	0.557	0.164	0.443	0.836	0.156	0.0440	−1.3565
8.	0.459	0.166	0.541	0.834	0.235	0.0987	−1.0057
9.	0.413	0.130	0.586	0.871	0.212	0.0962	−1.0164
10.	0.281	0.105	0.719	0.895	0.300	0.1937	−0.7329
11.	0.237	0.091	0.763	0.909	0.322	0.2270	−0.6884
12.	0.195	0.089	0.805	0.911	0.403	0.3144	−0.9011
13.	0.142	0.094	0.858	0.906	0.627	0.5622	−0 0255

From the values of equivalent ionic fractions at 30° and 60 °C, exchange isotherms were plotted and given in Fig. 1. The curves strongly deviated from the diagonal. Thus as compared to nicotine, aluminium was preferred throughout by kaolinite at both temperatures. This was in accordance with the separation factor whose values were lower than unity at both temperatures. An examination of the values of separation factor (Table I) further indicated that, in general, the preference of nicotine increased with a rise in its concentration while an increase in temperature was without any marked effect.

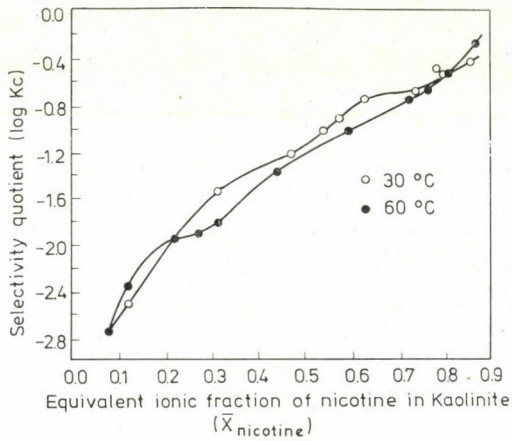

Fig. 2. Nicotine-aluminium selectivity in kaolinite

Using the trapezoidal rule, the plot of selectivity coefficients (Fig. 2) was used to calculate the thermodynamic equilibrium constant for the exchange reaction from the relationship

$$\ln K = (Z_A - Z_B) + \int_0^1 \ln K_C \, d\bar{X}_{nicotine} \tag{2}$$

A slightly higher value of K at 60° than at 30 °C indicated a somewhat greater preference by kaolinite for nicotine with a rise in temperature.

The values of $\Delta G°$, $\Delta H°$ and $\Delta S°$ were calculated from the following well known equations

$$\Delta G° = -RT \ln K \tag{3}$$

$$\ln \left(\frac{K_{T_2}}{K_{T_1}} \right) = - \frac{\Delta H°}{R} \left(\frac{1}{T_2} - \frac{1}{T_1} \right) \tag{4}$$

and $$\Delta G^\circ = \Delta H^\circ - T\Delta S^\circ \quad (5)$$

The results are given in Table II.

Table II

Thermodynamic values for the nicotine exchange with aluminium kaolinite at 30° and 60 °C

Thermodynamic parameters	Values at 30 °C	Values at 60 °C
K	0.135	0.155
ΔG° cal/mole	179.39	279.85
ΔH° cal/mole	−1018.21	
ΔS° cal/mole	−4.02	−4.02

The positive values of standard free energy indicated that at both temperatures the exchanges were non-spontaneous with a lower preference for nicotine. The enthalpy effect indicated that the reaction was temperature dependent and exothermic and that nicotine was more strongly bound on kaolinite as compared to aluminium. The non-spontaneity of exchange of nicotine found confirmation from entropy loss during the reaction. The greater order in the system in the final state of exchange as indicated by negative values of entropy, however, appeared to be due to binding of nicotine to fixed specific sites of kaolinite in the Stern layer.

Table III

The surface phase activity coefficient for different Al-nicotine compositions at the kaolinite surface at 30° and 60 °C

S. N.	Values at 30 °C			Values at 60 °C		
	$\bar{X}_{nicotine}$	f_{Al}	$f_{nicotine}$	$\bar{X}_{nicotine}$	f_{Al}	$f_{nicotine}$
1.	0.080	1.0000	1.0000	0.080	1.0000	1.0000
2.	0.149	1.2713	1.2586	0.149	1.2586	1.2461
3.	0.218	2.1383	2.0751	0.218	2.0751	2.0138
4.	0.309	3.0957	2.9154	0.269	2.5857	2.5093
5.	0.332	3.2871	3.1582	0.314	3.0957	2.9154
6.	0.475	5.5290	4.8067	0.443	5.1039	4.6182
7.	0.566	7.6141	5.7546	0.541	7.2427	5.8124
8.	0.623	9.2999	6.1105	0.586	8.3311	6.6851
9.	0.733	12.1825	7.4633	0.719	13.4637	8.4149
10.	0.780	16.9400	7.6906	0.763	14.8797	8.9352
11.	0.801	16.9000	8.0849	0.805	20.0855	9.3933
12.	0.848	21.1153	8.6711	0.858	34.8133	9.4877

The surface phase activity coefficients of aluminium and nicotine were calculated from the following expressions (HOWERY and THOMAS, 1965; SINGHAL *et al.*, 1975)

$$\ln f_{\text{nicotine}} = (\overline{X}_{\text{nicotine}} - 1) \ln K_C - \int_{\overline{X}_{\text{nicotine}}}^{1} \ln K_C \, d\overline{X}_{\text{nicotine}} \tag{6}$$

and

$$\ln f_{Al} = \overline{X}_{\text{nicotine}} \ln K_C - \int_{0}^{\overline{X}_{\text{nicotine}}} \ln K_C \, d\overline{X}_{\text{nicotine}} \tag{7}$$

The values are given in Table III. The values obtained were greater than unity and showed a consistent rise with an increase in the value of $\overline{X}_{\text{nicotine}}$. Such high values in solid state have been observed by other workers also (ROBINSON and STOKES, 1949; DEIST and TALIBUDEEN, 1967) and represented a very heterogeneous diffuse distribution of aluminium and nicotine ions on the kaolinite surface.

To study the deviation of the heterogeneous system from ideality the excess thermodynamic functions for the interaction were calculated from the equations (GAST and KLOBE, 1971; VANSANT and UYTTERHOEVEN, 1972):

$$\Delta G_m^x = RT \left[\overline{X}_{\text{nicotine}} \ln f_{\text{nicotine}} + \overline{X}_{Al} \ln f_{Al} \right] \tag{8}$$

$$\Delta H_m^x = - RT^2 \left[\overline{X}_{\text{nicotine}} \left(\frac{\delta \ln f_{\text{nicotine}}}{\delta T} \right) + \overline{X}_{Al} \left(\frac{\delta \ln f_{Al}}{\delta T} \right) \right] \tag{9}$$

and

$$\Delta G_m^x = \Delta H_m^x - T \, \Delta S_m^x \tag{10}$$

From the positive and rising values of ΔG_m^x (Table IV) it appeared that the heterogeneous mixture of ions during the exchange was less stable as compared to the pure forms and the stability decreased with a rise in nicotine concentration. A change from positive to negative in the enthalpies of mixing indicated an increase in strength of binding of the mixture of ions with an increase in the concentration of nicotine. Negative entropies were indicative of a more ordered distribution of the mixture of aluminium and nicotinium ions on the heteroionic exchanger with respect to the pure ionic forms. Thus the departure from ideality during the exchange reaction occurred in the form of a less stable though more ordered mixture of ions on the kaolinite surface.

Table IV

The excess free energies, enthalpies and entropies of mixing, ΔG_m^x, ΔH_m^x, ΔS_m^x for Al-nicotine exchange on kaolinite at 30° and 60 °C

30 °C

S. N.	$\overline{X}_{nicxtine}$	ΔG_m^X	ΔH_m^X	ΔS_m^X
1.	0.080	0.00	0.00	0.000
2.	0.149	142.50	53.02	−0.000
3.	0.218	446.07	194.39	−0.845
4.	0.309	659.26	1219.37	1.880
5.	0.332	504.07	494.82	−0.031
6.	0.475	977.47	477.14	−1.679
7.	0.566	1109.01	74.22	−3.472
8.	0.623	1166.17	−371.11	−5.159
9.	0.733	1271.49	−759.90	−6.817
10.	0.780	1313.42	−633.86	−6.602
11.	0.801	1328.01	−1042.65	−7.955
12.	0.848	1359.85	−1060.32	−8.121

60 °C

1.	0.080	0.00	0.00	0.000
2.	0.149	148.74	64.36	−0.261
3.	0.218	462.79	228.38	−0.726
4.	0.269	622.72	1498.83	2.576
5.	0.314	714.37	581.32	−0.412
6.	0.443	1017.70	581.32	−1.351
7.	0.541	1198.51	101.73	−0.561
8.	0.586	1279.43	−394.47	−5.183
9.	0.719	1448.16	−560.56	−6.219
10.	0.763	1489.17	−747.41	−6.924
11.	0.805	1531.98	−1224.93	−8.535
12.	0.858	1561.35	−1204.17	−8.563

*

The second author is indebted to U.G.C. (India) for the grant of a Post Doctoral Fellowship.

REFERENCES

[1] DEIST, J., TALIBUDEEN, O.: J. Soil Sci., **18,** 125—137. (1967)
[2] EL-SAYED, M. H., BURAU, R. G., BABCOCK, K. L.: Soil Sci. Soc. Amer. Proc., **34,** 397—400. (1970)
[3] FRINK, C. R., PEECH, M. (1963) Soil Sci. Soc. Amer. Proc., **27,** 527—530
[4] GAINES, G. L., THOMAS, H. C.: (1953). J. Chem. Phys., **21,** 714—718
[5] GAST, R. G., KLOBE, W. D. (1971). Clays and Clay Minerals, **19,** 311—319
[6] HELFFERICH, G. Ion Exchange. p. 153. McGraw-Hill Book Company, Inc. New York 1962
[7] HOWERY, S. G., THOMAS, H. C.: J. Phys. Chem., **69,** 331—537 (1965)
[8] LLOYD, M. K., CONLEY, R. F.: Clays and Clay Minerals, **18,** 37—46 (1970)
[9] ROBINSON, R. A., STOKES, R. H.: Trans. Faraday Soc., **45,** 612 (1949) (1949)
[11] SINGHAL, J. P., SINGH, R. P. (1973). J. Soil Sci., **24,** 271—276
[12] SINGHAL, J. P., SINGH, R. P., KUMAR, D. (1975). J. Ind. Chem. Soc , **52,** 380—384
[13] SINGHAL, J. P., SINGH, R. P., KUMAR, D. (1975). J. Ind. Chem. Soc., **52,** 1015—1019
[14] SINGHAL, J. P., SINGH, R. P., SINGH, C. P., GUPTA, G. K. (1976). J. Soil Sci., **27,** 42—47
[15] VANSANT, E. F. and UYTTERHOEVEN, J. B. (1972). Clays and Clay Minerals, **20,** 47—54

J. P. SINGHAL
R. P. SINGH
Aligarh Muslim University, Aligarh, India.

Acta Chimica Academiae Scientiarum Hungaricae, Tomus 93 (3—4), pp. 315—355 (1977)

INFRARED SPECTRA OF 1,2,3,5-TETRASUBSTITUTED BENZENE DERIVATIVES

G. VARSÁNYI*, G. HORVÁTH**, L. IMRE***,
J. SCHAWARTZ**, P. SOHÁR**** and F. SÓTI***

*(*Technical University, Budapest*
***Chinoin Pharmaceutical and Chemical Works, Budapest*
****Central Research Institute for Chemistry, Hungarian Academy of Sciences, Budapest*
*****Pharmaceutical Research Institute, Budapest)*

Received June 25, 1976

On the basis of the vibrations of the ring, 115 1,2,3,5-tetrasubstituted benzene derivatives can be classified into three groups, depending on whether all four substituents are 'light', or one or two of them are 'heavy'. The ring vibrations most closely resembling the 30 fundamental vibrations of benzene were first considered, and the intensity relations and frequency ranges of the relevant bands were given for each. In the second part an examination was made of the characters of the bands relating to the internal vibrations of the substituents. Particular attention was paid to the OH, C = O, NO_2 and amide groups, for intermolecular and chelate structures in the solid phase could be established from the features of the bands related to these groups. The intensities and frequencies were correlated with the electron shifts within the molecules.

Introduction

We earlier reported and discussed the infrared spectra of 50 1,2,3,5--tetrasubstituted benzene derivatives [1, 2]. The systematic investigation has now been extended to many further derivatives, permitting a more complete review of the vibrational properties of 115 1,2,3,5-tetrasubstituted benzene derivatives.

Below we list the compounds studied, including those reported previously, in three main groups: *(A)* all four substituents are 'light' [3, 4]; *(B)* there is a heavy halogen in position 1; *(C)* there are heavy halogens in positions 1 and 3.

Group A:

	Substituents in positions 1	2	3	5	
1.	CH_3	CH_3	CH_3	CH_3	1,2,3,5-tetramethylbenze [5,6]
2.	F	F	F	F	1,2,3,5-tetrafluorobenzene [7]
3.	CH_3	C_2H_5	CH_3	CH_3	1,3,5-trimethyl-2-ethylbenzene [8]
4.	CH_3	C_3H_7	CH_3	CH_3	1,3,5-trimethyl-2-n-propylbenzene [8]
5.	OH	OH	OH	CH_3	3,4,5-trihydroxytoluene
6.	OH	COOH	OH	OH	2,4,6-trihydroxybenzoic acid
7.	OH	OH	OH	COOH	3,4,5-trihydroxybenzoic acid
8.	OH	OH	OH	$COOCH_3$	methyl 3,4,5-trihydroxybenzoate
9.	OH	OCH_3	OH	CH_3	3,5-dihydroxy-4-methoxytoluene

10.	OH	OH	OCH_3	CHO	3,4-dihydroxy-5-methoxybenzaldehyde
11.	OH	$COOCH_3$	OH	OCH_3	methyl 2,6-dihydroxy-4-methoxybenzoate
12.	OH	OCH_3	OH	$COOCH_3$	methyl 3,5-dihydroxy-4-methoxybenzoate
13.	OCH_3	OH	OCH_3	CH_3	4-hydroxy-3,5-dimethoxytoluene
14.	OCH_3	OH	OCH_3	COOH	4-hydroxy-3,5-dimethoxybenzoic acid
15.	OCH_2	OH	OCH_3	$COOCH_3$	methyl 4-hydroxy-3,5-dimethoxybenzoate
16.	OH	$COOCH_3$	OCH_3	OCH_3	methyl 2-hydroxy-4,6-dimethocybenzoate
17.	OH	$CONH_2$	OCH_3	OCH_3	2-hydroxy-4,6-dimethoxybenzamide
18.	OCH_3	OCH_3	OCH_3	CHO	3,4,5-trimethoxybenzaldehyde
19.	OCH_3	OCH_3	OCH_3	COOH	3,4,5-trimethoxybenzoic acid
20.	OCH_3	OCH_3	OCH_3	$COOCH_3$	methyl 3,4,5-trimethoxybenzoate
21.	OCH_3	OCH_3	OCH_3	$CONH_2$	3,4,5-trimethoxybenzamide
22.	OCH_3	OC_2H_5	OCH_3	COOH	3,5-dimethoxy-4-ethoxybenzoic acid
23.	OCH_3	OC_3H_7	OCH_3	COOH	3,5-dimethoxy-4-n-propoxybenzoic acid
24.	OCH_3	OC_3H_5	OCH_3	$CONH_2$	3,5-dimethoxy-4-allyloxybenzamide
25.	OCH_3	OC_3H_5	OCH_3	CN	3,5-dimethoxy-4-allyloxybenzonitrile
26.	OCH_3	$OCOCH_3$	OCH_3	COOH	3,5-dimethoxy-4-acetoxybenzoic acid
27.	OH	COC_2H_5	$OCOCH_3$	$OCOCH_3$	2-propionyl-3,5-diacetoxyphenol
28.	OCH_3	$OCOCH_3$	$OCOCH_3$	CH_3	3-methoxy-4,5-diacetoxytoluene
29.	OCH_3	$OCOCH_3$	$OCOCH_3$	CHO	3-methoxy-4,5-diacetoxybenzaldehyde
30.	CH_2	NH_2	CH_3	CH_3	2,4,6-trimethylaniline [9]
31.	OH	$NO_2.H_2O$	OH	OH	2,4,6-trihydroxynitrobenzene hydrate
32.	OCH_3	OCH_3	OCH_3	NO_2	3,4,5-trimethoxynitrobenzene
33.	COOH	OH	NO_2	NO_2	3,5-dinitrosalicylic acid
34.	NO_2	OH	NO_2	CN	2,6-dinitro-4-cyanophenol
35.	NO_2	OH	NO_2	OH	2,6-dinitrohydroquinone
36.	NO_2	OCH_3	NO_2	CN	2,6-dinitro-4-cyanoanisole
37.	NO_2	OCH_3	NO_2	OH	4-methoxy-3,5-dinitrophenol
38.	NO_2	OH	NO_2	$OCOCH_3$	4-acetoxy-2,6-dinitrophenol
39.	NO_2	OH	NO_2	OSO_2CH_3	4-mesyloxy-2,6-dinitrophenol
40.	NO_2	OCH_3	NO_2	OSO_2CH_3	4-mesyloxy-2,6-dinitroanisole
41.	NO_2	NHC_2H_5	NO_2	CN	2,6-dinitro-4-cyano-N-ethylaniline
42.	NO_2	$N(CH_3)_2$	NO_2	CN	2,6-dinitro-4-cyano-N,N-dimethylaniline
43.	NO_2	$N(CH_2)_4O$	NO_2	CN	4-N-morpholino-3,5-dinitrobenzonitrile
44.	NO_2	OH	NO_2	NO_2	2,4,6-trinitrophenol

Group B:

45.	Cl	OH	CHO	$COOCH_3$	methyl 4-hydroxy-3-chloro-5-formylbenzoate
46.	Br	OH	OH	$COOCH_3$	methyl 3,4-dihydroxy-5-bromobenzoate
47.	I	OH	OH	CHO	3,4-dihydroxy-5-iodobenzaldehyde
48.	Cl	OCH_3	CN	$COOCH_3$	methyl 4-methoxy-3-chloro-5-cyanobenzoate
49.	Cl	OH	OCH_3	CHO	4-hydroxy-3-methoxy-5-chlorobenzaldehyde
50.	Br	CH_3	OH	OCH_3	2-hydroxy-4-methoxy-6-bromotoluene
51.	Br	OH	OCH_3	CHO	4-hydroxy-3-methoxy-5-bromobenzaldehyde
52.	I	OH	OCH_3	CHO	4-hydroxy-3-methoxy-5-iodobenzaldehyde
53.	Cl	OCH_3	OCH_3	COOH	3,4-dimethoxy-5-chlorobenzoic acid
54.	Cl	OCH_3	OCH_3	$CONH_2$	3,4-dimethoxy-5-chlorobenzamide
55.	Br	COOH	OCH_3	OCH_3	2,4-dimethoxy-6-bromobenzoic acid
56.	Br	$CONH_2$	OCH_3	OCH_3	2,4-dimethoxy-6-bromobenzamide
57.	Br	CN	OCH_3	OCH_3	2,4-dimethoxy-6-bromobenzonitrile
58.	I	OCH_3	OCH_3	$CONH_2$	3,4-dimethoxy-5-iodobenzamide
59.	Cl	OC_3H_5	OCH_3	COOH	3-methoxy-4-allyloxy-5-chlorobenzoic acid
60.	Br	OC_3H_5	OCH_3	COOH	3-methoxy-4-allyloxy-5-bromobenzoic acid
61.	Br	OC_3H_5	OCH_3	$CONH_3$	3-methoxy-4-allyloxy-5-bromobenzamide
62.	Br	CH_3	NH_2	OCH_3	4-methoxy-2-amino-6-bromotoluene

63.	Cl	OH	NO_2	CN	2-chloro-6-nitro-4-cyanophenol
64.	Br	CH_3	NO_2	OH	4-hydroxy-2-bromo-6-nitrotoluene
65.	Br	OH	NO_2	CN	2-bromo-6-nitro-4-cyanophenol
66.	I	OH	NO_2	CN	2-iodo-6-nitro-4-cyanophenol
67.	Br	CH_3	NO_2	OCH_3	4-methoxy-2-bromo-6-nitrotoluene
68.	Br	OCH_3	NO_2	CN	2-bromo-6-nitro-4-cyanoanisole
69.	Br	CH_3	NO_2	NH_2	4-amino-2-bromo-6-nitrotoluene
70.	Br	CH_3	NO_2	NO_2	2-bromo-4,6-dinitrotoluene
71.	Br	CH_2OH	NO_2	NO_2	2-bromo-4,6-dinitrobenzyl alcohol
72.	Br	$CONH_2$	NO_2	NO_2	2-bromo-4,6-dinitrobenzamide
73.	Br	CN	NO_2	NO_2	2-bromo-4,6-dinitrobenzonitrile
74.	Br	F	NO_2	NO_2	2-bromo-4,6-dinitrofluorobenzene
75.	Br	NH_2	NO_2	NO_2	2-bromo-4,6-dinitroaniline

Group C:

76.	Cl	OH	Cl	COOH	4-hydroxy-3,5-dichlorobenzoic acid
77.	Cl	OH	Cl	$COOCH_3$	methyl 4-hydroxy-3,5-dichlorobenzoate
78.	Cl	OH	Cl	$CONH_2$	4-hydroxy-3,5-dichlorobenzamide
79.	Br	OH	Br	COOH	4-hydroxy-3,5-dibromobenzoic acid
80.	Br	OH	Br	$COOCH_3$	methyl 4-hydroxy-3,5-dibromobenzoate
81.	Br	OH	Br	$CONH_2$	4-hydroxy-3,5-dibromobenzamide
82.	Br	OH	Br	CN	2,6-dibromo-4-cyanophenol
83.	I	OH	I	CH_3	4-hydroxy-3,5-diiodotoluene
84.	I	OH	I	CN	2,6-diiodo-4-cyanophenol
85.	Cl	OCH_3	Cl	$CH_2NH_3^+$	4-methoxy-3,5-dichlorobenzylammonium ion
86.	Cl	OCH_3	Cl	CHO	4-methoxy-3,5-dichlorobenzaldehyde
87.	Cl	OCH_3	Cl	$COCH_3$	4-methoxy-3,5-dichloroacetophenone
88.	Cl	OCH_3	Cl	COCl	4-methoxy-3,5-dichlorobenzoyl chloride
89.	Cl	OCH_3	Cl	COOH	4-methoxy-3,5-dichlorobenzoic acid
90.	Cl	OCH_3	Cl	$CONH_2$	4-methoxy-3,5-dichlorobenzamide
91.	Cl	OCH_3	Cl	CONHOH	4-methoxy-3,5-dichlorobenzohydroxamic acid
92.	Cl	OCH_3	Cl	CHNOH	4-methoxy-3,5-dichlorobenzaldoxime
93.	Cl	OCH_3	Cl	$CNHNH_2$	4-methoxy-3,5-dichlorobenzamidine
94.	Cl	OCH_3	Cl	CNHNHOH	4-methoxy-3,5-dichlorobenzohydroxyamidine
95.	Br	OCH_3	Br	COCl	4-methoxy-3,5-dibromobenzoyl chloride
96.	Br	OCH_3	Br	$CONH_2$	4-methoxy-3,5-dibromobenzamide
97.	Br	OCH_3	Br	$CONHCH_3$	4-methoxy-3,5-dibromo-N-methylbenzamide
98.	Br	OCH_3	Br	$CNHNH_2$	4-methoxy-3,5-dibromobenzamidine
99.	Br	OCH_3	Br	CNHNHOH	4-methoxy-3,5-dibromobenzohydroxyamidine
100.	Br	OCH_3	Br	CN	2,6-dibromo-4-cyanoanisole
101.	Br	OCH_3	Br	$CSNH_2$	4-methoxy-3,5-dibromothiobenzamide
102.	Br	OC_2H_5	Br	COOH	4-ethoxy-3,5-dibromobenzoic acid
103.	Br	OC_2H_5	Br	$CONH_2$	4-ethoxy-3,5-dibromobenzamide
104.	Br	OC_3H_7	Br	$CONH_2$	4-n-propoxy-3,5-dibromobenzamide
105.	Cl	OC_3H_5	Cl	COOH	4-allyloxy-3,5-dichlorobenzoic acid
106.	Cl	OC_3H_5	Cl	$CONH_2$	4-allyloxy-3,5-dichlorobenzamide
107.	Br	OC_3H_5	Br	$CONH_2$	4-allyloxy-3,5-dibromobenzamide
108.	Br	OC_3H_5	Br	$CONHCH_3$	4-allyloxy-3,5-dibromo-N-methylbenzamide
109.	I	$OCOCH_3$	I	COOH	4-acetoxy-3,5-diiodobenzoic acid
110.	Cl	OSO_2CH_3	Cl	OSO_2CH_3	2,6-dichloro-1,4-dimesyloxybenzene
111.	Cl	NH_2	Cl	$COOCH_3$	methyl 4-amino-3,5-dichlorobenzoate
112.	Cl	OCH_3	Cl	NH_2	4-methoxy-3,5-dichloroaniline
113.	Br	OCH_3	Br	NH_2	4-methoxy-3,5-dibromoaniline
114.	Br	OH	Br	NO_2	2,6-dibromo-4-nitrophenol
115.	Br	OCH_3	Br	NO_2	2,6-dibromo-4-nitroanisole

Bands originating from ring vibrations

In the following, using the numbering recommended by WILSON [10], we shall attempt in sequence to identify those vibrations from the spectra, the schematic picture of which *resembles* most closely the normal vibration of benzene as numbered by WILSON. Figure 1 shows the approximate co-ordinates of 30 normal vibrations of the ring, for compounds of group *A*.

Vibration 1. In the case of total symmetry, this belongs to species a_1. The original frequency in benzene is 992 cm^{-1}, but the mass of the substituents cause this to decrease considerably. The vibration picture depends on the nature of the substituents, and a separate treatment is therefore advisable in groups *A*, *B* and *C* of the compounds studied.

In group *A* the band is in general moderately strong or weak, but it may also be very weak. It is strong in the spectra of dimeric carboxylic acids, and also in the spectra of compounds 17 and 33. The overall frequency interval for this band is 440—580 cm^{-1}. In the case of single-atom substituents (not including hydrogen or hydrogens) it lies at 573—580 cm^{-1}; if the four substituents together comprise 5—8 atoms (similarly not including hydrogens), it is at 523—550 cm^{-1}; while with bulkier substituents it is at 485—505 cm^{-1} (though with ortho-acetoxy groups it is found at 525 or 532 cm^{-1}). The nitro group reduces the frequency, probably as a consequence of coupling with the β_{as} NO_2 vibration. In the spectra of mononitro compounds it lies at 475—490 cm^{-1}, and in those of dinitro compounds at 440—497 cm^{-1}. The frequency is particularly low in compounds with the bulky mesyloxy substituent.

In group *B* the band is generally weak or very weak. On many occasions it cannot even be identified. It is stronger in the spectra of dimeric carboxylic acids (see above) or if there is an OH group in position 3. Its overall frequency interval is 410—565 cm^{-1}. Here too, a nitro group decreases the frequency significantly. If there is neither a nitro nor a nitrile group in the molecule, then the frequency is 511—544 cm^{-1}, and indeed, in compound 62, in which the +M effect of the substituents is a maximum, it is 565 cm^{-1}. In nitriles, in the absence of the nitro group it is at 499—508 cm^{-1}, in mononitro compounds at 429—471 cm^{-1} (the frequency falls slightly in the sequence Cl, Br, I: *e.g.* 471, 467 and 464 cm^{-1} in compounds 63, 54 and 66), and in dinitro compounds at 410—423 cm^{-1}.

In group *C* the band is of medium intensity or strong. It is weak, however, in those cases where there are substituents of identical polarity in positions 2 and 5, *e.g.* in compounds 112 and 113 (OCH_3 and NH_2). The intensity is likewise decreased when there is a methylammonium, amidine, nitrile or nitro group in position 5. Its frequency interval is 441—553 cm^{-1}. The frequency generally decreases by 10—15 cm^{-1} in the sequence Cl, Br, I.

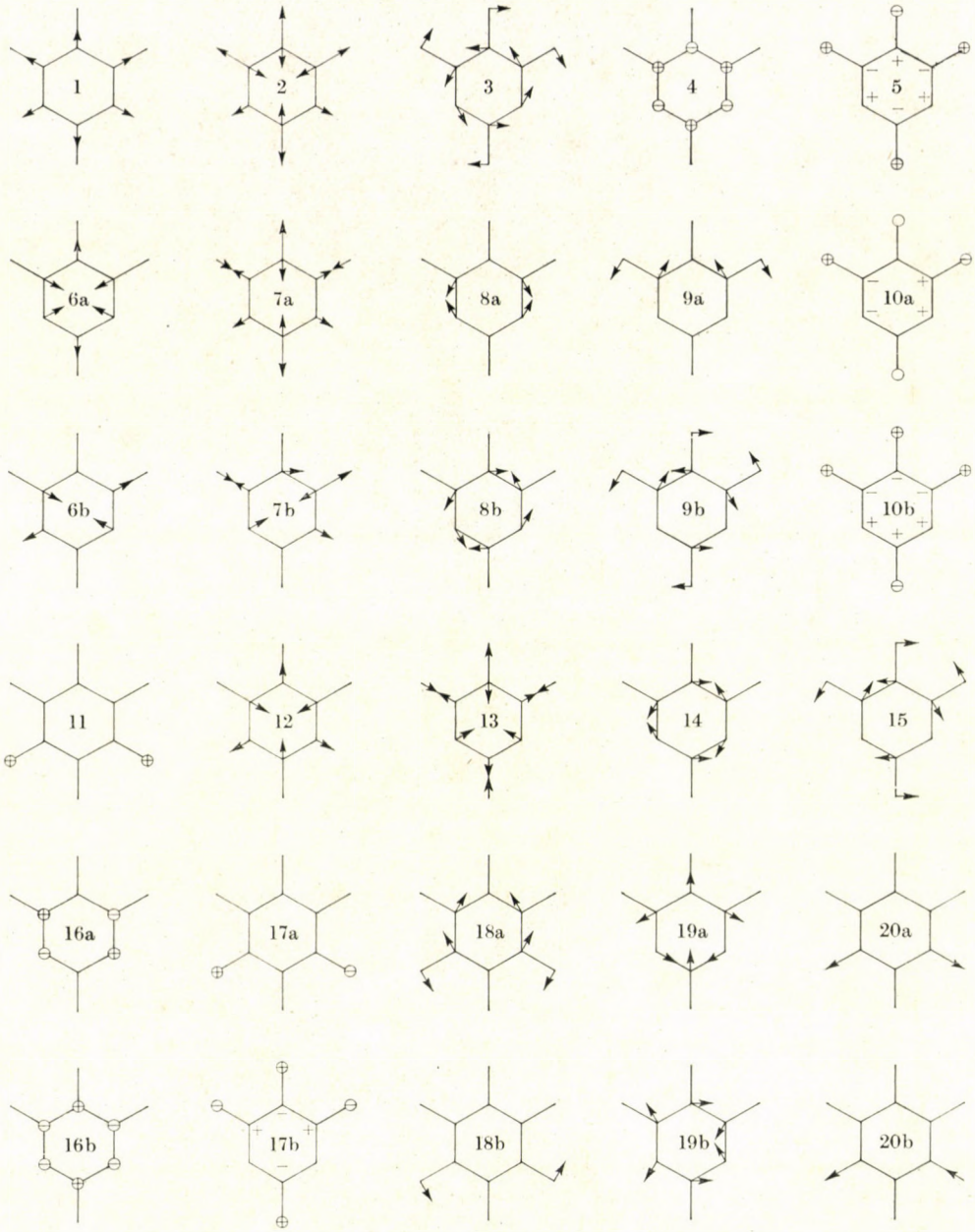

Fig. 1. Shematic picture of ring vibrations of group *A* compounds

The individual frequencies or ranges: 5-methyl derivative (83) 559 cm^{-1}; aldehyde 553 cm^{-1}; benzylammonium derivative (85) 540 cm^{-1}; acids (including I, Br and Cl derivatives) 502—536 cm^{-1}; nitriles, amines, amides, esters (with different halogens) 477—515 cm^{-1}; amidines 488—502 cm^{-1}; N-methylamides, nitro derivatives (only with bromine) 483—485 cm^{-1}; acetophenone derivative (87) (with chlorine) 493 cm^{-1}; hydroxyamidines 477—488 cm^{-1}; thiobenzamide (with bromine) 464 cm^{-1}; oxime (with chlorine) 478 cm^{-1}; and acid chlorides 441—462 cm^{-1}.

Vibration 2. This refers to in-phase stretching vibrations of light substituents relative to the ring. This type of internal motion is naturally accompanied by the internal vibration of the skeleton and by the in-plane bending vibration of the hydrogens, but the character of the vibration is given by the ν C–X mode

In group *A* the band is generally strong, or even very strong, but it may sometimes, be overlapped by a similarly strong adjacent band. Thus, it is covered in the spectrum of compound 27 by the ν_{as} OCC band of the acetoxy group; in the spectra of compounds 31, 41, 42 and 43 by the $\nu_s NO_2$; in the spectrum of compound 7 by the band of vibration 14 (which is always strong in the case of phenols because of the coupling with the β OH); and by the band of the β OH vibration itself in the spectrum of compound 12. Its overall frequency range is very broad: 1159—1405 cm^{-1}. If at least three substituents are monoatomic (not including hydrogens), the frequency is 1313—1405 cm^{-1}. If the four substituents together comprise 5—8 atoms* (in the following the asterisk always means that hydrogens are not included in the number), it is 1210—1296 cm^{-1}, while with more complex substituents it is 1200—1237 cm^{-1}. The frequencies of the 1,3-dinitro derivatives are mainly determined by the masses of the substituents in positions 2 and 5; the nitro groups participate to a minor extent in the vibration. (The mass effect does not prove that the polyatomic substituents are rigid, but that in these cases the coupling with internal vibrations of the substituents decreases the relevant frequency of the benzene ring). In the event of at most 4 atoms* in positions 2 and 5, the frequency is 1255—1280 cm^{-1}. In 3,5-dinitro compounds the frequency is substantially lower, because of coupling with the $\nu_s NO_2$: In compound 33 it is 1178 cm^{-1}, and in compound 44 1159 cm^{-1}.

In group *B* the band is of medium or high intensity. However, in the spectra of phenols and aniline derivatives it may be covered by the band of vibration *14*, which is strong in these spectra. The band is weak in dinitro or nitro cyano derivatives. Its overall frequency interval is 1186—1268 cm^{-1}. It is the light substituents in positions 2 an 5 that take part predominantly in this vibration. If there is no nitro or cyano group in these positions, then the frequency is 1221—1269 cm^{-1}; if there is, then it is 1186—1233 cm^{-1}.

In group *C* the band is always strong or very strong. The substituent in position 2 vibrates with the greatest amplitude. Its frequency range is 1204—1316 cm^{-1}. Variation of the halogens does not influence the frequency. In the case of an OH or NH_2 group it is at 1268—1316 cm^{-1} (it lies below 1300 cm^{-1} only if there is a nitro or cyano group in position 5, or if there is no intermolecular H-bond). The frequency is the lowest for the mesyloxy group: 1204 cm^{-1} (110). For the other substituents it is at 1256—1285 cm^{-1}, but at 1297 cm^{-1} in the spectrum of the thioamide (101) because of coupling.

Vibration 3. This is the in-phase in-plane bending vibration of the substituents. The band is very weak, and its frequency is very sensitive to the mass of the substituents; it is difficult to identify, all the more so as it appears in the far infrared in the event of more complex substituents.

Vibration 4. This is the puckering vibration of the ring. Carbon atoms 1, 3 and 5 vibrate with higher amplitude.

In group *A* the band exhibits very variable intensities. It is markedly weak in the spectra of 5-benzoate esters, 1,3-dinitro compounds and 5-methyl derivatives, and also in the case of compound 7. In the spectrum of compound 31 it is hidden under the γ OH band. In the other cases it is generally strong. Its overall frequency range is 674—739 cm^{-1}. In carbonyl compounds it is at 688—739 cm^{-1}, and in the others at 674—709 cm^{-1}. In the former group the frequency is increased by coupling with the γ CO.

In group *B* the intensity of the band is reduced by electron-attracting substituents, with the exception of the carboxyl (this occurs only in dimeric form) and aldehyde groups. If the carboxy group forms a weak dimer (55), the band is similarly weak. Its overall frequency range is 672—743 cm^{-1}. In the spectra of esters and acids it is at 673—714 cm^{-1}, and in those of amides at 718—743 cm^{-1}. In both cases, coupling with the γ CO band (see above) or the amide **VI** band increases the frequency. In the spectra of aldehydes and mononitro derivatives it is at 672—696 cm^{-1}, in those of dinitro derivatives at 702—709 cm^{-1}, and in the case of 5-methoxy derivatives at 700—726 cm^{-1} (without a carboxy or amide group at 700—715 cm^{-1}).

In group *C* the band is generally of medium intensity, but sometimes strong. In the spectrum of compound 99 it is overlapped by the γ C=N band. It may also be weak, however, if there is an amide, acetyl, hydroxamic acid, amidine or nitro group at position 5. Its frequency similarly depends on the nature of the 5-substituent. Its overall range is 653—738 cm^{-1}. Amines, amides, the benzylammonium derivative (85), the hydroxamic acid and nitriles absorb at 710—738 cm^{-1}, esters at 682—703 cm^{-1}, acids, acid chlorides, aldehydes, N-methylamides, the thioamide (101), amidines, hydroxyamidines, nitro derivatives and the dimesyloxy derivative (110) at 666—691 cm^{-1}, and the oxime (92) at 653 cm^{-1}. The different ranges develop as a

consequence of coupling with various out-of-plane vibrations of the substituens.

Vibration 5. This is the trigonally symmetric out-of-plane vibration of the substituents in the far infrared.

Vibration 6a. This is an in-plane bending vibration of the ring. If heavy halogens are present in positions 1 and 3, there is strong coupling with the stretching vibration of the halongens, as a consequence of which the vibration may be assigned to a much higher frequency than in groups *A* and *B* [3, 4].

In group *A* it appears as a medium, weak or even very weak band, in general below 400 cm^{-1}. It is difficult to identify. The band is also weak in the spectra of compounds of group *B*. It displays a moderate intensity in the spectra of ortho-nitrophenols. Its upper frequency limit is 445 cm^{-1}.

In the spectra of group *C* the band is generally of medium intensity; more rarely it is strong, but it may also be weak. It sometimes appears as a shoulder of the umbrella vibration (vibration 11). It is generally weak in the case of multiply bonded CN substituents (amidines, nitriles), and also when there are ethoxy, propoxy or allyloxy substituents in position 2. Its frequency range is 865—997 cm^{-1}. In the case of light and not rigidly bonded substituents (NH_2, CHO) in position 5, the frequency is higher: 925—952 cm^{-1}. With monoatomic* substituents in positions 2 and 5 (83) it is 997 cm^{-1}. If there is a bulkier or rigid (C≡N) substituent in position 5, together with OH or NH_2 in position 2, it is 880—917 cm^{-1}. With OCH_3 or OC_3H_5 groups it is 881—907 cm^{-1}, and with OC_2H_5 or $OCOCH_3$ groups 865—870 cm^{-1}. As the ether side-chain is lengthened, therefore, the frequency passes through a minimum.

Vibration 6b. This is similarly a deformation vibration of the ring, which even in the case of a single halogen is coupled with the C—Hal stretching vibration, and appears at a substantially higher frequency than in the spectra of group *A* [5, 6].

In the spectra, of group *A* the band is at best of medium strength, but it is generally weak or even very weak, and in some cases it cannot be identified. In the spectra of compounds 6, 7 and 8 it merges into the side of the γ OH band, and in the spectra of the two mesyloxy derivatives it appears as a shoulder of the band of vibration *1*. In the spectra of compounds 15, 18, 23, 31, the two 1,2-diacetoxy derivatives and compound 33, it is covered probably by the band of vibration *16a*, and in the spectrum of compound 11 by the band of vibration *16b*. In the spectrum of compound 19 it can be identified as a shoulder of the band of vibration *16a*. Its overall frequency range is 404—523 cm^{-1}. In the case of monoatomic* substituents in positions 1 and 3 (see the normal co-ordinate) the frequency is 491—523 cm^{-1}; with at most 6 atoms* in positions 1, 2 and 3 it is 455—503 cm^{-1};

in the spectra of the other compounds it is 416—465 cm^{-1}, but in picric acid (44) it is 404 cm^{-1}.

In the spectra of group *B* the band is moderately strong or strong. At times, however, it may be covered by the band of the umbrella vibration. The intensity is reduced by a 3-nitro group, if this is not chelating; in addition, the intensity also decreases with increasing mass of the halogens. In the spectra of 3,5-dinitro derivatives the band is again stronger, which shows that carbon atom 5 too has an appreciable amplitude. The overall frequency range is 768—866 cm^{-1}. In the spectra of nitro derivatives it is 768—797 cm^{-1}, in those of aldehydes 828—857 cm^{-1}, the frequency increasing in the sequence I, Br, Cl, and in the spectra of the other compounds 844—866 cm^{-1}.

In the spectra of the compounds of group *C* the band is of medium intensity or strong, and sometimes very strong. In the spectra of compounds 103 and 104 it appears as a shoulder of vibration *12*. It is weak in the spectra of compounds 83 and 101. Its frequency range is 725—818 cm^{-1}. It depends strongly on the mass of the halogen. In the spectra of chloro derivatives it is 805—818 cm^{-1}, but in the case of a 2-amino-group (111), which stiffens the C–Cl bond, it is 794 cm^{-1}.

Vibration 7a. The character of this vibration varies strongly, depending on the number of halogens. Without halogen or with one halogen atom, it is predominantly a stretching vibration of the light substituents relative to the ring, but the frequency is higher in group *B*, partly as a result of the changed normal co-ordinate compared with group *A*, and partly as a consequence of a weak coupling with the C–Hal stretching vibration. With two heavy halogens, it is the in-phase C–Hal stretching vibration that most closely resembles normal co-ordinate *7a* of benzene. This, however, has a very low frequency.

In the spectra of group *A* compounds the band is of medium strength or strong, and sometimes very strong. In the spectrum of compound 23 it is overlapped by the band of vibration *12*, while in the case of compounds 6 and 7 it merges into the γ OH band. In the spectra of compounds 22 and 26 it appears as a shoulder of the band of vibration *12*. Its overall frequency range is very broad: 763—997 cm^{-1}. In the case of at least 3 monoatomic* substituents it lies at 905—932 cm^{1-}, but in tetrafluorobenzene it is at 997 cm^{-1} [7]. In all other cases it is at 763—833 cm^{-1}, *i.e.* it is never found between 833 and 905 cm^{-1}.

In the compounds of group *B*, vibration 7a is predominantly a stretching vibration of the light substituents with respect to the ring, where the substituents in positions 2 and 5 vibrate in the same phase. The band is generally of high or medium intensity. However, in the spectrum of compound 53 it is overlapped by the umbrella vibration, and in the spectra of the allyloxy

derivatives by the band of the out-of-plane vibration of the hydrogens in the side-chain. The presence of an iodine atom reduces the amplitude of the vibration, and hence the intensity of the band. In five compounds (50, 62, 64, 67 and 69) there are groups of identical polarity in positions 2 and 5. However, the band is not weak in the spectra of these either, if the molecule contains an OH or NH_2 group (which vibrate with high amplitude) in position 3 or 5 (50, 62, 64 and 69). The corresponding band of compound 67, on the other hand, is weak. The overall frequency range is 900—992 cm^{-1}. In the spectra of dinitro derivatives and nitro-nitriles it is 900—917 cm^{-1}, in the spectra of the four aldehydes 966—992 cm^{-1}, with the frequency increasing in the sequence I, Br, Cl in the methoxy derivatives (49, 51 and 52), and in the other cases 920—970 cm^{-1}.

In the spectra of group *C* the band is of medium intensity or weak. In the spectra of the bromo and iodo derivatives it may be shifted into the far infrared, and is then difficult to identify. The band is very weak in the spectra of the aldehyde and benzophenone derivatives (86 and 87). It is relatively stronger if there is an allyloxy or amino group in position 2. Its frequency range is 215—415 cm^{-1}, the frequency depending strongly on the mass of the halogen. The frequency range for the chloro derivatives is 362—415 cm^{-1}, that for the bromo derivatives 270—354 cm^{-1}, while the frequency of the band to be assigned to this vibration in the Raman spectrum of 2,6--diiodo-4-cyanophenol (84) is 215 cm^{-1}. The 5-amino group increases the C–Cl force constant and the frequency (415 cm^{-1}). In all other cases the band appears below 400 cm^{-1}. As regards the bromo derivatives, the frequency is higher if there is a small substituent (*e.g.* OH) in position 2, *i.e.* between the two bromine atoms. At the same time, 5-nitro and 5-cyano groups strongly decrease the frequency (270 cm^{-1} in compound 82).

Vibration 7b. In the presence of heavy halogens this is predominantly a C–Hal stretching vibration, while in general it is the out-of-phase stretching vibration of the 1,3-substituents with respect to the ring.

In the spectra of group *A* the band is of medium strength, strong or very strong. It is weak only if the intensity is decreased by intermolecular association, *e.g.* in compounds 18, 19 and 31. Its overall frequency range is 820—1050 cm^{-1} (1050 cm^{-1} in the spectrum of tetrafluorobenzene [7], while in the case of chelates formed between the 2-hydroxy group and groups other than nitro it is 901—920 cm^{-1}. In the event of intermolecular association between 2-OR groups and 5-carboxyl or 5-acid amide (or *vice versa*) it is 905—944 cm^{-1}, but in the spectrum of compound 19 it is 968 cm^{-1}, in the spectra of *o,o'*-dinitrophenols it is 927—989 cm^{-1}, in the case of *o,o'*-dinitroanilines it is 915 or 916 cm^{-1}, with one monoatomic*, and one diatomic* substituent in positions 1 and 3 it is 946—951 cm^{-1}, and in all other cases it is 820—902 cm^{-1}.

In group *B* the band is weak in general, as a consequence of the low amplitude. The frequency range for chloro derivatives is 385—445 cm^{-1}, while within this it is 387—418 cm^{-1} in the spectra of the 3-methoxy derivatives; for the bromo derivatives it is 275—346 cm^{-1}, and for 2-iodo-6-nitro-4-cyanophenol (66) it is 245 cm^{-1} (Raman value). Within the individual intervals the nitro group decreases the frequency.

In group *C* the out-of-phase C–Hal stretching vibration plays the decisive role. The band is always weak, and can frequently not be identified. Its overall frequency range is 275—522 cm^{-1}, depending on the halogens. For the chloro derivatives it is 499—522 cm^{-1} (as in the case of vibration 7a, the maximum frequency is observed in the presence of the 5-amino group); for the bromo derivatives it is 315—389 cm^{-1}; while as regards the iodo derivatives the band is to be found at 275 cm^{-1} in the Raman spectrum of compound 84.

Vibration 8a. A skeletal stretching vibration characteristic of benzene derivatives. In group *A* the band is always strong or very strong. In the spectrum of compound 31 it is covered by the β OH band of water, while in the spectrum of compound 37 it merges into the side of the $\nu_{as}NO_2$ band. It appears as a shoulder in two cases: on the side of the β NH band in the case of compound 41, and on the side of the ν C=O band in the spectrum of compound 6. Its overall frequency range is 1577—1654 cm^{-1}. In the case of only monoatomic* substituents it is at 1605—1631 cm^{-1}, in the case of esters and amides at 1577—1601 cm^{-1}, in the spectra of aldehydes and acids (but without ethoxy or allyloxy groups in position 2) at 1593—1622 cm^{-1}, with ethoxy and allyloxy groups at 1580—1587 cm^{-1}, in the spectra of nitro derivatives at 1606—1654 cm^{-1}, and in other cases at 1601—1616 cm^{-1}.

In the spectra of group *B* the band is almost always very strong, and is in general stronger than vibration 8b, which appears at a somewhat lower frequency. Exceptions are the 5-amides, the 2,3-dihydroxy chelates and compound 73, in which all of the light substituents are negative in character and give rise to a uniform charge in the ring. Its overall frequency range is 1582—1623 cm^{-1}. In the presence of nitro and amino groups it is at 1595—1623 cm^{-1}, and in their absence at 1582—1607 cm^{-1}.

In the spectra of group *C* the band is not always as strong as in the previous two groups. In the case of amides and compound 85 it may be covered by the bending band of the amino group. In addition, the band is weak in the spectra of compounds 83, 91, 101, the nitriles and nitro derivatives, but in the latter two cases only if there is a methoxy and not a hydroxy group in position 2. Its overall frequency range is 1575—1637 cm^{-1}. Electron-repelling groups in positions 2 and 5 increase the force constant of the vibration and the frequency (1598 and 1613 cm^{-1} in the spectra of compounds

112 and 113, and even 1637 cm^{-1} for compound 83). In all the other cases the frequency remains in the interval 1575—1600 cm^{-1}.

Vibration 8b. This is similarly a skeletal stretching vibration. In the spectra of group *A* the band is rarely strong; it frequently merges into the band of vibration *8a*, and cannot be identified at all in some cases. The band is strong and strongly separated from band *8a* if there is an amino or substituted amino group in position 2 or if a 2-hydroxy group forms an intermolecular linkage with an ester or nitro group in position 5. The band is likewise strong and separated in the spectra of 1,2,3-trihydro derivatives. Sometimes, in the case of the dinitro derivatives, it appears as a shoulder of the $\nu_{as}NO_2$ band. Its overall frequency range is 1536—1614 cm^{-1}. In the spectra of polyalkylbenzenes [8] it is at 1579—1581 cm^{-1}, and in the case of nitro compounds at 1566—1601 cm^{-1} (except for the spectra of compounds 43 and 44, where it lies at 1552 and 1614 cm^{-1}, respectively).

In the spectra of group *B* it generally shows up as a strong band, but at times it merges into the band of vibration *8a* (49, 51, 70) or into the $\nu_{as}NO_2$ band (63, 68). The band is weak in the spectra of compounds 64 and 69, in which high-amplitude carbon atoms 2 and 5 have substituents of similar mass and similar character. Its frequency interval is 1553—1593 cm^{-1}. The frequency depends slightly on the mass of the halogen and of the 2-substituent (in 2-OH derivatives it is 1582—1593 cm^{-1}, but in the iodo compounds at 1570—1576 cm^{-1}). The presence of a nitro group decreases the frequency (1558—1577 cm^{-1}), but a second nitro group compensates this effect (1565—1593 cm^{-1}), presumably as a consequence of coupling with the $\nu_{as}NO_2$ vibration.

In group *C* the vibration is almost always indicated by a strong band. Exceptions are compound 83 and particularly compound 110, in the spectra of which the band is scarcely identifiable. Its overall frequency range is 1528—1576 cm^{-1}. The frequency falls by 10—15 and 20 cm^{-1} in the sequence Cl, Br, I. The minimum frequency for phenols is 1549 cm^{-1}; the nitro group and resultant coupling slightly increase the frequency. In the event of other 2-OR groups, the nitro derivative has the maximum frequency (1573 cm^{-1} in the spectrum of compound 115), while for amines, acids, esters, aldehydes, N-methylamides, and compounds 85 and 87 it is 1551—1565 cm^{-1} (about 1551 cm^{-1} for bromo, and about 1565 cm^{-1} for chloro derivatives), for acid chlorides, amides, nitriles, hydroxyamidines and compounds 91, 92 and 101 it is 1534—1555 cm^{-1} (depending on the mass of the halogen), and finally for amidines it is 1528—1529 cm^{-1}.

Vibrations 9a, 9b, 10a and *10b.* These are two in-plane and two out-of plane bending vibrations of the substituents, in the far infrared. The frequency of vibration *9a* is 170 cm^{-1} in the Raman spectrum of compound 82, and 135 cm^{-1} in that of compound 84. Vibration *9b* could be identified only in

the Raman spectrum of compound 82, at 275 cm^{-1}. Finally, the Raman frequency of vibration *10b* is 210 cm^{-1} in the case of the dibromo derivative 82, and 200 cm^{-1} in the diiodo derivative 84.

Vibration 11. This is the umbrella vibration. In group *A* it is generally a strong band, but in the spectra of 5-cyano and 5-nitro compounds it may be weak, or even very weak. In the spectra of group *B* the band is less strong; indeed, it is generally weak if there is a negative substituent in position 3. In this case too, however, the band is strong in the spectra of nitrophenols

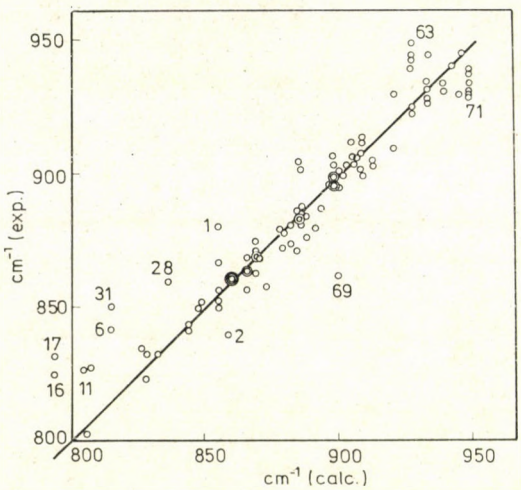

Fig. 2. Calculated and experimental frequencies of the umbrella vibration for 1,2,3,5-tetra-substituted benzene derivatives. 1. tetramethylbenzene; 2. tetrafluorobenzene; 3. 2,4,6-trihydroxybenzoic acid; 11. methyl 2,6-dihydroxy-4-methoxybenzoate; 16. methyl 2-hydroxy--4,6-dimethylbenzoate; 17. 2-hydroxy-4,6-dimethoxybenzamide; 28. 3-methoxy-4,6-diacetoxytoluene; 31. 2,4,6-trihydroxynitrobenzene hydrate; 63. 2-chloro-6-nitro-4-cyanophenol; 69. 4-amino-2-bromo-6-nitrotoluene; 71. 2-bromo-4,5-dinitrobenzyl alcohol

and nitroanilines. In group *C* the band is of strength medium or low in the spectra of acids, amides and thioamide, and strong in the other cases. In the spectra of some acids it may be overlapped by the band of vibration *6a*.

The formula to be found in Ref. [1] can be applied to the frequency of this vibration. Figure 2 shows the frequencies of vibration *11*. The vertical axis gives the experimental, and the horizontal axis the calculated values. A deviation greater than 10 cm^{-1} in the positive direction was found for compounds 1, 3, 28, 43, 62, 83 and 84, the 3,5-mononitro-nitriles, 3,5-dihydroxy, 3,5-hydroxy-methoxy and 3,5-dimethoxy derivatives. The probable cause of this is that the nitro and cyano groups do not reduce one another's electron-attracting effect, while in a 1,3,5-compound the third +M substituent plays a smaller role in the development of the alternating charges than

predicted by the formula. The difference of 35 cm^{-1} for compound 31 cannot be explained in this way. However, the formula does not take into consideration the substituents having no hydrogen atom in the ortho or para position. Thus, in compound 31 it neglects the nitro group, which otherwise has the highest negative spectroscopic moment and hence the strongest frequency-increasing effect.

A deviation greater than 10 cm^{-1} in the negative direction can be observed for compounds 2, 12, 32, 45, 67 and 69 and dinitro compounds. The difference is particularly high for the *m*-nitroaniline derivative [69], which shows that the nitro group exerts a substantially lower effect on the ring electrons here.

Vibration 12. This is a skeletal vibration in the radial direction, the amplitudes lying close to trigonal symmetry.

In group *A* the band is generally of medium intensity or strong. It is weak in the case of 2-allyloxy derivatives, dinitro compounds and 5-methoxy derivatives. In the spectrum of compound 31 it is covered by the very strong γ OH band, similarly as in the spectrum of compound 11. In the spectrum of compound 13 it is covered by the very low frequency umbrella vibration, and in the case of compound 33 by the γ C=O band. In the spectrum of picric acid (44) it appears as a shoulder on the band of vibration *4*. Its overall frequency range is 642–801 cm^{-1}, which is a very broad interval. In the spectrum of tetrafluorobenzene (2) its frequency is 786 cm^{-1}, and with the exceptions of alkylbenzenes [5, 6, 8] and nitro compounds is 732–780 cm^{-1} in all other cases. For compound 1 it is at 734 cm^{-1}, for the other alkylbenzenes at 710–721 cm^{-1} and for the dinitro compounds at 642–664 cm^{-1}, but for the 2-aniline derivatives it is 670–674 cm^{-1} and for picric acid (44) 685 cm^{-1}. The frequency of the vibration is anomalously high in the spectrum of compound 6: 801 cm^{-1}.

In group *B* the band is of medium strength, and occasionally strong. As in the case of vibration *6b*, a 3-nitro group decreases the intensity if it is not chelated (the band merges into the $\gamma_s NO_2$ band in the spectrum of compound 66), whereas in the case of 3,5-dinitro derivatives the band is again stronger. At the same time, 3,5-methoxy groups decrease the intensity. This supports the trigonal character of the vibration. Its overall frequency range is 658–808 cm^{-1}, again very broad. The nitro group reduces the frequency, but mainly in position 5. Otherwise, the 3-nitro group has only a slight effect on the frequency. The frequency for aldehydes is 788–808 cm^{-1} (increasing in the sequence I, Br, Cl), for esters and acids 766–772 cm^{-1}, for amides 770–789 cm^{-1}, and for the other non-nitro derivatives 790–808 cm^{-1}. For 3,5-dinitro derivatives it is 658–695 cm^{-1}.

In the spectra of group *C* it generally appears as a strong band. In the spectrum of compound 98 it merges into the bending band of the amino

group. Its overall frequency interval is 670—786 cm^{-1}. The nitro group decreases the frequency strongly: below 700 cm^{-1} only the bands of nitro derivatives are to be found. The frequency is also influenced by the mass of the halogens: there is a difference of about 20 cm^{-1} between the positions for the chloro and bromo derivatives. Apart from the nitro derivatives, relatively low frequencies are also observed for aldehyde 86 and hydroxamic acid 91: 743 and 746 cm^{-1}, respectively.

Vibration 13. This is a stretching vibration of trigonal symmetry, predominantly of light substituents, with the ring.

In the spectra of group *A* the band is generally strong or very strong. Exceptions are dinitro compounds not containing a cyano group. At times the band may be partially or completely covered by the β OH band (6, 7, 8 and 12). The overall frequency range is 1090—1195 cm^{-1}. With monoatomic* substituents in positions 1, 2 and 3 it is 1142—1195 cm^{-1}, and in the other cases, with the exception of the nitro derivatives, it is 1110—1148 cm^{-1}; in the nitro derivatives it is 1109—1126 cm^{-1}, but in compound 33 and picric acid (44) it is 1090 and 1093 cm^{-1}.

In group *B* it generally appears as a strong band. It is somewhat weaker in the spectra of 2-OH chelates. Its frequency range is 1062—1187 cm^{-1}. The nitro group reduces the frequency strongly. As regards the non-nitro derivatives, the frequency interval for acids and aldehydes is 1158—1187 cm^{-1}, for amides 1126—1134 cm^{-1}, and for the others 1144—1168 cm^{-1}. The frequency range for nitro compounds is 1062—1110 cm^{-1}, and within this is 1103—1110 cm^{-1} for the nitro-nitriles.

In group *C* it is a band of medium strength. It is weak, however, in the spectra of the amidines, thioamide 101 and compound 87. Its frequency range is 1122—1230 cm^{-1}. In the case of acids, esters, amides, N-methyl-amides and nitro derivatives the maximum frequency is 1156 cm^{-1}.

Vibration 14. A skeletal stretching vibration. In the spectra of the phenol derivatives of group *A* the band is strong or very strong, with the exception of compound 13, but it is sometimes partially or completely covered by another strong band. In the case of compound 5 it merges in the band of vibration *2*. In the spectra of compounds 33, 34, 35 and 37 it is covered by the $\nu_s NO_2$ band, and in that of compound 39 by the $\nu_{as} SO_2$ band. The band is strong in the spectrum of compound 30. It is similarly strong in the case of 1,2,3-trimethoxy and 1,3-dimethoxy-2-allyloxy derivatives, though it may be partially or completely covered by the band of vibration *2* (18, 20, 24). In the other cases the band is weak. The overall frequency range, 1206—1419 cm^{-1}, is very broad, but the reason for this is that the band is coupled with the β OH vibration in phenols, and appears at an anomalously high frequency. The highest frequency, 1419 cm^{-1}, is observed for compound 31. For the other phenols it is 1325—1386 cm^{-1}, but for picric acid (44) it

is only 1278 cm^{-1}. The corresponding frequency for compound 30 is 1309 cm^{-1}, and for tetramethylbenzene (1) 1294 cm^{-1}. In the spectra of the other compounds it is 1206—1279 cm^{-1}.

As regards the compounds of group *B*, the band is strong in the spectra of phenols, anilines and acid amides, but is otherwise weak. Its overall frequency interval is 1252—1331 cm^{-1}. For the ortho-nitrophenols it is 1326—1331 cm^{-1} (as a consequence of coupling with the high-frequency β OH vibration), for other phenols, anilines and dinitro derivatives it is 1270—1327 cm^{-1}, and for the other compounds it is 1252—1278 cm^{-1}.

In group *C* the band is moderately strong in the spectra of phenols and thioamide 101, and strong for 5-amines. It is otherwise weak, and in several cases cannot even be identified. In phenols it is coupled with the in-plane bending vibration of the OH group, and appears at an anomalously high frequency, particularly in the event of hydrogen bonds. The frequency range for phenols is 1310—1411 cm^{-1}. The band is found above 1400 cm^{-1} only for phenol esters 77 and 80. The vibration is also at a comparatively high frequency (1375 cm^{-1}) in compound 81. In the spectra of compounds not containing the OH group the frequency range is 1190—1275 cm^{-1}. The maximum frequency for the corresponding vibration of amides, N-methylamides, acid chlorides, nitriles and compound 85 is 1213 cm^{-1}.

Vibration 15. An in-plane bending vibration of the substituents relative to the ring. It is strongly sensitive to mass. The frequency of the vibration in the Raman spectrum of dibromo compound 82 is 140 cm^{-1}, and in that of the diiodo compound 84 it is 115 cm^{-1}.

Vibration 16a. In the case of only monoatomic or linear substituents, and if identical substituents are present in positions 1 and 3, the band would be forbidden in the infrared, since in the C_{2v} point-group the vibration belongs to the a_2 species. Otherwise, this is an out-of-plane, skeletal vibration. In the spectra of group *A* the band appears weakly or occasionally with medium strength in the case of asymmetric substituents. Its frequency range is 424—495 cm^{-1}. In the spectra of group *B* too, with a few exceptions it always gives a weak band. The exceptions are compounds containing 3-OH or 3-NH_2 groups. In accordance with the a_2 pseudo-symmetry, 2,5-substituents scarcely affect either the intensity or the frequency. Its frequency range is 453—520 cm^{-1}. In the case of a 3-methoxy group it is at 490—520 cm^{-1} (but in 3,5-dimethoxy derivatives at 459—475 cm^{-1}), in the event of 2-nitro and 3-aldehyde groups at 474—491 cm^{-1} (but for dinitro derivatives at 453—480 cm^{-1}), and with 3-OH and 3-NH_2 groups at 455—478 cm^{-1}. In the spectra of group *C* too the band is generally weak, with the exception of the strongly asymmetric dimesyloxy derivative (110). Its range of occurrence is 399—486 cm^{-1}. The minimum frequency in the case of 2-hydroxy or 2-amino-dichloro derivatives is 451 cm^{-1}.

Vibration 16b. The third out-of-plane skeletal vibration. In the spectra of group *A* the band is only strong if groups with moments of the same sign are situated in positions 2 and 5. Thus, a strong band appears in the spectra of tetramethylbenzene (1), tetrafluorobenzene (2), and compounds 9, 12, 28, 35, 37, 38, 39 and 40 (there are no infrared data for compounds 3 and 4, and the spectrum of compound 30 has been published only up to 700 cm^{-1}). Apart from these, only the corresponding band of compound 7 (gallic acid) is strong. The frequency range is 520—606 cm^{-1}.

In the spectra of group *B* the band is weak. An exception is compound 56, which differs from the others in that there is a 2-amide group. The frequency range is 543—636 cm^{-1}. The frequency is influenced mainly by the 2-substituent. In the case of an allyloxy group the frequency is 550—570 cm^{-1}, with a 2-carboxy group (55) it is 612 cm^{-1}, with a 2-cyano group (57) it is 636 cm^{-1}, with a hydroxymethyl group (71) it is 630 cm^{-1}, and otherwise it is 453—600 cm^{-1}.

In the spectra of group *C* the band is of medium strength, with a tendency to be weak; in a few cases, however, it may also be strong, if the amplitude of the vibration is increased for some reason. Examples are the nitriles, as a result of coupling with the out-of-plane vibration of the cyano group, and in addition compounds 78, 81 and 96. Its overall frequency range is 511—618 cm^{-1}, but it is to be found above 600 cm^{-1} only in the spectra of nitriles. It also appears at comparatively high frequencies due to coupling in propoxy and acetocy compounds (104, 109): 590 and 570 cm^{-1}. The nitro group decreases the frequency, because of coupling with the γ_S NO_2 vibration (511, 519 cm^{-1}). Further, frequency decreases due to coupling can be observed in acids, esters, amides. N-methylamides and amidines, involving out-of-plane C=O and C=N vibrations. The maximum frequency in this group is 559 cm^{-1}.

Vibration 17a. An out-of-plane CH vibration of species a_2 in point-group C_{2v}. It always gives a weak band, and is difficult to identify. Its expectable frequency range is 835—910 cm^{-1} [1]; it lies below or above 880 cm^{-1}, depending on whether the band of the umbrella vibration appears below or above 880 cm^{-1}.

Vibration 17b. An out-of-plane vibration of the substituents in the far infrared.

Vibration 18a. An in-plane C–H bending vibration. In group *A* the band is strong only if there is a 5-F or 5-OH group. It is otherwise weak, and can often not be identified at all. Its expectable frequency range is 1060—1110 cm^{-1}.

In group *B* it always gives a weak band in the event of a 3-nitro group. In addition, it may merge into the in-plane OH bending vibration band of phenols, or generally into the band of vibration *13*. Its overall frequency range is 1048—1140 cm^{-1}. With a 5-nitro or 5-cyano group it is at 1048—1057

cm^{-1}, in 3,5-dimethoxy derivatives at above 1118 cm^{-1}, and otherwise at 1102—1118 cm^{-1}. The sensitivity to substituents shows that not only the hydrogens take part in the vibration.

From the spectra of group *C* it may be established that the intensity of the band is considerably affected by the bulk of the substituent adjacent to the hydrogens; otherwise, this holds by and large for the first two groups too. In the case of chlorine derivatives and dimeric acids the band is stronger. In the spectra of phenols it often merges partly into the band of the in-plane deformation vibration of the OH group. Its frequency range is 1052—1098 cm^{-1}. The frequency too depends on the mass and bulk of the halogens. In chloro derivatives it is 1076—1098 cm^{-1}, in bromo derivatives 1057—1085 cm^{-1}, and in the three iodo compounds 1052—1064 cm^{-1}.

Vibration 18b. This is the other in-plane C–H bending vibration. It exhibits an appreciable intensity only if identical substituents are in positions 3 and 5, though in the spectra of compounds 16, 17, 31 and 33 it merges into the band of the in-plane bending vibration of the OH group, and in the case of compounds 55 and 56 into the band of vibration *13*. Its overall frequency range is 1135—1180 cm^{-1}.

Vibration 19a is a skeletal stretching vibration characteristic of benzene derivatives.

In the spectra of group *A* it generally appears as a strong or very strong band. Exceptions are the 1,2,3-trihydroxy compounds, the dinitroaniline derivatives, and compounds with an electron-attracting substituent in position 2. It is strong, however, in the case of an ester group forming a chelate with both of its neighbours (11). In two cases it is covered by the $\nu_{as}\,NO_2$ band (33, 37). Its overall frequency range is 1476—1546 cm^{-1}. In tetrafluorobenzene (2) it is at 1523 cm^{-1}, with only alkyl and amino substituents at 1478—1486 cm^{-1}, and in nitro compounds at 1476—1510 cm^{-1}. In the case of acids and acid amides the intermolecular association slightly increases the frequency: 1502—1546 cm^{-1}; in the other derivatives it is 1489—1540 cm^{-1}.

In the spectra of group *B* the intensity of the band depends on the difference between the polarities of the substituents in positions 2 and 3. The band is generally strong, but in 3-nitro derivatives it is weak if there is no OH, OCH_3, or NH_2 group in position 2. Its frequency range is 1448—1520 cm^{-1}. With monoatomic* substituents in positions 2 and 3 it is at 1494—1520 cm^{-1}, with polyatomic substituents at 1486—1493 cm^{-1}, and in the spectra of nitro derivatives at 1448—1486 cm^{-1}.

In group *C* the band is strong or very strong in most cases. Exceptions are the acids, where the band is of medium intensity, and also those amides containing an ethoxy, propoxy or allyloxy group in position 2. Its overall frequency range is 1452—1493 cm^{-1}, the frequency depending to a slight

extent on the halogens too. In chloro derivatives it is above 1469 cm^{-1} (with the exception of compound 110, where it is 1458 cm^{-1}), in bromo compounds 1458—1486 cm^{-1}, and in iodo compounds at 1452—1460 cm^{-1}.

Vibration 19b. This is similarly a skeletal stretching vibration characteristic of benzene derivatives.

In the spectra of group *A* the band is almost always strong, but it may sometimes be covered partially by neighbouring, likewise strong bands. Thus, in the case of dimeric acids it may be covered by the β OH band (22,

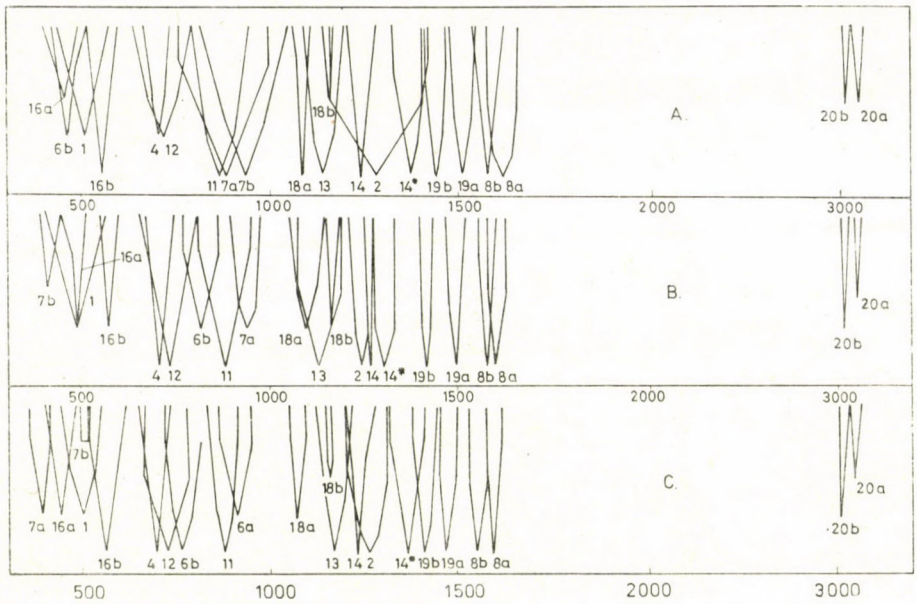

Fig. 3. Frequency ranges of ring vibrations of 1,2,3,5-tetrasubstituted benzene derivatives. 14* denotes normal vibration *14* of phenols

23, 26) or by the δ_{as}^{+} CH_3 band of the methoxy group (10, 19). Its overall frequency range is 1408—1465 cm^{-1}. If there are F or OH groups in positions 2 and 5 and there is no polyatomic* substituent it is at 1455—1465 cm^{-1}; in all other cases it is at 1408—1450 cm^{-1}.

In the spectra of group *B* too the band is generally strong. It is weak only in the spectra of those 3-nitro derivatives not containing an OH, OCH_3 or NH_2 group in position 2 (similarly as for the band of vibration *19a*). Its frequency range is 1390—1440 cm^{-1}. In dinitro compounds it is at 1390—1417 cm^{-1}.

In the spectra of group *C* it again appears as a strong band, with the exception of the amidines. In the spectra of the two anisidines it is covered by the bending band of the methyl group. Its overall frequency range is

1373—1438 cm^{-1}. It is influenced by the masses of the 2- and 5-substituents, and also by those of the halogens. It couples with the amide **III** band, and in amides, therefore, with the exception of the hydroxyamides, its frequency decreases; in the N-methylamides, however, it changes places with the amide **III** band and appears at higher frequency. In phenols the frequency is greater than 1395 cm^{-1}, in chloro derivatives above 1413 cm^{-1}, in bromophenols 1404—1438 cm^{-1}, and in iodophenols 1388—1395 cm^{-1}. In the spectrum of compound 111 it is 1402 cm^{-1}, whereas in those of the two anisidines it is a higher frequency than this, but the band is overlapped by the bending band of the methyl group. In the spectra of the methoxy, ethoxy, propoxy and allyloxy derivatives it is at 1373—1392 cm^{-1}, with the exception of the two N-methylamides, in the spectra of which the frequency is higher due to coupling (see above). As a consequence of coupling with the antisymmetric stretching vibration of the SO_2 group, the frequency is also comparatively high in the spectrum of compound 110: 1422 cm^{-1}.

Vibrations 20a and 20b are C–H stretching vibrations. The bands are always weak, and frequently superimposed on strong diffuse bands. Vibration *20a* is to be found at 3050—3102 cm^{-1}, and vibration *20b* at 2995—3050 cm^{-1}. In nitro derivatives a strong and sharp combination band often appears at the position of vibration *20a*.

A stylized picture of the spectrum originating from the vibrations of the ring, referred to the three compound groups, is to be seen in Fig. 3. The bands are also indicative of the intensity relations, but not *via* their areas, for the stylized bands are broad if the range of occurrence of the band is broad.

Internal frequencies of substituents

CH_3 group. The band of the symmetric stretching vibration is always weak, but it may be stronger in the presence of several methyl groups. Its frequency range in the CH_3, C_2H_5, C_3H_7, $COCH_3$, COC_2H_5, $COOCH_3$, OC_2H_5, OC_3H_7, $OCOCH_3$ and NHC_2H_5 groups is 2887—2926 cm^{-1}, and in the OCH_3, $N(CH_3)_2$ and OSO_2CH_3 groups 2828—2862 cm^{-1}.

The asymmetric stretching vibration generally has two bands, but both are weak. Their combined frequency range is 2932—2992 cm^{-1}. They are to be found above 2982 cm^{-1} only in the event of an ethyl group.

The band of the symmetric bending vibration is of very variable intensity. In OCH_3 and $OCOCH_3$ groups it is intense, but otherwise weak. It may sometimes be partially or completely covered by the band of vibration *14* of phenols, the band of the symmetric stretching vibration of the nitro group, or the band of the in-plane OH bending vibration of the COOH group. In the methyl group it is always weak. Its frequency range in the case of a methyl group is 1379—1385 cm^{-1}, and otherwise 1300—1398 cm^{-1}, but in the OCH_3

group it is always below 1360 cm^{-1}. If a methoxy group is situated between two nitro or two halogen groups, the frequency range is 1282—1320 cm^{-1}. The frequency is similarly very low in the OSO_2CH_3 group.

In theory, the asymmetric bending vibration has two bands per methyl group, between 1418 and 1475 cm^{-1}. The bands are of medium strength or weak, but in the $COOCH_3$ group they are generally strong. If a methoxy group is situated between two bulky substituents, then the lower-frequency component appears below 1430 cm^{-1}, whereas in all other cases both bands are to be found above 1430 cm^{-1}. In very many cases, one or the other band is overlapped by the band of vibration *19b*.

In principle, the rocking vibration similarly has two bands, between 957 and 1071 cm^{-1}. The bands are generally weak or of medium strength, with the exceptions of the methoxy or acetoxy groups. The rocking vibration occurs below 1008 cm^{-1} only if it originates from the methyl group of a mesyloxy group or a methoxy group situated between two bulky substituents. It is worth noting that the vibration has no low-frequency component in the spectrum of compound 19, presumably because the neighbouring methoxy groups in the ordered dimeric structure are situated in a fixed configuration beside each other.

CH_2 group. The band of the symmetric stretching vibration is almost always weak. An exception is compound 25, in the spectrum of which the symmetric stretching vibration of the $=CH_2$ group appears as a strong band, presumably because of the smaller bulk of the cyano group (higher amplitude). Its frequency range is 2857—2885 cm^{-1} in the $>CH_2$ group, and 2962—2990 cm^{-1} in the $=CH_2$ group.

The band of the antisymmetric stretching vibration is similarly weak in the $>CH_2$ group, with the exception of the morpholino derivative (43), which contains four methylene groups. In methoxy derivatives it may be covered by the symmetric stretching vibration of the methyl group, while in dimeric acids it may merge into the very diffuse band system of the OH stretching vibration. This latter also holds for the symmetric stretching vibration. Its frequency range is 2935—2942 cm^{-1} in the $>CH_2$ group (but a band is also to be found at 2995 cm^{-1} in the spectrum of compound 43), and 3068—3085 cm^{-1} in the $=CH_2$ group. In the latter case the band is generally of medium intensity.

The band of the scissoring vibration can barely be identified in the spectra of compounds also containing a methyl group. In the $=CH_2$ group it tends to separate from the band of the asymmetric bending vibration of the methyl group, but it may still be covered by the band of vibration *19b*. Its frequency range is 1447—1462 cm^{-1} in the $>CH_2$ group (but it also appears at 1407 cm^{-1} in the morpholino group beside the O atom), and 1410—1428 cm^{-1} in the $=CH_2$ group.

The band of the rocking vibration is almost always very weak, and most often cannot be identified. Its frequency range is 767–812 cm^{-1} in the $>CH_2$ group, and 1011–1025 cm^{-1} in the $=CH_2$ group.

In the $>CH_2$ group the wagging vibration appears with medium strength only if there is an allyloxy group between the halogens. Otherwise the band is very weak. It is strong, however, in the $=CH_2$ group if the vibration is perpendicular to the plane of the molecule. Its frequency range is 1320–1346 cm^{-1} in the $>CH_2$ group (but 1301 cm^{-1} in the ethylamino group), and 925–960 cm^{-1} in the $=CH_2$ group. In the spectrum of the dimeric compound 105 the band is interestingly split into two.

The twisting vibration can never be identified in the $>CH_2$ group. In the $=CH_2$ group the band is of medium strength, but in amides it may be covered by the amide V band. According to Raman spectra, its frequency range in the $>CH_2$ group is 1230–1260 cm^{-1}, while in the $=CH_2$ group it is 595–650 cm^{-1}.

CH group. The *stretching vibration* band is weak in the aldehyde, allyloxy and oxime groups. Its frequency range is 2732–2756 cm^{-1} in the aldehyde group, 3015–3022 cm^{-1} in the allyloxy group, and 2970–3000 cm^{-1} in the oxime group. The *in-plane bending vibration* defined by the C–H and the double bond appears as a strong or medium band only in the aldehyde group. Here too, however, the band is weak if the aldehydic carbonyl is involved in an intermolecular linkage with an OH group. This is particularly striking in the case of compounds 51 and 52. In the former the OH group forms a chelate with the bromine atom, but in the latter it does not with the iodine. This is also demonstrated by the large difference in the OH stretching frequencies. There is a corresponding large intensity difference between the CH bending vibration bands, in favour of the bromo compound. Its frequency range is 1394–1417 cm^{-1} in the aldehyde group, and 1300–1330 cm^{-1} in the allyloxy group; it could not be identified in the oximes. The band of the *out-of-plane vibration* is generally strong in all three groups. Exceptions are the halogen-benzaldehydes, in which the band becomes weaker with the increase of the number and mass of the halogens, but it is strong if the aldehyde group forms an intermolecular bridge. Its frequency range in the aldehyde group is 593–644 cm^{-1}, in the allyloxy group 974–997 cm^{-1}, and in the oxime group 600–630 cm^{-1}. Just as the wagging $=CH_2$ vibration, it is split into two in the spectrum of compound 105.

C–C bond. In the ethyl and acetyl groups the C–C stretching vibration appears at around 970 cm^{-1}. In the infrared spectrum it is generally a weak band.

C–C–C chain. In the propyl group, two stretching vibrations appear in the Raman spectrum, at around 890 and 1090 cm^{-1}. In the propionyl

group (27) the two vibrations result in strong bands in the infrared spectrum, at around 955 and 1065 cm^{-1}.

C=C bond. In the infrared spectrum the C=C stretching vibration always results in a weak band. Its frequency range in the allyloxy group is 1644—1655 cm^{-1}.

C–Cl bond. The stretching vibration appears as a strong band in the spectra of acid chlorides, at 669 and 682 cm^{-1}. Polarity of the bond decreases the frequency. The C–Cl bond is more polar in the dibromo compound 95 than in the dichloro compound 88. This is indicated not only by the smaller C–Cl stretching frequency, but also by the larger C=O stretching frequency (1762 cm^{-1} *vs.* 1746 cm^{-1}).

C–OH bond. The band of the alcoholic C–OH bond (71) is strong, at around 1020 cm^{-1}. The stretching vibration of the C–OH bond of the carboxyl group always appears as a strong band, though in group *C* it may partially merge in the band of vibration *2*. Its frequency interval can be divided into four parts.

1. If the carbonyl oxygen of the carboxyl group forms a hydrogen bond with a phenolic OH group, the frequency range is 1260—1268 cm^{-1}.

2. For dimeric acids in group *A* the range is 1271—1282 cm^{-1}.

3. For dimeric acids in groups *B* and *C* it is 1283—1302 cm^{-1}. In this case the frequency is increased by coupling with vibration *2*.

4. In group *C* if there is a 2-OH group, it is 1270—1278 cm^{-1}. In this case too coupling with vibration *2* is strong, but because of the light substituent the frequency of vibration *2* is very high and the two bands change places.

C–O–C chain. This occurs in esters and in the morpholino group (there is also a C–O–C chain in the methoxy group, but one of the carbon atoms is a member of the aromatic ring, and thus the stretching vibration of the oxygen atom towards this carbon atom is included among the 30 normal vibrations of the benzene ring). In esters two stretching bands appear; both are generally very strong. However, if the ester group is in position 2 the lower-frequency component appears only as a band of medium strength. The overall frequency ranges are 959—1010 cm^{-1} and 1261—1313 cm^{-1}. The frequency is affected by four circumstances.

1. Whether or not the carbonyl oxygen of the ester forms a hydrogen bond. If yes, then the frequency of the higher-frequency component increases (as the order of the C–O bond adjacent to the carbonyl oxygen increases).

2. Whether the ester group is in position 2 or 5. In the former case the range of the lower-frequency component is 959—967 cm^{-1}, while in the latter case it is 984—1010 cm^{-1}.

3. The magnitude of the frequency of vibration *2*, for the higher-frequency component is coupled with this. If the frequency of vibration *2* is high

because of the light substituents, this decreases the frequency of the C–O–C stretching vibration (1264 cm^{-1} in compound 8, in spite of the hydrogen bond, and 1264—1268 cm^{-1} in compounds 77, 80 and 111).

4. The presence of halogens in the molecule increases the frequency of the higher-frequency component. As a result of this, for example, in the spectra of compounds 45, 46 and 48 the higher-frequency stretching vibration changes places with vibration *2*, and appears at 1302—1313 cm^{-1}.

In the spectrum of the morpholino derivative a strong band can be found at 920 cm^{-1}, and a medium one at 1050 cm^{-1}. The strong band of an out-of-plane skeletal vibration at 454 cm^{-1} can also probably be assigned to the morpholine ring.

C=O bond. The band of the stretching vibration is always very strong. It is well known that a hydrogen bond decreases the frequency. The frequency of the stretching vibration of free C=O groups is 1707—1739 cm^{-1} in the ester group (maximum frequency in the spectrum of compound 48), 1693—1713 cm^{-1} in the aldehyde group, 1685 cm^{-1} in the acetyl group (87), 1664 cm^{-1} in the hydroxamic acid (91), 1746—1762 cm^{-1} in acid chlorides, and 1763—1788 cm^{-1} in the acetoxy group. In the latter case the C=O stretching frequency increases in one of the adjacent acetoxy groups, but if there is no nitro group in the molecule, then the maximum frequency in this case too is 1781 cm^{-1}.

A free COOH group did not occur in the series of compounds examined. In intermolecular bonding with an OH group, including carboxyl dimers, the C=O stretching frequency of the COOH group is 1668—1710 cm^{-1}. The actual value depends on the bond strength of the dimer. In intermolecular bonding with a phenolic OH group, the ester group absorbs at 1672—1695 cm^{-1}, and the aldehyde group at 1653—1679 cm^{-1}. In a chelate structure the frequency range is 1620—1674 cm^{-1}, similarly depending on the strength of the chelate bond. The 1674 cm^{-1} band is to be found in the spectrum of compound 33; otherwise, if there is no nitro group in the molecule, the maximum frequency is 1647 cm^{-1}. The lowest carbonyl frequency was found in the spectrum of compound 16.

The band of the in-plane bending vibration exhibits very variable intensity. In the spectra of acid chlorides it is strong, in those of dimeric carboxylic acids medium or strong, in the acetyl and propionyl group (27) medium, and in the ester group medium or weak, but very weak if the group is in position 2; it is also weak in the spectrum of the hydroxamic acid (91). In the acetoxy group it is generally strong, but if the C=O group is not in the plane of the ring as a consequence of steric hindrance, then the band is substantially weaker. In the case of the aldehyde group the band is very weak, and most often cannot even be identified. Its overall frequency range

is 718—866 cm^{-1}. In dimeric carboxylic acids and in the event of an intermolecular bridge, it is 718—751 cm^{-1}. If a para-OH group weakens the dimeric structure, or if there is an iodine atom in the molecule, the maximum frequency is 772 cm^{-1}. In all other cases it is found above 731 cm^{-1}. The frequency range for the ester group is 722—757 cm^{-1}, while in the case of a stronger intermolecular bonding with an OH group it is above 750 cm^{-1}. In the hydroxamic acid the frequency is 773 cm^{-1}. The aldehyde group absorbs at 777—809 cm^{-1}. The frequency here is determined by electron shift effects. Electron-repelling substituents ortho or para to the aldehyde group increase, while those meta to it decrease the frequency. Acid chlorides absorb at 803—804 cm^{-1}. The acetoxy group absorbs at 804—845 cm^{-1} but above 820 cm^{-1} only in the case of steric hindrance (two *ortho*-acetoxy groups). Finally, in the acetyl and propionyl groups the band is to be found at 866 and 842 cm^{-1}, respectively.

The band of the out-of-plane vibration is generally weak, and often diffuse. It may be comparatively strong, however, in the spectra of 2-carboxyl or 2-acetyl groups forming dimers or of the hydroxamic acid. The overall frequency range is 580—693 cm^{-1}. In the propionyl group it is at 587 cm^{-1}, and in the acetoxy group at 580—650 cm^{-1}. Steric hindrance and a nitro group reduce the frequency considerably. In the acetyl group the frequency is 625 cm^{-1}, in the hydroxamic acid 675 cm^{-1}, in acid chlorides 640—653 cm^{-1}, and in esters 633—685 cm^{-1}. Compound 8 forms intermolecular bonds of two different strengths, and accordingly two stretching and two out-of-plane vibrations appear, the latter at 645 and 675 cm^{-1}. The out-of-plane C=O frequency of the carboxyl group in the bound state is 636—693 cm^{-1}. The frequency is influenced by the strength of the dimer, but also by coupling with the out-of-plane OH vibration. This coupling is strongest in compound 53, as shown by the low frequency of 636 cm^{-1}.

C–N bond. The band of the stretching vibration is strong in the spectra of compounds 85 and 101, but weak in those of the amidines. Its frequency in the ammonium group (85) is 991 cm^{-1}, in the thioamide group (101) 930 cm^{-1}, and in the amidine group 1101—1102 cm^{-1}.

C–N–O chain. Of the two stretching vibrations, the lower-frequency one appears as a strong band, and the other as a weak band. The frequencies in the hydroxamic acid (91) are 952 and 1340 cm^{-1}, and in the hydroxyamidine group 943—946 and 1098—1100 cm^{-1}.

C=N bond. The stretching vibration gives a band of medium strength in the oxime group (92), and a very strong band in the amidine and hydroxyamidine groups, and also in the enol form of the thioamide group. Frequencies: in the enol form of the thioamide group 1409 cm^{-1}, in the oxime group 1630 cm^{-1}, in the hydroxyamidine group 1659—1664 cm^{-1}, and in the amidine group 1676 cm^{-1}.

The band of the in-plane bending vibration is weak in the oxime and in the enolic thioamide, moderately strong in the hydroxyamidine, and strong in the amidine group. Frequencies: in the enolic thioamide 541 cm^{-1}, in the oxime 743 cm^{-1}, and in the amidine and hydroxyamidine groups 708 – 725 cm^{-1}. In the last two groups the frequency is sensitive to the mass of the halogens in the molecule.

The band of the out-of-plane vibration can be identified only in the spectra of the amidine and hydroxyamidine compounds; in the former case it appears as a moderately strong band, and in the latter as a weak one. The frequency lies in the range 612 – 623 cm^{-1}, depending on the mass of the halogens.

C≡N bond. The band of the stretching vibration is always strong, except if there is an *ortho*-nitro group, decreasing by its electron attraction the polarity of the C≡N bond. Its frequency range is 2228—2256 cm^{-1}. The force constant of the bond and the frequency are decreased by electron-repelling groups in the ortho position, and increased by the nitro group. The minimum frequency for nitro derivatives is 2242 cm^{-1}, whereas the maximum frequency for compounds not containing a nitro group is 2245 cm^{-1}. The 2228 cm^{-1} band occurs in the spectrum of compound 57, in which there are two electron-repelling substituents in the vicinity of the cyano group.

The in-plane bending vibration is even more sensitive to conjugative effects. The nitro group increases both the frequency and the amplitude of the vibration. In these cases the band of the bending vibration is always strong. It is otherwise of medium strength or weak. The overall frequency range is 505—627 cm^{-1}. In nitro derivatives it is 583 – 627 cm^{-1}, and in compounds not containing a nitro group 505 – 563 cm^{-1}. In dihalogen derivatives it is 505 – 522 cm^{-1}.

C=S bond. In the spectrum of compound 101 two bands of medium strength can be assigned to this bond. The 1136 cm^{-1} band corresponds to the stretching vibration, and the 505 cm^{-1} band to the bending mode. Although some other bands permit the conclusion that this compound also exists in the enol form, the stretching band to be expected at around 600 cm^{-1} could not be identified.

OH bond. The stretching vibration nearly always produces very strong diffuse bands. In the case of some weak chelate bonds, however (phenolic OH with propionyl and aldehyde groups, or with the ether oxygen of the ester group), the band spreads out weakly.

The overall frequency range of the stretching vibration of the phenolic OH group is 3080 – 3595 cm^{-1}. In strong chelate structures with OH, nitro and carboxyl groups (6) and with the carbonyl oxygen of the ester group (12) it absorbs at 3080 – 3250 cm^{-1}. In chelates of moderate strength with neigh-

bouring OH groups, and with halogens (49, 51, 77, 78, 80, 81), the frequency range is 3300—3385 cm^{-1}; in weak chelates with propionyl, hydrated nitro, methoxy, amide, aldehyde and OH groups, with halogens, with the etheric oxygen of the ester group (on this basis it was possible to determine the configuration of compound 16, in which the carbonyl oxygen of the ester group is directed towards the methoxy group), and with the OH part of the carboxyl group the frequency range is 3335—3484 cm^{-1}. In an intermolecular bridge with carbonyl oxygen the range of appearance of the band is 3405—3490 cm^{-1} for the ester carbonyl, while with the carboxyl group (14) it is 3260 cm^{-1}. In compounds 47 and 52 a particularly strong intermolecular bond is formed due to the iodine atom, and the band appears diffusely at 3180 and 2700—3100 cm^{-1}. With OH, OCH_3, or NO_2 groups in an intermolecular bridge, the frequency range is 3180—3420 cm^{-1} (but below 3300 cm^{-1} only in the case of two neighbouring OH groups), while in the free OH group it is 3503—3595 cm^{-1}.

If the carbonyl oxygen forms an intermolecular bond with a phenolic OH group, the frequency of the OH stretching vibration of the carboxyl group is 3380 cm^{-1} (14). In the case of dimeric carboxylic acids a broad region characterized by several maxima is observed between 2500 and 3350 cm^{-1}. The position of the high-frequency end of the region depends on the stability of the dimer. In the event of a weak dimer (55) a single strong diffuse band occurs at around 3000 cm^{-1}. In compound 33 the free OH group absorbs at 3572 cm^{-1}.

The OH stretching frequency for the hydroxamic acid is 3240 cm^{-1}, for the oxime 3328 cm^{-1}, and for the hydroxamidines 3245—3280 cm^{-1}. Alcoholic OH absorbs at 3485 cm^{-1} in the case of a seven-membered chelate (71), and at 3290 cm^{-1} in an intermolecular linkage.

The bands of the in-plane bending vibration of phenolic OH are similarly very strong. Merely a weak band can be observed in the case of a simple hydrogen-bridged structure with an aldehyde group (52). In the strong chelation developing with the nitro group or with the carbonyl of the carboxyl or ester groups the frequency range is 1240—1266 cm^{-1}. In chelate structures of medium strength involving OH and halogens it is 1198—1244 cm^{-1}. In the weak chelates listed in connection with the stretching vibration it is 1152—1256 cm^{-1}, but lies above 1210 cm^{-1} only if the OH group is situated between two halogens. In intermolecular linkages the range of appearance of the band is 1134—1273 cm^{-1}, but it is above 1210 cm^{-1} only if two OH groups are in the ortho position, or if the vibration is hindered sterically by an iodine atom (at such time also the amplitude is lower and the band is weak). Finally, in the case of a free OH group the band lies at 1091—1169 cm^{-1}. Its overall frequency range is therefore 1091—1273 cm^{-1}; In the spectrum of compound 47 another band may be found at 1372 cm^{-1},

this can be correlated with the structure of the ν OH band, extending to 2700 cm^{-1}. It is likely that some symmetric cyclic structure develops between the two OH groups and the aldehyde group in the solid phase.

The band originating from the in-plane bending vibration of the carboxyl OH group is strong only if a dimeric structure has been produced; the stronger the bonding in the dimer, the stronger the band. Its frequency range in weak dimers is 1378—1395 cm^{-1}, and in stronger ones 1405—1420 cm^{-1}. In the particularly strong dimeric structure of compound 6 it is at 1482 cm^{-1}.

The OH in-plane bending vibration band of oxime, hydroxamic acid and hydroxyamidine groups cannot be identified with certainty. In seven-membered chelate rings an alcoholic OH absorbs at 1169 cm^{-1}, and in an intermolecular linkage with the NO_2 group at 1195 cm^{-1}.

The band of the out-of-plane vibration of phenolic OH is in general similarly strong and very diffuse. In the spectra of picric acid (44) and halogen-aldehydes, however, it is weak, presumably because of the lower amplitude. Its overall frequency range is 457—745 cm^{-1}, though free OH groups may also absorb below 457 cm^{-1}, however, these latter bands are difficult to identify. In strong chelate structures, depending on the strength of the chelate, the frequency range is 628—745 cm^{-1} (the highest value in the spectrum of compound 6, where the stretching band is found at 3170 cm^{-1}). In weak and medium-strength chelates it is at 501—637 cm^{-1}, though in the spectrum of compound 31 the strong and diffuse band appears at 693 cm^{-1}. (The diffuse nature of the band distinguishes it from the band of vibration 4, which is to be expected in this position, and with which it is clearly in accidental degeneracy.) In intermolecular bands the range is 463—700 cm^{-1}, but the band is above 620 cm^{-1} only in halogen derivatives, and below 500 cm^{-1} only in compound 84.

The out-of-plane vibration of the OH group of dimeric carboxyl appears at 900—940 cm^{-1}, in the form of a strong band; however, at times this may merge in the bands of other vibrations (*e.g.* vibration *7b* in group *A*, and also the vibrations of the allyloxy and ethoxy groups). In the spectrum of compound 33, which forms a loose dimer, the band occurs at 830 cm^{-1}. In some cases (19, 89, 102) the spectrum between 580 and 603 cm^{-1} indicates an OH group in a looser position.

The out-of-plane OH band of the likewise dimeric oxime is suspected to be at 702 cm^{-1}. A strong band is to be found at 406 cm^{-1} in the spectrum of the hydroxyamidine 94.

In the spectrum of compound 31 there is a broad absorption region of the hydrate water at 2650—3230 cm^{-1}, while the bending vibration of the water molecule yields a very strong band at 1652 cm^{-1}.

Alcoholic OH absorbs in chelates and in intermolecular bonds at 514 and at 565 cm^{-1}. The two types of OH linkage in compound 71 are confirmed

by the duplicate occurrence not only of every OH band, but also of the ν C–OH band.

From the mode of appearance of the C=O and OH vibrations the following hydrogen-bonded structures can be established in the crystalline phase (numbers refer to compounds):

5: a cyclic dimer, with a ten-membered ring, and a weak chelate;

6: a dimeric acid and a chelate between the carboxylic CO and phenolic OH groups;

7: a dimeric acid, an OH–OH chelate and an intermolecular bond;

8: an OH–OH chelate and an intermolecular CO–OH bond;

9, 46, 82, 84: an intermolecular linkage and a weak chelate;

10: intermolecularly bound and free OH groups;

11: a chelate formed *via* the carbonyl and ether oxygens of the ester group;

12, 37, 50, 51, 64: an intermolecular linkage;

13: a free OH and a weak chelate formed with the OCH_3 group;

14: an intermolecular CO–OH bond;

15: an intermolecular CO–OH bridge or a free OH;

16: a chelate with the ether oxygen of the ester group;

17: a weak chelate with the amide group;

19, 55, 59, 60, 89, 102: a loose dimeric acid;

22, 23, 26: a strong dimer;

27: in part a weak chelate between the OH and the propionyl carbonyl, and in part a free OH;

31: a six-membered ring between the nitro group and the hydrate water, a weak OH–NO_2 chelate, and a free OH;

33: a loose dimer and a weak chelate;

34, 38, 44: a strong chelate;

35: an OH–NO_2 chelate and an intermolecular linkage;

45: a chelate formed with the aldehyde group;

47: a strong intermolecular linkage, and presumably a cyclic structure;

49, 83: an intermolecular OH–OH linkage;

52: an intermolecular linkage with the aldehyde group, sterically hindered by the iodine;

53, 105, 109: a dimeric acid;

63, 65, 66: a strong chelate with the NO_2 group, but also an intermolecular linkage occurs;

71: a seven-membered chelate and an intermolecular linkage;

76: a weak OH–Cl chelate and a dimeric acid;

77: OH–Cl chelates of different strengths;

78, 80, 81: an OH–Cl or OH–Br chelate of medium strength;

79: an OH–Br chelate and a dimeric acid;

91: a dimeric hydroxamic acid;
92: a dimeric oxime;
94, 99: a loose hydroxyamidine dimer;
114: an intermolecular OH–NO_2 linkage.

O–C bond. The band corresponding to the O–C stretching vibration of the methoxy group is of appreciable intensity only if the OCH_3 group is in position 2 and if there is no halogen or nitro group in its neighbourhood. In general it is of opposite intensity to the band of the rocking vibration of the methyl group. It is frequently overlapped by other strong bands (vibrations *2* and *13*, and OH in-plane bending vibration). Its frequency range is 1170—1212 cm^{-1}. An adjacent nitro group raises the frequency: in the absence of a nitro group, the band always appears below 1200 cm^{-1}.

The band of the in-plane bending vibration is of very variable intensity. Its frequency range is 333—370 cm^{-1}. In dihalogen derivatives its frequency range is 352—370 cm^{-1} for the chloro compounds, and 338—355 cm^{-1} for the bromo compounds.

O–C–C chain. In accordance with its two stretching vibrations, it always produces two bands. In the ethoxy group it results in a modarately strong band at 903—912 cm^{-1}, and a weak band at 1104—1114 cm^{-1}. In the allyloxy group two bands can similarly be assigned to the O–C–C= chain, but these are at most of medium strength, and are generally weak. The two frequency ranges are 803—831 and 930—959 cm^{-1}. Both bands sometimes occur as a shoulder or in accidental degeneracy with a stronger band, in the latter case mainly with the CH_2 wagging vibration of the allyloxy group. Two bands also appear for the acetoxy group: a medium one at 905—925 cm^{-1}, and a very strong one at 1182—1205 cm^{-1}. In the case of ortho-acetoxy groups a further two bands can be found, corresponding to the sterically hindered acetoxy group. One is weak, at 945—965 cm^{-1}, and the other again very strong, at 1092—1099 cm^{-1}.

O–C–C–C chain. Three stretching bands originate from the propoxy group, a weak and two stronger ones. Clearly, in the latter two a greater role is played by the O–C bond. The frequency ranges are 800—820, 952—964 and 1125—1130 cm^{-1}. The latter is very strong in the spectrum of compound 23, but of medium strength in that of compound 104.

O–S bond. A strong band corresponds to the stretching vibration of the O–S bond in the spectrum of the mesyloxy group. The frequency is very sensitive to conjugative effects. The presence of an OH group in the neighbouring molecule favours the limiting polar structure, in which the order of the O–S bond increases. The vicinity of another mesyloxy group, however, strongly inhibits the limiting polar structure and decreases the O–S bond order. Accordingly, the frequencies are 656 cm^{-1} for compound 39, 641 cm^{-1} for compound 40, and 583 and 617 cm^{-1} for compound 10 (here the inter-

molecular interaction is so strong that the frequency is substantially lower; in addition, the vibration splits to components of the same and the opposite phase).

NH_3^+ group. In electrostatic bonding with the anion, this group produces six stretching bands of various strengths between 2000 and 3100 cm^{-1}. Some of these belong to the symmetric, and the others to the asymmetric components. The band of the symmetric bending vibration is strong. Its frequency in the spectrum of compound 85 is 1518 cm^{-1}. The asymmetric bending and rocking vibrations similarly give strong bands, at 1607 and 627 cm^{-1}.

NH_2 group. The bands of the symmetric and antisymmetric stretching vibrations are without exception very strong. The free amino group absorbs at 3320—3342 cm^{-1} (symmetric) and 3400—3440 cm^{-1}. In intermolecular bonding with another amino group, the ranges are 3225—3255 and 3300—3340 cm^{-1}. In acid amides the symmetric and antisymmetric vibrations appear only in intermolecular structures. Both bands are very strong, their frequency ranges being 3165—3195 and 3335—3395 cm^{-1}. The higher the C—N bond order in the amide group, the greater the separation of the two frequencies. Accordingly, the frequency difference can be correlated with the frequency of the amide **I** band (C = O stretching vibration), insofar as the C—N bond order varies in the opposite direction to the C = O bond order. The correlation formula is:

$$\nu_A = 1750 - 0.5\,\Delta\,\nu_{NH_2} \pm 5 cm^{-1}$$

Both electron-repelling groups in the ortho position and heavy halogens in general all increase the internal conjugaton, and thereby the frequency difference: 187—212 cm^{-1}. In the other cases the difference is 170—175 cm^{-1}. In the spectra of four compounds the NH_2 stretching vibrations can be differentiated from one another not as symmetric and antisymmetric modes, but as the stretching vibrations of bound and free N–H bonds. In compound 17 one of the hydrogens of the NH_2 group forms a chelate with the *ortho*-methoxy group, while in compounds 78 and 81 the NH_2 group forms an intermolecular bridge with the OH group. These three molecules do not form the customary amide—amide linkage. Compound 96 contains an amide—amide linkage of a different nature, but in part it forms an intermolecular bridge with the oxygen of the methoxy group of the molecule in the other layer (Fig. 4). The frequency of the N–H stretchings vibration in the amide—amide linkage is 3175—3298 cm^{-1}. In the spectrum of compound 96 the 3298 cm^{-1} band indicates the N–H bond linked to the methoxy group, while the 3175 cm^{-1} band denotes the N–H bond in the amide—amide linkage. The frequencies of the free N–H stretching vibrations in these four molecules are 3438—3465 cm^{-1}. In compound 72, in addition to the intermolecularly bound structure, a chelate formed with a

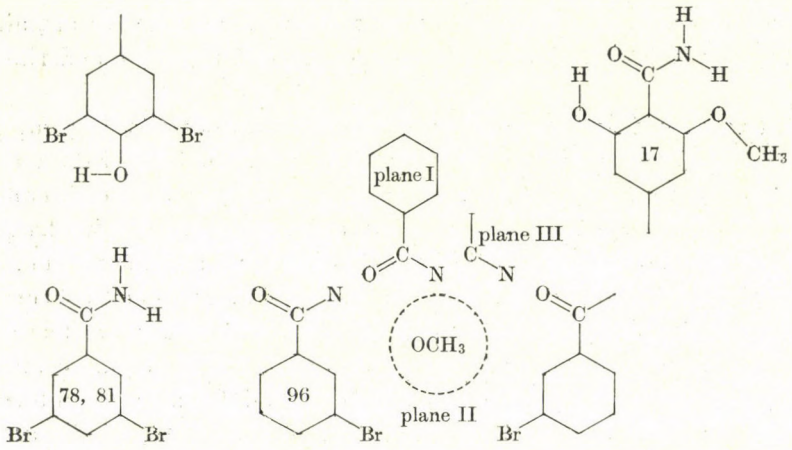

Fig. 4. Assumed structures of some amides in the crystalline phase

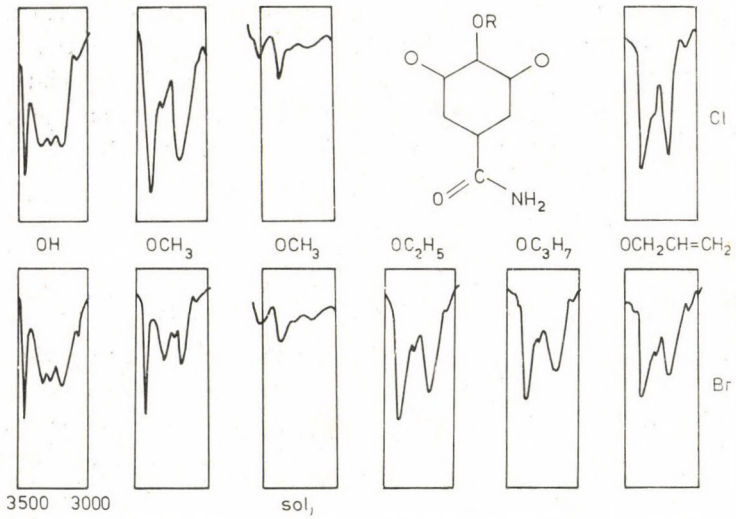

Fig. 5. Spectral ranges of NH_2 stretching vibrations of some amides between 3000 and 3500 cm^{-1}

nitro group or a bromine atom also occurs. Accordingly, five NH_2 stretching bands are to be found.

In compounds 72 and 96 the NH_2 group is presumably bent out of the plane of the ring. In compound 72 both neighbours of the amide group are bulky substituents, and the protrusion is therefore due to intramolecular steric reasons. In the case of the other compound the cause must be sought in the various crystal structures. It is interesting that the spectrum of compound 96 (dibromomethoxybenzamide) is similar to those of dichloro- and dibromo-hydroxybenzamides, but different from those of dibromo-ethoxy-, propoxy-

and allyloxy-, and dichloromethoxybenzamides. At the same time, the structure of dichloromethoxybenzamide in the crystalline state is similar to those of dibromoethoxy-, propoxy- and allyloxybenzamides, but differs from those of dibromomethoxy- and dichlorohydroxybenzamides (Fig. 5). The essential difference between the two groups may be that in one of them the 2-substituent does not stand out from between the halogens (dichloro- and dibromohydroxy-, and dibromomethoxybenzamides), whereas in the other

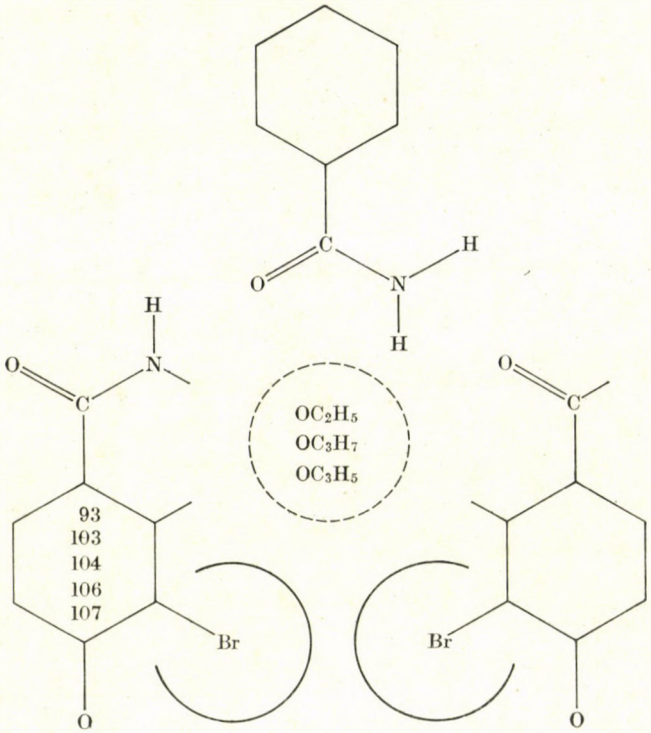

Fig. 6. Assumed structures of some amides in the crystalline phase

group it does (Fig. 6). The two groups are also differentiated by the frequency of the amide **III** band, insofar as the frequency is below 1390 cm^{-1} in the case of bent-out NH_2 groups, but otherwise above 1398 cm^{-1}. It is worth noting that the spectra of dichloro- and dibromo-methoxybenzamide are very different in the crystalline phase, but the same in solution (Fig. 5).

In amidines the frequency ranges for the two bands are 3055—3060 and 3225—3230 cm^{-1}. In the spectrum of the thioamide 101 the two bands appear at 3190 and 3382 cm^{-1}.

The band of the scissoring vibration is very strong in the spectra of anilines, and is found at 1618—1637 cm^{-1}. In the amides, this vibration will be discussed among the amide bands. In the amidines the band of the scissor-

ing vibration merges into the band of the C = N stretching vibration. In the spectrum of compound 101 it is to be found at 1642 cm^{-1}, similarly as a very strong band.

The rocking vibration is difficult to identify in the spectra of the anilines. It is expected to appear between 1000 and 1100 cm^{-1}. In the spectra of compounds 21 and 24 a band of medium strength was identified at 747 cm^{-1}, but in the spectra of the other amides it is probably overlapped by the bands of vibrations *4* or *12*. It can be identified at 823 cm^{-1} in the spectrum of the thioamide.

The band of the wagging vibration is very weak in the spectra of the anilines in the case of a free amino group, but it may also be strong if the amino group is situated between halogens or forms an intermolecular linkage. It appears at 614—630 cm^{-1} in the event of a free amino group, and at 700—730 cm^{-1} when there is an intermolecular linkage. Bands of both the free and the bound group can be found in the spectrum of compound 98. The NH_2 wagging vibration of amidines gives a strong band at 705—710 cm^{-1}. The corresponding strong band for the thioamide is found at 591 cm^{-1}.

N–H bond. The band of the stretching vibration is always very strong. It is to be found at about 3200 cm^{-1} in the ethylamino group, at 3175 cm^{-1} in the hydroxamic acid (99) as a shoulder of the diffuse OH band, at 3350 cm^{-1} in the amidines as a shoulder of the antisymmetric NH_2 stretching band, at 3296—3300 cm^{-1} in the N-methylamides as an independent very strong band, and at 3290 cm^{-1} in the enol form of the thioamide. There are two types of NH bond in the hydroxyamidine group, one involving singly bonded, and the other doubly bonded nitrogen. The former absorbs at 3488—3490 cm^{-1}, and the latter at 3390—3392 cm^{-1}.

The quasiplanar $>$NH and planar =NH bending vibrations give a strong band in the ethylamino group, but in the other cases it can be observed only as shoulders. In all derivatives it occurs in a narrow frequency interval, between 1640 and 1655 cm^{-1}, but it may be covered by the C = N stretching vibration or, in the spectrum of the thioamide, by the band of the NH_2 scissoring vibration. In the N-methylamides it may be classified among the amide bands.

The band of the out-of-plane vibration in the hydroxyamidines and the enol form of the thioamide may also be identified as a strong or medium band. The frequency of the former is 648—660 cm^{-1}, and of the latter 675 cm^{-1}.

N–C bond. In the spectra of the N-methylamides the stretching and bending vibration each yield one weak band, in the regions of 980—988 and 340—345 cm^{-1}.

N–C–C chain. In the ethylamino group the two stretching vibrations are characterized by a medium and a very weak band, at 966 and 1195 cm^{-1}.

$N\lessdot^{C}_{C}$ *group.* The stretching vibrations of the dimethylamino group appear in the form of two bands that are so weak that they could not be identi-

fied from a single spectrum. In the spectra of other dimethylanilines they are found at 935—965 and 1170—1200 cm^{-1}.

N–O bond. The N–O stretching vibration of oxime 92 gives a band of medium strength, at 957 cm^{-1}.

NO_2 group. The symmetric and antisymmetric stretching vibrations of the nitro group are found in the form of two very strong bands. The positions of the bands are determined mainly by conjugative effects. From this aspect, separate attention must be paid to both the average frequencies of the bands and the frequency splitting. In the event of undisturbed conjugation of the nitro group with the ring, the average frequency and the frequency splitting decrease, because the N–O bond order and the O—N—O bond angle are smaller.

In mononitro derivatives (excluding the anilines) the frequency splitting is 171—200 cm^{-1}, and within this is 184—200 cm^{-1} in OH chelates. Chelation always increases the frequency splitting, for it creates a difference between the two oxygen atoms. In the spectrum of compound 69 the splitting is 159 cm^{-1}. In dinitro derivatives (again excluding the aniline derivatives) the splitting is 177—240 cm^{-1}. In chelates it is 195—240 cm^{-1}. An appreciable splitting of 237 cm^{-1} can be observed in the spectrum of compound 31, which points to the asymmetry of the hydrate structure. In strong chelates (34, 38, 39) the symmetric stretching vibration (and in one case the antisymmetric stretching vibration too) is split into two components, corresponding to the chelating and the other nitro group. In aniline derivatives the symmetric and antisymmetric stretching vibrations are similarly split, but to vibrations of the same and of the opposite phase. From the intensity relations the lower-frequency (stronger) band may be assigned to the out-of-phase vibration. The frequency splitting of the in-phase vibration is 172—183 cm^{-1}, and of the out-of-phase vibration is 211—217 cm^{-1}. Finally, in the trinitro derivative (44) splitting can be observed over 207—214 cm^{-1}.

The average frequencies are as follows:

1. In mononitro derivatives with the nitro group in position 5 the range is 1420—1434 cm^{-1} (but the 1420 cm^{-1} is taken from the spectrum of compound 114, in which the nitro group forms an intermolecular bond with the OH group of a second molecule).

2. Mononitro derivatives with the nitro group in position 2 or 3 may be divided into two groups, depending on whether they contain a CN group or not. If they do, then the average frequency is 1453—1458 cm^{-1}. If not, then it is 1438—1447 cm^{-1} (here too the lowest frequency is observed in the spectrum of a compound (64) forming an intermolecular bridge).

3. In 3,5-dinitro derivatives the average frequency is 1441—1447 cm^{-1}.

4. In 1,3-dinitro derivatives the average frequency of a chelating nitro group is 1438—1442 cm^{-1}.

5. In non-chelating 1,3-dinitro derivatives the average frequency is 1450—1468 cm^{-1} (the 1450 cm^{-1} is calculated from the spectrum of compound 37, which forms an intermolecular linkage).

6. In the spectra of *ortho*- and *para*-nitroaniline derivatives, the average value calculated from the frequency averages of the in-phase and out-of-phase symmetric and antisymmetric stretching vibrations is 1404—1410 cm^{-1}.

7. Finally, in the spectrum of picric acid (44) the average frequency of the chelated nitro group is 1429 cm^{-1}, while that of the others is 1452 cm^{-1}.

In the event of a 5-nitro group the band of the scissoring vibration is always weak. For the 3-nitro group too it is strong only if there is no CN group in the molecule. Its overall frequency range is 802—902 cm^{-1}.

1. In mononitro derivatives with the nitro group in position 5 it is 802—828 cm^{-1}.

2. In mononitro derivatives with the nitro group in position 3 it is 855—885 cm^{-1}.

3. In 1,3-dinitro derivatives it is 845—890 cm^{-1} in the event of chelation, and 804—830 cm^{-1} in the case of a free nitro group (including the aniline derivatives too).

4. In 3,5-dinitro derivatives the frequency of the scissoring vibration of the 3-nitro group is 850—867 cm^{-1} (the band of the 5-nitro group can be identified only in the spectra of compounds 71 and 75, at 820 and 824 cm^{-1}).

5. In the spectrum of picric acid a weak band is found at 836 cm^{-1}.

6. In the spectrum of compound 31 the frequency is 902 cm^{-1}.

The band of the rocking vibration is always very weak, and can often not even be identified. Only in the spectrum of compound 31 is a strong band found corresponding to this vibration. Its frequency range is 498—549 cm^{-1}.

The band of the wagging vibration is always strong. In every case where at least two nitro groups are present in the molecule, the band is split into two (though in the spectrum of compound 73 the splitting is so minute that the two bands merge). Its overall frequency range is 717—775 cm^{-1}. However, only nitro groups which are strongly chelated or linked to hydrate water absorb above 760 cm^{-1}. The frequency depends to a slight extent on the mass of the other substituents too: the lowest frequencies are to be found in the spectra of the mesyloxy derivatives, while further, the bromo and iodo derivatives absorb at lower frequencies than the corresponding chloro derivative.

Characteristic and strong combination bands appear in the spectra of nitro derivatives. Not including the *o*-nitroanilines, a strong or very strong band is found between 3080 and 3110 cm^{-1}; this probably corresponds to the overtone of the antisymmetric stretching vibration. In the spectra of 3-mononitro derivatives not containing a CN group this overtone is weak. In the spectra of *o*, *o*'-dinitroaniline derivatives, in addition to the overtone of the antisymmetric stretching vibration, the combination of the split antisym-

metric vibrations and the combination of the in-phase symmetric and antisymmetric vibrations also result in strong and diffuse bands, which merge to various extents.

S–C bond. In the mesyloxy group the stretching vibration of the S–CH_3 bond yields bands of medium strength, while in the spectrum of compound 110 it results in one weak and one strong band. The frequencies are 764—768 cm^{-1} in the spectra of compounds 39 and 40, and 732 and 750 cm^{-1} in that of compound 110. Because of intermolecular effects in the latter compound, the polar structure of the group and the hyperconjugation of the methyl group are suppressed.

SO_2 group. This also occurs in the mesyloxy group. Its symmetric and antisymmetric stretching vibrations result in strong, and sometimes very strong bands. The frequency range for the symmetric stretching vibration is 1166—1187 cm^{-1}, while that in the antisymmetric case is 1371—1383 cm^{-1}. The frequency splitting depends slightly on the polar structure: the more polar the structure, the smaller the splitting. In the spectrum of compound 39 the splitting is 191 cm^{-1}, for compound 40 it is 196 cm^{-1}, and for compound 110 the average frequency splitting is 201 cm^{-1}. In the latter case the bands of both the symmetric and the antisymmetric stretching vibrations are split into two.

The scissoring vibration also leads to strong bands. The frequency range is 529—537 cm^{-1}. Two bands are found in the spectrum of compound 110.

The wagging vibration similarly gives a strong band, at 504—515 cm^{-1}. In compound 110 the two bands merge and appear at 504 cm^{-1}.

Amide bands. In the literature on infrared spectroscopy the amide bands are included in a special category. None of them can be assigned completely to the vibration of any one bond, but rather to the amide group as a whole.

Nevertheless, the amide **I** band is mainly characteristic of the stretching vibration of the CO group. The band is always very strong. With two exceptions, its frequency range in the spectra of primary acid amides is 1645—1662 cm^{-1}. These two exceptions are compounds 78 and 81, in the spectra of which the NH_2 stretching vibrations too betray the free NH group, while the frequency of the amide **I** band at 1688—1690 cm^{-1} permits the conclusion that the amide–amide structure is totally absent. Two types of intermolecular structure could be established from the NH_2 bands in compounds 72 and 96 too, but here the amide—amide structure predominates, since apart from the 1655—1658 cm^{-1} amide **I** band only a small shoulder towards higher frequencies reveals that another structure is also present. The frequency is a little influenced by the bulk of the halogens: the amide **I** bands of the dichloro derivatives are at 1657 and 1659 cm^{-1}, while those of the dibromo derivatives are at 1648—1651 cm^{-1} (with the exception of the phenols, see above). In compound 17 the carbonyl forms a chelate with the ortho-OH group. Here

the amide **I** band can be identified as a shoulder of the amide **II** band, at 1645 cm^{-1}. The amide **I** band of the secondary amides appears at 1637 and 1638 cm^{-1}.

The amide **II** band originates to a fairly large extent from the NH_2 scissoring vibration and, in the case of secondary amides, from the N–H in-plane bending vibration. The band is always strong or very strong. The frequency range for the amide **II** band of primary amides is 1600—1627 cm^{-1}, but it occurs above 1620 cm^{-1} only if the carbonyl of the amide group forms a chelate. In the spectra of secondary amides the band is found at 1537 and 1538 cm^{-1}.

A considerable role is played in the amide **III** band by the C–N stretching vibration, the bond order of which is fairly high because of internal conjugation. With the exception of compound 56, the band is always strong, and sometimes very strong. The only exception can be attributed to the ortho-bromo atom. In the spectra of primary amides the frequency range is 1386—1420 cm^{-1}, the same as that for vibration *19b*. Consequently, various band shifts can be observed due to coupling. Thus, in the spectra of compounds 90, 96, 103, 104, 106 and 107 the band of vibration *19b* changes places with the amide **III** band, and the latter is therefore to be found at higher frequencies: 1389—1405 cm^{-1}. The frequency is anomalously high in the spectrum of compound 17, but here the carbonyl oxygen forms a chelate and this increases the C—N bond order (1420 cm^{-1}). The band appears below 1400 cm^{-1} in all other cases. In the spectra of secondary amides the frequency is 1327 and 1328 cm^{-1}.

The amide **IV** band corresponds to a significant extent to the C = O in-plane bending vibration. It is strong only in the spectrum of the single iodine derivative (58), and is otherwise of medium strength or weak; it is often covered by the various vibrations of the ring (vibrations *6b*, *11* and *12*). Its frequency range is 783—840 cm^{-1}. In group *A* the frequency is 839 and 840 cm^{-1}, in group *B* 800—820 cm^{-1} (but 820 cm^{-1} only in compound 56, in which the force constant of the vibration may be increased by the repulsion of the *ortho*-bromo atom), and in group *C* 783—792 cm^{-1}. Accordingly, the vibration is coupled with some motion of the halogens. As regards the secondary amides, the amide **IV** band could be identified only in the spectrum of compound 97, at 798 cm^{-1}.

The amide **V** and amide **VI** bands belong to the out-of-plane vibrations of the group. The two are generally distinguished by the fact that the amide **VI** band is more diffuse. From the widths of the bands and from the frequency, it may be concluded that the major role is played in the amide **V** band by the wagging vibration of the NH_2 group (or by the N–H vibration perpendicular to the NHR plane in secondary amides), and in the amide **VI** band by the out-of-plane vibration of the carbonyl group. The amide **V** band is of medium intensity or strong, and is very often superimposed on the amide **VI** band.

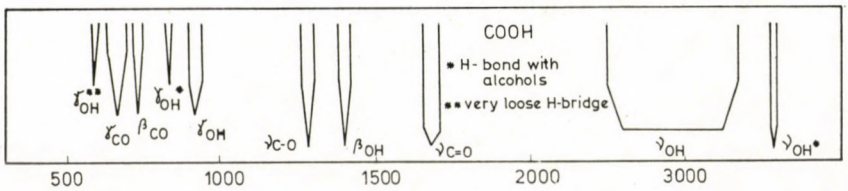

Fig. 7. Frequency ranges of internal vibrations of the COOH group

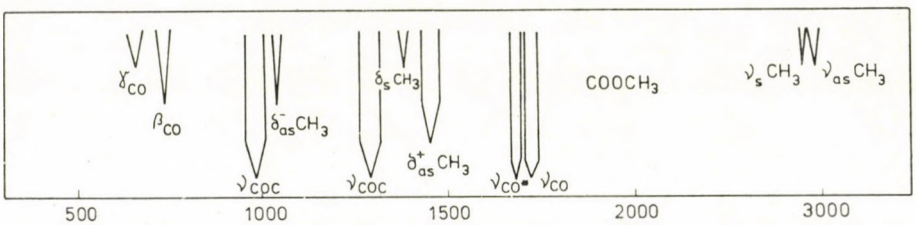

Fig. 8. Frequency ranges of internal vibrations of the $COOCH_3$ group

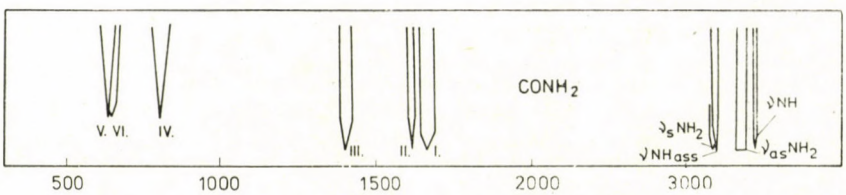

Fig. 9. Frequency ranges of internal vibrations of the $CONH_2$ group

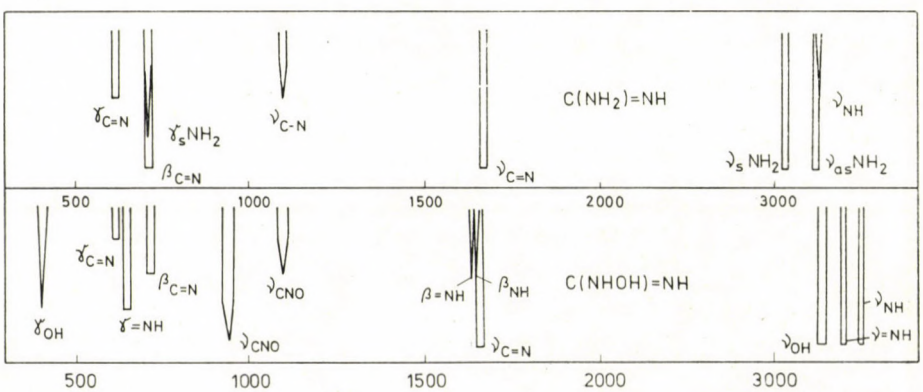

Fig. 10. Frequency ranges of internal vibrations of the $C(NH_2)=NH$ and $C(NHOH)=NH$ groups

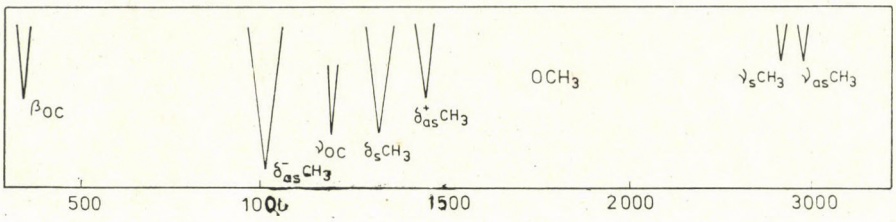

Fig. 11. Frequency ranges of internal vibrations of the OCH_3 group

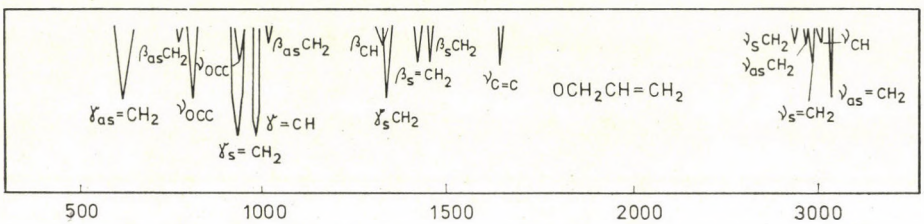

Fig. 12. Frequency ranges of internal vibrations of the $OCH_2CH{=}CH_2$ group

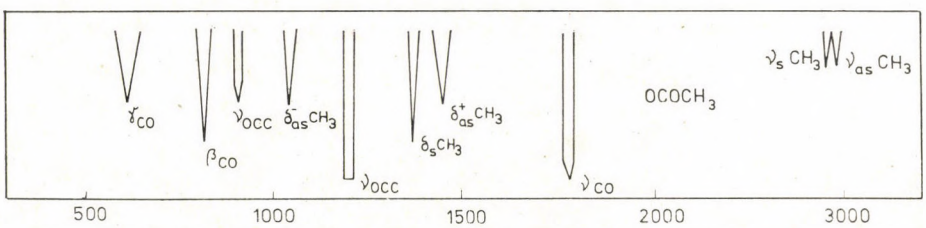

Fig. 13. Frequency ranges of internal vibrations of the $OCOCH_3$ group

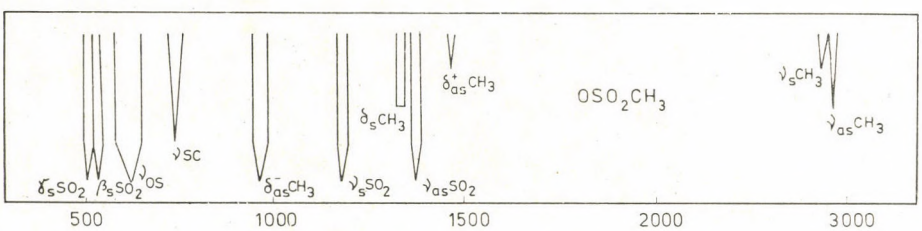

Fig. 14. Frequency ranges of internal vibrations of the OSO_2CH_3 group

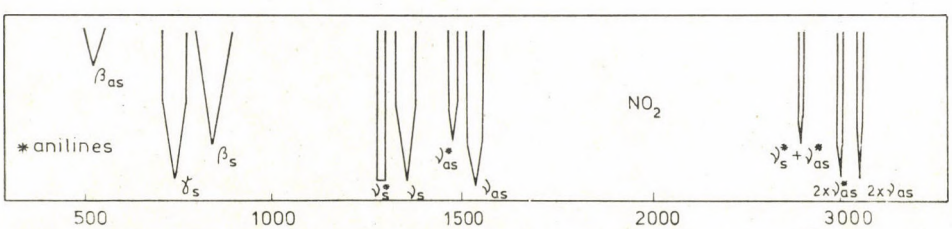

Fig. 15. Frequency ranges of internal vibrations of the NO_2 group

In the spectrum of compound 17, however, which forms a weak association, it is weak and less sharp. The overall frequency range is 587—666 cm^{-1}. If only one of the hydrogens of the NH_2 group is bound, then the frequency is 587—640 cm^{-1}, but if it is not possible to distinguish between the two hydrogens in the associated structure (the carbonyl oxygen is situated symmetrically between the two hydrogens), then the minimum frequency is 647 cm^{-1} (or 638 cm^{-1} in compound 17). The amide **VI** band is always diffuse and strong; it is very difficult to give its mean frequency. The diffuse band sometimes extends over the entire interval 615—680 cm^{-1}.

The stylized spectra of the bands originating from the internal vibrations of the substituents are given for the various substituents in Figs 7—15.

REFERENCES

[1] VARSÁNYI, G., SOHÁR, P.: Acta Chim. (Budapest), **74**, 315 (1972)
[2] VARSÁNYI, G., SOHÁR, P.: Acta Chim. (Budapest), **76**, 243 (1973)
[3] VARSÁNYI, G.: Vibrational Spectra of Benzene Derivatives. Academic Press, New York, London 1969
[4] VARSÁNYI, G.: Assignments for Vibrational Spectra of 700 Benzene Derivatives. Akadémiai Kiadó, Budapest 1973
[5] STERIN, KH. E., ALEKSANIAN, V. T., UKHOLIN, S. A., BRAGIN, O. V., GAVRILOVA, A. E., ZOTOVA, S. V., LIBERMANN, A. L., MIKHAILOVA, E. A., SMIRNOVA, E. N., STERLIGOV, O. D., KAZANSKII, B. A.: Izv. Akad. Nauk. SSSR, Ser. Khim., 1444 (1961)
[6] L. M., SVERDLOV, M. A., KOVNER, E. P. KRAINOV: Kolebatel'nye Spektry Mnogoatomnykh Molekul. Nauka, Moscow 1970
[7] STEELE, D.: Spectrochim. Acta, **18**, 915 (1962)
[8] ALEKSANIAN, V. T., STERIN, KH. E., LIBERMANN, A. L., MIKHAILOVA, E. A., PRAINISHNIKOVA, M. A., KAZANSKII, B. A.: Izv. Akad. Nauk. SSSR, Ser. Fiz., **19**, 225 (1955)
[9] BARUAH, G. D., SINGH, K., RAI, D. K.: Ind. J. Pure Appl. Phys., **8**, 678 (1970)
[10] WILSON, E. B.: Phys. Rev., **45**, 706 (1934)

György VARSÁNYI 1111-Budapest, Műegyetem rkp. 3.
GÁBOR HORVÁTH Chinoin, Budapest, Tó u. 1—5.
LAJOS IMRE Központi Kémiai Kutatóintézet
Budapest, Pusztaszeri út 57—69.

József SCHAWARTZ Chinoin, Budapest, Tó u. 1—5.
Pál SOHÁR Gyógyszerkutató Intézet, Budapest,
Szabadságharcosok útja 47/49.

Ferenc SÓTI Központi Kémiai Kutatóintézet
Budapest, Pusztaszeri út 57—69.

Acta Chimica Academiae Scientiarum Hungaricae, Tomus 93 (3—4), pp. 357—369 (1977)

NACHTRÄGLICHE ERHÖHUNG DES INFORMATIONSGEHALTES VON SPEKTRALPHOTOPLATTEN IN DER OPTISCHEN EMISSIONSSPEKTRALANALYSE

K. DANZER und A. SONNTAG

Technische Hochschule Karl-Marx-Stadt, Sektion Chemie und Werkstofftechnik, DDR-90 Karl-Marx-Stadt, Postschließfach 964

Eingegangen am 26. Juli, 1976

Ausgehend von theoretischen Grundlagen photographischer Informationen wird die Möglichkeit abgeleitet, photographisch gespeicherte Informationen nachträglich im Sinne einer besseren Informationsausnutzung zu beeinflussen. Es wurde die Anwendung des Entwicklungsdetailfilterverfahrens nach Lau und der Gradationsverstärkung durch hartes Umkopieren von photographisch registrierten Spektren untersucht. Beide Verfahren führen für Spektrallinien geringer Schwärzung zu einer Steigerung des Signal-Rausch-Verhältnisses und damit auch zu einer Verbesserung des Nachweisvermögens bestimmter Spektrallinien.

Die photographische Registrierung von Spektren besitzt auch gegenwärtig, trotz der gewaltigen Fortschritte auf dem Gebiet photoelektrischer Detektoren, eine breite Bedeutung, insbesondere für die wissenschaftliche Forschungsarbeit. Eine wesentliche Ursache dafür ist die große Informationskapazität von Photoplatten. Während in der optischen Emissionsspektralanalyse einerseits große Anstrengungen unternommen werden, durch Optimierung des Anregungsvorganges die Informationsgewinnung zu erhöhen, vor allem das Nachweisvermögen zu verbessern, bleibt andererseits eine beträchtliche Menge an Informationen, die in der photographischen Schicht gespeichert sind, ungenutzt. Ziel dieser Arbeit soll es sein, Möglichkeiten der besseren Informationsausnutzung photographisch registrierten Spektren zu zeigen.

1. Parameter zur Kennzeichnung photographischer Informationen

Photographische Informationen werden in der Regel eingeteilt in Großflächen- und Detailinformationen [1]. *Großflächeninformationen* werden beschrieben durch die charakteristische *Schwärzungskurve*

$$S = f(\log E \cdot t) = f(\log H) \tag{1}$$

S = photopraphische Schwärzung
E = Beleuchtungsstärke, $[E] = lx = cd \cdot sr \cdot m^{-2}$
H = Belichtung, $[H] = lx \cdot s$

bzw. entsprechende Transformationen [2] [3] [4] [5] sowie durch den *Kontrast* (vgl. Bild 2)

$$K = \frac{H_{\max} - H_{\min}}{H_{\max} + H_{\min}} . \tag{2}$$

Demgegenüber werden *Detailinformationen* beschrieben durch die Größen *Auflösungsvermögen:*

A_L lineares bzw. laterales Auflösungsvermögen, $[A_L] = \mathrm{mm}^{-1}$, Linien, die pro mm gerade noch getrennt wahrgenommen werden können; $A_F = A_L^2$ Flächenauflösungsvermögen, $[A_F] = \mathrm{mm}^{-2}$;

Konturenschärfe:

Friesersche k-Zahl, $[k] = \mu\mathrm{m}$, entspricht dem Abstand von der Stelle einer wahren Kante, wo die Maximalbelichtung $H_{\max}$ auf 0,1 $H_{\max}$ abgesunken ist;

und *Körnigkeit:*

$K = 100 \log Q$; $Q = S_{\shortparallel}/S_{\#}$ Callier-Quotient der Schwärzung bei Messung der optischen Dichte mittels parallelen bzw. diffusen Lichtes.

Auf Detailinformationen bezieht sicht auch die *Speicherkapazität (Informationskapazität) C* [6] [7] photographischer Schichten, die durch das Auflösungsvermögen bestimmt wird

$$C = A_F = A_L^2 . \tag{3}$$

$$[C] = \mathrm{bit} \cdot \mathrm{mm}^{-2}$$

Für die gebräuchlichen Spektralplattensorten ORWO Blau Extrahart WU 3, Rot Extrahart WO 3, Gelb Extrahart WP 3 beträgt die Informationskapazität etwa $C = 10^4$ bit $\cdot$ mm^{-2}.

Die Einteilung in Großflächen- und Detailinformationen trägt u. a. der auch dem Spektrochemiker bekannten Tatsache Rechnung, daß die "Makro"-Schwärzungskurve für kleine Details nicht mehr gilt [8].

Eine einheitliche Betrachtung sowohl von Großflächen-, als auch von Detailinformationen unter allgemeinen Gesichtspunkten wird ermöglicht durch die Einführung des Begriffes *Ortsfrequenz R*

$$R = \frac{1}{g} , \quad [R] = \mathrm{mm}^{-1} \tag{4}$$

g Rasterabstand (vgl. Abb. 2)

Damit wird die Analyse jeder beliebigen Intensitätsverteilung durch Fourieranalyse möglich. Abb. 1 zeigt die Objekt- und Bildverteilungen in Orts- und Ortsfrequenzdarstellung; beide sind durch die folgenden Fourierintegrale ineinander überführbar:

$$B(\mathbf{w}) = \int_{-\infty}^{+\infty}\int b(\mathbf{r}')\ \mathrm{e}^{-2\pi i(\mathbf{r}',\mathbf{w})}\,\mathrm{d}x'\,\mathrm{d}y' \tag{5a}$$

$$D(\mathbf{w}) = \int_{-\infty}^{+\infty}\int d(\mathbf{r}')\ \mathrm{e}^{-2\pi i(\mathbf{r}',\mathbf{w})}\,\mathrm{d}x'\,\mathrm{d}y' \tag{5b}$$

$$O(\mathbf{w}) = \int_{-\infty}^{+\infty}\int o(\mathbf{r})\ \ \mathrm{e}^{-2\pi i(\mathbf{r},\mathbf{w})}\,\mathrm{d}x\,\mathrm{d}y \tag{5c}$$

$$b(\mathbf{r}') = \int_{-\infty}^{+\infty}\int B(\mathbf{w})\,\mathrm{e}^{2\pi i(\mathbf{r}',\mathbf{w})}\ \ \mathrm{d}u\,\mathrm{d}v \tag{6a}$$

$$\mathrm{d}(\mathbf{r}') = \int_{-\infty}^{+\infty}\int D(\mathbf{w})\,\mathrm{e}^{2\pi i(\mathbf{r}',\mathbf{w})}\ \ \mathrm{d}u\,\mathrm{d}v \tag{6b}$$

$$o(\mathbf{r}) = \int_{-\infty}^{+\infty}\int O(\mathbf{w})\,\mathrm{e}^{2\pi i(\mathbf{r},\mathbf{w})}\ \ \mathrm{d}u\,\mathrm{d}v \tag{6c}$$

$\mathbf{r} = \{x, y\}$ Ortsvektor
$\mathbf{w} = \{u, v\}$ Ortsfrequenzvektor

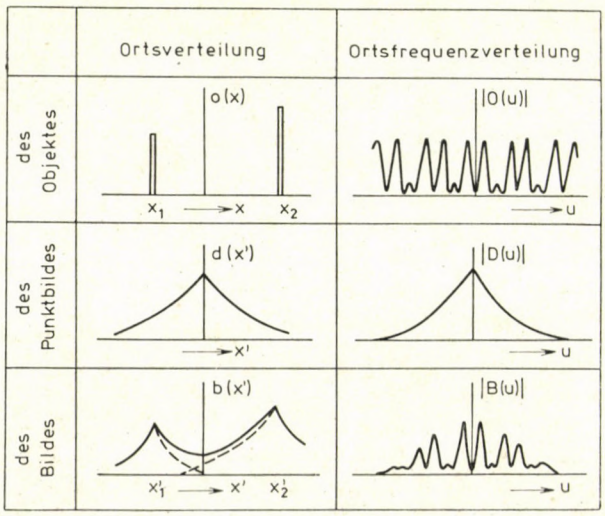

Abb. 1. Informationsübertragung beim photographischen Prozeß in Orts- und in Orstfrequenzdarstellung (vereinfachte eindimensionale Darstellung)

Gl. (5b) beschreibt die Ortsfrequenzverteilung idealer Punktbilder und stellt damit eine allgemeine Übertragungsfunktion photographischer Informationen dar. Wie aus Abb. 1 hervorgeht, sind die Funktionen $O(u)$, $D(u)$ und $B(u)$ als Fouriertransformierte reeller Funktionen symmetrisch, d. h. $|O(u)| = |O(-u)|$, so daß in der Regel nur die Kurven für $+u$ dargestellt werden [9].

Die Ortsverteilung des Bildes entspricht einer Faltung der Objektfunktion mit der Übertragungsfunktion

$$b(\mathbf{r}) = \mathrm{d}(\mathbf{r}) * o(\mathbf{r}), \tag{7a}$$

so daß die Ermittlung der Objektfunktion, die eigentliche Aufgabe der optischen Informationsübertragung, mit

$$B(\mathbf{w}) = D(\mathbf{w}) \cdot O(\mathbf{w}) \tag{7b}$$

möglich wird nach der Beziehung

$$o(\mathbf{r}) = \int_{-\infty}^{+\infty}\int \frac{B(\mathbf{w})}{D(\mathbf{w})} e^{2\pi i(\mathbf{r},\mathbf{w})}\, \mathrm{d}u\, \mathrm{d}v \tag{8}$$

Aufgrund der Faltung mit der Übertragungsfunktion, die nur innerhalb eines endlichen Gebietes von $\{u, v\}$ von Null verschiedene Werte annimmt und damit die Bandbreite der zur Abbildung verwendeten Ortsfrequenzen darstellt [10], ist die Rekonstruktion des Objektes nur mit einer bestimmten Unschärfe möglich.

Durch die Fourieranalyse lassen sich alle zweidimensional gespeicherten Informationen auf Signale zurückführen, die durch Angabe zweier Größen, der *Ortsfrequenz* R und den *Kontrast* K eindeutig bestimmt sind (Abb. 2). Da als Details häufig bereits sinusförmige Intensitätsverteilungen vorliegen, erübrigt sich eine weitere Fourierzerlegung.

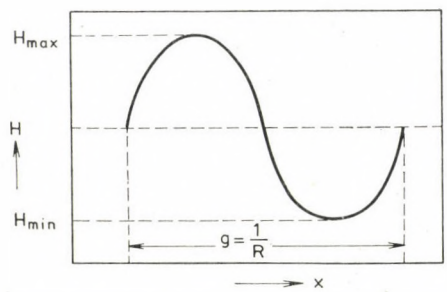

Abb. 2. Bestimmungsgrößen eines Bildelementes mit sinausförmigem Intensitätsverlauf

Eine wichtige Größe, die den Zusammenhang zwischen dem Kontrast und der Ortsfrequenz beschreibt, ist die *Modulationsübertragungsfunktion* (MTF) photographischer Schichten. Sie stellt die Änderung des Modulations-(Kontrast-)übertragungsfaktors $M(R)$ mit der Ortsfrequenz dar

$$M(R) = \frac{K_B(R)}{K_O(R)} \tag{9}$$

K_B Bildkontrast, K_O Objektkontrast

Abbildung 3 zeigt die Modulationsübertragungsfunktionen photographischer Schichten mit hohem bzw. geringem Auflösungsvermögen.

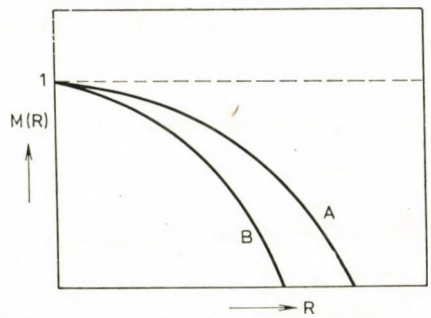

Abb. 3. Modulationsübertragungsfunktionen (A) einer photographischen Schicht hoher Auflösung und (B) einer Schicht niedriger Auflösung

2. Möglichkeiten der nachträglichen Informationsaufbereitung photographischer Informationen

Zu den Vorteilen photographischer Informationsträger gehört neben der hohen Speicherkapazität vor allem die Tatsache, daß sich die gespeicherten Informationen nachträglich nach verschiedenen Methoden umformen und aufbereiten lassen. Dabei werden an dem normal entwickelten und fixierten Material auf chemischem oder physikalischem Wege Veränderungen vorgenommen, die sich mathematisch als Transformationen der Schwärzungsfunktion bzw. der Modulationsübertragungsfunktion darstellen.

In Abbildung 4 ist das Schema der photographischen Informationsübertragung dargestellt. Als objektive physikalische Ursachen für Unschärfe und Rauschen kommen hauptsächlich in Betracht [1]:

- Lichtstreuung in der photographischen Schicht,
- Korngröße,
- chemische Diffusionseffekte,
- mechanische Effekte.

Sie werden hauptsächlich beeinflußt durch Art, Menge, Konzentration und Temperatur des Entwicklers sowie durch die Entwicklungszeit und die Dynamik des Entwicklungsvorganges [11] [12].

Für die optische Emissionsspektralanalyse ist eine nachträgliche Verbesserung der Informationsausnutzung grundsätzlich auf drei verschiedenen Wegen in Erwägung zu ziehen:

(1) Empfindlichkeitssteuerung, und zwar

(a) aller Bereiche der Schwärzungskurve durch verschiedene Verstärkungsverfahren [13] [14] [15] sowie durch Holokopie [1], [16],

b) des geradlinigen Teiles der Schwärzungskurve,

(2) Kontraststeuerung durch Masken- bzw. Ortsfrequenzfilterverfahren, insbesondere durch Entwicklungsdetailfilterverfahren (EDFV) [1] [17] [18],

(3) Schwärzungstransformationen und -markierungen, z. B. durch Äquidensitometrie und Schwärzungsreliefverfahren [1] [19].

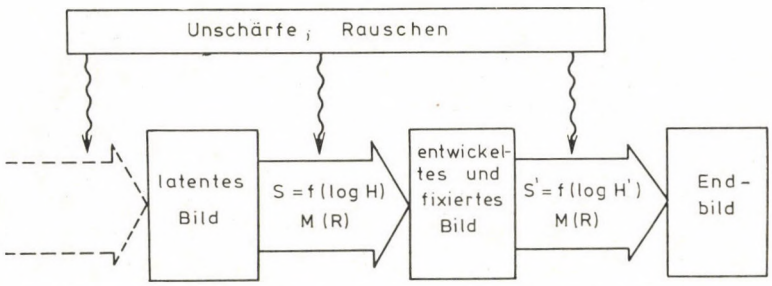

Abb. 4. Informationsübertragung im Verlaufe des photographischen Prozesses

Von den angegebenen Verfahren erschien für die Verbesserung des Signal-Rausch-Verhältnisses und damit für eine Erhöhung des Nachweisvermögens spektrographischer Methoden besonders zwei Verfahren aussichtsreich: das Entwicklungsdetailfilterverfahren nach Lau [17] sowie eine nachträgliche Erhöhung der Gradation γ, d. h. ein Umkopieren der Spektralphotoplatte auf hart arbeitendes Photomaterial [20].

3. Das Entwicklungsdetailfilterverfahren (EDFV)

Das Problem der ungenügenden Informationsausschöpfung von Photographien ergibt sich u. a. aus der charakteristischen Schwärzungskurve, von der nur ein Teil, der geradlinige, zur Auswertung geeignet ist. Die in "Schwelle" und "Schulter" der Kurve enthaltenen Informationen gehen in der Regel verloren, da hier Kontraste schwer meßbar sind.

Um die für die Spektralanalyse relevanten Informationen besser auszuschöpfen, ist es nicht unbedingt erforderlich, den Gesamtkontrast auszugleichen, sondern vielmehr die hohen Ortsfrequenzen zu verstärken und damit eine Verbesserung der Detailwiedergabe zu erzielen.

Praktisch erreicht man das durch sogenannte Maskenverfahren. Unter Masken versteht man photographische Schichten, die mit dem Originalnega-

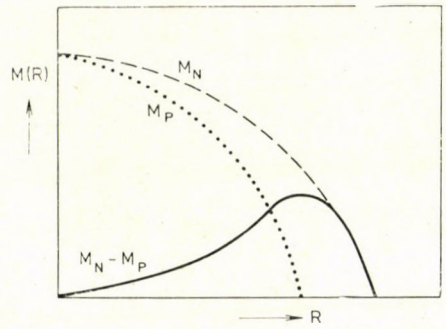

Abb. 5. Veränderung der Modulationsübertragungsfunktion durch eine unscharfe Maske

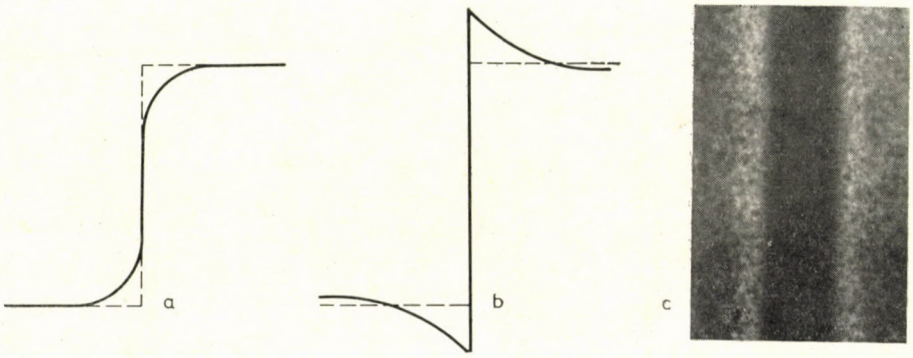

Abb. 6. Schwärzungsverlauf auf der Photoschicht (a) für eine ideal scharfe Kante und (b) bei Wirkung des Eberhardteffektes; (c) zeigt eine Originalspektrallinie bei Wirkung des Eberhardt-Effektes

tiv zusammenwirken, um bestimmte Effekte zu erhalten [1]. Oft sind Masken besonders verarbeitete Positive des Originalnegativs. Für die Verstärkung hoher Ortsfrequenzen besitzen unscharfe Masken besondere Bedeutung, wie Abb. 5 anhand der Modulationsübertragungsfunktionen deutlich zeigt.

Das Entwicklungsdetailfilterverfahren ist ein photochemisches Maskenverfahren, bei dem eine unscharfe, steuerbare Maske durch Belichten von entwicklergetränktem Photomaterial in einer Kopierschicht erzeugt wird. Dabei werden Nachbareffekte, speziell die unter der Bezeichnung "Eberhardt-Effekt" [21] zusammengefaßten, die man bei normalen Entwicklungen gerade auszuschalten sucht [22], bewußt ausgenutzt und hochgezüchtet.

Die Wirkung des Eberhardt-Effektes ist schematisch in Abb. 6b dargestellt, 6c zeigt die Diffusionswirkungen an einer Spektrallinie anschaulich und deutlich. Die gegenläufigen Diffusionen von frischem Entwickler und entwicklungshemmenden Oxidationsprodukten sind letztlich verantwortlich für die Verstärkung hoher Ortsfrequenzen. Abb. 7 zeigt, daß es möglich ist, auf diesem Wege schwache Spektrallinien zu verstärken.

Bei der praktischen Durchführung des EDFV wurde so vorgegangen, daß von der Original-Spektralplatte, die nach Möglichkeit bis zu 5fach überbelichtet sein kann, Kontaktkopien angefertigt wurden, und zwar entweder

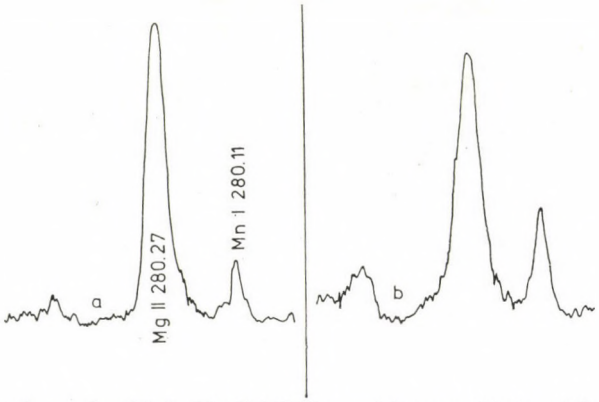

Abb. 7. Verstärkung der Linie Mn I 280,11 nm (a) normal behandelte Photoplatte, (b) EDF-behandelte Platte

auf Photoplatten oder Filme. Dabei müssen sich die Schichtseiten berühren, um Diffusionslichthofwirkungen gering zu halten. Der feste planparallele Andruck von Original und Kopiermaterial wurde am besten mittels einer Photokassette des verwendeten Spektrographen erreicht. Nach der Belichtung wurde die Kopie kurze Zeit normal anentwickelt, gegebenenfalls nachbelichtet [29] und anschließend unter Entwicklermangel ausentwickelt. Dazu wurde auf die entwicklerfeuchte Kopie eine Folie aufgewalzt, so daß für den Ausentwicklungsprozeß nur der dünne Entwicklerfilm zwischen Kopie und Folie zur Verfügung stand [23—28].

Die detaillierten Kopierbedingungen sind in Tabelle II zusammengestellt.

4. Gradationsverstärkung (GV) durch hartes Umkopieren

Eine Empfindlichkeitsverstärkung über eine Beeinflussung der Gradation γ führt in der Regel zu einer allgemeinen Kontrastverstärkung bis zu einer gewissen Grenze. Die Verstärkung von Spektrallinien kann dabei so weit gehen, daß Signale, die auf der Originalplatte unterhalb der Nachweisgrenze

liegen, sich nach der Kopie oberhalb der Nachweisgrenze befinden, wie folgende Überlegungen zeigen.

Auf der Originalplatte sei die Schwärzung einer schwachen Spektrallinie

$$S_{L+U} = S_U + \Delta S_0 \,. \tag{10}$$

Die zugehörige Erfassungsgrenze ergibt sich zu

$$S_E = S_U + 6\,\sigma_U \,, \tag{11}$$

wobei gelten soll

$$\Delta S_0 < 6\,\sigma_U \tag{12a}$$

und damit auch

$$S_{L+U} < S_E \,. \tag{12b}$$

Nach zweifacher harter Kopie beträgt die Schwärzung dieser Linie

$$S'_{L+U} = S'_U + \Delta S_2 \tag{13a}$$

bzw. wenn ΔS_2 als Vielfaches von ΔS_0 ausgedrückt wird

$$S'_{L+U} = S'_U + k \cdot \Delta S_0 \,. \tag{13b}$$

Für die Erfassungsgrenze gilt mit $\sigma_U \approx \sigma'_U$

$$S'_E = S'_U + 6\,\sigma_U \,. \tag{14}$$

Der Wert von k läßt sich aus den Gradationen der Kopiermaterialien abschätzen. Es gilt

$\Delta S_0 = \gamma_0 \Delta Y_0$	für die Originalplatte	(15a)
$\Delta S_1 = \gamma_1 \Delta Y_1 \approx \gamma_0 \gamma_1 \Delta Y_0$	für die 1. Kopie	(15b)
$\Delta S_2 = \gamma_2 \Delta Y_2 \approx \gamma_0 \gamma_1 \gamma_2 \Delta Y_0$	für die 2. Kopie	(15c)

Mit der in Gl. (13b) eingeführten Beziehung $\Delta S_2 = \Delta S_0 \cdot k$ ergibt sich aus den Gln. (15a) und (15c)

$$k \approx \gamma_1 \gamma_2 \,. \tag{16}$$

Für das bei unseren Untersuchungen verwendete Filmmaterial ORWO FU5 beträgt $\gamma \approx 5$, so daß $k \approx 25$ zu erwarten ist. Praktisch wurde ermittelt [20]

$$k = 13{,}8 \pm 3{,}6.$$

Für schwache Spektrallinien mit einer Schwärzung S_{L+U} nach Gl. (10) im Schwärzungsbereich

$$S_U + 0{,}5\,\sigma_U < S_{L+U} < S_U + 6\,\sigma_U \tag{17a}$$

bzw.

$$0{,}5\,\sigma_U < \Delta S_0 < 6\,\sigma_U \tag{17b}$$

ergibt sich mit dem ermittelten k-Wert

$$k \cdot \Delta S_0 > 6\,\sigma_U \tag{18a}$$

und damit auch

$$S_{L+U} > S_E\,. \tag{18b}$$

Diese Überlegungen konnten experimentell bestätigt werden.

5. Ergebnisse

Als Modellproben wurden Spektralkohlen der Reinheit TO (VEB Elektrokohle Lichtenberg, DDR) verwendet, da diese erfahrungsgemäß Spektrallinien mehrerer Elemente mit Schwärzungen in der Nähe ihrer Nachweisgrenzen zeigen können. In Tabelle I sind die Anregungs- und Aufnahmeparameter zusammengestellt.

Tabelle I

Anregungs- und Aufnahmebedingungen

Spektrograph	2 m – Plangitterspektrograph PGS 2 (VEB Carl Zeiss Jena) Gitter: 651 Striche/mm 1. Ordnung theoretisches Auflösungsvermögen 45 6000 Dispersion: 7,37 Å/mm
Spaltbreite	15 μm
Lichtführung zum Spektrographen	Zwischenabbildungssystem Zeiss; Elektroden ausgeblendet, Zwischenblende 5 mm
Anregung	UBI 1 (VEB Carl Zeiss Jena) Gleichstromdauerboden 10 A, 300 V
Elektroden	Universalelektroden TO Form 119 (VEB Elektrokohle Lichtenberg), Elektrodenabstand 2 mm
Belichtungszeit	180 s
Photomaterial	ORWO WU 3, spektral blau extrahart
Entwicklung	Metol–Hydrochinon 1 : 4, 20 °C, 4 min Schaukelentwicklung
Schwärzungsmessung	Schnellphotometer G II (VEB Carl Zeiss Jena)

Der unmittelbaren Anwendung des EDFV auf die Entwicklung der Originalplatte standen einige Gründe entgegen. Einmal ist die Gradation der verwendeten Spektralplatten ORWO spektral blau extrahart WU 3 mit $\gamma \approx 1$ zu gering, um effektive EDF-Wirkungen zu erzielen. Außerdem läßt sich die erforderliche Überbelichtung zwar im konkreten Modellfall, nicht aber allgemein verwirklichen. Schließlich sollte auch die Möglichkeit ausgeschlossen werden, die Originalplatte durch Fehler beim EDFV zu beeinträchtigen. Aus dem zuerst angeführten Grund erwies sich auch die Herstellung von zwei Kopien nach dem EDFV mittels Spektralplatten als ungünstig.

Es wurde deshalb die Anwendung von zwei Verfahren untersucht, wobei einmal das EDFV mit der Gradationsverstärkung durch hartes Umkopieren kombiniert wurde, zum anderen beide Kopien nach Gradationsverstärkung erzeugt wurden. Tabelle II gibt einen Überblick über die Parameter der beiden angewandten Verfahren.

Tabelle II

Kopierbedingungen (alle Zeitangaben in s)

Verfahren	Entwicklerkonzentration	Belichtungszeit	Zeit der normalen Entwicklung	Zeit der Entwicklung unter Entwicklermangel
1 Erstkopie: EDFV	1 : 4	60	10	120
Zweitkopie: GV	1 : 4	90	180	—
2 Erstkopie: GV	1 : 4	10	180	—
Zweitkopie: GV	1 : 4	180	180	—

In Abb. 8 ist ein Spektrenausschnitt auf der Originalplatte und nach den beiden Kopierverfahren dargestellt. Daraus geht hervor, daß zwei im ausgewählten Bereich befindliche Linien, die im Original im Rauschen des Untergrundes verschwinden, nach den speziellen Kopierverfahren deutlich hervortreten.

Die Auswertung für die Linie Co 287,96 nm, die in Abb. 9 veranschaulicht ist, zeigt, daß diese sowohl durch EDFV, verbunden mit Gradationsverstärkung, als auch durch zweifache Gradationsverstärkung beträchtlich über die Erfassungsgrenze angehoben wird.

Ein Vergleich der beiden angewandten Verfahren zeigt, daß der Verstärkungsgrad einer Linie von der Schwärzungsdifferenz auf dem Original abhängt. Aus Abb. 10 geht hervor, daß für hartes Umkopieren die Verstärkung v mit wachsendem ΔS bis zu einer Sättigungsgrenze zunimmt, während sie für EDFV + GV mit ΔS abnimmt.

*

Herrn Prof. em. Dr. E. LAU, Zentralinstitut für Optik und Spektroskopie der Akademie der Wissenschaften der DDR, danken wir für förderliche Diskussionen und Hinweise.

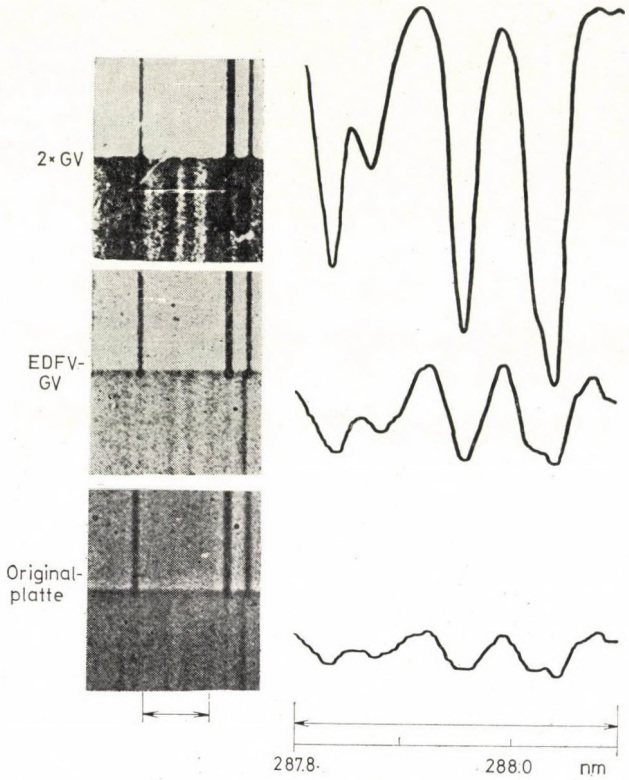

Abb. 8. Spektrenausschnitt einer Original-Spektralplatte und von Kopien nach dem EDVF, verbunden mit Gradationsverstärkung sowie nach zweifacher GV

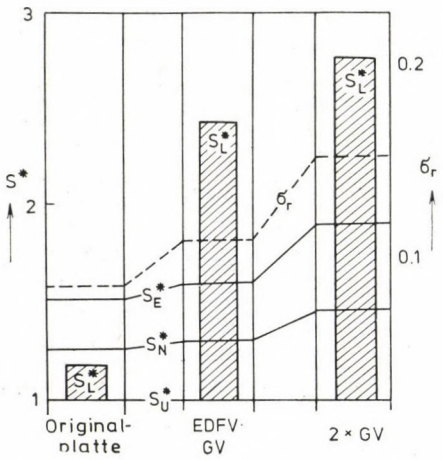

Abb. 9. Auf die Untergrundschwärzung bezogene Linienschwärzungen S_L^* in Relation zu den jeweiligen Nachweisgrenzen (S_N^* nach dem 3 σ-Kriterium) und Erfassungsgrenzen (S_E^*, nach dem 6 σ-Kriterium) der Linie Co 287,96 nm für die Originalplatte und die beiden untersuchten Kopierverfahren

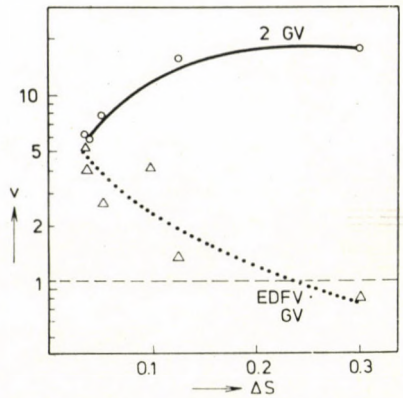

Abb. 10. Verstärkung des Signal-Rausch-Verhältnisses nach EDFV + GV und nach hartem Umkopieren (2×GV)

LITERATUR

[1] Krug, W., Weide, H. G.: Wissenschaftliche Photographie in der Anwendung. Leipzig 1972
[2] Kaiser, H.: Spectrochim. Acta **3** (1947) 159
[3] Török, T.: Proc. XIV. Coll. Spectr. Internat. Debrecen 1967, 155. London: Hilger
[4] Zimmer, K.: ibid., 435
[5] Török, T., Zimmer, K.: Quantitative Evaluation of Spectrograms by Means of 1-Transformation. Budapest 1972
[6] Zweig, H. J., Higgins, G. C., MacAdam, D. I.: J. Opt. Soc. Amer., **48** (1958) 926
[7] Jones, R. C.: J. Opt. Soc. Amer., **51** (1961) 1159
[8] Mika, J., Török, T.: Analytical Emission Spectroscopy. Budapest 1973
[9] Röhler, R.: Informationstheorie in der Optik. Stuttgart 1967
[10] Schober, H.: Wiss. Z. Hochsch. Elektrotechn. Ilmenau, **3** (1957) 273
[11] Török, T., Heltai, G., Moharos, I.: Acta Chim. (Budapest), **77**, (1973) 11, 117
[12] Török, T., Heltai, G.: Spectrochim. Acta **27** B (1972) 215
[13] Belchev, S. M., Burgudzhiev, Z., Petkova, T. S.: God. Sofii. Univ., Chim. Fak., 1970—1971, 65, 397
[14] Kalyanam, M., Rajagopalan, S. R., Rajagopal, C.: Trans. Soc. Advan. Electrochem. Sci. Technol., **7** (1972) 56
[15] Petrakiev, A., Dimitrov, G.: Talanta, **16** (1969) 1583
[16] Lau, E.: Optik, **21** (1964) 637
[17] Lau, E.: Bild u. Ton, **25** (1972) 149
[18] Stutzke, G., Hess, G.: J. Signalaufzeichnungsmat., **1** (1973) 193
[19] Lau, E., Krug, W.: Die Äquidensitometrie. Berlin 1957
[20] Sonntag, A.: Diplomarbeit, Techn. Hochsch. Karl-Marx-Stadt 1975
[21] Eberhardt, G.: Physikal. Z., **12** (1912) 288
[22] Nikolaevskii, L. S.: Zh. prikl. Spektrosk., **20** (1974) 924
[23] Lau, E.: Bild u. Ton, **22** (1969) 66; 196; **23** (1970) 357; **24** (1971) 363; **26** (1973) 23; 209; **27** (1974) 11
[24] Lau, E., Weide, H.-G., Stutzke, G.: Bild u. Ton, **19** (1966) 290
[25] Weide, H.-G.; Bild u. Ton, **22** (1969) 2
[26] Lau, E., Stutzke, G.: Bild u. Ton, **22** (1969) 322
[27] Lau, E., Hicke, H.-G.: Bild u. Ton, **24** (1971) 165; **25** (1972) 71
[28] Lau, E., Stutzke, G., Wotzka, K. H.: Bild u. Ton, **24** (1971) 101
[29] Lehmann, J., Lehmann, N.: Diplomarbeit. Techn. Hochsch. Karl-Marx-Stadt 1976

K. Danzer DDR—90 Karl-Marx-Stadt, Postschließfach 964.

Acta Chimica Academiae Scientiarum Hungaricae, Tomus 93 (3—4), pp. 371—394 (1977)

A MODEL OF LIQUID WATER

TETRAGONAL CLUSTERS: DESCRIPTION AND DETERMINATION OF PARAMETERS

F. HAJDU

(Central Research Institute for Chemistry, Hungarian Academy of Sciences)

Received July 26, 1976

Based on the radial distribution functions of water at three temperatures obtained from X-ray diffraction experiments, a tetragonal cluster model is proposed for the structure. Besides reproducing the experimental RDF's, and the reduced intensities, the model can describe the volume effects, and other physical correlations between water and some ice polymorphs.

1. Introduction

In a previous paper, it had been pointed out that the radial distribution function (RDF) of water obtained from X-ray diffraction measurements have some features not found, or neglected in earlier works on this topic. These are following:

i) The first coordination number of molecules (or of O nuclei) as calculated from the experimental radial density function, is slightly below 4 and hardly depends on temperature in the range 4° to 50° C — provided that the 'symmetrical' procedure is applied to determine the area under the first intermolecular peak of the radial density curve.

ii) The second peak in the RDF's is found at about 3.6 Å, partly overlapping the main peak at 2.83 Å, and causing the obvious asymmetry of the latter. The peak at 3.6 Å is the only one that gets more pronounced with rising temperature.

iii) The next peak — described in previous works as unique round 4.6 Å — was found by present author and colleagues (see the paper referred to above) to be a doublet with peaks round 4.3, and 4.8 Å, respectively. While the distance 4.6 Å was regarded as the edge of a regular tetrahedron formed by the four nearest neighbours of a central molecule, the two peaks can be assigned to the edges of a non-regular tetrahedron of similar origin [1, 1a].

These observations led the author to suggest a new model for water structure.

As to the survey of numerous structural models of water proposed by many previous authors, we refer to the books of EISENBERG and KAUZMANN [2] and those edited by F. FRANKS [3] W. A. P. LUCK [4] and T. ERDEY-GRÚZ [5]

respectively. The chemical physics of ice is thoroughly dealt with by FLETCHER [6].

According to the present model, water consists of clusters with a tetragonal network formed by hydrogen bonds. Geometrically, the tetragonal lattice is closely related to the diamond-like cubic lattice of ice I_c from which it can be derived by combined contraction and dilatation. The positions of O atoms are displayed on a ball-and-spike model in Fig. 1 representing a typical cluster of 54 molecules.

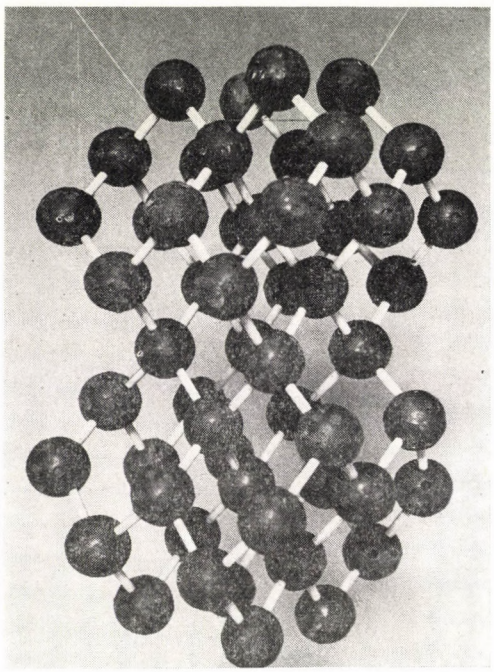

Fig. 1. Ball-and-spike model of a tetragonal water cluster (54 balls, long spikes, $2\alpha = 90°$)

The clusters must be thought of as formations unceasingly changing their shape and dimensions the mean life-time of which is long compared with the duration of interaction between the X-photon and the molecule but short relative to the measuring time of intensity. One may assume that the boundaries of the clusters coincide with the planes of the tetragonal lattice (*i.e.* the planes of six-membered puckered rings formed by water molecules). This assumption conforms with the ideas about cooperative breaking and establishing of the hydrogen bonds firstly proposed by FRANK and WEN in 1957 [12] and confirmed by some recent ab initio calculations as *e. g.* [13].

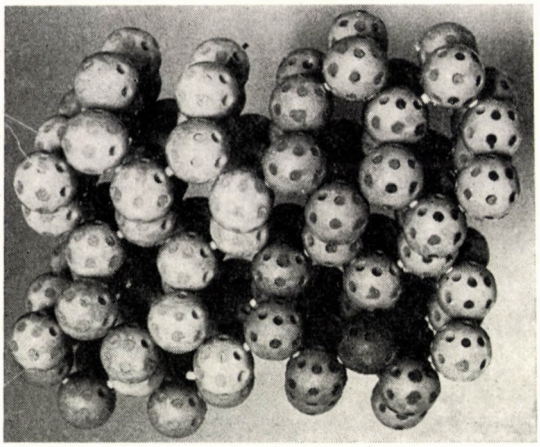

Fig. 2. Volume decrease by cluster adhesion, I. A cluster of 108 molecules (short spikes applied)

The average size of the cluster decreases with increasing temperatures. The clusters attract each other by van der Waals forces acting between the molecules of their adjacent surface layers. In our assumption, the neighbouring clusters are displaced relative to one another on the model of a slip-dislocation in a crystal. In this shifted position the surface layers can get somewhat closer, their molecules mutually filling in the cavities of the adjacent framework. Thus, the packing of the molecules becomes closer in these layers than inside the cluster, resulting in two observable effects:

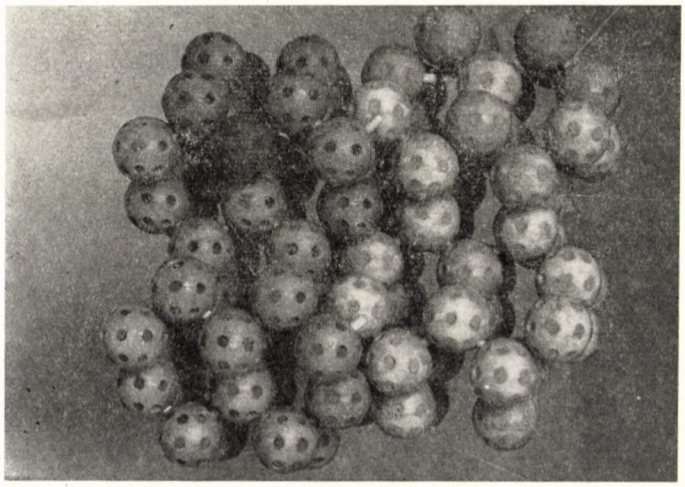

Fig. 3. Volume decrease by cluster adhesion, II. Two adhered clusters with 108 molecules in the aggregate: Volume decrease as compared with Fig. 2.

i) Contraction takes place as illustrated by ball models in Figs 2 and 3 where a cluster consisting of 108 molecules (Fig. 2) is compared with an ensemble of two displaced clusters of 54 molecules (Fig. 3).

ii) There must appear 'extra' (*i.e.* interstitial) pair distances as compared to a regular ice-like network. One of these lies between the first (2.83 Å), and the second (4.3 Å) network distance values.

We may think with reason that the zone of interaction of the clusters where the molecules partly free from hydrogen bonds are concentrated plays an important role in the transport phenomena such as diffusion, viscosity, and proton conductivity as well as in dissociation.

In explaining the volume contraction of H_2O on melting and the existence of interstitial pairs in the liquid, the present model contradicts both interstitial and distorted bond models. In the interstitial models, the coexistence of two phases is assumed, *i.e.* molecules in the ice-like and in the gas-like state (SAMOILOV [7], NARTEN, DANFORD and LEVY [8]) and, on the other hand, according to the distorted bond model (POPLE [9]) all hydrogen bonds of the ice structure are preserved, but their angles must be, on the average, very strongly distorted in order to approach the actual molecule density of water.

2. Some geometrical aspects of the tetragonal lattice

In the present model H positions are not taken into account. Accordingly in the treatment below, lattice points mean always the centers of O atoms — or those of the water molecules regarded as spherically symmetrical.

Table 1 gives a comparison of ice lattices I_h, I_c, and the proposed tetragonal lattice of water. Fig 4. shows a picture of the three cells.

In the following treatment instead of cell dimensions a, and c, we use the O–O distance or H-bond length R, and the O–O–O angle or H-bond angle 2α. The parameters are interconnected through the relationships

$$a = 2R \cdot \sin\alpha, \quad \text{and} \quad c = 4R \cdot \cos\alpha$$

On substituting $\cos\alpha = 1/\sqrt{3}$ (*i.e.* 2α is the tetrahedral central angle) we obtain the cubic cell parameters.

Both lattices I_h, and I_c require the regular tetrahedral symmetry of the pentamer pattern consisting of a central molecule and its four nearest neighbours. Namely one of the bond lines in I_h, and all four in I_c play the role of three-fold symmetry axes which are essential elements of hexagonal and cubic lattices, respectively. The free water molecule exhibits the lower mm2 (C_{2v}) symmetry.

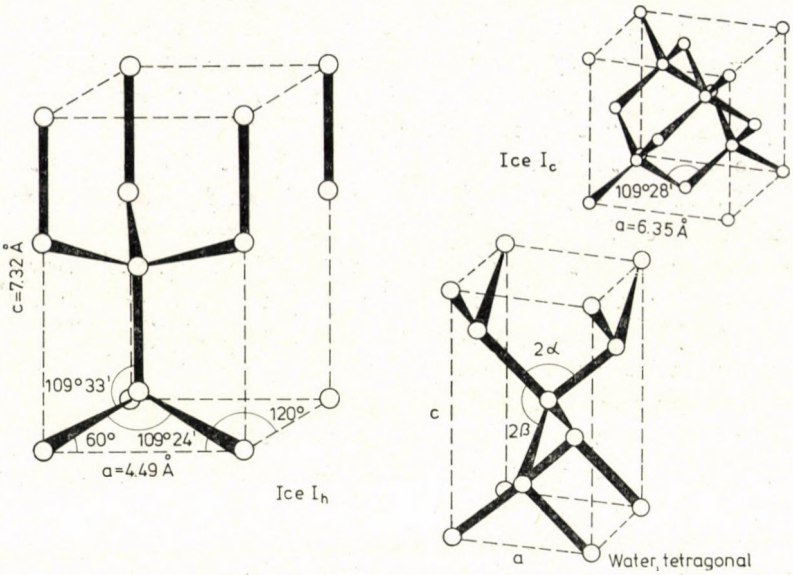

Fig. 4. Unit cells of ices I_h, I_c, and tetragonal water

Table I

Characteristics of the ice lattices I_h, I_c and the tetragonal lattice of water

	I_h	I_c	Tetragonal
Space group	$P6_3/mmc$	$Fd3\ m$	$I\bar{4}2\ d$
a	4.498 Å	6.358 Å	4.235 Å
c	7.328 Å		7.508 Å
	(−130 °C	(−130 °C)	(+4 °C)
R	*2.76 Å, 2.75 Å	2.75 Å	2.83 Å
2α	*109.47° ±0.16	109.47°	97°
$x-y$ angle	60°	90°	90°
V_{cell}	128.4 Å^3	257.02 Å^3	134.7 Å^3
n	4	8	4

* The difference between the two R values and the deviation of 2α are not due to random errors, but to the significant departure of the I_h lattice from the ideal hexagonal symmetry. The shorter R belongs to O–O distances parallel to the c-axis.

The $\widehat{\text{H-O-H}}$ angle is 104,5°, less than the tetrahedral central angle. The proposed tetragonal lattice has a symmetry higher than the molecule following from the neglection of the H atoms and from the assumption that OH. . .$\widehat{\text{O}}$. . . . . .HO angles are equal to O. . .$\widehat{\text{HOH}}$. . .O angles with their planes perpendicular. The four bond-lines meeting in an O center subtend altogether six angles.

Regarding the two bond-types covalent (OH) and H-bond (O. . .H), both angles mentioned above are symmetrical to their bisector, the other four angles (O. . .HO. . .HO) are asymmetrical. If the two former angles are equal with planes perpendicular, then the latter four angles are also equal. Denoting the symmetric angle with 2α, the asymmetric angle with 2β, we find that $\cos\beta = \sin\alpha/\sqrt{2}$. If $\alpha = 48{,}5°$ which value was found by curve fitting (as seen later), then $\beta = 58°$.

The difference between the symmetries of ice I_c and the tetragonal lattice can be characterized as the difference between a regular tetrahedron ($2\alpha = 109{,}47°$) inscribable into a cube and a bisphenoid ($2\alpha \leqslant 109{,}47°$) which can be inscribed into a tetragonal prism.

While the proposed tetragonal lattice can be derived from ice I_c lattice by simple topological transformation equivalent to the bending of the H-bonds, the transformation $I_h \rightleftharpoons$ tetragonal (and similarly $I_c \rightarrow I_h$) requires the instantaneous rupture of every fourth hydrogen bond and their recombination after geometrical rearrangement.

Unlike both ices I_h and I_c, the tetragonal network is compatible with whatever value of the angle 2α which makes the lattice very elastic. The states corresponding to different 2α values can continuously go over in each other by cooperative bond bending. From this geometrical condition it can be concluded that finite tetragonal clusters might perform cooperative intermolecular vibrations of relatively large amplitude, without rupture. Eventually, the Raman band of frequency 60 cm^{-1} (WALRAFEN [3]) can be assigned to such a vibration mode. This type of vibration means simultaneously a density fluctuation of the cluster because the cell volume is a simple single-valued function of angle α (at constant R).

The volumes/molecule, in terms of α and R, are the following. For the ice lattices I_h and I_c:

$$v_h \approx v_c = \frac{8\sqrt{3}}{9} R^3 = 1.5395\, R^3 \text{ Å}^3/\text{molecule} \qquad (1)$$

Here v_h means the volume of an ideal hexagonal cell. In reality, ice I_h deviates from this form by its shorter c-value by about 0.25%. The volume of the tetragonal cell is

$$v_t = 4R^3 \cdot \sin^2\alpha \cdot \cos\alpha = 4R^3(\cos\alpha - \cos^3\alpha) \text{ Å}^3/\text{molecule} \qquad (2)$$

Again, on $\cos\alpha = 1/\sqrt{3}$, $v_t = v_c$. One can easily show that the tetrahedral bond angle is the abscissa of a maximum in the $v_t = f(\cos\alpha)$ function, since

$$\left(\frac{\partial v_t}{\partial \cos\alpha}\right)_{R=\text{const.}} = 4R^3(1 - 3\cos^2\alpha) = 0 \qquad \text{if } \cos\alpha = \frac{1}{\sqrt{3}}$$

and the second derivative is $-24R^3/\sqrt{3} < 0$.

Thus, all possible tetragonal cells (with $2\alpha \leqslant 109.47°$) possess smaller volume, than the cubic or hexagonal cells with identical R values.

The empirical value for 2α is 97° as obtained from a least square fit of the RDF's (see below). The departure of this angle from 109.47° is too small to explain the big jump of density of melting, the more so, since the strong volume-increasing effect of the sudden change in the first neighbour distance from R = 2.75 to 2.83 Å must also be overbalanced. The big volume effect (altogether −17%) can only be explained by the closer packing of clusters as stated above. Nevertheless, the cell volume decrease on bond angle changes is an important feature of the present model. Among others, it points to the mechanism, how pressure promotes melting: under the influence of external mechanical pressure, the molecules of ice I_h get closer to each other by bond bending, rather than by bond breakage or shortening, since bending is energetically more favourable. The hexagonal ice lattice is, however, incompatible with non-tetrahedral bond angles and responds to a greater angle change by breaking up, that is, by melting. With this an even stronger volume decrease takes place, the system obeying thus in two steps the principle of Le Chatelier — Braun.

The assumed elasticity of the tetragonal lattice (together with other possibilities like the shortening of the O–O distance, and the closer packing of the clusters) can explain the compressibility, and other high pressure properties of water deviating from the behaviour of normal liquids. In spite of its greater density, the isothermal compressibility of water is four times greater than that of ice I_h: in the neighbourhood of the melting point we find namely

$$\varkappa_{T,\,\mathrm{water}} = \frac{-1}{V}\left(\frac{\partial V}{\partial p}\right)_T = 50\times 10^{-6}\,\mathrm{bar}^{-1}\,(\mathrm{at}\ 0°\mathrm{C}),\ \text{and}$$

$\varkappa_{T,\,\mathrm{ice}} = 12\times 10^{-6}\,\mathrm{bar}^{-1}\ldots 9\times 10^{-6}\,\mathrm{bar}^{-1}$ in the whole range $0 \geqslant t \geqslant -$ —253° C, respectively.

By partially differentiating eq. (2) we obtain the relative volume changes on varying α and R, respectively:

$$\frac{1}{V}\left(\frac{\partial V}{\partial \alpha}\right)_R = -\sin\alpha\,\frac{1-3\cos^2\alpha}{\cos\alpha-\cos^3\alpha} = 0.0108\,\mathrm{deg}^{-1},\ \text{and}$$

$$\frac{1}{V}\left(\frac{\partial V}{\partial R}\right)_\alpha = \frac{3}{R} = 1.06\ \mathrm{Å}^{-1},$$

the numerical values are obtained by taking $\alpha = 48.5°$, $R = 2.83$ Å. Thus, a bond angle decrease by 1°, and the abbreviation of the H-bond length by 0.01 Å, both correspond to a volume change caused by 220 bar external pressure.

The much smaller compressibility *i.e.* the rigidity of ice I_h may be due to the resistance of this lattice to both bond bending, and bond shortening. The rigidness of this structure is clearly demonstrated by the other fact that I_h does not exist at all under pressures higher than 2.2 kbar. In the temperature range $0 > t > -22°$ C it melts on the influence of a pressure 1 bar $< p \leq 2{,}2$ kbar, and water (supercooled) is produced; at temperatures lower than $-22°$ C, a transformation into ice III(tetragonal) or ice II(rhombohedral) takes place, depending on temperature.

The difference between the topology of the I_h lattice on the one hand and that of the lattices I_c and tetragonal on the other hand, can be illustrated from an other point of view. All three networks are very open structures with a good deal of empty space, but the geometry of the cavities in them is different. In ice I_h, the cavities are formed by 12 surrounding molecules; in ice I_c and the tetragonal lattice, the cavities are formed by 10 molecules. Their configuration is the analogue of that of carbon atoms in the molecule adamantane ($C_{10}H_{16}$). This compound has its condensed homologues diadamantane, triadamantane, etc. containing 14, 18 etc. carbon atoms. Similarly, the number of the cavities in the lattices of ice I_c and water can be augmented by one when properly adding 4 farther molecules. This rule has been utilized in a computer program simulating water clusters and also in building up the ball models (Figs 1—3.). In this way, we obtain clusters with a chamfered shape where each molecule is at least 2-bonded.

In Table II, the radial distances r_i, the coordination numbers C_i, and cell volumes v_h, v_c, v_t are compared for the three lattice types. The trigonometric relationships yielding the r_i's by the aid of R and α are also given. It can be seen that, beginning with the second neighbours, each radial distance in I_c splits up into two distinct values in the tetragonal network.

3. Model calculations, RDF fitting

We have computed the RDF of the model structure by varying its parameters to yield an optimal fit to the experimental function. The agreement of the RDF's is considered as a necessary, though not sufficient evidence for the adequacy of the model. Recently, S. N. BAGCHI has outlined a cluster theory of liquids and suggested a method for calculating the model RDF that seems to increase the probative force of a successful fit [10]. BAGCHI's procedure had to be modified in some respects because of the anomalous features of water. (Details are described in the Appendix of this paper.)

We have chosen the pair correlation function $g(r)$ as the object of the fitting procedure. The resolution of peaks is the sharpest and the sensitiveness to errors in the model parameters is the highest in this function as compared

Table II

Radial distances, coordination numbers and specific volumes of the lattices ice I_h, I_c and tetragonal water
(Expressions in terms of the bond length and the half bond angle, R, α)

a) Distances and coordination numbers

	I_h*		I_c		Tetragonal	
	$\cos\alpha = 1/\sqrt{3}$ $\sin\alpha = \sqrt{2/3}$				$\cos\alpha = 0.6633$ $\sin\alpha = 0.7483$	
i	r_i/R	C_i	r_i/R	C_i	r_i/R	C_i
1	1	4	1	4	1	4
2	$\sqrt{8/3} = 1.633$	12	$\sqrt{8/3} = 1.633$	12	$2 \sin \alpha = 1.497$	4
3	$5/3 = 1.667$	1	$\sqrt{11/3} = 1.915$	12	$\sqrt{2 + 2\cos^2\alpha} = 1.697$	8
4	$\sqrt{11/3} = 1.915$	9	$4/\sqrt{3} = 2.309$	6	$\sqrt{1 + 4\sin^2\alpha} = 1.800$	8
5	$4/\sqrt{3} = 2.309$	3	$\sqrt{19/3} = 2.516$	12	$\sqrt{8}\sin\alpha = 2.117$	4
6	$7/3 = 2.333$	9			$\sqrt{1 + 8\cos^2\alpha} = 2.126$	4
7	$\sqrt{19/3} = 2.516$	9			$\sqrt{1 + 8\sin^2\alpha} = 2.341$	4
8					$\sqrt{5 + 4\cos^2\alpha} = 2.600$	8
9					$4\cos\alpha = 2.654$	2

b) Volumes per molecule

v/R^3	v/R^3	v/R^3
$\frac{8\sqrt{3}}{9} = 1.5395$	$\frac{8\sqrt{3}}{9} = 1.5395$	$4\cos\alpha \cdot \sin^2\alpha = 1.486$

$v_h = 32.36$ Å^3/molecule $= v_c$
$\approx v_{\text{ice, exp}}$ $(R = 2.76$ Å$)$

$(R = 2.83$ Å$)$
$v_t = 33.68$ Å^3/molecule
$v_{\text{water, exp}} = 29.95$ Å^3/molecule
$\Delta v = 3.73$ Å^3/molecule

* I_h data are valid for the ideal hexagonal lattice.

to other expressions of the radial distribution (as *e.g.* $D(r) = 4\pi\,\varrho_0 r^2 g(r)$). The goodness of the fit has also been checked in the $D(r)$ as well in the $si(s)M(s)$ functions. The analytical form of the model pair correlation function is the following:

$$g(r) = g_d(r) + g_c(r) \tag{3}$$

where $g_d(r)$ is the sum of contributions furnished by distinct pair separations r_i, according to the relationship:

$$g_d(r) = \sum_i C_i [(32\pi^3)^{1/2}\varrho_0 l_i r_i r]^{-1} \times \left\{\exp\left[-\frac{(r_i - r)^2}{2l_i^2}\right] - \exp\left[-\frac{(r_i + r)^2}{2l_i^2}\right]\right\} \tag{4}$$

and $g_c(r)$ is a term describing the transition between the range of discrete pair distances, and that of the structureless, continuous distribution where $g(r) \equiv 1$. For this term, we have chosen the half side of a Gaussian

$$g_c(r) = \exp\left[-\frac{(r_c - r)^2}{2l_c^2}\right], r \leq r_c \tag{5}$$

$$g_c(r) = 1, \qquad r > r_c$$

The parameters varied were the discrete distances r_i, the corresponding coordination numbers C_i, the m.s. vibration amplitudes l_i^2, the radius of the structureless sphere r_c, and the m.s. vibration amplitude of this radius l_c^2. In eq.(4), ϱ_0 denotes the molecule number density of water, $\varrho_0 = 0.0334$ at 4° C. In the final run the number of discrete distances was 9 and the total number of parameters 29.

The fitting procedure was performed in two steps. 1) In a preliminary trial and error process, the values R, α and r_8, that is the H-bond length, the H-bond angle, and the first observable interstitial pair distance ($r_8 \sim$ $\sim$ 3.6 Å), respectively, had been established for the three temperatures and then fixed. As only the first 7 distances were taken from the network, r_8 and r_9 included in least squares fitting denote inter-cluster distances. (They are not identical with r_8 and r_9 in Table II.)The trials for R, α, r_8 were based on the first four peak positions in the experimental $g(r)$. The optimal values that yielded the best results in the following least squares procedure, could mostly be found at once.

Together with R, α, and r_8, also the pair separations r_1 through r_7 were fixed, since they are defined by R, α and the trigonometric relationships of Table II. In the final runs of the fitting program an additional interstitial distance $r_9 \sim 5.3$ Å was involved which has improved the fits as compared with the previous runs with 8 distances. The introduction of the two interstitial distances r_8 and r_9 by a voluntary and empirical way, could be justified later on by computer simulation of assemblies of clusters (see below).

2) The 9 distinct r_i values having been fixed, the least squares procedure was performed with 20 parameters (9 coordination numbers C_i and m.s. vibration amplitudes l_i^2, r_c, and l_c^2), by fitting $g(r)$ values over the range $2.5 \leq$ $\leq r \leq 8$ Å at intervals of $\Delta r = 0.05$ Å. The range below 2.5 Å in the experimental curve contains O-H peaks, not considered in the present model. Above 8 Å the structure was neglected, the distribution assumed to be perfectly disordered. Table III shows the values of 29 parameters and the standard deviations of the fits (σ) for the three temperatures. The goodness of the fits is illustrated also by the Figs 5, 6, 7.

A remark must be made as to the reliability of the parameters. It is known that the expansion of an arbitrary function in Gaussians is not unambiguous. In the course of our least squares calculations, we experienced that the fit was extremely sensitive for variations in the peak positions, *i.e.*, the values of R, α, r_8. The sharp optimum of these parameters seems to support the adequacy of the geometry. On the other hand, a comparatively wide range of the parameters C_i, and l_i^2 could yield the same least squares sum. Thus,

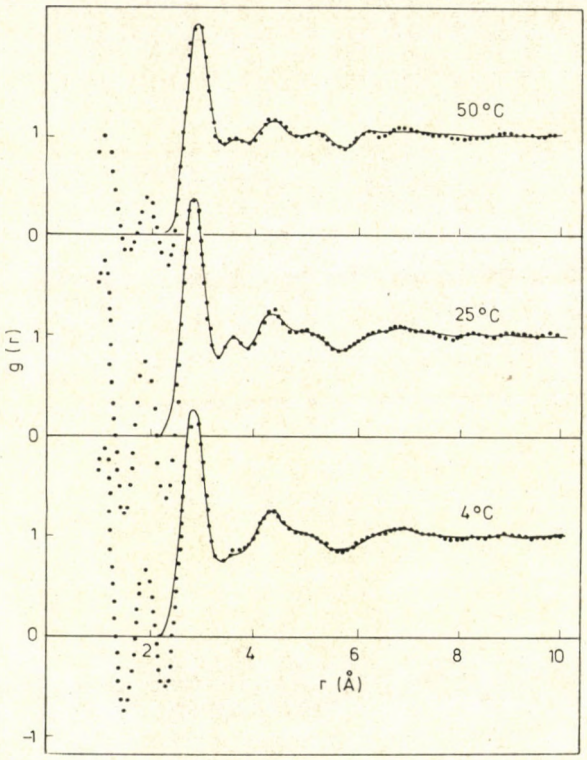

Fig. 5. Pair correlation functions $g(r)$ of water at 4°, 25° and 50 °C, respectively. Full line (—) is the best fit calculated from the model. Dots (. . .) show the experimental curves of the author and colleagues

the first decimals of the C_i values and the second decimals in the l_i^2's are not quite reliable, which accounts for some of the seemingly illogical deviations in Table III between 4° and 25° data. The differences between the values for 50° C and the first two data sets seem to be above the limits of error.

A deficiency of the above parameter set is that none of these parameters define explicitly the sizes of the clusters. Indirect indications, however, can be read out of these data which support the cluster hypothesis and the assumption on the temperature dependence of the clusters. The following data are worth mentioning.

Table III

Parameters of the model g(r) function for 4°, 25° and 50 °C

i	4°			25°			50°		
	r_i Å	C_i	l_i Å	r_i Å	C_i	l_i Å	r_i Å	C_i	l_i Å
1	2.83	3.76	0.21	2.83	3.93	0.20	2.86	3.45	0.21
2	4.24	3.13	0.26	4.24	3.18	0.26	4.28	2.40	0.24
3	4.80	6.22	0.47	4.80	6.51	0.43	4.85	6.15	0.43
4	5.09	5.88	0.64	5.09	5.87	0.67	5.15	5.93	0.65
5	5.99	2.71	0.49	5.99	3.18	0.37	6.05	2.88	0.36
6	6.02	2.46	0.44	6.02	2.82	0.48	6.08	2.81	0.44
7	6.62	1.30	0.89	6.62	1.25	0.85	6.70	1.05	1.11
8	3.56	3.43	0.35	3.56	3.27	0.28	3.60	4.81	0.40
9	5.30	1.99	0.51	5.30	1.34	0.24	5.34	1.20	0.21
r_c	6.95			6.96			7.09		
l_c			0.73			0.71			0.85
σ		0.023			0.023			0.022	

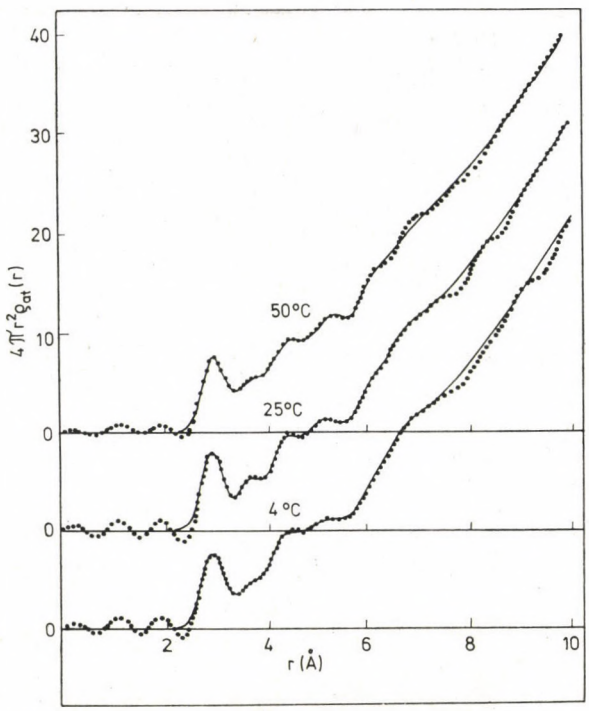

Fig. 6. Radial density functions $D(r) = 4\pi\varrho_0 r^2 g(r)$ of water. Notation is the same as in Fig. 5

i) The radius r_c of the sphere of continuous, structureless distribution is about 7 Å. This value must not be considered as the radius of the cluster because the loss of correlation between distant particles is a general feature of amorphous systems. The correlation length, and the average edge length of the clusters must be distinguished (BAGCHI [10]). The value $2r_c \sim 14$ Å may be regarded only as a rough lower limit for the cluster dimensions.

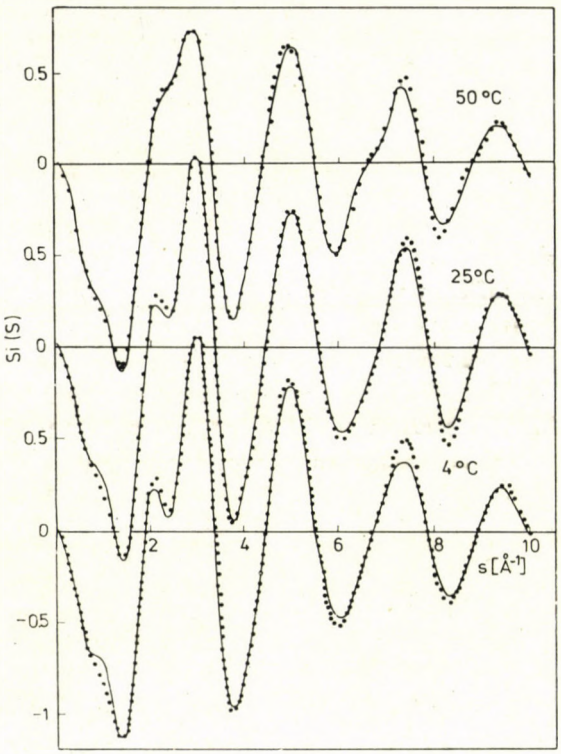

Fig. 7. Reduced intensity functions (multiplied by s) of water, $si(s) = 4\pi\varrho_0 \int_0^{I_m} r[g(r)-1] \times \sin(sr)dr$. Notation is the same as in Figs 5 and 6. (In the intramolecular range $0 \leq r \leq 2$ Å, $g(r)$ made equal to 0.)

ii) The coordination number C_8 pertaining to the first observable 'interstitial' *i.e.* non-H-bonded pair distance ~ 3.56 Å is a measure of the specific surface of the clusters because the molecules in the interior of the clusters are excluded from this type of interaction. Table III shows a significant rise of C_8 between 25°, and 50° C, in accordance with the assumption on cluster size decrease with rising temperature.

iii) The effective coordination numbers C_2 to C_7 pertain to pair distances in the network. Their values related to the corresponding coordination number

in the infinite lattice show a monotonic decrease with growing r. The decrease of the quotients $C_{i,\text{eff}}/C_{i,\infty}$ (where $C_{i,\infty}$ denotes the value of C_i in the infinite lattice) is the consequence of finite cluster dimensions. The mean density of water, however, cannot be reconciled with the loss of distant neighbours. In our model they are supplied by the term $g_c(r)$. This can be regarded as the common envelopping curve of all distances between 5.5 and 7 Å the residual preference of some distances appearing as small ripples on it.

iv) An indirect but strong evidence for the clusters in the sense used in this model, is the volume change on melting. The difference between the specific cell volume and the actual specific volume of water slowly increases with rising temperature. Starting from these differences a more detailed estimation can be given for cluster dimensions. (See below.)

The first coordination number C_1 behaves differently from $C_2 \ldots C_7$ as it is very close to the ideal figure 4, and hardly depends on temperature. This fact seems to speak against the cluster hypothesis which demands the collective breaking of a significant part of the H-bonds. This contradiction between experience and hypothesis can be resolved. In agreement with WERES and RICE [11], we assume that not only H-bonds, but also van der Waals interactions have a potential energy minimum at an O–O pair distance of about 2.9 Å. Accordingly, the majority of broken H-bonds seems to be replaced immediately in the distance statistics by van der Waals interactions of similar length. The main difference between H-bond and the shortest van der Waals bond is, thus not in their length, but in their orientations which is, however, not to be observed in the RDF's. It follows from this that the peak at 3.6 Å represents the second nearest van der Waals pairs, not the nearest ones. The reality of the supposition on the existence of first, second, third, etc. not H-bonded neighbours as well as the composition of C_1 of an intra-cluster and an inter-cluster component, could be supported by the computer simulation of cluster assemblies.

By the aid of an integral test, one can make sure whether the above parameters of molecular distribution reproduce the bulk density. According to a known relationship

$$4\pi\varrho_0 \cdot \int_0^\infty (g(r) - 1)r^2\,dr = kT\varrho_0\varkappa - 1$$

where k is the Boltzmann constant, T the absolute temperature, $\varkappa$ the isothermal compressibility of the liquid.

The infinite upper limit may be replaced by a finite one ($r_m \geq r_c$), since our assumed $g(r) \equiv 1$ if $r \geq r_c$. The finite integral can be expressed by, and computed from, the 29 parameters of eqs (3, 4, 5). The values obtained are the following: -0.623 (at 4°), -0.486 (at 25°), -0.261 (at 50°). The deviation

from the expected value is 0.3. . .0.7 which means a relative error of about 1%, since the total number of molecules within the sphere of radius r_c amounts to 50.

4. Estimation for cluster dimensions from the volume effect

To make an estimation for cluster dimensions, we start from the volume effect, *i.e.* from the difference between the cell volume calculated from the corresponding lattice parameters, and the empirical specific volume of water, because this is the most pregnant effect which directly depends on cluster sizes, more precisely on the specific surface area of the clusters. As it will be clear below, we must adopt several simplifying assumptions and estimative values for some intermediate numerical quantities, so, we are not speaking of a calculation but only of an estimation of cluster sizes.

The molecular volume of the tetragonal cell is calculated according to the formula: $v_t = 1.486\ R^3$ Å^3 assuming that the $\widehat{\text{O-O-O}}$ angle remains 97°, independently of temperature. Table IV shows the volume effects in the range $4° \leq t \leq 100°$ C. The R values for 4°, 25° and 50° C were taken from own results, that for 100° C is an extrapolated figure with regard to the Oak Ridge data.

Table IV

Some parameter values of the tetragonal lattice of water at different temperatures

Parameter	Temperature (centigrade)			
	4°	25°	50°	100°
R Å	2.83	2.84	2.86	2.90
v_t Å /molecule	33.68	34.04	34.76	36.24
$\varrho_t = v_t^{-1}$ Å^{-3}	0.02969	0.02938	0.02877	0.02759
v_{exp} Å^3	29.95	30.02	30.25	31.13
ϱ_{exp} Å^{-3}	0.0334	0.0333	0.0331	0.0321
$v_t - v_{exp}$ Å^3	3.73	4.02	4.51	5.11

According to the present model, the tetragonal clusters adhere to each other in such a way that the molecules in the contacting surface layers are more closely packed than in the interior of the clusters. Denoting the particle density in the lattice by $\varrho_t = 1/v_t$ Å^{-3}, we can express the density in the adhering layers by giving a multiplicative factor: $\varrho_i = q \cdot \varrho_t$ where ϱ_i denotes the interstitial or intercluster density, $q \sim 1.5$ seems very probable. We use below this value with the remark that a deviation from this figure would though change all other numerical values too, but not the tendencies of the parameters.

Let us divide in thought the volume of the liquid in two components: part V_t is filled out by the tetragonal lattice of density ϱ_t (molecule volume v_t), and the inter-cluster part $V_i = v - V_t$, filled out by the surface layers of density $\varrho_i(= 1/v_i)$, v denoting the actual molecule volume of water. The following equations are valid:

$$\varrho_t V_t + q\varrho_t(v - V_t) = 1, \quad \text{or} \quad \varrho_t\left[\frac{V_t}{v} + \mathrm{q}\,1 - \frac{V_t}{v}\right] = \frac{1}{V} = \varrho$$

where ϱ means the empirical particle density of water. $\frac{V_t}{v}$ and $\frac{V_i}{v}$ can be expressed from these as :

$$\frac{V_t}{v} = \frac{q - v_t/v}{q - 1} \quad \text{and} \quad \frac{V_i}{v} = 1 - \frac{V_t}{v} = \frac{v_t/v - 1}{q - 1}$$

So, we obtain the partial quantities for the two kinds of volume, (Table V). Below, we shall need the quotient $V_i/V_t = \dfrac{v_t/v - 1}{q - v_t/v}$ too, so, this value is also figuring in the Table.

The partition of the water molecules differs naturally from this proportion, since the particle densities in V_i and V_t are different. The molar ratio of the molecules within the interior of the clusters, μ_t and that of the molecules in the surface layers, μ_i are furnished by the following relationships:

$$\mu_i = \frac{1}{1 + qV_i/V_t} \quad \mu_i = 1 - \mu_t = \frac{1}{\dfrac{V_t}{qV_i} + 1}$$

These values are also given in Table V.

μ_t and μ_i are closely related to the fraction of broken hydrogen bonds. According to our somewhat simplifying assumptions, the surface molecules take part instead of 4, in 3 or 2 H-bonds (*i.e.* we neglect one-bonded species) which means that 1 or 2 bonds of these molecules had been broken during the formation of the cluster. Simulated models have shown that the occurrence of 3- and 2-bonded molecules is not equal, but their ratio can be taken with good approximation as 2 : 1, and so, the average number of broken H-bonds per molecule is 1.333. Thus, finally we obtain for the fraction of broken H-bonds p_b:

$$p_b = \frac{1{,}333\,\mu_i}{4} = 0{,}333\,\mu_i$$

The p_b values for the four temperatures are also given in Table V. These figures are very close to our other estimation made on the basis of the effective first coordination number of the cluster (see below).

Our next step is the calculation of the average sizes (diameter or edge length) of the clusters. To be able to do this, further simplifying assumptions must be adopted. Although the above parameters implicitly include the specific surface area of the clusters, the dimensions of a body corresponding to such a value, depend also on the shape of the body. Let us therefore assume that the average tetragonal cluster exhibits approximately the shape of a cube, the surface layers being monomolecular on the faces of the cube. We take the area of these monomolecular layers as being equal to the area of the faces of

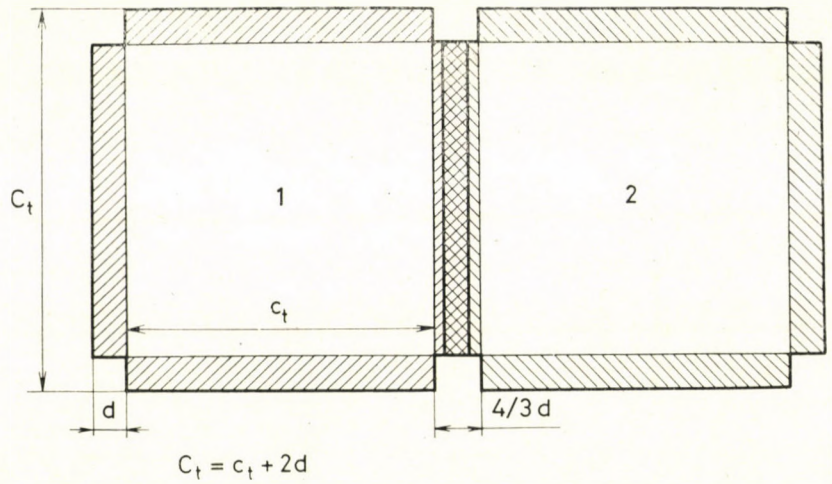

Fig. 8. Scheme of the contact with interpenetration between two clusters (cross-section)

the inner cube, *i.e.* the edges and the corners of the outer cube are omitted. Although this assumption seems unnatural, it corresponds to our previous assumption on the chamfered shape of the clusters, not containing 1-bonded molecules. The simplified cluster shape is illustrated by Fig. 8.

To calculate the edge length c_t of the cube with tetragonal lattice density, one needs one more datum, the effective thickness of the contacting layers, denoted by d^*. The thickness of a monomolecular layer of the tetragonal lattice can be taken as $d = 2.15$ Å and the thickness of two interpenetrating layers — taking into account the assumed density ratio of the pure network and the common layers, $\varrho_i/\varrho_t = 1.5$ — must be 4/3 times greater as the value mentioned, $d^* = 1.333 \times 2.15 = 2.86$ Å. Using these notations and the numerical values, the edge length c_t of the cube with purely tetragonal lattice structure, can be determined from the following equation:

$$\frac{V_i}{V_t} = \frac{3c_t^2 d^*}{c_t^3} = \frac{3d^*}{c_t}, \quad \text{and so, } c_t = 3d\frac{V_t}{V_t}$$

The total edge length of a cluster, C_t, is obtained by adding to c_t twice the thickness of the monomolecular layer, 4.3 Å (neglecting the temperature dependence of this value).

$$C_t = c_t + 4.3 \text{ Å}$$

According to the above, in Table V the lengths C_t, and the average cluster volumes V_c are given where $V_c = c_t^3 + 6\ c_t^2\ d$. The number of molecules in the average cluster is naturally given as $N_c = V_c\ \varrho_t$.

Let us call attention to the following features of the data sets of Table V making also use of similar data sets not presented here, based on different values of $q = \varrho_i/\varrho_t$.

Table V

Parameters of the tetragonal clusters of water at different temperatures ($\varrho_i/\varrho_t = q = 1.5$)

Parameter	4°	25°	50°	100°
V_i/v	0.248	0.268	0.300	0.328
V_t/v	0.752	0.732	0.700	0.672
V_i/V_t	0.330	0.366	0.428	0.488
μ_i	0.33	0.35	0.39	0.42
μ_t	0.67	0.65	0.61	0.58
p_b	0.111	0.116	0.13	0.14
C_t Å	30.3	27.7	24.3	21.9
V_c Å^3	26300	19900	13160	9500
N_c	780	585	380	265

All data pertaining to cluster sizes strongly depend on the value of q. For a given q, several calculated parameters seem to depend weakly on temperature. These are V_t/v, V_i/v, μ_t, μ_i, p_b. In spite of this fact, the final geometrical characteristics of the clusters, C_t, V_c, and N_c change very markedly in the temperature range investigated. This is due to the fact that the latter variables depend on the ratio of two, slowly but oppositely changing quantities, namely on V_t/V_i. The moderate variation of the fraction of broken H-bonds, p_b between 4° and 100° C, is in accordance with the results of the spectroscopic studies of LUCK [4] and of WALRAFEN [3].

From the point of view of justificating the present model, the fact that relatively small changes in the fraction of broken H-bonds involve well-marked variations in cluster dimensions within the temperature range 4 – 100° C, seems important. The latter phenomenon can serve as the starting point for the explanation of properties possessing strong temperature dependence like surface energy, diffusion, viscosity, etc.

5. Modelling of clusters and cluster assemblies

In order to complete our knowledge about the properties of the clusters and their assemblies, we tried to gain some additional pieces of information from simulated models.

5.1. Ball models. A set of drilled balls allowed building up tetragonal network fragments with a bond angle 90° which is not far from the empirical 97° . (The accurate value is irrelevant for the topology of the network.) The

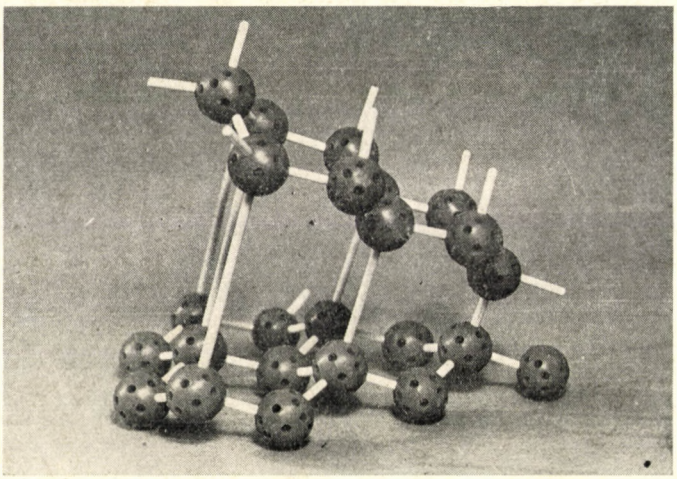

Fig. 9. The model of the moment of melting: lattice is destroyed when topology of ice I_h is combined with non-tetrahedral bond angles

use of longer spikes allows observing the adamantane-like cages and counting the number of 4-,3-,2-bonded molecules in a cluster of given shape and size (Fig. 1). A similar model could demonstrate the incompatibility of the hexagonal mirror-symmetric arrangement with non-tetrahedral bond angles. Fig. 9 can be regarded in this sense as the illustration for the moment of melting: the planes of puckered rings cannot be parallel when the bond angle is not tetrahedral and the topology of ice I_h is preserved. After rotating the planes by 60° relative to each other, they get parallel and can form a new lattice (the tetragonal one).

In an other set of ball models, we let the balls touch each other. These models give a picture of the possible dislocations between two or more clusters and allow an estimation about the volume decrease by the adhesion of the clusters (Figs 2 and 3). In this example with two clusters of 54 molecules the volume effect amounts to -10% which must be multiplied by 3 when a system of clusters is assumed to be repeated infinitely in three dimensions.

Since −30% is nearly double of the empirical −17%, either the average cluster sizes can be taken higher, or a lower efficiency of the packing of clusters may be assumed.

5.2. Computer simulated models

With the help of a special program, tetragonal clusters with arbitrary shape and size as well as aggregates of equal clusters with arbitrary displacements could be modelled on the computer. Clusters containing 54 to 712 molecules and assemblies consisting of 2 to 9 identical clusters have been computed. The computed clusters of 54 molecules have the same configuration as those seen in Figs 1 and 3. The larger ones (259, 388 and 712 molecules) roughly approach the estimated values for 100, 50, and 4° C, given above (Table V). Displacement vectors between two clusters were chosen by trials based on visual observation of the ball models. The output of the program consists of a list of the coordinates of all latice sites (and the number of their first neighbours in addition), the list of the occurring pair distances, their frequencies and the average coordination numbers (for distances below 10 Å), and the total number of points with 1, 2, 3, 4 and 5 neighbours. Table VI shows the list of coordination numbers for clusters with different sizes. From the effective first coordination number C_1 of a cluster the number and fraction of broken bonds can easily be calculated. Denoting the number of molecules in the cluster by N, the number of broken bonds r_b and their fraction p_b can be obtained as

$$r_b = (4 - C_1) \cdot N, \text{ and } p_b = 1 - \frac{C_1}{4}.$$

For example, $C_1 = 3.50$ yields $p_b = 0.15$, a figure near to the values given by LUCK [4] from infrared band intensities and to those by HAGGIS *et al.* (HASTED [3, 4]) interpreting dielectric properties. The numbers and the temperature dependence of the numbers of 4-, 3- and 2-bonded molecules can also be compared between the present work and that of HAGGIS *et al.*

By comparing the radial distances of different aggregates with those of the single cluster, we can form a notion of the effect of cluster aggregation on the RDF. Table VII shows the changes in the distance statistics for assemblies made from different clusters. Two important facts can be read from Table VII.

i) The effective coordination numbers — especially C_1 — are greater in the aggregate than in the single cluster, so that by extrapolating the figures to a complete system of clusters (where each cluster is surrounded by others), we obtain $C_1 \gtrsim 4$. Thus, our explanation for the apparent constancy of C_1 — given in §3 above, seems to be justified.

ii) The distance spectrum of an aggregate contains new items, *i.e.* interstitial pair distances, dispersed among the network values in the whole

Table VI

Pair distances and coordination numbers in simulated tetragonal clusters of different size

		Number of molecules in the cluster									
		10(1)		54(2)		259(3)		388(4)		712(5)	
i	r_i Å	C_i	$C_i/C_{i\infty}$	C_i	$C_i/C_{i\infty}$	C_i	$C_i/C_{i\infty}$	C_i	$C_i/C_{i\infty}$	C_i	$C_i/C_{i\infty}$
1	2.83	2.4	0.60	2.96	0.74	3.34	0.835	3.40	0.85	3.50	0.875
2	4.25	1.2	0.30	2.37	0.59	3.10	0.78	3.27	0.82	3.38	0.85
3	4.82	2.4	0.30	4.15	0.52	5.44	0.68	5.67	0.71	6.07	0.76
4	5.11	1.6	0.20	3.55	0.44	5.19	0.64	5.57	0.70	5.93	0.74
5	5.99	1.2	0.15	3.48	0.43	5.13	0.64	5.45	0.68	5.85	0.74
6	6.01										
7	6.64	—	—	1.48	0.37	2.50	0.62	2.72	0.68	2.92	0.73
8	7.38	—	—	2.37	0.34	4.20	0.52	4.54	0.56	5.12	0.64
9	7.54	0.2	0.1	1.07	0.50	1.37	0.68	1.38	0.69	1.52	0.76
p_b		0.4		0.26		0.166		0.149		0.123	

(1) The configuration of this cluster is similar to that of adamantane
(2) One repetition of the adamantane cell in 3 perpendicular directions
(3) Corresponds approximately to water about 100 °C (Table V.)
(4) Corresponds approximately to water about 50 °C (Table V.)
(5) Corresponds approximately to water about 4 °C (Table V.)

Table VII

Pair distances and coordination numbers in simulated cluster assemblies as functions of cluster dimensions

(C_i: coordination numbers; ΔC_i: increment of C_i compared to the single cluster)

	Number of molecules in the cluster							
	54		259		388		712	
r_i Å	C_i	ΔC_i	C_i	ΔC_i	C_i	ΔC_i	C_i	ΔC_i
2.83—2.92	3.70	0.74	4.00	0.66	4.00	0.60	4.00	0.50
3.25—3.85	6.70	6.70	4.79	4.79	4.14	4.14	3.22	3.22
4.25	3.11	0.74	3.38	0.18	3.50	0.23	3.45	0.07
4.82	4.15	0.00	5.43	0.00	5.67	0.00	6.07	0.00
5.05—5.12	6.32	2.82	6.30	1.10	6.53	0.96	6.51	0.58
5.40—5.70	6.15	6.15	5.69	5.69	4.96	4.96	4.38	4.38
5.95—6.05	9.26	5.78	6.30	1.17	6.70	1.25	7.03	1.18
6.20—6.40	9.25	9.25	3.76	3.76	3.07	3.07	2.45	2.45
6.55—6.65	5.26	3.78	4.69	2.19	4.89	2.17	4.55	1.63
6.80—7.26	10.22	10.22	5.96	5.96	5.25	5.25	3.60	3.60
7.33—7.38	6.88	4.51	8.80	4.60	9.64	5.10	8.41	3.29
7.47—7.54	7.81	6.74	6.69	5.32	5.89	4.51	4.74	3.22
etc.								

r-range investigated. Thus our assumption that cluster aggregation fills up the large gaps in the distance spectrum of ice-like network, could also be verified. Interstitial distances are present in the intervals $3 \leq r \leq 4$, and $5 \leq \leq r \leq 6$ Å, and so on (but none between 3.9 and 5.1 Å). The out-of-lattice distances figuring in our fitted RDF's ($r_8 \sim 3.6$, $r_9 \sim 5.4$ Å), correspond to the weighted averages within the two groups mentioned.

Arguments for the physical reality of the model as well as the analysis of the formation of some ice polymorphs, the structure of supercooled water, and the melting of ice I_h will be presented in a following paper.

Appendix

Deviations of the applied $g(r)$ fit from Bagchi's original method.

In the theory of liquid structures, and the RDF fitting procedure suggested by S. N. BAGCHI [10], the interatomic distances in (atomic) liquids are not free variables, they are (in a first approximation) taken from the crystalline state of the substance at 0 K. The mean square vibration amplitudes are supposed to vary linearly with the number of convolutions by which the i'th atom is reached from the origin using uncorrelated fundamental lattice vectors. Bagchi has successfully applied his method to liquid metals and argon by taking into account 10—12 discrete pair distances. BAGCHI's formula for the pair correlation function is as follows:

$$g(r) = \sum_{i=1}^{p} C_i[(4\pi)^{3/2} m_i^{1/2} b \varrho_0 r_i r]^{-1} \times \left[\exp\left(-\frac{(r-r_i)^2}{m_i b^2}\right) - \exp\left(-\frac{(r+r_i)^2}{m_i b^2}\right)\right]$$

where the m_i's are integers denoting the number of convolutions as mentioned above, b^2 is the m.s. amplitude of the first neighbours' distance.

Some modifications introduced by us in this expression can be justified by the molecular structure and the anomalous features of water. The following modifications should be mentioned:

i) None of the known ice polymorphs offered itself as the starting structure at 0 K, the more so, since in both ices I_h and I_c the O–O distance is round 2.75 Å which suffers a sudden change to 2.83 Å on fusion. No such change takes place in the case of normal substances.

The missing structure has been replaced by the tetragonal lattice described above, which had been found out in a heuristic way. We have seen nevertheless that this lattice is actually a generalized form of ice I_c, a structure existing at low temperatures.

ii) Beside the radial distances derived from the tetragonal lattice, two additional interstitial distances had to be introduced in the $g(r)$. In summary we may state that owing to the very open character of ice and water structures,

the packing of molecules becomes closer in the disordered (liquid) state than it is in the ordered (solid) forms. Normal substances behave just the other way.

iii) As described in the text, the series of contributions of discrete distances had to be terminated with a continuous term. We were led to this point by experience. In the course of our fitting computations we have found namely that increasing the number of discrete terms in eq. (3) (*e.g.*, taking 11 distances instead of 7) did not improve the fit, and what is worse, the parameter values and their dependence on r became physically inconsistent (*e.g.* negative coordination numbers, etc.). We could attribute this behaviour of the model to the existence and adhesion of clusters giving rise to a whole series of interstitial pairs. Whereas the introduction of two discrete items (3.6, 5.4 Å) has explicitly solved this problem in the range $r < 6$ Å, all the interstitial distances above 6 Å could be expressed by the single Gaussian term which acts as the envelopping curve of all distances in the range $6 \text{ Å} < r \leq r_c \approx 7$ Å. The omission of this term affects especially strikingly the reduced intensity function of the model within the range $1 < s < 3 \text{ Å}^{-1}$.

It is also understandable that for normal atomic liquids deriving from a close-packed or nearly close packed crystalline lattice, the distance spectrum of the lattice is sufficiently dense and complete, so that the overlapping broad Gaussian-like terms can reproduce the $g(r)$ even in the high r-range. In this case the use of the somewhat arbitrary continuous term is not necessary.

iv) We had to vary the mean square amplitudes l_i^2 independently, since BAGCHI's rule on their linear increase with the vectorial distance from the origin proved to be inoperative for water. Although this rule makes an essential feature of BAGCHI's general liquid model, the deviation of the RDF of water from the rule is explicable by the nature of the H-bond. The intermolecular vibrations of the H-bonded molecules are certainly not isotropic, their amplitude in the direction of the bond (stretching) must be smaller than in the perpendicular directions (bending). The existence of H-bonded neighbours within, and van der Waals bonded neighbours on the surfaces of the clusters, means that the vibration amplitudes cannot be ordered into a single monotonic series. We must note, however, that BAGCHI allowed the variation of the discrete radial distances in the second approximation whereas in our fitted RDF's the distances are never varied after having been defined by the H-bond length, the bond angle, and the geometry of the tetragonal lattice. This fact strongly supports the quasicrystalline nature of the clusters in water.

*

The author wishes to thank Prof. G. SCHAY and Prof. S. LENGYEL for their careful and critical discussing the manuscript and Prof. S. N. BAGCHI for his remarks and encouraging discussions during his stay in Budapest; Mr. G. PÁLINKÁS and Mr. T. RADNAI are gratefully thanked for their assistance, especially in adapting the necessary computer programs. Acknowledgements are due to Mrs. É. JABLÁNCZY for revising the English text, to Mrs. M. LUKÁCSY Mrs. M. BERCELI, and Mr. I. TARLÓS for their technical assistance.

REFERENCES

[1] HAJDU, F., LENGYEL, S., PÁLINKÁS, G.: J. of Appl. Cryst., **9**, 134 (1976)
[1a] HAJDU, F., LENGYEL, S., PÁLINKÁS, G.: Acta Chimica (Budapest). **91** (3), 273 (1976)
[2] EISENBERG, D., KAUZMANN, W.: The Structure and Properties of Water (1969) Oxford, Clarendon Press
[3] FRANKS, F. (editor): Water. A Comprehensive Treatise Vol. I. The Physics and Physical Chemistry of Water, Plenum Press, New York—London (1972)
[4] LUCK, W. A. P. (editor): The Structure of Water and Aqueous Solutions, Verlag Chemie-Physik Verlag, Weinheim (1974)
[5] ERDEY-GRÚZ, T.: Transport Phenomena in Aqueous Solutions, Akadémiai Kiadó, Budapest (1974)
[6] FLETCHER, N. H.: The Chemical Physics of Ice, Cambridge University Press (1970)
[7] Самойлов, О. Я.: Структура водных растворов электролитов и гидратация ионов — Издательство АН СССР, Москва (1957)
[8] NARTEN, A. H., DANFORD, M. D., LEVY, H. A.: Disc. Faraday Soc., **43**, 97 (1967)
[9] POPLE, J. A.: Proc. Roy. Soc., A **205**, 163 (1951)
[10] BAGCHI, S. N.: Acta Cryst., A **28**, 560 (1972)
[11] WERES, O., RICE, S. A.: J. Am. Chem. Soc., **94**, 26, 8983 (1972)
[12] FRANK, H. S., WEN, W. Y.: Disc. Faraday Soc., **24**, 133 (1957)
[13] DEL BENE, J., POPLE, J. A.: J. Chem. Phys., **52**, 4858 (1972)

Ferenc HAJDU H-1088 Budapest, Puskin u. 11—13.

Acta Chimica Academiae Scientiarum Hungaricae, Tomus 93 (3—4), pp. 395—401 (1977)

POLYATOMIC CATIONS OF SELENIUM IN CHLOROSULFURIC ACID

S. A. A. ZAIDI, Z. A. SIDDIQI and N. A. ANSARI

(Division of Inorganic Chemistry, Department of Chemistry, Aligarh Muslim University, Aligarh 202001 U.P. India)

Received July 26, 1976

Selenium dissolves in chlorosulfuric acid to give a green solution which changes to yellow after a few hours. The green and the yellow colours are due to the formation of the cations Se_8^{2+} and Se_4^{2+}, respectively. It has been shown by conductometric and spectrophotometric studies that at moderate concentrations of appropriate oxidizing agents selenium can be oxidized to the oxidation state +1 yielding the Se_4^{4+} cation.

Introduction

During recent years it was shown that the coloured solutions of sulfur, selenium and tellurium in sulfuric, disulfuric and fluorosulfuric acids [1—6] are due to the formation of polyatomic cations, viz. S_{16}^{2+}, S_8^{2+}, S_4^{2+}, Se_4^{2+}, Se_8^{2+}, Te_4^{2+} and Te_4^{4+}, containing the elements in low valence states. In a few cases further oxidation of these cations to higher valence states by appropriate oxidizing agents has also been reported. There is no mention of the formation of the Se_4^{4+} ion in any of the above acidic media. No such study has so far been undertaken in chlorosulfuric acid which is stronger than sulfuric acid. It was, therefore, considered worth-while investigating the possibility of the oxidation of selenium yielding polyatomic cations especially Se_4^{4+} as a stable entity.

Experimental

Pure chlorosulfuric acid (Riedel) was used. All the materials were commercially pure samples and were used after drying in vacuum at 80° C excepting selenium dioxide which was purified by evaporating with fuming nitric acid and then subliming in a dry atmosphere at 200°C.

The design of the conductivity cell, meaning and significance of the notations γ and ω and the determination of γ have been described elsewhere [7—9].

The conductance measurements were carried out by using a Systronics type 302- S.R. No. 306 conductivity bridge thermostatted at 25 ± 0.1° C. The ultraviolet-visible spectra of the solutions were recorded on a Beckman Model DU 2 spectrophotometer.

The conductance of the green solutions of selenium in HSO_3Cl was found to vary with time becoming stable only after a few hours. A graph of the specific conductance *vs.* time was plotted for each set of measurements. This graph was extrapolated to zero time to get the specific conductance of the green solution for a particular concentration of selenium in HSO_3Cl. The specific conductance values thus obtained after a number of experiments and the corresponding stable values were then plotted against concentration expressed in g-atom of Se per kg of the solution (ω) and are shown in Fig. 1.

Results and discussion

Conductometric measurements

Selenium dissolved readily in chlorosulfuric acid yielding green conducting solutions. Both the conductance and the colour changed with time and after a few hours a yellow solution of stable conductance was obtained. Figure 1 represents the specific conductance vs. concentration curves of the green

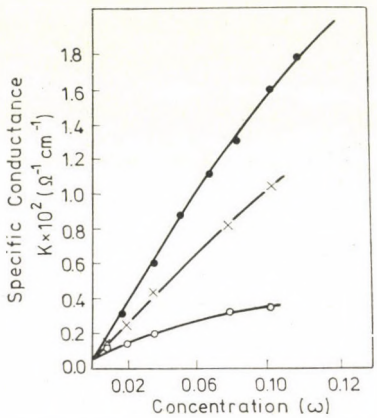

Fig. 1. Specific conductance *vs.* concentration curves of solutes in HSO_3Cl at 25 °C ● Potassium chloride; × Yellow solution of selenium; ○ Green solution of selenium

and the stable yellow solutions. The value of γ has been found to be 0.23 for the green and 0.58 for the yellow solutions. The formation of green and yellow solutions in sulfuric acid and disulfuric acid [1, 2, 6] has been attributed to the cationic species Se_8^{2+} and Se_4^{2+}, respectively. It is reasonable to suggest that in chlorosulfuric acid, selenium is oxidized to form polyatomic cations and the formation of these species may be expressed according to the following general reaction.

$$Sc + 2X\,HSO_3Cl \rightarrow Se_n^{X+} + \frac{X}{2}SO_2 + \frac{X}{2}H_2SO_4 + X\,HCl + X\,SO_3Cl^- \qquad (1)$$

$$\gamma = \frac{X}{n}$$

The theoretically expected values of γ for the formation of Se_8^{2+} and Se_4^{2+} according to the above reaction come out to be 0.25 and 0.50, respectively. The experimentally observed values of γ are very close to the estimated values and support the above suggested general reaction. The ionization of selenium

involving the formation of Se_8^{2+} and Se_4^{2+} ions may then be represented by equations (2) and (3)

$$8Se + 4HSO_3Cl \rightarrow Se_8^{2+} + SO_2 + H_2SO_4 + 2HCl + 2SO_3Cl^- \quad (2)$$

$$4Se + 4HSO_3Cl \rightarrow Se_4^{2+} + SO_2 + H_2SO_4 + 2HCl + 2SO_3Cl^- \quad (3)$$

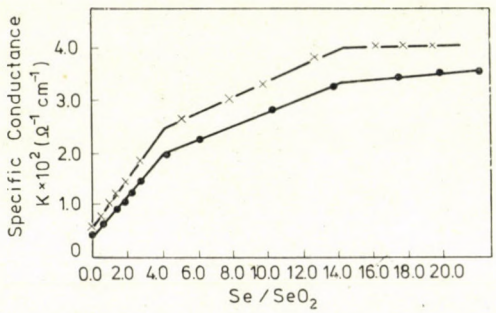

Fig. '. Conductometric titrations of the green solutions of selenium with selenium dioxide in HSO_3Cl at 25 °C ● Concentration of SeO_2 0.0317 ω; × Concentration of SeO_2 0.0372 ω

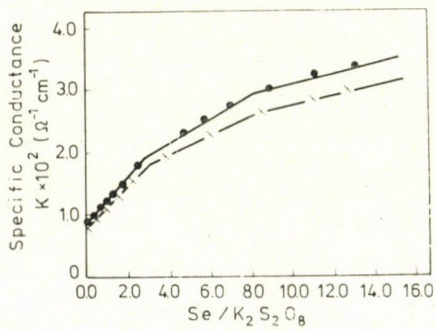

Fig. 3. Conductometric titrations of the green solutions of selenium with potassium persulfate in HSO_3Cl at 25 °C. ● Concentration of $K_2S_2O_8$ 0.0268 ω; × Concentration of $K_2S_2O_8$ 0.0294 ω

The green species Se_8^{2+} can be oxidized to higher valence states by oxidizing agents like SeO_2 and $K_2S_2O_8$. This is clear from the conductometric titrations (Figs 2 and 3). As the green species gradually changes to yellow after a few hours, instead of titrating the green solution with successive additions of the oxidizing agents, the titration was carried out by successive addition of selenium metal to a solution of the oxidizing agent in HSO_3Cl. Initially the addition of selenium produced a green solution which was immediately converted to yellow and then finally to a colourless solution. This indicates that selenium metal first reacts with the solvent HSO_3Cl producing Se_8^{2+},

which is then oxidized in the presence of the oxidizing agent to the yellow species Se_4^{2+}, but due to the high concentrations of the oxidizing agents it is further oxidized to the higher valence state Se(IV), presumably SeO_2, which corresponds to the colourless solutions. As soon as the concentrations of selenium reached the ratios of $Se/SeO_2 \approx 4$ and $Se/K_2S_2O_8 \approx 3$, the solutions became light red, which at even higher ratios acquired some yellowish tinge probably due to the formation of the Se_4^{2+} ion. It is reasonable to ascribe the light red colour to the existence of some cationic species in a valence state intermediate between Se(IV) and Se_4^{2+}, presumably Se_4^{4+}. This may be further confirmed by the analysis of the conductometric titration data. From Figs 2 and 3 it is apparent that changes in the slope occur at the ratios $Se/SeO_2 = 4$ and 14.0 and $Se/K_2S_2O_8 = 2.9$ and 8.0. This may be interpreted in the following way.

Selenium dioxide oxidizes Se_8^{2+} to Se_4^{2+} and is itself reduced to Se_4^{2+} according to the following equation.

$$7Se_8^{2+} + 4Se(IV) \rightarrow 15Se_4^{2+} \tag{4}$$

and the reaction occurring in HSO_3Cl may be given as

$$7Se_8^{2+} + 4SeO_2 + 24HSO_3Cl \rightarrow 15Se_4^{2+} + 8HCl + 8H_2SO_4 + 16SO_3Cl^- \tag{5}$$

The equation for the overall reaction may be obtained by combining Eqs (2) and (5)

$$56Se + 4SeO_2 + 52HSO_3Cl \rightarrow 15Se_4^{2+} + 7SO_2 + 15H_2SO_4 + 22HCl + 30SO_3Cl^- \tag{6}$$

The calculated ratio of $Se/SeO_2 = 14.0$ at the equivalence point of Se_4^{2+} formation is in excellent agreement with the observed value. From the conductivities of the end point solutions the value of γ was determined and the experimental value of 0.60 (Table I) is in good agreement with the value of 0.53 predicted by Eq. (6). At moderately higher concentrations of the oxidizing agent SeO_2, Se_8^{2+} is oxidized presumably to Se_4^{2+} responsible for the light red solution. The reaction of Se_8^{2+} with SeO_2 under these conditions may be written as

$$2Se_2^{8+} + 4SeO_2 + 24HSO_3Cl \rightarrow 5Se_4^{4+} + 8HCl + 8H_2SO_4 + 16SO_3Cl^- \tag{7}$$

and the overall reaction is given as

$$16Se + 4SeO_2 + 32HSO_3Cl \rightarrow 5Se_4^{4+} + 2SO_2 + 10H_2SO_4 + 12HCl + 20SO_3Cl^- \tag{8}$$

Table I

Specific conductances and γ values of the end point solutions from titrations of Se with SeO_2 in HSO_3Cl at 25 °C

Se/SeO_2	SeO_2 (mol)	Se (mol)	Total Se (mol)	Sp. Cond. $K \times 10^2$	Observed γ	Calculated γ
4.0 : 1.0	0.03171	0.12684	0.14930	2.066	1.05	
					(1.12)*	1.25
4.0 : 1.0	0.03718	0.14872	0.17510	2.528	1.20	
14.0 : 1.0	0.03171	0.44394	0.46650	3.330	0.55	
					(0.60)*	0.53
14.0 : 1.0	0.03718	0.052052	0.54697	4.000	0.65	

* Average value of γ.

The observed ratio of $Se/SeO_2 = 4$ at the equivalence point for the formation of Se_4^{4+} is the same as the predicted value. The γ value of 1.12 for the end point solution is quite consistent with the reaction represented by Eq. (8).

Attempts to check the oxidation of Se_8^{2+} by $K_2S_2O_8$ to Se_4^{2+} and Se_4^{4+} have also been made. Potassium persulfate behaves as a strong oxidizing agent because of its ability to accept two electrons according to the following reaction

$$S_2O_8^{2-} + 2e^- \rightarrow 2SO_4^{2-}$$

The formation of the cations Se_4^{2+} and Se_4^{4+} from selenium in chlorosulfuric acid solution containing $K_2S_2O_8$ may be represented by Eqs (9) and (10), respectively

$$8Se + K_2S_2O_8 + 8HSO_3Cl \rightarrow 2Se_4^{2+} + 3H_2SO_4 + 2HCl + SO_2 + 2K^+ + 6SO_3Cl^- \quad (9)$$

and

$$8Se + 3K_2S_2O_8 + 16HSO_3Cl \rightarrow 2Se_4^{4+} + 7H_2SO_4 + 6K^+ + SO_2 + 2HCl + 14SO_3Cl^- \quad (10)$$

The observed ratios of Se $K_2S_2O_8 = 8.0$ and 2.9 are very close to the values predicted by Eqs (9) and (10), respectively. The conductometric values of the end point solutions (Table II) are also very close to those predicted by Eqs (9) and (10).

It is thus obvious from the above that the green species Se_8^{2+} formed in HSO_3Cl can be further oxidized to Se_4^{2+} or Se_4^{4+} depending upon the relative concentrations of the oxidizing agents used. In excess of the oxidizing agents, however, SeO_2 is formed.

Table II

Specific conductances and γ values of the end point solutions from titration of Se with $K_2S_2O_8$ in HSO_3Cl at 25 °C

$Se/K_2S_2O_8$	$K_2S_2O_8$ (mol)	Se (mol)	Sp. Cond. $K \times 10^2$	Observed γ	Calculated γ
2.9 : 1.0	0.02683	0.08049	1.825	1.49	
				(1.52)*	1.75
2.9 : 1.0	0.02938	0.08226	1.924	1.54	
8.0 : 1.0	0.02683	0.21464	2.627	0.90	
				(0.90)*	0.75
8.0 : 1.0	0.02938	0.23504	2.957	0.90	

* Average value of γ.

Absorption spectra

The absorption spectrum of the green species obtained by dissolving selenium in cold HSO_3Cl is shown in Fig. 4. (Curve A). This species has an intense absorption maximum at 450 nm and a broad weak absorption at 730 nm. A similar spectrum was reported by GILLESPIE *et al.* [1] for the green solution obtained by dissolving Se in H_2SO_4 and HSO_3F. The intense absorption at 295 nm reported by these authors could not be observed in HSO_3Cl. It might be due to a blue shift of this peak in HSO_3Cl to such an extent that it crosses the solvent cut-off at 280 nm. The absorption spectrum of the HSO_3Cl solution of the yellow species obtained by oxidizing the green solution with $K_2S_2O_8$ is shown in Fig. 4. (Curve B). This has only one intense absorption at 400 nm although, in addition to the intense band at 410 nm a very weak band at 330 nm has bean reported in H_2SO_4 and HSO_3F [1].

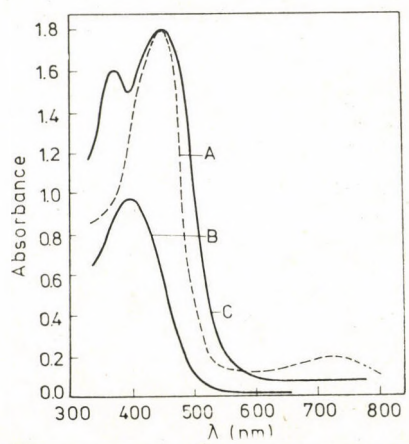

Fig. 4. Absorption spectra of the solutions of selenium in HSO_3Cl. A Green solution; B Yellow solution; C Light red solution

The absorption spectrum of the solution containing Se_4^{4+} obtained by oxidizing selenium at moderate concentrations of $K_2S_2O_8$ $Se/K_2S_2O_8 = 1.5$ is shown in Fig. 4. (Curve C). This has two absorption maxima of about equal intensities at 370 and 450 nm. A similar absorption spectrum for the Te_4^{4+} species in HSO_3F [4] has been reported, which contains two bands of nearly equal intensities at 360 and 420 nm. The similarity in the absorption spectra of the two analogous species Se_4^{4+} and Te_4^{4+} supports the tentative assignment for the formation of Se_4^{4+} ion in HSO_3Cl.

*

Professor W. RAHMAN is thanked for providing facilities. One of us (N.A.A.) is thankful to Aligarh Muslim University, Aligarh, for financial assistance.

REFERENCES

[1] BARR, J., GILLESPIE, R. J., KAPOOR, R., MALHOTRA, K. C.: Can. J. Chem., **46,** 149 (1968)
[2] BARR, J., CRUMP, D., GILLESPIE, R. J., KAPOOR, R., UMMAT, P. K.: Can. J. Chem., **46,** 3607 (1968)
[3] GILLESPIE, R. J., BARR, J., KAPOOR, R., PEZ, G. P.: J. Amer. Chem. Soc., **90,** 6855 (1968)
[4] BARR, J., GILLESPIE, R. J., PEZ, G. P., UMMAT, P. K., VAIDYA, O. C.: Inorg. Chem., **10,** 362 (1971)
[5] GILLESPIE, R. J., PASSMORE, J., UMMAT, P. K., VAIDYA, O. C.: Inorg. Chem., **10,** 1327 (1971)
[6] GILLESPIE, R. J., PEZ, G. P.: Inorg. Chem., **8,** 1229 (1969)
[7] ZAIDI, S. A. A., SIDDIQI, Z. A.: J. Inorg. Nucl. Chem., **37,** 1806 (1975)
[8] ZAIDI, S. A. A., SIDDIQI, Z. A.: J. Inorg. Nucl. Chem. **38,** 1404 (1976)
[9] ZAIDI, S. A. A., SIDDIQI, Z. A.: Acta Chim. (Budapest) (In press)

S. A. A. ZAIDI
Z. A. SIDDIQI
N. A. ANSARI
Division of Inorganic Chemistry,
Department of Chemistry, Aligarh
Muslim University, Aligarh 202001 U. P. India

Acta Chimica Academiae Scientiarum Hungaricae, Tomus 93 (3–4), pp. 403–407 (1977)

SYNTHESIS OF 2*H*- AND 4*H*-1,3-BENZOTHIAZINE DERIVATIVES

STUDIES OF THE 1,3-BENZOTHIAZINE RING CLOSURE REACTION OF N-(3,4-DIALKOXYPHENYLTHIOMETHYL) ACID AMIDES

J. SZABÓ, L. FODOR, I. VARGA, E. VINKLER and P. SOHÁR*

*(Pharmaceutical Chemical Department, Medical University, Szeged, and * Pharmaceutical Research Institute, Budapest)*

Received March 23, 1976

In contrast with our earlier findings being in agreement with the observation of other authors, it is now shown that the 1,3-benzothiazine ring closure reaction of N-(3,4-dialkoxyphenylthiomethyl) acid amides (**I**) in acid medium proceeds in two directions. Besides the 4*H*-1,3-benzothiazine derivatives (**III**), varying amounts of 2*H*-1,3-benzothiazine derivatives (**II**) are also formed, as isomers, their actual quantities depending on the structure of **I**.

In the course of our studies on the 1,3-benzothiazine ring closure reaction of N-(3,4-dialkoxyphenylthiomethyl) aroyl amides (**I**) it was found [1] that compounds **Ia-c** yielded the isomeric 2-aryl-4*H*-1,3-benzothiazine derivatives (**IIIa-c**) instead of the expected 4-aryl-2*H*-1,3-benzothiazine derivatives (**IIa-c**), when the cyclization reaction was carried out in phosphorus oxychloride solution, *i.e.* in acid medium. Later Japanese researchers [2] arrived at the same result when attempting the cyclization of compound **Ia** with polyphosphoric acid.

According to our recent investigations [3, 4], in the presence of pyridine as a proton-acceptor agent, acid amides **I** are cyclized exclusively to 2*H*-1,3-benzothiazine derivatives (**II**) by the effect of phosphorus oxychloride.

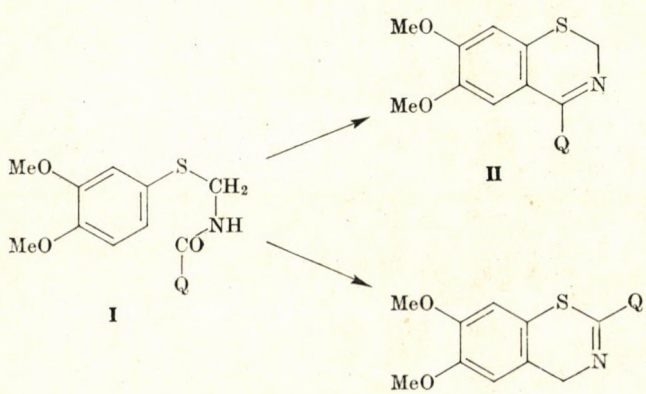

a Q = Ph
b Q = 3,4-$(MeO)_2C_6H_3$—
c Q = 4-$MeOC_6H_4$—
d Q = 4-ClC_6H_4
e Q = Me—
f Q = Et—
g Q = $PhCH_2$—
h Q = 3,4-$(MeO)_2C_6H_3CH_2$—
i Q = H

It was therefore assumed that the cyclization reaction of acid amide thioethers **I** in acid medium may take place in two different ways, so 2*H*-1,3-benzothiazine isomers (**II**) can also be formed together with 4*H*-1,3-benzothiazine derivatives (**III**). Consequently, this cyclization reaction was re-examined also including such acid amide thioethers (**Id-h**) where cyclization had not been attempted earlier, or the reaction had failed. In acid medium the 1,3-benzothiazine cyclization reaction with all acid amide thioethers (**Ia-h**) examined by us, was found to take place in two different directions that is, both the 2*H*- and 4*H*-1,3-benzothiazine isomers were formed. However, in the cyclization reaction of the aromatic acid amide thioethers **Ia-d**, the 2*H*-1,3-benzothiazine isomers (**IIa-d**) were formed in such a low yield that they could only be isolated by a special procedure described in Experimental.

The acid amide thioether **Ii** could not be synthesized by general methods. Therefore the synthesis of compounds **IIi** and **IIIi** was attempted by the cyclization of N-(hydroxymethyl)formamide and 3,4-dimethoxythiophenol with

Table I

Compound	IR data cm^{-1} (KBr)		NMR data ($CDCl_3$) $\delta_{TMS} = 0$ ppm				
	ν OCH_3	ν C=N*	δ CH_2 s (2H)	δ OCH_3	δ H—5	δ N—8	Signals of substituent Q
IIIb	2835	1580	4.65	3.82	6.37		δ H—5' = 6.75, *d*** (1H)
				3.85	6.77		δ H—2' ≈ 7.48, *d*** (1H)
				3.88	2x*s*(2x1H)		δ H—6' ≈7.52, 2x*d* (1H)
				3x*s*(12H)			$J_{5',6'}$ = 9Hz**,
							$J_{2',6'}$ = 2Hz**
IIId	2840	?*	4.68	3.85	6.80		δ H—3',5'-7.35• (2H)
				s(6H)	6.83		δ H–2',6' = 7.94• (2H)
					2x*s*(2x1H)		$J_{2'',3'} \equiv J_{5',6'} \equiv$ 9Hz•
IIIf••	2830	1630	4.93	3.95	6.85	7.03	δ CH_3 = 1.50 ppm, t^{∇} (3H)
				3.97	*s*(1H)	*s*(1H)	δ CH_2 = 3.25 ppm, qa^{∇} (2H)
				2x*s*(6H)			J_{AX} = 7.5 Hz$^{\nabla}$
IIIg••	2840	1630	4.97	3.85	6.70	6.95	δ CH_2 = 4.58 ppm, *s*(2H)
	2830			3.90	*s*(1H)	*s*(1H)	ν ArH = 435—460 Hz, *m*(5H)
				2x*s*(6H)			

• Data calculated from the multiplet AA'BB' by the AB approximation
•• ν(=N$^+$H) bands are at 2800–2100 and ~ 1900 cm^{-1}
* Group vibration of νC=N character coupled with the aromatic skeletal vibration at 1600 cm^{-1}.
** Data calculated from the multiplet AMX, $J_{2',5'} \equiv J^{para} \approx 0$
∇ Data calculated from the multiplet A_2X_3

phosphorus oxychloride. However, the isomer **IIIi** expected to form besides **IIi** could not be isolated from this reaction, presumably because it underwent a rapid decomposition in the acid medium existed in the course of work-up.

The structures of the compounds which had not been described in our earlier papers [3, 4], were confirmed by elemental analysis and, in some cases, by IR and NMR spectra. The spectroscopic data are given in Table I.

Experimental

M. p.'s are uncorrected

The IR spectra were recorded with a Perkin-Elmer 457 instrument; the NMR spectra were obtained at room temperature with a JEOL 60-HL (60MHz) spectrometer, using TMS internal standard.

1. Cyclization of N-(3,4-dimethoxyphenylthiomethyl)benzamide (Ia)

N-(3,4-Dimethoxyphenylthiomethyl) benzamide (101 g; 0.33 mole) was heated with phosphorus oxychloride (100 ml) on a boiling water bath for 1 hr. After cooling, the reaction mixture was decomposed with ice, neutralized with sodium carbonate and extracted with benzene. The benzene solution was dried over sodium sulfate and the solvent evaporated. The residue was dissolved in hot ethanol (60 ml) and crystallized. A colourless crystalline substance, 2-phenyl-6,7-dimethoxy-4*H*-1,3-benzothiazine (**IIIa**) (39.5 g) was obtained, m. p. 99—100° C; no m. p. depression was observed with an authentic sample [1].

The ethanol was evaporated from the mother liquor. The residue was dissolved in benzene (100 ml) and extracted with 10% hydrochloric acid (50 ml). The acid solution was neutralized with sodium carbonate and extracted with benzene. The benzene solution was again extracted with hydrochloric acid, neutralized with sodium carbonate, extracted with benzene again, and the substance obtained from benzene was crystallized from ethanol. 4-Phenyl-6,7-dimethoxy-2*H*-1,3-benzothiazine (**IIa**) was obtained (1.83 g) as pale yellow crystals, m.p. 141—142° C; no m. p. depression was observed with an authentic sample [3].

2. Cyclization of N-(3,4-dimethoxyphenylthiomethyl)veratric acid amide (Ib)

N-(3,4-Dimethoxyphenylthiomethyl)veratric acid amide (3.63 g; 0.01 mole) was heated with phosphorus oxychloride (4 ml) on a hot water bath for 1 hr. The reaction mixture was processed further as given in Expriment 1. Colourless crystals of 2-(3',4'-dimethoxyphenyl)-6,7-dimethoxy-4*H*-1,3-benzothiazine (**IIIb**) (1.22 g), were obtained from ethanol, m. p. 126—127° C; no m. p. depression was observed in admixture with an authentic sample [1]. In the crystalline state, on storage for years, this compound undergoes conversion to a modification having a melting point of 135—136° C; in the molten state, the conversion takes place rapidly. Both substances have identical R_f values (silica gel layer; benzene–ethanol 9 : 1); they yield the same picrate from ethanol solution [m. p. 198—200° C (d.)] Dimorphism, as well as the structure of **IIIb**, was also confirmed by the IR and NMR spectra.

In addition to this, 4-(3',4'-dimethoxyphenyl)-6,7-dimethoxy-2*H*-1,3-benzothiazine (**IIb**) (0.06 g) was obtained as pale yellow prisms from benzene; m. p. 152—153° C. No m. p. depression was observed with an authentic sample [4].

3. Cyclization of N-(3,4dimethoxyphenylthiomethyl)anisic acid amide (Ic)

N-(3,4-Dimethoxyphenylthiomethyl) anisic acid amide (3.33 g; 0.01 mole) was treated as described in Experiment 1. to obtain 2-(4'-methoxyphenyl)-6,7-dimethoxy-4*H*-1,3-benzothiazine (**IIIc**) (1.02 g), which crystallized as colourless radial needles from ethanol, m. p. 92—93° C; no m. p. depression was observed with an authentic sample [1].

The product obtained by extraction with hydrochloric acid was purified chromatographically on a silica gel layer (benzen–chloroform–ethanol, 10 : 5 : 1) and crystallized from ethanol to yield 4-(4'-dimethoxyphenyl)-6,7-dimethoxy-2*H*-1,3-benzothiazine (**IIc**) (0.02 g) as pale yellow crystals, m. p. 144—145° C; no m. p. depression was observed in admixture with an authentic sample [4].

4. Cyclization of N-(3,4-dimethoxyphenylthiomethyl)-4'-chlorobenzamide (Id)

N-(3,4-Dimethoxyphenylthiomethyl)-4'-chlorobenzamide (33.8 g; 0.1 mole) was treated as described in Experiment 1, to give 2-(4'-chlorophenyl)-6,7-dimethoxy-4*H*-1,3-benzothiazine (**IIId**) (15.5 g) in the form of colourless radial needles from ethanol; m. p. 129—130° C.

$C_{16}H_{14}ClNO_2S$ (319.81). Calcd. C 60.09; H 4.41; N 4.38; S 10.02. Found C 59.79; H 4,50; N 4.32; S 10.22%.

4-(4'-Chlorphenyl)-6,7-dimethoxy-2*H*-1,3-benzothiazine (**IId**) (0.12 g) was also obtained from the reaction as colourless needles from ethanol, m. p. 139—140° C; no m. p. depression was observed with an authentic sample [4].

5. Cyclization of N-(3,4-dimethoxyphenylthiomethyl)acetamide (Ie)

N-(3,4-Dimethoxyphenylthiomethyl) acetamide (24.1 g; 0.1 mole) was refluxed with phosphorus oxychloride (40 ml) in carbon dioxide atmosphere for 2 hrs. The reaction mixture was decomposed with ice, neutralized with sodium carbonate and extracted with benzene. The alkaline substances were extracted from the benzene solution with 10% hydrochloric acid (100 ml), the hydrochloric acid solution was neutralized with sodium carbonate and extracted with benzene. The solution was dried over sodium sulfate and the solvent evaporated. The residue was subjected to chromatographic purification on a preparative silica gel layer (benzene–ethanol, 9 : 1). 2-Methyl-6,7-dimethoxy-4*H*-1,3-benzothiazine (**IIIe**) (2.4 g) was obtained as a colourless viscous oil.

$C_{11}H_{13}NO_2S$ (223.29). Calcd. C 59.17; H 5.87; N 6.27; S 14.36. Found C 58. 99; H 6.09; N 5.99; S 14.20%

The hydrochloride was precipitated from the ethanol solution with ether, to obtain pale yellow crystals, m. p. 180—181° C (d.).

$C_{11}H_{14}ClNO_2S$ (259.75). Calcd. C 50.87; H 5.43; N 5.39; Cl 13.65. Found C 50.64; H 5.68; N 5. 39; Cl 13.55%.

Besides this product, 4-methyl-6,7-dimethoxy-2*H*-1,3-benzothiazine (**IIe**) was obtained as a yellow viscous oil; this was converted into the hydrochloride in ethanol solution to obtain yellow crystals of 4-methyl-6,7-dimethoxy-2*H*-1,3-benzothiazinium chloride (2.8 g), m. p. 190—191° C (d.); no m. p. depression was observed with an authentic sample [3].

6. Cyclization of N-(3,4-dimethoxyphenylthiomethyl)propionic acid amide (If)

N-(3,4-Dimethoxyphenylthiomethyl) propionic acid amide (5.1 g; 0.02 mole) was treated as described in Experiment 5, to obtain 4-ethyl-6,7-dimethoxy-2*H*-1,3-benzothiazine (**IIf**) (0.56 g) as a pale yellow viscous oil. The picrate separated in the form of yellow crystals from ethanol, m. p. 180—182° C (d.); no m. p. depression was observed with an authentic sample [3]. The other product was 2-ethyl-6,7-dimethoxy-4*H*-1,3-benzothiazine (**IIIf**) (0.49 g), a colourless oil that undergoes colouration when standing exposed to air.

$C_{12}H_{15}NO_2S$ (237.32). Calcd. C 60.74; H 6.37; N 5.91; S 13.51. Found 60.26; H 6.11; N 5.72; S 13.41%.

The picrate separated from ethanol as yellow needles, m. p. 173—174° C (d.).

$C_{18}H_{18}N_4O_9S$ (466.43). Calcd. C 46.35; H 3.89; N 12.01; S 6.87. Found C 46.20; H 3.80; N 11.90; S 6.70%.

The hydrochloride separated from ethanol as pale yellow crystals, m. p. 194—195° C (d.).

$C_{12}H_{16}ClNO_2S$ (273.78). Calcd. C 52.64; H 5.89; S 11.71. Found C 51.94; H 5.88; S 11.47%.

7. Cyclization of N-(3,4-dimethoxyphenylthiomethyl)phenylacetamide (Ig)

N-(3,4-Dimethoxyphenylthiomethyl)phenylacetamide (3.17 g; 0.01 mole) was treated as described in Experiment 5, to obtain 4-benzyl-6,7-dimethoxy-2*H*-1,3-benzothiazine (**IIg**)

(0.20 g) as pale yellow crystals from ether, m. p. 81—82° C; no m. p. depression was observed with an authentic sample [4].

The other product from this reaction was 2-benzyl-6,7-dimethoxy-4*H*-1,3-benzothiazine (**IIIg**) (0.12 g), a colourless viscous oil that suffered colouration when standing in air.

$C_{17}H_{17}NO_2S$ (299.38). Calcd. C 68.20; H 5.72; N 4.68; S 10.71. Found C 67.76; H 6.09; N 4.45; S 10.55%.

The hydrochloride separated from ethanol solution with ether as pale yellow crystals, m. p. 178—180 °C (d.).

$C_{17}H_{18}ClNO_2S$ (335.85). Calcd. C 60.80; H 5.40; Cl 10.56; N 4.17; S 9.55. Found C 60.67; H 5.64; Cl 10.76; N 4.25; S 9.70%.

8. Cyclization of N-(3,4-dimethoxyphenylthiomethyl)homoveratric acid amide (Ih)

N-(3,4-Dimethoxyphenylthiomethyl)homoveratric acid amide (3.77 g; 0.01 mole) was converted into 4-(3',4'-dimethoxybenzyl)-6,7-dimethoxy-2*H*-1,3-benzothiazine (**IIh**) (0.07 g) as described in Experiment 5. Pale yellow crystals separated from ether, m. p. 144—145° C; no m. p. depression was observed with an authentic sample [4].

The other product of the reaction was 2-(3',4'-dimethoxybenzyl)-6,7-dimethoxy-4*H*-1,3-benzothiazine (**IIIh**) (0.05 g). When crystallized from a mixture of ether and methanol (9 :1), colourless crystals separated, m. p. 93—94° C.

$C_{19}H_{21}NO_4S$ (359.45). Calcd. C 63.50; H 5.89; N 3.90. Found C 63.12; H 5.75; N 3.85%.

Lemon yellow crystals of the picrate were obtained from ethanol, m. p. 166—167° C (d.).

$C_{25}H_{24}N_4O_{11}S$ (588.55). Calcd. C 51.02; H 4.41; N 9.52; S 5.45. Found C 50.41; H 4.60; N 9.25; S 5.40%.

9. 6,7-Dimethoxy-2*H*-1,3-benzothiazine (IIi)

3,4-Dimethoxythiophenol (1.7 g; 0.01 mole) was mixed with N-(hydroxymethyl) formamide (0.75 g; 0.01 mole) and phosphorus oxychloride (5 ml) was added in small portions. After the vigorous evolution of hydrogen chloride, the reaction mixture was refluxed 10 min. on a hot water bath. After cooling, the reaction mixture was decompensed with ice, neutralized with sodium carbonate and extracted with benzene. The benzene solution was extracted with 10% hydrochloric acid (20 ml), the hydrochloric acid solution was neutralized with sodium carbonate, extracted with benzene, then the benzene solution was dried over sodium sulfate and the solvent evaporated. The pale yellow oily residue was dissolved in ethanol (2 ml) and ether containing hydrochloric acid was added in order to precipitate 6,7-dimethoxy-2*H*-1,3-benzothiazinium chloride (0.25 g) as orange yellow crystals, m.p. 194—195° C (d.); no m.p. depression was observed with an authentic sample [3].

*

The authors' thanks are due to Mrs. J. SZABÓ (Pharmaceutical Chemical Department of he Medical University, Szeged) for the microanalyses, to Mrs. B. CSÁKVÁRI and Mr. A. FÜRJES (Pharmaceutical Research Institute, Budapest) for their assistance in recording the spectra.

REFERENCES

[1] VINKLER, E., SZABÓ, J.: Acta Chim. Acad. Sci. Hung. **6**, 323 (1955)
[2] ITO, I., TAKEDA, K., TANAKA, K.: Chem. Abstr., **75**, 129492 (1971)
[3] SZABÓ, J., FODOR, L., VARGA, I., SOHÁR, P.: Acta Chim. (Budapest), **88**, 149 (1976)
[4] SZABÓ, J., FODOR, L., VARGA, I., VINKLER, E., SOHÁR, P.: (In press)

János SZABÓ
Lajos FODOR
István VARGA
Elemér VINKLER
H-6720, Szeged, Pf. 121.

Pál SOHÁR
H-1045, Budapest, Újpest 1, Pf. 82.

Acta Chimica Academiae Scientiarum Hungaricae, Tomus 93 (3—4), pp. 409—414 (1977)

AN ALTERNATIVE ROUTE FOR THE SYNTHESIS OF SOME NEW 5-DISUBSTITUTED-AMINO-3-SUBSTITUTED-IMINO-1,2,4-DITHIAZOLINES: OXIDATIVE DEALLYLATION AND CYCLIZATION OF 1,1,5-TRISUBSTITUTED-2-S-ALLYLISO-4-THIOBIURETS

RAJENDRA SINGH and V. K. VERMA

(Applied Chemistry Section, Institute of Technology, Banaras University, Varanasi-221005, India)

Received March 26, 1976,
in revised form 25 August, 1976

5-Methylphenylamino-3-*p*-tolylimino-, 5-methylphenylamino-3-*p*-ethoxyphenylimino-, 5-methylphenylamino-3-*p*-Cl-phenylimino-5-diphenylamino-3-*p*-tolylimino and 5-diphenylamino-3-*p*-ethoxyphenylimino-1,2,4-dithiazolines have been prepared by the oxidative deallylation and cyclization of the corresponding 1,1,5-trisubstituted-2-S-allyliso-4-thiobiurets with iodine in boiling chloroform. Mechanism of the reaction is proposed.

A survey of the literature reveals that although a number of 5-disubstituted-amino-3-imino-1,2,4-dithiazoline salts have been prepared [1, 2] there are only a few 5-disubstituted-amino-3-substituted-imino-1,2, 4-dithiazolines, synthesized by the oxidative debenzylation of 1,1,5-trisubstituted-2-S-benzyliso-4-thiobiurets, on record [3]. Recently, we have reported the preparation of a number of 3,5-disubstituted-imino-1,2,4-dithiazolidines [4] by the oxidative deallylation of 1,5-diaryl-2,S-allyliso-4-thiobiurets.

In view of these interesting results, now we report the successful extension of the oxidative deallylation and cyclization reaction as an alternative route to the synthesis of some new 5-disubstituted-amino-3-substituted-imino-1,2,4-dithiazolines.

1,1-Disubstituted-thiocarbamides were allylated with allyl bromide. The expected 1,1-disubstituted-2-S-allylisothiocarbamide free base (**I**) so obtained was condensed with the appropriate aryl isothiocyanate to afford the desired 1,1,5-trisubstituted-2-S-allyliso-4-thiobiuret (**II**). These isodithiobiurets (**II**) on oxidation with iodine in boiling chloroform gave the related 5-disubstituted-amino-3-substituted-imino-1,2,4-dithiazolines (**III**). The structure of **III** was finally settled as they were also obtained by the direct oxidation of the related 1,1,5-trisubstituted-2,4-dithiobiurets (**IV**). Compounds **IV** were obtained by the reductive deallylation of the corresponding isodithiobiurets (**II**) with dry hydrogen sulfide in pyridine–triethylamine and also by the reduction of the related dithiazoline (**III**) with ethanolic ammonical hydrogen sulfide. In all the cases compounds **III** and **IV** were characterized by the mixed

melting point technique and by their identical IR spectra. The scheme of the reactions can be depicted as follows:

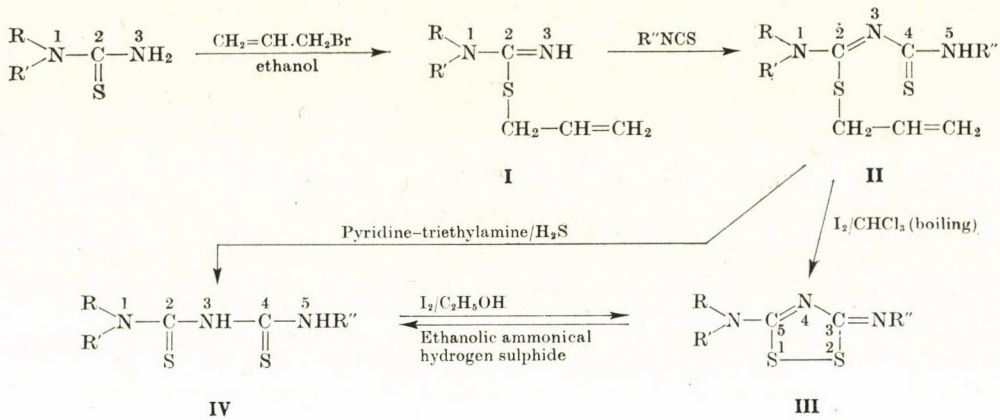

where R and R' = methyl or phenyl

R" = *p*-tolyl-, *p*-Cl-phenyl- or *p*-ethoxyphenyl group.

The following mechanism of the reaction can be suggested:

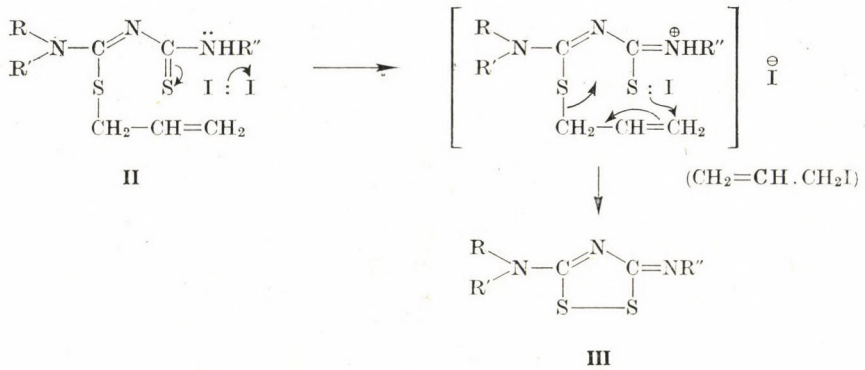

Experimental

1,1,5-Trisubstituted-2-S-allyliso-4-thiobiurets (II)

Following WERNER's procedure [5], the appropriate 1,1-disubstituted thiocarbamides were refluxed with allyl bromide in ethanol for about 1 hr cooled, made alkaline with ammonium hydroxide and the free base was extracted with benzene. The desired benzene extract of 1,1-disubstituted-2-S-allylisothiocarbamide free base was refluxed with the appropriate aryl isothiocyanate (1 : 1 mole) on a water bath for 1 hr. The excess of benzene was evaporated and the semi-solid product, on washing with petroleum ether and treatment with ethanol afforded the expected 1,1,5-trisubstituted-2-S-allyliso-4-thiobiuret as a crystalline solid. The products **II** were recrystallized from ethanol (Table I).

Table I

Synthesis of 1,1,5-*trisubstituted*-2-*S*-*allyliso*-4-*thiobiurets* (*II*)

1,1-Disubstituted-2-S-allylisothiocarbamide-	Isothiocyanate	1,1,5-Trisubstituted-2-S--allyliso-4-thiobiuret formed	M. p., °C	Yield, %	Molecular formula	Analysis	
						Found	Calcd.
1-methyl-1-phenyl--2-S-allyliso-	*p*-tolyl-isothiocyanate	1-methyl-1-phenyl-5-*p*--tolyl-2-S-allyliso-	136	67	$C_{19}H_{21}N_3S_2$	C: 64.49 H: 6.01 N: 12.03	C: 64.22 H: 5.91 N: 11.88
1-methyl-1-phenyl--2-S-allyliso-	*p*-ethoxy-phenylisothiocyanate	1-methyl-1-phenyl-5-*p*--ethoxyphenyl-2-S--allyliso-	132	63	$C_{20}H_{23}N_3S_2O$	C: 62.16 H: 6.10 S: 16.49	C: 62.33 H: 5.97 S: 16.62
1-methyl-1-phenyl--2-S-allyliso-	*p*-Cl-phenyl-isothiocyanate	1-methyl-1-phenyl-5--*p*-chlorophenyl-2--S-allyliso-	152	64	$C_{18}H_{18}N_3S_2Cl$	C: 57.30 H: 4.84 S: 16.93	C: 57.52 H: 4.78 S: 17.07
1,1-diphenyl-2-S--allyliso-	*p*-tolyl-isothiocyanate	1,1-diphenyl-5-*p*-tolyl-2-S-allyliso-	125	70	$C_{24}H_{23}N_3S_2$	C: 67.53 H: 5.96 N: 10.68	C: 67.50 H: 5.79 N: 10.5
1,1-diphenyl-2-S--allyliso-	*p*-ethoxy-phenylisothiocyanatae	1,1-diphenyl-5-*p*--ethoxy-phenyl-2-S--allyliso-	94	73	$C_{25}H_{25}N_3S_2O$	C: 67.76 H: 5.50 N: 9.51	C: 67.11 H: 5.59 N: 9.39

Typical IR frequencies (cm^{-1}) of 1-methyl-1-phenyl-5-*p*-ethoxyphenyl-2-S-allyliso-4-thiobiurets: 3200 m, NH stretching (lit. [8] 3400—3100); 1120m, 1145vs, 1200w, N—C-(=S)-N grouping (lit. [7a] 1200—1100); 1590 w, N—C=N grouping (lit. [7b] 1686—1582)

5-Diaryl(arylalkyl)amino-3-arylimino-1,2,4-dithiazolines (III)

(i) *Oxidative deallylation of* 1,1,5-*trisubstituted-2-S-allyliso-4-thiobiurets with iodine in boiling chloroform*

The details of a representative experiment are as follows:

1-Methyl-1-phenyl-5-*p*-chlorophenyl-2-S-allyliso-4-thiobiuret (3 g) was dissolved in boiling chloroform (20 ml) and a hot solution of iodine (4 g) in chloroform (20 ml) was added; the iodine was used in excess. The solvent was evaporated and the residue washed with ether. On the addition of a small amount of ethanol, the expected 1,2,4-dithiazoline hydriodide (yield 80%, 2.1 g) crystallized. Treatment of the hydriodide with ammonia afforded the free base, which was recrystallized from chlorobenzene, m. p. 192° C. The experiments are summarized in Table II.

Table II

5-*Diaryl/alkylarylamino*-3-*arylimino*-1,2,4-*dithiazoline* (**III**): *oxidation of* 1,1,5-*trisubstituted*-2--*S-allyliso*-4-*thiobiurets with iodine in boiling chloroform*

1,1,5-Trisubstituted-2-S--allyliso-4-thiobiurets: oxidized	5-Diaryl/alkylarylamino--3-arylimino-1,2,4-dithiazoline formed	M. p., °C	Yield, %	Molecular formula	Analysis	
					Found	Calcd.
1-methyl-1-phenyl--5-*p*-tolyl-	5-methylphenyl-amino-3-*p*-tolyl--imino-	129	82	$C_{16}H_{15}N_3S_2$	C: 61.31 H: 4.64 N: 13.31	C: 61.34 H: 4.79 N: 13.41
1-methyl-1-phenyl--5-*p*-ethoxy-phenyl-	5-methylphenyl-amino-3-*p*-ethoxy-phenylamino-	110	75	$C_{17}H_{17}N_3S_2O$	C: 58.79 H: 5.08 N: 12.36	C: 59.47 H: 4.95 N: 12.18
1-methyl-1-phenyl--5-*p*-chlorophenyl	5-methylphenyl-amino-3-*p*-chloro-phenylimino-	192	80	$C_{15}H_{12}N_3S_2Cl$	C: 53.83 H: 3.47 N: 12.71	C: 53.97 H: 3.59 N: 12.59
1,1-diphenyl-5-*p*--tolyl-	5-diphenylamino--3-*p*-tolylimino-	180	70	$C_{21}H_{17}N_3S_2$	C: 66.93 H: 4.92 S: 17.51	C: 67.20 H: 4.53 S: 17.33
1,1-diphenyl-5-*p*--ethoxy-phenyl-	5-diphenylamino-3-*p*-ethoxyphenyl-imino-	165	78	$C_{22}H_{19}N_3S_2O$	C: 65.15 H: 4.65 S: 15.71	C: 65.19 H: 4.69 S: 15.88

Typical IR frequencies (cm^{-1}) of 5-methylphenylamino-3-*p*-chlorophenylamino-1,2,4--dithiazoline: C=N (1620 s) [7] ring —S—S-linkage (480 s) [9]. The absence of IR band for —NH is remarkable.

(ii) *Oxidation of* 1,1,5-*trisubstituted* 2,4-*dithiobiurets with iodine in dilute ethanol*

The 2,4-dithiobiurets listed in Table III were oxidized with iodine in ethanolic solution and ether was added, where upon the hydriodides of the respective dithiazolines precipitated. The free bases were obtained by treating these products with ammonia. The bases were recrystallized from ethanol and chlorobenzene. No depression in the mixed melting points were observed with the respective 5-disubstituted-amino-3-substituted-imino-1,2,4-dithiazolines recorded in Table II. The compounds further characterized by identical IR spectra.

Preparation of 1,1,5-trisubstituted 2,4-dithiobiurets

(i) *Reduction of* **II** *with hydrogen sulfide in pyridine-triethylamine medium*

The isodithiobiurets (**II**) were reduced with hydrogen sulfide (for 4 hrs) in pyridine–triethylamine (6 : 1) medium [6]. The reaction mixture was poured onto crushed ice and acidified with hydrochloric acid, to obtain the related 2,4-dithiobiurets which were filtered off and recrystallized from ethanol (Table III).

Table III

Synthesis of 1,1,5-*trisubstituted* 2,4-*dithiobiuret* (**IV**) *by reductive deallylation of* 1,1,5-*trisubstituted* —2-*S*-*allyliso*-4-*thiobiurets with hydrogen sulfide in pyridine-triethylamine*

1,1,5-Trisubstituted-2-S--allyliso-4-thiobiurets	1,1,5-Trisubstituted-2,4--dithiobiurets formed	M. p., °C	Yield, %	Molecular formula	Analysis	
					Found	Calcd.
1-methyl-1-phenyl--5-*p*-tolyl-2-S--allyliso-	1-methyl-1-phenyl--5-*p*-tolyl-2,4-di--thiobiuret	123	70	$C_{16}H_{17}N_3S_2$	S: 20.03 N: 13.51	S: 20.31 N: 13.33
1-methyl-1-phenyl--5-*p*-ethoxyphenyl--2-S-allyliso-	1-methyl-1-phenyl-5-*p*-ethoxyphenyl--2,4-dithiobiuret	167	68	$C_{17}H_{19}N_3S_2O$	C: 59.27 H: 5.71	C: 59.13 H: 5.50
1-methyl-1-phenyl--5-*p*-chlorophenyl -2-S-allyliso-	1-methyl-1-phenyl--5-*p*-chlorophenyl 2,4-dithiobiuret	118	74	$C_{15}H_{14}N_3S_2Cl$	N: 12.37 S: 15.89	N: 12.51 S: 16.09
1,1-diphenyl-5-*p*--tolyl-2-S-allyliso-	1,1-diphenyl-5-*p*--tolyl-2,4-dithio-biuret	138	65	$C_{21}H_{19}N_3S_2$	C: 67.03 H:. 5.19 N:.11.50	C: 66.84 H:. 5.04 N: 11.14
1,1-diphenyl-5-*p*--ethoxy-phenyl--2-S-allyliso-	1,1-diphenyl-5-*p*--ethoxyphenyl-2,4--dithiobiuret	116	63	$C_{22}H_{21}N_3S_2O$	C: 64.99 H: 5.36	C: 64.86 H: 5.16

Typical IR frequencies (cm^{-1}) of 1-methyl-1-phenyl-5-*p*-ethoxyphenyl-2,4-dithiobiurets: 3395w, NH-stretching (lit. [8] 3400—3100); 1150m shows N—C(=S)-N grouping (lit. [7a] 1200—1100).

(ii) *Reduction of* 1,2,4-*dithiazoline* (**III**) *with ethanolic ammonical hydrogen sulfide*

The dithiazolines (**III**) (Table II) were dissolved in hot ethanolic ammonical hydrogen sulfide, and hydrogen sulfide was passed through the solution for about 45 min. On dilution and acidification, the corresponding 2,4-dithiobiuret was obtained, which was recrystallized from ethanol. No depression in m. p. was observed in admixture with the respective 2,4-dithiobiurets listed in Table III. Identity was further confirmed by the identical IR spectra.

The IR spectra were recorded in Nujol with a Perkin-Elmer spectrophotometer (Model-720).

*

The authors thanks are due to the Incharge, Applied Chemistry Section, the Director' Institute of Technology and the Head, Department of Chemistry, Banaras Hindu University for the facilities. One of us (R.S.) also expresses his gratitude to the Council of Scientific and Industrial Research, New Delhi, for a Junior Research Fellowship.

REFERENCES

[1] FROMM, E., BAUMHAUR, H.: Ann., **361,** 319 (1908)
[2] FROMM, E., JUNIUS, E.: Ber., **28,** 1100 (1895)
[3] VERMA, V. K.: J. Indian Chem. Soc., **47,** 547 (1970)
[4] SINGH, R., VERMA, V. K., AGARWAL, C. V.: J. Indian Chem. Soc., **52,** 444 (1975)
[5] WERNER, E. A.: J. Chem. Soc., **57,** 299 (1890)
[6] FAIRFUL, A. E. S., PEAK, D. A.: J. Chem. Soc., **1955,** 796
[7] COLTHOP, N. B., DALY, L. H., WIBERLY, S. E.: "Introduction to Infrared and Raman Spectroscopy" (a) p. 322, (b) p. 284, Academic Press, New York and London, 1964
[8] KATRITZKY, A. R., "Physical methods in Heterocyclic Chemistry" Vol. II, p. 325. Academic Press, New York and London, 1963
[9] PARANJPE, M. G., Indian J. Chem., **6,** 132 (1968)

Rajendra SINGH, V. K. VERMA
Institute of Technology, Banaras Hindu University, Varanasi-221005, India.

Acta Chimica Academiae Scientiarum Hungaricae, Tomus 93 (3—4), pp. 415—418 (1977)

OXIDATION OF SOME HYDROXYARYLPYRAZOLINES WITH MANGANESE DIOXIDE

T. C. SHARMA, VINITA SAKSENA and N. J. REDDY

(School of Studies in Chemistry, Vikram University Ujjain, India)

Received May 16, 1976

Manganese dioxide oxidation of hydroxyarylpyrazolines (**I**) give the corresponding pyrazoles (**III**) accompanied by very small amounts of unidentified yellow solids. The structures of the pyrazoles have been confirmed by their synthesis from chalcone dibromides (**IV**) and hydrazine hydrate.

A variety of reagents such as chromic oxide [1], bromine [1, 2], potassium permanganate [2, 3], silver nitrate [4], potassium ferricyanide [5], lead dioxide [1, 6] and nickel peroxide [7] have been employed to effect the oxidation of variedly substituted pyrazolines. GLADSTONE and NORMAN [8] oxidized pyrazolines using lead tetraacetate and suggested an ionic mechanism for this reaction. In a recent study, BHATNAGER and GEORGE [9] oxidized some 1,3,5-trisubstituted pyrazolines by manganese dioxide and suggested a free radical mechanism for this oxidation reaction. In all these oxidation reactions the corresponding pyrazole is either the only end product or one of the products. Transition metal oxides [10—13] have also been employed in the oxidation of phenols. The products formed during these oxidations depend upon the nature of the oxidant, substrate and the reaction conditions. In most cases quinones are the major products.

In the present investigations, we have examined the manganese dioxide oxidation of some 3,5-disubstituted Δ^2-pyrazolines (**I**) having a phenolic nucleus at C-3. In every case two products have been obtained from the reaction mixture. Pyrazoles (**III**) are the major products accompanied by very small amounts of unidentified, yellow coloured solids. These compounds, however, had negative ferric chloride test, whereas the pyrazoles gave positive ferric chloride test. The structures of pyrazoles are further confirmed by their synthesis from 2'-hydroxychalcone dibromides (**IV**) and hydrazine hydrate.

Since manganese dioxide oxidations proceed *via* free radicals [14] and when a free radical is formed by loss of a hydrogen atom from either nitrogen or carbon, loss from nitrogen ordinarily takes precedence [15], so a likely mechanism for these reactions is as follows.

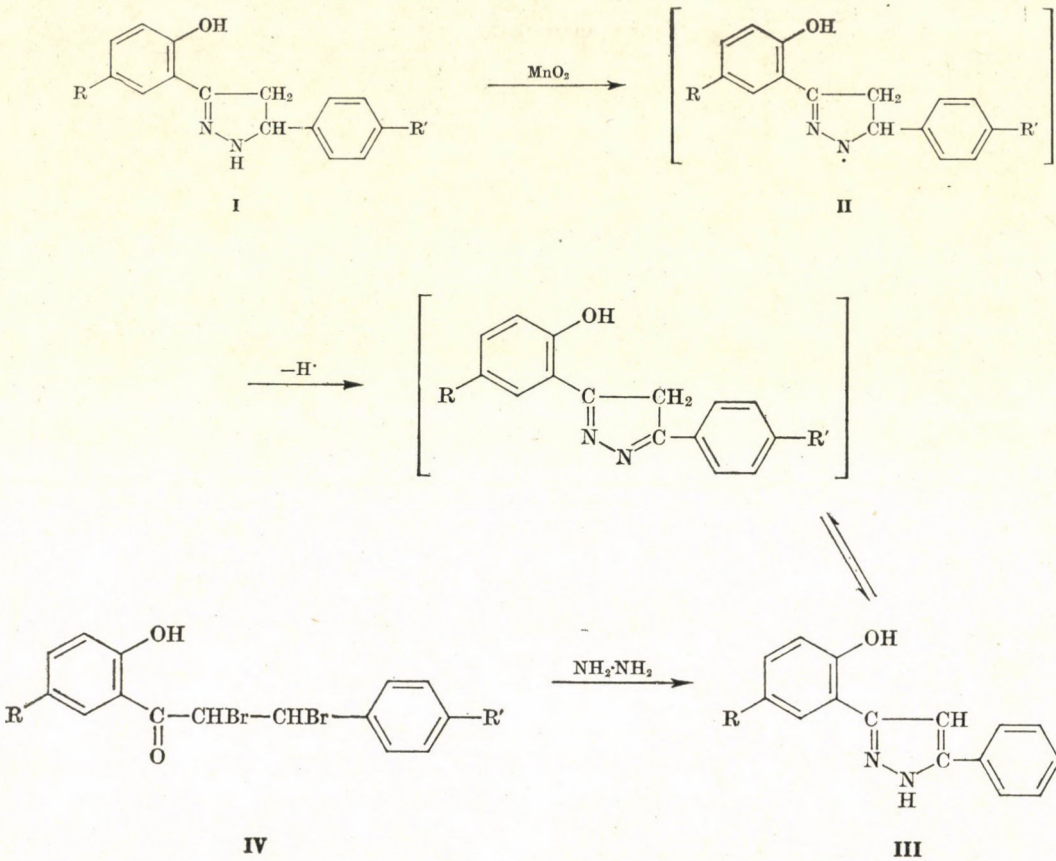

(**a**) R = R′ = H (**b**) R = H, R′ = Cl
(**c**) R = H, R′ = OCH_3 (**d**) R = CH_3, R′ = OCH_3

The IR spectra of the pyrazoles show three to four absorption bands in the region 1620—1500 cm^{-1} and it is, therefore, difficult to ascribe any of these to either C = C or to C = N stretching vibrations with certainty [16]. Absorption peaks due to the OH group appear in the region 3430—3300 cm^{-1}. This shift to longer wavelength from the normal position (3650—3590 cm^{-1}) indicates hydrogen bonding in these compounds.

Further evidence for chelation is obtained from a study of the NMR spectra. The NMR spectra of the pyrazoles show no signals due to NH and OH protons in 1.7—10.0 τ region (for which spectra have been determined). It is on record [17] that the NH proton of pyrazoles absorb at —3.2 to —3.6 τ, but the absence of OH signal can only be explained if there is chelation in these molecules.

The complexing ability of these compounds is under investigation.

Experimental

General Procedures

(a) Active manganese dioxide was prepared by using manganese sulfate dihydrate and potassium permanganate according to the reported procedure [18].

(b) Chalcones

The appropriate aldehyde and acetophenone were mixed in equimolar proportions in alcohol solution and treated with sodium hydroxide (20% aqueous). The mixture was heated on a water bath at 60° C for about 3 hrs. The chalcone was isolated by acidification; crystallization was effected from alcohol.

(c) Chalcone Dibromides

The chalcone (0.01 mole) in aceteic acid or carbon disulfide was treated with bromine (0.01 mole) solution in the same solvent with cooling and shaking. The resulting solid was filtered off, washed with cold ether and crystallized from alcohol.

(d) Pyrazolines

These compounds were prepared following the literature procedure [19].

A mixture of 2'-hydroxychalcone (2 g), hydrazine hydrate (26 ml, 50%) and ethanol (50 ml) was refluxed for 3 hr. and allowed to cool at room temperature. White needles separated, which were filtered off, washed with water and recrystallized from alcohol (1.4g), m. p. 89° (lit. [19] m.p. 89—90.5°).

The other products of this series prepared similarly are listed in Table I.

Table I

Compound No.	Solvent of crystallization	M. p., °C	Yield, %	Formula	N %	
					Calcd.	Found
Ib	Alcohol	135—136	70	$C_{15}H_{11}N_2OCl$	10.3	10.2
Ic	Alcohol	101—102	68	$C_{16}H_{16}N_2O_2$	10.4	10.2
Id	Alcohol	113	69	$C_{17}H_{18}N_2O_2$	9.9	10.0

Oxidation of 3-(2-hydroxyphenyl)-5-phenylpyrazoline (Ia)

Pyrazoline (**Ia**, 2 g) was dissolved in dry chloroform (200 ml) and manganese dioxide (4 g) was added. The mixture was shaken at 25° C for 30 min., after which the excess manganese dioxide was filtered off. The solvent was removed to leave a solid which was shown to be a mixture of two components as revealed from two spots on TLC. The solid was chromatographed on a silica-gel column. Elution with a mixture (1 : 1) of benzene and petroleum ether (b. p. 40—60° C) gave a small amount of a yellow solid which showed negative ferric chloride test. Further elution with benzene gave (**IIIa**), m. p. 144° C (lit. [20] m. p. 144° C).

The identity of this compound was further confirmed by mixed m. p. with a sample prepared by the action of hydrazine hydrate on 2'-hydroxychalcone dibromide as described below.

Synthesis of 3-(2-hydroxyphenyl)-5-phenylpyrazole (IIIa)

A solution of 2'-hydroxychalcone dibromide (**IVa**, 1 g, m. p. 190° C) in alcohol (20 ml) was mixed with hydrazine hydrate (6 ml, 50%). The reaction mixture was allowed to stand at room temperature for 24 hrs and diluted with water. The solid which separated was filtered off, washed with water and crystallized from benzene to give **IIIa** (0.4 g), m. p. 144° C.

C 76.3; H 5.1; N 11.8 Found C 76.2;H 5.0; N 11.6%

$C_{15}H_{12}N_2O$. Calcd.

IR: νmax(KBr), 3350, 3120, 1610, 1535, 1505, 1490, 1450, 1380, 1260, 1240, 1180, 1110, 1048, 1030, 970, 900, 825, 800, 760, 745, 725, 695, 685 and 600 cm^{-1}.

UV (ethanol): 212 mμ (logε 4.60) and 257 mμ (logε 4.53).

Oxidation of Ib

A mixture of the pyrazoline **Ib** (2 g), active manganese dioxide (4 g) and chloroform (200 ml) was shaken at room temperature for 1 hr. The reaction mixture was then worked up as described in the previous experiment to afford a small quantity of a yellow compound and the pyrazole **IIIb**, which was crystallized from benzene to obtain 0.6 g of the product m. p. 190—191° C

C 66.6; H 4.1; N 10.4%. Found C 66.3; H 4.0; N 10.2%

$C_{15}H_{11}N_2OCl$. Calcd.

Synthesis of 3-(2-hydroxyphenyl)-5-(4-chlorophenyl)-pyrazole (IIIb)

2'-Hydroxy-4-chlorochalcone dibromide [21] (**IVb**, 1 g) and hydrazine hydrate (50%, 4 ml) were refluxed in ethanol (20 ml) for 30 min. The reaction mixture was then allowed to cool to room temperature, where upon white needles separated. These were filtered off, washed with water and recrystallized from benzene to give 0.5 g of **IIIb**, m. p. 191° C; mixed m. p. with a sample prepared by the oxidation of pyrazoline (**Ib**) showed no depression.

IR: νmax(KBr), 3350, 1630, 1615, 1595, 1510, 1490, 1455, 1395, 1285, 1260, 1240, 1190, 1120, 1090, 1050, 1035, 1010, 970, 825, 800, 770, 750, and 735 cm^{-1}.

UV (ethanol): 211.5 mμ (log ε 4.64) and 259.8 mμ (log ε 4.62).

The NMR spectrum ($CDCl_3$ + DMSO) had only multiplets centered at about τ 2.5 due to aromatic and ethylenic protons.

Oxidation of Ic

A mixture of the pyrazoline **Ic** (2 g), active manganese dioxide (4 g) and chloroform (150 ml) was shaken at room temperature for 30 min. Working up as usual gave a yellow solid and the pyrazole **IIIc** (0.8 g), m. p. 148—149° C.

Synthesis of 3-(2-hydroxyphenyl)-5-(4-methoxyphenyl)-pyrazole (IIIc)

2'-Hydroxy-4-methoxychalcone dibromide [22] (**IVc**, 1 g) and hydrazine hydrate (50%, 4 ml) were allowed to react in ethanol (10 ml) for 24 hrs. Dilution of the reaction mixture with water gave a white solid. It was filtered off, washed with water and crystallized from benzene to obtain white needles (0.7 g), m. p. 149° C. Mixed m. p. determination with a sample prepared by oxidation of the pyrazoline **Ic** showed no depression.

C 72.1; H 5.3; N 10.6 Found C 72.0; H 4.9; N 10.3% $C_{16}H_{14}N_2O_2$. Calcd.

IR: ν max(KBr), 3300, 1620, 1590, 1585, 1500, 1465, 1448, 1415, 1395, 1270, 1235, 1175, 1115, 1090, 1050, 1020, 970, 930, 825, 790, 740, 710 and 675 cm^{-1}.

UV (ethanol): 212 mμ (log ε 4.64) and 258.5 mμ (log ε 4.60).

The NMR spectrum (CD_3COCD_3) had a singlet at τ 6.5 (3H) due to OCH_3 group and a multiplet centered at about τ 3.0 (9H) owing to aromatic and ethylenic protons.

Oxidation of Id

A mixture of the pyrazoline **Id** (2g) and active manganese dioxide (4 g) was shaken in chloroform (150 ml) for 30 min. at room temperature. Work-up as in the previous cases gave traces of a yellow compound and the pyrazole **IIId** (0.8 g), m. p. 170—171° C (from benzene).

Synthesis of 3-(2-hydroxy-5-methylphenyl)-5-(4-methoxyphenyl)-pyrazole (IIId)

2'-Hydroxy-5'-methyl-4-methoxychalcone dibromide [22] (1 g) and hydrazine hydrate (50%, 6 ml) were allowed to react in alcohol (10 ml) at room temperature. After 24 hrs the reaction mixture was diluted with water. The solid thus separated was filtered off, washed with water and crystallized from benzene to give 0.5 g of **IIId** m. p. 170—171° C. No m. p. depression was observed in admixture with a sample obtained in the previous experiment.

C 66.6; H 4.1, N 10.4. Found C 66.5; H 4.0, N 10.2% $C_{15}H_{11}N_2OCl$, Calcd.

IR: νmax (KBr), 3430, 1615, 1530, 1505, 1450, 1435, 1420, 1300, 1275, 1240, 1175, 1130, 1105, 1050, 1025, 975, 960, 835, 810, 770, 700 and 600 cm^{-1}.

UV: 210.5 mμ (logε 4.70) and 259.5 (logε 4.63).

The NMR spectrum (CD_3COCD_3) showed a multiplet centered at about τ 3.0 (8H) due to aromatic and ethylenic protons, a singlet at τ 6.6 (3H) due to OCH_3 group and another sharp singlet at τ 8.16 (3H) due to CH_3 protons.

*

The authors thank Professor M. M. Bokadia for providing laboratory facilities and Dr. R. P. Sharma for providing the spectroscopic data. Thanks are also due to the U.G.C. for the award of Junior Research Fellowships (to V.S. and N. J. R.).

REFERENCES

[1] Von Auwers, K., Heimke, P.: Liebigs Ann., **458**, 186 (1927)
[2] Smith, L. I., Howard, K. L.: J. Am. Chem. Soc., **65**, 159 (1943)
[3] Strauss, F., Miffat, C., Heitz, W.: Ber., **51**, 1547 (1918)
[4] Dodwadmath, R. P., Wheeler, T. S.: Proc. Ind. Acad. Sci., **2A**, 438 (1935)
[5] Buchner, E., Dessauer, H.: Ber., **26**, 258 (1893)
[6] Beech, S. G., Turnbull, J. H., Wilson, W.: J. Chem. Soc., **4686** (1952)
[7] Balachandran, K. S., Bhatnager, I., George, M. V.: J. Org. Chem., **33**, 3891 (1968)
[8] Gladstone, W. A. F., Norman, R. O. C.: J. Chem. Soc., (C) **1536** (1966)
[9] Bhatnager, I., George, M. V.: Tetrahedron **24**, 1293 (1968)
[10] Konaka, R., Terabe, S., Kuruma, K.: J. Org. Chem., **34**, 1334 (1969)
[11] Blanchard, H. S.: J. Org. Chem., **25**, 264 (1960)
[12] Cook, C. D., English, E. S.: J. Org. Chem., **23**, 755 (1958)
[13] George, M. V., Balachandran, K. S.: Chem. Rev., **75**, 491 (1975)
[14] Meth-Cohn, O. H., Suschijtky, H.: Chem. and Ind., **1969**, 443
[15] Braude, E. A., Brook, A. G., Linstead, R. P.: J. Chem. Soc., **3574**, (1954)
[16] Bellamy, L. J.: The Infrared Spectra of Complex Molecules, pp. 263, 270 John Wiley, New York, 1962
[17] Williams, J. K.: J. Org. Chem., **29**, 1377 (1964)
[18] Pratt, E. F., McGovern, T. P.: J. Org. Chem., **29**, 1540 (1964)
[19] Kállay, F., Janzsó, G., Koczor, I.: Tetrahedron **21**, 19 (1965)
[20] Baker, W., Harborne, J. B., Ollis, W. D.: J. Chem. Soc., **1303**, (1952)
[21] Krishnamurthy, A., Krishnamohan Rao, K. S. R., Subba Rao, N. V.: J. Indian Chem. Soc., **50**, 213 (1973)
[22] Von Auwers, Anschutz, K. L.: Ber., **54**, 1543 (1921)

T. C. Sharma
Vinita Saksena
N. J. Reddy
Vikram University, Ujjain (M.P.) India.

Acta Chimica Academiae Scientiarum Hungaricae, Tomus 93 (3—4), pp. 421—424 (1977)

POLYETHYLENE GLYCOL DERIVATIVES AS COMPLEXING AGENTS AND PHASE-TRANSFER CATALYSTS, I

(PRELIMINARY COMMUNICATION)

L. TŐKE and G. T. SZABÓ

(Department of Organic Chemical Technology, Technical University, Budapest)

Received March 26, 1977

According to PEDERSEN [1, 2] macrocyclic compounds containing repeating —O—CH_2—CH_2 units give stable complexes with alkali and alkaline earth cations.

This phenomenon provides a possibility of employing the cyclic polyethers in nucleophilic substitutions as activators of anions accompanying these cations. This is especially advantageous in heterogeneous reactions [3] when they can transport 'naked' anions through phase barriers. Cryptates, phosphoramidates and polyamino compounds can also be used for this purpose [4].

As the complexing abilities of compounds containing —OCH_2CH_2 units is not limited to cyclic derivatives [5], we started a research on the characterization and usage of acyclic polyethers and their derivatives.*

It was the complexing ability of the materials with Na^+ ions which was studied first. For measuring the stability constants in ethanol a potentiometric method was employed using a Radelkis OP Na 7113 Na^+-electrode and Radelkis OP 8203 double-junction $Ag^+/AgCl$ reference electrode. Between $5 \cdot 10^{-5}$ and $5 \cdot 10^{-3}$ *M* concentrations the cell worked reproducible.

Among the materials examined by us were oligo- and polyethylene glycols and derivatives shown in Fig. 1.

Materials **1** and **4** are commercial products; the other ones were prepared in our laboratory using Na^+-free circumstances.

In the c ' ulations we have considered the polyethylene glycol derivatives to be materi s consisting of identical molecules defined by the average molecular weig t.

Varying the polyether: Na^+ ratio between 1 and 9, an essentially stable 1 : 1 complexing stoichiometry was found. So the equilibrium constant of the reaction

$$Na^+ + L \rightleftharpoons [Na^+L] \text{ can be defined}$$

* Recently we have taken notice of a preliminary communication dealing with polyethylene glycols as phase transfer catalysts [6].

as stability constant of the complex:

$$K_{1C} = \frac{C_{[NaL]^+}}{C_{Na^+} C_L} .$$

Table I.

*Complex stability constants**

Material	K_{1C} $\frac{1}{\text{mole}}$ **
1	110
2	20 ± 4
3	100
4	2200
5	2700
6	1400
7	2000

* Oligoethylene glycols examined are omitted because of the low values of K_{1c}
** Uncertainty is ±15%, unless otherwise stated

The stability constants measured are shown in Table I. The data of Table I reveal the following:

(1) Polyethylene glycol derivatives form stable complexes with Na^+ ion.

(2) Stability of the complexes depends upon the length of the chain. For polyethers $\overline{M} \approx 2000$ the stability constants are higher (even if it is calculated for one OCH_2CH_2 unit) than those of polyethers $\overline{M} \approx 300$. The results may be explained using Ugelstad and Rokstad's [9] theory: because of the higher number of statistical combinations among the oxygen atoms, the conformation needed for the complex formation can be achieved more easily.

(3) The values of the stability constants for the polymer–Na^+ complexes can be influenced by modifying the end group of the chain; *e.g.*, when exchanging the OH groups, by tertiary nitrogen (**2** and **6**), the value of K_{1c} decreases; when protecting the OH groups by dihydropyran (**5**), the stability constants increase.

The effect of $(CH_3)_3Si-O$ groups is not significant.

Polyethylene glycol derivatives **4**, **5** and **6** have been tried in preparing alkali salt solutions in apolar solvents.

In a series of inorganic salts having the same cation (*e.g.* Na^+) the hardness of the anion [10] was found to effect solubility in apolar solvents. Under identical circumstances, the concentrations of the solutions decrease in the following order:

$$I^- > Br^- > Cl^- .$$

Polyethylene glycol derivatives have also been employed as solid-liquid phase transfer catalysts. Among the reactions examined so far were the nucleophilic substitution of bromine and chlorine in benzyl halides by cyano and acetate ions.

A typical example is given for the preparation of an inorganic salt solution in an apolar solvent, and another for a solid-liquid phase transfer reaction.

HO—PEG 300—OH

1

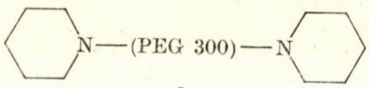

2

$(CH_3)_3SiO$—(PEG 300)—$OSi(CH_3)_3$

3

HO—PEG 2000—OH

4

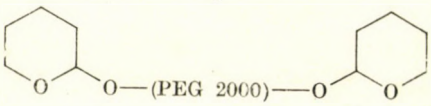

5

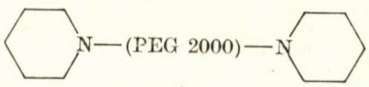

6

$(CH_3)_3SiO$—(PEG 2000)—$OSi(CH_3)_3$

7

Fig. 1. Code numbers of studied materials

Preparation of NaI solution in benzene

Dry NaI (0.0075 g; $5 \cdot 10^{-5}$ mole) and 0.5 g ($2.3 \cdot 10^{-4}$ mole) **6** were dissolved in 20 ml of dry ethyl alcohol. The clear solution was evaporated in vacuum to dryness. The solid residue was dissolved in 20 ml of dry benzene $\left(c = 2.5 \cdot 10^{-3} \frac{\text{mole}}{l.}\right)$. The clear solution proved to be stable.

Preparation of benzyl acetate

Compound **1** (1 g; $2.3 \cdot 10^{-3}$ mole) and 4.8 g ($4.8 \cdot 10^{-2}$ mole) of potassium acetate were added to 10 ml of dry acetonitrile. After stirring for 30 min at 40°C, benzyl chloride (5.7 ml; 0.05 mole) was added. The mixture was stirred at 40°C and the reaction was followed by GLC analysis.

After 4.5 hrs the conversion was practically complete. The precipitate was filtered off, washed with acetonitrile, and the combined acetonitrile solution was distilled to yield 5.78 g (79%) of benzyl acetate b.p. 212—216°C.

REFERENCES

[1] PEDERSEN, C. J.: J. Am. Chem. Soc. **89,** 7017 (1967)
[2] PEDERSEN, C. J.: J. Am. Chem. Soc. **92,** 386 (1970)
[3] DIETRICH, B., LEHN, J. M.: Tetrahedron Lett. **1973,** 1225
[4] NORMANT, H., CUVIGNY, T., SAVIGNAC, P.: Synth. **1975,** 805
[5] DAVIDOVA, S. L., BARABANOV, V. A., ALIMOVA, N. V., PLATE, N. A.: Izv. Akad. Nauk SSSR **1975,** 1441
[6] LEHMKUHL, H., RABOT, F., HAUSCHILD, K.: Synth. **1977,** 189
[7] PUNGOR, E.: MTA Kém. Közlemények **30,** 1 (1968)
[8] FRENSDORF, H. K.: J. Am. Chem. Soc. **93,** 600 (1971)
[9] UGELSTAD, J., ROKSTAD, O. A.: Acta Chem. Scand. **18,** 474 (1964)
[10] PEARSON, R. G.: J. Chem. Educ. **45,** 581 (1968)

László TŐKE
Gábor Tamás SZABÓ
} H-1521 Budapest, Műegyetem

Acta Chimica Academiae Scientiarum Hungaricae, Tomus 93 (3—4), pp. 425—426 (1977)

A NEW SYNTHESIS OF THIO-SUGARS *VIA* THIO-KETONES

(PRELIMINARY COMMUNICATION)

M. M. A. ABDEL-RAHMAN

(Department of Chemistry, Faculty of Science, Alexandria University, Alexandria, Egypt)

Received April 7, 1977; in revised form, July 13, 1977

Because of the considerable interest in the biochemistry of thio-sugars [1], a search for their synthesis was considered *via* the corresponding thio-ketones as intermediates.

Aliphatic thioketones, unlike their aromatic analogues, have not been extensively studied and there is inconsistent information about their properties and methods of synthesis. Although there are ideas about their preparation by reacting the appropriate ketone with phosphorus pentasulfide, hydrogen sulfide, or other thionating agents, it has been shown [2] that, according to the ketone used and the conditions of the reaction, the product may be a thio-ketone, a dimer or a higher polymer, or a *gem*-dithiol.

Sugar thioketones have not been described before, which would be useful synthetic intermediates for the synthesis of thio-sugars by the action of a reducing agent. In the present communication, the synthesis of 1,2 : 5,6-di-*O*-isopropylidene-3-thio-α-D-allo-furanose from 1,2 : 5,6-di-*O*-isopropylidene-α-

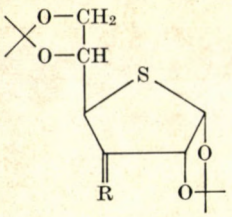

1

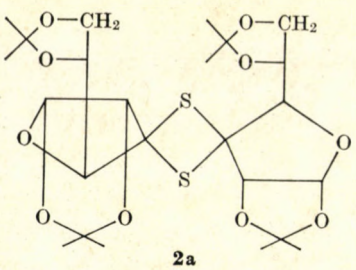

2a

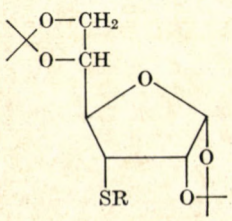

3

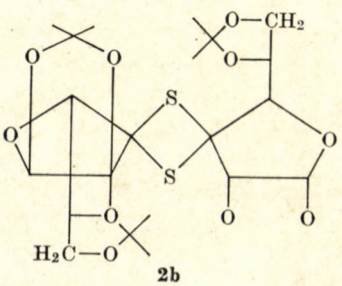

2b

D-ribo-hexafuranos-3-ulose is described. Thus, boiling 1,2 : 5,6-di-*O*-isopropylidene-α-D-ribo-hexofuranos-3-ulose [3] (**1**, R=O) with phosphorus pentasulfide in aqueous pyridine resulted in the production of a white crystalline material, crystallized from ethanol, m.p. 267—270°C, $[\alpha]_D^{20}$ + 42.5° (c 1.0, chloroform). In spite of the agreement of its micro-analytical data (Found: C, 52.2; H, 6.4; S, 11.4. $C_{12}H_{18}O_5S$ requires: C, 52.5; H, 6.6; S, 11.7%) with those required for the thioketone (**1**, R=S), its UV spectrum did not show the characteristic thione [2] bands. On the other hand, the mass spectrum showed a molecular ion (*m/e* 548), which ascertained the compound to be a dimer, which may exist in the two stereoisomeric forms **2**a and **2**b.

On the other hand, treatment of a solution of **1** (R=O) in DMF containing triethylamine at 100°C with a stream of hydrogen sulfide resulted in the formation of a yellow oil, possessing maxima at 227 and 268 nm in its UV spectrum, indicating the presence of the thioketone (**1**, R=S). Storage or warming of the material afforded the crystalline dimer **2**. The freshly prepared, crude thioketone (**1**, R=S) was reduced using sodium in liquid ammonia to afford 1,2:5,6-di-*O*-isopropylidene-3-thio-α-D-allo-furanose (**3**, R=H), b.p. 92—95°C (10^{-3} torr, n^{21} 1.51, $[\alpha]_D^{20}$ + 38°C (c 1.0, chloroform), ν_{max} 2600 cm^{-1} (SH), (Found: C, 52.0; H, 7.1; S, 11.3. $C_{12}H_{20}O_5S$ requires: C, 52.2; H, 7.3; S, 11.6%). On benzoylation it gave the S-benzoyl derivative (**3**, R=COPh), m.p. 79—82°C, $[\alpha]_D^{21}$ + 110° (c 0.9, chloroform), ν_{max} 1670 cm^{-1} (SBz). These constants and the NMR spectrum were in accordance with those reported earlier [4]. It seems that reduction of the thioketone (**1**, R=S), as expected, follows the same stereochemical way as the reduction [5] of the ketone (**1**, R=O), where the attack occurs from the least hindered side of the double bond.

REFERENCES

[1] PITTS, M. J., CHEMIELEWSKI, M., CHEN, M. S., ABDEL-RAHMAN, M. A., WHISTLER, R.: Arch. Biochem. Biophys. **169**, 384 (1975)
[2] MAYER, R., MORGENSTERN, J., FABIAN, J.: Angew. Chem. Int. Ed. Engl. **3**, 277 (1964)
[3] ONODERA, K., HIRANO, S., KASHIMURA, N.: J. Am. Chem. Soc. **87**, 4651 (1965); Carbohyd. Res. **6**, 276 (1968); BRIMACOBE, J. S., BRYAN, J., HUSAIN, A., STACEY, M., TOLLEY, M.: *ibid.*, **3**, 318 (1967)
[4] HEAP, J., OWEN, L.: J. Chem. Soc. (C), **1970**, 712
[5] THEANDER, O.: Acta Chem. Scand. **18**, 2209 (1964)

M. M. A. ABDEL-RAHMAN University of Minnesota
The Hormel Institute 801—16th Avenue N. E.
Austin, Minnesota 55912 USA.

INDEX

ANALYTICAL CHEMISTRY

PHYSICAL AND INORGANIC CHEMISTRY

ORGANIC CHEMISTRY

Printed in Hungary

A kiadásért felel az Akadémiai Kiadó igazgatója — Műszaki szerkesztő: Zacsik Annamária

A kézirat nyomdába érkezett: 1977. III. 17. — Terjedelem: 18,90 (A/5) ív, 91 ábra

77.4332 Akadémiai Nyomda, Budapest — Felelős vezető: Bernát György

ACTA CHIMICA

ТОМ 93 – ВЫП. 3 – 4

РЕЗЮМЕ

Некоторые характеристики холографических пластинок и применение их в спектральном анализе

З. БУРГУДЖИЕВ, К. ЦИММЕР и Е. БОБОЛИНА

Возможности использования фотоматериала в спектральном анализе могут быть надлежаще оценены, если основные свойства этого материала, в частности форма кривой почернения и отношение сигнала к шуму, известны. Согласно требованиям, обычные спектральные пластинки должны обладать разрашающей силой порядка 100 линий/мм; этот вопрос можно считать уже достаточно выясненным. Однако, это не характерно для холографических пластинок, разрешающая способность которых сильно отличается. Оценка последней, представляющая практический интерес, является предметом этой статьи.

Исследование газофазного терморазложения бромированных производных метана

Б. А. КИШ, Т. ДЁЙЧ, О. КАПОШИ и Л. ЛЕЛИК

Экспериментально были определены изменения концентрации продуктов газофазного пиролиза метилбромида, метиленбромида и бромоформа в инетрвале температур 720—1170°К.

На основе предварительных термодинамических соображений и расчетов были отмечены вероятные направления терморазложения. Вслед за этим, используя экспериментальные наблюдения, были определены наиболее вероятные реакционные ступени. В случае разложения бромоформа и, используя толуол в качестве газа-носителя, была определена сила связи C—Br в молекуле, исходя из температурной зависимости константы скорости реакции расщепления связи. Согласно расчетам это 51,0 ккал/моль.

Отдельные ступени цепных процессов подтверждались термохимическими данными, полученными с помощью метода МС.

Расчет фактора реактивного поля в диэлектрике с шаровой симметрией слоев

(Уточнение модели Онсагера)

Я. ЛИСИ и Л. МЕСАРОШ

Модель Онсагера, относящаяся к статистической относительной проницаемости жидкостей была модифицирована таким образом, что гомогенный диэлектрик, фигурирующий в модели Онсагера, был заменен гетерогенным диэлектриком. В новой модели полость окружена шаровой оболочкой с относительной проницаемостью ε_{loc}, а последняя, в свою очередь, залегает в диэлектрике бесконечной протяженности с относительной проницаемостью ε_0. Был определен фактор реактивного поля, соответствующего новой модели, а также было изучено влияние среды, непосредственно окружающей полость, на фактор реактивного поля.

Сорбция смесей растворитель-нерастворитель на фенолрезитольных гелях

Э. ВОЛЬФРАМ, Й. ДЬЁРДИ-ЭДЕЛЕНИ и М. НАДЬ

Степень набухания (определенная весовым путем) пластинок фенол-резитольных смол, полученных из пленок высушиванием из бинарных жидких смесей, содержащих различные количества одного растворяющего компонента (ацетон, 1,4-диоксан, метанол, н-пропанол) и одного нерастворяющего компонента (вода или н-гептан), были определены в равновесии набухания. Из полученных данных для всего интервала состава были рассчитаны количество растворителя, связанного полимерной фазой, и сорбционный параметр.

Как правило, нерастворитель понижает поглощение растворителя полимером, за исключением водных смесей как ацетона, так и диоксана, где наблюдается синергетический эффект. Было найдено, что т. наз. обратная сорбция, т. е. относительное обогащение сорбционного слоя нерастворителем, что вытекает из отрицательных величин сорбционного параметра, происходит в системах, где взаимодействие двух растворяющих компонентов не слишком слабо.

Результаты находятся в согласии с более ранними данными, полученными для поливинилового спирта, и могут быть объяснены на основе теоретических соображений Поукли.

Свойства смесей спирт–амин, XII

Электропроводность смесей три(н-бутил)-амин-спирт

Ф. РАТКОВИЧ и М. ЛАСЛО

Удельная электропроводность смесей три(н-бутил)-амина с метанолом, этанолом, 1-пропанолом и 1-бутанолом была исследована в полном интервале концентраций при температурах 20 и 45°С. Полученные результаты интерпретируются, исходя из модели диссоциации ассоциатов типа A_iB, содержащих несколько молекул спирта на одну молекулу амина. Было найдено, что концентрация смешанных ассоциатов практически не зависит от спиртовых компонентов смесей и максимум удельной электропроводности зависит от диэлектрической постоянной спирта, используемого в качестве растворителя — как это предсказывается на основе теории Бъеррума об ассоциированных ионах. Было рассчитано число спиртовых молекул в смешанных ассоциатах и, исходя из его температурной зависимости, можно было делать заключения относительно циклического или цепного характера ассоциатов чистых спиртов. Было найдено, что в изученном интервале температур чистый метанол характеризуется цепной ассоциацией, в то время как ассоциаты более высоких членов гомологического ряда являются скорее циклическими. Эти результаты находятся в согласии с полученными более ранее.

Свойства смесей спирт–амин, XIII

Электропроводность растворов первичных и вторичных аминов в спиртах

Ф. РАТКОВИЧ и М. ЛАСЛО

Электропроводность смесей н-бутиламин—спирт и ди(н-бутил)-амин—спирт была исследована при 20 и 45°С. Результаты рассчитывали, исходя из модели, полагающей электролитическую диссоциацию смешанных ассоциатов типа A_nB. Полученные результаты указывают на то, что в случае ди(н-бутил)-амина в основном присутствуют ассоциаты типа A_nB и лишь в меньших количествах ассоциаты типа A_iBA_j. В случае же смесей н-бутиламин—спирт, помимо ассоциатов типа A_nB, необходимо также считаться с ассоциатами типа A_iB_j, особенно в области средних концентраций спирта. Число молекул спирта в смешанных ассоциатах было исследовано в зависимости от температуры. Полученные результаты подтверждают более ранние заключения, а именно, что в гомологическом ряду от метанола до 1-бутанола циклическая структура становится все более характерной.

Модель отталкивания электронных пар валентной оболочки и геометрия тетраэдрических и подобных молекул

И. ХАРГИТТАИ и А. БАРАНИ

Представлена простая модель, с помощью которой демонстрируются изменения в валентных углах. Эта модель использует точечные заряды на сфере для тетраэдрических систем. Современные геометрические данные соответствуют многим, хотя и не всем, предсказаниям простых правил модели отталкивания электронных пар валентной оболочки.

Исследование реакций хемосорбированного водорода и кислорода на платиновых катализаторах без носителей

Д. МОГЕР, М. ХЕГЕДЮШ, Т. БЕШЕНЕИ и Ф. НАДЬ

На основе исследований с использованием термодесорбционной хроматографии и техники импульса были сделаны следующие заключения относительно реакционной способности стабильно хемосорбированных водорода и кислорода:

1. Хемосорбированный кислород может быть удален с поверхности катализатора с помощью газообразного водорода уже при комнатной температуре.
2. Хемосорбированный водород, однако, удаляется с помощью газообразного кислорода лишь при таких повышенных температурах, при которых и десорбция имеет конечную скорость. Таким образом, можно полагать, что при комнатной температуре протеканию реакции препятствует кинетический (вероятно стерической) барьер.
3. В свете этих исследований, обычная интерпретация «кислородно-водородного» титрования, широко используемая в практике катализа, становится сомнительной, по крайней мере, для случая металлических платиновых катализаторов.

Обменные равновесия на алюминий-никотине, III

Каолинит

ДЖ. П. СИНГАЛ и Р. П. СИНГ

На основе термодинамических исследований обменных разновесий между никотином и Al-каолинитом были получены изотермы, факторы разделения, коэффициенты селективности и изменения стандартных свободных энергий, которые указывают на то, что реакция протекает неспонтанно с предпочтением в отношении к никотину. Неспонтанность реакции получает подтверждение, исходя из потери энтропии. Было, однако, обнаружено, что никотин сильно связан с фиксированными специфическими местами каолинита в слое Штерна. Коэффициенты активности и избыточные термодинамические функции указывают на то, что реакция протекает в сильно гетерогенной неидеальной системе.

Инфракрасные спектры 1,2,3,5-тетразамещенных производных бензола

ДЬ. ВАРШАНИ, Г. ХОРВАТ, Л. ИМРЕ, Й. ШАВАРЦ, П. ШОХАР и Ф. ШОТИ

Исходя из колебаний в кольце, 115 1,2,3,5-тетразамещенных производных бензола могут быть подразделены на три группы согласно тому, что все четыре заместителя «легкие», либо один или два среди них «тяжелые». Вначале были проанализированы 30 колебаний кольца бензола, которые наиболее вероятно могут быть отнесены к основным колебаниям. Для каждого колебания приводятся интенсивности относимых полос и интервалы частот. Во-вторых был рассмотрен характер полос, относимых к внутренним колебаниям заместителей. Особое внимание уделяли группам OH, C=O, NO_2 и амида, т. к. на основе характеристик их полос можно делать заключения относительно межмолекулярной и хелатной структуры в твердой фазе. Интенсивности и частоты этих полос приводились в корреляцию с электронными сдвигами внутри молекулы.

Повышение содержания информаций спектральных фотопластинок в оптической эмиссионной спектроскопии

К. ДАНЦЕР и А. ЗОНТАГ

Исходя из теоретических основ фотографических информаций, показывается возможность дополнительной обработки фотографически зарегистрированной информации для улучшения использования резервов информации. Исследовано применение фильтров при проявлении и усиление градации путем твердого копирования фотографически зарегистрированных спектров. Оба метода улучшают отношение сигнала к шуму при спектральных линиях слабого почернения, и таким образом, улучшают детектирование некоторых спектральных линий.

Модель жидкой воды

Тетрагональнные кластеры: описание и определение параметров

Ф. ХАЙДУ

Для описания структуры воды предлагается модель тетрагональных кластеров, основанная на функциях радиального распределения, полученных из рентгенодиффракционных исследований при трех температурах. Помимо воспроизведения экспериментальных функций радиального распределения и приведенных интенсивностей, модель хорошо описывает объемные эффекты и другие физические корреляция между водой и некоторыми ледяными полиморфами.

Полиатомные катионы селена в сульфонилхлориде

С. А. А. ЗАИДИ, З. А. СИДДИКИ и Н. А. АНСАРИ

Селен растворяется в сульфонилхлориде, давая зеленый раствор, которой после стояния в течение нескольких часов переходит в желтый. Зеленый и желтый растворы являются следствием образования катионов Se_8^{+2} и Se_4^{+2}, соответственно. На основе кондуктометрических и спектрофотометрических исследований было показано, что в присутствии средних количеств соответствующих окислительных реагентов селен окисляется до валентного состояния $+1$, приводя к образованию катиона Se_4^{+4}.

Получение производных 2Н- и 4Н-бензотиазина

Исследование замыкания 1,3-бензотиазинового кольца в амидах N-(3,4-диалкоксифенилтиометил)-кислот

Й. САБО, Л. ФОДОР, И. ВАРГА, Э. ВИНКЛЕР и П. ШОХАР

Было установлено, что, в противоположность ранним исследованиям, но в согласии с некоторыми наблюдениями других авторов, замыкание 1,3-бензотиазинового кольца в амидах N-(3,4-диалкоксифенилтиометил) кислоты (I), проводимое в кислых средах, представляет собой реакцию в двух направлениях, где наряду с производными 4Н-1,3-бензотиазина (III) образуются также в различных количествах — в зависимости от строения (I) — изомеры 2Н-1,3-бензотиазина (II).

Альтернативный путь синтеза некоторых новых 5-аминодизамещенных и 3-иминозамещенных 1,2,4-дитиазолинов: окислительное деаллилирование и циклизация 1,1,5-тризамещенных 2-S-аллилизо-4-тиобиуретов

Р. СИНГ и В. К. ВЕРМА

5-Метилфениламино-3-п-толилимино-, 5-метилфениламино-3-п-этоксифенилимино-, 5-метилфениламино-3-п-хлорфенилимино-, 5-дифениламино-3-п-толилимино- и 5-дифениламино-3-п-этоксифенилимино-1,2,4-дитиазолины были получены окислитетельным деаллилированием и циклизацией соответствующих 1,1,5-тризамещенных 2-S-аллилизо-4-тиобиуретов йодом в кипящем хлороформе. Приводится механизм этой реакции.

Окисление некоторых гидроксиарилпиразолинов двуокисью марганца

Т. С. ШАРМА, В. САКСЕНА и Н. И. РЕДДИ

Окисление гидроксиарилпиразолинов двуокисью марганца приводит к образованию соответствующих пиразолов (III), сопровождаемых очень небольшими количествами неидентифицируемого желтого осадка. Строение пиразолей подтверждалось на основе их синтеза из дибромистого халкона (IV) и гидрата гидразина.

Les Acta Chimica paraissent en français, allemand, anglais et russe et publient des mémoires du domaine des sciences chimiques.

Les Acta Chimica sont publiés sous forme de fascicules. Quatre fascicules seront réunis en un volume (4 volumes par an).

On est prié d'envoyer les manuscrits destinés à la rédaction à l'adresse suivante:

Acta Chimica
H-1521 Budapest, Hongrie

Toute correspondance doit être envoyée à cette même adresse.

La rédaction ne rend pas de manuscript.

Le prix de l'abonnement est de $ 32,00 par volume.

Abonnement — en Hongrie à Akadémiai Kiadó (1363 Budapest, P.O.B. 24, C.C.B Bankszámla 215 11488), à l'étranger à l'Entreprise pour le Commerce Extérieur «Kultúra» (1389 H-Budapest 62, P.O.B. 149 Compte-courant No. 218 10990) ou l'étranger chez tous les représentant ou dépositaires.

Die Acta Chimica veröffentlichen Abhandlungen aus dem Bereich der chemischen Wissenschaften in deutscher, englischer, französischer und russischer Sprache.

Die Acta Chimica erscheinen in Heften wechselnden Umfanges. Vier Hefte bilden einen Band. Jährlich erscheinen 4 Bände.

Die zur Veröffentlichung bestimmten Manuskripte sind an folgende Adresse zu senden:

Acta Chimica
H-1521 Budapest, Ungarn

An die gleiche Anschrift ist auch jede für die Redaktion bestimmte Korrespondenz zu richten.

Manuskripte werden nicht zurückerstattet.

Abonnementspreis pro Band: $ 32,00.

Bestellbar für das Inland bei Akadémiai Kiadó (1363 Budapest, Postfach 24, Bankkonto Nr. 215 11488), für das Ausland bei dem Außenhandelsunternehmen »Kultúra« (H-1389 Budapest 62, P.O.B. 149. Bankkonto Nr. 218 10990) oder bei seinen Auslandsvertretungen und Kommissionären.

«Acta Chimica» издают статьи по химии на русском, английском, французском и немецком языках.

«Acta Chimica» выходит отдельными выпусками разного объема, 4 выпуска составляют один том и за год выходят 4 тома.

Предназначенные для публикации рукописи следует направлять по адресу:

Acta Chimica
H-1521 Budapest, ВНР

Всякую корреспонденцию в редакцию направляйте по этому же адресу.

Редакция рукописей не возвращает.

Подписная цена — $ 32,00 за том.

Отечественные подписчики направляйте свои заявки по адресу Издательства Академии Наук (1363 Budapest, P.O.B. 24, Текущий счет 215 11488), а иностранные подписчики через организацию по внешней торговле «Kultúra» (H-1389 Budapest 62, P.O.B. 149. Текущий счет 218 10990) или через ее заграничные представительства и уполномоченных.

Reviews of the Hungarian Academy of Sciences are obtainable at the following addresses:

AUSTRALIA
C.B.D. LIBRARY AND SUBSCRIPTION SERVICE, Box 4886, G.P.O., *Sydney N.S.W. 2001*
COSMOS BOOKSHOP, 135 Ackland Street, *St. Kilda (Melbourne), Victoria 3182*

AUSTRIA
GLOBUS, Höchstädtplatz 4, *1200 Wien XX*

BELGIUM
OFFICE INTERNATIONAL DE LIBRAIRIE, 30 Avenue Marnix, *1050 Bruxelles*
LIBRAIRIE DU MONDE ENTIER, 162 Rue du Midi, *1000 Bruxelles*

BULGARIA
HEMUS, Bulvar Ruszki 6, *Sofia*

CANADA
PANNONIA BOOKS, P.O. Box 1017, Postal Station "B", *Toronto, Ontario M5T 2T8*

CHINA
CNPICOR, Periodical Department, P.O. Box 50, *Peking*

CZECHOSLOVAKIA
MAD'ARSKÁ KULTURA, Národní třida 22, *115 33 Praha*
PNS DOVOZ TISKU, Vinohradská 46, *Praha 2*
PNS DOVOZ TLAČE, *Bratislava 2*

DENMARK
EJNAR MUNKSGAARD, Norregade 6, *1165 Copenhagen*

FINLAND
AKATEEMINEN KIRJAKAUPPA, P.O. Box 128, *SF-00101 Helsinki 10*

FRANCE
EUROPERIODIQUES S. A., 31 Avenue de Versallies, *78170 La Celle St. Cloud*
LIBRAIRIE LAVOISIER, 11 rue Lavoisier, *75008 Paris*
OFFICE INTERNATIONAL DE DOCUMENTATION ET LIBRAIRIE, 38 rue Gay-Lussac, *75240 Paris Cedex 05*

GERMAN DEMOCRATIC REPUBLIC
HAUS DER UNGARISCHEN KULTUR, Karl-Liebknecht-Strasse 9, *DDR-102 Berlin*
DEUTSCHE POST ZEITUNGSVERTRIEBSAMT, Strasse der Pariser Kommüne 3—4, *DDR-104 Berlin*

GERMAN FEDERAL REPUBLIC
KUNST UND WISSEN ERICH BIEBER, Postfach 46, *7000 Stuttgart 1*

GREAT BRITAIN
BLACKWELL'S PERIODICALS DIVISION, Hythe Bridge Stteet, *Oxford OX1 2ET*
BUMPUS, HALDANE AND MAXWELL LTD., Cowper Works, *Olney, Bucks MK46 4BN*
COLLET'S HOLDINGS LTD., Denington Estate, *Wellingborough, Northants NN8 2QT*
WM. DAWSON AND SONS LTD., Cannon House, *Folkestone, Kent CT19 5EE*
H. K. LEWIS AND CO., 146 Gower Street, *London WC1E 6BS*

GREECE
KOSTARAKIS BROTHERS, International Booksellers, 2 Hippokratous Street, *Athens-146*

HOLLAND
MEULENHOFF-BRUNA B.V., Beulingstraat 2, *Amsterdam*
MARTINUS NIJHOFF B.V., Lange Voorhout 9—11, *Den Haag*
SWETS SUBSCRIPTION SERVICE, 473b Heereweg, *Lisse*

INDIA
ALLIED PUBLISHING PRIVATE LTD., 14/13 Asaf Ali Road, *New Delhi 110001*
150 B-6 Mount Road, *Madras 600002*
INTERNATIONAL BOOK HOUSE PVT. LTD., Madame Cama Road, *Bombay 400039*
THE STATE TRADING CORPORATION OF INDIA LTS., Books Import Division, Chandralok, 36 Janpath, *New Delhi 110001*

ITALY
EUGENIO CARLUCCI, P.O. Box 252, *70100 Bari*
INTERSCIENTIA, Via Mazzé 28, *10149 Torino*
LIBRERIA COMMISSIONARIA SANSONI, Via Lamarmora 35, *50121 Firenze*
SANTO VANASIA, Via M. Macchi 58, *20124 Milano*
D. E. A., Via Lima 28, *00198 Zoma*

JAPAN
KINOKUNIYA BOOK-STORE CO. LTD., 17-7 Shinjuku-ku 3 chome, Shinjuku-ku, *Tokyo 160-91*
MARUZEN COMPANY LTD., Book Department, P.O. Box 5056 Tokyo International, *Tokyo 100-31*
NAUKA LTD., IMPORT DEPARTMENT, 2-30-19 Minami Ikebukuro, Toshima-ku, *Tokyo 171*

KOREA
CHULPANMUL, *Phenjan*

NORWAY
TANUM-CAMMERMEYER, Karl Johansgatan 41—43, *1000 Oslo*

POLAND
WĘGIERSKI INSTYTUT KULTURY, Marszalkowska 80, *Warszawa*
CKP I W ul. Towarowa 28 *00-958 Warsaw*

ROUMANIA
D. E. P., *Bucureşti*
ROMLIBRI, Str. Biserica Amzei 7, *Bucureşti*

SOVIET UNION
SOJUZPETCHATJ — IMPORT, *Moscow*
and the post offices in each town
MEZHDUNARODNAYA KNIGA, *Moscow G-200*

SPAIN
DIAZ DE SANTOS, Lagasca 95, *Madrid 6*

SWEDEN
ALMQVIST AND WIKSELL, Gamla Brogatan 26, *101 20 Stockholm*
GUMPERTS UNIVERSITETSBOKHANDEL AB, Box 346, *401 25 Göteborg 1*

SWITZERLAND
KARGER LIBRI AG, Petersgraben 31, *4011 Basel*

USA
EBSCO SUBSCRIPTION SERVICES, P.O. Box 1934, *Birmingham, Alabama 35201*
F. W. FAXON COMPANY, INC., 15 Southwest Park, *Westwood, Mass, 02090*
THE MOORE-COTTRELL SUBSCRIPTION AGENCIES, *North Cohocton, N. Y. 14868*
READ-MORE PUBLICATIONS, INC., 140 Cedar Street, *New York, N. Y. 10006*
STECHERT-MACMILLAN, INC., 7250 Westfield Avenue, *Pennsauken* N. J. 08110

VIETNAM
XUNHASABA, 42, Hai Ba Trung, *Hanoi*

YUGOSLAYIA
JUGOSLAVENSKA KNJIGA, Terazije 27, *Beograd*
FORUM, Vojvode Mišiča 1, *21000 Novi Sad*

8. XI. 1977 Index: 26.007